

2006 Annual Report

“Emergence of Adaptive Motor Function through
Interaction among the Body, Brain and Environment
- A Constructive Approach to the Understanding of
Mobiligence - ”

Project Leader: Hajime Asama (The University of Tokyo)



March, 2007

Area No. 454
Under Grant-in-Aid for Scientific Research
on Priority Area
from the Japanese Ministry of Education, Culture, Sports,
Science and Technology

Academic Year from 2005 to 2009

2006 Annual Report

“Emergence of Adaptive Motor Function through
Interaction among the Body, Brain and Environment
- A Constructive Approach to the Understanding of
Mobiligence - ”

Project Leader: Hajime Asama (The University of Tokyo)



March, 2007

Area No. 454
Under Grant-in-Aid for Scientific Research
on Priority Area
from the Japanese Ministry of Education, Culture, Sports,
Science and Technology

Academic Year from 2005 to 2009

Contents

Part 1: Report of Steering Committee

| | | |
|---|--|---------|
| Introduction of the <i>Mobiligence</i> Project | Emergence of Adaptive Motor Function through Interaction among the Body, Brain and Environment - A Constructive Approach to the Understanding of <i>Mobiligence</i> - Hajime Asama | 1 |
| Steering Committee Report on the <i>Mobiligence</i> Project | Hajime Asama, Kazuo Tsuchiya, Koji Ito, Masafumi Yano, Koichi Osuka, Kaoru Takakusaki, Ryohei Kanzaki, Hitoshi Aonuma, Akio Ishiguro, and Jun Ota | 3 |

Part 2: Report of Group A

| | | |
|--|--|---------|
| Group A: Adaptation to Environment Annual Report | Koji Ito | 5 |
| Voluntary Movements Controlled by “Mi-Nashi” created in the Motor Cortices | Masafumi Yano | 7 |
| Modeling of Intra-cerebral Mechanisms for the Motor Adaptation to Unknown Environments | Koji Ito and Toshiyuki Kondo |11 |
| The Roles of Implicit and Explicit Processes in Vision | Satoshi Shioiri, Kazumichi Matsumiya and Ichiro Kuriki |15 |
| Behavior Induction and Recall under an Unknown Situation based on Multimodal Mirror Neuron Model | Tetsunari Inamura |19 |
| Visuomanual Coordination in Ball Catching Task | Yasuharu Koike |23 |
| Analysis of Human Skills in Manipulation with Interaction with Environment | Hidden Markov Modeling of Human Pivoting Operations - Yusuke Maeda and Hajime Sugiuchi |27 |
| Optimal Foraging Strategy: Representation of Anticipated Rewards and Optimal Work Cost Investment in Hippocampus Striatum Optic Tectum | Toshiya Matsushima |31 |
| Complementality between the Feedback and Feedforward Mechanisms | Yasuhiro Takachi and Yasuji Sawada |35 |
| Classification of Object-Shape by a Supple Finger Robot with a Tactile Sensing Array | Sumiaki Ichikawa, Kenshi Watanabe, Ken-ichi Ohkubo and Fumio Hara |39 |
| Mirror Neuron System Related to Bodily Self | Akira Murata and Hiroaki Ishida |43 |
| Constructive Approach to Understanding the Active Learning Process of Adaptation within a Given Task Environment | Hiroaki Arie, Shigeki Sugano and Jun Tani |47 |

Part 3: Report of Group B

Group B: Research Report

| | | |
|---|----------------|----|
| | Kazuo Tsuchiya | 51 |
| Cortical Motor Areas & Postural and Locomotor Synergies | | |
| Katsumi Nakajima, Futoshi Mori, Masahiko Inase, Dai Yanagihara, Taizo Nakazato, Shigeru Kitazawa and Kaoru Takakusaki | | 53 |
| System Biomechanics of Locomotion in the Japanese Monkey: Exploration of Principal Mechanism for Generating Adaptive Locomotion based on a Neuro- Musculoskeletal Model | | |
| Naomichi Ogihara, Shinya Aoi, Yasuhiro Sugimoto, Masato Nakatsukasa and Kazuo Tsuchiya | | 57 |
| Realization of Adaptive Locomotion based on Dynamic Interaction between Body, Brain, and Environment | | |
| Koh Hosoda, Hiroshi Kimura, Katsuyoshi Tsujita and Kousuke Inoue | | 61 |
| Hypothalamic Regulation of Muscular Tonus Involvement of GABAergic Neurons - | | |
| Yoshimasa Koyama, Kazumi Takahashi and Tohru Kodama | | 65 |
| Study on Brain Adaptation in Rat-machine Fusion Systems | | |
| Takafumi Suzuki and Kunihiro Mabuchi | | 69 |
| Detection with BMI Methods How Body Movements are Involved in Neural Coding in the Brain | | |
| Yoshio Sakurai | | 73 |
| A Multi-disciplinary Study of Adjustment Mechanisms of Human Bipedal Gait | | |
| Takashi Hanakawa, Kazumi Iseki, Kazuo Hashikawa and Manabu Honda | | 77 |
| Neural Mechanisms of Integration of the Somatic and Autonomic Nervous Functions in the Emergence of Motor Behaviors | | |
| Kiyoji Matsuyama and Mamoru Aoki | | 81 |
| A Locomotor CPG Model based on Phase Dynamics | | |
| Ikuko Nishikawa | | 85 |
| Sensing while Moving: Exploring a Neural Correlate of Sensorimotor Gating during Voluntary Movement | | |
| Kazuhiko Seki | | 89 |

Part 4: Report of Group C

Group C: Social Adaptation

| | | |
|--|----------------|----|
| | Hitoshi Aonuma | 93 |
| Systematic Understanding of Neuronal Mechanisms for Adaptive Behavior in Changing Environment | | |
| Hitoshi Aonuma and Ryohei Kanzaki | | 95 |
| Modeling of Neuronal Mechanism of Fighting Behavior in Crickets | | |
| Jun Ota, Hajime Asama and Kuniaki Kawabata | | 99 |
| Analysis of Adaptive Behaviors Emerged by Functional Structures in Interaction Networks | | |

| | |
|----------------------------|-----|
| Publications, Awards | 167 |
| Activity Record | 182 |

Introduction of the *Mobiligence* Project

Emergence of Adaptive Motor Function through Interaction among the Body, Brain and Environment

- A Constructive Approach to the Understanding of *Mobiligence* -

Hajime Asama

Director of the *Mobiligence* Project
The University of Tokyo

1. Introduction

The *Mobiligence* project is a five-year project started from 2005[1], which was accepted as a program of Scientific Research on Priority Areas of Grant-in-Aid Scientific Research from the Japanese Ministry of Education, Culture, Sports, Science and Technology (MEXT). In addition to the planned research groups which started in 2005, new two-years-research groups (applied research groups) will be selected and start from 2006. This paper presents the abstract of the project.

2. Objective of the *Mobiligence* Project

Human can behave adaptively even in diverse and complex environment. All the animals can perform various types of adaptive behaviors, such as a locomotive behavior in the form of swimming, flying walking, a manipulation behaviors such as reaching, capturing, grasping by using hands and arms, a social behavior to the other subjects, etc. Such adaptive behaviors are the intelligent sensory-motor functions, and most essential and indispensable ones for animals to survive.

It is known that the function of such adaptive behaviors is disturbed in patients with neurological disorders. Parkinson disease is a typical example of disorders on adaptive motor function, and autism or depression can also be considered as a disorder on social adaptive function.

Recently, due to aging or environmental change of society, the population of people who are suffering from these diseases is growing rapidly, and it is urgent to cope with this problem. However, the mechanisms for the generation of intelligent adaptive behaviors are not thoroughly understood. Such an adaptive function is considered to emerge from the interaction of the body, brain, and environment, which requires that a subject acts or moves. Base on the consideration, we call the intelligence for generating adaptive motor function *mobiligence*.

The present project is designed to investigate the mechanisms of *mobiligence* by closely collaborative research of biology and engineering. In the course of this collaborative project, the following processes will be carried out:

1. Biological and physiological examinations of animals;
2. Modeling of biological systems;
3. Construction and experiments on artificial systems by utilizing robotic technologies; and
4. Creation of a hypothesis and its verification.

The final goal of this project is to establish the common principle underlying the emergence of *mobiligence*.

3. Research Approach of the *Mobiligence* Project

In this project, the *mobiligence* mechanism is to be elucidated by the constructive and systematic approaches, through the collaboration of biologists and engineering scientists who developed biological models by integrating physiological data and kinetic modeling technologies as shown in figure 1. In other words, the *Mobiligence* Project is pursued by integrating biology and engineering, i.e., physiological analysis (biology), modeling and experiments on artificial systems (engineering), verification of models (biology), and discovery and application of principles (engineering).

In the following discussion, the focus is on three adaptive mechanisms:

1. Mechanism whereby animals adapt to recognize environmental changes;
2. Mechanism whereby animals adapt physically to environmental changes; and
3. Mechanism whereby animals adapt to society.

Research groups for each of the categories listed above are organized. The three groups conduct their respective research and clarify the universal, common principle underlying the mechanism of *mobiligence*. The Planned Research Team studies the following specific subjects: analysis of the environmental cognition and the adaptive mechanism in reaching movements; analysis of the physical adaptive mechanism in walking; and analysis of the adaptive mechanism observed in the social behaviors of insects. In addition, the Planned Research Team clarifies the common principle underlying *mobiligence* from a dynamic viewpoint. Furthermore, we study adaptive mechanisms relating to various objects by publicly inviting proposed topics and clarify the universal, common principle therein.

4. Research Activities till the *Mobiligence* Project

The *Mobiligence* project is highly motivated by the previous project on emergent systems, which was carried out from 1995 to 1997 and directed by Prof. Shinzo Kitamura of Kobe University. Although the system theory on emergent function formation was actively discussed in the project, the principle it couldn't be revealed enough how to design the emergent systems. After the project on emergent systems, a special interest group on System Principle on Emergence of *Mobiligence* and Its Engineering Realization was organized in the System and Information Division of the Society of Instrument and Control Engineers (SICE) in 2003, and the research activities have been continued.

We held a workshop sponsored by the Tohoku University Nation-wide Cooperative Research Project from 2001, and a workshop on the development of the emergence system of *mobiligence* and its control system under the sponsorship of the Nissan Science Foundation.

Before starting the *mobiligence* project, we planned and held organized sessions in international conferences and in lecture meetings of academic societies

- IFAC Intelligent Autonomous Vehicles (IAV)
- International Symposium on Distributed Autonomous Robotic Systems (DARS)
- International Symposium on Adaptive Motion of Animals and Machines (AMAM)
- IEEE/RSJ International Conference on Intelligent Robots and Systems (IROS)

- SICE Annual Conference
- SICE System and Information Division Annual Conference (SSI)
- SICE System Integration Division Annual Conference (SI)
- SICE Symposium on Decentralized Autonomous Systems

5. Expected Impact of the *Mobiligence* Project

Various types of adaptive motor function mechanisms performed by animals are expected to be elucidated. In the medical field, the results of our research will contribute to the discovery of a method to improve motor impairment and develop rehabilitation systems. In addition, in the engineering field, the results of our research will contribute to the derivation of the design principles of artificial intelligence systems. Furthermore, we will explore the new research field, *mobiligence*, establish a research organization that integrates biology and engineering, and implement programs to foster young engineering scientists and biologists to conduct collaborative and interdisciplinary research between biological and engineering research, respectively.

References

- [1] http://www.arai.pe.u-tokyo.ac.jp/mobiligence/index_e.html

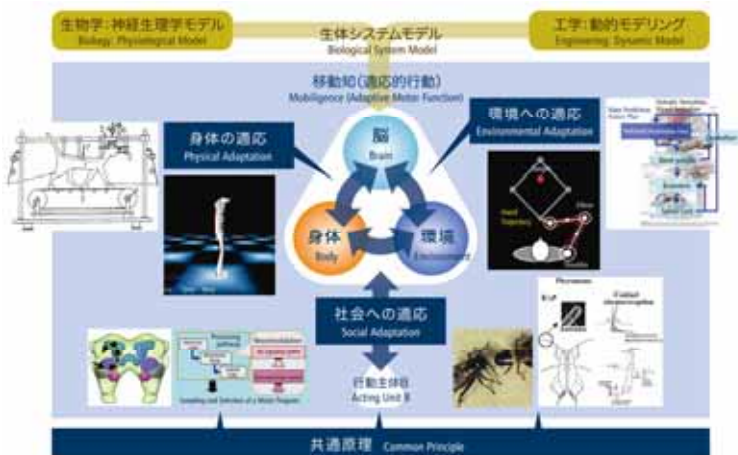


Fig. 1 Framework of the *Mobiligence* Project



Fig. 2 Expected Impact of the *Mobiligence* Project

Steering Committee Report on the *Mobiligence* Project

Hajime Asama*¹, Kazuo Tsuchiya*², Koji Ito*³, Masafumi Yano*⁴, Koichi Osuka*⁵,
Kaoru Takakusaki*⁶, Ryohei Kanzaki*¹, Hitoshi Aonuma*⁷, Akio Ishiguro*⁸, Jun Ota*¹

*¹The University of Tokyo, *²Kyoto University, *³Tokyo Institute of Technology, *⁴Tohoku University,
*⁵Kobe University, *⁶Asahikawa Medical College, *⁷Hokkaido University, *⁸Nagoya University

1. Missions

The missions of the steering committee are as follows:

- Establish goals for the *Mobiligence* Project
- Plan and coordinate research
- Evaluate research progress and consult
- Determine the procedures for the public invitation of proposed topics
- Organize symposia and research meetings for the purpose of developing related research
- Plan publicity of research results
- Encourage close collaboration among researchers, i.e., information exchange, mutual understanding, and communication
- Plan international research and lectures by members of academic societies and announce interim and ex post evaluations of progress
- Devise programs to encourage fused collaboration among biologists and engineering scientists and establish a research center and research organization

2. Summary of 2006 Activities of the Steering Committee

Research subjects were coordinated in each group to facilitate the fused collaboration between biologists and engineering scientists, which characterizes this project, and joint group meetings and open group meetings were organized to promote the inter-group collaboration effectively. Many events were organized as follows; a domestic symposium, an open symposium, a closed symposium, practice programs, tutorials, and seminars. The internal evaluation was performed twice. Many organized sessions are organized at international and domestic conferences. The homepage for publicity and the database to record the activities in the project were maintained and updated. Research report was edited and published. Junior Academy of the *mobiligence* project was established and their activities were supported.

3. Steering Committee Meetings

The following Steering Committee meetings were held:

- [1] 1st Steering Committee Meeting
June 25th, 2006, 12:00-14:30
at Toya Sunpalace
- [2] 2nd Steering Committee Meeting
Mar. 10th, 2007, 12:00-14:00
at Toya Sunpalace

4. Organization of Symposia

4.1 Domestic Symposium

A domestic symposium was held in Toya Sunpalace, Hokkaido, Japan, on June 23-25, 2006. Group meetings were held on the first day. On the second day, the objective of the project was introduced by Prof. Hajime Asama, director of the project, followed by presentation of current research progress by each group leaders, Prof. Koji Ito, Prof. Kazuo Tsuchiya, Prof. Hitoshi Aonuma, and Prof. Koichi Osuka, and Prof. Tateo Shimodate (Hokkaido Univ.) and Dr. Hiroaki Gomi (NTT Communications) gave invited talks. A night session was also organized by Junior Academy of the *Mobiligence* project. On the last day, six research leaders presented their research subjects, and three domestic reviewers, Prof. Shinzo Kitamura (Kobe University), Prof. Shigemi Mori (National Institute for Physiological Sciences), and Prof. Ryoji Suzuki (Kanazawa Institute of Technology) presented their review comments. Total number of participants was 106.

4.2 Open Symposium for Publicity

An open symposium was held in RIKEN (The Institute of Physical and Chemical Research), Wako, Japan, on Dec. 1, 2006. At first, the objective of the project was introduced by Prof. Hajime Asama, director of the project, followed by presentation on the social impact and medical application of the project by Prof. Kaoru Takakusaki. Prof. Tadashi Isa (NIPS: National Institute for Physiological Sciences) a member of Integrative Brain Research project, gave an invited talk. Prof. Toshiyuki Kondo presented the concept of adaptiveness in the *Mobiligence* project, and Prof. Naomichi Ogihara, Prof. Ryohei Kanzaki, and Prof. Jun Ota presented the approaches on how to understand the mechanisms of biological systems by collaboration of biologists and robotics researchers from viewpoints of system biomechanics, neuron-informatics, bionomics and physiology. At last, Prof. Akio Ishiguro introduced the common principle to be obtained from the project. Total number of participants was 93. The presentations and discussions were recorded and edited, which can be seen at [1].

4.3 Closed Symposium for Internal Evaluation

A closed symposium for internal evaluation was held in Toya Sunpalace, Hokkaido, Japan, on Mar. 8-10, 2007. Presentation on the research progress in 2006 of all the

subjects in the *Mobiligence* project was made by each research leader, and reviewed by steering committee members. A night session was also organized by Junior Academy of the *Mobiligence* project. Total number of participants was about 90.

5. Tutorials

To accelerate the fused collaboration and to foster young scientists and students who are doing *mobiligence* research, the following tutorial programs including practice and experiments were arranged and held:

- [1] 2nd Experimental Practice Program
Seminar with Practice for measurement and signal processing, Sep. 4-5, 2006 at Tokyo Inst. Of Tech., Tokyo
- [2] 3rd Experimental Practice Program
Tutorial lectures on technology to measure biogenic amine in the cricket brain, Dec. 4-9, 2006, at Kanazawa Institute of Institute.
- [3] Seminars and Tutorials
 - Seminar by Prof. Morasso, Genoa University, DIST, Oct. 31, 2006, at Genoa University.
 - Seminar by Dr. Tiaza Bem-Sojka and Dr. Pierre Meyrand, Nov. 27, 2006 at Kyoto University
 - Tutorial from modeling, analysis and control of human locomotion to understanding of disorders, Apr. 15, 2006 at Kyoto University
 - Tutorial on multi-robot systems and internal model of insects, Apr. 18, 2006 at Hokkaido University
 - Tutorial on brain physiology and collaboration between biology and robotics, June 9-10, 2006 at Asahikawa Medical College
 - Tutorial on oscillators and networks, July 21, 2006 at Hokkaido University
 - Tutorial on scientific papers reading on biology, Sep. 18-20, 2006 at Shikotsuko Kanko Hotel

In addition to the list, nine group meetings and 43 local meetings were held. Group D performed interview to the *mobiligence* researchers for eight times to investigate the common principle.

6. Review

At the domestic symposium mentioned above, three domestic members of reviewers evaluated the research subjects according to their presentation. Because this is the first research year for the subscribed research groups, the internal evaluation was carried out mainly based on the research plan.

At the closed symposium mentioned above, steering committee members in addition to the three domestic members of reviewers evaluated the research progress and grade of collaboration between biology and robotics. The review results are feedback to the research leaders toward successful research execution.

7. Arrangement of Special Issue and Organized Sessions

Following organized sessions in international and domestic conferences were organized:

- [1] 2006 Annual Conference of JSME Robotics and Mechatronics Division (Robomec '06) (Domestic) May 27th, 2006, Tokyo, Japan (11 papers)
- [2] 2006 Annual Conference of Robotics Society of Japan (RSJ '06) (Domestic), Sep. 26th, 2006, Okayama, Japan (4 papers)
- [3] 16th Intelligent Systems Symposium (FAN Symposium '06) (Domestic), Sep. 26th, 2006, Kashiwa, Japan (1 keynote speech and 7 papers)
- [4] IEEE/RSJ Int. Conference on Intelligent Robots and Systems (IROS 2006), Oct. 11th, 2006, Beijing, China (4 papers)
- [5] SICE-ICCAS Joint Conf. 2006 (SICE-ICCAS), Nov. 21st, 2006, Busan, Korea (1 invited speech and 9 papers)
- [6] 2006 SICE Symposium on Systems and Information (SSI '06) (Domestic), Nov. 28th, 2006, Tsukuba, Japan (4 papers)
- [7] 2006 SICE Symposium on System Integration (SI '06) (Domestic), Dec. 15th, 2006, Sapporo, Japan (15 papers)
- [8] 2007 SICE Symposium on Autonomous Decentralized Systems (Domestic), Jan. 29th, 2007, Tokyo, Japan (23 papers)

8. Activity Support for Junior Academy of the *Mobiligence* project

The steering committee supported the following activities of the Junior Academy of the *mobiligence* project:

- [1] Planned and held an organized session in SICE Symposium on Systems and Information 2006(SSI2006), November 28, 2006
- [2] Planned and held an organized session in 19th SICE Symposium on Decentralized Autonomous Systems, January 29, 2007
- [3] Creating Glossaries(ongoing project)

9. Publicity and Others

For publicity, a home page of the *Mobiligence* project was updated accordingly[2], database on research achievements[3] and activity records was maintained and presented on the web site.

The brochure of the *Mobiligence* project including subscribed research groups was published and distributed. The report, this volume, on the research activities of the *Mobiligence* project in 2006 was edited and published.

The research results on locomotion control based on CPG and the outline of the *mobiligence* project were publicized to the press in Apr., 2006 at University of Electro-Communications.

References

- [1]<http://www.netrush.jp/idou.htm>.
- [2]http://www.arai.pe.u-tokyo.ac.jp/mobiligence/index_e.html
- [3]http://www.arai.pe.u-tokyo.ac.jp/mobiligence/act/index_e.html

Group A: Adaptation to Environment Annual Report

Koji ITO

Tokyo Institute of Technology, Japan

1. RESEARCH PROJECT

The aim of Group A is 1) to clarify the intelligence mechanisms for creating appropriate hypotheses (“Mi-Nashi” information) based on the accumulated experiences under unpredictable environments, 2) to analyze the motor control mechanisms producing adaptive behaviors corresponding to dynamical environments, and 3) to construct mathematical models of the adaptive motor control composed of the brain, body and environment. In order to perform the above subjects, the project organizes the following subgroups.

Subgroup A01: Real time formation of constraint conditions for adaptive motor actions in dynamical environments.

Motor control system consists of <Body> with various action outputs and sensory inputs, <Brain> as the central controller, and <external environment>. The body includes large number of sensors and actuators, and connects the brain with the environment. The interaction between the body and environment imposes some constraints on the redundant degree of freedom in the total dynamical system. Then, the body and environment are the controlled object and builds up the external dynamics to the brain. Accordingly, it is essential in the motor control to self-adjust the dynamic relations among the brain, body and environment corresponding to the purpose of his/her action or movement under an infinite variety of environments. That is, in the dynamical system with the redundant degree of freedom composed of the brain, body and environment, it is the most important problem in the adaptation to environment to find some constraints (“Mi-Nashi” information) from the spatiotemporal contexts and to create the internal dynamics appropriate to the forthcoming environment.

Subgroup A02: Understanding of intra-cerebral mechanisms for the motor adaptation to unknown environments.

In order to create adaptive behaviors in various environments, it is necessary to integrate the redundant degrees of freedom in the brain, body and environment based on changing contexts of situation. Subgroup A02 aims to elucidate the brain mechanisms of the sensorimotor coordination corresponding to the dynamical environments by the experimental, constructive and systematic approaches.

Subgroup A03: Computational modeling and understanding of sensorimotor integration.

Subgroup A03 aims to analyze the mechanisms of the environment cognition and motor constraint based on the perceptual dynamics of visual, auditory sensations, etc., and to construct the computational model of real time sensorimotor integrations.

2. RESEARCH GROUPS

- Planned Research Groups

- 1) M. Yano (Tohoku University)
- 2) K. Ito (Tokyo Institute of Technology)

- Subscribed Research Groups

- 3) S. Shioiri (Tohoku University)
- 4) T. Inamura (National Institute of Informatics)
- 5) Y. Koike (Tokyo Institute of Technology)
- 6) Y. Maeda (Yokohama National University)
- 7) T. Matsushima (Hokkaido University)
- 8) Y. Sawada (Tohoku Institute of Technology)
- 9) S. Ichikawa (Tokyo University of Science, Suwa)
- 10) A. Murata (Kinki University, School of Medicine)
- 11) J. Tani (Brain Science Institute, RIKEN)

3. RESEARCH RESULTS

Subgroup A01: Real time formation of constraint conditions for adaptive motor actions in dynamical environments.

(1) A voluntary movement is an action that the biological system makes for carrying out an aim with adapting unpredictable environments. The aim of the movement can be acquired by the system having “Mi-Nashi”. As a higher constraint for resolving the ill-posedness in motor control, “Mi-Nashi” has to set practical constraints in various levels of control mechanisms in real time. Here, we focused attentions on the reaching movement and modeled the following two decentralized autonomous mechanisms:

1. Real time transformation of the desired hand velocity into the angular velocity of each joint: By using “Mobility Measure” estimated from the kinematical state of the system in real time, the controller can solve the ill-posedness of the transformation from the hand velocity space to the joint velocity space.
2. Real time transformation of the desired torque of each joint to the muscle forces: By using information about the efficiency of energy consumption of each muscle in real time, the controller can solve the ill-posedness of the transformation from the joint torque space to the muscle force space.

Each mechanism works as a constraint that emerges in real time from the sensory information about the kinematical and dynamical properties of the system during the movement. Thus, the proposed mechanisms enable the system to adapt to the unpredictable changes in the environment and the system itself, and can be considered as the mechanism for constraint self-emergence/self-satisfaction based on “Mi-Nashi”.

(2) Thanks to a mutual interaction among a variety of chemical substances, real neural networks in our brain-nervous systems is not merely an electric circuit, but a complicated dynamical system, which can be changed depending on neuromodulators, such as acetylcholine, dopamine, 5-HT, and so on. This suggests that the polymorphism of the neural network is dominated by a small number of neuromodulators, and the activities of the chemical substances should be intrinsically self-regulated according to a sensorimotor context. Based on this, we proposed a neural network

model with intrinsic neuromodulator bias. The proposed model was applied for an arm-reaching movement controller under various viscous curl force fields. Simulation results demonstrated that the neural circuit structure of proposed model was changed depending on the contents of sensorimotor mappings and could adapt to changing environments in real time.

Subgroup A02: Understanding of intra-cerebral mechanisms for the motor adaptation to unknown environments.

(1) When manipulating objects or using tools, humans must compensate for the resultant forces arising from interaction with the physical environment. Recent studies have shown that humans can acquire a neural representation of the relation between motor command and movement, i.e. learn an internal model of the environment dynamics. Then, we can generate a motor command in a feedforward manner.

This year, we investigated whether humans could identify a simple dynamics from the complex body-environment dynamics. Humans memorize the time series of the hand reaction force and the hand velocity and displacement through the somatosensory feedback. Then, if the force vectors loaded to the hand are orthogonal each other or there are the phase differences between the peak values of external forces, humans could decompose the mixed environment dynamics into different simple dynamics, i.e., could make separate internal models. After this, it will be necessary to analyze the relations between the separate identification and the tool use.

(2) We investigated the brain mechanisms of recognition bodily self and others. Basically, the parietal-premotor network is considered to be related to the sensory motor control, but our results suggested that this network has crucial roles for matching the efference copy with the sensory feedback through the internal model and has a part in forming body images. We speculate that the mirror neuron responds to both visual images of one's own body and others, then the visual signal and motor command are integrated in the process of motor learning, and finally the visual representation of action may trigger the motor programs in mirror neuron system. This hypothesis provides important concepts for imitation learning or simulation of other's mind in the computational modeling. On the other hands, it is not clear how the brain represents other's body. Our data in VIP suggests that other's body is recognized by referring to self body mapping in the manner of mirror image. This provides an important suggestion for computational modeling of imitation or recognition of other's body.

Subgroup A03: Computational modeling and understanding of sensorimotor integration.

(1) Humans interact with many different objects and environments. The motor control system must be capable of providing appropriate motor commands for the multitude of distinct contexts that are likely to be experienced.

In the experiments, the virtual ball moving was shown vertically downward on the display. The SPIDER system simulated the contact force, which was given to the subject with five different timings from -60 to 60 msec. The subject was asked to catch the virtual ball at a fixed hand position. After learning, the subjects received the ball at a fixed timing advanced by the contact force feedback. We found that subjects learned new environments in which the ball was falling by different timings even though the visual information was invariant. These results suggest that the somatosensory feedback

plays an important role to form a timing in the feedforward manner.

(2) In our daily life, we frequently perform coordinated movements using right and left hands and fingers. To explore coordinated control mechanisms, subjects performed forefinger movements of two patterns (in-phase and anti-phase movements). During these movements, new external force field was inflicted to the left finger tip by a manipulandum. We observed a strong inter-finger cooperation in the in-phase movement and independent control feature in the anti phase movements. Additionally, we found that the adaptation characteristics to the force field in the in-phase and anti-phase movements are different with each other. It will be necessary to investigate the relations between the spatiotemporal characteristics of right and left coordinated movements and the motor control system by using brain imaging methods.

4. MEETING AND OTHERS

- Meeting of Group A

Date: 13:30-17:30, 23 June, 2006.

Place: Meeting room, Toya Sunpalace.

Attendee: 20 members.

Contents: Report on the research plans and results by all members of planned and subscribed research groups and frank and fruitful discussions on "Mi-Nashi".

- Joint meeting of Group A and B

Date: November 20, 13:00 – 21, 16:30, 2006.

Place: Meeting room, The Research Institute of Electrical Communication, Tohoku university.

Attendee: 50 members of group A and B.

Contents: Report on the research results by group members and the general discussions on adaptation to environments including the following invited lectures.

1) Dr. Kikuro Fukushima (Hokkaido University, School of Medicine): "Frontal cortical control of pursuit eye movements".

2) Dr. Rieko Osu (National Institute of Information and Communications Technology (NICT) / ATR Computational Neuroscience Labs): "Motor control and learning".

3) Tiaza Bem-Sojka (Department of Bionics, Institute of Biocybernetics and Biomedical Engineering, Polish Academy of Sciences): "Multistability and neuro-modulation: two mechanisms of network activity reconfiguration".

4) Pierre Meyrand (Laboratoire de Neurobiologie des Reseaux, CNRS/ University of Bordeaux1): "Reconfiguration of a rhythmic motor program by a mechanoreceptor neuron".

- Invited lecture

Date: 16:30-17:45, 21 March, 2006.

Place: Dept. of Informatics, Systems, Telecommunications (DIST), University of Genova, Italy.

Attendee: 15 PhD students and researchers.

Lecturer: Koji ITO.

Title: Adaptive Motor Functions through Dynamic Interactions among the Body, Brain and Environment.

Voluntary Movements Controlled by “Mi-Nashi” created in the Motor Cortices.

Masafumi Yano, Research Institute of Electrical Communication, Tohoku University

I. INTRODUCTION

A voluntary movement is an action that the biological system makes for carrying out an aim with adapting unpredictable environments. The aim of the movement can be acquired by the system having “Mi-Nashi”. As a higher constraint for resolving the ill-posedness in motor control, “Mi-Nashi” has to set practical constraints in various levels of control mechanisms in real time. Furthermore, for adapting unpredictable changes in conditions of the system and the environment, “Mi-Nashi” should emerge from the system-itself depending on interactions between the system and the environment, and the system have to evaluate whether the emerged “Mi-Nashi” would be satisfied every moments. These are computational problems that the motor control system, i.e., the motor cortices, has to solve during the voluntary movement control in the real world. Here, we focused attentions on the human reaching movement of the redundant arm.

II. IMPEDANCE MAP FOR VOLUNTARY MOVEMENT

Fig.1 shows an impedance map of the body [1]. Elements in upper and lower rows correspond to dimensions of ‘motion’ and ‘force’, respectively, and three columns represent configuration spaces of the body (left, hand-space; middle, joint-space; right, muscle-space). To transform one dimension to the other or one space to the other, respective matrices are needed. A computational task for the reaching movement control is to calculate commands for the muscle force from the information about the hand position. For this task, some of the matrices have to be determined. However, this problem is ill-posed because the biological system is redundant. To determine the necessary matrices, there must be a constraint.

In conventional approaches [2]–[6], it was supposed that dynamical and environmental parameters would not change during the movement. Thus, only in such condition, previously proposed constraints could determine the appropriate matrices for the reaching movement. These imply that the existing constraints have no adaptability by themselves to the unpredictable changes of system or environment. Although a learning strategy was proposed to estimate the dynamical and environmental parameters through the repeated trials and errors of reaching movement, the adaptability of such strategy would be limited to the case that the conditions of system or environment change rather slowly compared to the time scale for the learning strategy.

For the reaching movement in the real world, the constraint itself should be adaptable to the unpredictable changes. In the followings, we propose two mechanisms, in which constraints

emerge in real time from interactions between the system and environment during the movement.

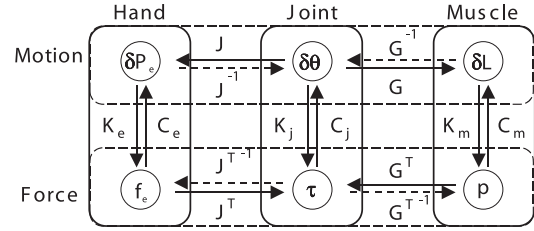


Fig. 1. An impedance map of the body for reaching movement.

III. A DECENTRALIZED AUTONOMOUS MECHANISM TO OPTIMALLY TRANSFORM THE DESIRED HAND VELOCITY TO THE ANGULAR VELOCITY OF EACH JOINT IN REAL TIME

We propose a reaching movement controller that uses kinematical information of the system during movements. Suppose 3 joints - 3 links model of a redundant arm moving in 2D plane (Fig.2A). As a higher constraint, the controller calculates a desired hand velocity, v_d , in real time from sensory information about a desired hand position, x_d , and a current hand position, x_h (Fig.2B):

$$v_d = (x_d - x_h)/t_d, \quad (1)$$

where, t_d is a time gain.

A. Decentralized autonomous controller

To satisfy v_d , the controller determines the velocity command of each joint, \tilde{v}_{di} , through decentralized autonomous interactions written as:

$$\begin{aligned} \tilde{v}_{d1} &= (1 - k_2)(1 - k_3)v_{d1}^l + k_2v_{d1}^{c2} + k_3v_{d1}^{c3} \\ \tilde{v}_{d2} &= (1 - k_1)(1 - k_3)v_{d2}^l + k_1v_{d2}^{c1} + k_3v_{d2}^{c3} \\ \tilde{v}_{d3} &= (1 - k_2)(1 - k_1)v_{d3}^l + k_2v_{d3}^{c2} + k_1v_{d3}^{c1}, \end{aligned} \quad (2)$$

where, v_{di}^l , v_{di}^{cj} are local commands and coupling commands of each joint, respectively (Fig.2B, C). ‘ k_i ’ is an index for evaluating mobility of each joint, as we call ‘Mobility Measure’, defined as follows:

$$k_i = \exp[-\ln 2 \|v_{di}^l - v_i\|^2 / (\|v_{di}^l\|/2)^2]. \quad (3)$$

\tilde{v}_{di} in Eq. (2) is transformed to the desired joint torque by the following equations.

$$\dot{\theta}_{di} = \tilde{v}_{di} \cdot e_{xi} / \|a_i\| \quad (4)$$

$$\tau_{di} = G_i(\dot{\theta}_{di} - \dot{\theta}_i), \quad (5)$$

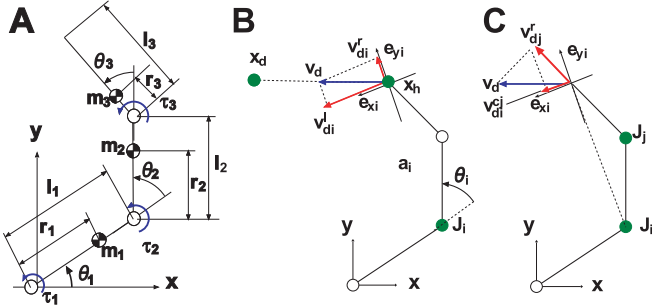


Fig. 2. Three joints arm model (A) and definitions of a local command, its residual (B), and coupling commands (C).

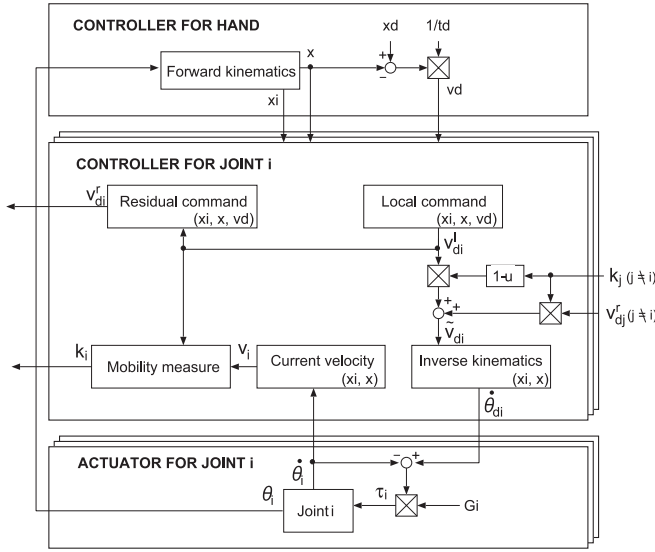


Fig. 3. A block diagram of the decentralized autonomous controller.

where, G_i is a proportional gain of joint i . A block diagram of the controller is shown in Fig.3.

B. Matrix-form description of decentralized autonomous controller

With regard to the system as a whole, the controller written as a decentralized autonomous form in Eqs. (1)-(4) can be generally transformed into a matrix form by using Jacobian, $\mathbf{J} = [\mathbf{J}_1 \cdots \mathbf{J}_m]$, $\mathbf{J}_i = \partial \mathbf{x}_h / \partial \theta_i \in \mathbb{R}^{n \times 1}$ [7].

$$\dot{\theta}_d = \mathbf{K}_l \text{diag}(\mathbf{J}^T \mathbf{J})^{-1} \mathbf{J}^T \mathbf{v}_d + \text{diag}(\mathbf{J}^T \mathbf{J})^{-1} \mathbf{J}^T (\mathbf{K}_c \mathbf{V}_d^r)^T, \quad (6)$$

where, $\mathbf{K}_l = \text{diag}[\prod_{j \neq 1}^m (1 - k_j), \cdots, \prod_{j \neq m}^m (1 - k_j)] \in \mathbb{R}^{m \times m}$, $\mathbf{K}_c = [k_1 \cdots k_m] \in \mathbb{R}^{1 \times m}$, $\mathbf{V}_d^r = [v_{d1}^r \cdots v_{dm}^r] \in \mathbb{R}^{m \times m}$. First and second terms of the right-hand side in Eq. (6) correspond to the local and coupling commands in Eq. (2), respectively. Eq. (6) implies that the controller would have distinctive features depending on the values of k_i . When k_i for all joints is 0, only the first term will be left and it pulls the hand to the desired hand position in a spring-like manner. Since Eq. (6) does not include inverse Jacobian matrix, the

controller would work well regardless of any initial configuration including a singular configuration. When k_i for all joints is 1, only the second term will be left, and consequently the calculated $\dot{\theta}_d$ will be an analytical solution which satisfies the direction of \mathbf{v}_d [8]. During movements, k_i would have a value between 0 and 1, and the above two strategies would be combined. So, if ' k_i ' evaluates the kinematical and dynamical mobility of each joint, appropriate motor pattern would emerge in real time even when unpredictable changes occur in the environment or the system.

C. Simulated results

Fig.4A and Fig.4B show simulated results in the normal case and in the case that the first link was lengthened, respectively. In both cases, the hand trajectories were almost straight regardless of movement directions. ' f_i ' in Fig.4 shows the kinematical mobility of each joint calculated from configurations of the links during movements. These results indicate that the mobility measure, k_i , appropriately evaluates the changes of the kinematical mobility caused by the change of the link length, and the controller autonomously shifted the dominant joint depending on the movement directions. Further simulated results (data are not shown) confirmed that the mobility measure, k_i , can appropriately evaluate the dynamical mobility of the joint, and that the controller can adapt the target shift during the movement or can carry out the movement from the fully-stretched, singular configuration.

IV. MECHANISMS FOR AN EMERGENCE OF CONTROL COMMANDS FOR THE HAND VELOCITY AND FOR TRANSFORMING THE DESIRED JOINT TORQUE TO THE MUSCLE FORCES IN REAL TIME

In this section, we propose two mechanisms, i.e. one for an emergence of control commands for the hand velocity and the other for transforming the transforming the desired joint torque to the muscle forces, that accomplish the reaching movement even when the target position would be changed during the movement. Suppose an arm model of 2 joints - 2 links with 6 muscle types moving in 2D plane (Fig. 5)

A. Emergence of control commands for the hand velocity

A higher center for the motor control has to generate the control commands that carry out the movement purpose with making the movement smooth. Suppose that t_0, t_{now}, t_d, X_d are the start time, the present time, the desired end time and the desired hand position for the reaching movement. The 6 boundary conditions can be obtained as follows: $\dot{X}(t_0) = 0, X(t_{now}), \dot{X}(t_{now}), X(t_d) = X_d, \dot{X}(t_d) = 0, \ddot{X}(t_d) = 0$. From the following equation, the higher center calculates a profile of the hand velocity from the present time to the desired end time that satisfies the 6 boundary conditions and the condition for the smooth movement:

$$X(t) = \sum_{i=0}^5 \frac{1}{i!} C_i t^i, \quad (7)$$

where, C_i is a coefficient vector determined by the boundary conditions. Based on Eq. (7), desired vectors of the hand

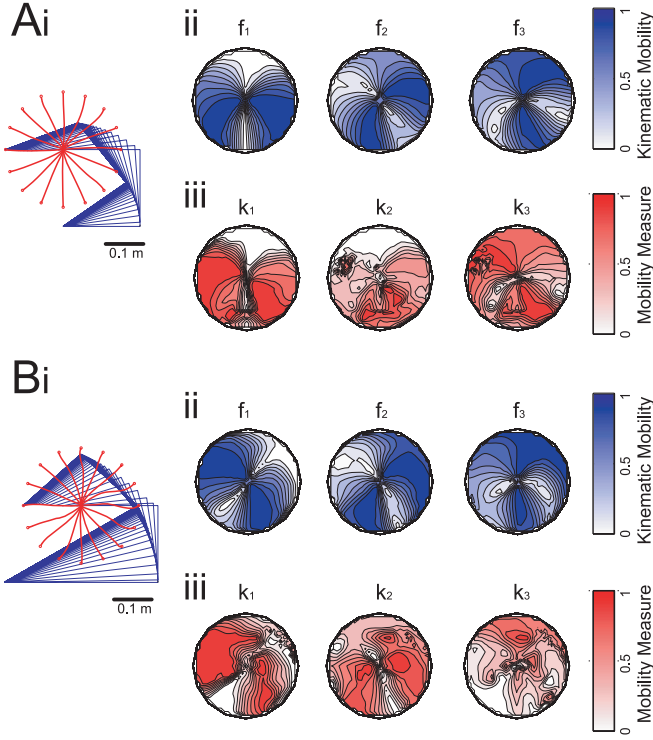


Fig. 4. Simulated results of normal reaching with different arm geometries. Ai: Hand trajectories with one example of arm postures traced every 0.1 s with stick lines. Aii: Spatial map of kinematical mobility measures for the shoulder (f1), elbow (f2), and wrist (f3). Aiii: Spatial map of joint mobility measures for the shoulder (k1), elbow (k2) and wrist (k3). B: Corresponding results when the first link was lengthened.

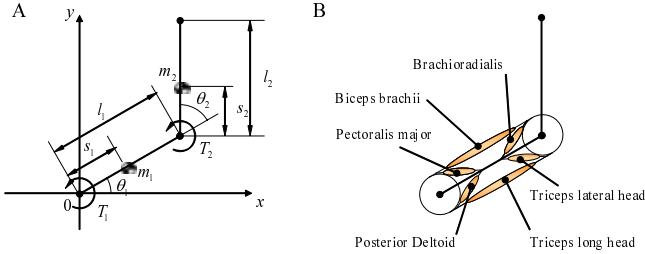


Fig. 5. Arm model of 2 joints - 2 links with 6 muscle types moving in 2D plane. A: Two joints arm model. B: Muscle configuration.

velocity, \dot{X}_d and of the hand acceleration, \ddot{X}_d , for $t+\Delta t[s]$ are calculated as:

$$\dot{X}_d = \sum_{i=1}^5 \frac{1}{(i-1)!} C_i (t_{now} + \Delta t)^{i-1}, \quad (8)$$

$$\ddot{X}_d = \sum_{i=2}^5 \frac{1}{(i-2)!} C_i (t_{now} + \Delta t)^{i-2}. \quad (9)$$

These commands work well as constraints for the controller of joints even when the target position would change.

B. Transformation from the desired hand velocity to the desired joint torques

\dot{X}_d and \ddot{X}_d are transformed into the desired joint torques by the following equation:

$$T_{d,i} = I_{v,i} \ddot{\theta}_{d,i} + K_i \left(\ddot{\theta}_{d,i} - \frac{d\dot{\theta}_i}{dt} \right). \quad (10)$$

where, $\ddot{\theta}_{d,i}$ and $I_{v,i}$ are the desired angular acceleration of the joint i and the inertia moment of the links estimated from the muscular-sensory information, respectively. First and second terms of the right hand side of Eq. (10) are the feed-forward and the feed-back components, respectively. K_i is the proportional gain for the feed-back component.

C. A decentralized autonomous mechanism to optimally determine the muscle forces based on the muscle-efficiency function

A problem to optimally transform the desired joint torque to the force vector of redundant muscles of each joint is described as the following mathematical programming problem (MP problem):

Objective function:

$$\max_{\mathbf{p}} f(\mathbf{p}, \dot{\mathbf{p}}, t) = \mathbf{P}_0^t \boldsymbol{\eta}(\mathbf{p}). \quad (11)$$

Constraint:

$$\mathbf{g}(\mathbf{p}, \dot{\mathbf{p}}, t) = \mathbf{T} - \mathbf{R}\mathbf{p} = \mathbf{O}, \quad (12)$$

where, $\mathbf{P}_0 \in \mathbb{R}^{n \times 1}$, $\boldsymbol{\eta} \in \mathbb{R}^{n \times 1}$, $\mathbf{R} \in \mathbb{R}^{r \times n}$, $\mathbf{p} \in \mathbb{R}^{n \times 1}$, $\mathbf{T} \in \mathbb{R}^{r \times 1}$, and r, n are the numbers of joints and muscles. $P_{0,i}$, η_i , p_i , T_j and R_{ji} are the maximum force of the muscle i , the muscle-efficiency function, the muscle force, the desired joint torque and the moment-arm of muscle i for joint j , respectively. Because the muscle-efficiency function is convex and the constraint for the MP is linear, the locally optimal solution corresponds to the globally optimal solution. Based on Lagrange's method of indeterminate coefficient, the requirement to provide the optimal solution is defined by the following equation:

$$P_{0,1}^b \frac{\partial \eta_1^b}{\partial p_1^b} = \dots = P_{0,k}^b \frac{\partial \eta_k^b}{\partial p_k^b} = \sum_i^l P_{0,i}^m \frac{\partial \eta_i^m}{\partial p_i^m}, \quad (13)$$

where, b, m , are the indices of biarticular and monarticular muscles, and k, l are the numbers of biarticular and monarticular muscles, respectively. Eq. (13) can be satisfied by the decentralized autonomous interactions among the muscles, and thus, the interactions can be thought as the dynamical constraint for determining the redundant muscle forces (Fig. 6).

D. Simulated results

Fig.7 shows typical examples, indicating that the smooth hand velocity profile emerges even when the target was suddenly changed just after the movement onset. Comparison between the analytical solution and the simulated muscle forces during the movement confirmed that the proposed mechanisms optimally transform the desired joint torque to the redundant muscle forces (Fig. 8).

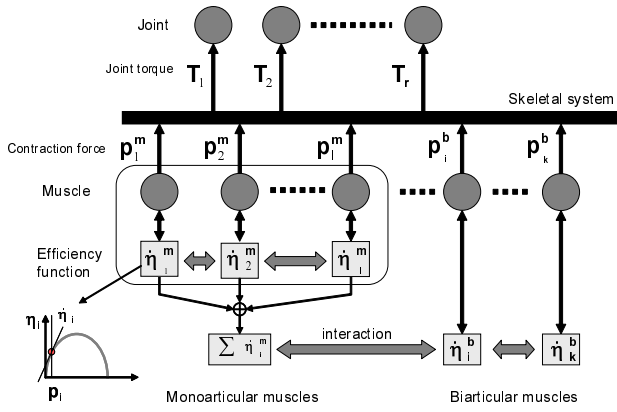


Fig. 6. Decentralized autonomous interactions among the muscles using the information about the muscle efficiency.

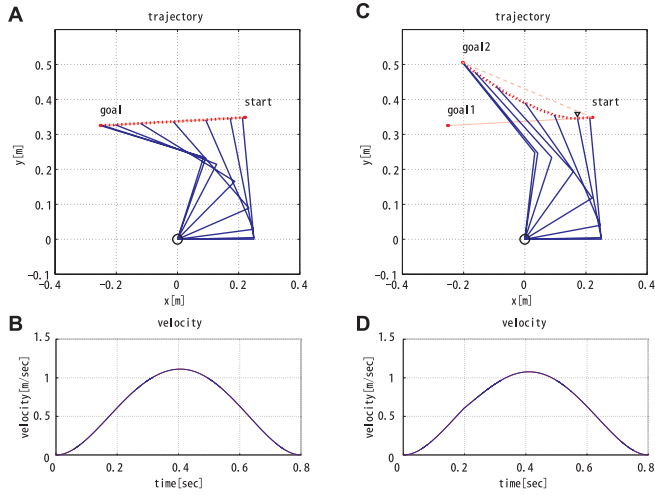


Fig. 7. Typical arm movements (A, C) and hand velocity profiles (B, D). A, B: Normal case. C, D: Case when the target was shifted.

V. CONCLUSION

The proposed mechanisms are summarized as Fig.9. The mechanism described in Section 3 can be thought as the constraint for the transformation from the hand velocity space to the joint velocity space (Fig.9, Arrow 2). The emergent mechanism for desired hand velocity (Fig.9, Arrow 1), proposed in Section 4, works as the constraint for determining the trajectory of the hand in real time even when conditions of the system or environment suddenly change during the movement. Furthermore, the decentralized autonomous mechanism proposed in Section 4 (Fig.9, Arrow 3) works as the constraint for transforming the joint torque to the muscle forces, and dynamically optimizes the movements in real time. Thus, we conclude that the proposed mechanisms solve the ill-posed problem in the motor control for reaching movement and simultaneously enable the system to adapt to the unpredictable environment in real time.

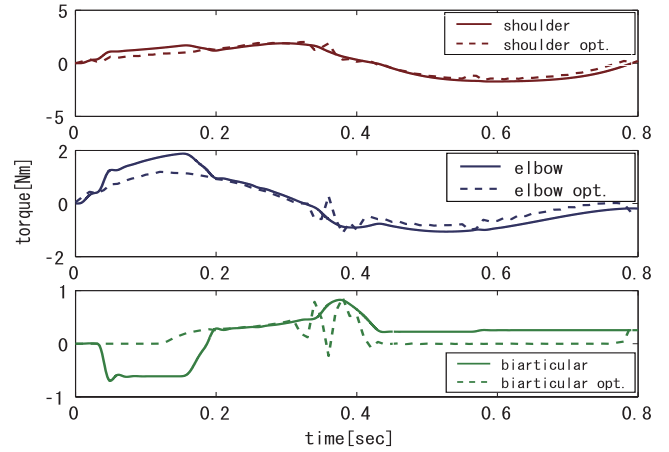


Fig. 8. Comparison between the analytical solution and the simulated forces of each muscle.

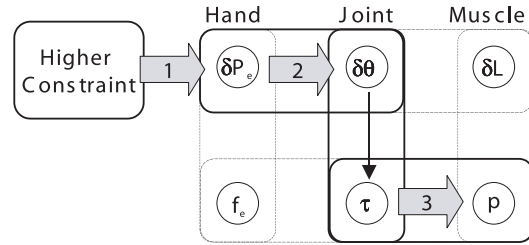


Fig. 9. Summary of the proposed decentralized autonomous mechanisms in the impedance map.

REFERENCES

- [1] Mussa-Ivaldi FA et al. (1988) *Biol. Cybern.*, 60, 1-16
- [2] Flash T & Hogan N (1985) *Journal of Neuroscience*, 5, 1688-1703
- [3] Uno Y et al. (1989) *Biol. Cybern.*, 61, 89-101
- [4] Harris CM & Wolpert DM (1998) *Nature*, 394, 780-784
- [5] Bizzi E et al. (1976) *Journal of Neurophysiology*, 39, 435-444
- [6] Arimoto S et al. (2005) *Advanced Robotics*, 19, 401-434
- [7] Yoshihara Y, Tomita N, Asano T, Makino Y, & Yano M (2007) *Proceedings of 19th SICE-DAS*, 31-36 (in Japanese)
- [8] Yoshihara Y, Tomita N, Asano T, Makino Y, & Yano M (2006) *Proceedings of SICE-ICASE International Joint Conference 2006*, SP02-2(CDROM)
- [9] Tomita N, Asano T, & Yano M (2007) *Proceedings of 19th SICE-DAS*, 37-42 (in Japanese)

A02 Annual Report 2006: Modeling of Intra-cerebral Mechanisms for Motor Adaptation to Unknown Environments

Koji ITO

Tokyo Institute of Technology

Toshiyuki Kondo

Tokyo University of Agriculture and Technology

I. INTRODUCTION

Even if we situated in unknown, diverse, complicated and dynamically-changing environments, we can adapt in several trials-and-errors. As a consequence of the motor learning processes, we can acquire a neural representation of the relation between motor command and movement, i.e. learn an *internal model* of the environment dynamics. However it is still open question to explain the neural representation, i.e. how the internal models are represented in a brain. For example, we can instantly manipulate any objects by using any tools even though there are a number of combinational possibilities.

In addition, we can select an appropriate internal model according to the contextual information of the environments. It implies that there is an intrinsic prediction and motor adaptation mechanisms in the motor area of our brain.

The group A02 aims to clarify the intra-cerebral mechanisms to recognize unknown environments and generate suitable motor commands through psychophysical experiments and computational modeling of human arm-reaching movement learning.

In this annual report we will explain our recent research topics entitled; "Decomposition of internal models in motor learning under mixed dynamic environments" and "Polymorphic neural networks model."

II. DECOMPOSITION OF INTERNAL MODELS IN MOTOR LEARNING UNDER MIXED DYNAMIC ENVIRONMENTS

In daily life, we utilize many kinds of tools to achieve various tasks. The tool connects the body with the environment. In order to realize the task quickly, smoothly or efficiently, it is required to adjust the kinematic and dynamic relations among the body, tool and environment according to the task. Now, to manipulate objects or to use tools, humans must compensate for the resultant forces arising from interaction with the physical environment.

Recent studies have shown that humans can acquire a neural representation of the relation between motor command and movement, i.e. learn an internal model of the environment dynamics. Then, we can compensate for the mechanical perturbation in a feedforward manner. Humans can learn an enormous number of motor behaviors in different environments. Then, it is required to construct multiple internal representations of various dynamic environments, which can be recollected corresponding to each environment. The concept of multiple models implies the ability to adapt to diverse perturbations

with different contexts and to make efficient use of redundancy by performing the same task in different ways under different environments[1].

In this study, we consider two environments that have different dynamics ("V"elocity-dependent and "P"osition-dependent force Fields). Through the psychophysical experiment of arm-reaching movement, the effect of the experience in the mixed force field (V+P) to the following learning processes is discussed.

A. Experimental setup

The experimental apparatus is shown in Fig.1. The manipulandum (x-y table) is actuated by a couple of linear direct drive motors (x axis: max. 599 N, y axis: 197 N; NSK Ltd), which are controlled by the digital servo at the sampling rate 2 KHz and can generate various mechanical impedances against the grip grasped by the subject. The subject was seated on the chair with adjustable height in front of the experimental equipment and the trunk was fixed on the back of the chair by the strap. Therefore, the elbow and shoulder joints could only move in the horizontal plane (two degrees of freedom). The subject was instructed to reach the target from the initial position with a velocity within the range of 300 ± 50 ms.

The target position was located at 0.125 m from the start point in the y-axis direction. The hand position during movement including the initial and final positions was displayed on the front screen by the projector.

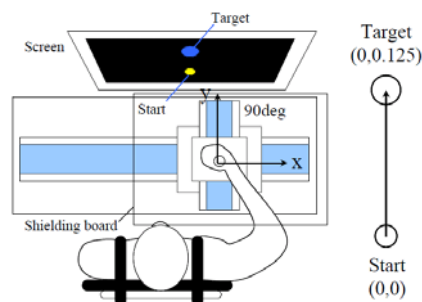


Fig. 1. Experimental setup.

The manipulandum generated two kinds of dynamic environments V and P as shown Fig.2, which were loaded to the grip grasped by the subject. Here, V is a resistive viscosity force field in proportion to the velocity in the direction of

movement (Eq.(1)), P is a resistive position dependent force field in proportion to the displacement in the direction of movement (Eq.(2)).

$$F = B\dot{X} \quad (1)$$

$$F = KX \quad (2)$$

where, $X=[x, y]^T$ and $F=[F_x, F_y]^T$ represent hand position and perturbation force to the hand, respectively. In the experiment, $B=[12 \ -12; -12 \ -12]$ N/(m/s), and $K=[50 \ 50; 50 \ -50]$ N/m.

The subjects are separated into two groups (group A and B), and the experiments have been executed during two days. The procedure of the experiment is as follows. First, sufficient successful trials are asked under the null field (NF) for training. Next, 160 trials were performed under the viscosity force field V . Then, for the group A, 160 trials were performed under the mixed force field $V+P$. For the group B, 160 trials were performed under the viscosity force field V instead of $V+P$. Finally, for both groups, 160 trials were performed under the force field P .

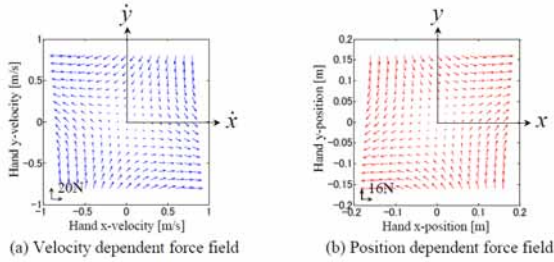


Fig. 2. Force fields.

The performance of the arm-reaching movement was evaluated based on the Eq.(3) and (4). Here, t_0 and t_{f1} are start time and termination time of the reaching movement, and t_{f2} is $t_{f1}+600$ ms.

$$E_1 = \int_{t_0}^{t_{f1}} |x|\dot{y}|dt \quad (3)$$

$$E_2 = \int_{t_{f1}}^{t_{f2}} \frac{\sqrt{(x_d - x(t))^2 + (y_d - y(t))^2}}{t_{f2} - t_{f1}} dt \quad (4)$$

B. Results

Fig.3 shows the hand trajectories of a subject in the mixed force field $V+P$ (the group A). Also Fig.4 depicts the hand trajectories of a subject in the velocity-dependent force field V (the group B). These figures represent three stages of learning, i.e., 1) before learning (1–10 trials), 2) after learning and 3) the after-effect. In the final stage of learning, the force field was unexpectedly removed on selected trials to examine the after-effects of learning.

The learning process seems to be same for both force fields V and $V+P$. The hand trajectory is slipped out from the straight line toward the target at the beginning of learning, which indicates that it is an unknown dynamics for the subject. Especially, it should be noticed that the force field $V+P$ is an unknown dynamics even after having learned the force field V .

On the other hand, when coming to the end of learning, the hand trajectory could be kept near the straight line to the target in both force fields V and $V+P$. It indicates that the subject performs the reaching motion based on the identified environment dynamics V and $V+P$ respectively. This is confirmed by the after-effect. The hand trajectories are curved to the clockwise direction even under no force field, which suggests that the reaching motion is performed by a feedforward manner based on the internal representation of the environment dynamics.

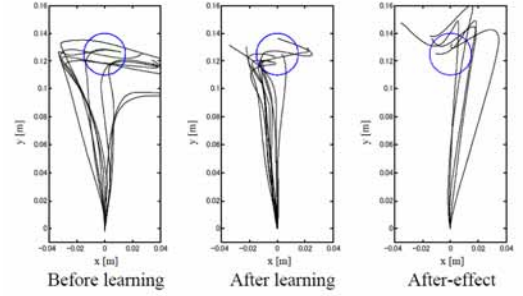


Fig. 3. Trajectories under force field $V+P$ (Group A).

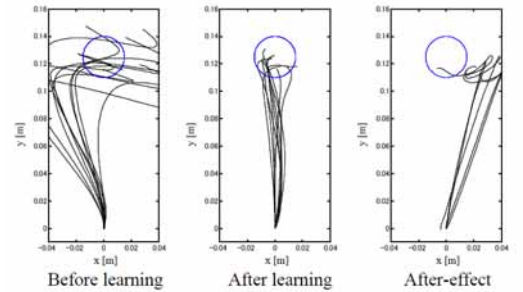
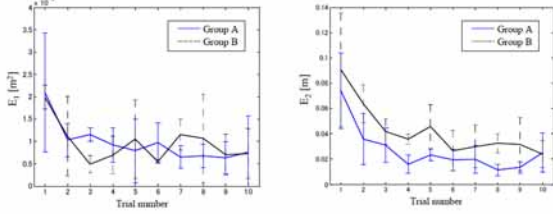


Fig. 4. Trajectories under force field V (Group B).

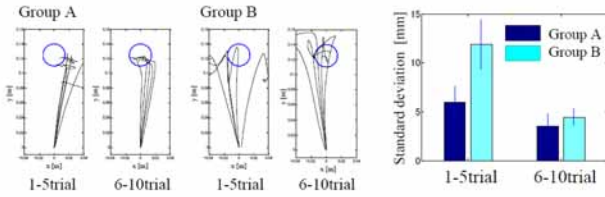
After the learning experiments for the force field V and $V+P$, the subject was asked to perform the reaching motion under the force field P . Fig.5 (a) shows the performance index during early stage of learning, which determined by Eq.(3) and (4). As in Fig.5(b), it is seen that the trajectory of the subject (group B) is deviated from the straight line to the target during 1–5 trials. On the contrary, the trajectory of the subject (group A) seems stable during the trials. These results imply that the subject (group A) could partially identify the force field P through those learning processes.

In addition, Fig.5(c) demonstrates the reaction force of the hand at 1–10 trials of the both groups. In the figure, the horizontal axis is x -directional components of the hand force,

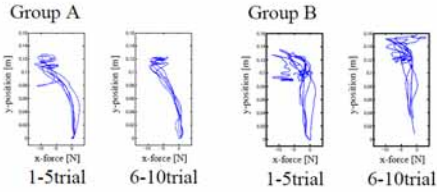
and vertical axis is the y-position of the hand. From these figures, it can be seen that the subject (group A) can produce opposite force to compensate the force field P even in early stage of the learning (i.e. 1–5 trials).



(a) Learning curve E_1 and E_2 during 1-10 trials



(b) Hand trajectory during 1-10 trials



(c) Hand force during 1-10 trials

Fig. 5. Analysis of the experiment .

III. POLYMORPHIC NEURAL NETWORKS MODEL

Recent neurophysiology has revealed that a variety of chemical substances called neuromodulators (NMs) play crucial roles to regulate the dynamic characteristics of neural networks. Even in the case of higher level animals, the ability of environment cognition and motor adaptation should be influenced by internal/external hormones.

Based on the physiological background, we proposed a polymorphic neural networks model for the environment cognition and motor adaptation. In the proposed model, the sensorimotor mappings represented by the neural networks can be modulated according to the density of the diffused chemical substances. In addition, the diffusion of the neuromodulators is regulated by the same monolithic neural networks. Therefore, the proposed model intrinsically has self-reference structure.

A. CTRNN with NM bias

In this study, a polymorphic neural networks model is proposed based on a continuous time recurrent neural networks

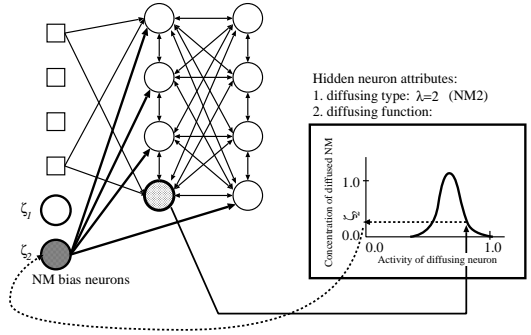


Fig. 6. CTRNN with Intrinsic Bias

(CTRNN). Thus the neural networks model is called CTRNN with NM (neuromodulator) bias.

Fig.6 schematically shows the CTRNN with NM bias. The network basically consists of fully-connected hidden neurons, each of which has the following dynamics (leaky-integrator dynamics).

$$T_i \frac{ds_i(t)}{dt} = -s_i(t) + \sum_{j=1}^{N_h} w_{ij} h_j(t) + \sum_{k=1}^{N_s} w_{ik} I_k(t) \quad (5)$$

$$h_j(t) = \frac{1}{1 + \exp[-(s_j(t) - \theta_j)]} \quad (6)$$

where $s_i(t)$ and $h_i(t)$ are the internal state and output of the neuron i , respectively. N_s and N_h are the number of sensors and hidden units. T_i is the time constant of the neuron, w_{ij} and w_{ik} are the synaptic weights, and θ_j is the threshold of the neuron. These parameters (T , w , θ) are the target to be optimized.

As can be seen in the figure, the proposed model has additional bias inputs named NM bias ζ_i . The characteristics of the CTRNN can be altered by modulating the NM bias ζ_i like RNNPB (recurrent neural networks with parametric bias) proposed by Tani[2].

One of the crucial point to be noted is how the bias inputs can be regulated. In neurophysiology, the self-recursive modulation is known as ‘‘intrinsic neuromodulation[3].’’ In the proposed model, we adopted the self-regulation method proposed in [4], i.e. the NM bias is controlled by the identical network itself.

As schematically shown in Fig.6, each hidden neuron has the capability to diffuse its specific (i.e. genetically-determined) type of NM ($\lambda_j = \{1, 2, \dots, M\}$) in accordance with its activity and the diffusing function given by Eq.(7) is also genetically-optimized.

$$\zeta_i(t) = \exp \left[\frac{(h_j(t) - \mu_j)^2}{2\sigma_j^2} \right] \quad (7)$$

In this example, the shaded hidden neuron can diffuse NM2 ($\lambda_j = 2$) with the concentration ζ_2 depending on its activity.

B. Simulation

To investigate the validity of the proposed model, it is applied to two dimensional arm-reaching movement control in various viscous force fields (Fig.2). In the simulation, we modeled the human arm as a planar two-link manipulator with antagonistic muscles. Moreover the external forces in the hand coordinate F is given by the following equation.

$$F = B\dot{X} \quad (8)$$

$$B = \begin{pmatrix} b_{11} & b_{12} \\ b_{21} & b_{22} \end{pmatrix} = n \begin{pmatrix} 0 & -1 \\ 1 & 0 \end{pmatrix} \quad (9)$$

where F described by Eq.(8) is a viscous curl force field, in which the hand suffers an orthogonal force in proportion to the hand velocity \dot{X} . In the simulation, we optimized the neural controller modeled by the CTRNN with NM bias model under both of two environments (F_{Env_1} and F_{Env_2}). Here, F_{Env_1} is a null field, i.e. $n=0.0$ in Eq.(9). On the other hand, F_{Env_2} corresponds to a viscous curl force field, i.e. $n=5.0$.

C. Results

After the parameters optimization process, the evolved CTRNN+NM-based neural controller was evaluated in the following four environments, i.e. $n=0.0$, 2.5, 5.0, and 7.5 in Eq.(9), because we are interested in the robustness of the neural controller. Note that $n=0.0$ and $n=5.0$ are the training environments, and $n=2.5$ and $n=7.5$ are un-experienced (i.e. unknown) environments. Fig.7 demonstrate the resultant hand trajectories in the four kinds of viscous curl force fields.

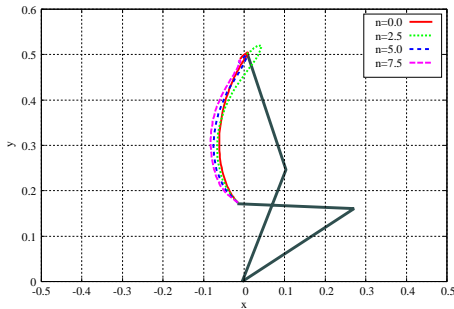


Fig. 7. Resultant trajectory .

As can be seen in Fig.7, the optimized neural controller based on the proposed model can recognize environmental change via its sensorimotor context, and it can appropriately modulate sensorimotor mapping so as to keep an optimal hand trajectory.

For further investigation about the robustness of the proposed CTRNN+NM model, we measured the performance of the optimized neural controller while the viscous parameters (b_{12} and b_{21} in Eq.(9)) are exhaustively changed in a range ($b_{12} \in [-3.0, -7.0]$, $b_{21} \in [3.0, 7.0]$). Fig.8 shows the results of the exhaustive evaluation.

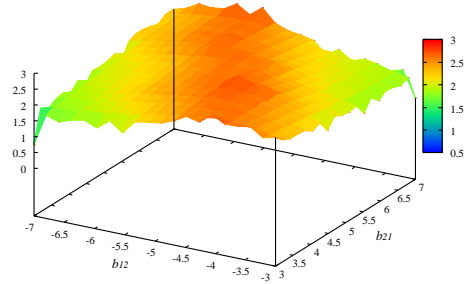


Fig. 8. Robustness of the trained neural controllers while viscous parameters (b_{12} and b_{21}) are exhaustively changed.

According to the verification experiments, the proposed CTRNN+NM model has demonstrated high robustness against not only b_{12} but also b_{21} . Especially, the diagonal line keeps high performance. This implies that the proposed CTRNN with NM bias model evolved “adaptation strategy” (i.e. sensorimotor constraints and their elicitation procedure) instead of “sensorimotor mapping” as it is (i.e. an optimal inverse dynamics of the experienced environment).

IV. CONCLUSION

In the paper, we shortly reported two research examples in the group A02; psychophysical experiments of arm-reaching motor learning and proposal of a computational polymorphic neural networks model with self-reconfigurable feature, called CTRNN with NM bias.

ACKNOWLEDGMENT

This research has been partially supported by a Grant-in-Aid for Scientific Research on Priority Areas (No.454, 2005–2010), (C) (No.,2006–2007) and Young Scientists (B) (No.18700195, 2006–2007) from the Japanese Ministry of Education, Culture, Sports, Science, and Technology.

REFERENCES

- [1] J. R. Flanagan et al.: Composition and decomposition of internal models in motor learning under altered kinematic and dynamic environments, *J.Neuroscience* **19**, RC34, 1/5, 1999.
- [2] J. Tani, M. Ito and Y. Sugita: Self-organization of distributedly represented multiple behavior schemata in a mirror system: review of robot experiments using RNNPB, *Neural Networks*, **17**, 1273/1289, 2004.
- [3] Marder, E. and Thirumalai, V.: Cellular, synaptic and network effects of neuromodulation, *Neural Networks*, vol.15, pp.479–493, 2002.
- [4] T. Kondo, Evolutionary design and behavior analysis of neuromodulatory neural networks for mobile robots control, *Applied Soft Computing*, **7**, 189–202, 2007.

The Roles of Implicit and Explicit Processes in Vision

Satoshi Shioiri, Matsumiya Kazumichi, Kuriki, Ichiro
Tohoku University

Abstract—We investigated the differences between processes of explicit and implicit learning related to visual perception, measuring facilitation effect by learning stimulus configuration in visual search experiments (contextual cueing effect). Explicit learning was found to be less efficient than implicit learning when evaluated by visual search time even the participants had similar time of period for learning for both type of learning. This result suggests that the learning and/or memory process in seeing repeatedly without explicit knowledge of the repeats is different from the process with explicit learning. The implicit and explicit processes may have different role in visual perception and the former is perhaps useful for memorizing or familiarizing complex scenes, with which active visual processing such as visual searches performed efficiently

I. INTRODUCTION

When we perceive the world, we usually think we are aware what we are seeing. This feeling of visual awareness suggests that the visual system works with processes that are explicit to us. However, through the history of the visual science, much of visual processing has been revealed to be done without consciousness. Indeed, there is variety of counter intuitive visual perception. For example, motion is seen in the opposite direction to that of actual displacement in the visual stimulus¹ and perceived motion direction changed with stimulus temporal conditions². The visual system, and perhaps other sensation systems also, has processes that we are not aware. It is important and possible to differentiate conscious and unconscious processes to understand the brain functions, which in turn is important to develop interfaces to machines and/or education system suitable for the human brains. However, we have little knowledge of the role of consciousness in vision and of the method to investigate it. Our approach for the issue is to measure the differences in performance between the conditions, which we assume that the explicit and implicit processes concerns based on the experimental manipulations.

In the present study, we focus on a phenomenon called contextual cuing effect. Contextual cuing effect is a type of unconscious or implicit learning of visual images. Although implicit processes for motor control have been investigated for decades^{3, 4}, those for perception and recognition is not much known. Contextual cuing effect is one of a few implicit learning effect known for visual perception^{5, 6}. It is found when participants search a target among similar distracters repeatedly in a visual search task. In the original condition of the first report of contextual cueing⁵, half of the displays (the location of the target and distracters) are unique to each trial, whereas the remaining displays are repeated throughout the experiment. There were twelve different repeated displays, where the locations, but not the identities, of the target and distracters are held. The contextual cuing effect is the

fastening of the target detection time in the repeated displays. This is an example of implicit learning since participants are often unaware that any repetitions have occurred. When an recognition test of the displays is performed at the end of the search sessions, performance is at chance even for participants who report being consciously aware of the repetitions during.

The purpose of the present study is to investigate how implicit and explicit learning/memory of stimulus images differ in performing visual search tasks. We measured the reaction time and eye movements of participants when they were searching a target in repeated or new displays. Participants were told to search the target without being informed of the repetition of displays in the implicit condition. In the explicit condition, in contrast, participants were told to memorized the display so that they would be able to use the information to search the target in later trials in the session. Possible differences in the learning processes could cause differences between the two conditions in the degree of the shortening of reaction, in time course of the learning, and in eye movements properties.

Before the experiment comparing explicit and implicit learning, we examine whether contextual cueing effect is found by learning of preceding displays. The reason why we did this experiment was because we wished to show the generality of the effect. Temporal contexts should be important in everyday life to predict the events later and the effect should be considered more important if it occurs with the preceding display.]

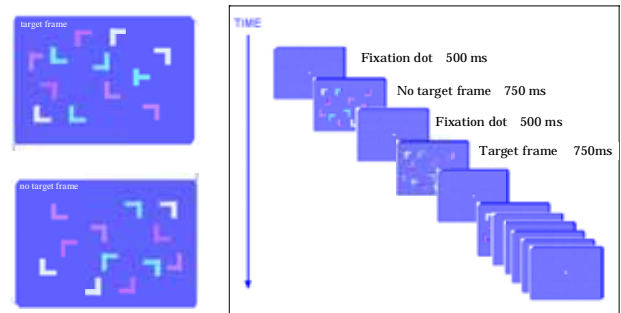


Fig 1. Examples of the target frame (top) and no target frame (left). Five frames (one target frame and four no target frames) were presented sequentially.

II. EXPERIMENT 1: TEMPORAL EFFECT

A. Method

Figure 1 shows the example of search stimuli. The target was a T among eleven Ls. To investigate the temporal effect, five displays were sequentially presented and a target was in one of the displays. Each block had twenty four trials, half of which were old and the other half was new displays. In old displays, stimulus configurations

was fixed so the locations of the target and distracters were the same while the orientation and color differed from one to the other.

Participants searched a target in the five displays and pressed one of two keys to indicate the direction of target T when he found the target in whichever of the displays. Each participant ran twenty five blocks. Five students from Tohoku University participate in the experiment. Stimuli were displayed on a 21 inch CRT display under control of a video board (ViSaGe, Cambridge Research Inc.), after careful calibration of luminance linearity and viewed from 38 cm distance.

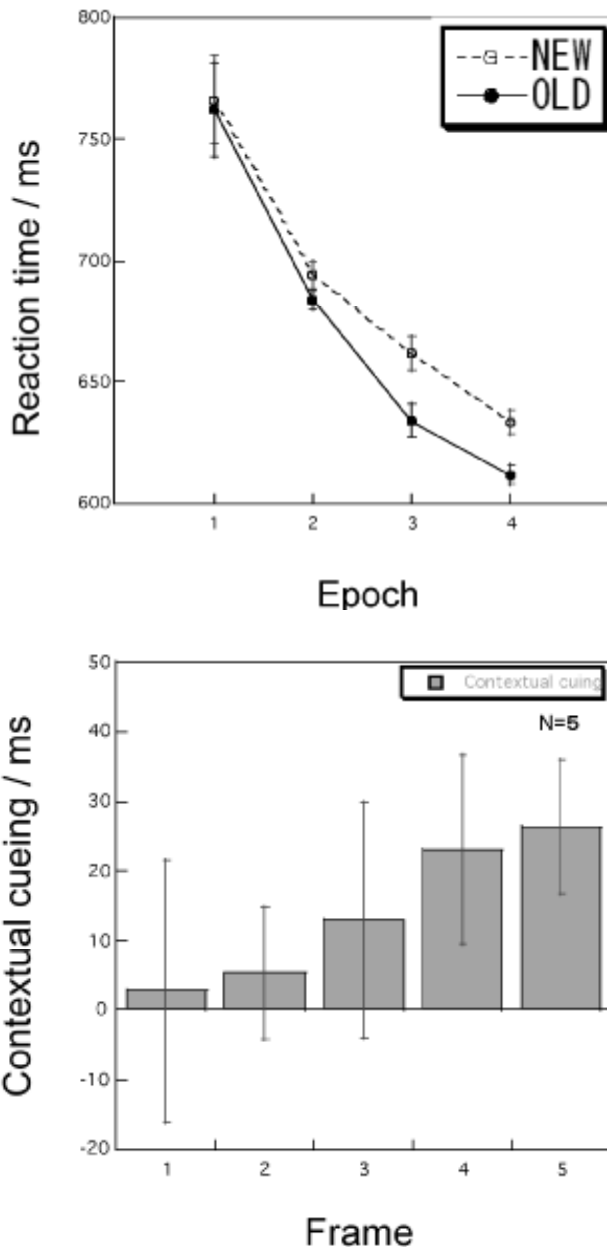


Fig. 2 Reaction time as a function of epoch (group of five blocks) for new and old sets of frames (top). The difference between the new and old sets (amount of contextual cueing effect) for each target frame (bottom).

B Results

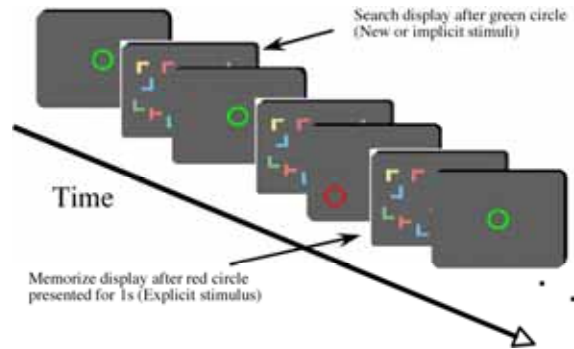
Figure 2 (a) shows reaction times averaged over participants as a

function of epoch (which is a sum of five blocks) separately for new and old displays and (b) shows reaction time for different temporal target locations (the frame number with the target in the five displays). These results showed, first that contextual cueing effect was found in the present condition, and second that the effect was larger in later displays. They suggest that context of the previous display influences the present target localization. The visual system may use spatiotemporal context for visual search, which is perhaps a useful in the everyday life, for examples, driving a car on familiar roads and finding food in the refrigerator.

III. EXPERIMENT 2: EXPLICIT AND IMPLICIT MEMORY

A. Method

Search stimuli were similar to the one used in Experiment 1 (the target was T among eleven Ls) but only one frame was used for each trial. There were two types of sessions: one is called memory session and the other is called no memory session. First eight blocks of a total of 32 blocks in each session are for learning (learning phase) and the rest blocks are for search (search phase). There were implicit, explicit and new display conditions in each session. Each block consisted six explicit, six implicit and six new display trials. There were differences in the learning phases among different stimulus



conditions.

Fig.3 Sequence of trials in the learning phase. A pre-cue frame with a red (in the explicit display) or a green circle (implicit and new displays) was presented before each stimulus display.

The explicit stimulus display was presented for 1s after a uniform field with a red circle at the location of the target in the stimulus display. The stimulus display replaced the field when participants initiated the trial by pressing a key. The memory and the no memory sessions used different instructions for explicit stimulus display. In the memory condition, participants were told to memorize the configuration (the location of the target and distracters) so that the knowledge was used to find target later in the search phase. Participants were assumed to memorize the image configurations explicitly in this session. In the no memory session, participants were told to respond the direction of the target T (left or right) without being told the configurations were used later in the search phase. Participants were assumed to memorize the image configurations explicitly in this condition.

The no memory condition was a control to see the effect of seeing stimulus without memorization. Seeing the images with neither memorizing nor searching target may still facilitate the search in later trials and such effect can be identified in this condition. The implicit and new displays were presented after a uniform field with a green circle at the center of the display and participants simply searched the target when it was presented. These two displays were the same in the all three conditions. There was no difference among

stimulus conditions in the search phase.

Only a fixation point was displayed at the center of the display before the search display. At the end of a session, participants performed a recognition task. The recognition task consisted of 6 new and 12 repeated displays (explicit and implicit ones).

The same apparatus as in Experiment 1 was used and eye movements were recorded with an eye tracker (Cambridge Research Ltd.) with a 50-Hz sampling rate. Ten students from Tohoku University participate in the experiment. Five of them participated in the memory session and the other five did in the no memory session.

B. Results

Figure 4 shows reaction times averaged over participants as a function of epoch (which is a sum of four blocks) separately for memory (a) and no memory (b) conditions and Figure 5 shows relative values of reaction time to that of new displays. The relative values are shown here to cancel the individual differences in reaction time in order to see the differences between the implicit and explicit conditions independent of individual differences. First and the second epochs are in the learning phase,

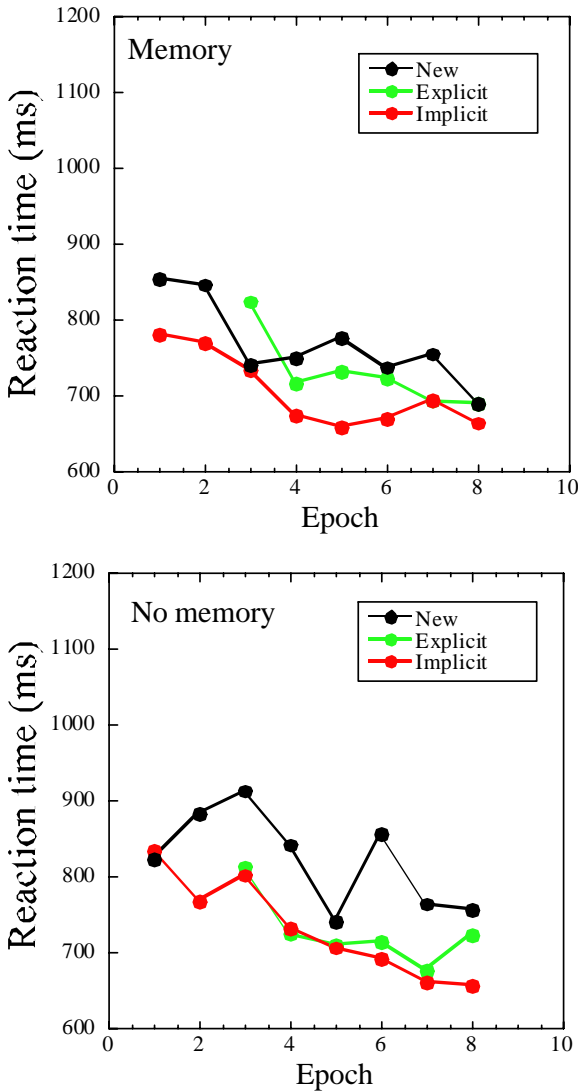


Fig. 4 Reaction time as a function of epoch (group of four blocks) for

three stimulus types in the memory condition (top) and in the no memory condition (bottom).

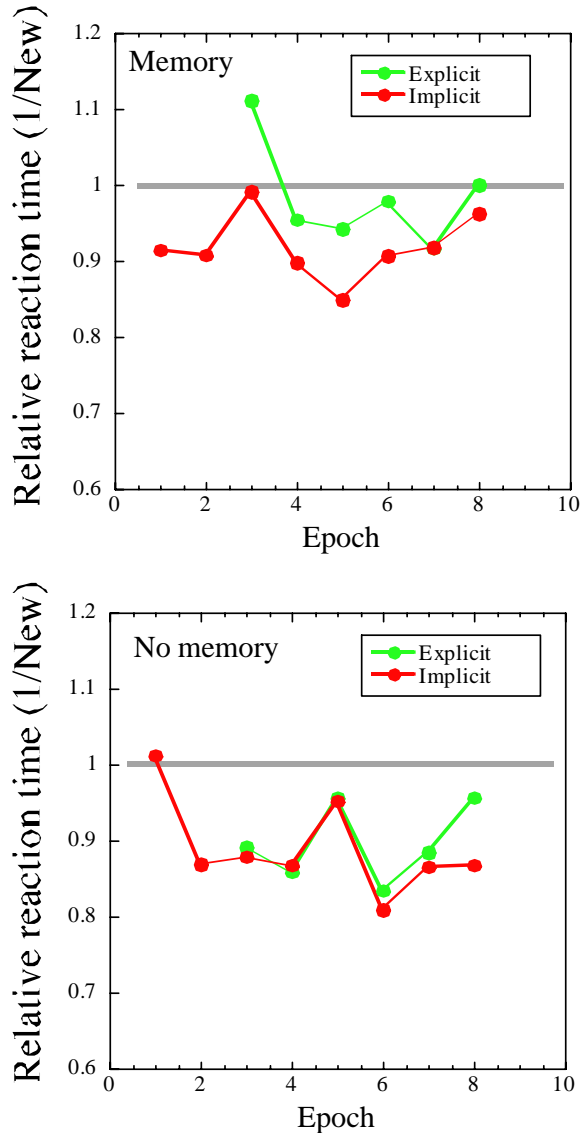


Fig. 5 Reaction time relative to that of new stimulus for explicit and implicit stimulus types as a function of in the memory condition (top) and in the no memory condition (bottom).

The results in the memory session show that shortest reaction time was found in the implicit display, then explicit display followed. The differences between the explicit and implicit conditions cannot be attributed to the difference in time for memorizing because the reaction time of epochs 1 and 2 for implicit display is shorter than 1 s, which was presentation time for explicit display. The results, therefore, suggests that explicit effort to memorize the display configuration is not as effective as simple repeats of searching displays. Interestingly, the results in the no memory condition showed that the reaction time is similar between the explicit and implicit displays, both of which are shorter than the time for new displays. This suggests that amount of contextual cueing is similar with and without searching. Since longer reaction time for explicit display in the memory session, the explicit effort to memorize display configuration may have suppressed the contextual cueing effect in the memory session.

Figure 6 shows the recognition rate in each condition. The performance is at about chance in all but one conditions. The exception is the explicit display of the memory condition, where recognition rate is over 60%. Although the recognition rate for the condition is not very high, the value higher than that in the other conditions suggests that explicit learning contribute to memory that is used in the recognition. The results of reaction time and recognition rate support the notion that there are qualitative differences between the explicit and implicit learning.

Figure 7 shows the results of eye movements. Relative values to the new display of average fixation duration and fixation numbers are shown. Reduction of reaction time can be attributed to reduction of either/both of fixation duration or/and fixation numbers. There are differences in fixation duration and fixation numbers among conditions. Decrease of fixation numbers in the implicit learning condition has been reported^{7,8} and the present results are consistent with the previous report. Fixation duration is usually unchanged when visual search time became short. The results of implicit display in the memory condition show some reduction of fixation duration in our experiment, while they may be within the individual differences. Although it is not clear that how these factors are related to explicit and implicit processes, the data suggest that explicit and implicit processes influence differently on the eye movements during the search phase.

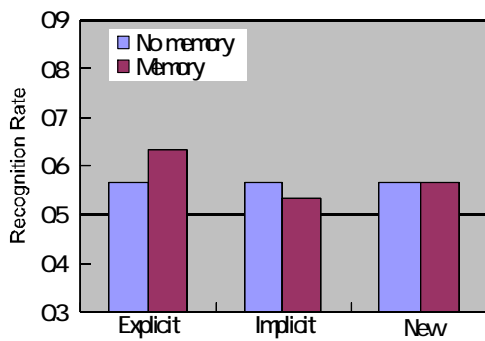


Fig. 6 Recognition rates for three stimulus types in the memory and no memory conditions.

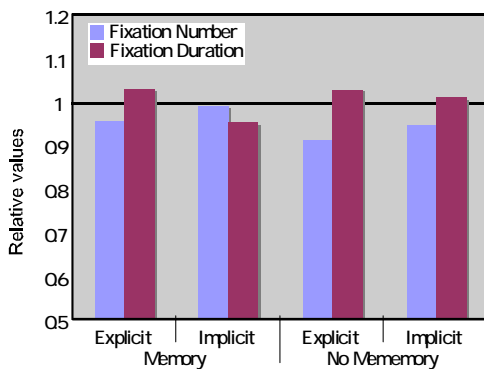


Fig. 7 Eye movement results for explicit and implicit stimuli. Fixation numbers and fixation duration relative to those for new stimuli are shown for explicit and implicit stimuli.

and implicit processes work very differently for memorizing spatial configuration of images. Most importantly, the memory through explicit effort to memorizing display configurations is not as efficient as implicit memory obtained from repeating for visual search whereas the opposite is the case for recognition. Since eye movements are related to the differences, this may not be solely for perception but may also be related to action.

There are several important issues remained for future research. First, the time of 1s may not be long enough for explicit memory and longer learning time may provide more efficient effect in the explicit memory condition. Second, the effect on eye movements is not clear in the present results. This is perhaps because of the small number of participants and experiments with additional participants should reveal the details. Third, measurements of brain activities, such as event related potential, related to each of implicit and explicit processes are important to understand physiological processes. We are conducting experiments considering these issues. Additionally, we are interested in effects of probability fluctuations between implicit and explicit learning and are planning to investigate the effects.

REFERENCES

- [1] S. Shioiri and P. Cavanagh, "ISI produces reverse apparent motion," *Vision Res* **30**(5), 757-768 (1990).
- [2] S. Shioiri and K. Matsumiya, "High spatial frequency superiority of motion aftereffect," presented at the Vision Science Society, Sarasota, FL, 2006.
- [3] P. Mazzoni and J. W. Krakauer, "An implicit plan overrides an explicit strategy during visuomotor adaptation," *J Neurosci* **26**(14), 3642-3645 (2006).
- [4] D. B. Willingham, "Becoming aware of motor skill," *Trends Cogn Sci* **5**(5), 181-182 (2001).
- [5] M. M. Chun and Y. Jiang, "Contextual cueing: implicit learning and memory of visual context guides spatial attention," *Cognit Psychol* **36**(1), 28-71 (1998).
- [6] M. M. Chun, "Contextual cueing of visual attention," *Trends Cogn Sci* **4**(5), 170-178 (2000).
- [7] M. S. Peterson and A. F. Kramer, "Attentional guidance of the eyes by contextual information and abrupt onsets," *Percept Psychophys* **63**(7), 1239-1249 (2001).
- [8] J. R. Brockmole and J. M. Henderson, "Recognition and attention guidance during contextual cueing in real-world scenes: evidence from eye movements," *Q J Exp Psychol (Colchester)* **59**(7), 1177-1187 (2006).

IV. DISCUSSION

Results of reaction time and eye movements suggest that explicit

Behavior Induction and Recall under an unknown Situation based on Multimodal Mirror Neuron Model

Tetsunari Inamura*[†]

*National Institute of Informatics / The Graduate University for Advanced Studies, JAPAN

Abstract—Memorization, abstraction, and generation of a time-series of sensors and motion patterns are some of the most important functions for intelligent robots, because these memories are useful for situation recognition and behavior decision making. In conventional research, recurrent neural networks are often used for such memory functions. However, they cannot memorize a lot of patterns and its learning algorithm is unreliable. In this paper, I propose a method for the induction of behavior and situational estimation based on Hidden Markov Models, which is currently one of the most useful stochastic models. With the proposed method, I show the feasibility of: (1) Both recognition and association are executed at the same time, and (2) A multiple degrees of freedom and multiple sensorimotor patterns are acceptable.

I. INTRODUCTION

For intelligent robots, the description and memorization of time-series sensorimotor patterns are important, such as for sound, image, and force of action. Robots should be able to decide the necessary behavior based on the current uncertain and insufficient sensory data, especially in real environments. In such cases, experience and a memory of the time-series of the sensorimotor pattern would be effective for situation recognition and behavior induction. Figure 2 shows the concept of a situation estimation and behavior induction. It is important that robots generate entire sensorimotor patterns using short-period and imperfect triggers. It is also useful that the motion pattern acts as trigger for the sensor association, and the sensor patterns also act as triggers for the motion association, as shown in Fig. 2. With this type of function, humanoid robots could generate various behaviors with on-site and realtime interaction between humans and robots.

Recently, dynamics-based pattern memorization and generation/association methods have been proposed. However, these methods need certain mapping functions between several of the internal states of the dynamics and the actual sensorimotor patterns. Another difficulty that these approaches have is that the design of their dynamics depends on the developer, such as the number of dimensions for the internal state space and the arbitration for multiple situations, namely the multiple dynamics.

I have focused on a Hidden Markov Models (HMMs) based approach rather than the methods presented above. Inamura *et al*[1] have proposed a symbol emergence model using HMMs, in which the HMMs act as recognizers, abstractors, and generators for humanoids' motion patterns. I propose in this paper a novel method based on HMMs that can recognize current situations, estimate future situations, and invoke multimodal sensorimotor patterns.

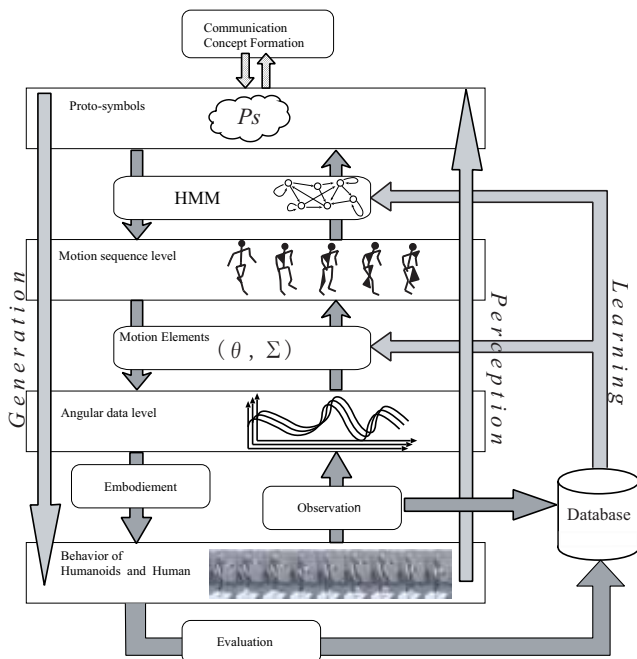


Fig. 1. An outline of mirror neuron model (mimesis model)

II. UNKNOWN SITUATION RECOGNITION AND NOVEL BEHAVIOR INDUCTION USING GEOMETRIC SYMBOL REPRESENTATION

A. Abstract of multimodal sensorimotor patterns using continuous HMM

I have proposed a mathematical model for a development of mirror neuron model from engineering viewpoint[2]. The concept of the model is shown in Fig.1 In the model, HMM is used as a key technology. HMM is a probabilistic modeling method that can recognize time-series patterns, learn the probabilistic dynamical system, and generate the original patterns. HMM consists of a finite number of states and connection arcs between each state node. In this framework, state transition occurs probabilistically and delivers a sequence of multi-dimensional vectors (Fig. 3). The difference between normal and Continuous HMMs(CHMM) is their output information. Discrete indices are output from normal HMMs, and continuous vectors are output from continuous HMMs[3].

In conventional research, HMMs are used for simple modality like speech recognition and the motion pattern of

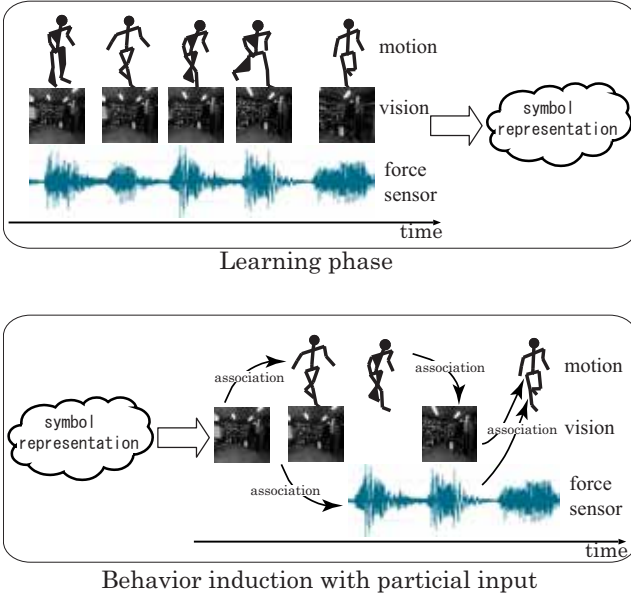


Fig. 2. Concept of situation estimation and induction of behavior by multimodal sensorimotor patterns

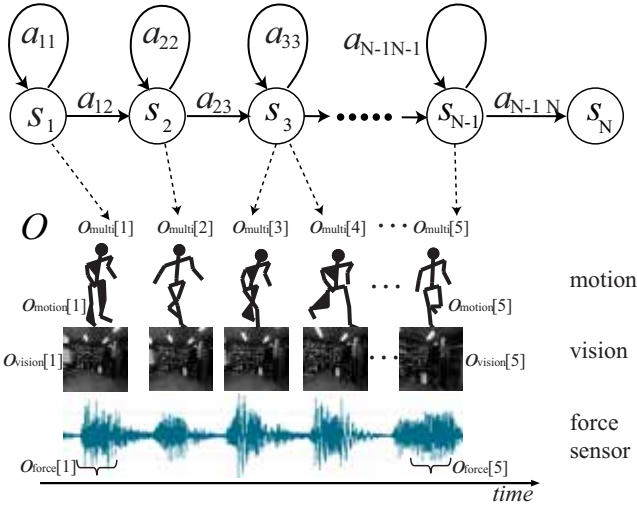


Fig. 3. Concept for adaptation of continuous hidden Markov models for integration of multimodal sensorimotor patterns

humanoid robots. However, HMMs do not have any limitations against the combination of several kinds of physical quantities. Therefore, we propose CHMM for combined multimodal sensorimotor patterns. Figure 3 shows the outline of our proposed CHMM. For the output of the CHMM, multimodal sensorimotor vector $\mathbf{o}_{multi}(t)$ is used, that is simple combination of several different patterns like motion, image, and the force sensor.

B. Construction of geometric symbol representation

Although some distance is needed for construction of space, the distance between two HMMs is not easily de-

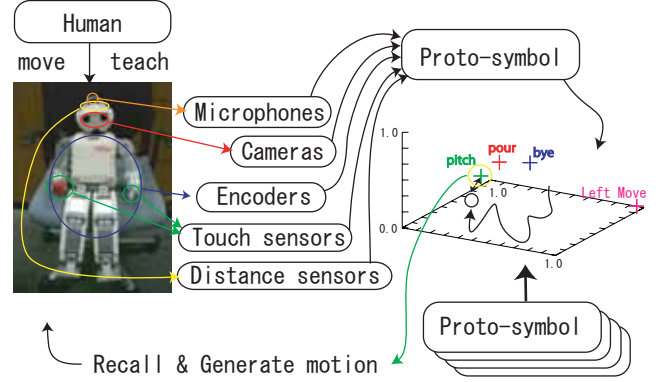


Fig. 4. Proto-symbol space based on time-series patterns of multi-modal sensors

finable because it is a stochastic model. For such stochastic models, there is a method for expressing the distance information. In this paper, we have adopted Kullback-Leibler information as the representation for the distance between HMMs. Strictly speaking, the Kullback-Leibler information is not for distance because it does not satisfy the property of the distance, triangle inequality and symmetry; therefore, we say the Kullback-Leibler information is a degree of similarity between the HMMs. The following equation is usually used to calculate the distance between HMM λ_1 and λ_2 .

$$D(\lambda_1, \lambda_2) = \sum_n \frac{1}{T_n} [\log P(y_1^T | \lambda_1) - \log P(y_1^T | \lambda_2)] \quad (1)$$

As the Eq.(1) does not satisfy the distance axiom, we use following improved information:

$$Ds(\lambda_1, \lambda_2) = \frac{1}{2} (D(\lambda_1, \lambda_2) + D(\lambda_2, \lambda_1)) \quad (2)$$

In order to construct the symbol space from the distance information, multidimensional scaling (MDS) is used. MDS is a method that accepts the distance information among elements, and the output is position of each element in the generated space. In the case of HMMs, the Kullback-Leibler information Ds is used for the similarity f_{ij} . Let the position of each HMMs as $\mathbf{x} = \{x_1, x_2, \dots, x_n\}$ where n is the number of dimension of the space. Using the least-squares method, each position \mathbf{x} is calculated.

C. Recognition of unknown sensorimotor patterns and Induction of novel behavior

To recognize the temporal multimodal sensorimotor patterns $\mathbf{O} = [\mathbf{o}[1], \mathbf{o}[2], \dots, \mathbf{o}[t]]$, where $[t]$ is the index of discrete time, the position of the target pattern in the symbol space is used. Using an algorithm described by Inamura[1], a short sensorimotor pattern of the current situation is transformed as a point in the symbol space. In other words, a total sensorimotor pattern is successively transformed as a curved line in the space.

Situation recognition is executed sequentially by calculating the distances between the assigned points of the known

behavior and a point that indicates the current situation. When the closest distance becomes less than the threshold, the system recognizes that the current situation corresponds with the behavior of the closest point. Since the recognition process is sequentially executed, it is similar to the entrainment into an attractor in nonlinear dynamics.

After the recognition, novel sensorimotor patterns are generated by creation of a HMM parameter which corresponds to the recognition result. To calculate the novel HMM parameter, several known HMM parameter are combined as follows:

$$b_i(\mathbf{y}) = \sum_{m=1}^M \frac{1}{d_l \sum_l \frac{1}{d_l}} cN(\boldsymbol{\mu}_{im}^l, \boldsymbol{\rho}_{im}^{l^2})$$

$$a_{ij} = \sum_{m=1}^M \frac{1}{d_l \sum_l \frac{1}{d_l}} a_{ij}^l \quad (3)$$

where, d_l indicates a distance between known proto-symbol position and input sensorimotor pattern, $\boldsymbol{\mu}_{im}$ and $\boldsymbol{\rho}_{im}$ indicate mean vector and covariance matrix for m -th Gaussian function of output probability $b_i(\mathbf{y})$.

III. APPLICATION FOR MULTI-MODAL SENSORIMOTOR PATTERNS

A. Application for sound recognition

One of the most typical behavior of humanoid robots is support task in daily-life environments and handling of humans' tools. In such a situation, not only vision but also auditory is effective information to accomplish the tasks. I have thus performed an experiment that several kinds of collision noises are used for the construction of the proto-symbol space.

Three kinds of collision noises are recorded when a humanoid robot grasp P.E.T. bottle, aluminum and steel cans, then hit them with a desk. 20-dimensional cepstrum feature vector is calculated for 30[ms] time length, at every 10[ms]. 58 vectors for 600[ms], that is full length of the noise, are used to construction of proto-symbol. The recognition rate was 93.3% for aluminum can, 96.7% for steel can, and 93.3% for P.E.T. bottle, respectively.

B. Application for gesture imitation

I have developed an gesture imitation system that uses a stereo images to recognize human's gesture under an assumption that the robot could not observe joint angle sensor directly[4]. The position of end effector (hand) is measured by stereo image processing. The number of dimension thus become to be 6, for both hands. A created proto-symbol space is shown in Fig.5.

C. Learning and mutual association of huge amounts of dimensional sensorimotor data

Next, we confirmed the feasibility of multimodal learning and the association function for huge amounts of dimensional data. For a huge amount of dimensional sensorimotor data, we chose the relationship between the motion pattern and a raw image pattern for the humanoid behavior.

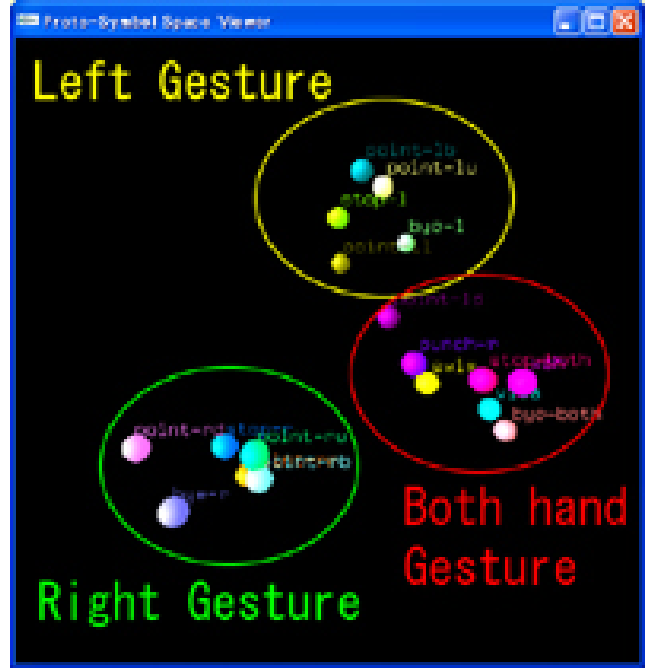


Fig. 5. A Proto-symbol space created by observation of gesture patterns

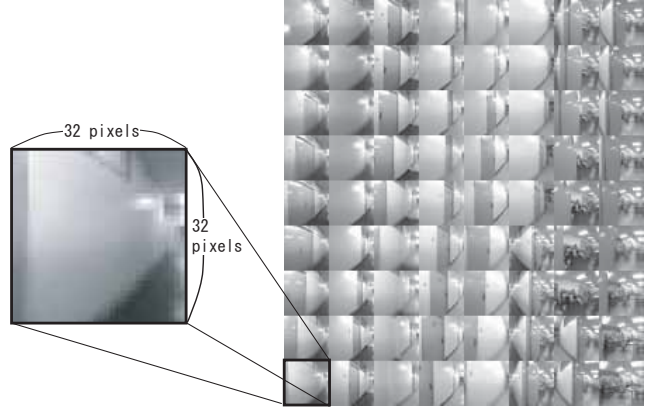


Fig. 6. Used raw image pattern

For the raw image pattern, a sequence of gray scale images was used. The gray scale image was $32pixels \times 32pixels$ for each moment. Therefore, the image vector is indicated as follows:

$$\mathbf{o}_{vision} = (I_{11}, I_{12}, \dots, I_{32 \ 32}), \quad (4)$$

where I_{ij} indicates the intensity of the (i, j) pixel.

Sequences of joint angles are used for the motion patterns, that is, the size of the joint angle vector was 20:

$$\mathbf{o}_{motion} = (\theta_1, \theta_2, \dots, \theta_{20}). \quad (5)$$

Therefore, the size of the multimodal sensorimotor vector \mathbf{o}_{multi} is 1044.

$$\mathbf{o}_{multi} = \begin{pmatrix} \mathbf{o}_{vision} \\ \mathbf{o}_{motion} \end{pmatrix} \quad (6)$$

A sequence of vision and motion patterns for some walking behaviors was recorded for about a ten second period, at a sampling rate of 10[Hz]. The used image sequence that was recorded by humanoid is shown in Fig.6. The number of nodes was set up at ten, and the number of mixture of Gaussian was set at 20. The learning process took about 10 minutes on an Intel Xeon 3.2[GHz] processor.

For the association, the first frame image was input for the humanoid, and the association output of the motion pattern was analyzed. Figure 7 shows the trajectory of the left hip's pitch joint, the left knee joint, and the left shoulder's pitch joint, for both the original and associated motion patterns. As the result shows, both the original and the generated motion patterns are almost equivalent. This indicates the ability of the prediction and evocation from exiguous sensor inputs as a tip-off. The induction process took about one second on an Xeon 3.2[GHz] processor.

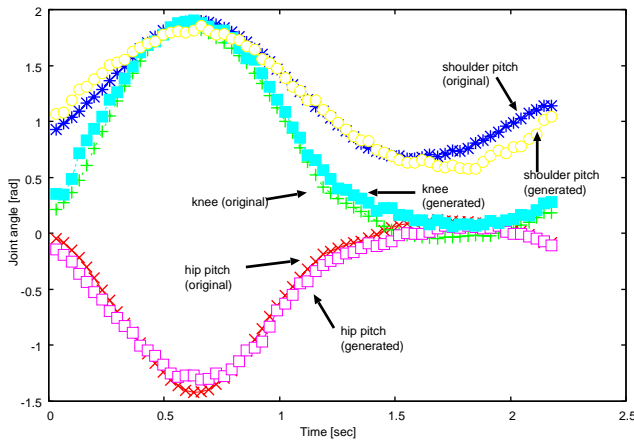


Fig. 7. Original motion pattern and generated motion pattern

IV. BEHAVIOR INDUCTION EXPERIMENT USING MULTIMODAL SENSORIMOTOR DATA

Next, we have confirmed the feasibility of the behavior induction function based on the geometric symbol representation using a real humanoid robot[5]. The humanoid has 20 degrees of freedom in its two arms, head, and torso. Two six-axes force sensors are embedded in both wrists; two binocular cameras are set in the head.

In the learning phase, a human takes the robot by the hand and teaches it to move step by step. The teacher (human) can easily and directly move the robot's arms because the servo gain is set quite low. During the teaching phase, the robot observes the joint angles θ_{motion} , and object detection using its vision and force sensors with a 10-Hz sampling rate. For object detection, the robot detects the 3D positioning of three colored objects, red, blue and green.

In the behavior induction phase, the humanoid tries to recognize the current situation using the ongoing sensor patterns. A short interval of 20 samples is cut from the sensorimotor pattern stream, and then they are transformed as a state point in the geometric symbol space. After calculating

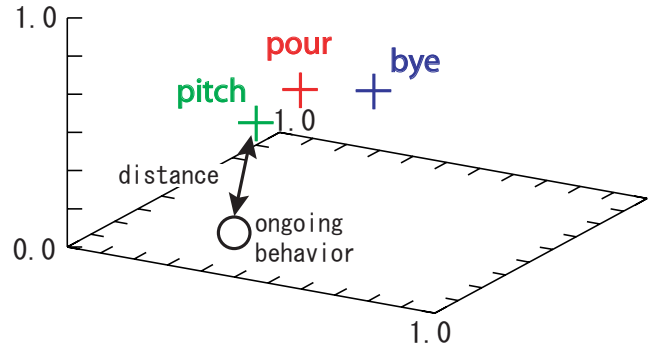


Fig. 8. Constructed symbol space for three behaviors

of distances between each point (symbol of each behaviors) and the ongoing motion's point, the robot can recognize which is the most similar behavior by searching for the closest distance.

V. CONCLUSIONS

Realtime situation recognition and behavior induction are achieved by using the introduction of geometric symbol representation and online transformation from ongoing behaviors into the space representations. A robot can generate entire sensorimotor patterns using short-period time and imperfect triggers. Through experiments, we proved the feasibility of the behavior learning and induction methods based on on-site and realtime interaction between humans and robots.

This year, I have improved the mirror neuron model to treat multimodal sensorimotor patterns like sound, image sequence and position of end effectors. I have also performed a confirmation experiment that the robot recognize and generate not only known behavior but also unknown/novel behavior. Furthermore, I will improve the system to integrate each modality so that the system could recognize unknown situation and generate novel behavior with combination of recalled behavior for each known situation. That will be the research issue in the next year.

REFERENCES

- [1] Tetsunari Inamura, Hiroaki Tanie, and Yoshihiko Nakamura. From stochastic motion generation and recognition to geometric symbol development and manipulation. In *International Conference on Humanoid Robots*, 2003. (CD-ROM).
- [2] Tetsunari Inamura, Yoshihiko Nakamura, Iwaki Toshima, and Hiroaki Tanie. Embodied symbol emergence based on mimesis theory. *International Journal of Robotics Research*, 23(4):363–378, 2004.
- [3] Steve Young et al. *The HTK Book*. Microsoft Corporation, 2000.
- [4] Naoki Kojo, Tetsunari Inamura, Kei Okada, and Masayuki Inaba. Gesture recognition for humanoids using proto-symbol space. In *IEEE International Conference on Humanoid Robots*, pages 76–81, 2006.
- [5] Tetsunari Inamura, Naoki Kojo, and Masayuki Inaba. Situation recognition and behavior induction based on geometric symbol representation of multimodal sensorimotor patterns. In *IEEE/RSJ International Conference on Intelligent Robots and Systems*, pages 5147–5152, 2006.

Visuomanual coordination in ball catching task

Yasuharu Koike

Abstract—Humans show a variety of motor behavior which enables us to interact with many different objects under different environments. Considering the number of objects and environments which influence the dynamics of the arm, the corresponding motor control system must be capable of providing appropriate motor commands for the multitude of distinct contexts that are likely to be experienced.

In the experiments, we showed a virtual ball moving vertically downward on a 50 inch plasma display with five different force timing from -60 msec to 60 msec at intervals of 30 msec. The ball catching was simulated by a force-feedback system, provided by the SPIDAR. The subject was asked to catch the virtual ball at an initial hand position. The hand position and Electromyographic (EMG) signals of flexor carpi radialis were recorded.

At the beginning, subjects caught the ball at the same timing as gravitational acceleration for all condition. The subjects came to receive the ball of any timing gradually as training advanced by force feedback. We found that subjects learned new environments in which the ball was falling by a different timing even though the visual information was same. These results suggest that humans can learn different timing by force feedback.

I. INTRODUCTION

Catching a falling ball task was investigated in order to reveal mechanisms that estimate time-to-contact (TTC) [1], [2], [3], [4].

From our previous experiment [5], human can learn the different acceleration conditions and they can discriminate the different acceleration using visual or haptic information. Is the dynamics of falling ball with different acceleration acquired?

Almost of all experiments used the physically consistent conditions. So at the ball contact, the visual and haptic stimuli were displayed simultaneously. How do we detect the TTC by visual or haptic information?

In this experiments, we showed a virtual ball moving vertically downward on a 50 inch plasma display with five different force timing from -60 msec to 60 msec at intervals of 30 msec. The ball catching was simulated by a force-feedback system.

At the beginning, subjects caught the ball at the same timing as gravitational acceleration for all condition. The subjects came to receive the ball of any timing gradually as training advanced by force feedback. We found that subjects learned new environments in which the ball was falling by a different timing even though the visual information was same. These results suggest that humans can learn different timing by force feedback.

P & I Laboratory, Tokyo Institute of Technology, R2-15, 4259, Nagatsuta-cho, Midori-ku, Yokohama, 226-8503 koike@pi.titech.ac.jp

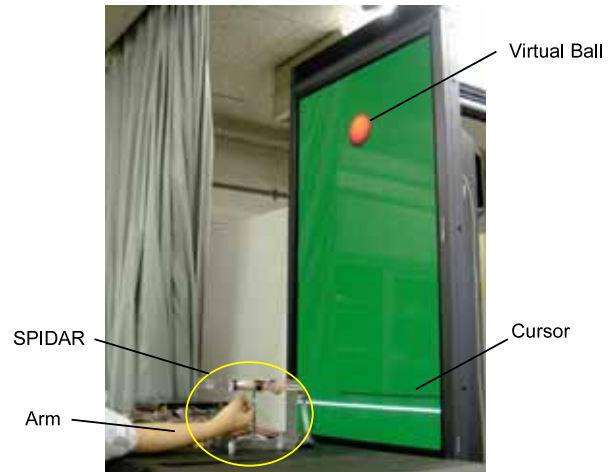


Fig. 1. Experimental environment.

II. EXPERIMENT

A. Subjects

3 healthy subjects (2 men and 1 woman, 23 ~ 17 years old) participated in the study. The subjects were right-handed, had normal vision or vision that was corrected for normal. Experiments were conformed to the Declaration of Helsinki on the use of human subjects in research.

B. Visual and haptic display using virtual reality environment

Figure 1 shows a experimental environment. We use a haptic device “SPIDAR” which use four motors (Maxon DC motor, RE25) to strain by strings for applying the force to a hand. OPTOTRAK (Northern Digital) was used for measuring a hand position in 200 Hz.

Figure 2 shows system configuration.

We also measure Electromyographic (EMG) signals (Bagnoli-16 system Delsys inc.) for measuring a intention for catching, because EMG signals activate about 100 msec before exerting a force. Active electrode was put on palmaris longus and EMG signals was sampled at 2 kHz with 16bit. In order to show the visual stimuli to the subject, plasma display (PDP503-CMX, 50 inches, Pioneer) was used. Virtual ball was falling from 80 [cm] height with 0 [m/sec] initial velocity, was same color and size, and applied 4.9 [N] force to right hand for 1.1 sec for different perturbation conditions.

C. Experimental procedure

Subjects were asked to catch the ball at the initial position. At the beginning of the trial, beep signal sounded and after

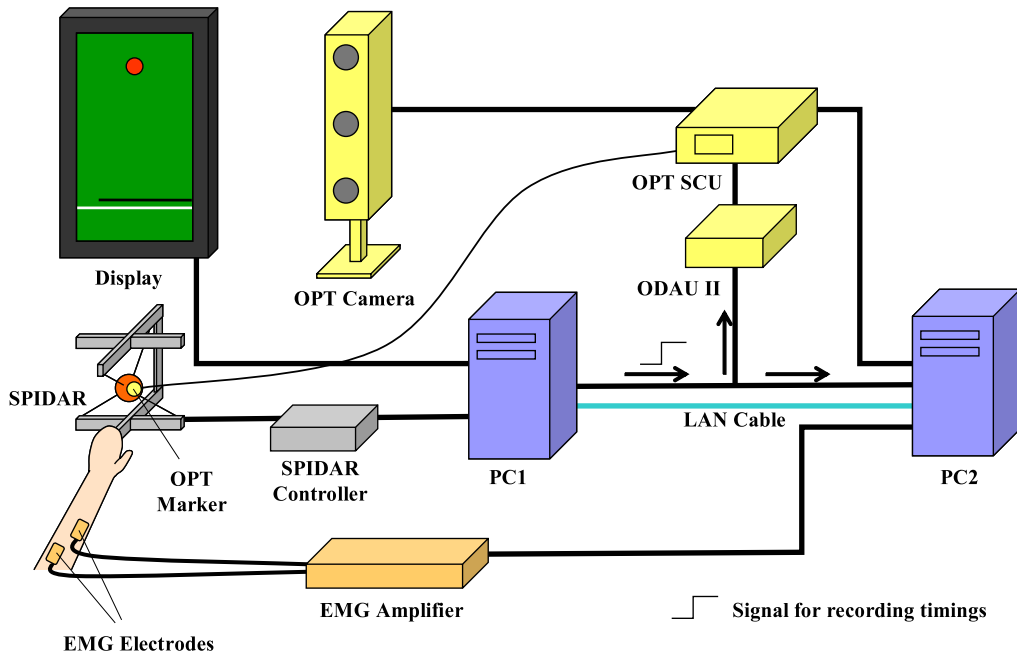


Fig. 2. system configuration

a random delay ranging from 0.75 to 1.25 sec, the virtual ball was falling with 0 m/s initial velocity and 9.8 m/s^2 acceleration.

Subjects performed 5 different experiments. Each experiment consisted of 100 trials. In the first block, there were 10 trials without delay. In the second block, there were 80 trials with delay. In this block one delay period was randomly selected from 5 conditions (-60, -30, 0, 30, 60 msec). In the third block, there were 10 trials without delay. Each experiment therefore consisted of 100 repetitions per 5 conditions. Last 10 trials were used to reveal the presence of aftereffects and wash out.

Few trials were excluded from the analysis attributed the presence of artifacts during the trial as marked in the notebook.

III. RESULTS

In five conditions, all subjects were not aware that the force timing was changed during the task. In spite of unperceived conditions, the subjects adapted into different delay timing.

Figure 3 shows time series of the filtered EMG signals of wrist and elbow. The time when the force was applied to the hand was shown as 0.

In the case of zero delay, EMG activities increased 100 msec before applying the force.

In the case of another delay, the onset of the filtered EMG signal was changed and the timing of the onset gradually became the same as the case of zero delay.

Figure 4 shows the time series of hand position .

As same as EMG activation, hand position also move 100 msec before the force onset, and the timing gradually shifted

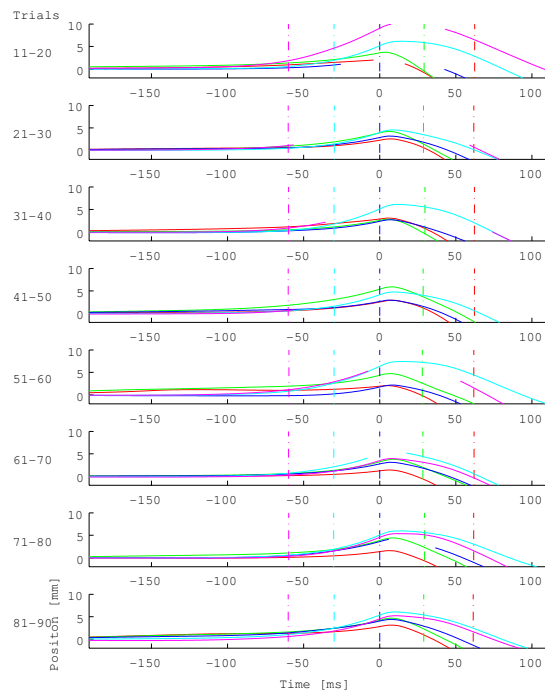


Fig. 4. Hand position

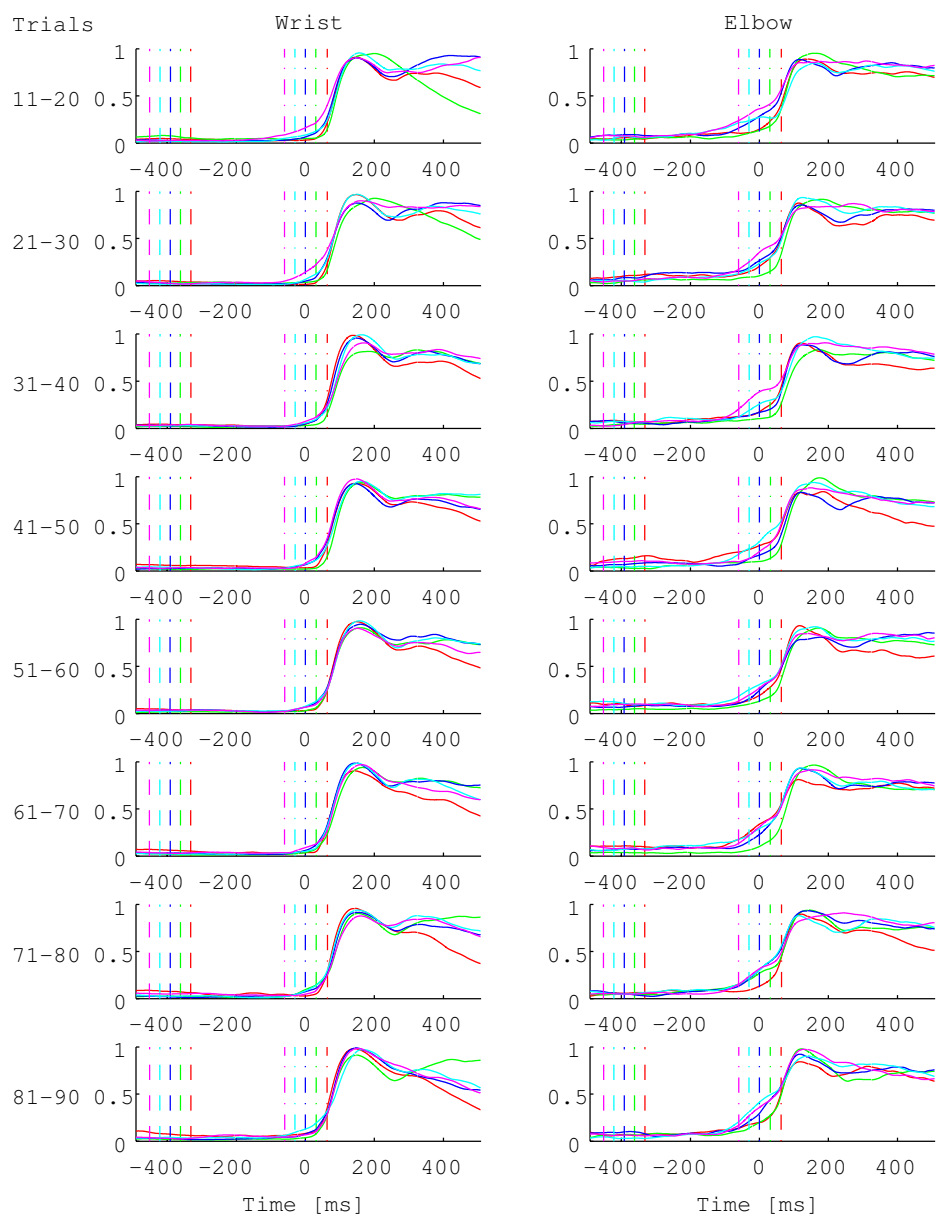


Fig. 3. time series of the filtered EMG signals of wrist and elbow

to the same timing as 0 delay.

IV. DISCUSSION

We showed that the subject could adjust the timing of the EMG onset without perceive the delay. Visual stimulus was followed the normal gravitational environment and only the timing of force was changed. If we use the internal model which estimated the time-to-contact from visual information, we could not estimate different timing. However, the subjects learned the different timing.

We can assume two hypotheses for explaining this phenomena. One is that the subject learned the different timing by using visual stimuli. They would become to estimate the different TTC with same visual stimuli as they learned the different acceleration. The other one is that the subject learned the delay between the motor command and muscle tension.

Whichever hypotheses being correct, the force information would be crucial role for learning the TTC.

V. ACKNOWLEDGMENTS

This work has been partially supported by a Grant-in-Aid for Scientific Research on Priority Areas "Emergence of Adaptive Motor Function through Interaction between Body, Brain and Environment" from the Japanese Ministry of Education, Culture, Sports, Science and Technology.

REFERENCES

- [1] G. J. K. Alderson, D. J. Sully, et al. : An Operational Analysis of a One-Handed Catching Task Using High Speed Photography, *Journal of Motor Behavior*, vol.6, no.6, 217/226 (1974)
- [2] F. Lacquaniti and C. Maioli: The Role of Preparation in Tuning Anticipatory and Reflex Responses during Catching, *The journal of neuroscience*, vol.9, no.1, 134/148 (1989)
- [3] D. N. Lee, D. S. Young, et al. : Visual Timing in Hitting an Acceleration Ball, *Quarterly Journal of Experimental Psychology*, vol.35A, 333/346 (1983)
- [4] G. J. P. Savelsbergh, H. T. A. Whiting, et al. : The Role of Predictive Visual Temporal Information in the Coordination of Muscle Activity in Catching, *Exp. Brain and Res*, vol.89, 223/228 (1992)
- [5] Y.Koike, S.Hong, D.Shin: Learning and switching between multiple nonzero - gravity environments for catching task, *Neuroscience abstract*, 2005
- [6] M. Ishii and M. Sato: A 3D Spatial Interface Device Using Tensed Strings, *Presence*, vol.3, no.1, 81/86 (1984)
- [7] J. McIntyre, M. Zago, et al. : Does the Brain Model Newton's Law?, *nature neuroscience*, vol.4, no.7, 693/694 (2001)
- [8] A. M. Brouwer, E. Brenner, et al. : Perception of Acceleration with Short Presentation Times: can Acceleration be Used in Interception? , *Percept Psychophys*, vol.64, no.7, 1160/1168 (2002)

Analysis of Human Skills in Manipulation with Interaction with Environment

—Hidden Markov Modeling of Human Pivoting Operations—

Yusuke MAEDA and Hajime SUGIUCHI

Abstract—In this paper, a method to model human operations using Hidden Markov Models (HMM) is presented. The “optimal” HMM with an appropriate number of states is determined based on the MDL (Minimum Description Length) criterion. Human pivoting operations, a typical grasplless manipulation, are modeled using Gaussian mixture HMMs. The obtained HMMs are analyzed by metric MDS (Multidimensional Scaling) to reveal individual characteristics in the operations.

I. INTRODUCTION

Human dexterity is highly remarkable and still a mystery to current robotics. There is a great demand for robotization of human skillful operations, and therefore explorations into such operations are important. The hidden Markov model (HMM) [1] is widely used as a powerful tool for modeling of human operations [2]–[7]. Because human operations usually have a considerable variation, stochastic approaches like HMM are convenient in modeling.

A problem in using HMMs is how to determine their topology. If we use an HMM with a complicated topology, we can model operation data accurately. However, too complicated HMMs lead to overfitting. In the above literatures, the topology was empirically determined by considering the balance of the accuracy and the complexity. On the other hand, in this paper, we use the MDL criterion [8] for the topology determination. The MDL gives an objective measure to obtain the “best” HMM that has a balance between the accuracy and the complexity.

The modeled operation in this paper is human pivoting [9]. A vertex of the manipulated object is used as a pivot around which the object is rotated (Fig. 1(a)). The object is

in one-point contact with the ground in pivoting and therefore the human operator does not have to support all the weight of it. Thus, pivoting is suitable for manipulation of heavy objects. Repeating small rotations around two vertices of the object by turns, the object can be moved to any locations (Fig. 1(b)) The pivoting operation is a typical grasplless manipulation that requires an interaction between humans and the environment.

II. APPLICATION OF MDL CRITERION TO HMM

A. MDL Criterion

Let us consider modeling of a sequence of T data, \mathbf{O} . When we apply the i -th model of M_c candidates to the data, the MDL criterion can be expressed as follows [8]:

$$l_R^{(i)} = -\log p_{\hat{\theta}^{(i)}}^T(\mathbf{O}) + \frac{L_i}{2} \log T + \log M_c, \quad (1)$$

where $\hat{\theta}^{(i)}$ is the maximum likelihood estimator of the parameters of the i -th model; $p_{\hat{\theta}^{(i)}}^T$ is its likelihood, and L_i is the model dimension of the i -th model. The model that minimizes (1) can be considered as the “best” model. When L_i is increased, the first term of (1), $-\log p_{\hat{\theta}^{(i)}}^T(\mathbf{O})$, will be decreased, but the second term, $\frac{L_i}{2} \log T$ will be increased. The best balance of the two terms gives us the best model of the data. Note that the third term, $\log M_c$, is constant and therefore we ignore it hereafter.

B. MDL Criterion for Gaussian Mixture HMMs

Let us consider a Gaussian mixture HMM described by the following parameters:

$$\begin{aligned} \lambda &= (\mathbf{A}, \mathbf{w}, \boldsymbol{\mu}, \boldsymbol{\Sigma}, \boldsymbol{\pi}) \\ \mathbf{A} &= [a_{ij}] \in \mathbb{R}^{N \times (N+1)} \\ \mathbf{w} &= \{\mathbf{w}_1, \dots, \mathbf{w}_N\} \\ \mathbf{w}_n &= \{w_{n1}, \dots, w_{nM}\} \\ \boldsymbol{\mu} &= \{\boldsymbol{\mu}_1, \dots, \boldsymbol{\mu}_N\} \\ \boldsymbol{\mu}_n &= \{\mu_{n1}, \dots, \mu_{nM}\} \\ \boldsymbol{\Sigma} &= \{\boldsymbol{\Sigma}_1, \dots, \boldsymbol{\Sigma}_N\} \\ \boldsymbol{\Sigma}_n &= \{\Sigma_{n1}, \dots, \Sigma_{nM}\} \\ \boldsymbol{\pi} &= [1, 0, \dots, 0] \in \mathbb{R}^N, \end{aligned}$$

where \mathbf{A} is the state transition matrix and therefore $\sum_{j=1}^{N+1} a_{ij} = 1$; $\boldsymbol{\pi}$ is the initial state distribution; N is the number of states; M is the number of mixture components in each state; S is the number of the elements of an observation

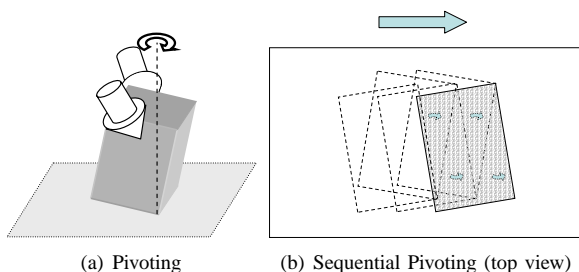


Fig. 1. Pivoting Operation

Yusuke MAEDA and Hajime SUGIUCHI are with Division of Systems Research, Faculty of Engineering, Yokohama National University, 79-5 Tokiwadai, Hodogaya-ku, Yokohama 240-8501, Japan {maeda, sugi}@ynu.ac.jp

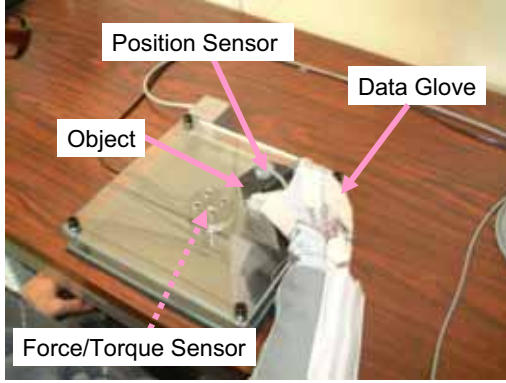


Fig. 2. Data Acquisition Setup

vector \mathbf{o} (i.e., $\mathbf{o} \in \mathbb{R}^S$); $w_{nm} \in \mathbb{R}$, $\boldsymbol{\mu}_{nm} \in \mathbb{R}^S$ and $\boldsymbol{\Sigma}_{nm} \in \mathbb{R}^{S \times S}$ are the parameters for the Gaussian probability density function of the m -th mixture component of the n -th state as follows:

$$b_n(\mathbf{o}) = \sum_{m=1}^M w_{nm} \mathcal{N}(\mathbf{o}; \boldsymbol{\mu}_{nm}, \boldsymbol{\Sigma}_{nm}) \quad (2)$$

$$\mathcal{N}(\mathbf{o}; \boldsymbol{\mu}, \boldsymbol{\Sigma}) = \frac{1}{\sqrt{(2\pi)^S \det \boldsymbol{\Sigma}}} \exp\left(-\frac{1}{2}(\mathbf{o} - \boldsymbol{\mu})^T \boldsymbol{\Sigma}^{-1}(\mathbf{o} - \boldsymbol{\mu})\right), \quad (3)$$

where w is a weight coefficient ($\sum_{m=1}^M w_{nm} = 1$), $\boldsymbol{\mu}$ is a mean vector, and $\boldsymbol{\Sigma}$ is a covariance matrix. Because of the implementation of HTK (Hidden Markov Model Toolkit) [10], which we used for HMM calculation, the HMM has an additional non-emitting exit state, and therefore the size of \mathbf{A} is not $N \times N$, but $N \times (N + 1)$.

For simplicity, we assume that the covariance matrix $\boldsymbol{\Sigma}_{nm}$ is diagonal. Then, if we do not impose any constraints on the topology of the HMM, the model dimension of the HMM is given by $N^2 + (M - 1)N + 2SMN$. When we generate an HMM by Baum-Welch algorithm from K observation sequences, $\mathbf{O}^{(1)}, \dots, \mathbf{O}^{(K)}$, the MDL criterion (1) is given by the following equation:

$$-\sum_k \log p(\mathbf{O}^{(k)} | \boldsymbol{\lambda}) + \frac{N^2 + (M - 1)N + 2SMN}{2} \log \sum_k T^{(k)}, \quad (4)$$

where $p(\mathbf{O}^{(k)} | \boldsymbol{\lambda})$ is the likelihood that $\mathbf{O}^{(k)}$ is produced by the HMM $\boldsymbol{\lambda}$, and $T^{(k)}$ is the data length of $\mathbf{O}^{(k)}$. If we generate various HMMs with different topology (e.g., different number of states), we can choose the “best” HMM that minimizes (4) among them.

III. MODELING OF HUMAN PIVOTING OPERATIONS

A. Pivoting Data Acquisition

We prepared a data acquisition setup for human pivoting operations as shown in Fig. 2. The manipulated object is a rubber cuboid of 0.36 [kg] and its size is $50 \times 50 \times 100$ [mm].

TABLE I
OVERVIEW OF PIVOTING DATA

| Operator | Operation Time [s] | | | |
|----------|--------------------|------|------|------|
| | average | S.D. | max | min |
| A | 4.45 | 0.44 | 5.58 | 3.75 |
| B | 3.62 | 0.42 | 4.70 | 2.85 |
| C | 3.54 | 0.52 | 5.73 | 3.06 |
| D | 5.58 | 0.55 | 7.50 | 4.82 |
| E | 3.13 | 0.37 | 3.76 | 2.58 |
| F | 5.07 | 0.50 | 6.18 | 4.26 |
| G | 4.23 | 0.51 | 5.69 | 3.67 |
| H | 4.72 | 0.79 | 6.37 | 3.49 |
| I | 3.69 | 0.36 | 4.61 | 3.13 |
| J | 6.34 | 0.58 | 7.41 | 5.44 |
| K | 6.83 | 0.74 | 9.44 | 5.53 |
| L | 4.94 | 0.51 | 6.61 | 4.36 |

TABLE II
OBTAINED HMMs

| Operator | # of States | Log Likelihood | MDL [nat] |
|----------|-------------|--------------------|---------------------|
| A | 36 | 4.96×10^3 | -1.44×10^5 |
| B | 29 | 2.71×10^3 | -0.77×10^5 |
| C | 25 | 1.81×10^3 | -0.51×10^5 |
| D | 34 | 5.25×10^3 | -1.48×10^5 |
| E | 22 | 3.01×10^3 | -0.86×10^5 |
| F | 32 | 5.96×10^3 | -1.71×10^5 |
| G | 38 | 2.90×10^3 | -0.79×10^5 |
| H | 34 | 2.43×10^3 | -0.64×10^5 |
| I | 35 | 3.42×10^3 | -1.00×10^5 |
| J | 42 | 7.29×10^3 | -2.05×10^5 |
| K | 28 | 7.35×10^3 | -2.14×10^5 |
| L | 35 | 4.92×10^3 | -1.43×10^5 |

This object is appropriate for pivoting because its weight is too heavy to pick it up by two-fingered pinching.

The position and orientation of the object were acquired by Polhemus Fastrak. The motion of the human fingers was measured by a data glove, Teiken StrinGlove. We calculated a time series of finger joint angles from the measured data and operators’ finger dimensions. We also measured ground reaction forces by a force/torque sensor (Nitta IFS-67M25A 50-I). All the data were sampled at 120 [Hz] by a Linux PC.

The target task was 300 [mm] transportation of the object by pivoting as fast as possible. Twelve male subjects (Operator A through L) performed two-fingered pivoting operations 30 or more times for each, after a few trials for practice. A brief overview of the obtained data is shown in Table I.

B. Hidden Markov Modeling

In this study, we used only the following crucial data for hidden Markov modeling:

- MP, PIP and DIP joint angles (flexion/extension) of index finger,
- IP and MP joint angles (flexion/extension) of thumb.

A set of these data forms a observation vector ($S = 5$). Then the time sequences of the observation vector was modeled by a Gaussian mixture HMMs. The number of mixture components was two ($M = 2$).

We used HTK [10] for HMM parameter estimation. Because Baum-Welch algorithm used for the parameter estimation can find only local optima, we repeated it six times

TABLE III
HMM DISSIMILARITY

| | A | B | C | D | E | F | G | H | I | J | K | L |
|---|-------|-------|-------|-------|-------|-------|------|-------|------|------|------|-----|
| A | 0.0 | | | | | | | | | | | |
| B | 31.3 | 0.0 | | | | | | | | | | |
| C | 39.2 | 25.9 | 0.0 | | | | | | | | | |
| D | 57.5 | 67.2 | 70.6 | 0.0 | | | | | | | | |
| E | 96.4 | 69.0 | 33.5 | 157.7 | 0.0 | | | | | | | |
| F | 104.4 | 123.6 | 200.0 | 190.7 | 114.8 | 0.0 | | | | | | |
| G | 45.3 | 45.2 | 36.5 | 62.3 | 41.5 | 59.0 | 0.0 | | | | | |
| H | 53.3 | 90.5 | 36.7 | 127.5 | 101.7 | 150.8 | 17.9 | 0.0 | | | | |
| I | 21.2 | 44.6 | 40.5 | 26.0 | 121.1 | 53.5 | 27.5 | 54.7 | 0.0 | | | |
| J | 44.5 | 45.9 | 73.0 | 65.0 | 70.9 | 86.6 | 16.0 | 18.7 | 52.8 | 0.0 | | |
| K | 32.7 | 107.9 | 168.3 | 46.9 | 303.8 | 129.6 | 96.3 | 188.9 | 38.2 | 94.9 | 0.0 | |
| L | 9.3 | 18.7 | 27.3 | 36.9 | 66.8 | 133.3 | 33.4 | 33.5 | 20.2 | 46.4 | 37.5 | 0.0 |

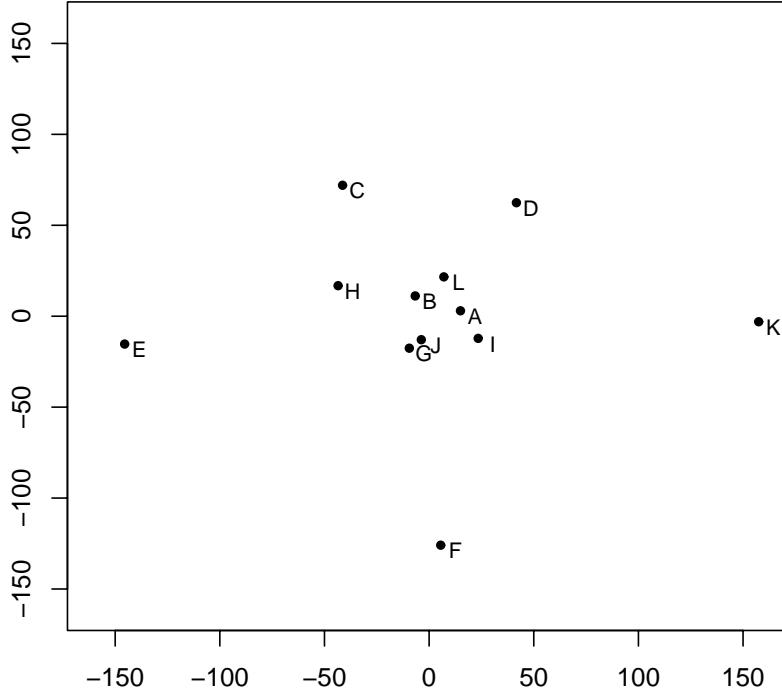


Fig. 3. MDS Result

by changing the initial conditions. Then we increased the number of the states of HMMs step by step to find the HMM that minimizes the MDL criterion (4). The obtained “best” HMMs for the human operators are shown in Table II. Although we did not impose any constraints on the topology of the HMMs in this paper, we can also deal with HMMs with restricted topology such as left-right models using the MDL principle.

C. Dissimilarity Analysis

We can define a stochastic dissimilarity measure between two HMMs, $D_s(\lambda_1, \lambda_2)$, as follows [1]:

$$D(\lambda_1, \lambda_2) = \frac{\sum_k \{\log p(O_1^{(k)} | \lambda_1) - \log p(O_1^{(k)} | \lambda_2)\}}{\sum_k T_1^{(k)}} \quad (5)$$

$$D(\lambda_2, \lambda_1) = \frac{\sum_k \{\log p(O_2^{(k)} | \lambda_2) - \log p(O_2^{(k)} | \lambda_1)\}}{\sum_k T_2^{(k)}} \quad (6)$$

$$D_s(\lambda_1, \lambda_2) = \frac{1}{2} \{D(\lambda_1, \lambda_2) + D(\lambda_2, \lambda_1)\} \quad (7)$$

The dissimilarity can be used for analysis of the relationship of human operation skills [5], [7].

Table III shows the dissimilarity values calculated by (7). However, the table is not intuitive, thus we plot the HMMs on a plane by metric multidimensional scaling (MDS) so that we can easily grasp their dissimilarities. Fig. 3 is the result of metric MDS by cmdscale() of R [11].

The figure shows that pivoting operations by Operator E, F, and K have striking personalities. Typical joint data in their operation is presented in Fig. 4~6. The average operation time of pivoting by Operator E is the smallest (3.13 [s]) of

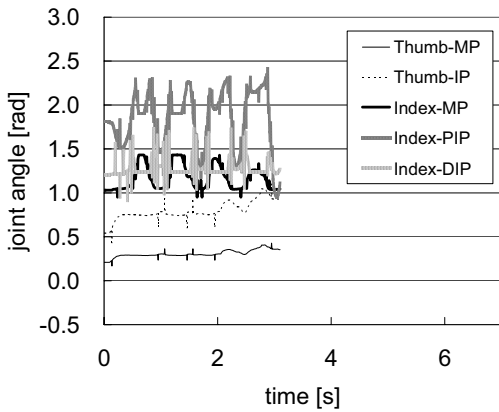


Fig. 4. Typical Joint Data of Operator E

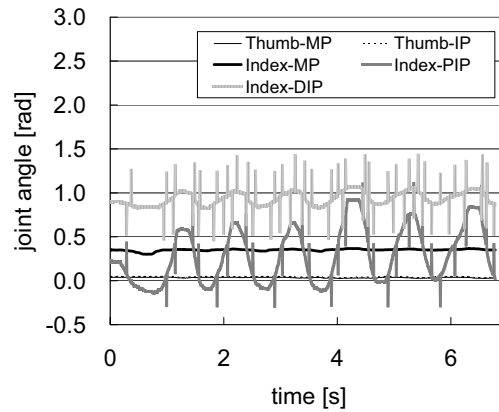


Fig. 6. Typical Joint Data of Operator K

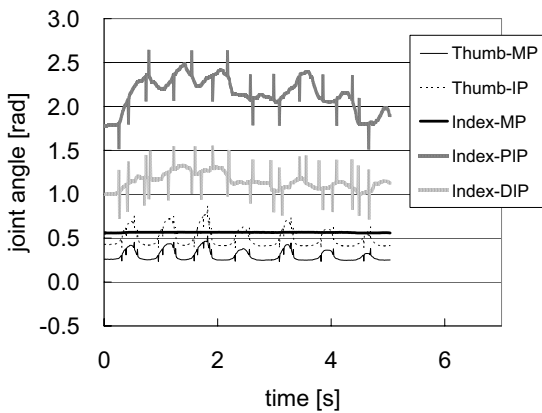


Fig. 5. Typical Joint Data of Operator F

twelve operators (see Table I), and the number of the states of his HMM is also the smallest ($N = 22$). On the other hand, the average of the operation time of pivoting by Operator K is the longest, 6.83 [s] (see Table I). Consequently, it is natural that the HMMs of Operator E and K are located at the both ends of the plane.

Operator F is not special in terms of operation time. However, his pivoting operations are different from those of other operators in that he rarely uses the MP flexion/extension of his index finger in pivoting.

IV. CONCLUSION

In this study, we performed a hidden Markov modeling of human pivoting operations. Finger motions in pivoting were collected and modeled using Gaussian mixture HMMs. The number of the states of the HMMs are determined by MDL (Minimum Description Length) criterion. The obtained HMMs are analyzed by metric MDS (Multidimensional Scaling) based on the HMM dissimilarity measure. Future work should address the application of the obtained HMMs to the implementation of human-like skills on robots.

REFERENCES

[1] Lawrence R. Rabiner. A tutorial on hidden Markov models and selected applications in speech recognition. *Proc. of IEEE*, Vol. 77, No. 2, pp. 257–286, 1989.

[2] Blake Hannaford and Paul Lee. Hidden Markov model analysis of force/torque information in telemanipulation. *Int. J. of Robotics Research*, Vol. 10, No. 5, pp. 528–539, 1991.

[3] Jie Yang, Yangsheng Xu, and C. S. Chen. Hidden Markov model approach to skill learning and its application. *IEEE Trans. on Robotics and Automation*, Vol. 10, No. 5, pp. 621–631, 1994.

[4] M. C. Nechyba and Yangsheng Xu. Stochastic similarity for validating human control strategy models. *IEEE Trans. on Robotics and Automation*, Vol. 14, No. 3, pp. 437–451, 1998.

[5] Kaiji Itabashi, Sehoon Yea, Tatsuya Suzuki, and Shigeru Okuma. Acquisition of the human skill with hidden Markov model. *T. of Soc. of Instrument and Control Engineers*, Vol. 34, No. 8, pp. 890–897, 1998. (in Japanese).

[6] Tetsunari Inamura, Hiroaki Tanie, and Yoshihiko Nakamura. From stochastic motion generation and recognition to geometric symbol development and manipulation. In *Proc. of IEEE-RAS Int. Conf. on Humanoid Robots*, 1b–02, 2003.

[7] Kazuaki Hirana, Takeshi Nozaki, Tatsuya Suzuki, Shigeru Okuma, Kaiji Itabashi, and Fumiharu Fujiwara. Quantitative evaluation for skill controller based on comparison with human demonstration. *IEEE Trans. on Control Systems Technology*, Vol. 12, No. 4, pp. 609–619, 2004.

[8] Te Sun Han and Kingo Kobayashi. *Mathematics of Information and Coding*. American Mathematical Society, 2001.

[9] Yasumichi Aiyama, Masayuki Inaba, and Hirochika Inoue. Pivoting: A new method of grasping manipulation of object by robot fingers. In *Proc. of IEEE/RSJ Int. Conf. on Intelligent Robots and Systems*, pp. 136–143, Yokohama, Japan, 1993.

[10] HTK (Hidden Markov Model Toolkit). <http://htk.eng.cam.ac.uk/>.

[11] R. <http://www.r-project.org/>.

Optimal foraging strategy: representation of anticipated rewards and optimal work cost investment in hippocampus – striatum – optic tectum

Toshiya Matsushima, Animal Behavior and Intelligence, Department of Biology, Faculty of Science, Hokkaido University

Abstract—Do animals have mind? Do non-mammalian vertebrate animals in particular have mental processes similar to ours? The issue of “animal mind” has long been unchallenged simply because it was ill-defined. Recent progresses in behavioral studies in birds, however, revealed that they have cognitive process analogous to ours. In this report, we will show data obtained from a series of experimental psychological studies using chicks of domestic chickens as subjects. Bio-psychological studies revealed; (1) Optimal patch-use model in behavioral ecology was reproduced in the form of laboratory behavioral tasks. The patch stay time followed the matching law, in contrast to those found in binary choices based on anticipated profitability. (2) Optimal diet menu model was also mimicked in the form of binary choices between a small-immediate food item and a large-delayed food item. The degree of impulsiveness was given by the ratio of chicks choices of the former (immediate) food among total trials available. The choices proved to be context dependent, and the choices turned out to be more impulsive when the proximity of food item varied and had to be anticipated at the time of making choices. (3) The assumption of “omniscient forager” is unrealistic for most of natural foragers; instead, the amount (therefore the profitability) of anticipated food items varies making it a risky choice. In binary choice between an amount-varying feeder (risky feeder) and an amount-invariant feeder (non-risky feeder), chicks consistently preferred the non-risky alternative. From these series of studies, it is concluded: i) Foraging choices follow a complex evaluation function with multiple factors such as amount, delay, consumption cost, and risk. ii) These multiple factors are dissociable in different regions in the brain. iii) The foraging choices do not necessarily maximize the gain rate, thus violating the economical rationality.

I. INTRODUCTION

RECENT progress in behavioral studies of birds suggested that they have cognitive processes analogous to ours, humans [1]. Pepperberg [2] reported that African Grey Parrots are able to manipulate vocal labeling for communication with human. Clayton [3] has studied food storing behaviors and assumed that blue jays (corvids in general) could have episodic-like memory. Furthermore, Emery [4] has suggested that jays organize their behaviors based on assumption of other individuals' cognitive process, indicative of “theory of mind” in birds. All these cases were

Toshiya Matsushima, Department of Biology, Faculty of Science, Hokkaido University (corresponding author), phone & fax: +81-11-706-3523; e-mail:matusima@mail.sci.hokudai.ac.jp).

successful in showing that the birds have cognitive processes similar to primates. Does it mean that they have “mind” that is identical to ours?

This issue of the animal mind is however, terribly ill-defined, simply because many topics and concepts still remain highly ambiguous; without specifying human mind, for example, we are unable to precisely argue the “similarity” to ours. It is also highly controversial whether elementary brain processes in animals (and humans) mind process can be categorized in the same fashion. Purely materialistic approaches have limited applicability to the issue of mind.

In this report, I will introduce some of the experimental psychology of domestic chicks as subjects. The idea is that the ecological backgrounds of foraging choice can be related to the neural bases and cognitive processes. Through viewing the issue in both ecology and neuroscience, we will be prepared to discuss the issue of animal mind (or evolution of intelligence) with minimal assumptions.

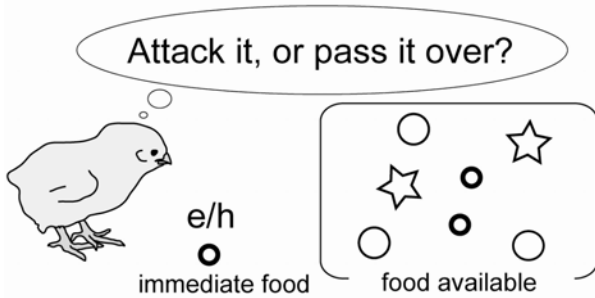
Accompanying phenomenal convergence of dynamics, a given equation often yields a diverging spectrum of solutions. Neuroscience has been a powerful tool, because we could omit and disregards solutions that were physiologically unrealistic. Similarly, through filtering the possible solutions by ecological / evolutionary realisms, we will be given additional constraints, thus making our arguments on animal minds highly practical (less imaginary) than it used to be. The present series of study thus aims at the foundation of neuro-ecology.

II. OPTIMAL FORAGING THEORY

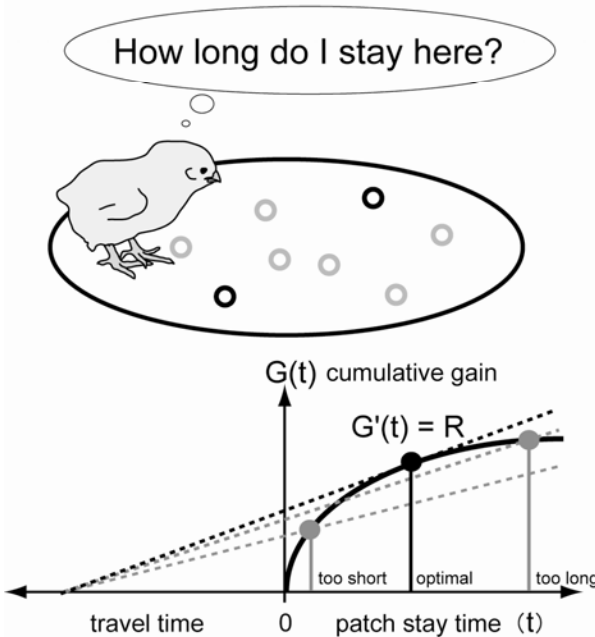
Based on insect behaviors, Charnov [5] proposed two classical models for foraging behaviors based on foraging behaviors, both of which are quantitatively formulated and are highly sensitive to experimental verifications; they are, optimal diet menu model (or optimal prey menu model) and optimal patch use model (or optimal patch stay time model). Both of these two models are organized based on an assumption that rational decision makers adopt the optimization strategy, so that subjective gain rate (in the long term) should be maximized after each microscopic actions. In other words, the theory tried to formulate decisions that subsequently lead the animal to maximize the long-term gain. In both of these models, the point is how do animals have to

do with the lost opportunity, the possible gain that was lost by making a choice. No one can take two exclusive options in foraging choices. One takes an option and gives up another. The question is whether the immediate one could give rise to a better consequence than the other, or the lost opportunity.

A Optimal Diet Menu Model



B Optimal Patch-use Model



Let us assume a forager in an environment (space), in which food of several different types is randomly scattered. The omniscient forager (single individual in the environment) knows the gain and the handling time for each type of the food. However, the encounter is randomized, and the subject forager does not know what type of food the subject will encounter next, and when. Decision to attack it will give rise to a certain gain at the expense to the lost opportunity, in which the handling time was invested to further searching food, yielding a possibly better food item.

The situation the forager faces in natural condition is actually much more complicated. Food items are often

scattered in a patchy fashion. In between food patches, the forager must move, searching for a new patch of food. The point is that the subject must invest locomotor work cost in a situation where no immediate food reward was available. Once the subject encountered a patch, it will stay there and start to collect the food items. Initially, the gain rate will be very high, because the patch is fresh and filled with a certain amount of food. Subsequently, however, the density of food items gradually decrease as the subject forage, making the gain rate (instantaneous gain rate) monotonically decreasing. What if the forager stayed until the patch is exhausted? Does this strategy optimal? The answer is definitely “no.” Optimal forager must leave the patch on the way, much early before the food is exhausted. At certain point of time in the stay time, the lost opportunity (the gain available in the next patch) will exceed the immediate gain, making the move-out from the food patch an economically rational action, even though the patch still contains some food. The law of “diminishing return” hold true in animal economics as in ours.

Ecological and ethological studies in insects, birds and fish revealed that these two models are realistic, as they are powerful in predicting some of the foraging behaviors [6]. The molar properties of foraging behaviors follow general rules irrespective of the species, and the rule of long-term gain maximization hold true. What behavioral actions and cognitive processes at the molecular level are thus responsible? Are these molecular phenomena uniquely determined under the optimal strategy?

III. CHOICE THEORY

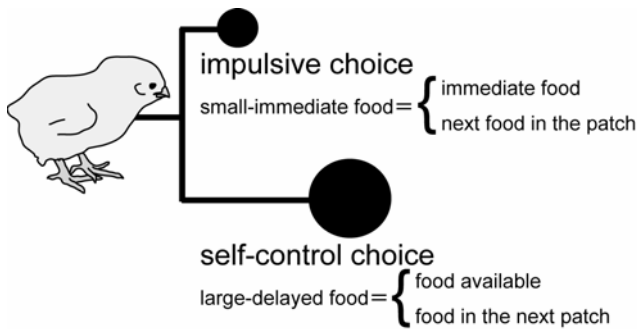
Birds do not learn aerodynamics in order to fly. Similarly, economical decision makers do not need to learn economics in order to achieve the optimal foraging. The point is whether the action at its microscopic level leads to the long-term gain, what-so-ever the immediate consequence is.

It should be noted that the foragers face a binary choice, namely, choices between “small-but-immediate reward” (immediate food or the food available within reach) and “large-but-delayed food” (lost opportunity). In psychological framework for human behaviors, the former is assumed to be *impulsive*, while the latter is *self-control*. At least in human society, we have a social agreement that the self-control choice is a matured alternative and the impulsive choice is to be hatred violation of rules.

When viewed from the ecological standpoint, however, it does not hold true. Actually, in many situations, foraging animals show a strong level of impulsiveness in their choices, suggesting that the distance (as a spatial factor) or delay (a temporal factor) is a critical factor. Why?

Under natural condition, in contrast to our human society, the immediate food is available for a limited short period of time. The food item may move away, or captured by other conspecific individuals, thus making the value only short-term lasting. Definitely, the prey items are living

organisms that must survive to reproduce, so that they develop counter-predatory strategy against the foragers. In such situation, the impulsive choice makers can maximize the long-term gain rate. It is therefore possible to claim that the adaptive behaviors in choice situation are achieved when the level of impulsiveness is appropriately adjusted, instead of being highly self-controlled.



IV. CONTEXT AND RISK

Our previous experimental analyses (localized brain lesion and single neuron recording experiments) have suggested that various aspects of food rewards such as amount, delay (or inverse of spatio-temporal proximity; distance or delay time for food delivery), and consumption time (or work cost for handling food) are separable, so that the neural representations in brain are discrete [7-10]. In other words, the optimal foraging theory is *homologous* to the choice theory in that they are formulating the same issue in different terminology. In both cases, the situations that the subjects face are strongly simplified. However, in naturally occurring situations, the spatio-temporal distribution of food items is not fixated, but is varied in every instance, leading to that the amount, delay and cost are only probabilistically given. In the following, we will see how chicks do for the variation.

Subjective value of food reward decreases when the amount is small. Devaluation occurs also when the food delivery is delayed. Animals thus try to find significant cues that could signal the *presence*, the *amount* and the *proximity* of food items. With its economical consequences kept identical, we can arrange two cognitively distinct choice situations; *i.e.*, a situation where the amount varied and is anticipated by the immediate cues, and a situation where the proximity varies and anticipated. In the former situation, the chicks learned to associate the colored beads with the distance of fixed amount of food items in fixed feeders. Chicks thus made choices based on the recalled association between cue colors and the associated food amount. In this condition, the chicks showed considerable degree of self-control, or disregarded the discount of food items by

distance. On the other hand, when the proximity of food items (distance between the choice to the feeders) varied, but signaled by color cues, the chicks made choices based more on the proximity, while the food amount was somehow disregarded. These results indicate that the choice is context dependent, and the context can be made explicit in terms of the concerns the subjects have in choices, or the factor that varies and is anticipated.

What comes out if the food amount varied but not anticipated? In the next step of study, a situation was set so that the amount varied at every trial but was not signaled by any cues. The choice was in between two alternative feeders, the expected gain rate was set identical; the economically rational decision makers would have chosen these two alternatives equally, at 50-to-50%. However, the chicks consistently showed an aversion to the varying feeder; e.g., a feeder with 0 or 10 pellets of food (5 pellets expected) was balanced with another feeder with 2.8-3.2 pellets of food. This suggest that the subjective value follows a skewed function (non-linear function) of subjective value, as could have been assumed from the Weber's law. The second derivative of the subjective value against the objective value (food amount) could thus be given as a logarithm, and the function being shaped in convex.

These results confirm the idea that the foraging choice in domestic chicks, even after a long history of domestication, remains highly cognitive. As the organizing principle of behaviors, however, the optimal foraging theory gives only a partial account, with their choices being highly context-dependent. Clearly, the chick choices deviate from gain rate maximization. One of the possible interpretations may be to state that "chicks do not live *solely* on breads," or chicks have some hidden fitness that makes the choices deviated from the caloric (energetic) gain maximization. Alternative idea is to state that "Darwinian fitness is an incomplete account of behaviors," or chicks follow totally different logic in their decisions.

V. CONCLUSION

1. Foraging choice follow evaluation function composed of multiple factors, such as amount, delay, cost and risk of anticipated food reward.
2. These factors are represented separately in different regions in the brain, and values might not be singly represented as a scalar value.
3. Foraging choices do not maximize the gain rate. Optimal strategy may not uniquely give a single solution in choice situation.

REFERENCES

- [1] Watanabe, S. "Pigeon views highlight human mind." Kyoritsu-Publications, Japan, 1997.
- [2] Pepperberg, I.M. The Alex Studies. Cambridge, Massachusetts: Harvard University Press, 1999.

- [3] Clayton, N. & Dickinson, A. Episodic-like memory during cache recovery by scrub jays. *Nature*, 395, 272-274, 1998.
- [4] Emery, H.J. & Clayton, N. Effects of experience and social context on prospective caching strategies by scrub jays. *Nature*, 414, 443-446, 2001.
- [5] Charnov, E.L. Optimal foraging: the marginal value theorem. *Theoretical Population Biology*, 9, 129-136, 1976 .
- [6] Stephens, D.W. & Krebs, J.R. *Foraging Theory*. Princeton, New Jersey: Princeton University Press. 1986.
- [7] Izawa, E.I., Zachar, G., Yanagihara, S., & Matsushima, T. Localized lesion of caudal part of lobus parolfactorius caused impulsive choice in the domestic chick: evolutionarily conserved function of ventral striatum. *Journal of Neuroscience*, 23, 1894-1902, 2003.
- [8] Aoki, N., Suzuki, R., Izawa, E.-I., Csillag, A., Matsushima, T. Localized lesions of ventral striatum, but not arcopallium, enhanced impulsiveness in choices based on anticipated spatial proximity of food rewards in domestic chicks. *Behavioural Brain Research* 168, 1-12, 2006.
- [9] Izawa, E.-I., Aoki, N., Matsushima, T. Neural correlates of the proximity and quantity of anticipated food rewards in the ventral striatum of domestic chicks. *European Journal of Neuroscience*, 22, 1502-1512, 2005.
- [10] Aoki, N., Csillag, A., Matsushima, T. Localized lesions of arcopallium intermedium of the lateral forebrain affected the choice of costly food reward without impairing reward-amount discrimination in the domestic chicks. *European Journal of Neuroscience* 24, 2314-2326, 2006.

Complementarity between the feedback and feedforward mechanisms

Yasuhiro Takachi & Yasuji Sawada, Tohoku Institute of Technology

Abstract—We studied the characteristics of human hand motion in a visual tracking experiments by FFT. The feedback component has a wide spectrum typically ranging from 1 Hz and higher. The feedforward component appears with sharp peaks located at twice of the target frequency. We found the component which represents feedback mechanism decreases, while the component which is related to the feedforward mechanism increases with increasing target frequency. This complementary relation between the two mechanism was reproduced by a simple model.

1. INTRODUCTION

From a series of tracking experiments, the author has proposed “proactive control”(1,2) as the optimization strategy for the dynamic error, developed in animals through evolution. The experiment of reference(1) was done for a sinusoidal one dimensional motion. A question remained if one obtains the same results when the target moves in two or higher dimensional space. Furthermore it was left unclear why the proactive behavior appears at a frequency of the target higher than 0.3Hz. The present research was intended to clarify these questions.

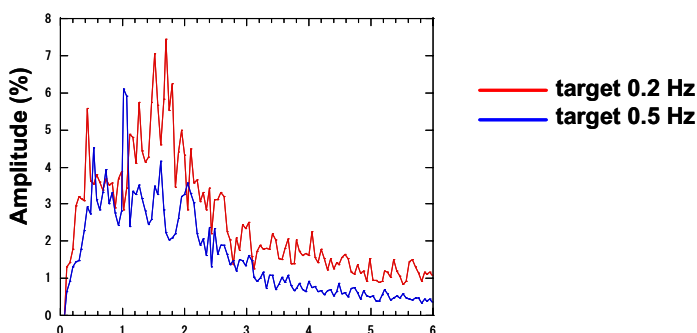


Fig.1 Fourier spectrum of the hand speed when the hand tracks a circular orbit. The abscissa is the frequency and the ordinate represent the Fourier component.

2. EXPERIMENTALS

A target moves in a circular orbit with a constant speed on a computer screen. A subject was asked to track the target as accurate as possible. The subjects are 10 healthy young men with age from 22 to 31

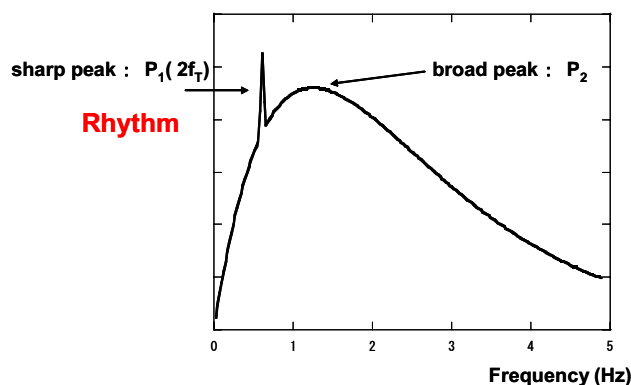


Fig.2 A schematic drawing of the power spectrum showing that it is composed of the broad spectrum and a sharp rhythmic spectrum.

A typical power spectrum is shown in Fig.1. One can see a broad peak over 1~3Hz region and a sharp rhythmic peak at $2f_T$ (twice of the target frequency). The strengths of the two components vary with the target frequency.

The global feature shown in Fig.2 is unanimous over all the subjects. The ratio of the strength of the two power obtained experimentally is shown in Fig.3

This result suggests an interesting problem: why an aperiodic component appears in hand motion when one is asked to move in a circular orbit with a constant speed.

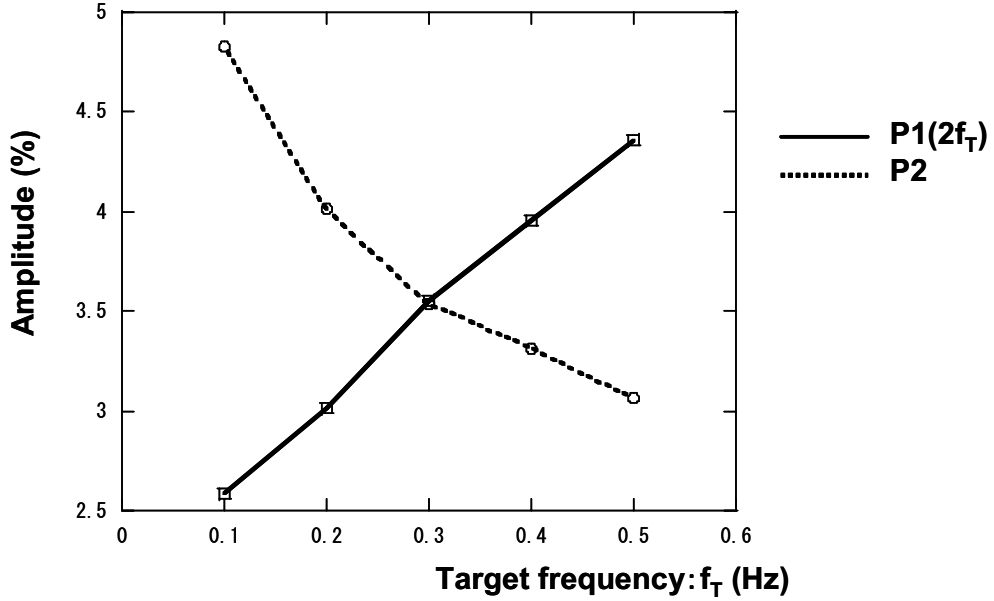


Fig 3 The experimentally observed strengthes of the spectra for the Feedback(P2) and feedforward (P1)components

3. COMPLEMENTALITY SHOWN BY A MODEL EQUATION

We write a coupled equations for the hand position $\varphi(t)$ in physical space and the hand position $\xi(t)$ in the cognitive space.

$$\frac{d\xi(t)}{dt} = \frac{\alpha(\theta_E)}{\tau_1} (\theta(t-\delta) - \varphi(t-\delta)) + (1 - \alpha(\theta_E)) \gamma \frac{d\theta(t-\delta)}{dt} \quad (3)$$

$$\frac{d\varphi(t)}{dt} = \frac{1}{\tau_2} (\xi(t-\delta) - \varphi(t)) \quad (4)$$

Where $\theta(t)$ is the target coordinate. τ_1 and τ_2 are the time constants for the visual processing and muscle motion. δ is the time delay for the visual processing. α is the effective parameter of the feedback mechanism which depends on the distance between the center of fovea and the position of the target. It was found that the departure of the fovea increases with increasing frequency of the target, and thereby

the value of α decreases with increasing target frequencies, as shown in Fig.4. Furthermore, it was found that the eye motion becomes ellipsoidal with long and short axis in the horizontal and vertical, therefore the amount of departure depends on the eye position θ_E .

The reason why the feedback mechanism becomes inefficient, and why the feedforward mechanism becomes efficient with increasing frequency of the target motion are important problems. We have obtained a preliminary data which explains these behavior by assuming a temporal switching between the two mechanisms. The detail will be reported elsewhere.

Apart from the microscopic mechanism, we obtain a similar behavior in the spectrum of the velocity of the hand motion. from the present model with some appropriate noise, as shown in Fig.4 (right)

Fig.5 shows the complementality of the two mechanisms obtained from the model, similar to the one obtained experimentally. Although this complementality is essentially reproduced by the effectiveness factor α , the result suggested that the two mechanism works together with the ratio $\alpha / 1 - \alpha$. It seems that the results strongly supports a probabilistic switching between the two mechanism with a statistical weight depending on the speed of the target.

We studied what effects this automatically created rhythmic component exerts in the mutual tracking experiments.

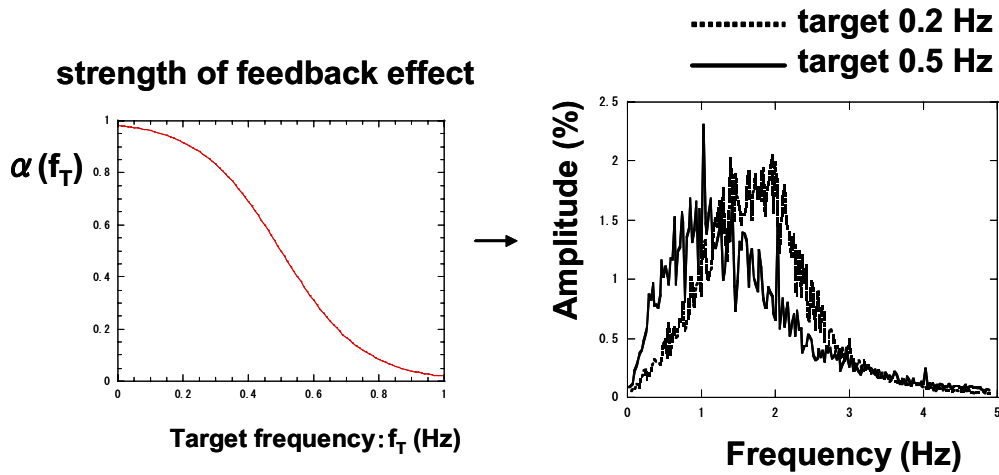


Fig.4 (Left) The strength assumed for the feedback factor as a function of the target frequency

Right) The Fourier spectrum of the hand velocity calculated by the model

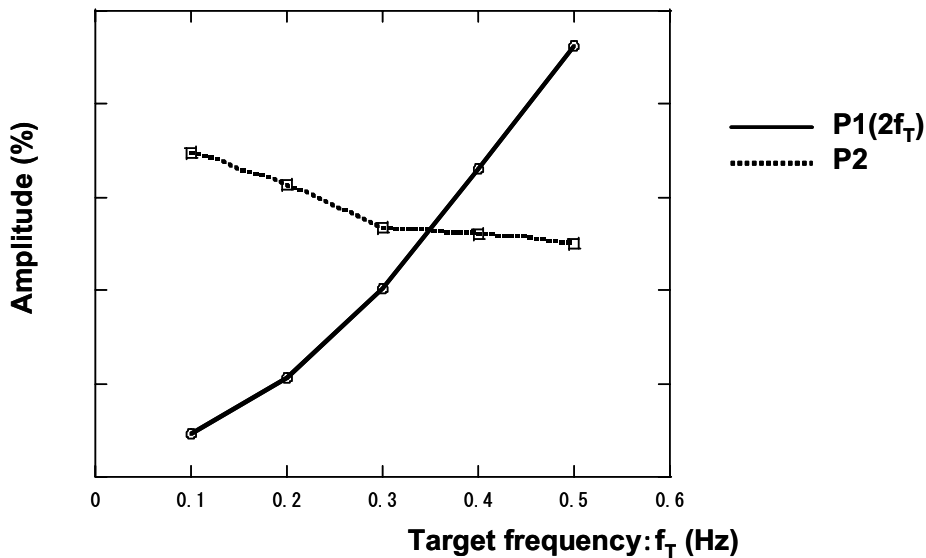


Fig.5 The strengthes of the spectra for the feedback(P2) and feedforward (P1)components calculated by the model used here.

4 . MUTUAL TRACKING AND A COMMUNICATION DYNAMICS

In the above sections we learned that a rhythmic component is created automatically without any external rhythmic stimuli at a target frequency higher than ~ 0.3 Hz.

In this section we present evidence that the rhythmic components created automatically helps the two subjects tracks each other with high correlation. Fig. 6 shows an examples of the hand speed as a function of time. Blue and green lines show the two subjects. The figures on the left and

right correspond to the case when the training frequency before the mutual tracking experiment is 0.2 Hz and 0.5 Hz

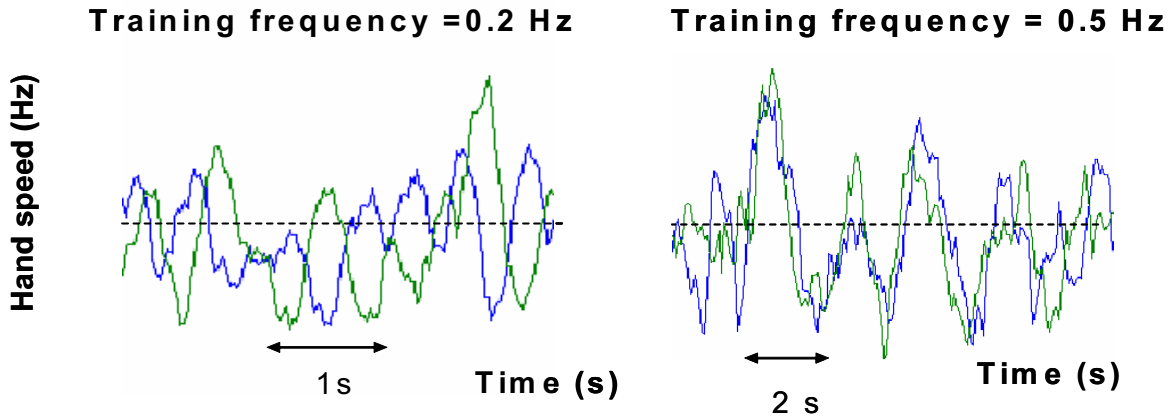


Fig.6 Examples of the time sequence of the speed of the hand motion in mutual tracking.

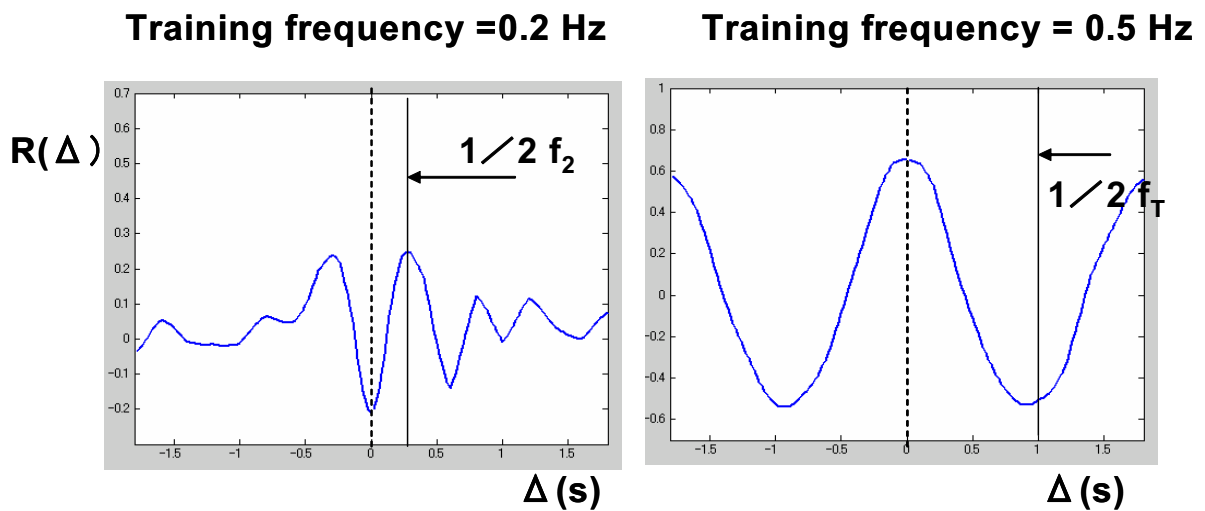


Fig.7 Correlation function between the speed of the hand motion.

The correlation of the case when training frequency is at 0.5 Hz where we know that a rhythmic component is automatically created.

6. Reference

1) F. Ishida and Y. Sawada: Human hand moves proactively to the external stimulus: An evolutionary strategy for minimizing transient error. *Physical Review Letter*, 93, 168105 (2004)

2) Yasuhiro Takachi* and Yasuji Sawada: The enhancement of proactivity in hand tracking by the discretization of visual information (refereed 2006)

Classification of Object-Shape by a Supple Finger Robot with a Tactile Sensing Array

- Tactile feature in neighborhood-information around the contact points on finger skin -

ICHIKAWA, Sumiaki* WATANABE, Kenshi* OHKUBO, Ken-ichi* HARA, Fumio*

* Tokyo University of Science

1. Introduction

It is anatomically said that there are two types in somatosensor in a human body. One is a tactile sensing of finger skin, the other is bathyesthesia in posture sense. In general, our posture image of the body will vanished in keeping bed rest, on the other hand, as soon as slightly moving the body, we can get the posture image in clear. Focusing on a tactile perception with a finger or hand sense, we almost need moving our finger, stroking or rubbing. It is said that there is close connection between getting somatosensory and moving body. From the viewpoint of anatomy, a report in cutaneous sensation of a human-body said that a stimulation input from skin surface goes to the medulla through synapse associated with reflection in a spinal cord, and it goes to primary somatosensory area through inhibitory synapse in the medulla, then, those link to making the hand feeling or the stereognostic sense. Other reports also pointed out their relationship and anatomical area, but information processing from the stimulation to the body image is still not clear.

In this research, we have a viewpoint that quick processing of environmental perception is a starting point of flexible and adaptive performance in animal behavior. As the amount of stimulation from skin sense whole the body concentrating to the central nerve is too large, it needs a rational processing mechanism for the numerous stimulation between the sensory receptor on the skin and the brain.

This research focuses on two types of adaptation in the cutaneous mechanoreceptor of the human finger, one is slowly adapting corresponding to static contacting and the other is rapidly adapting corresponding to dynamic contacting[1][2]. We are standing on the following assumption; These two types of stimulus signal from the receptors with different adapting speed will make information about spatial and temporal coding in the brain or in the neural circuit before the brain, it then contribute to the higher brain function and quick adaptive behavior. Under the assumption, the spatial information of the stimulus signal is not so important. The frequency of analogical contacting situation between skin and an object is treated, that is, important things are feature at very local area around the receptive field of the mechanoreceptor on the skin.

Based on the assumption, we manufactured a supple finger robot with tactile sensor array and evaluated the performance of its classification accuracy for the object shape by the statistical method which depends on the frequency of local feature with temporal and spatial infor-

mation. We have a policy that what is able to classify means what is used in the classification has enough information to classify. We show discussion about relationship between cutaneous sensation and tactile feature of neighborhood contacting information.

The classification of an object shape by a robot hand or finger was researched in the robotics. They were almost using spatial position information of the tactile contact point and the angle of finger links[3][4][5]. In this research, we think the information which can obtained by biological method is different from such engineering measurement.

2. Data processing of contact state

Our manufactured supple finger robot consists of five links those are related to human fingers such as forefinger, palm and thumb (Fig. 1). The size and mass of each link is shown in Table 1. The ratio of the size among five links is corresponding to that of a human finger. To pull a wire connecting to the top of the robot finger the finger links being to grasp an object. It just modeled to a muscle grasping a finger. At first, first link begins to bend, next, the second link begins to bend, finally the third link begin to bent, it is along the mechanical balance.

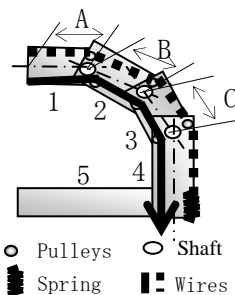


Fig.1 Finger-type link model

Table 1 Dimension and mass of the links

| | Dimension[mm] | Mass[kg] |
|---|---------------|----------|
| 1 | 80 x 30 x 40 | 0.12 |
| 2 | 135 x 30 x 40 | 0.2 |
| 3 | 150 x 30 x 40 | 0.26 |
| 4 | 225 x 30 x 40 | 0.47 |
| 5 | 165 x 30 x 40 | 0.33 |
| A | 65 | - |
| B | 105 | - |
| C | 120 | - |

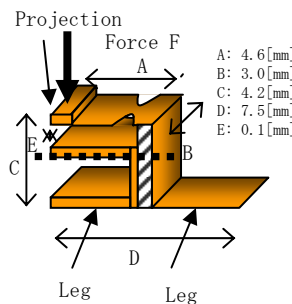


Fig.2 Structure of a mechanical Projection

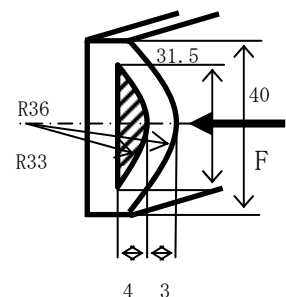


Fig.3 Sectional view of a touch-sensor switch (Complisemi-circular soft silicone base; Comp.=0.004[m/N])

2.1 Mechanical sensor on robot skin

The robot finger is made of silicon and has a round arch as a cross-sectional shape which is in mid with a shape and a suppleness of a human finger (Fig.3). A number of contact switch sensors (Fig.2) are arranged on the surface of the robot finger skin. When a point, "Projection" shown in Fig. 2, is press by contacting force, the switch sensor becomes "on". The switches are put on the round arch at 10 mm intervals in the long direction of the finger link, and at 7 mm intervals in the across direction. The number of the switches on each link is, from the top finger link, 35, 35, 45 and 75 respectively. The total number of the switches with 5 lows and 47 columns is 235. The number of "on" switch in each 5 lows means the level of the contact force. That is, the number of "on" switch is one at a beginning of contacting to an object then the number is in increase in accelerating the contact force, because the cross-sectional shape is a round arch and the silicon finger is with suppleness. The number of the switches is corresponding to the area size of contacting region.

Fig. 4 (a) shows panoramic view of the finger links with a number of contact switches from the top finger link. In Fig. (b) a circular cylinder is grasped by finger robot.



Fig. 4 Finger-type link equipped with soft tactile sensors (a) and the state of object-grasping (b)

2.2 Capturing the contact data

A tension wire contacting the top of finger links winded up at a constant speed. The robo finger slowly moves to the end of its movable range for 12.5 second. The movement duration is represented in 250 steps for sampling data. Then, the sampling rate is 0.05 second. The states of switches are shown in time-series data for the 250 steps.

A contact switch has two states. One is "on" represented in 1, the other is "off" in 0. The number of data at every time step is 235 because of 5 lows and 47 columns. To accumulate the switch sates among the 5 lows in each columns the 5 x 47 data is represented in 47 columns data with contact force level. Finally, the total contact data is a two dimensional map with 47 columns long and 250 steps wide. The two dimensional contact map include two index, that is, the direction of columns shows spatial and the direction of time step shows temporal.

2.3 Characteristic vector by 8-neighborhood cells

Here, a point of a single value in the contact data with 47 x 250 is called "cell". The value of each cell is representing the degree of the contact force in 5 levels. As a beginning of this research, the 5 levels of the contact

force are reduced to 2 levels, that is, contacting or not contacting. Focusing on the "on" cell with above 1 degree of contact force and 8-neighborhood cells around the "on" cell (**Fig. 5**), the 8-neighborhood cells are represented in specific pattern with 256 varieties. Here, symmetric specific-patterns in spatial direction are regarded as identical pattern. In Fig. 5 the 6 patterns of middles with 2 columns, named p1, p2 and p3, are examples of the symmetric specific-pattern. Then, the number of varieties is reducing 256 varieties into 144 varieties. Here, the reduced patterns with 144 varieties are called with characteristic pattern p_i ($i = 1 - 144$).

The 144-dimensional vector represented by the frequency of the p_i in the contact data, which is obtained through grasping an object, shows a specific value strongly relating to the grasped object shape. It is called with characteristic vector, here.

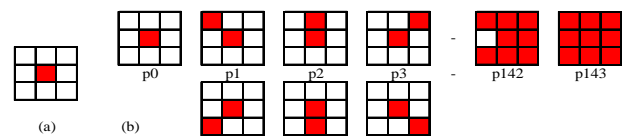


Fig. 5 8-cells pattern (a), and example of 144 contracted patterns (b)

2.4 Representation in lower dimensional characteristic vector

The characteristic vector consists of p_i with 144 varieties. But, all of the p_i are not always needed. It is though that some p_i are not counted in a grasping and that some p_i have very little contribution for classification from the statistical viewpoint. The principal component analysis method applies on the p_i that are sampled for some object shapes. The p_i are ranked by the contribute rate of the components and the absolute characteristic value in the component. New characteristic vector is made by some of the ranked p_i . The count of selected p_i means the degree of the dimension in the new characteristic vector. When the count of p_i is limited to low number it means the new characteristic vector consists of low dimension.

To evaluate the degree of separation among the characteristic vectors of each object in that vector space, we conduct discrimination analysis using the Mahalanobis distance to calculate classification accuracy.

3. Experiment of shape classification

3.1 Convex polygonal objects

Experiments are carried out with 12 varieties of shapes. The objects can be enough grasped by the finger robot. That is, one is a circular, SC, with 100 mm in diameter, the others are 11 varieties of polygon inscribed in a circle with 100 mm in diameter, S3, S4, S5, S6, S8, S10, S12, S15, S18, S20 and S24. The suffix number for 3 to 20 means the number of sides of the convex polygon.

3.2 Identification class and positional convergence

In a few times of grasping, an object, which was ini-

tially placed at random location, the final location and position of the object was converged into some specific position and location. The numbers of them are 1 piece in SC, 2 pieces in S3, 1 piece in S4, 2 pieces in S5 and 1 piece in S6, respectively. The polygons for S8 to S24 have no discriminable convergence position and location.

In this research each discriminable position and location of convergence is treated as a class of identification. Basically, the name of the class are called the object name. In the case of the multi-convergence, they are called with extra suffix number such as S#-1 or S#-2. They were 14 classes (SC, S3-1, S3-2, S4, S5-1, S5-2, S6, S8, S10, S12, S15, S18, S20 and S24) for 12 types of object shape from experimental results.

3.3 Results of classification

In the experiments, with respect to each object shape, the object are initially placed with the convergence position and location by pre-grasping of itself. Table 3 shows the results of the principal component analysis for the 14 classes. This shows for the 5th components in order of the major value in the contribution ratio. The cumulative contribution ratio was 0.9999 until the 5th components. The pi are selected by major ranked pi with respect to the absolute value of the contribution factor among elements of the component vector. The absolute value is above 0.3. The major ranked pi in the 5th components are 12 pieces,

Table 3 Results of PCA for selecting dominant patterns for S objects (Main coefficients of eigenvectors of principal components)

| P.C. | 1st | 2nd | 3rd | 4th | 5th |
|--------------------------------|------------|-----------|------------------------|--|--|
| Patterns and Their Coefficient | p143 0.945 | p91 0.926 | p21 0.909 p91 0.349 | p53 0.524 p122 0.391 p138 0.391 p55 0.367 p140 0.308 | p62 0.510 p51 0.484 p67 0.317 p36 0.305 |
| A.Proportion | 0.6147 | 0.9102 | 0.9997 | 0.9998 | 0.9999 |

Fig. 6 Dominant patterns for S objects

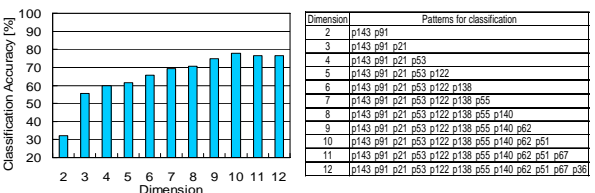


Fig. 7 Classification accuracy of dimensional characteristic about S objects

Table 4 Classification results at 10-dimensional vector space for S objects

| | S3-1 | S3-2 | S4 | S5-1 | S5-2 | S6 | S8 | S10 | S12 | S15 | S18 | S20 | S24 | SC | N.A. | A.R. | C.A.(%) |
|------|------|------|----|------|------|----|----|-----|-----|-----|-----|-----|-----|----|------|------|---------|
| S3-1 | 8 | | | | | | 3 | | | | | | | | | | 80 |
| S3-2 | | 10 | | | | | | | | | | | | | | | 100 |
| S4 | | | 10 | | | | | | | | | | | | | | 100 |
| S5-1 | | | | 10 | | | | | | | | | | | | | 100 |
| S5-2 | | | | | 10 | | | | | | | | | | | | 100 |
| S6 | | | | | | 10 | | | | | | | | | | | 100 |
| S8 | | | | | | | 10 | | | | | | | | | | 100 |
| S10 | | | | | | | 1 | 9 | | | | | | | | | 90 |
| S12 | | | | | | | 1 | 1 | 7 | 1 | | | | | | | 70 |
| S15 | | | | | | | 1 | 5 | | 5 | | | | | | | 50 |
| S18 | | | | | | | 1 | 3 | | 2 | 4 | | | | | | 40 |
| S20 | | | | | | | 1 | 1 | | 1 | 6 | 1 | | | | | 40 |
| S24 | | | | | | | 2 | | 3 | | 1 | 4 | | | | | 60 |
| SC | | | | | | | 3 | | | 1 | | | 6 | | | | 60 |

p143, p91, p21, p53, p122, p138, p55, p140, p62, p51 and p67. These characteristic pattern pi are shown in Fig. 6.

The number of elemental pieces including the characteristic vector of pi , that is dimension number of the characteristic vector, is increasing from 2 to 12. The order to increase is along the order in Fig. 6. The results of classifying accuracy for the 14 classes by the characteristic vector with respect to the dimension number. The left graph in Fig. 7 shows the classification accuracy to the dimension number of the characteristic vector. The right table shows included pi to the dimension number.

It is inclined to increasing the accuracy for increasing the dimension number. The increasing degree between 2-dimension and 3-dimension is larger, that is 30% to 55%. After the 3-dimension to the 10-dimension the accuracy is slightly increasing into 75% and then, it is in saturation. Table 4 shows the cross-tabulation table for the classification with the 10-dimensional vector. The classes of test objects show in portrait orientation, and the classification classes show in landscape orientation. The numbers in the table mean the number of the objects classified to the class. AR in column shows the accuracy in percentage. The accuracy for S3 to S8 are almost 100%. But the other object classes are in low degree. The object in class S8 is 100% in the accuracy, but the other objects in the classes, S10, S12, S18, S20 and SC, are also classified to S8 in same cases as mistake. Such cases of mistake classification are frequently shown in the area right and bottom corner in the table. The classes in mutual mistake are almost without the convergence position and location.

4. Discussion

4.1 Classification accuracy among 7 classes with positional convergence

Almost all of mistakes were seen in the classes without convergence position and location. Classifying experiments and the principal component analysis for them are carried out anew within the 7 classes with positional convergence. The classes in experiments are SC, S3-1, S3-2, S4, S5-1, S5-2 and S6. As the results, the cumulative contribution ratio within the 6th components is 0.9999 and the major ranked pi are 14 pieces, p143, p91, p21, p53, p138, p122, p51, p55, p129, p140, p4, p62, p36 and p67. The classification results with these new pi shows that the accuracy is 90% with only 3-dimension, and is almost 100% with 6-dimension.

4.2 Implication of characteristic pattern

From viewpoint of dynamical implication, the pi are grouped in 4 types with respect to temporal change of contacting. They are “start”, “continuation”, “increase” and “decrease”. The 4 groups of pi in the section 4.1 are shown in Fig. 8. For implementing this grouping manner to the results shown in Fig. 6, The “continuation” is top of three pi , those are the most significant factor of these component vectors, and is the dominant group of pi in the classification. The 3 pi can be grouped into 3 kinds further. These are p143 in persistent contact, p91 in edge contact and p21 in point contact. Adding p21, the point

contact, the accuracy is increasing above 50 %, and adding the “increase” group then increasing more. It is shown that the groups, “continuation” and “increase”, are significant types of the groups.

| Type | Dominant patterns | | | | |
|--------------|---|---|---|--|--|
| Continuation |  p143 |  p91 |  p21 | | |
| Increase |  p53 |  p138 |  p122 |  p51 |  p62 |
| Decrease |  p55 |  p129 |  p140 |  p36 |  p67 |
| Start |  p4 | | | | |

Fig. 8 Pattern types segmented by contact dynamics

4.3 Relationship among 7 classes with positional convergence

With respect to the 7 classes with positional convergence Fig. 9 graphically shows the frequency and the standard deviation of each p_i , which is the significant 6 p_i (p143, p91, p21, p53, p138, p122) in the characteristic vector. The solid hexagonal polygon shows the frequency and the outline around the polygon shows the standard deviation. Here, the scaling factor of p143, p91 and p21, they are grouped within “continuation” is 1/100 to the other scale of p_i .

The shapes of the polygons are enough different each other to look them. It is corresponding to statistical properties. On the other hand, looking at the outline, which means the standard deviation, it is very narrow and then is shows enough reproducibility of classification in each class.

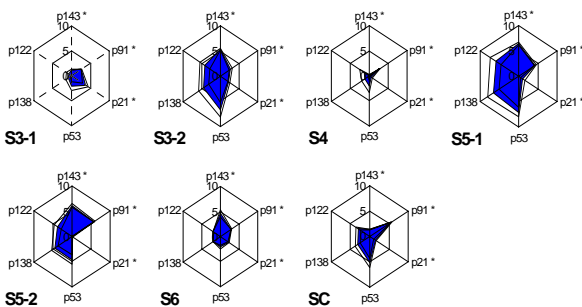


Fig. 9 Averages and standard deviations of feature vectors for 7 classes (* : Their frequencies are adjusted to 1/100.)

4.4 Relationship among 7 classes in frequent mistakes

Focusing on the 7 classes, which have mistake in classification shown in Table 4, that is with respect to S8, S10, S12, S15, S18, S20 and S24, graphical results, which are equivalent to the manner in section 4.3, are shown in Fig.10. The shapes of the polygons in Fig. 10 are similar

to each other comparing to the results of Fig.9. It is corresponding to the mutual mistakes of classification among the objects without positional convergence in Table 4.

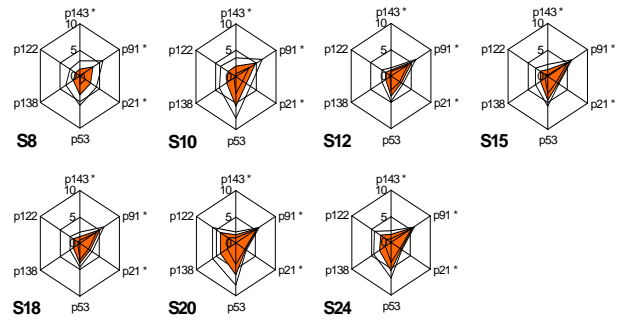


Fig. 10 Averages and standard deviations of feature vectors for error classes (* : Their frequencies are adjusted to 1/100.)

5. Conclusions

This research focused on two types of adaptation in the cutaneous mechanoreceptor of the human finger. One is concerning to temporal feature and the other is to spatial one. With respect to process in cutaneous sensation of a human finger, the assumption was given that stimulation signals from the mechanoreceptor were simplified into frequency data with temporal and spatial information. The 8-neighborhood data pattern represents temporal and spatial feature around contacting point on the skin. A characteristic vector is made of the frequency of the pattern in the whole skin. From viewpoint of engineering the statistical work was carried out to investigate the classification accuracy.

As the results, the three significant characteristic patterns can enough classify the polygonal shapes with 3 edges to 8 edges. Looking at the significant characteristic pattern, the most significant pattern among them is continuation type. The next significant pattern is the type of increase. The dominant feature of the shape to classify is the density of the polygonal edge represented in number of edge. The mutual mistakes of classification are frequently seen in above 8 edges of the polygon. It is visually shown by comparing between good classifying class and frequent mistaking class.

The experimental result show that the polygons within 6 edges are enough classified by the frequency of characteristic pattern on the skin. In the future work, softness of the object feature will be investigated by this analysis.

References

- [1] Iwamura, “ヒト触覚受容器の構造と特性”, journal of RSJ, Vol.2, No.5, pp. 438-444, 1984.
- [2] Maeno, “ヒト指腹部と触覚受容器の構造と機能”, journal of RSJ, Vol.18, No.6, pp. 772-775, 2000.
- [3] Kinoshita, “人工触覚による対象物体の特徴抽出”, journal of the Society of Instrument and Control Engineers, Vol.14, No.1, pp. 90-96, 1978.
- [4] Okada, “つかみによる物体認識”, bulletin of the electrotechnical Laboratory, Vol.40, No.9, pp. 733-747, 1976.
- [5] Kudoh, Satoh, Takada, “感覚器官を持った人工の指による物体の認識”, journal of the Society of Instrument and Control Engineers, Vol.10, No.3, pp. 378-384, 1974.

Mirror neuron system related to bodily self

Murata A and Ishida H., Department of Physiology, Kinki University School of Medicine

Abstract— We will discuss neurophysiological mechanisms of bodily self and others distinction in the parieto-premotor network. Integration of efference copy and sensory feedback is an essential factor for agency recognition. The parietal cortex may have a crucial role for these mechanisms. We also discuss shared representation of self and others in the brain.

I. INTRODUCTION

THE body is not separable from action control. Recently, it is claimed that the body representation is also important for the social cognitive function, like communication, imitation, and/or theory of mind. In this process, self and other should be represented in the brain on the basis of the body. Self consciousness is based on the corporeal awareness. There are two components in bodily self-recognition. One is ownership of one's own body parts in the sense that one's body parts belongs to the self. The other one is the sense of agency of action, in which an executed action is recognized as being generated by one's own body parts. Although there are many definitions, we think that corporeal awareness involves internal representation about the spatiotemporal dynamic organization of one's own body that is constructed by the processes of the consciousness of the body. As we will discuss later, interaction between intrinsic motor signal (efference copy) and sensory feedback contributes to both motor control and corporeal awareness (Fig 1). Accordingly, we suggest that the process of corporeal awareness share components with the sensory motor control system in the parieto-premotor network.

Further, in the social cognitive function such as imitation, communication or theory of mind, it is necessary to recognize other's action. This function is considered to be involved in

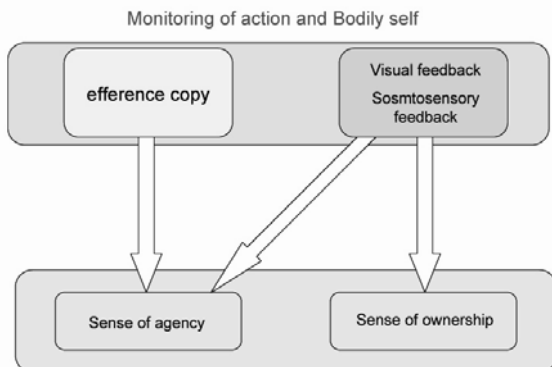


Fig.1

mirror neuron system. For this function, representation of other's body should exist in the brain. In this paper we report our studies how the brain represents own body and others.

II. BRAIN NETWORK FOR GRASPING OBJECTS

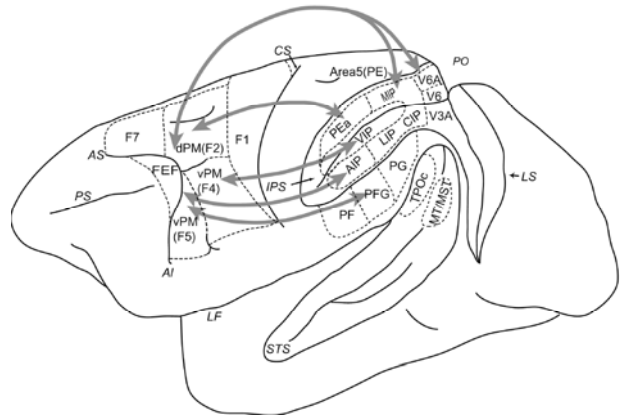


Fig.2 parieto-premotor networks (with permission of IEICE, ref [24])

A behavioral experiment revealed that visual properties of 3D objects had an important role for hand manipulation [1]. The parietal and premotor cortices have strong anatomical connections with each other. As shown in Figure 2, there are several parallel pathways between the parietal and premotor cortices [10]. Recent physiological studies have revealed that these parallel pathways have different roles, such as arm reaching and/or hand grasping, along with corporeal awareness. Especially, it is well known that network between parietal area AIP and ventral premotor cortex (F5) has predominant roles for distal hand movements. Neurons in both of these areas were active during grasping objects, namely hand manipulation neurons. Furthermore, some of these neurons showed activity mainly related to motor signals and/or visual response during fixation on the objects to be grasped [2][4].

As concerned to hand manipulation neurons area AIP, it was revealed that visual response for the objects was selective for 3D properties of the objects (shape, size and /or orientation) by Murata et al [2]. This visual response was also found in the neurons that showed motor component, because of activity during grasping movements in visually occluded condition. These results suggested that area AIP was involved in matching 3D visual properties and motor components. Furthermore, grasping related activity in F5 was found by Rizzolatti's group. Activity of these neurons showed

selectivity for the type of hand movement, such of precision grip, finger prehension, and whole hand grasping [3]. They coined the term “motor vocabulary” for these different types of movements. Functional properties of neurons in this area were similar to those of AIP [2] [4]. A group of grasping-related neurons in F5 was activated when the monkey fixated on the objects to be grasped [29].

However, there are also differences in the functional properties of neurons between AIP and F5. Activity during fixation on the objects in F5 was rather selective for hand configuration during grasping objects than visual properties of the objects. Furthermore, neurons in F5 showed sustained activity (so-called set-related activity) preceding the hand movement after the object presentation. This may reflect the process of visuo-motor transformation before execution of a particular movement. This set-related activity was less common in AIP neurons than in F5 neurons [23]. F5 receives visual information about three-dimensional objects, such as shape, orientation, and size from AIP. In F5, the motor program or motor pattern that is appropriate for presented objects is selected. This motor information is then sent to the primary motor area [5]. At the same time, this copy of motor representation, i.e. the efference copy, is returned to AIP to be matched with the visual object representation [23]. The results also reflected computational modeling of affordance learning [26].

III. SENSORY FEEDBACK AND CORPOREAL AWARENESS

In the sensory-motor control, sensory feedback is also an important component. The parietal association cortex stands very important position for feedback control, because the area receives both visual and somatosensory inputs. Many of the grasping neurons in AIP have strong visual properties, showing less activation in the dark than in than light. Some of these visual neurons did not respond to the view of the objects, suggesting sensitivity to the particular visual hand configuration during grasping [2]. The hypothesis is that the area may be concerned with the monitoring of ongoing hand movement. To test this hypothesis, we recorded single cell activity from PFG and AIP of the monkey while it performed the hand manipulation task and the fixation task with the guidance of a spotlight on a monitor screen. In the hand manipulation task, the monkey could not see its own hand as well as an object to be grasped directly, but their images were presented on a screen using a video camera. The monkey was required to reach and grasp the object while watching the screen. In the fixation task, the monkey was required to fixate on the screen and we presented movies of the monkey’s own hand movement. We found that some neurons related to the hand manipulation task in both AIP and PFG responded to the movie of the monkey’s own hand movement (hand-type neurons) [10]. Many of these visual neurons (hand-type) did not show much activity during fixation on the objects. For example, a neuron recorded from PFG showed activity during

manipulation both in the light and in the dark. This neuron responded to the movie of the monkey’s own hand holding an object. The neuron remained active when we erased the image of the object from the movie, and thus the response could be considered as responding to the configuration of hand movement. As we discussed in the previous section, the motor-related activity might reflect an efference copy that might have originated from the ventral premotor cortex F5. We consider that a comparator in AIP and/or PFG has a crucial role for distinction between own body and other’s by matching the efference copy with visual feedback.

In PFG, Rizzolatti’s group found the mirror neurons that were originally found in the F5 [16]. These neurons were activated during execution of hand or mouth action and also during observation of the same action made by another individual. The functions of these neurons were designated in terms of the human cognition, for example, “action recognition”, “theory of mind”, “origin of language”, “imitation”, and “empathy”. A recent study revealed that mirror neurons in PFG contributed to recognition of observed motor acts and prediction of what will be the next motor act of the complete action, that is, understanding the intentions of the agent’s action [25].

Because the mirror neurons were included in the visuo-motor control system, we need to discuss their functional role with respect to the motor control. These neurons respond to the image of action. We postulated that the function of the mirror neuron to be the monitoring of self-generated action. To study if the hand-type neurons in PFG or AIP have properties of mirror neurons, we studied activity of the neurons during watching a movie of hand action by the experimenter. We found the hand-type of neurons in PFG responded to the movie of the experimenter’s hand [10]. These results showed that some of the mirror neurons in the inferior parietal cortex were sensitive to both the view of the monkey’s own hand action and that of others’ actions as well. We suggest that mirror neurons in PFG correlated with the monitoring of self-generated action by collaboration with F5 in the ventral premotor cortex. In the process of development of the infants, mirror neurons in the parietal cortex may be one of source of visual feedback, then the neurons associate with intrinsic motor representation. Finally, visual representation of action may trigger the motor programs in mirror neuron system.

The inferior parietal cortex also receives proprioceptive feedback. Temporal contingency of the efference copy, somatosensory feedback, and visual feedback are crucial for agency recognition [10]. In our experiment, we introduced temporal delay in the visual feedback during actual hand movement. When the monkey reached and grasped the object looking at the monitor, movement of the hand on the monitor was presented with 500ms delay. As the results, although the data was very preliminary, we found some modulation in visual response of hand-type neurons with temporally distorted visual feedback.

In the human, it was revealed that activity in the parietal cortex was modulated by temporal mismatching between visual feedback and somatosensory feedback during passive hand movement [20]. Neuropsychological and imaging experiments revealed that the inferior parietal cortex was involved in the sense of agency. Patients who had damage in the inferior parietal cortex showed difficulty in judgment of agency of hand action on the monitor screen during executing hand action [12]. It is possible that the efference copy influences sensory feedback in PFG, suggesting a contribution of PFG to self/other distinction. In conclusion, it is suggested that sensory motor control system contribute to construct body image monitoring own action [13]. Iriki et al. (1996) recorded neurons of the PEa in the anterior bank of the intraparietal sulcus of a monkey trained to use a rake to get food pellets [14]. Neurons in this area showed tactile receptive field on the hands and visual receptive fields close to the hand. Interestingly, visual receptive fields of some bimodal neurons expanded to include the rake some minutes after the monkey started retrieving food with it. This may be also results of integration among efference copy, visual feedback and somatosensory feedback.

In the computational modeling of sensory-motor control, internal model is the model for the cerebellum [23], however it is also possible to adopt the concept of internal model for the cerebral cortex. Further, the system also contributes to distinction of self and others. In the development infants, distinction between self action and other's action is the bases of imitation or communication [15]. The parietal cortex may have crucial roles in this process sharing sensory motor control system [17] [21]. Thus if the concept of internal model is adopted in the mechanism for self other distinction, the idea is expanded to the humanoid robots who acquire body consciousness or ability of imitation, further simulation of the mind.

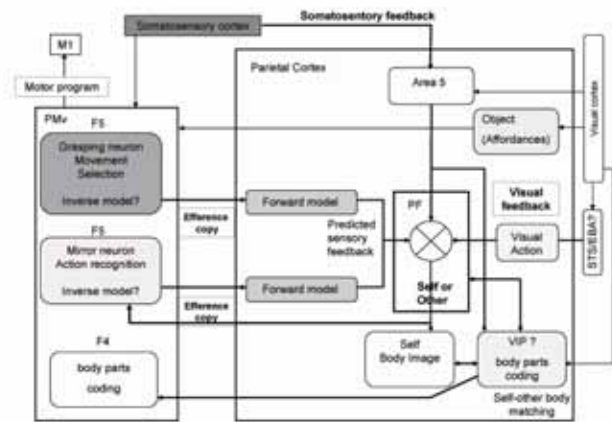
IV. REPERSENTAION OF OTHER'S BODY IN THE BRAIN

As described in the previous session, the parietal cortex and premotor cortex are much involved in self body representation. In the parietal association cortex, there are several areas where multimodal neurons are found, for example visual-tactile bimodal neurons. In these areas, properties of area VIP have been well studied. The tactile receptive fields of the neurons are usually located on the face, head or sometimes limbs and the visual receptive fields are in locations congruent with the tactile receptive fields. In many cases, the visual receptive fields are located very close to the body [18], namely in the peripersonal space. These neurons may encode body parts centered frame of reference.

On the other hand, for the recognition of others action, imitation or communication, representation of other's body is necessary in one's own brain. For moment, it is not clear how the brain represent other's body. Decety et al. suggested that self body and other's body were represented in the shared brain network [8]. Further, it was reported a female subject

for whom the observation of another person being touched was experienced as tactile stimulation on the equivalent part of own body [19].

We expect that other's body map in the brain may be influenced by own body map. As we described before, the neurons in area VIP code own body parts and peripersonal space. We studied neuronal activity in the VIP whether these neurons are related to other's body representation [22]. In this study, an experimenter confronted the monkey and we presented visual stimuli close to experimenter's body. The stimuli were just simple moving objects or scrolling on the experimenter's body by himself or third person. As the results, we found the bimodal neurons that showed receptive fields (RFs) on the monkey's body, not only on the face but also on the limbs. Some of these neurons also showed visual RFs on the experimenter's body which were congruent with RFs on the monkey's body parts in a manner of mirror image. For example in the case that vidual-tactile RFs of the monkey were on the right face, visual RF of the experimenter was on the left face. These results suggest that coding of other's body parts is in the same area that codes own body parts, and a map of self body parts is referred for recognition of other's body. In the humanoid robots, there is a problem how the system recognizes other's body. In the imitation learning, the system should superimpose other's body on one's own. Our data will provide important idea for matching system between one's own body and other's.



V. CONCLUSION

We reported our results concerning brain mechanisms of recognition bodily self and others. Basically, parietal-premotor network which is considered to be related to sensory motor control, but our results suggested that this network is also involved in sense of agency and mapping of the body. In this system, internal model may have crucial roles for matching efference copy with sensory feedback. We speculate that mirror neuron respond to visual image both of own body and others, then in the process of motor learning motor and visual signal is integrated. Finally, visual representation of action may trigger the motor programs in

mirror neuron system. This hypothesis provides important concepts for imitation learning or simulation of other's mind in the computational modeling [27]. On the other hands, it is not clear how the brain represent other's body. Our data in VIP suggests that other's body is recognized by referring to self body mapping in the manner of mirror image. This provides an important suggestion for computational modeling of imitation or recognition of other's body.

REFERENCES

- [1] Castiello U, Bonfiglioli C and Bennett K. Prehension movements and perceived object depth structure. *Percept Psychophys* 60: 662-672., 1998.
- [2] Murata A, Gallese V, Luppino G, Kaseda M and Sakata H. Selectivity for the shape, size, and orientation of objects for grasping in neurons of monkey parietal area AIP. *J Neurophysiol* 83: 2580-2601, 2000.
- [3] Rizzolatti, G., Camarda, R., Fogassi, L., Gentilucci, M., Luppino, G. and Matelli, M. Functional organization of inferior area 6 in the macaque monkey. II. Area F5 and the control of distal movements, *Exp Brain Res*, Vol.71,No.3, pp.491-507, 1988
- [4] Raos, V., Umilta, M-A., Murata, A., Fogassi, L. and Gallese V. Functional properties of grasping-related neurons in ventral premotor area F5 of the Macaque monkey. *J Neurophysiol.* 95(2).709-729, 2006
- [5] Sakata H, Taira M, Kusunoki M, Murata A and Tanaka Y. The TINS Lecture. The parietal association cortex in depth perception and visual control of hand action [see comments]. *Trends Neurosci* 20: 350-357, 1997.
- [6] Murata A. Contribution of ventral premotor cortex to hand and arm movement in the space *Shinkei Kenkyu no Shinpo* Vol. 42 No.1 49-58 1998
- [7] Murata, A. Self and others representation in the parietal cortex based on sense of body *JPS(J Psysiol Science)* Vol. 56 Suppl. S170 The proceedings of the 83rd annual meeting, 2006
- [8] Decety, J. and Sommerville, J. A. Shared representations between self and other: a social cognitive neuroscience view, *Trends Cogn Sci*, Vol.7,No.12, pp.527-533, 2003
- [9] Keysers, C. and Perrett, D. I. Demystifying social cognition: a Hebbian perspective, *Trends Cogn Sci*, Vol.8,No.11, pp.501-7, 2004
- [10] Murata, A. and Ishida, H. Representation of bodily self in the multimodal parieto-premotor network. In: *Representation and Brain*, edited by Shintaro Funahashi, Springer Verlag In press 2007
- [11] 村田 哲 模倣の神経回路と自他の区別 *SOBIM* Vol.29, No.1,pp.14-19 2005
- [12] Sirigu, A., Daprati, E., Pradat-Diehl, P., Franck, N. and Jeannerod, M. Perception of self-generated movement following left parietal lesion, *Brain*, Vol.122 (Pt 10), pp.1867-74, 1999
- [13] 村田 哲 ミラーニューロンとボディイメージ 21世紀の科学をつくる 脳の謎に挑む 第4回 数理科学, Vol. 39, No.12, pp. 69-77 2001
- [14] Iriki, A., Tanaka, M. & Iwamura, Y.: Coding of modified body schema during tool use by macaque postcentral neurones. *Neuroreport*, 7, 2325-30, 1996
- [15] Meltzoff, A. N. and Decety, J. What imitation tells us about social cognition: a rapprochement between developmental psychology and cognitive neuroscience, *Philos Trans R Soc Lond B Biol Sci*, Vol.358,No.1431, pp.491-500 2003
- [16] Gallese, V., Fadiga, L., Fogassi, L. and Rizzolatti, G. Action recognition in the premotor cortex, *Brain*, Vol.119,No.Pt 2)(pp.593-609, 1996
- [17] Murata A and Kumashiro M. Links between mirror neurons in the ventral premotor cortex of the macaque and Broca's area of the human. *Shinkei Kenkyu no Shinpo* Vol.47,No5, 684-693 2003
- [18] Colby CL, Duhamel JR, Goldberg ME Ventral intraparietal area of the macaque: anatomic location and visual response properties. *J Neurophysiol* 69: 902-914 , 1993
- [19] Blakemore SJ, Bristow D, Bird G, Frith C, and Ward J. Somatosensory activations during the observation of touch and a case of vision-touch synaesthesia. *Brain* 128: 1571-1583, 2005.
- [20] Shimada S, Hiraki K, Oda I The parietal role in the sense of self-ownership with temporal discrepancy between visual and proprioceptive feedbacks. *Neuroimage* 24: 1225-1232, 2005
- [21] Murata A. Function of mirror neurons originated from motor control system *The brain & neural networks* Vol.12, No.1: 52-60, 2005
- [22] Ishida H and Murata A recognition of other's body parts by visuo-tactile bimodal neuron in area VIP. 19 the SICE Symposium on Decentralized Autonomous Systems 1-4 2007
- [23] Wolpert DM, Doya K and Kawato M A unifying computational framework for motor control and social interaction. *Philos Trans R Soc Lond B Biol Sci* 358: 593-602 2003
- [24] Murata A and Ishida H Representation of bodily self and others in the brain. *IEICE technical Report* 106 (410): 41-44 2006
- [25] Fogassi L, Ferrari PF, Gesierich B, Rozzi S, Chersi F and Rizzolatti G Parietal lobe: from action organization to intention understanding. *Science* 308: 662-667 2005
- [26] Oztop E, Imamizu H, Cheng G and Kawato M A computational model of anterior intraparietal (AIP) neurons *Nuerocomputing* 69 (10-12) 1354-1361 2006
- [27] Oztop E, Kawato M, and Arbib M. Mirror neurons and imitation: A computationally guided review. *Neural Netw* 19: 254-271, 2006.
- [28] Murata A, Fadiga L, Fogassi L, Gallese V, Raos V, Rizzolatti G Object representation in the ventral premotor cortex (area F5) of the monkey. *J Neurophysiol* 78: 2226-2230 , 1997

Constructive Approach to Understanding the Active Learning Process of Adaptation within a Given Task Environment

Hiroaki Arie, Shigeki Sugano
Science & Engineering, Waseda University

Jun Tani
RIKEN Brain Science Institute

I. INTRODUCTION

We humans learn our behavior skills through repetitions of own behavior experiences. We learn to manipulate object, to use tools and to navigate to desired location.

The compositionality is an essential issue in considering human skilled behaviors. If the mission of a particular robot is just to repeat the same goal-directed behavior, all the things to do for the robot is to acquire a single motor scheme to generate the target behavior. However, it will be not the case if robots or humans are required to adapt to various goals under diverse situations. In this case, the motor schemes should be organized in a compositional manner such that compositions of various motor schemes can generate diverse actions adaptively corresponding to required goals. For example, an attempt of drinking a cup of water might be decomposed into multiple motor schemes such as reaching to a cup, grasping the cup and moving the cup toward own mouth. Each motor scheme can be utilized as a component for other goal-directed actions as like reaching to a cup can do for the goal of clearing it away.

This idea of decomposition of whole behaviors into sequences of reusable primitives are originally considered by [1] as the motor schemata theory. However, when we think about the behavior primitives, they should not be treated as concrete objects. Instead, each behavior primitive should be acquired as enough “elastic” such that it can be utilized flexibly in various situations. For example, a behavior primitive of grasping an object should be utilized enough adaptively to variations of the object positions as well as their shapes. This requires generalization in learning of the skills. In addition, the context-dependent aspects in generating motor act sequences are important, which was metaphorically termed as “kinetic melody” by [2]. For example, exact motor trajectories of grasping a cup should be affected by next motor act to follow them as well as the entire goals of whether to drink a cup of water or to clean off the cup. The whole motor behaviors should be generated fluently by capturing the context-dependent nature of intended action goals. Then, the essential question here is that how this sort of “organic” compositionality can be achieved through learning processes.

In the brain science perspective, we speculate that such “organic” compositional structures responsible for generating skilled behaviors might be acquired in inferior parietal lobe (IPL) through the repeated sensory-motor experiences. Our ideas have been inspired by [3] who suggested that the world

models are firstly stored in parietal cortex and then they are consolidated into cerebellum. Conventionally, parietal cortex has been viewed as a core cite to associate and integrate the multi-modality of the sensory inputs [4], [5]. However, the neuropsychological studies investigating various apraxia cases, including ideomotor apraxia and ideational apraxia [6], [7], have suggested that IPL should be also an essential site to represent a class of behavior skills, especially related to object manipulations. We speculate that this region might function as internal models by having certain anticipatory mechanisms for coming sensory inputs as related to motor acts. Furthermore, it has been speculated that IPL might function both for generating and recognizing the goal-directed behaviors [8] by having dense interactions with cells in ventral premotor (PMv) which are known as mirror neurons [9].

Our group have investigated how the “organic” compositionality can be attained in modeling of IPL and PMv interactions for several years. One of our original neural network models is so-called the recurrent neural network with parametric biases (RNNPB)[10], [11]. In this modeling, a recurrent neural network (RNN) learns various forward models of motor-related sensory inputs sequences as parameterized by the parametric biases (PBs). This means that the forward dynamics of the RNN can be modulated by values of the PBs that function as bifurcation parameters of the dynamics.

The PBs can be used to encode the goal information both for behavior generation by means of prediction and its recognition by postdiction. Once the goal is set by means of setting a specific value for the PBs, the forward model autonomously generates prediction of the sensory inputs sequence reaching to the goal. In this model, we assume that the PB is manipulated in PMv and that the forward model predicts sensory inputs sequences in IPL. The prediction of the sensory image includes that of proprioception regarding to postures of limbs. We assume that this prediction for the time-development for the posture might be sent to M1 as well as cerebellum where exact motor commands to achieve the posture changes might be obtained by inverse models.

The goals or intentions by others can be recognized by making match between the sensory sequence imaginary generated by the forward model and the observed actual one [10], [12]. The PB value of minimizing the error in this match is inversely computed through iterative search. The PB value obtained by this postdiction scheme represents the goal or the intention for the observed behavior.

This year we reported further extensions of our models. We have shown that on-going behavior can be adapted to the contextual changes in the environment in real time by simultaneously conducting the prediction and the postdiction interactively for modulating the PB value dynamically [13]. We also found that different goal-directed behaviors can be embedded in a single continuous-time recurrent neural network with utilizing its initial sensitivity characteristics of which mechanism seems to be much simpler than the parameter bifurcation mechanism of the PB [14]. Furthermore, we found that the forward model can be scaled significantly by self-organizing level structures with having different time-constant dynamics in the networks [15]. Our robotics experiments showed that behavior primitives are self-organized in the lower level dynamics with fast time-constant and combinational manipulations of them are learned in the higher one with slower time constant. The analysis of these experiments indicated that the composition mechanism attained in the level-structured dynamics is “organic” in a sense that it captures generalization through learning of various sensory-motor experiences as well as contextual natures of the goal-directed skilled behaviors.

Another new challenge of this year was to introduce the exploration-based learning paradigm to acquisitions of behavior skills, which turns to be the main focus in the following sections in the current report. It is widely assumed that basal ganglia (BG) plays important roles for the exploration-based learning [16]. Although BG seems to involve deeply with the on-line learning mechanisms assumed in reinforcement learning scheme, it is not well known that whether the skills consolidated after long time period still stay in BG or they are transformed to other cortex areas. From the reviews of neuropsychological studies [6], [7], [2], [17], it is natural to consider that behavior skills especially for manipulating objects and tools are initially acquired in BG through the on-line exploration and then they are consolidated in IPL after the long run through incremental off-line learning during sleep. It is furthermore assumed that the behavior skills might be consolidated in IPL with association of their goal information, presumably represented in PMv, as have been discussed previously. Based on these assumptions on human brain mechanisms, the current report introduces our novel models that could explain how exploration-based experiences can be transformed to structured skills through the memory consolidation processes.

Before closing this introduction section, we briefly describe our motivation to build physical robot platforms for our experiments. Main reason to conduct robot experiments is to show that the proposed model can work in more realistic setting compared to simulation ones. Although the real physical experiments have limitations in searching for adequate parameter values through iterative experiments, the fact that the robot actually works inversely would prove that the proposed model is robust enough to function with only limited amounts of the parameter adjustments. In order to conduct the long time exploration-based learning experiments with a physical robot, there was necessity to build a durable

robot. Therefore, we built a novel robot with a tendon-based actuation mechanism which can afford elasticity at each joint of the robot. The following sections will describe, our brain-inspired model for the exploration-based learning of goal-directed behavior skills, its implementation in neural network models and their early stage experiments both in simulations and with our developed real robot.

II. BIOLOGICAL MODEL

This section describes more details of our biological brain model. The model basically consists of two parts (see Figure1). One part is PMv-IPL-M1 network that works as a

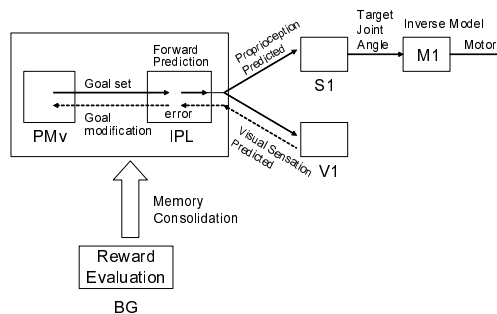


Fig. 1. brain model

mirror system both to generate and recognize goal-directed skilled behaviors. The cases with supervised training of this network have been reported in [12], [13], [14]. In the generation pathway, PMv provides the goal information to the forward model assumed in IPL by means of setting its internal state (it could correspond to PB or context state in RNN implementation). The prediction of proprioception inputs are sent to primary sensor (S1) and its conversion to target joint angles are further sent to M1 as well as cerebellum to compute corresponding motor commands. At the same time, the prediction of visual sensation is computed in IPL and it is compared with the real visual sensation in early vision area including v1. If the error is generated, the error is fed-back to PMv to modify the internal state in direction of minimizing error. In this way, the goals of current behaviors can be adapted to contextual changes in environment [13].

The other part is BG that evaluates the cumulative reward of on-going behavior trials. In our model, it is assumed that BG memorizes only sensory-motor sequence patterns with good cumulative rewards in its short-term memory. The memorized patterns are later transferred to PMv-IPL network as teaching patterns to train the network in off-line. It is expected that multiple behavior schemes of gaining the higher cumulative rewards will be consolidated in PMv-IPL network through the iterative trials of the robot.

Currently, this whole model is still under construction. The current report describes parts of this global picture, namely BG-IPL interactions and IPL-M1 interactions. For the study of BG-IPL interactions, we investigate a reinforcement learning scheme which realizes the memory consolidation of well-rewarded behavior patterns in simulations. For the study of

IPL-M1 interactions, we examine how the forward model in IPL and the inverse model in M1 or cerebellum can function cooperatively through their learning.

III. BG-IPL INTERACTION MODEL

A. Proposed neural network model

We utilized the actor-critic method which is one of the temporal difference (TD) family of reinforcement learning methods. As shown in Figure 2, the model consists of two parts called actor and critic. In this method, actor plays the role of IPL whose output decides the behavior of a robot, and the critic, which is corresponding to a part of BG, approximates the value function $V(t)$ and compute the TD error.

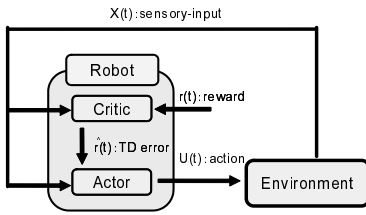


Fig. 2. Actor-Critic Model

The goal of this algorithm is to find a policy (control law) $U(t)$ that maximizes the expected cumulative rewards for a certain period in the future defined by the next equation:

$$V(t) = \int_t^{\infty} \frac{1}{\tau} e^{-\frac{s-t}{\tau}} r(s) ds \quad (1)$$

where $r(t)$ is the immediate reward for the state at time t . $V(t)$ is called value function of state $X(t)$ and τ is the time constant for discounting future rewards. The basic idea in TD learning is to predict future reinforcement. By differentiating the equation (1) with respect to time t we have

$$\tau \frac{d}{dt} V(t) = V(t) - r(t). \quad (2)$$

The TD error $\hat{r}(t)$ is defined as a prediction error from equation (2)

$$\hat{r}(t) = r(t) - \frac{1}{\tau} V(t) + \frac{d}{dt} V(t) \quad (3)$$

If the current prediction for $V(t)$ is accurate, the TD error should be equal to zero. In addition, if the prediction value for the current state is small, the TD error becomes positive. Accordingly, in the Actor-Critic method, the TD error is used as the reinforcement signal for policy improvement.

We introduce the Actor-Critic method into a CTRNN learning algorithm. In our algorithm, an actor and a critic are implemented into one CTRNN to share the context loop which plays an important role in state recognition.

Input and output neurons represent three types of information: the value function $V(t)$, observation of the state $X(t)$, and action $U(t)$. The learning method of the CTRNN is based on the gradient descent optimization of connection weight values and biases of each neuron to minimize the

learning error of a given set of teaching data. The delta errors of the connection weight and biases are computed by using the conventional back-propagation through time (BPTT) algorithm. In our method, the teaching data and propagating error are modulated by the TD error to introduce reinforcement learning.

First, we consider the learning of the value function. The TD error indicates the inconsistency between the ideal and predicted value functions, therefore, the teaching data for the neuron representing value function $V(t)$ is updated using the following equation:

$$V^*(t) = V(t) + \hat{r}(t) \quad (4)$$

where $V^*(t)$ is the teaching data and $V(t)$ is the value predicted by the current CTRNN.

Next, we consider a way for improving the action using its associated value function $V(t)$. It is shown that, in the actor-critic method, the TD error can be used as the reinforcement signal for the improvement of action. A random noise signal is added to the output of the controller. Under such conditions, if the TD error is positive, then the output has to be shifted to a good direction. From this cause, the output has to be learned substantially where the TD error is positive. The error signal corresponding to the output neuron for action is modulated according to the following equation:

$$e(t) = \{\hat{U}(t) - U_{real}(t)\} \times \sigma(\hat{r}(t) \times \phi) \quad (5)$$

where $\hat{U}(t)$ is the action calculated by the CTRNN, and $U_{real}(t)$ is the actual action including a noise signal. Sigmoid function $\sigma(x)$ is used to ensure that the magnification range is limited between 0 and 1.

In reinforcement learning, CTRNN has to learn a new sequence generated in each trial, which is inherently incremental learning. We use a database, which is corresponding to BG, to store sequences and the CTRNN is trained using these sequences. A sequence, stored in the database, is selected by the total reward of the trial. The maximal total reward in passed trials is stored and the total reward of a new trial is compared to it. If the total reward of a new trial is greater than a certain rate of a passed maximal one, then the new sequence is stored in the database.

B. Experiment

To test the effectiveness of the proposed method, we applied it to the task of swinging up a pendulum with limited torque. The experiment was carried out using a physical simulation. In this task, a robot has to bring a pendulum to an inherently unstable upright equilibrium by controlling the torque $U(t)$ around the rotational axis. Furthermore, the maximal torque is smaller than mgl , so the robot has to swing the pendulum several times to build up sufficient momentum to bring it upright. The state of the pendulum is defined by the joint angle $\theta(t)$ and the pendulum's rotational speed $\dot{\theta}(t)$. Here, a partially observable environment is considered, in which the robot cannot observe the state information corresponding to the rotational speed $\dot{\theta}(t)$. The

robot has to learn to approximate this information using its internal state to solve the task.

The time course of the total reward through learning is shown in Figure 3. In this figure, only a trial which is used in the learning phase is counted and others are discarded. The initial performance is about 2.5, but quickly increased to above 20 within the first 30 trials. The performance of the CTRNN increase gradually when there are more learning iterations, and in trial 342, the performance of the CTRNN reached its peak. In this trial, the CTRNN can swing up the pendulum and maintain the pendulum in upright position successfully. The time course of system dynamics is shown in Figure 4. The learning algorithm proposed in this paper

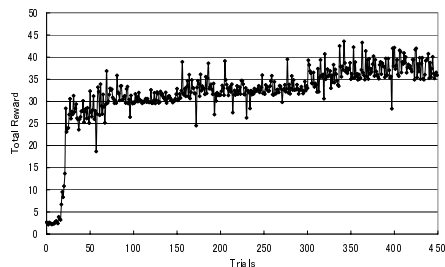


Fig. 3. Learning curve

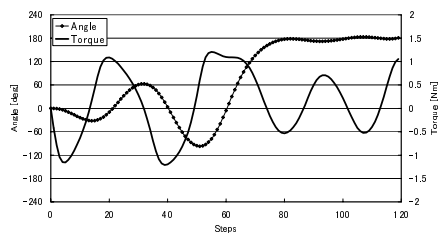


Fig. 4. Time course of system dynamics in trial 342

allowed the CTRNN to organize its internal state space successfully and to use that information to achieve the given task.

IV. IPL-M1 INTERACTION MODEL

At present, a humanoid upper-torso robot is being developed to serve as a research platform. The hardware allows for real exploratory behavior experiments in the sense that it is "collision safe", i.e. it can hit obstacles as well as other parts of its own body, much like a human infant, and learn about its environment in this interactive way.

Each of the arm joints is actuated by an antagonistic pair of two motor-spring assemblies. By controlling the tension in the spring with a classic PID controller, the joints are being torque-controlled. The spring-like property gives the arm a sensible "natural" behavior: if it is disturbed, or hits an obstacle, the arm simply deflects out of the way.

Because of inherent nonlinear characteristics of the developed control system, standard PID control schemes cannot be applied to the system. Therefore, we implemented the IPL-M1 model into the robot system with employing the CTRNNs to construct both of the forward model and the

inverse model. After the performance of this part is evaluated, BG as well as PMv parts will be added to the system.



Fig. 5. tendon-driven robot

REFERENCES

- [1] M.A. Arbib. Perceptual structures and distributed motor control. In *Handbook of Physiology: The Nervous System, II. Motor Control*, pages 1448–1480. Cambridge, MA: MIT Press, 1981.
- [2] Luria A.R. *The Working Brain*. Penguin Books Ltd., 1973.
- [3] M. Ito. Bases and implications of learning in the cerebellum - adaptive control and internal model mechanism. *Progress in Brain Research*, 148:95–109, 2005.
- [4] C.L. Colby, J. Duhamel, and M.E. Goldberg. Ventral intraparietal area of the macaque: anatomic location and visual response properties. *Journal of Neurophysiology*, 69:902–914, 1993.
- [5] H. Sakata, M. Taira, A. Murata, and S. Mine. Neural mechanisms of visual guidance of hand action in the parietal cortex of the monkey. *Cereb Cortex*, 5:429–438, 1995.
- [6] H. Liepmann. Apraxie. *Erg ges Med*, 1:516–543, 1920.
- [7] K.M. Heilman. Ideational apraxia - a re-definition. *Brain*, 96:861–864, 1973.
- [8] L. Fogassi, P.F. Ferrari, B. Gesierich B, S. Rozzi, F. Chersi F., and G. Rizzolatti. Parietal lobe: from action organization to intention understanding. *Science*, 308:662–667, 2005.
- [9] G. Rizzolatti, L. Fadiga, V. Gallese, and L. Fogassi. Premotor cortex and the recognition of motor actions. *Cognitive Brain Research*, 3:131–141, 1996.
- [10] J. Tani and M. Ito. Self-organization of behavioral primitives as multiple attractor dynamics: a robot experiment. *IEEE Trans. on Sys. Man and Cybern. Part A*, 33(4):481–488, 2003.
- [11] J. Tani, M. Ito, and Y. Sugita. Self-organization of distributedly represented multiple behavior schemata in a mirror system: reviews of robot experiments using RNNPB. *Neural Networks*, 17:1273–1289, 2004.
- [12] M. Ito and J. Tani. On-line imitative interaction with a humanoid robot using a dynamic neural network model of a mirror system. *Adaptive Behavior*, 12(2):93–114, 2004.
- [13] M. Ito, K. Noda, Y. Hoshino, and J. Tani. Dynamic and interactive generation of object handling behaviors by a small humanoid robot using a dynamic neural network model. *Neural Networks*, 19:323–337, 2006.
- [14] R. Nishimoto. *Learning to Generate Combinatorial Action Sequences Utilizing the Initial Sensitivity of Deterministic Dynamical Systems*. PhD thesis, PhD thesis, Graduate School of Arts and Sciences, University of Tokyo, 2007.
- [15] R. Paine and J. Tani. How hierarchical control self-organizes in artificial adaptive systems. *Adaptive Behavior*, 13(3):211–225, 2005.
- [16] K. Doya, K. Samejima, K. Katagiri, and M. Kawato. Multiple model-based reinforcement learning. *Neural Computation*, 14:1347–1369, 2002.
- [17] N. Geschwind and E.A. Kaplan. Human cerebral disconnection syndromes. *Neurology*, 12:675–685, 1962.

Group B: Research Report

Kazuo Tsuchiya

Dept. of Aeronautics and Astronautics, Graduate School of Engineering, Kyoto University

I. RESEARCH PROJECT

Animals generate locomotion adaptive to various environments by cooperatively manipulating their complicated and redundant musculoskeletal systems. So far, biomechanical studies have investigated the mechanical and dynamical characteristics of cooperative muscle activities. On the other hand, neurophysiological studies have examined neural activities during various motions and evaluated their functional roles based on animal experiments. Animal skillful behaviors emerge through dynamical interactions between brain, nervous system, and musculoskeletal system. Group B consists of biologists who study exercise physiology and engineers who study biomechanics and conducts cooperative research aiming to elucidate how the mechanisms of selection and realtime generation of motion patterns adapt themselves to environmental variations (Fig. 1). In particular, biologists record neural activities related to locomotor behaviors and investigate the functional roles of the neural activities based on such animals as monkeys, cats, and rats as well as humans. On the contrary, engineers construct neuromusculoskeletal models founded on anatomically based whole-body musculoskeletal and mathematical models of locomotor nervous systems based on neurophysiological findings. They clarify the nervous system mechanism that generates adaptive behaviors founded on a constructive approach by simulating locomotion based on the constructed models and comparing simulation results with physiological experimental results. This group wants to open a new research field called 'System Biomechanics' that integrates biomechanics and neurophysiology. Furthermore, this group aims to construct a new robotics called 'Biorobotics' and establish applications to anthropology and rehabilitation. This report shows the representative studies of this group. Further details are shown in the report of each subgroup.

A. Elucidation of functional roles of cortical motor areas in locomotor behaviors

In primates, cortical motor areas in the frontal lobe are one of the major sources of efferents projecting to both the brainstem and spinal cord. Since these areas are functionally separated in the primary motor cortex (M1), the supplementary motor area (SMA) and the premotor area (PM) in terms of controlling hand and digit movements, the purpose of the present study is to elucidate whether each of these areas plays specific roles for the execution of locomotor behaviors. Two series of experiments were performed on two macaque monkeys which were trained to perform quadrupedal and bipedal locomotion on treadmill without any constraints.

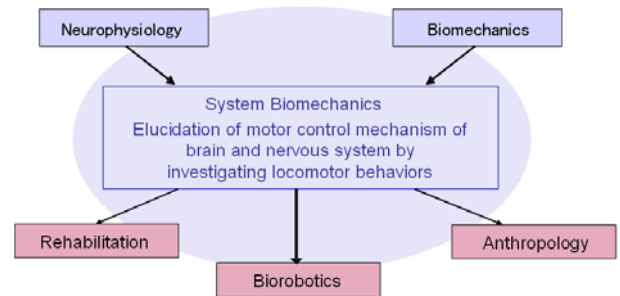


Fig. 1. Research project of Group B

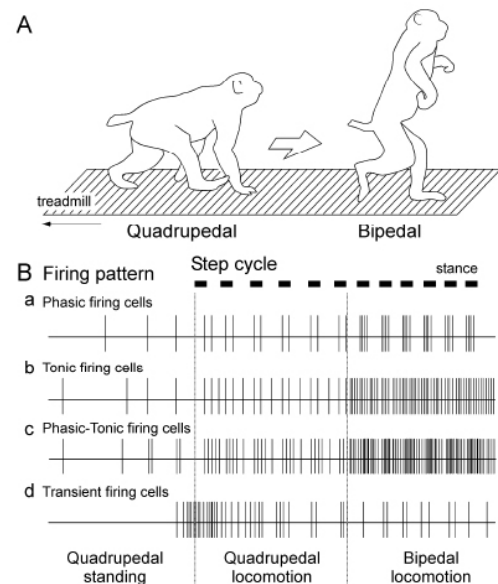


Fig. 2. Schematic presentation of representative firing patterns of cortical neurons during locomotor behaviors.

First, we recorded neuronal activities in these areas during treadmill walking so that we could determine whether neurons in each area had their own specific firing property. We also tested how the firing pattern is altered by the transition from quadrupedal to bipedal locomotion (Fig. 2). Next, we injected muscimol, a GABA_A-receptor agonist, into each of cortical motor areas to determine whether deficit of locomotor behaviors specific to each area was evoked. Based on the present findings, role of cortical motor areas in the modulation of subcortical motor systems is discussed in relation to the control of postural and locomotor synergies.

Firing properties of recorded neurons during standing and locomotor behaviors are summarized as follows: (1) Firing rate of most neurons in each area was lower when animal was standing with quadruped. (2) Immediately before initiating locomotion with either quadruped or biped, a population of PMd neurons started to discharge. (3) Neurons in M1

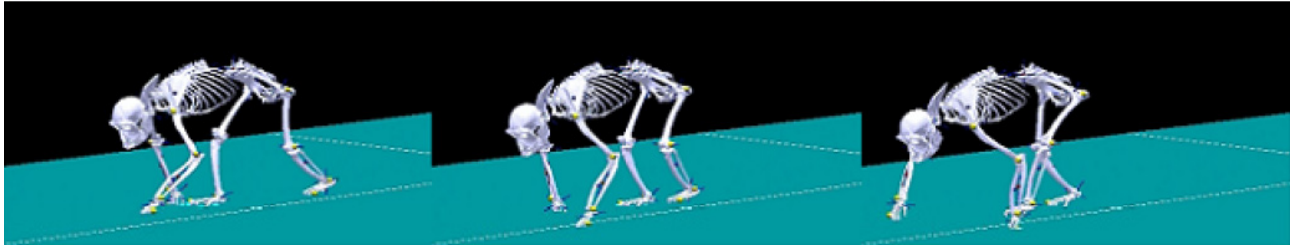


Fig. 4. Forward dynamic simulation of quadrupedal locomotion of a Japanese monkey based on musculoskeletal model

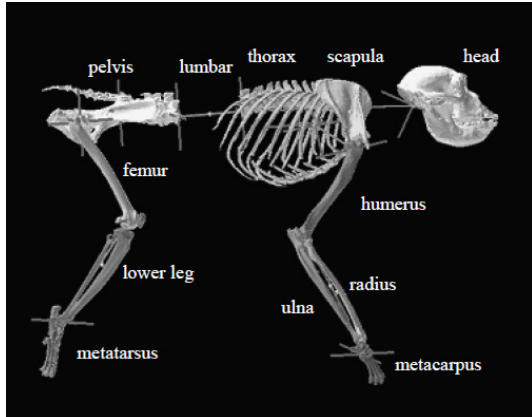


Fig. 3. Kinematic description of the whole-body skeleton of a Japanese monkey as a chain of links. Only right fore and hindlimb are shown.

mainly exhibited rhythmic discharge during locomotion in relation to step cycles. (4) Majority of SMA neurons tonically discharged during locomotion. (5) Majority of PMd neurons displayed either phasic or phasic-tonic firing during locomotion. (6) Firing frequency of most neurons recorded in all three areas was higher in locomotion with biped than quadruped.

This study is the first to provide direct evidence that neurons in the trunk/hindlimb region of the cortical motor areas in primates contribute to the execution of quadrupedal and bipedal locomotion. Present findings suggest that each area plays specific role in the control of locomotor behaviors. The M1 is possibly involved in the rhythmic movements of contralateral hindlimb during locomotion. The SMA may play a role in the postural control, while the PMd may contribute to the initiation of locomotion in addition to the control of postural and locomotor (rhythmic leg movements) synergies. Bipedal locomotion requires the intense activation of cortical motor areas than quadrupedal locomotion.

II. CONSTRUCTION OF A NEURO-MUSCULOSKELETAL MODEL OF THE JAPANESE MONKEY

The present study constructed a biologically plausible computer simulation of animal locomotion. In particular, it created a neuro-musculoskeletal model for quadrupedal and bipedal locomotion in the Japanese monkey (*Macaca fuscata*). A kinematic skeleton of the Japanese monkey was mathematically described as a chain of 20 links connected by revolute joints, as illustrated in Figure 3. Joints connecting the trunk segments (head, thorax, lumbar vertebrae, and pelvis) were represented as 3-degree-of-freedom (DOF)

joints. The scapula is usually modeled as immobile with respect to the thorax, although the relationship between the scapula and forelimb is functionally equivalent to the femur and hindlimb, thus representing an important element for propulsion. A new approach was thus used to mathematically model the translational motion of the scapula along the rib cage using three revolute joints.

A fresh cadaver of a female Japanese monkey was dissected to mathematically describe the path of each muscle and the associated capacity to generate force. Each muscle in the fore and hindlimbs was carefully exposed to observe points of origin and insertion. The muscle was then removed and mass and fascicle length were systematically recorded to calculate the physiological cross-sectional area (PCSA). The path of each muscle was defined using a series of points connected by line segments. The capacity of each muscle to generate force was assumed to be proportional to PCSA. Each muscle was basically modeled as a line segment connecting origin and insertion.

CPG was hypothesized to represent a set of oscillators corresponding to each of the limbs and the trunk segment, and oscillator phase was considered to encode the orientation and length of the limb axis, with the spinal circuitry of interneurons somehow generating muscle activation patterns based on output signals from the CPG. For now, we modeled this transformation using a PD feedback control law, and joint torque was applied instead of muscle force to generate locomotion. Orientation and length profiles of limbs were provided based on measured kinematic data. The CPG phase was reset in response to the timing of hand or foot-ground contacts. To realize coordinated interlimb movements, appropriate dynamic interactions among the oscillators were assumed (Fig. 4).

A nine-year old male Japanese monkey walking quadrupedally/bipedally on a treadmill at three km/h was videotaped using four digital cameras and locomotion was analyzed. A total of 16 reflexive markers (eight on one side) were placed at: 1) the head of 5th metatarsal; 2) the lateral malleolus of fibula; 3) the lateral epicondyle of the femur; 4) the greater trochanter; 5) the acromion; 6) the lateral epicondyle of humerus; 7) the styloid process of the ulna; and 8) the head of 5th metacarpal. These markers were manually digitized frame-by-frame, and their coordinates were calculated using 3D motion analysis software. A new treadmill was constructed in which a force plate was embedded, and we started to synchronously capture locomotor kinematics and kinetics.

Cortical Motor Areas & Postural and Locomotor Synergies

Katsumi NAKAJIMA¹, Futoshi MORI², Masahiko INASE¹, Dai YANAGIHARA³, Taizo NAKAZATO⁴, Shigeru KITAZAWA⁴ and Kaoru TAKAKUSAKI⁵.

1. Department of Physiology, Kinki University School of Medicine, Sayama, Japan

2. Department of Veterinary Physiology, Yamaguchi University, Yamaguchi, Japan

3. Department of Life Science, Graduate School of Arts and Science, University of Toyo, Tokyo, Japan

4. Department of Physiology, School of Medicine, Juntendo University, Tokyo, Japan

5. Department of Physiology, Asahikawa Medical College, Asahikawa, Japan

Abstract: *The present study was designed to understand how cortical motor areas in primates contribute to the gait control. In freely-moving macaque monkeys, firing property of cortical neurons in the motor-related areas was first examined during locomotion on moving treadmill. In quadrupedal locomotion, most neurons in the primary motor cortex (M1) rhythmically discharged in relation to step cycles, while those in the supplementary motor area (SMA) tonically discharged. Neurons in these areas increased their firing rate when the animal walked bipedally. While a majority of neurons in the dorsal part of the premotor cortex (PMd) tonically and phasically discharged during locomotion, a portion of the PMd neurons transiently increased their firing rates when the monkey initiated walking. Microinjection of muscimol into the hindlimb region of M1 resulted in local paresis of the contralateral hindlimb. However, muscimol injection into trunk/hindlimb region of the SMA did not paralyze the limb movement but disturbed postural control. When the PMd was a target of muscimol injection, the monkey seemed to lack the capability of initiating locomotor behaviors in response to external events. These findings suggest that cortical motor areas in macaque monkeys are functionally organized in relation to the execution of locomotor behaviors. Possibly they are involved in the initiation (PMd), postural control (SMA) and rhythmic limb movements (M1). Because firing rates of neurons recorded in these areas were much higher in bipedal than quadrupedal locomotion, bipedal locomotion may require enhanced activities of cortical motor areas.*

Keywords; motor cortex, bipedal and quadrupedal locomotion postural control, basal ganglia, brainstem, spinal cord

1. INTRODUCTION

The term motor control refers to the study of postures and movements, and also the functions of mind and body that govern posture and movements. Postures of the limbs, the trunk and the whole body are maintained by muscular effort. On the other side, "movements" are transition from one posture to another [1]. One of the most representative movements that require dynamic postural changes is locomotion. For initiation of locomotion, maintenance and transition of one's body weight against the gravity are essential. Therefore dynamic postural changes are thought to the initial stage of purposeful movements.

Basic neural systems responsible for the control of posture and locomotion are located in the brainstem and spinal cord [2].

Adaptive locomotor behaviors triggered by cerebral cortex and the limbic system are therefore mediated by the activation of the brainstem-spinal cord systems and regulated by the basal ganglia and the cerebellum. The motor cortex is involved in the control of precise stepping movements in visually-guided walking. Although experimental lesions of the cat motor cortex do not prevent animals from walking in a smooth floor, they severely impaired tasks requiring a high degree of visuomotor coordination, such walking on the rungs of horizontal ladder and stepping over a series of barriers [3]. Such skilled walking is associated with considerable modulation in the activity of a large number of neurons in the motor cortex [4]. Clinically, bipedal gait of Parkinson disease patients is seriously disturbed. Typically they hesitate to start walking (frozen gait) and walk slowly with diminished arm swing and flexed forward posture [5, 6]. However the gait disturbance is improved and normalized by visual input (paradoxical gait). The improvement has been shown to be brought about by the enhanced activities of parietal and frontal cortices by visual stimuli [7].

In primates, cortical motor areas in the frontal lobe are one of the major sources of efferents projecting to both the brainstem and spinal cord. Since these areas are functionally separated in the primary motor cortex (M1), the supplementary motor area (SMA) and the premotor area (PM) in terms of controlling hand and digit movements [8, 9, 10], the purpose of the present study is to elucidate whether each of these areas plays specific roles for the execution of locomotor behaviors. Two series of experiments were performed on two macaque monkeys which were trained to perform quadrupedal and bipedal locomotion on treadmill without any constraints. First, we recorded neuronal activities in these areas during treadmill walking so that we could determine whether neurons in each area had their own specific firing property. We also tested how the firing pattern is altered by the transition from quadrupedal to bipedal locomotion. Next, we injected muscimol, a GABA_A-receptor agonist, into each of cortical motor areas to determine whether deficit of locomotor behaviors specific to each area was evoked. Based on the present findings, role of cortical motor areas in the modulation of subcortical motor systems is discussed in relation to the control of postural and locomotor synergies.

2. MATERIALS AND METHODS

The experiments were performed on two macaque monkeys (7.5 and 8.5kg). All of the procedures were approved in the Guide

for the Care and Use of Laboratory Animals (NIH Guide), revised 1996. During the investigation every effort was made to minimize animal suffering and to reduce the number of animals used.

Surgery: Before surgery, animals were trained to perform quadrupedal and bipedal locomotion on a moving treadmill. Surgery was made under pentobarbital anesthesia (20mg/kg, i.p.). The head was fixed in a stereotaxic apparatus. Two stainless steel pipes were mounted in parallel on the skull using acrylic resin and small screws. A chamber was then attached to the skull over cortical motor areas for the single-unit recording and muscimol injection.

Recording of cortical neurons: After recovery of the surgery, a tungsten microelectrode were inserted into trunk/hindlimb regions of M1, SMA and dorsal part of PM (PMd) using a custom-made micro-manipulator. Extracellular activity of neurons was recorded from the monkey walking freely with both quadrupedal and bipedal on the treadmill. Intracortical microstimulation (ICMS, 5.0-50 μ A, 333 Hz, 12-22 pulse trains) was carried out at the end of each experimental session.

Muscimol injection: Prior to the injection, locations of trunk/hindlimb regions of M1, SMA and PMd were examined by ICMS. Muscimol (5.0~10.0 μ g/ μ l, 1.0~4.0 μ l), a GABA_A-receptor agonist, was then injected into the trunk/hindlimb region of each area using Hamilton microsyringe (10 μ l) attached with Teflon-coated tungsten wire. Effects of the injection were confirmed by the reduction of spontaneous activity of the neurons. The monkey was then encouraged to walk on the treadmill and its locomotor figure was compared before and after the injection.

3. RESULTS

3-1. Firing property of cortical neurons during locomotion

To date, activity of 82 neurons was recorded from trunk/hindlimb region of the M1, SMA and PMd of the monkey (Fig.1A) walking quadrupedally or bipedally on a moving treadmill belt. Of these, 54 neurons showed task-related activity during quadrupedal and/or bipedal locomotion. To analyze firing property of the task-related neurons, peri-event time histograms were constructed in relation to single step cycles of the hindlimb contralateral to the recording side (Fig.1B and 1C).

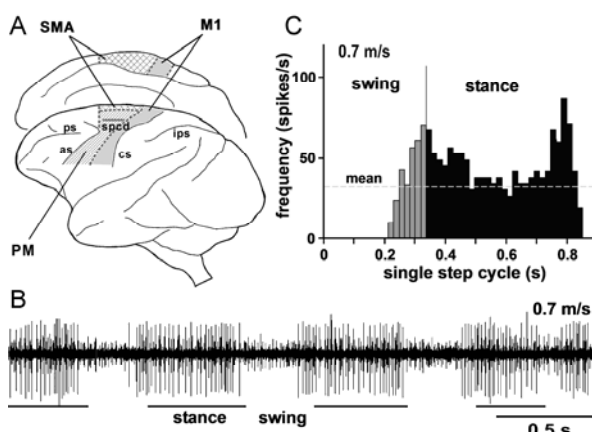


Figure 1. Activity of an M1 neuron during locomotion

A. Cortical motor areas in the cerebral cortex of macaque monkeys. B Example of M1 neuron discharging phasically during quadrupedal locomotion. C. Firing histogram of this cell in relation to step cycles of the hindlimb contralateral to the recording side. Periods of stance and swing phases are indicated by filled and hatched bars. Bin width is 18 msec. Abbreviations, cs; central sulcus, ps; principal sulcus, ips; intraparietal sulcus, spcd; superior precentral dimple, as; arcuate sulcus.

Before starting locomotion, standing with quadrupedal, the neurons in all areas exhibited sporadic or tonic firing with lower rate. When a monkey started to locomote, a majority of the neurons altered their firing patterns. Firing property of the cortical neurons was divided into four patterns as shown in Fig. 2B. They discharged either phasically (phasic cells; a) or tonically (tonic cells; b), or both (phasic-tonic cells; c).

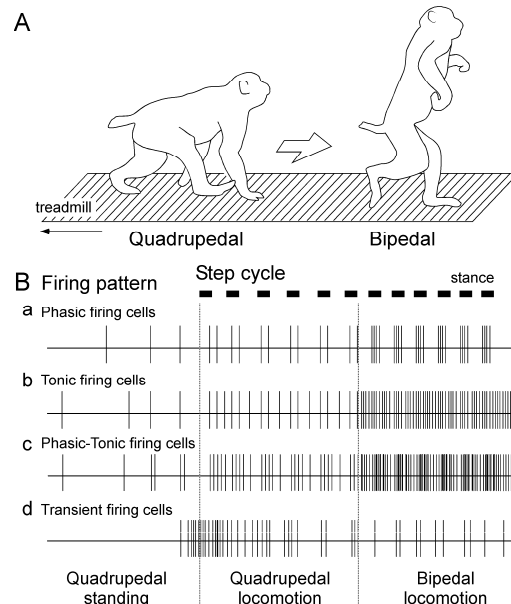


Figure 2. Schematic presentation of representative firing patterns of cortical neurons during locomotor behaviors.

A. Postural changes of quadrupedal (left) and bipedal (right) locomotor behaviors in monkey. B. Schematic illustration of firing property of motor cortical neurons. See text for explanations.

Relative proportion of each firing pattern was shown in Fig. 3 in relation to the locations of recorded motor areas during quadrupedal (A) and bipedal locomotion (B). During quadrupedal locomotion (Fig. 3A), in the M1, 15 out of 21 task-related neurons were the phasic cells. An example is shown in Fig.1B. The peak activity occurred at widely different times during the step cycle in different cells. In contrast, majority of neurons in the SMA (7/13) and the PMd (8/20) were the tonic or phasic-tonic cells. Noteworthy is that 4 neurons in the PMd displayed bursting discharges preceding the initiation of locomotion (Fig.2Bd, 3B).

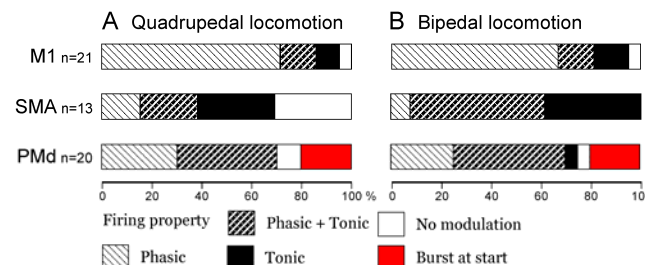


Figure 3. Firing patterns of cortical neurons during locomotion

Relative proportion of motor cortical neurons with different firing properties during quadrupedal (A) and bipedal (B) locomotion.

When the monkey converted its locomotor pattern from quadrupedal to bipedal walking (Fig.2A), most neurons in all areas increased their firing frequency. Compared with quadrupedal locomotion, one of the prominent features was

that proportion of tonic and phasic-tonic cells in the SMA and PMd was larger in bipedal locomotion. In addition, 5 out of 7 cells in these areas, which had no modulatory firing during quadrupedal locomotion, showed tonic firing pattern during bipedal locomotion. In the PMd, a group of neurons generated bursting firing preceding the onset of bipedal locomotion as in the case of quadrupedal locomotion (Fig. 3B).

3-2. Changes in bipedal locomotor patterns following in-activation of motor cortical areas by muscimol injections

Further to elucidate functional roles played by each area, muscimol was selectively injected into trunk/hindlimb region of the M1, SMA and PMd. When muscimol was injected unilaterally into the M1 region, flaccid paresis was observed in the contralateral hindlimb without any postural disturbance. In contrast, bilateral injection of muscimol into the SMA region produced truncal or postural sway together with a tottering gait pattern, i.e., postural disturbance was prominently induced. However, such disturbance was not prominent if muscimol was injected unilaterally. When the PMd region was a target of muscimol injection, the animal could not initiate locomotion against either the presentation of rewards or abrupt movement of the treadmill belt. In this case, however, the monkey seemed to be able to start locomotion volitionally.

4. DISCUSSION

Firing properties of recorded neurons during standing and locomotor behaviors are summarized as follows: (1) Firing rate of most neurons in each area was lower when animal was standing with quadruped. (2) Immediately before initiating locomotion with either quadruped or biped, a population of PMd neurons started to discharge. (3) Neurons in M1 mainly exhibited rhythmic discharge during locomotion in relation to step cycles. (4) Majority of SMA neurons tonically discharged during locomotion. (5) Majority of PMd neurons displayed either phasic or phasic-tonic firing during locomotion. (6) Firing frequency of most neurons recorded in all three areas was higher in locomotion with biped than quadruped.

4-1. Descending signals from the cerebral cortex involved in the control of postural and locomotor synergies

It is generally agreed that rhythmic limb movements during locomotion are induced by the activity of central pattern generators (CPG) in spinal cord (Fig.4A) [11]. Therefore rhythmic firing of M1 neurons may not contribute to rhythmogenicity, but to modulate the excitability of target motoneurons and interneurons through corticospinal tract (Fig.4B) so that the excitability of spinal reflex loops of particular spinal segments could be appropriately regulated during locomotion. However, the M1 receives inputs from the somatosensory cortex, and from the basal ganglia and the cerebellum through thalamus. Modulated activity in the M1 may be attributed to cortical interconnections among the motor areas, somatosensory inputs or convergent inputs from the basal ganglia and the cerebellum. This could be the case in the SMA and PMd activity.

Neurons in the SMA tonically discharged during locomotion. The SMA is involved in programming the sequence

of movements through loops with the basal ganglia and cerebellum [7, 12, 13]. Output neurons in the SMA project to the midbrain and the pontomedullary reticular formation where basic neural structures responsible for controlling postural reflexes, postural muscle tone and locomotion are located [2]. Because muscimol injection into the SMA disturbed postural control during bipedal locomotion, the tonic firing property of the SMA neurons may contribute to the postural equilibrium during locomotion via brainstem and spinal cord pathways, particularly the reticulospinal tract (Fig.4C).

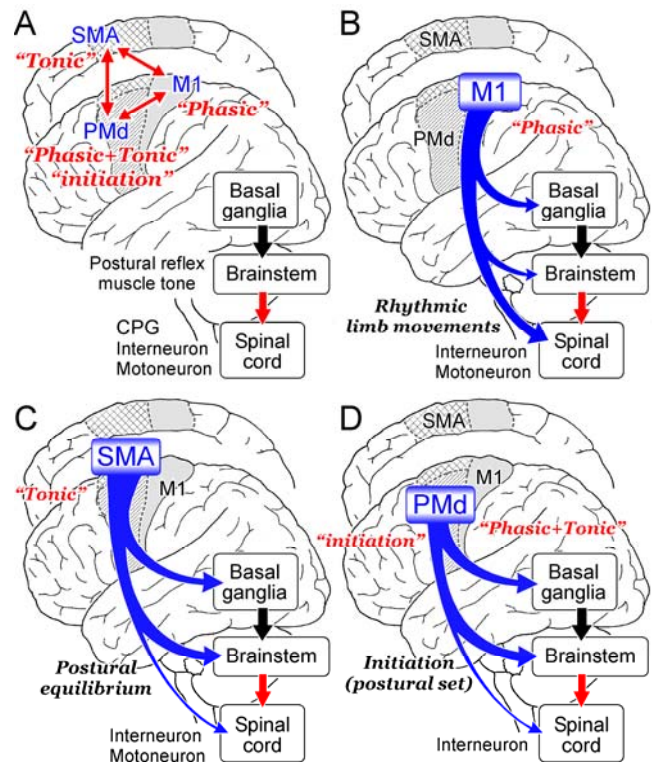


Figure 4 Possible neuronal mechanisms of cortical control of locomotor behaviors

A. Interconnections among cortical motor areas. B-D. Descending corticoreticular, corticostriatal and corticospinal locomotor control from the M1 (B), SMA (C), and PMd (D). See text for explanations.

A majority of PMd neurons displayed both tonic and phasic firing. We speculate that the firing property may be partly ascribed to the convergent inputs from the SMA and the M1. A small portion of the PMd neurons only transiently discharged before onset of locomotion. By injecting muscimol into the PMd, the monkey seemed unable to initiate locomotion that was triggered by external events, such as presentation of rewards (food) and alteration of somatosensory information generated by moving the treadmill. The PMd receives multimodal sensory inputs arising from the parietal cortex. This area, in turn, provides dense projections to the brainstem in addition to the basal ganglia (Fig.4D).

We have previously suggested that cortical motor areas control locomotor behaviors by direct cortico-brainstem projections and indirect projections via the basal ganglia to the brainstem [2]. The former provides glutamatergic excitatory drive and the latter provides GABAergic inhibitory control to the brainstem motor systems. Accordingly, an increase in the cortical activity may enhance the brainstem activity by

the direct excitation and by the indirect disinhibition.

It follows that the tonic activity in the SMA and PMd may be responsible for the generation of steady rhythmic limb movements and the maintenance of postural muscle tone during locomotion. On the other hand, transient firing of the PMd neurons may provide strong cortical excitation and transient reduction of the basal ganglia inhibition acting on brainstem motor systems, which lead to the “motor set” before initiation of locomotor movements.

In Parkinson disease patient, visual input improves gait disturbance such as frozen gait, fast-tiny steps and postural instability (paradoxical gait), and the visual input enhances the PMd activity, which may normalize locomotor program [7]. Accordingly, the PMd may play crucial role for initiation and programming of the locomotor behaviors.

4-2. Functional organization of cortical motor areas responsible for locomotor behaviors

In primates, there exist several cortical motor areas related to execution and control of voluntary movements in the frontal lobe. With respect to hand movements, these motor cortical areas have both functional and anatomical organizations [8, 9]. There are also dense inter-cortical connections among them (Fig.4A) [10]. As to the descending projection from these areas, the M1, SMA and PM project directly to the brainstem and/or spinal cord (Fig.4B-D) [8, 14].

In this study, neurons in the M1 (phasic), SMA (tonic) and PMd (phasic-tonic) showed different firing properties during locomotion. In addition, locomotor deficits produced by muscimol injection were peculiar to each of these areas. All these results prompt us carefully to discuss different functional roles played by each of these areas in the control of locomotor behaviors, although have not yet identified output of recorded neurons and samples are still small in number.

One of noteworthy findings is that most cortical neurons had higher firing rates during locomotion with biped than quadruped. This indicates that bipedal locomotion requires higher cortical activity. This finding agrees well with our preliminary results obtained by a positron emission tomography study showing that activity of the M1 and SMA in macaque monkeys has been more pronounced during bipedal than quadrupedal locomotion. We presume that the enhanced activity of the motor areas may strengthen contractions of postural muscles in trunk and hindlimbs so that the subject can maintain its body equilibrium during bipedal standing and locomotion.

5. SUMMARY & CONCLUSION

This study is the first to provide direct evidence that neurons in the trunk/hindlimb region of the cortical motor areas in primates contribute to the execution of quadrupedal and bipedal locomotion. Present findings suggest that each area plays specific role in the control of locomotor behaviors. The M1 is possibly involved in the rhythmic movements of contralateral hindlimb during locomotion. The SMA may play a role in the postural control, while the PMd may contribute to the initiation of locomotion in addition to the control of postural and locomotor (rhythmic leg movements)

synergies. Bipedal locomotion requires the intense activation of cortical motor areas than quadrupedal locomotion.

REFERENCES

- [1] V.B. Brooks: “What is Motor Control?” In: *The Neural Basis of Motor Control*. Oxford Univ. Press, pp. 5-17, (1986).
- [2] K.Takakusaki, K.Saitoh, H.Harada and M.Kashiwayanagi: “Role of basal ganglia-brainstem pathways in the control of motor behaviors”, *Neurosci. Res.*, vol. 50, pp.137-151 (2004).
- [3] K. Pearson, J. Gordon: “Locomotion” In: *Principles of Neural Science*, Chapter 37, (4th edition, Kandel ER, Schwartz JH, Jessell TM eds.), McGraw-Hill Press, New York pp 737-755 (2000).
- [4] T. Drew: “Motor cortical cell discharge during voluntary gait modification”. *Brain Res.* 457: 181-187 (1988).
- [5] P.A.Pahapill and A.M.Lozano: “The pedunculopontine nucleus and Parkinson’s disease”, *Brain*, vol.123, pp.1767-1783, (2000)
- [6] C.D. Marsden: The mysterious motor function of the basal ganglia: The Robert Wartenberg Lecture. *Neurology* 32, 514-539 (1982)
- [7] T.Hanakawa, Y.Katsumi, H.Fukuyama, M.Honda, T. Hayashi, J.Kimura and H.Shibasaki: “Mechanisms of underlying gait disturbance in Parkinson’s disease: a single photon emission computed tomography study”, *Bain*, vol.122, pp.1271-1281, (1999).
- [8] R.P. Dum, P.L. Strick; “The corticospinal system: a structural framework for the central control of movement”. In: *Handbook of physiology*, Sec 12, Exercise: regulation and integration of multiple systems (Rowell LB, Shepard JT, eds), pp 217–254. New York: American Physiological Society (1996).
- [9] J. Tanji: Sequential organization of multiple movements: involvement of cortical motor areas. *Annu. Rev. Neuroci.* 24: 631-651 (2001)
- [10] R.P. Dum, P.L. Strick: Frontal lobe inputs to the digit representations of the motor areas on the lateral surface of the hemisphere. *J. Neurosci.*, 25:1375–1386 (2005)
- [11] S. Grillner: “Control of locomotion in bipeds, tetrapods, and fish”. In: Brooks, V.B. (Ed.), *The Nervous System II*, Am. Physiol. Soc. Press, Bethesda, pp. 1179-1236 (1981).
- [12] G.E.Alexander,M.R.Delong, P.E.Strick: “Parallel organization of functionally segregated circuits linking basal ganglia and cortex,” *Ann. Rev. Neurosci.*, vol.9, pp.357-381, (1986).
- [13] F.A.Middleton, P.L.Strick: “Basal ganglia and cerebellar loops: motor and cognitive circuits”, *Brain Res. Rev.* 31, 236-250 (2000).
- [14] K. Keizer, H.G.J.M Kuypers: “Distribution of corticospinal neurons with collaterals to the lower brain stem reticular formation in Monkey (*Macaca fascicularis*),” *Exp. Brain. Res.*, 74: 311-318 (1989).

System Biomechanics of locomotion in the Japanese monkey: Exploration of principal mechanism for generating adaptive locomotion based on a neuro-musculoskeletal model

Naomichi Ogihara, Shinya Aoi, Yasuhiro Sugimoto, Masato Nakatsukasa, and Kazuo Tsuchiya

I. INTRODUCTION

Animals are capable of generating locomotion adaptive to diverse environments by coordinately controlling complex musculoskeletal systems. Mechanisms underlying the emergence of such intelligent adaptive behavior have conventionally been attributed to the sophisticated control mechanism of a biological sensorimotor nervous system. However, the suggestion has recently been made that animals achieve such adaptive yet efficient locomotion by exploiting intrinsic designs and properties of the musculoskeletal structures acquired through evolutionary history. A fundamental limitation may thus exist in attempts to clarify how the nervous system adaptively functions during locomotion based solely on neurophysiological studies; towards elucidating the mechanisms, the mechanisms of information processing emerging from appropriate dynamic interactions among the neuro-control system, musculoskeletal system and environment must be thoroughly investigated.

The present study constructed a biologically plausible computer simulation of animal locomotion by integrating physiological findings from the locomotor nervous system and the anatomy and biomechanics of the musculoskeletal system, with the aim of illuminating the dynamic principles underlying the emergence of adaptive locomotion in animals. Particular focus was placed on modeling quadrupedal and bipedal locomotion in the Japanese monkey (*Macaca fuscata*), as Japanese monkeys have recently been used for neurophysiological studies on adaptive locomotor mechanism [1-2], allowing direct comparisons between experimental data and simulation results. Moreover, the transition from quadrupedalism to bipedalism in Japanese monkeys is regarded to some extent as a modern analogue of the evolution of bipedal locomotion and therefore offers an interesting subject for research in the field of physical anthropology [3-7]. Furthermore, inferences gained by analyses of phylogenetically close animals such as primates might be more directly extensible to the understanding of human locomotion and associated clinical applications.

We call this constructive approach to elucidate the locomotor intelligence in the dynamic interactions among body, brain and environment “system biomechanics”. While conventional biomechanics studies mechanical behaviors and loads imposed

on the musculoskeletal system from a mechanical engineering perspective, system biomechanics treats the combination of musculoskeletal and neuro-information processing systems as a dynamic system, and analyzes the mechanisms underlying the emergence of adaptive locomotion based on system methodology. Obviously, the mechanics of the musculoskeletal system constitute a crucial element of the dynamical system, so the system biomechanics are inclusive of conventional biomechanics.

Herein we report current progress in our system biomechanics study of quadrupedal/bipedal locomotion in the Japanese monkey, i.e., three-dimensional gait analysis and forward dynamic simulation based on an anatomically based whole-body musculoskeletal model.

II. WHOLE-BODY ANATOMICAL MODEL OF JAPANESE MONKEY

For a realistic representation of body motion, a fresh cadaver of an adult male Japanese monkey underwent whole-body computed tomography, and a total of 1935 cross-sectional images were obtained, and three-dimensional (3D) surface models of the entire skin surface and skeletal system were constructed. The skeleton was divided into the following bone segments: head; thorax (with cervical vertebrae); lumbar vertebrae; pelvis; scapula; humerus; ulna; radius; hand (carpals and metacarpals); femur; tibia (with fibula); and foot (tarsals and metatarsals). A bone coordinate system embedded in each of the bones was defined by principal axes. Each joint was approximated as a combination of hinge joints, joint centers and rotational axes estimated by joint morphology based on joint surface approximation using a quadric function. Joint centers were determined from the position of the apex of the fitted quadric surface and the two principal radii of curvature at the apex, and rotational axes were determined from the

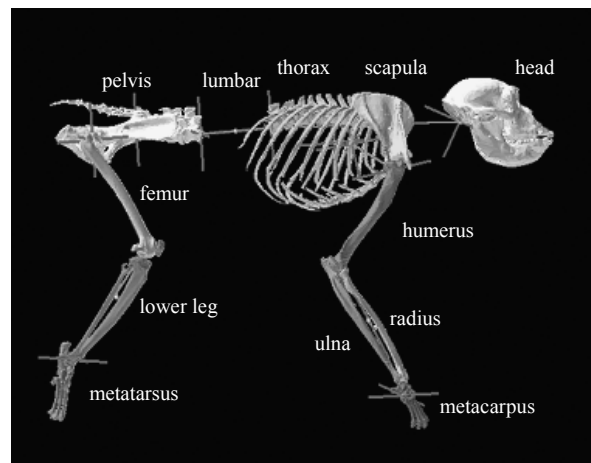


Fig 1. Kinematic description of the whole body skeleton of a Japanese monkey as a chain of links. Only right fore- and hindlimb are shown.

N. Ogihara and M. Nakatsukasa are with Laboratory of Physical Anthropology, Graduate School of Science, Kyoto University, Kitashirakawa-oiwakecho, Sakyo, Kyoto 606-8502, Japan (e-mail: {ogihara, nakatsuk}@anthro.zool.kyoto-u.ac.jp).

S. Aoi, Y. Sugimoto, and K. Tsuchiya are with Department of Aeronautics and Astronautics, Graduate School of Engineering, Kyoto University, Yoshida-honmachi, Sakyo, Kyoto 606-8501, Japan (e-mail: {shinya_aoi, yas, tsuchiya}@kuaero.kyoto-u.ac.jp).

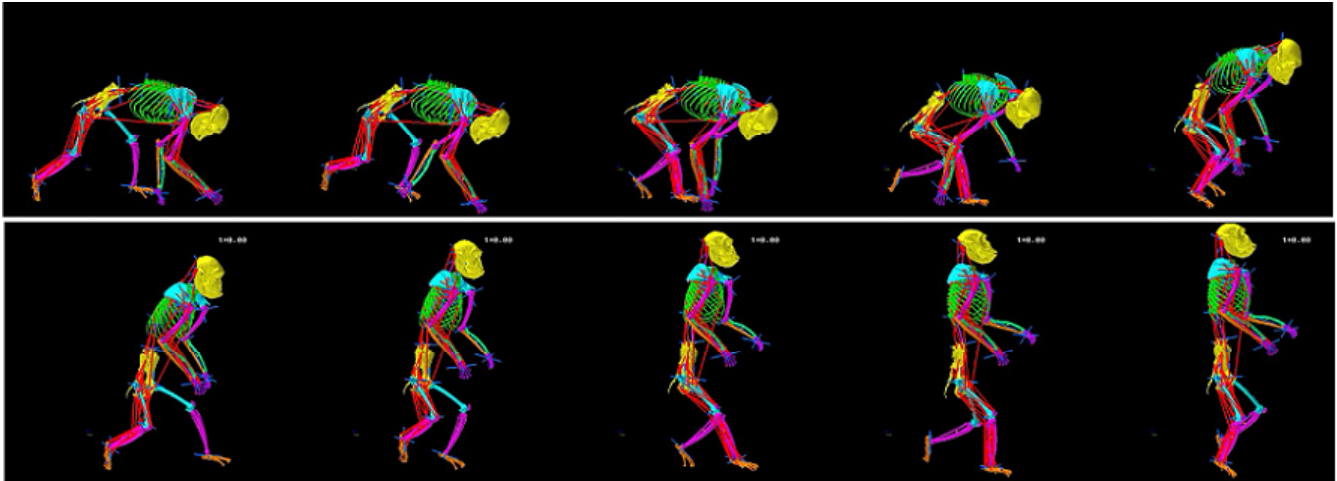


Fig 2. Reconstructed whole-body kinematics of a Japanese monkey in transition from quadrupedal to bipedal walking.

principal directions in which the principal curvatures occurred. A kinematic skeleton of the Japanese monkey was thus mathematically described as a chain of 20 links connected by revolute joints as illustrated in Figure 1. Joints connecting the trunk segments (head, thorax, lumbar vertebrae and pelvis) were represented as 3-degree-of-freedom (DOF) joints. The scapula is usually modeled to be immobile with respect to the thorax, although the relationship between scapula and forelimb is functionally equivalent to that of the femur and hindlimb, thus representing an important element for propulsion [8]. A new approach was thus used to mathematically model translational motion of the scapula along the rib cage using 3 revolute joints. Shoulder (glenohumeral), elbow, radioulnar, and wrist joints were modeled as 2-, 1-, 1- and 2-DOF joints, respectively. Hip, knee and ankle joints were represented as 3-, 1- and 2-DOF joints, respectively. The total number of DOF for the skeletal system was thus 45. As a result of morphologically accurate description of the joint kinematics based on quadric function approximation, rotational axes of the joints did not coincide with bone coordinate axes, unlike robots.

To calculate inertial properties necessary for biomechanical studies (i.e., mass, position of the center of mass of the segment, and inertial tensor about the center of mass), the body surface was divided into 20 segments by planes passing through the joint centers. One exception was the scapular segment, which was separated from the thoracic volume by a rounded surface so as to include muscles of the shoulder girdle. Inertial properties of the segment were then numerically calculated using 3D CAD software, assuming that segment composition is homogeneous and density is 1.0 g/cm^3 . This resulted in a body mass of 10.0 kg, nearly equal to the average body mass of an adult male Japanese monkey.

Several studies have quantified the musculature of the Japanese monkey [9-10]. However, no complete quantitative data on whole-body musculature have been reported. A fresh cadaver of a female Japanese monkey was thus dissected to mathematically describe the path of each muscle and the associated capacity to generate force. Each muscle in the fore- and hindlimbs was carefully exposed and points of origin and insertion were observed. The muscle was then removed and mass and fascicle length were systematically recorded to calculate physiological cross-sectional area (PCSA). The path

of each muscle was defined using a series of points connected by line segments. Capacity of each muscle to generate force was assumed to be proportional to PCSA. Each muscle was basically modeled as a line segment connecting origin and insertion.

III. GAIT ANALYSIS USING THE MUSCULOSKELETAL MODEL

Locomotion is an elaborate physical phenomenon generated by dynamic interactions between a complex chain of musculoskeletal elements and the changing outside world. To understand the mechanism underlying the generation of adaptive locomotion, actual locomotion must be thoroughly investigated from the outset. For this reason, a male Japanese monkey (9-years-old) walking quadrupedally/bipedally on a treadmill at 3 km/h was videotaped using 4 digital cameras and locomotion was analyzed. A total of 16 reflexive markers (8 on one side) were placed at: 1) head of 5th metatarsal; 2) lateral malleolus of fibula; 3) lateral epicondyle of femur; 4) greater trochanter; 5) acromion; 6) lateral epicondyle of humerus; 7) styloid process of ulna; and 8) head of 5th metacarpal. These markers were manually digitized frame-by-frame and the coordinates of markers were calculated using 3D motion analysis software. The change in position of each coordinate over time was low-pass filtered at 8 Hz.

If the musculoskeletal model described could be matched to the temporal history of digitized marker coordinates, all body



Fig 3. Synchronous measurement of locomotor kinematics and kinetics using a new treadmill in which a force plate could be embedded.

skeletal motion could be reconstructed as in video fluoroscopy. For this, the musculoskeletal model was firstly scaled to the size of the monkey in the video based on segment lengths, and the 45 DOF of the skeletal system were adjusted frame-by-frame to minimize the sum of distances between corresponding markers while minimizing deviations of joint angles from the anatomically natural position (midpoints of the ranges of joint rotations). The quasi-Newtonian method was used to solve this minimization problem. Figure 2 illustrates results of matching, indicating that the whole-body kinematics of a Japanese monkey walking on a treadmill was successfully reconstructed using an anatomically based musculoskeletal model and the model-based matching technique. To determine the position and orientation of any bone segment, 6 DOF have to be defined. As a result, 16 marker coordinates are insufficient to prescribe the complete posture of the entire skeleton. However, by introducing kinematic constraints defined by joint morphology, the present study successfully yielded anatomically reasonable, natural skeletal motion from a limited number of external markers. Unrealistic solutions such as dislocation and collision were thus avoided.

Reconstruction of skeletal motion contributes to interpretation and comprehension of locomotor mechanisms. From this reconstructed skeletal motion, changes in state variables of muscles such as muscle length and contractile velocity during locomotion can be estimated. If a ground reaction force profile could be measured in synchronization with kinematic data, joint torque profiles could be calculated based on calculation of inverse dynamics. Furthermore, muscular force profiles in addition to motor command profiles sent to muscles during locomotion could also be estimated if a mechanical model of the muscle were employed. Conversely, activity profiles of exteroceptors such as cutaneous receptors on the plantar surface of a foot and proprioceptors such as muscle spindles and Golgi tendon organs could also be roughly estimated from changes in state variables and forces in the musculoskeletal model. Overall behavior of the peripheral sensorimotor nervous system might thus be macroscopically reconstructed from the measurable set of kinematic and kinetic data. We planned to approach the information processing of locomotion by analyzing correlations among estimated neural activities. For this reason, a new treadmill was constructed in

which a force plate could be embedded, and we started to synchronously capture locomotor kinematics and kinetics (Fig. 3).

IV. FORWARD DYNAMIC SIMULATION OF LOCOMOTION

Animal locomotion, including that of primates, is generally accepted as being generated by a rhythm-generating neuronal network in the spinal cord known as the central pattern generator (CPG), with locomotion evoked by stimulus input from the mesencephalic locomotor region in the brainstem [11-13]. However, rhythmic signals produced by the CPG alone do not generate adaptive locomotion. Afferent proprioceptive information is also essential for generating locomotion, and must be mutually coordinated in the spinal cord to construct appropriate intra- and interlimb coordination.

Exactly what are encoded specifically in the output and state variables of the CPG remain unclear. However, recent neurophysiological studies on spinocerebellar neurons have reported that sensory feedback signals from proprioceptors in muscles and joints are integrated in the spinal circuitry to encode global parameters of the limb movement, i.e., orientation and length of the axis connecting the most proximal joint and the distal position of a limb (limb axis) [14-16]. This finding implies that global parameters describing limb kinematics, along with individual local proprioceptive inputs, are actually utilized as important sensory inputs for locomotion.

Conversely, limb movements such as kicking and locomotion are also suggested to be generated by a combination of small numbers of invariant synergistic muscle activation patterns, each created by a functional module located in the spinal cord. Control of such combination patterns alters movement kinematics, i.e., position and direction of limb movement [17-19]. Grasso et al. also suggested that muscle activation patterns in locomotion were generated primarily based on kinematics, after demonstrating that the kinematic patterns of human forward and backward locomotion are basically the same while muscle activations are quite different [20]. Furthermore, activities of Purkinje cells in the cerebellum during arm movement, typically linked to arm dynamics, have recently been suggested to represent kinematic information of

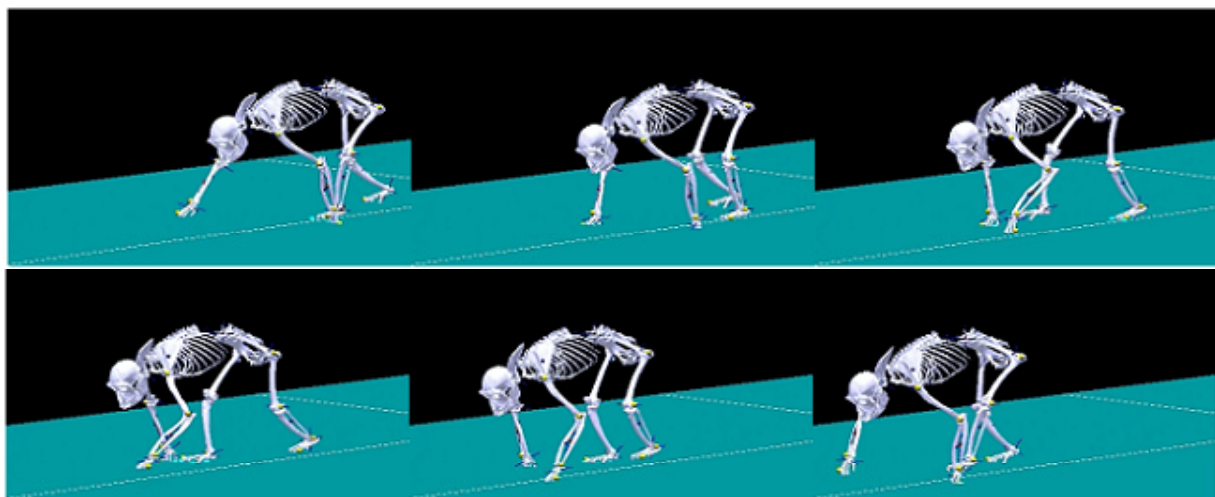


Fig 4. Forward dynamic simulation of quadrupedal locomotion of a Japanese monkey based on the musculoskeletal model.

hand movements, indicating that muscle activation patterns are generated primarily based on global kinematic parameters at the spinal cord level, even in arm movements [21].

These findings suggest that: 1) in the spinal cord, a global parameter may exist representing limb kinematics, i.e., orientation and length of the limb axis, and this global representation is used for coordinated control of the limb musculoskeletal system and information exchange between central and peripheral nervous systems; 2) state variables of the CPG may represent the phase of global limb kinematics, and muscle activation patterns are generated based on these variables at the spinal modules; and 3) phase dynamics of the CPG network are autonomously regulated by mutual interactions among CPGs in addition to global sensory information, to adapt to various environments and cope with external perturbations.

In this study, the CPG was thus hypothesized to represent a set of oscillators corresponding to each of the limbs and the trunk segment, and phase of the oscillator was considered to encode the orientation and length of the limb axis, with the spinal circuitry of interneurons somehow generating muscle activation patterns based on output signals from the CPG. For now, we modeled this transformation using a PD feedback control law, and joint torque was applied instead of muscle force to generate locomotion. Orientation and length profiles of limbs were provided based on measured kinematic data (Fig. 2). Phase of the CPG was reset in response to the timing of hand/foot-ground contacts. To realize coordinated interlimb movements, appropriate dynamic interactions among the oscillators were assumed.

Figure 4 illustrates the generated quadrupedal locomotion pattern. Although many problems remain, the results show that locomotion was successfully generated due to dynamic interactions among the body mechanical system, the nervous system consisting of the oscillators, and the environment. The importance of computer simulation studies based on biologically relevant neuro-musculoskeletal modeling has gained particular emphasis in recent years for truly elucidating adaptive mechanisms of locomotion in animals [22-23]. Based on our current model, we aim to further improve our simulation study, particularly that of the locomotor neuro-control system with the collaboration of neurophysiologists to achieve biologically plausible simulations.

V. CONCLUSION

Herein we report our system biomechanics studies of quadrupedal/bipedal locomotion in the Japanese monkey based on an anatomically based whole-body musculoskeletal model. Such a physically realistic musculoskeletal model may reproduce actual mechanics of the body system during locomotion, allowing in-computer analysis of locomotor mechanisms. We hope to elucidate the dynamic principles underlying the emergence of adaptive locomotion by analyzing the behavior of neuro-musculoskeletal dynamics recreated in a computer from a system engineering perspective.

ACKNOWLEDGMENT

We would like to express our gratitude to all the staff of the

Suo Monkey Performance Association for their generous collaborations in experiments.

REFERENCES

- [1] F. Mori, K. Nakajima, A. Tachibana, C. Takasu, M. Mori, T. Tsujimoto, H. Tsukada and S. Mori, "Reactive and anticipatory control of posture and bipedal locomotion in a nonhuman primate", *Progress in Brain Research*, vol. 143, pp.191-198, 2004.
- [2] K. Nakajima, F. Mori, C. Takasu, M. Mori, K. Matsuyama and S. Mori, "Biomechanical constraints in hindlimb joints during the quadrupedal versus bipedal locomotion of M-fuscata", *Progress in Brain Research*, vol. 143, pp.183-190, 2004.
- [3] S. Hayama, M. Nakatsukasa and Y. Kunimatsu, "Monkey performance: The development of bipedalism in trained Japanese monkeys", *Acta Anatomica Nipponica*, vol. 67, pp.169-185, 1992.
- [4] E. Hirasaki, N. Ogihara, Y. Hamada, H. Kumakura and M. Nakatsukasa, "Do highly trained monkeys walk like humans? A kinematic study of bipedal locomotion in bipedally trained Japanese macaques", *Journal of Human Evolution*, vol. 46, pp.739-750, 2004.
- [5] M. Nakatsukasa, N. Ogihara, Y. Hamada, Y. Goto, M. Yamada, T. Hirakawa and E. Hirasaki, "Energetic costs of bipedal and quadrupedal walking in Japanese Macaques", *American Journal of Physical Anthropology*, vol. 124, pp.248-256, 2004.
- [6] N. Ogihara, H. Usui, E. Hirasaki, Y. Hamada and M. Nakatsukasa, "Kinematic analysis of bipedal locomotion of a Japanese macaque that lost its forearms due to congenital malformation", *Primates*, vol. 46, pp.11-19, 2005.
- [7] M. Nakatsukasa, E. Hirasaki, and N. Ogihara, "Energy expenditure of bipedal walking is higher than that of quadrupedal walking in Japanese macaques", *American Journal of Physical Anthropology*, vol. 131, pp.33-37, 2006.
- [8] M.S. Fischer, "Locomotory organs of mammals: New mechanics and feed-back pathways but conservative central control", *Zoology*, vol. 103, pp.230-239, 2001.
- [9] H. Ishida, "On the muscular composition of lower extremities of apes based on the relative weight (in Japanese)", *Journal of Anthropological Society of Nippon*, vol. 80, pp.125-142, 1972.
- [10] K. Fujino, "Statics and function of the shoulder muscle morphology in macaques: A three-dimensional analysis and its theoretical basis (in Japanese)", *Primate Research*, vol. 12, pp.113-131, 1996.
- [11] S. Grillner, "Locomotion in vertebrates: central mechanisms and reflex interaction", *Physiological Reviews*, vol. 55, pp.274-304, 1975.
- [12] M.L. Shik and G.N. Orlovsky, "Neurophysiology of locomotor automatism", *Physiological Reviews*, vol. 56, pp.465-501, 1976.
- [13] E. Eidelberg, J.G. Walden and L.H. Nguyen, "Locomotor control in macaque monkeys", *Brain*, vol. 104, pp.647-663, 1981.
- [14] G. Bosco and R.E. Poppele, "Proprioception from a spinocerebellar perspective", *Physiological Reviews*, vol. 81, pp.539-568, 2001.
- [15] R.E. Poppele, G. Bosco and A.M. Rankin, "Independent representations of limb axis length and orientation in spinocerebellar response components", *Journal of Neurophysiology*, vol. 87, pp.409-422, 2002.
- [16] R. Poppele and G. Bosco, "Sophisticated spinal contributions to motor control", *Trends in Neurosciences*, vol. 26, pp.269-276, 2003.
- [17] E. Bizzi, M.C. Tresch, P. Saltiel and A. d'Avella, "New perspectives on spinal motor systems", *Nature Reviews Neuroscience*, vol. 1, pp.101-108, 2000.
- [18] A. d'Avella, P. Saltiel and E. Bizzi, "Combinations of muscle synergies in the construction of a natural motor behavior", *Nature Neuroscience*, vol. 6, pp.300-308, 2003.
- [19] Y.P. Ivanenko, R.E. Poppele and F. Lacquaniti, "Motor control programs and walking", *Neuroscientist*, vol. 12, pp.339-348, 2006.
- [20] R. Grasso, L. Bianchi and F. Lacquaniti, "Motor patterns for human gait: Backward versus forward locomotion", *Journal of Neurophysiology*, vol. 80, pp.1868-1885, 1998.
- [21] S. Pasalar, A.V. Roitman, W.K. Durfee and T.J. Ebner, "Force field effects on cerebellar Purkinje cell discharge with implications for internal models", *Nature Neuroscience*, vol. 9, pp.1404-1411, 2006.
- [22] K. Pearson, O. Ekeberg and A. Buschges, "Assessing sensory function in locomotor systems using neuro-mechanical simulations", *Trends in Neurosciences*, vol. 29, pp.625-631, 2006.
- [23] A. Frigon and S. Rossignol, "Experiments and models of sensorimotor interactions during locomotion", *Biological Cybernetics*, vol. 95, pp.607-627, 2006.

Group B-3: Realization of Adaptive Locomotion based on Dynamic Interaction between Body, Brain, and Environment

Koh Hosoda, Graduate School of Engineering, Osaka University
Hiroshi Kimura, Graduate School of Information Systems, University of Electro-Communications
Katsuyoshi Tsujita, Faculty of Engineering, Osaka Institute of Technology
Kousuke Inoue, Faculty of Engineering, Ibaraki University

Abstract—The behavior of a robot is emerged from the interaction between body, control, and environmental dynamics. The research group B-3 aims to design body and control dynamics for emerging adaptive locomotion. We investigate three types of locomotion, biped, quadruped, and snake-like and developed robots. In 2006, we have realized Walking speed control by tuning tonus, jumping and running experiments of a biped robot, Oscillator-controlled Bipedal Walk with Pneumatic Actuators, adaptive running of a quadruped robot, and construction of a snake-like robot mimicking musculo-skeleton system of snakes.

I. INTRODUCTION

The research program entitled Emergence of Adaptive Motor Function through Interaction between Body, Brain, and Environment - Understanding of Mobiligence by Constructive Approach - started in 2005, as a MEXT Grant-in-Aid for Scientific Research on Priority Areas. One of the main goals of the project is to find a principle of emergence of adaptive locomotion. To approach the issue from the constructivist viewpoint, our research group B-3 aims to develop locomotive agents with various modalities based on dynamic interaction between body, control and environment.

In 2006, we have realized Walking speed control by tuning tonus, jumping and running experiments of a biped robot, Oscillator-controlled Bipedal Walk with Pneumatic Actuators, adaptive running of a quadruped robot, and construction of a snake-like robot mimicking musculo-skeleton system of snakes.

II. WALKING SPEED CONTROL BY TUNING TONUS

When a biped robot is controlled by electric motors, its speed is determined by the given desired trajectory of each joint. However, in human walking, walking speed is emerged by the interaction between body, control, and environment. Especially, the body tonus plays a great role to change the speed. Emergence of walking by such interaction between the body tonus and the environment is supposed to be a key issue for realizing adaptive walking.

In this section, experimental results of a biped robot driven by pneumatic actuators (Fig.1) demonstrate that it can change the walking velocity by regulating the tonus of the joints.

The valve operation for walking is shown in Fig.2. After the touch information of a foot, the agonistic actuator is supplied with the compressed air for T_s [s], and then, the valve is closed. Whereas, the antagonistic actuator is expelled



Fig. 1. A biped robot driven by agonistic and antagonistic pneumatic actuators

for T_e [s], and then, the valve is closed. The relation between the walking speed and the control parameters T_s and T_e is shown in Fig.3. T_e has a strong relation with the tonus of the hip joint. From Fig.3, the walking speed increases when the joint tonus is high.

III. JUMPING AND RUNNING EXPERIMENTS OF A BIPED ROBOT

An antagonistic muscle mechanism that can regulate the joint compliance contributes enormously to human dynamic locomotion. The antagonism is supposed to be a key to realize more than one locomotion mode. In this paper, we demonstrate how antagonistic pneumatic actuators are utilized for three dynamic locomotion modes of a biped robot, walking, jumping, and running.

To demonstrate the effectiveness, a biped robot is built by utilizing McKibben pneumatic actuators (Fig.4). Since we intend to utilize the dynamics of the robot, we adopt simple feedforward manner valve operation initiated by touch information for each locomotion mode. Then, we mainly investigate the relation between the joint compliance realized by the antagonistic drive and the resultant behavior.

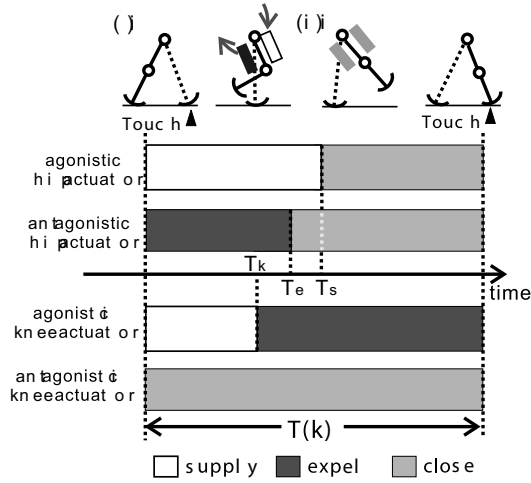


Fig. 2. Valve operation for walking with a compliant hip joint

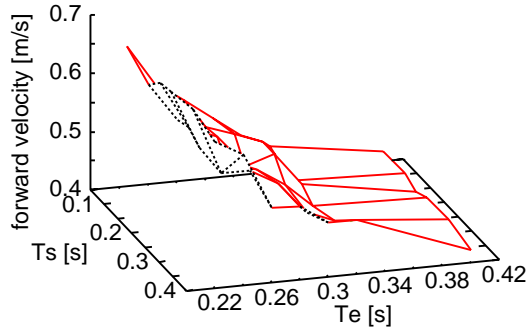


Fig. 3. Relationship between supply duration of agonistic hip actuator T_s , expel duration of antagonistic hip actuator T_e , and walking velocity

IV. OSCILLATOR-CONTROLLED BIPEDAL WALK WITH PNEUMATIC ACTUATORS

Bipedal locomotion has two essential stages in leg motions. One is swinging stage and the other is supporting stage. In the swing stage, the actuator forces are relaxed; stiffness of the joints decreases and becomes passive. When in the supporting stage, stiffness of the joints increases due to generated forces of the antagonistic pair of actuators. By controlling and tuning the stiffness of the joints through the balanced adjustment of the generated force of such pair of actuators, it is expected that the robot obtains adaptability to variances of the environment or of physical properties of the ground surface.

This section deals with development of oscillator controller for the bipedal robot with antagonistic pairs of pneumatic actuators. In the proposed controller, nonlinear oscillators are assigned for each joint. Periodic motions of the legs are switched between swinging stage and supporting stage according to the phase of oscillators. Oscillators compose network architecture and have mutual interactions to each other. These oscillators receive touch sensor signals at the end of the legs when the end of the leg touches the ground as feedback signals. At the contact moment of the leg,

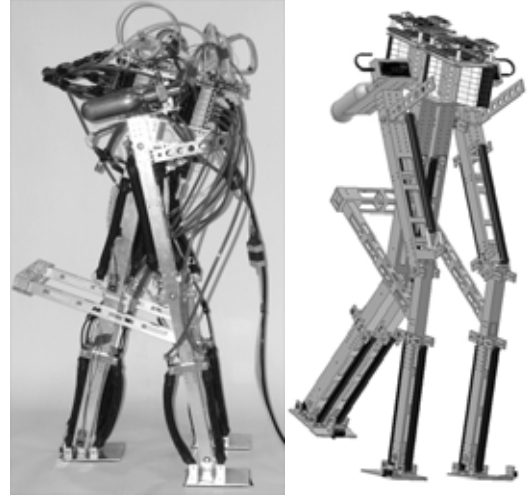


Fig. 4. A biped robot driven by agonistic and antagonistic pneumatic actuators for running and jumping



Fig. 5. Jumping experiment: the flight time and height were 270[ms] and 120[mm], respectively. Air pressure was 0.6[MPa]. The robot could jump several times.

the oscillator phase is reset, and swinging stage is forced to change to supporting stage. These dynamic interactions make mutual entrainments between oscillators and compose a steady limit cycle of the total periodic dynamics of the bipedal locomotion.

A. Control Architecture

The controller has a nonlinear oscillator network with individual oscillators assigned to joints. The antagonistic pairs of pneumatic actuators are driven by timing signals as functions of the oscillator phases. The contact sensor signals are feedback for the oscillator network. These dynamic interactions cause the entrainment and generate a stable limit cycle for locomotion. With the oscillator phase defined as $\phi_m^{(k)}$, the oscillator network can be expressed in the following equations;

$$z_m^k = \exp(j\phi_m^{(k)}) \quad (1)$$

$$\dot{\phi}_m^{(k)} = \omega + K(\phi_m^{(l)} - \phi_m^{(k)} - \gamma_{lk}) + \delta(\phi_{Ak} - \phi_m^{(k)}) \quad (2)$$

$$\gamma_{12} = \gamma_{21} = \pi \quad (3)$$

$$T_{mn}^{(k)} = F(\phi_m^{(k)}) \quad (4)$$

Fig.7 shows the results of the numerical simulation and indicates walking cycle time. We found that the system



Fig. 6. Running experiment: the flight time and speed were 0.12[s] and 1.13[m/s], respectively. Air pressure was 0.6[MPa]. It could run 5 steps at most.

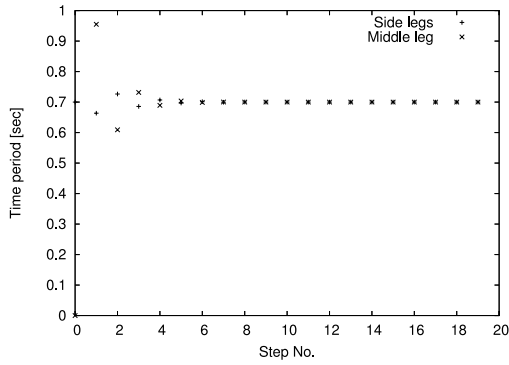


Fig. 7. Walking cycle of a CPG driven biped robot

reached a stable limit cycle and achieved steady locomotion with the proposed control system. Fig.8 shows the actual cycle times when the nominal time periods for the oscillators are changed during locomotion. These results show that the system can continue stable locomotion over various lengths of time. This means the system has a considerably wide basin of attraction for limit cycle.

V. ADAPTIVE RUNNING OF A QUADRUPED ROBOT

We tried the design and stability analysis of a simple quadruped running controller that could autonomously generate steady running of a quadruped with good energy

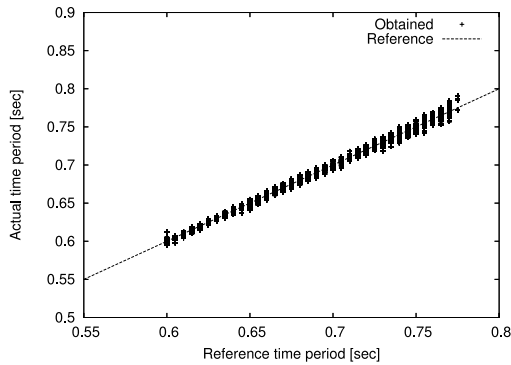


Fig. 8. Basin of attraction of walking cycle of a CPG driven biped robot

efficiency and suppress such disturbances as irregularities of terrain. In this study, we first considered the fixed point of quasi-passive running based on a sagittal plane model of a quadruped robot. Next, we regarded friction and collision as disturbances around the fixed point of quasi-passive running, and proposed an original control method to suppress these disturbances.

A. Motion Generation and Control

1) *Rhythm Generator*: We define the phase of each leg in the n^{th} step ϕ_l as expressed by Eq.(5). The timing for each leg to switch between the stance and swing phase is: $\phi_l > 0$:swing phase, $\phi_l \leq 0$:stance phase.

$$\phi_l = \sin(\omega_l[n]t + \psi_l) + \phi_{0l}, \quad \omega_l[n] = \frac{2\pi}{T_l[n]} \quad (5)$$

where $T_l[n]$ and $\omega_l[n]$ are the cyclic period and the angular frequency of the leg l in the n^{th} step, respectively. The initial phase ψ_l is defined for the generation of the gait¹. The offset ϕ_{0l} determines the duty factor. $T_l[n]$ is calculated by using the Delayed Feedback Control (DFC) method described in Section V-A.3.

2) *Torque Generator*: Depending on the leg phase ϕ_l generated by the rhythm generator, following different control actions are assigned.

- In the swing phase ($\phi_l > 0$), the PD control expressed by Eq.(6) is performed.

$$\tau_l(t) = -K_p(\gamma_l - \gamma_l^{td}) - K_d\dot{\gamma}_l \quad (6)$$

- In the stance phase ($\phi_l \leq 0$), constant torque $\tau_l^{st}[n]$ of the hip joint in each leg is output, as expressed by Eq.(7).

$$\tau_l(t) = \tau_l^{st}[n] \quad (7)$$

In the control action of the swing phase, γ_l^{td} is the touchdown angle corresponding with the fixed point. K_p and K_d are the gains of PD control. In the control action of the stance phase, the DFC method described in Section V-A.3 determines $\tau_l^{st}[n]$.

3) *DFC Using Stance Phase Period*: We use the following definitions to express the state variables (\mathbf{x}) and the measured variables (\mathbf{y}) of discrete dynamical system.

$$\mathbf{x}[n] = [T_f[n], T_h[n], \tau_f[n], \tau_h[n]]^T \quad (8)$$

$$\mathbf{y}[n] = [t_f^{st}[n], t_h^{st}[n]]^T \quad (9)$$

where $t_l^{st}[n]$ represents the n^{th} stance phase period measured by a contact sensor. We use this stance phase period to propose the following DFC methods.

$$T_l[n+1] = T_l[n] - K_{DF.T}(t_l^{st}[n] - t_l^{st}[n-1]) \quad (10)$$

$$\tau_l^{st}[n+1] = \tau_l^{st}[n] - \delta(l)K_{DF.\tau}(t_l^{st}[n] - t_l^{st}[n-1]) \quad (11)$$

$$\delta(l) = \begin{cases} -1, & l = f : foreleg \\ 1, & l = h : hindleg \end{cases}$$

¹The bounding gait: $\psi_f = 0$, $\psi_h = \pi$ and the pronking gait: $\psi_f = \pi$, $\psi_h = \pi$, where 0 and π mean that the leg begins to move from the swing phase and stance phase, respectively.

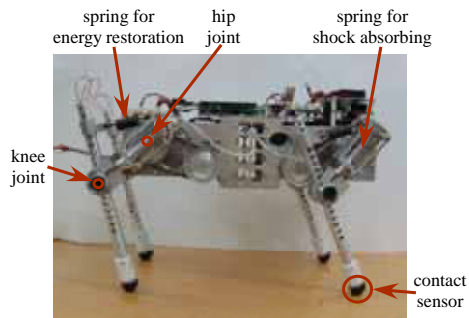


Fig. 9. Quadruped robot: Rush. The size is 30 (cm) in length and 20 (cm) in width. The height of leg is 20 (cm). The total weight is 4.3 (Kg).



Fig. 10. Snapshots of Rush running over a step in the bounding gait.

where $K_{DF.T}$ and $K_{DF.\tau}$ are DFC gains. Eq.(10) and Eq.(11) are used to calculate the cyclic period of the leg phase and hip joint torque of the next stance phase, respectively. $K_{DF.T}$ and $K_{DF.\tau}$ are determined by trial and error in simulations and experiments.

The effectiveness of the proposed control method was validated by simulations.

B. Experiments

We developed a quadruped robot; Rush (Fig.9). Each leg of Rush has two rotational joints (i.e. hip and knee) and a contact sensor at the toe. At this moment, Rush is not power autonomous, and a rate gyro sensor is not equipped. A DC motor of 27.5 (W) power with 19 reduction ratio is equipped at hip joint. Knee joint is passive.

We applied the control method above described to Rush. The control parameters and the initial values of the DFC method used in the experiment were same with those in the simulation. Rush successfully shifted from the standing to the steady running. Rush autonomously run over a step 2cm in height while just using contact sensor information. The snapshots of running are shown in Fig.10.

At low and medium speeds, the rhythm generator was dominant and it was possible to realize the generation of the bounding gait from the standing and the energy accumulation by the mutual entrainment. At high-speed running, the role of the rhythm generator became small since the spring mechanism mostly generated the rhythm of the steady running.

VI. CONSTRUCTION OF A SNAKE-LIKE ROBOT MIMICKING MUSCLO-SKELETRO SYSTEM OF SNAKES

Snakes have long cord-shaped body and propel by winding its body to generate mechanical interaction with the environment (friction and pressure between abdomen or side of the



Fig. 11. A Snake robot prototype driven by pneumatic actuators

body and the environment). This locomotion is essentially different from other legged animals. Based on this type of locomotion, living snakes exhibit highly adaptive behaviors in diverse environments such as rough ground, water, mud, sand, or tree branches. By investigating mobiligence of snakes underlying such adaptability, information about dependencies of intelligence to locomotion types can be obtained.

In this fiscal year, as a first-step to throw light on mobiligence in snakes, firstly we are developing a new snake-like robot with flexible body structure based on anatomy and bio-mechanics on snakes. Additionally, we modeled central pattern generator (CPG), that is expected to exist in spinal cord of snakes and governing lower control of rhythmical locomotion (such as meandering), and constructing a neural controller adaptable to environmental changes using information about mechanical interaction with the environment.

A. Construction of a snake-like robot mimicking musculo-skeletro system of snakes

In order to construct a mechanical model reproducing flexible body of snakes, instead of electrical motors that are usually used for robots, we use AirMuscle (Hitachi Medical Corp.), a pneumatic actuator that has viscoelasticity. We designed a snake-like robot that has AirMuscle actuators on ventral, dorsal and both sides to mimic musculo-skeletro structure of real snakes (Fig.11).

B. Construction of adaptive neural controllers

Snakes can flexibly adapt its locomotion to surrounding situations. One our main purpose is to investigate biological principle to realize this ability. In this fiscal year, as a basis for this purpose, we constructed a neural model to realize adaptation of meandering locomotion to changing ground friction. We use two CPG models (Ekeberg's model that is obtained from physiology on lamprey and Matsuoka's model constructed based on engineering.

Hypothalamic regulation of muscular tonus

-Involvement of GABAergic neurons-

Yoshimasa Koyama, Kazumi Takahashi and Tohru Kodama

Abstracts - Regulation of muscular tonus in the brainstem is under the control of the hypothalamus and basal ganglia. The experiment was performed to show that (1) the cholinergic neurons in the muscular tonus inhibitory system (pedunculopontine tegmental nucleus :PPN) were activated directly by orexin when it was applied in the vicinity of the neurons, while they were inhibited when orexin was applied to wider area around the neurons. (2) the cholinergic neurons in the PPN were under the tonic inhibition from the GABAergic neurons . (3) orexin applied into the PPN induced GABA release in the PPN. orexinergic projection from the hypothalamus activates the GABAergic neurons in the basal ganglia or brainstem, then inhibits the muscular tonus inhibitory system. These results suggest that the GABAergic neurons in the basal ganglia or the brainstem mediate the orexinergic influences from the hypothalamus and by inhibiting the muscular inhibitory system, contribute to maintain the muscular tonus.

I. INTRODUCTION

THE regulation of muscular tonus that underlies locomotion or other movements is made cooperative interaction of muscular tonus regulation system and locomotion system. As is shown in Figure 1, muscular tonus is maintained or facilitated by the noradrenergic (NA) neurons in the locus coeruleus (LC), serotonergic (5HT) neurons in the raphe magnus (RM), while muscular relaxation is induced by the cholinergic neurons in the pedunculopontine tegmental nucleus (PPN). The output of the PPN cholinergic neurons, mediating the reticulo-spinal tract, suppresses the motoneurons in the spinal cord, then reduces muscular tonus. The glutaminergic neurons in the midbrain locomotion inducing region (MLR) have a crucial role in inducing locomotion pattern[1].

Yoshimasa Koyama is with Department of Science and Technology, Fukushima University. 1 Kanaya-gawa, Fukushima 960-1296, Japan (e-mail, koyamay@sss.fukushima-u.ac.jp).

Kazumi Takahashi is with Department of Physiology, Fukushima Medical University. 1 hikari-ga-oka, Fukushima 960-1295, Japan (e-mail, takahasi@fmu.ac.jp).

Tohru Kodama is with¹Department of Psychology, Tokyo Metropolitan Institute for Neuroscience, 2-6 Musashidai, Fuchu, Tokyo 183-8526, Japan (e-mail, hiro@tmin.ac.jp).

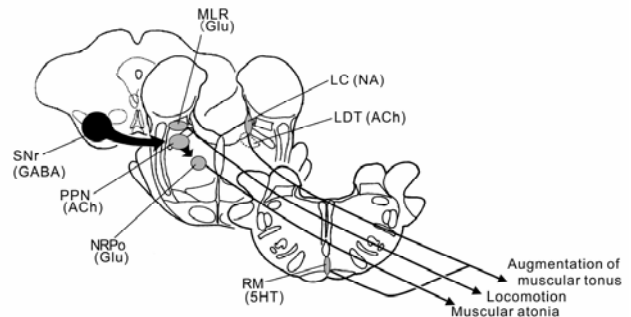


Fig. 1 Muscular tonus regulation system in the brainstem

The muscular tonus regulatory system receives descending influences from the hypothalamus and basal ganglia[2]. For example, when the orexinergic afferents from the hypothalamus is in deficient, sudden attack of muscular tonus disappearance (cataplexy) is induced by emotional stimuli such as food, fear or laughing. Cataplexy is one of the characteristic symptoms of narcolepsy, a serious sleep disorder[3,4]. Using decerebrated cats, we examined the influence of orexin on the muscular tonus regulatory system in the brainstem, and proposed the hypothesis as shown in Figure 2 [5], that is,

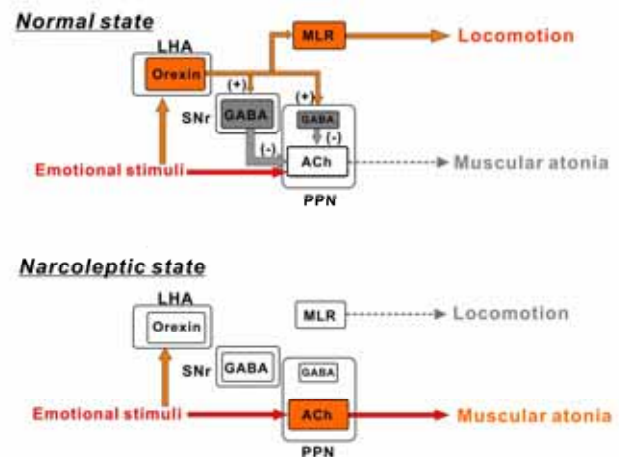


Fig. 2 Schematic diagram of muscular tonus regulation through the hypothalamus-basal ganglia- brainstem. Upper, normal animals; lower, orexin deficient animals. See text for abbreviations.

The orexinergic neurons in the hypothalamus (LHA) (1) activate the MLR and induce locomotion, (2) inhibit the muscular tonus inhibitory system in the brainstem (PPN) through the GABAergic neurons in the substantia nigra pars reticulata (SNr) or the PPN, leading to increase in muscular

tonus. (3) Finally, in normal animals, emotional stimuli including food or fear induce locomotion by activating the orexinergic system in the hypothalamus, but the muscular tonus regulating system in the brainstem, receiving inhibition from the orexinergic system, is not activated, then muscular atonia does not occur. On the other hand, when the orexinergic system is in deficiency (in narcoleptic state), inhibition on the muscular tonus inhibitory system does not work, the emotional stimuli preferentially activate the PPN, then cataplexy occurs. To verify this hypothesis, Influences of GABAergic system on the muscular tonus regulating system in the brainstem were examined in the following experiments.

1. Inhibitory influence of orexin on the brainstem cholinergic neurons

It is well known that orexin affects excitatory on almost all of the neurons[6]. It has also been reported that the brainstem cholinergic neurons are excited by orexin [7,8]. However, the results obtained in our experiment are not consistent with these reports[4]. Since orexin augments muscular tonus, the brainstem cholinergic neurons are supposed to be inhibited. To solve this discrepancy, effects of orexin applied by two different ways were compared.

METHODS

Urethane anesthetized rats were fixed to the stereotaxic apparatus, and single neuronal activity was recorded through a glass pipette microelectrode. Orexin was applied by the following two ways and effect on the neuronal activity was examined (Fig. 3).

(1) To examine the direct effect of orexin, orexin was applied to the vicinity of the recorded neurons.

(2) To detect the indirect effect of orexin, large amount was applied far away from the neurons.

In case of (1), multibarreled glass pipette with a diameter of less than 5 μm was glued to the recording electrode. The recording tip was extruded 20 μm from the multibarrel. In case of (2), single glass pipette with a diameter of 50 μm was used for orexin application. This was glued to the recording electrode separated from the recording tip about 100 μm .

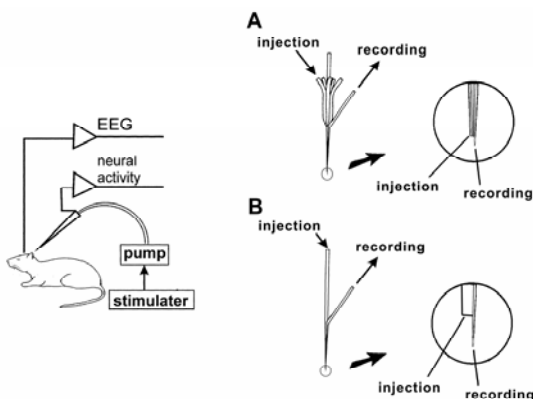


Fig. 3. Experimental set up to examine the effect of orexin on the brainstem cholinergic neurons

RESULTS

Figure 4 shows the effect of orexin applied by the method (1). After orexin application, a slow and slight increase of firing rate was observed. The effect was dependent on the amount of pressure used for application; by the maximum pressure (40 psi) the excitatory effect continued for more than 2 minutes. The long lasting excitation such as shown in Figure 4 was observed in 6 among 8 cholinergic neurons. The remaining two was not affected and no inhibitory response was observed.

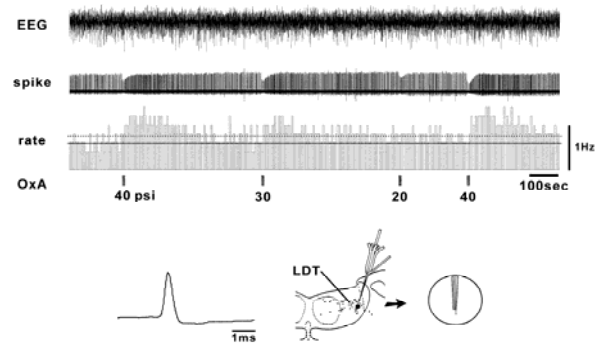


Fig. 4. Response of the brainstem cholinergic neurons to orexin applied in the close vicinity of it. OrexinA (OxA) was applied by pressure at the period of vertical bar. Numbers indicate pressure (psi) used for application of orexin. EEG, electroencephalogram; spike, action potentials; rate, firing rate of the neuron

When orexin was applied far away from the recording neuron by the method (2), no excitatory response was observed, instead about 2 minutes after the application, the neuronal firing gradually decreased and the inhibition lasted for more than 10 minutes (Fig. 5A). When the electrode was advanced by oil drive manipulator, the same amount of orexin induced remarkable excitation with a latency of several seconds, then the long lasting inhibition followed (Fig. 5B).

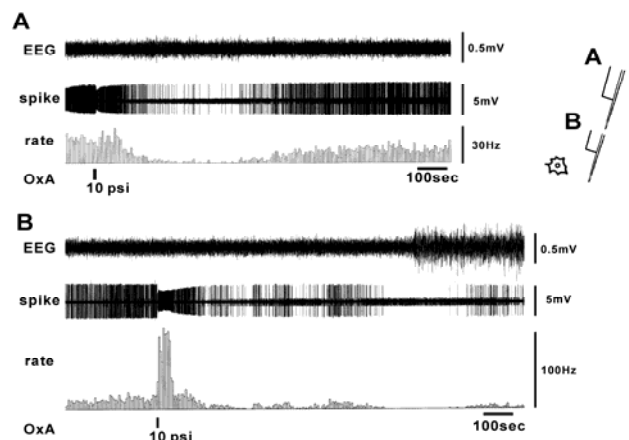


Fig. 5. Effect of orexin when large amount was applied around the recorded neuron. A, Inhibitory effect of orexin. B, Excitatory effect of orexin when the electrode was approached to the neuron.

These results suggest that orexin applied by the method (1) affect directly on the recorded neuron, while when orexin was applied by the method (2), it diffused to the surroundings of the recorded neuron, and excites the inhibitory interneurons locating around the recorded neuron, then exerts indirect inhibitory influence on the recorded neuron. It has been reported that large amount of GABAergic neurons are locating around they PPN[9], and that the orexinergic neurons in the hypothalamus project widely to the various brain areas, including the PPN and its surrounding area[10,11]. It is highly probable that, *in vivo*, the orexinergic neurons excite the GABAergic neurons around the PPN.

2. Tonic GABAergic inhibition on the brainstem cholinergic neurons

The orexinergic neurons are most active during waking and become less active or silent during sleep[12]. The cholinergic neurons in the PPN are most active during REM sleep and are deeply involved in induction of muscular atonia during REM sleep. During waking they become silent and contribute to maintain muscular tonus[13-15]. If the GABAergic neurons are influenced by the orexinergic neurons and affect on the cholinergic PPN neurons, the effect would result in suppression of the firing during waking. So, in the next experiment was performed to check whether the cholinergic neurons ion the PPN receive GABAergic inhibition during waking.

METHODS

Unanesthetized rats were fixed painlessly to the stereotaxic instrument using an acrylic plate mounted on the head of the animals. Under this condition, the rats showed normal sleep-waking cycles. Using a multibarreled electrode as shown in Figure 3A, the neuronal activity was recorded and drugs were applied iontophoretically.

RESULTS

As is shown in Figure 6, this neuron shows almost no firing during waking. Since the firing increase during REM sleep, this neuron are considered to be involved in muscular atonia during REM sleep. When bicuculline (GABA_A antagonist) was applied by current of 80 nA during waking, the neuron, which was silent, started to discharge even during waking. This indicates that the cholinergic PPN neurons receive tonic inhibitory influence during waking from the GABAergic neurons.

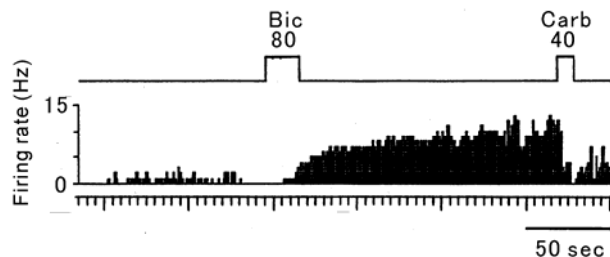


Fig. 6. Effect of bicuculline (Bic) on the cholinergic PPN neuron. Bic was applied during silent period (waking). Numbers indicate the current (nA) to eject the drugs. The neuron activity was inhibited by carbachol (Carb), which is a nature of the cholinergic neurons.

3. Release of GABA in the PPN induced by orexin

If the orexinergic neurons modulates the activity of GABAergic neurons, GABA release in the PPN would be modulated by orexin. To assess this assumption, GABA release in the PPN was measured using microdialysis technique.

METHODS

After one week of operation for implanting a guide tube, microdialysis probe was inserted through the guide tube to the PPN (Fig. 7). Three hours after the implantation, sampling under freely moving condition was performed every 10 minutes. After one hour of control sampling, orexin A(1 mM, 0.25 μ l) was applied through the injection cannula which was glued to the microdialysis probe. GABA content in the dialysates were measured using high power liquid chromatography (HPLC) method.

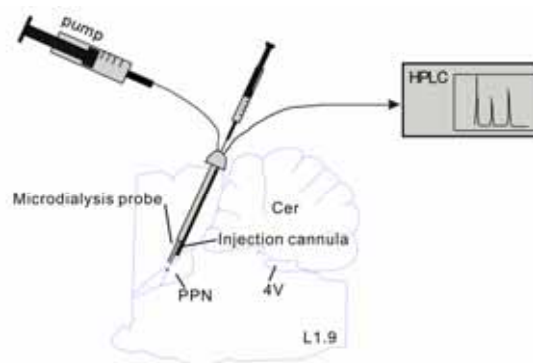


Fig. 7. Experimental diagram for the measurement of GABA and injection of orexin. Location of the probe is shown on the side view of the brain.

RESULTS

As is shown in Figure 8, after the injection of orexin to the PPN, GABA release in the PPN increased about 40 % from the baseline at the first 10 minutes period. From the next 10 minutes period (10 to 20 minutes after the injection) to the fourth 10 minutes period (30 to 40 minutes after the injection), GABA release significantly increased ($p < 0.05$) when compared with the control group to which artificial

cerebrospinal fluid (ACSF) was injected. When orexin was injected to the reticular formation posterior to the PPN, increase of GABA release was not detected. Release of glutamate measured in the same dialysate did not increase after the injection. The result indicates that the orexinergic afferents to the PPN increase the release of GABA in the PPN.

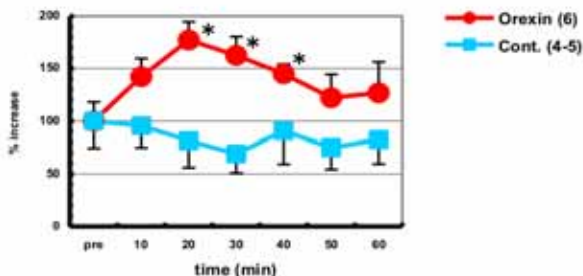


Fig. 8. GABA release in the PPN when orexin was injected to the PPN. The value measured one hour before the orexin injection was indicated as 100 % (pre). Asterisks (*) indicate statistical significance ($p < 0.05$) between orexin injected group (Orexin) and control group (Cont.) obtained by t-test.

SUMMARY AND FUTURE WORK

The present study demonstrates the GABAergic influences on the brainstem cholinergic neurons that is involved in regulation of muscular tonus. In normal animals, through this GABAergic inhibition, the orexinergic neurons suppress the muscular tonus inhibitory system, then work to maintain muscular tonus, make it possible to induce locomotion when the animals receive emotional stimuli. In orexin deficiency (narcoleptic) state, lack of activation of the GABAergic neurons results in induction of emotion-induced muscular atonia (cataplexy). The orexinergic system is a neural substrate that induces an appropriate behavior when the animals respond to a variety of stimuli in the environment. The future work has to elucidate how the emotional stimuli affect on the muscular tonus regulation system including the hypothalamus, basal ganglia and brainstem.

REFERENCES

- [1] K. Takakusaki, T. Habaguchi, J. Ohtinata-Sugimoto, K. Saitoh and T. Sakamoto. "Basal ganglia efferents to the brainstem centers controlling postural muscle tone and locomotion: a new concept for understanding motor disorders in basal ganglia dysfunction," *Neuroscience*, vol.119, pp.293-308, 2003.
- [2] K. Saitoh, S. Hattori, W.J. Song, T. Isa and K. Takakusaki. "Nigral GABAergic inhibition upon cholinergic neurons in the rat pedunculopontine tegmental nucleus," *Eur J Neurosci*, vol.18, pp.879-886, 2003.
- [3] R.M. Chemelli, J.T. Willie, C.M. Sinton, J.K. Elmquist, T. Scammell, C. Lee, J.A. Richardson, S.C. Williams, Y. Xiong, Y. Kisanuki, T.E. Fitch, M. Nakazato, R.E. Hammer, C.B. Saper and M. Yanagisawa. "Narcolepsy in orexin knockout mice: molecular genetics of sleep regulation," *Cell*, vol.98, pp.437-451, 1999.
- [4] L. Lin, J. Faraco, R. Li, H. Kadotani, W. Rogers, X. Lin, X. Qiu, P.J. de Jong, S. Nishino and E. Mignot. "The sleep disorder canine narcolepsy

- is caused by a mutation in the hypocretin (orexin) receptor 2 gene," *Cell*, vol.98, pp.365-376, 1999.
- [5] K. Takakusaki, K. Takahashi, K. Saitoh, H. Harada, T. Okumura, Y. Kayama and Y. Koyama. "Orexinergic projections to the cat midbrain mediate alternation of emotional behavioural states from locomotion to cataplexy," *J Physiol*, vol.568, pp.1003-1020, 2005.
- [6] C.B. Saper, T.C. Chou and T.E. Scammell. "The sleep switch: hypothalamic control of sleep and wakefulness," *Trends Neurosci*, vol.24, pp.726-731, 2001.
- [7] S. Burlet, C.J. Tyler and C.S. Leonard. "Direct and indirect excitation of laterodorsal tegmental neurons by hypocretin/orexin peptides: Implication for wakefulness and Narcolepsy," *J Neurosci*, vol.22, pp.2862-2872, 2002.
- [8] K. Takahashi, Y. Koyama, Y. Kayama and M. Yamamoto. "Effects of orexin on the laterodorsal tegmental neurons," *Psychiatry Clin Neurosci*, vol.56, pp.335-336, 2002.
- [9] C.J. Holmes, L.S. Mainville and B.E. Jones. "Distribution of cholinergic, GABAergic and serotonergic neurons in the medial medullary reticular formation and their projections studied by cytotoxic lesions in the cat." *Neuroscience*, vol.62, pp.1155-1178, 1994.
- [10] T. Nambu, T. Sakurai, K. Mizukami, Y. Hosoya, M. Yanagisawa and K. Goto. "Distribution of orexin neurons in the adult rat brain," *Brain Res*, vol.827, pp.243-260, 1999.
- [11] C. Peyron, D.K. Tighe, A.N. van den Pol, L. de Lecea, H.C. Heller, J.G. Sutcliffe and T.S. Kilduff. "Neurons containing hypocretin (orexin) project to multiple neuronal systems," *J Neurosci*, vol.18, pp.9996-10015, 1998.
- [12] M.G. Lee, O.K. Hassani and B.E. Jones. "Discharge of identified orexin/hypocretin neurons across the sleep-waking cycle," *Journal of Neuroscience*, vol.25, pp.6716-6720, 2005.
- [13] A.E. El-Husseini, C. Bladen, J.A. Williams, P.B. Reiner and S.R. Vincent. "Nitric oxide regulates cyclic GMP-dependent protein kinase phosphorylation in rat brain," *J Neurochem*, vol.71, pp.676-683, 1998.
- [14] Y. Kayama, M. Ohta and E. Jodo. "Firing of 'possibly' cholinergic neurons in the rat laterodorsal tegmental nucleus during sleep and wakefulness," *Brain Res*, vol.569, pp.210-220, 1992.
- [15] M. Steriade, S. Datta, D. Pare, G. Oakson and R.C. Curro Dossi. "Neuronal activities in brain-stem cholinergic nuclei related to tonic activation processes in thalamocortical systems," *J Neurosci*, vol.10, pp.2541-2559, 1990.

Annual Report B-12:

Study on brain adaptation in rat-machine fusion systems

Takafumi Suzuki*, Kunihiko Mabuchi*

Abstract— The goal of this research project is to elucidate the brain adaptation function in rat-machine fusion systems. To achieve this goal, we have developed fundamental techniques. These techniques include A) a method for improving the accuracy of walking parameters estimated using neural signals measured in the primary motor cortexes of rats, and B) elemental techniques for long-term stable neural recording using devices such as B-1) an electrode array, B-2) a flexible neural probe with micro fluidic channels for injecting medicines and B-3) an electrode array with a hydraulic positioning system.

I. INTRODUCTION

THE goal of this project is to elucidate the ability of the brain (specifically the motor center) to adapt to a variable body environment by using a rat-machine fusion system in which the body's environmental conditions are changeable. We plan to construct a "rat car" vehicle system in which the car is controlled by neural signals in the motor cortexes of rats. The system allows us to change the relationship between the motor command signals and the effectors (muscles or the vehicle) arbitrarily. By using multi-recordings of neural signals together with injections of certain medicines into the system, we plan to elucidate the brain property mentioned above.

This year, we have been engaged in developing fundamental techniques to achieve this goal. The techniques includes A) a method for improving the accuracy of walking parameters, such as speed, estimated using the neural signals measured in the primary motor cortexes of rats, and B) elemental techniques for long-term stable neural recording such as B-1) a tungsten multi-electrode array, B-2) a flexible neural probe integrated with micro fluidic channels for injecting medicines such as Neural Growth Factor and B-3) an electrode array with a hydraulic positioning system.

II. RESULTS

A) Rat-car system

We have developed a BMI in the form of a small vehicle, which we call the 'RatCar'. A unique point of our RatCar system is that a neural signal source (i.e., a rat) is mounted on the vehicle body and the two components move around as a unit. The rat is therefore provided with somatosensory feedback as the vehicle moves. This enables the rat to realize that its desire to move has been satisfied through the vehicle

movement. We expect this condition to increase the ability of the rat to adapt to the system. Our ultimate goal is to illude the rat into recognizing the vehicle as corresponding to its own original limbs, and this will enable use of the RatCar as a platform for future neuroscience research. In addition, the movement of the vehicle system causes electromagnetic noise and artifacts in the recorded signals, an inevitable problem for real applications in hospitals and day to day society. The development of the RatCar system will help us investigate and solve these problems. Here, we focus on basic control of the vehicle movements. We previously built a linear model based on a least squares error approach to estimate the locomotion speed. We have expanded this model to estimate a more generalized locomotion state which includes the speed and changes of directions of a rat's movements. We compared these estimated values to the actual recorded ones, and attempted to control the vehicle.

METHODS

A flow diagram of the RatCar system is shown in Fig. 1. First, neural signals are recorded by neural electrodes implanted in the motor cortexes of the rat's brain. These are amplified, filtered, and transferred to the A/D converter. Next, neural spikes are detected from the raw signals. A simple template matching technique is used to reduce noises and artifacts. In principle, this part of the system corresponds to the neurons which generated the spike waveform. Finally, the locomotion speed and changes in direction are estimated from the firing rates of spikes in each category.

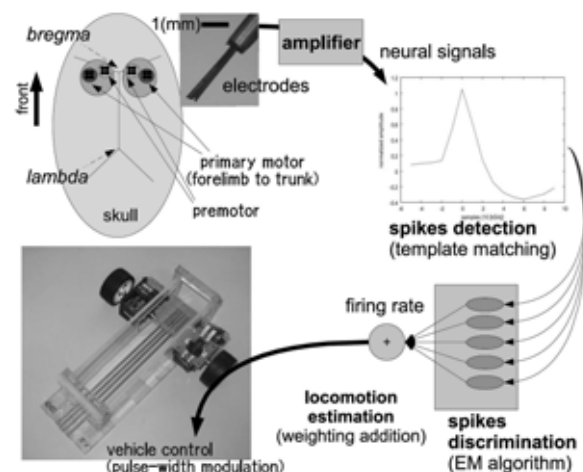


Fig. 1. Flow diagram of the RatCar system

*Graduate School of Information Science and Technology,
The University of Tokyo

Signal Recording

We determined the coordinates of the recording sites according to a stereotaxic atlas of the rat brain and functional localization maps. The areas corresponding to the forelimbs and the trunk in the primary motor cortices and the nearby premotor cortices were selected to represent the body movement during locomotion. Next, we fabricated and implanted bundled electrodes consisting of tungsten wires to record signals in the areas described above. Each wire was 40um in diameter and coated with Parylene-C polymer. Its tip was cut off to gain 50 to 100 [kohm] in impedance, which enabled us to simultaneously record the activities of several neurons around each electrode. The electrodes were tightly fixed on the skull using a resin adhesive and screws cut into the brain. Through the electrodes, the electrical potentials between any two wires were differentially recorded. The signals obtained from the electrodes were amplified by 10,000 times voltage, filtered through 500 Hz to 3kHz (Nihon Kodan MEG-6116), and transmitted to an A/D converter (National Instruments PCI-6071E) installed in a computer. The acquisition rate was 10 kHz for each channel.

Spikes Detection and Discrimination

We applied template matching to the signals acquired in the computer to reduce noise and artifacts. We then detected spike waveforms at the peak amplitudes (i.e., a relative maximum or minimum).

We applied a Gaussian-mixture model (GMM) to the distribution of spike heights, assuming that spikes having similar peak amplitudes originated from the same neuron. The parameters for the Gaussian-mixture were estimated by the expectation-maximization (EM) algorithm while a number of Gaussians were empirically determined. Linear Model for Locomotion Estimation

The muscle activity of the body is expected to change during locomotion. This suggests that variation in the neuronal firing rate will be either positively or negatively correlated to the walking speed. Consequently, we assumed a model,

$$v(t) = \sum_{n=1}^N a_n x_n(t), \quad (1)$$

where the values of a_n are the contribution factors of neuron n having a firing rate of x_n at time t to the locomotion state v . This is the simplest representation describing the correspondence between neural activity and actual movements.

This linear model can be described in matrix form as,

$$X\vec{A} = \vec{V}, \quad (2)$$

where vector $A = (a_1, a_2, \dots, a_i, \dots, a_n)T$ for the contribution factors, matrix $X = (x_{k,i}) = (x_i(t = t_k))$ representing the firing rate of each neuron at each time t , and estimated speed vector $V = (.v(t = t_1), \dots, .v(t = t_k))T$ at each time t . Therefore, vector A can be estimated by minimizing the square error of the actual walking speed V as follows:

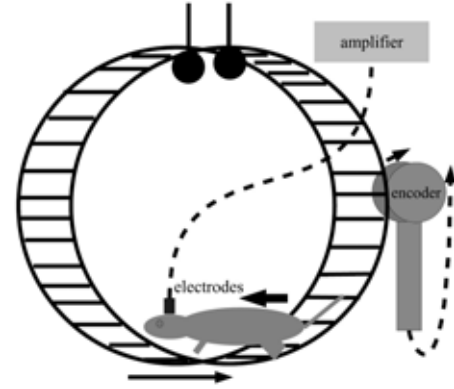


Fig. 2. A rat in exercise wheel. The wheel was supported by bearings that allowed it to rotate freely in both directions. The neural signal of the rat and the rotation speed of the wheel were simultaneously recorded while the rat walked inside of the wheel.

$$\vec{A} = (X^T X)^{-1} X^T \vec{V}. \quad (3)$$

For all of these procedures, we used the same channels on the same rat for each trial, but the period of time for the estimation differed from that used to calculate weights (i.e., an open dataset).

1) Forward Speed: We used an animal exercising wheel (Fig. 2) to observe the locomotion speed of a rat as in our previous work. The rat walked without interruption inside the wheel and an encoder attached to the wheel recorded its rotation speed. Neural signals were simultaneously recorded and a firing rate for each neuron was calculated every 100 ms.

2) Changes in Direction: To find the correspondence between neural spikes and changes in direction during locomotion, we built a Y-branch passage for a rat to walk

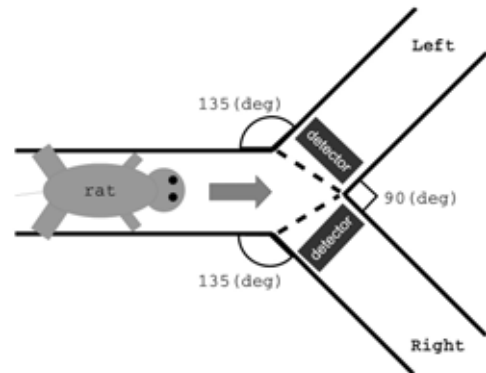


Fig. 3. A rat in a Y-branch passage. A rat was released at one end of the passage (left side of the figure) and guided to walk through one of the branches. Neural signals were recorded for 1 s before a rat passed over the detector installed at the entrance of each branch.

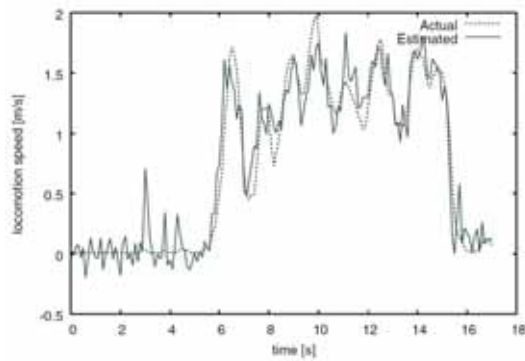


Fig. 4. Actual (black) and estimated (gray) walking speed of a rat

through (Fig. 3).

While a rat was guided to walk through one of the branches (left or right), neural signals were recorded for 1 s before the rat stepped on the detector at the start of each branch. We then assigned a value of -1 or 1 to the locomotion state to specify the weights for a rat walking into either the left or right passage.

We attempted to discriminate which side (left or right) that a rat went to and calculated the sequence of locomotion state values every 100 ms to investigate their variation.

Vehicle Control

According to the estimated locomotion speed and changes in direction, the vehicle was controlled to trace the actual movement of a rat. The vehicle had two DC motors connected to the driving wheels. These were controlled by pulse-width modulated (PWM) signals generated by a D/A converter (National Instruments PCI-6071E) attached to the personal computer.

RESULTS

Forward Speed

Fig. 4 shows the estimated locomotion speed (gray) and the actually recorded locomotion speed (black) during a trial. These were coincident with each other. The mean square

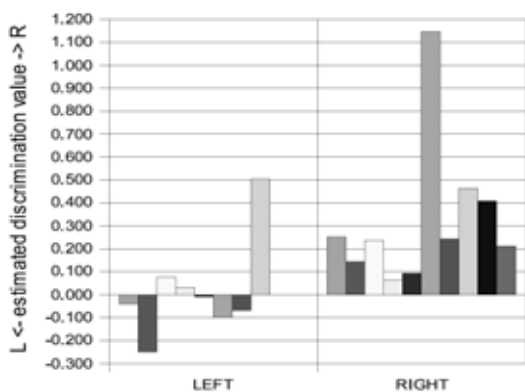


Fig. 5. Estimated direction values, which should be -1 for left and 1 for right

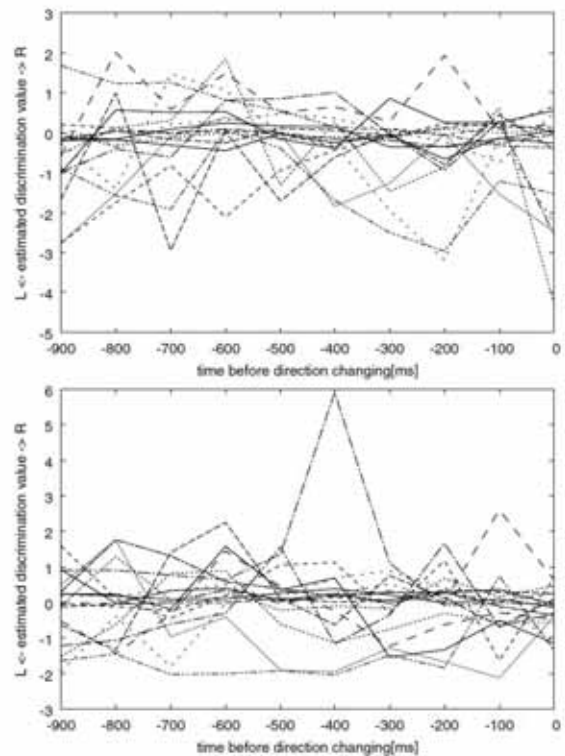


Fig. 6. Estimated direction values for each 100 (ms) as a rat walked toward the detectors. The upper and lower figures are for trials where a rat walked respectively to the left or to the right. The times on the x-axis indicate the remaining time until a rat stepped on either detector.

error for this trial was 0.032 and the correlation coefficient was 0.965.

Changes in Direction

Fig. 5 shows the estimated locomotion state values for left-turning and right-turning. Although these values are far from the desired values (1 or -1) especially for left-turning, the values tended to be discriminated for most trials. Fig. 6 shows the estimated locomotion state values for every 100 ms. These values differed remarkably between trials. Some trials showed large shifts towards extreme values, although the overall value tended to be localized around zero.

DISCUSSION

Neural Measurement

Our electrodes were redesigned to have a smaller diameter (50 μm) than in previous experiments to reduce invasiveness when they penetrated the brain. The possibility of recording from more channels was increased to the degree that some neurons could be clearly recorded even after several months. However, many channels became disabled soon after the implant. The reasons for this are still unclear and histological investigation around the electrodes will be needed.

We implanted electrodes in the primary motor and premotor cortices to read the intention of a rat regarding

locomotion. The implanted areas were determined based on previous studies, but the position control was not accurate because of individual differences and obstacles such as blood vessels. In addition, we could record obvious neural signals from all recording regions for only a few of the rats. These problems prevented us from comparing the properties of each area and from finding the busy recording sites to estimate the locomotion states. We need to develop a system which is more robust with regard to individual differences and recording sites, and we may have to increase the number of trials.

Signal Processing and Estimation

In this work, we implemented an automatic spike discrimination method based on GMM and the EM algorithm. This method suppressed the influence of the manual configuration of parameters, and increased the reliability of the results. However, there are some parameters that an experimenter still has to set empirically: the initial GMM condition, the selection of reliable neurons, etc. In the future, these should also be automatically determined to enable more reliable results.

While the results from estimation of the locomotion speeds showed the ability of the simplified linear model to work as an intention translator, the results for changes in direction included large errors and variances. Some large errors were caused by calculation inaccuracy due to attempts to divide by zero or to zero determinants of matrices. The introduction of a more reliable calculation technique and the automatic elimination of ill-natured signals (e.g., those having no correlation to the locomotion or that are too uniform) in advance will be effective measures to prevent such errors.

Our current locomotion state estimator depends only on the adjacent firing rates. The use of temporal changes in the firing rates may increase the estimation accuracy. In particular, we need to reduce the excessive variation in the estimated values which was caused by neural activity unrelated to locomotion. This can be done by using a finite impulse response (FIR) filter (e.g., the AR model) or infinite impulse response (IIR) filters (e.g., Kalman filters).

Vehicle Control

Some rats tended to stop moving when left in the wheel or on the Y-branch passages used to record the locomotion states. This reduced the number of samples and the recorded neural firings were useless in these cases. Advance selection of rats more likely to move or the application of methods to motivate a rat to walk is needed. Possible methods include stimulation methods using electrical stimulus, flashing lights, or sounds, and feeding techniques. So far, we have developed methods for independently estimating locomotion speed and changes in direction. Therefore, although the rat's intention was unconfirmed when we attempted to move vehicle using the neural signals of a rat mounted on it, the vehicle did actually move. In future, we will apply an event recorder system using video cameras to monitor the intention while a rat is freely moving.

The RatCar system consists of a vehicle controlled by the neural signals from the motor cortices of a rat, and we have estimated the rat's walking speed and changes in direction from these signals. Stronger correlation than in previous experiments was achieved between the actual and the estimated walking speeds. In addition, an approximate discrimination of changes in direction was achieved. Those results made it possible to realize some control of the vehicle.

A relatively large degree of error still remains, though, especially in the estimation of changes in direction. An improved method to determine the implanting positions and a better model for estimating locomotion states will need to reduce errors.

B) Elemental techniques for long-term stable neural recording

In this study, we focused on optimal electrode alignment for brain recording from the motor cortex for Brain-Machine Interface (BMI) application. We fabricated multi-electrode arrays covering primary motor cortex. The neural signal of the rat and its walking speed were simultaneously recorded. Estimation of the walking speed was conducted from neural signals using four different recording sites and evaluated anterior electrodes group and posterior electrodes group provided a good estimation, on the other hand two electrode groups around the center gave a bad estimation however it was possible to record neural signals. These result therefore suggested improving estimation using the electrodes which concentrated on the both sides.

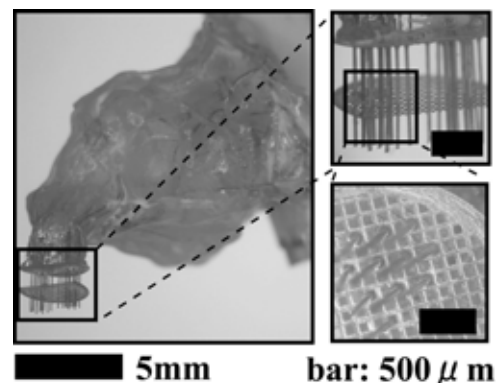


Fig. 7. Tungsten multi-electrode array

III. CONCLUSION

We report the results, up to this point, of this project such as A) an improvement in the accuracy of walking parameters estimated from the neural signals measured in the primary motor cortex of rats, and B) elemental techniques for long-term stable neural recording such as B-1) an electrode array, B-2) a flexible neural probe with micro fluidic channels for injecting medicines and B-3) an electrode array with a hydraulic positioning system. By using these fundamental techniques we are going to invest in a study of the ability function of the brain next year as scheduled.

Detection with BMI methods how body movements are involved in neural coding in the brain

Yoshio Sakurai

Graduate School of Letters, Kyoto University

Abstract — The present study is detecting, with multineuronal recording and brain-machine interfaces (BMI), how body movements are involved in neural coding in the brain. In the present year, we have established behavioral learning tasks for rats and have developed a BMI system. We report here that neuronal activity was remarkably changing when the brain was working with the BMI and sharp synchrony of firing among closely neighboring neurons was valid for neuronal coding.

I . INTRODUCTION

Recognition and detection of valid information in the environments are must for animals to behave adaptively, that necessarily require neural coding in the brain. Recent neuroscience studies have suggested that the essential feature of neural coding is highly dynamic and distributed information processing by activity of functional neuron groups, as the famous psychologist D.O.Hebb suggested. However, as the other famous psychologist J.J.Gibson indicated, recognition and detection of valid information need action to and interaction with the environments of much information. This suggests that real features of neuronal coding could be experimentally uncovered by investigating how body movements are involved in neural activity of coding in the working brain of behaving animals.

. PURPOSE

The present study is detecting, with multineuronal recording and brain-machine interfaces (BMI), how body movements are involved in neural coding in the brain. For that, we establish behavioral learning tasks for rats and develop a BMI system with long-term multineuronal recording. The main brain regions are hippocampal-cortical systems.

. ORIGINALITY

The present study rejects the classical neuroscience framework, i.e., recognizing the brain as a simple device which passively percepts and processes incoming information in the environments. Instead, we focus on interactions between neural coding and body movements and aim to experimentally investigate them. To establish the BMI system for the present study, developing and integrating new hardwires and software and collaboration between psychological behavior experiments and neurophysiological recording experiments are required. That is surely a new multidisciplinary project among different fields of science.

. METHODS

We construct a novel system consisting of automatic and real-time spike sorting with independent component analysis (ICA) in combination with a newly developed multi-electrodes for long-term recording from multi-sites of the brain. Then we connect the system with appropriate behavioral tasks for rats and look for valid neuronal activity and synchrony, which can be used as neuronal codes to work the BMI system. We especially focus on the firing synchrony in the neuronal networks.

. RESULTS

We developed a task apparatus (Fig. 1) and several behavioral tasks, i.e., simple free-response task, response with inter-trial interval task, visual discrimination task, auditory-location association task, right-left alternation task for rats with nose-poke reposes. Then we developed an unique multi-electrode (dodecatrode) with microdrive (Fig.

2) and a real-time spike sorting system RASICA (Real-time and Automatic Sorting with Independent Component Analysis) (Fig. 3). The RASICA can automatically separate multi-neuronal activity recorded with the dodecatrodes and detect firing frequency and synchrony of the sorted neurons with any parameters for analysis. This system has been applied for patents by Kyoto University.



Figure 1 Apparatus of behavioral tasks. In the operant box located in the center, rats are trained to perform behavioral tasks. The interface box to control the operant box and other apparatuses is set behind the box. The loud speaker and cables with head-amplifiers are attached near the ceiling. All are in the sound-proofed shielded box .

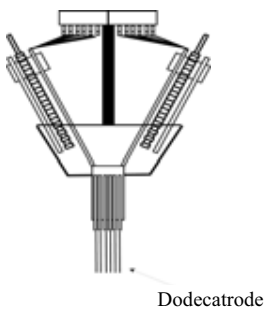


Figure 2 Microdrive with dodecatrodes. Each dodecatrode consist of 12 microwires and the microdrive operates each dodecatrode independently.

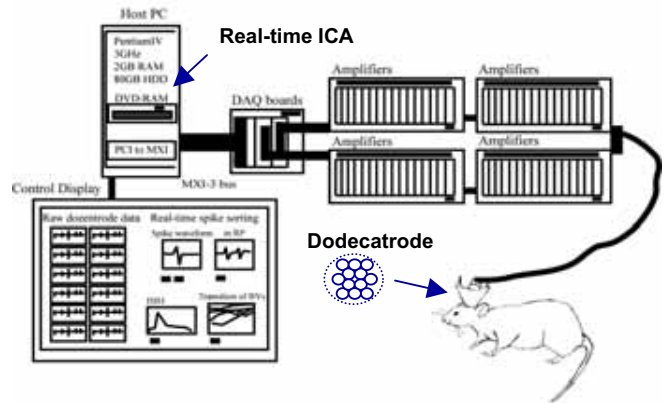


Figure 3 A schematic diagram of RASICA system. A host computer for the RASICA controls the two A/D boards and data storage, transmitted from the A/D boards to the personal computer via the high speed bus, and is responsible for the real-time spike sorting with ICA (see Experimental procedures). The data files are written to backup DVD-RAMs in a DVD drive.

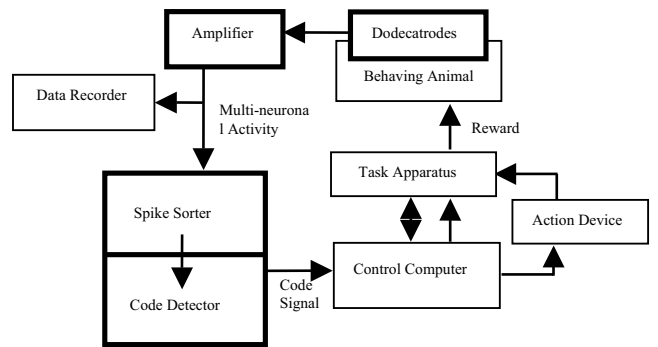


Figure 4 A schematic diagram of the BMI system. Thick lines are implicated in the RASICA.

We have constructed the whole system for BMI with the RASICA (Fig. 4) and are investigating how hippocampal neuronal activity change when the rat brain is connected to the BMI system. In a preliminary experiment, multi-neuronal activity was recorded from the hippocampal CA1 and 10 single neurons were automatically separated. The neuronal code instead of nose-poke behavior is certain firing frequency and synchrony in a 40 msec time window. The rat soon did not try to access the holes for nose-pokes and the neuronal code frequently appeared only 30 min after the experiment started (Fig. 5).

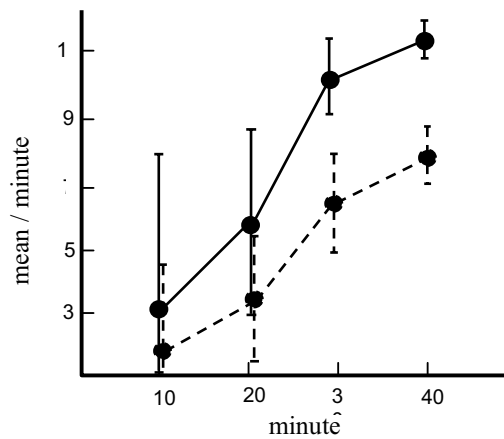


Figure 5 Firing frequency and synchrony of hippocampal CA1 neurons when connected to BMI. situation. The solid line means the firing frequency and the dotted line means firing synchrony.

In the next task, a guillotine door sometime opened to make the response holes for nose-pokes available (trial period). Inter-trial intervals between the trials were 8 sec during which the neuronal codes were not effective. Firing frequency and synchrony during the trials soon increased in the first day and maintained the level in 4 days of sessions but those during the inter-trial intervals gradually decreased (Fig. 6). This means that the rat's brain gradually learned to regulate to the neuronal codes.

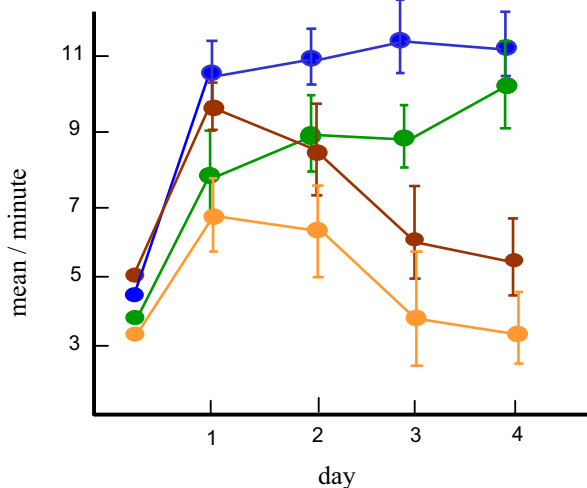
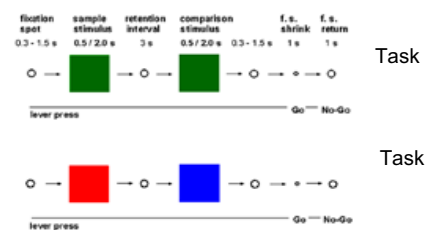


Figure 6 Firing frequency and synchrony of hippocampal CA1 neurons when connected to BMI. situation in the task with inter-trial intervals. Blue line and brown line mean firing frequency during the trials and inter-trial intervals respectively. Green and orange lines mean firing synchrony during the trials and inter-trial intervals respectively.

To make the significance of firing synchrony more clearly, we investigated features of firing synchrony in the prefrontal cortex of monkeys while they were successively performing two tasks in which working memory for either stimulus duration or color was required (Fig. 7) with the unique spike-sorting with ICA and multi-neuronal recording (Fig. 8). About eighty percent of the total pairs of neighboring neurons showed precise firing synchrony during the performance of the tasks and some of the neuronal pairs showed task-dependent synchrony that appeared in only one of the tasks (Figs, 9 and 10). These results suggest that some closely neighboring neurons have dynamic and sharp synchrony to make local and functional neuronal groups to represent information in the working brain. These functional groups have a possibility to be effective neuronal codes for BMI.



Task A
Task B

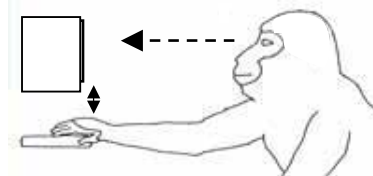


Figure 7 Two behavioral tasks for the monkeys. The first square is a sample stimulus and the second one is a comparison stimulus in each task. See ref. (4).

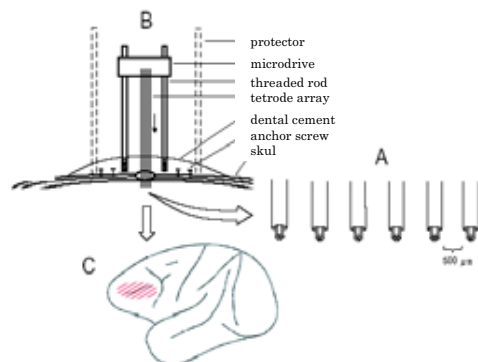


Figure 8 Recording methodology and recorded area. A, Array of tetrodes. B, Microdrive assembly. C, Recorded principal sulcus area (red diagonals). See ref. (4).

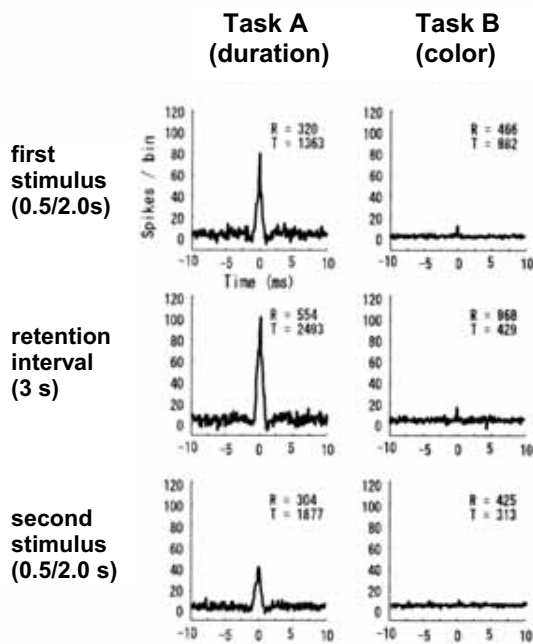


Figure 9 An example of difference correlograms from a pair of neighboring neurons showing dynamic and precise synchrony. Bin width is 1 msec and the horizontal values indicate time in milliseconds between -100 and +100. See ref. (4).

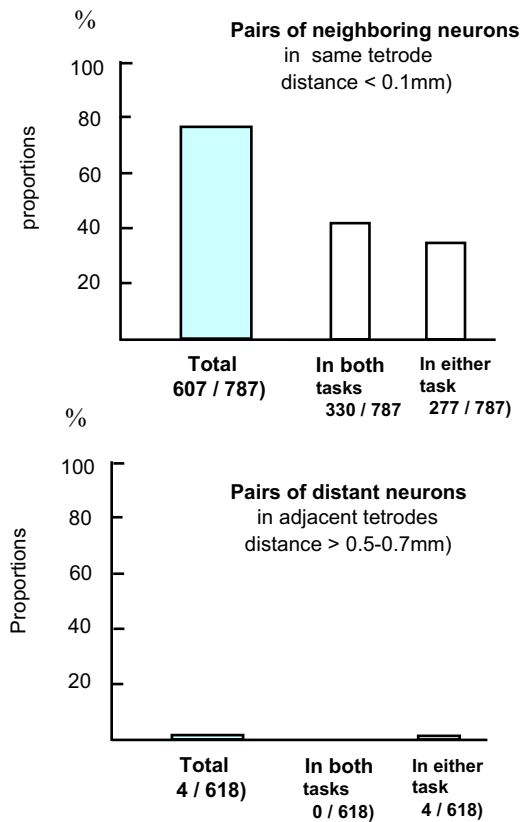


Figure 10 Proportions of neuronal-pairs showing precise synchrony. See ref. (4)

ACKNOWLEDGEMENTS

The author thanks Dr. Susumu Takahashi, a post-doc researcher of Japan Science and Technology Agency, for collaborating for the present research project.

REFERENCES

- (1) Sakurai, Y. (2007) *Search for Representation in the Brain*. Kyoto University Press, In press. (In Japanese)
- (2) Sakurai, Y. (2007) How can we detect ensemble coding by cell assembly. In Funahashi, S. (Ed.). *Representation and Brain*. Springer, Tokyo, In press.
- (3) Sakurai, Y. (2007) Brain-machine interface to detect real dynamics of neuronal assemblies in the working brain. In Wu, J.L., Ito, K., Tobimatsu, S., Nishida, T. & Fukuyama, H. (Eds.). *Complex Medical Engineering*. pp.407-412, Springer, Tokyo.
- (4) Sakurai, Y., and Takahashi, S. (2006) Dynamic synchrony of firing in the monkey prefrontal cortex during working memory tasks. *Journal of Neuroscience*, 26, 10141-10153.
- (5) Sakurai, Y. (2006) Multi-neuronal activity and brain-machine interface. *Seitai No Kagaku*, 57(4), 292-297. (In Japanese)
- (6) Sakurai, Y. (2006) Multi-neuronal activity - cell assembly - brain-machine interface. *Japanese Journal of Physiological Psychology and Psychophysiology*, 24(1), 57-67. (In Japanese)
- (7) Koike, Y., Hirose, H., Sakurai, Y. and Iijima, T. (2006) Prediction of arm trajectory from a small number of neuron activities in the primary motor cortex. *Neuroscience Research*, 56, 146-153

A multi-disciplinary Study of Adjustment Mechanisms of Human Bipedal Gait: Annual Report 2006

Takashi Hanakawa, Kazumi Iseki, Kazuo Hashikawa, and Manabu Honda

Abstract—Toward the better understanding of adjustment mechanisms of human bipedal gait, we have proposed a hypothetical model of its functional neuroanatomy, which incorporates both cortico-basal ganglia and basal ganglia-brainstem pathways. To test the feasibility of this model, we performed a cerebral blood flow study in patients with subcortical vascular encephalopathy with and without gait disturbance. A preliminary result supported a role of multiple cortical motor areas in maintaining gait.

I. INTRODUCTION

SENESCENCE may be regarded as the process in which mobility and intelligence that had been acquired through long-term learning from infancy are gradually being lost. Especially, loss of ability to adjust locomotion according to the walking environment, or in response to perturbations, is a significant problem leading to falling and resultant disability in elderly. As the unprecedented aging society is rapidly approaching in Japan, strategies must be developed to deal with problems of locomotion as well cognitive decline, leading causes of disability in elderly people. To invent new effective strategies, we must first understand accurately the neural mechanisms of locomotor adjustment and their interaction with the environment. Unfortunately, however, the relevant knowledge is very limited and fragmented.

A fundamental machinery subserving human gait is considered to exist at the level of the brainstem and the spinal cord, as does that of quadruped animals. To fit into new walking circumstances, however, higher neural systems such as the cerebellum, basal ganglia, and cerebral cortex are likely to be recruited. This notion is consistent with the development of locomotion in each individual. From infancy to adolescence, a walking pattern develops from unstable and immature toddling to easily adjustable, sophisticated adult type. Such evolution of the locomotor and postural regulation system seems to parallel with the maturation of the cerebellum and higher-order cortical

This work was supported by the Grant-in-Aid for the Priority Areas (“Emergence of adaptive motor function through interaction among body, brain and environment”; area 454) from the Ministry of Education, Science, Sports and Culture of Japan.

T. H. is with the Department of Cortical Function Disorders, National Institute of Neuroscience, National Center of Neurology and Psychiatry, Kodaira, Tokyo 187-8522, Japan (corresponding author, phone: 042-341-2711; fax: 042-346-1748; e-mail: hanakawa@ncnp.go.jp).

K. I. is with Human Brain Research Center, Kyoto University Graduate School of Medicine, Kyoto 606-8507, Japan (e-mail: iseki@kuhp.kyoto-u.ac.jp).

K. H. is with Human Brain Research Center, Kyoto University Graduate School of Medicine, Kyoto 606-8507, Japan (e-mail: hashikawa@kuhp.kyoto-u.ac.jp).

M. H. is with the Department of Cortical Function Disorders, National Institute of Neuroscience, National Center of Neurology and Psychiatry, Kodaira, Tokyo 187-8522, Japan (e-mail: honda@ncnp.go.jp).

motor areas. On the other hand, the ability of adaptive locomotor behavior is gradually getting declined during senescence. Peculiarly, gait disturbance in patients with Parkinson’s disease, a neurologic disease which is closely related to aging, can be ameliorated by the interaction with the walking environment. This phenomenon tells us that the relationship between the intelligent and mobile organism and the environment is not simple. Many factors potentially affect such a relationship – development, aging, and disease. We need to take these dynamically changing factors into account.

This research program aims at clarifying the neural mechanisms of human adaptive locomotor behavior and its changes due to aging and disease processes. For this purpose, multiple non-invasive brain mapping techniques such as functional magnetic resonance imaging (fMRI), positron emission tomography (PET), single photon emission computed tomography (SPECT), transcranial magnetic stimulation (TMS) will be used in various combination. For the first step, we have proposed hypothetical models that were originally developed by incorporating the model proposed by Takakusaki and colleagues [1] and the findings from our own studies. As one of the projects to test the feasibility of these models, we have launched a SPECT activation experiment in which the pathophysiology of gait disturbance in patients with subcortical vascular encephalopathy was investigated.

II. HYPOTHETICAL MODELS OF NEURAL MECHANISMS FOR HUMAN BIPEDAL GAIT

A. A normally functioning system (Figure 1)

Indirect evidence from patients with spinal cord injury strongly supports the existence of central pattern generators (CPG), similar to the ones in quadruped animals or lamprey, in the human spinal cord. CPG is regarded as a neural network that can generate periodic motor commands without requiring inputs from other areas. In normal circumstances, however, CPG is regulated by inputs from the central and peripheral systems and thus does not produce autonomous stepping movement.

A midbrain or metencephalic locomotor region (MLR) has been extensively studied in quadruped animals such as cats. In proximity of the MLR, there is another important structure termed the pedunculopontine nucleus (PPN) that is shown to regulate muscle tones. MLR and PPN appear to be the essential brainstem structures that regulate locomotion. Although there is no direct proof of the same MLR/PPN functionality in humans, we previously showed that parts of dorsal midbrain and pons are activated during human gait [3]. Therefore, it should be reasonable to

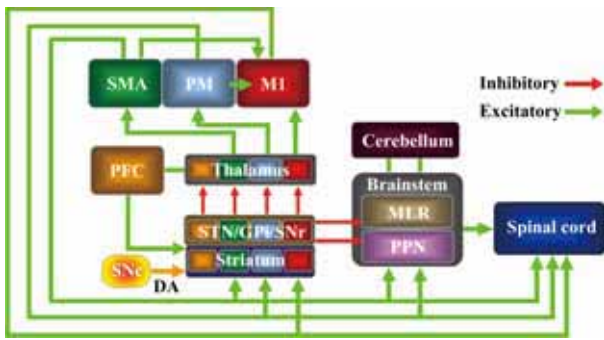


Fig. 1. A hypothetical neuroanatomy of human gait (modified from [2])

assume that the MLR/PPN play pivotal roles in regulating locomotion and related postural changes in humans, too. Rich evidence indicates the significance of the cerebellum in controlling locomotion and posture in humans.

MLR/PPN receive inhibitory inputs from the substantia nigra pars reticulata (SNr). Together with the subthalamic nucleus (STN) and the internal segment of globus pallidus (GPi), the SNr constitutes output nuclei of the basal ganglia. The outputs from the basal ganglia modulate the excitability of the motor-related cortices, such as the primary motor cortex (M1), supplementary motor areas (SMA), and lateral premotor areas (PM), via the thalamus. The motor-related cortices project not only to the brainstem reticular formation and the spinal cord but also to the striatum. The latter projection works as a feedback to the basal ganglia. In other words, the copy of output signals from the motor-related cortex to the motor effectors serves as the signal controlling the status of motor-related cortices at the next stage of the behavior. Of special note is that motor-related areas project to different sub-sectors of the striatum, thereby constituting independent multiple circuits. Those motor-related areas are likely important for human gait as activation of these areas have been observed during gait [2]-[3]. However, the specific role subserved by each area is still unclear. Finally, one of the most important regulator of the status of the basal ganglia is dopaminergic (DA) projection from the substantia nigra pars compacta (SNc).

B. Pathophysiology of Parkinsonian gait

In patients with Parkinson's disease (PD), degeneration of SNc DA neurons leads to overwhelming inhibitory outputs from the basal ganglia, and this change results in hypokinesia due to the failure for the motor cortices to be

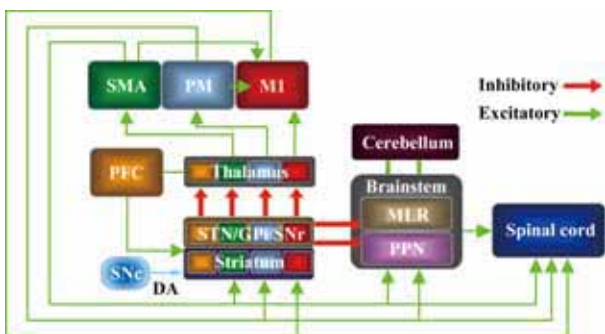


Fig. 2. Pathophysiology of Parkinsonian gait (modified from [2])

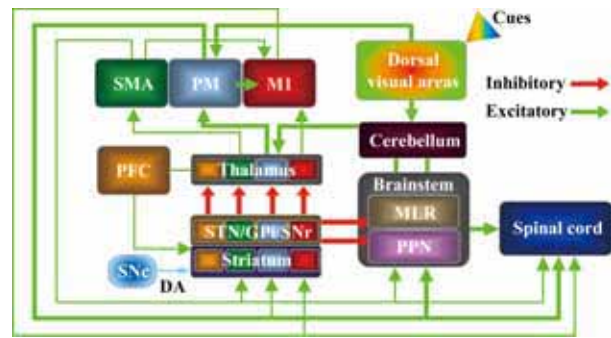


Fig. 3. Mechanisms generating paradoxical gait (modified from [2])

energized on demand. Further, it is proposed that the over-inhibition from the basal ganglia to the PPN may result in increased muscle tonus (rigidity) in PD patients. Gait disturbance in PD seems to be a result from combined dysfunctions of these basal ganglia-cortical and basal ganglia-brainstem systems [1]. Partly in consistent with this hypothesis, hypofunction of SMA is shown during Parkinsonian gait [3].

C. Mechanisms of paradoxical gait in PD (Figure 3)

Even advanced PD patients with frequent freezing phenomena may be able to overcome their disability when exposed to strong emotional stimuli or such visual stimuli as transverse lines placed with adequate intervals. This phenomenon is sometimes called “kinesie paradoxale” as apparently more task demands make the task less difficult. We previously showed that the cerebellum, dorsal visual areas, and lateral premotor cortex were activated during the amelioration of Parkinsonian gait under the influence of visual stimuli [4].

Certain visual stimuli as transverse lines are preferentially processed in the dorsal visual areas and the cerebellum. The dorsal visual areas are interconnected with the PM, and these two areas are the key substrates for visuomotor behavior. During walking under visual guidance, the two pathways (dorsal visual areas-cerebellum-thalamus-PM and dorsal visual areas-PM) potentially enhance the PM functionality. It seems possible that the activation of the PM overcome the suppression of the locomotor-related regions brainstem and spinal cord, and thus restore near-normal gait in PD.

III. PATHOPHYSIOLOGY OF GAIT DISTURBANCE IN PATIENTS WITH ISCHEMIC SUBCORTICAL LESIONS

A. Parkinson-like gait disturbance in patients with ischemic subcortical lesions

It has been long known that pronounced “leukoariosis” often as a result from microvasculopathy is associated with gait disturbance. A survey of in-hospital patients showed that SAE/SVE (subcortical arteriosclerotic encephalopathy or subcortical vascular encephalopathy) was the second most frequent cause of gait disturbance only after PD [5]. A subtype of SAE/SVE presenting primarily with cognitive decline (“Binswanger's disease”) sometimes manifests “lower-body parkinsonism [6].” Especially, periventricular

white-matter lesions are reported to be associated with lower body Parkinsonism. Lower-body Parkinsonism refers to akinetic-rigid syndrome almost limited to the lower half of the body, especially gait. Cerebrovascular disorder including SAE/SVE is considered the most frequent etiology of so-called “frontal gait disorder.”

Gait disturbance in SAE/SVE is characterized by both locomotor insufficiency and postural instability [7]. Gait analyses of SAE/SVE patients revealed decreases in cadence and marked increases of the time for double support phase [8].

Previously proposed mechanisms of gait disturbance in SAE/SVE include disconnection between the frontal cortex and the subcortical locomotor centers. Unfortunately, there has been no direct evidence to date. As subcortical lesions can be detected by standard clinical imaging like MRI or X-ray computed tomography, it seems worthwhile taking a look at the relationship between lesions and gait disturbance. However, a cross-sectional study failed to find the significant relationship between gait disturbance and white matter lesions on T2-weighted anatomic MRIs in SAE/SVE patients [6]. Some SAE/SVE patients who had pronounced lesions on MRIs showed marked gait disturbance whereas some with marked MRI lesions were not so severely affected. SAE/SVE patients often have multiple lacunar infarcts in the basal ganglia, and it is difficult to determine if white matter lesions or basal ganglia infarcts are responsible for gait disturbance. Another point is that abnormal intensities on MRI may include non-specific changes such as leakage of the cerebrospinal fluid from the ventricles or the enlargement of perivascular space.

To clarify the pathophysiology of gait disturbance in SAE/SVE patients, we performed a cerebral blood flow (CBF) activation study in patients with SAE/SVE with various degrees of gait disturbance. This study was also to test the proposed hypothesis of the neuroanatomy of human gait. A split-does method was employed for the two injections of SPECT tracers. ^{99m}Tc -ECD (^{99m}Tc -ethylcysteinate dimer) was used as a radiotracer. ^{99m}Tc -ECD is fixed within the brain in proportion to regional cerebral blood flow and stay there for hours in a stable form. Further, ^{99m}Tc -ECD is easier to handle than is ^{99m}Tc -PAO (^{99m}Tc -hexamethyl-propyleneamine oxime).

B. Methods

1) Subjects: The evaluation of white matter lesion was based on the criteria proposed by Fazekas and colleagues [9]. Included SAE/SVE patients were those whose Fazekas' grade were 3 or more; namely, periventricular white matter abnormal intensities, irregular in shape, extended into the deep white matter and those deep white matter lesions widely joined together. Exclusion criteria were: 1) patients who were hospitalized due to recent episodes of acute stroke within 1 month of the enrollment; 2) patients who underwent surgery due to degenerative lumbar spinal disorder within 6 months of the enrollment; 3) patients who complained of lumbago or knee pain at the time of

enrollment. Eighteen subjects were found eligible for the study (10 men, 8 women). The mean age of the subjects was 75 years old (range, 68-81 years old). Subjects gave informed consent for the enrollment.

2) Evaluation of gait disturbance: A gait analysis was performed to evaluate the severity of gait disturbance of the enrolled patients. By means of force plate and joint-motion capture systems, following parameters were calculated: cadence, gait speed, step length, double support phase, single support phase, and step width. FOGQ score [10], a subjective scale reflecting freezing phenomena, was also assessed by questionnaire.

The gold standard does not exist as yet for the assessment of gait disturbance in SAE/SVE patients. Hence, we asked three neurologists to evaluate the appearance of gait of the enrolled patients. They evaluated and scored several aspects of gait, through a video monitor. The patients were classified into a gait impaired group and an unimpaired group.

3) A CBF activation study was conducted on a 3-head SPECT scanner (Prism3000, Picker). CBF measurements were performed in two behavioral conditions (gait and rest). In half of the patients, the gait condition was studied first, and in the rest of the patients the rest condition was studied first. In the gait-rest conditional order, for example, the patients were first asked to walk on a treadmill under the supervision of a medical doctor. When treadmill walking was judged to reach a stable state, a bolus of ^{99m}Tc -ECD (300 MBq) was administered intravenously (gait condition). They kept walking for 5 minutes after the injection. Then they were moved onto the SPECT scanner, and scanning was commenced about 10 minutes after the tracer injection. Scanning lasted for 24 minutes for the first injection. After 5 minutes of the scan completion, the subjects received another bolus of ^{99m}Tc -ECD (500 MBq) while lying on the scanner bed (rest condition). Scanning started 10 minutes after the second injection and lasted for 24 minutes.

Reconstructed CBF images were analyzed with SPM2. Images were motion corrected, spatially normalized to fit into a standard stereotaxic space, and were smoothed. Statistical analysis was performed voxel-by-voxel, which produced statistical parametric mapping of *t*-statistics.

C. Results

Ten patients were classified into the gait-impaired group and 8 patients were judged have normal locomotor ability. There were significant differences in the gait parameters between the two groups (data not shown).

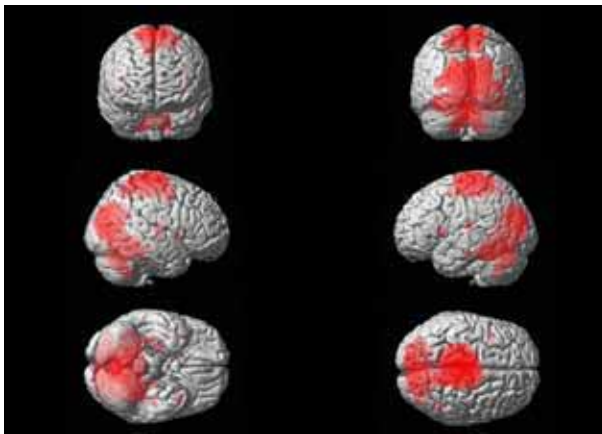


Fig. 4. Significant activation during the walking condition as compared with the rest condition ($P < 0.05$, FDR corrected).

A preliminary analysis of CBF data is presented below. First, all patients were pooled together and CBF increase during the gait condition was assessed as compared with the rest condition (Figure 4). The gait-related activation included medial fronto-parietal cortices (M1, SMA, dorsal parts of PM, somatosensory cortex), visual association areas, and infratentorial areas (vermis and para-median parts of cerebellar hemisphere).

When gait-related activation was compared between the gait-impaired group and the unimpaired group, the impaired group showed reduction of gait-related CBF increases in the left PM and visual association areas. On the other hand, the gait-impaired group showed increase in gait-related activation in SMA as compared with the unimpaired group.

D. Discussion

The overall pattern of gait-related activity was quite similar to that was reported for elderly volunteers in our previous experiment [3]. This finding supports the roles of multiple motor areas and the cerebellum for human gait. Interestingly, the decreased PM activity and increased SMA activity seems the opposite of the activity changes observed in PD patients as compared with control subjects. A more detailed analysis using parameters from the gait analysis is now underway.

IV. CONCLUSION

By combining the proposed neuroanatomy of gait and the preliminary results from the SAE/SVE patients, we can hypothesize that dysfunction of either PM or SMA causes

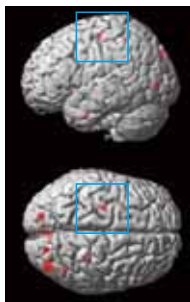


Fig. 5. Reduction of gait-related activation in the gait-impaired groups as compared with the impaired group ($P < 0.005$, uncorrected). Cyan square includes left PM activity.

gait impairment, with accompanying a compensatory overactivity of the other area.

ACKNOWLEDGMENT

The authors would like to thank Dr Manabu Nankaku at the Kyoto University Hospital for his technical help, Dr Hidekazu Tomimoto at Department of Neurology, Kyoto University Graduate School of Medicine for referring patients, and also Professor Hidenao Fukuyama at Human Brain Research Center, Kyoto University Graduate School of Medicine for his general support.

REFERENCES

- [1] K. Takakusaki, T. Habaguchi, J. Ohtinata-Sugimoto, K. Saitoh, T. Sakamoto. "Basal ganglia efferents to the brainstem centers controlling postural muscle tone and locomotion: a new concept for understanding motor disorders in basal ganglia dysfunction," *Neuroscience*, vol. 119, no. 1, pp. 293-308, January 2003.
- [2] T. Hanakawa. "Neuroimaging of standing and walking: Special emphasis on Parkinsonian gait," *Parkinsonism Relat. Disord.*, vol. 12, suppl. 2, pp. S70-S75, October 2006.
- [3] T. Hanakawa, Y. Katsumi, H. Fukuyama, M. Honda, T. Hayashi, J. Kimura, H. Shibasaki. "Mechanisms underlying gait disturbance in Parkinson's disease: a single photon emission computed tomography study," *Brain* vol. 122, part 7, pp. 1271-1281, July 1999.
- [4] T. Hanakawa, H. Fukuyama, Y. Katsumi, M. Honda, H. Shibasaki. "Enhanced lateral premotor activity during paradoxical gait in Parkinson's disease," *Ann. Neurol.*, vol. 45, no.3, pp. 329-226, March 1999.
- [5] H. Stolze H, S. Klebe, C. Baecker, C. Zechlin, L. Friege, S. Pohle, G. Deuschl. "Prevalence of gait disorders in hospitalized neurological patients," *Mov. Disord.* vol. 20, no. 1, pp 89-94, January 2005.
- [6] L. Sudarsky. "Gait disorders: Prevalence, morbidity, and etiology," *Adv. Neurol.*, vol. 87, pp. 111-117.
- [7] J. Jankovic, J. G. Nutt JG, L. Sudarsky. "Classification, diagnosis and etiology of gait disorders," *Adv. Neurol.* vol. 87, pp. 119-133, 2001.
- [8] H. Bazner, M. Oster, M. Daffertshofer, M. Hennerici. "Assessment of gait in subcortical vascular encephalopathy by computerized analysis: a cross-sectional and longitudinal study," *J. Neurol.*, vol. 247, no. 11, pp. 841-849, November 2000.
- [9] F. Fazekas, J. B. Chawluk, A. Alavi, H. I. Hurtig, R. A. Zimmerman. "MR signal abnormalities at 1.5T in Alzheimer's dementia and normal aging," *AJR Am. J. Roentgenol* vol. 149, no. 2, pp. 421-426, August 1987.
- [10] N. Giladi, H. Shabtai, E. S. Simon, S. Biran, J. Tal, A. D. Korczyn. "Construction of freezing of gait questionnaire for patients with Parkinsonism," *Parkinsonism Relat. Disord.*, vol. 6, no. 3, pp. 165-170, July 2000.

Neural mechanisms of integration of the somatic and autonomic nervous functions in the emergence of motor behaviors

Kiyoji MATSUYAMA and Mamoru AOKI

Summary: Coordinated movements between left and right limbs and between fore- and hind-limbs are essential for locomotion in quadrupeds. During locomotion evoked by stimulation to the cuneiform nucleus in decerebrate rabbits, the hindlimbs exhibited left-right in-phase hopping gaits with strong backward extensions, while the forelimbs showed left-right alternating movements, thus indicating that locomotor pattern-generating networks (CPGs) for fore- and hind-limbs are constituted in a different manner. Despite such differences, locomotor cycles of the forelimbs were well synchronized with those of the hindlimbs when the hindlimb hopping was evoked. This suggests that fore- and hind-limb CPGs are tightly coupled via ascending propriospinal systems. Such divergent coordination mechanisms in the spinal cord are suitable for elaborating wider motor synergies of all limbs during locomotion in rabbits.

I. Introduction

All animals can behave freely and volitionally under various conditions of external environments surrounding them. For smooth emergence of such behaviors, it is essential to coordinate functions of the somatic and autonomic nervous systems, each of which is involved in the control of animal motions and internal body environments, respectively. In this study, to understand neural mechanisms for coordination of these systems, we focus attention on “locomotion” and “respiration” as a representative somatic and autonomic nervous function, respectively, and aim to investigate neural mechanisms

Kiyoji Matsuyama: Dept. of Physiology, Sapporo Medical University School of Medicine, South-1, West-17, Chuo-ku, Sapporo 060-8556, Japan. (TEL: +81-11-611-2111, FAX: +81-11-644-1020, e-mail: matsuk@sapmed.ac.jp)

Mamoru Aoki: Dept. of Physical Therapy, Hokkaido Bunkyo University, Faculty of Human Science, Kogane-cho, Eniwa 061-1408, Japan

for the control and regulation of these functions.

Locomotion and respiration are characterized by their rhythmic movements, and their basic neural control systems are commonly located in the brainstem and spinal cord. In this year, we have studied the following two points: 1) neural mechanisms for generating coordinated quadrupedal locomotion in rabbits, 2) involvements of medullary raphe nuclei in respiration control in rats [1]. In particular, in the former study, we have developed a locomotor preparation using decerebrate rabbits and characterized their evoked-locomotor patterns. Below, we summarized the findings from this study.

II. Research achievements

Neural mechanisms for generating coordinated quadrupedal locomotion in rabbits

1. Purpose

In quadrupedal locomotion, coordinated movements between left and right limbs and between fore- and hind-limbs are essential. Many quadrupeds such as cats and dogs usually exhibit left-right alternation between two limbs of the same girdle and also synchronous movements of fore- and hind-limbs during locomotion [2]. However, rabbits usually exhibit “hopping” gaits, which are characterized by left-right nonalternation of the hindlimbs. Similar nonalternating gaits appear in other quadrupeds when they move at high speed in “gallop”. This study was aimed to 1) characterize coordination patterns of the left and right limbs and also those of the fore- and hind-limbs during locomotion in rabbits, and 2) reveal neural mechanisms for generating the coordination.

2. Materials and Methods

a. Surgical procedures

Experiments were performed on 15 adult male rabbits (New Zealand White) weighing 2-3 kg. Under halothane

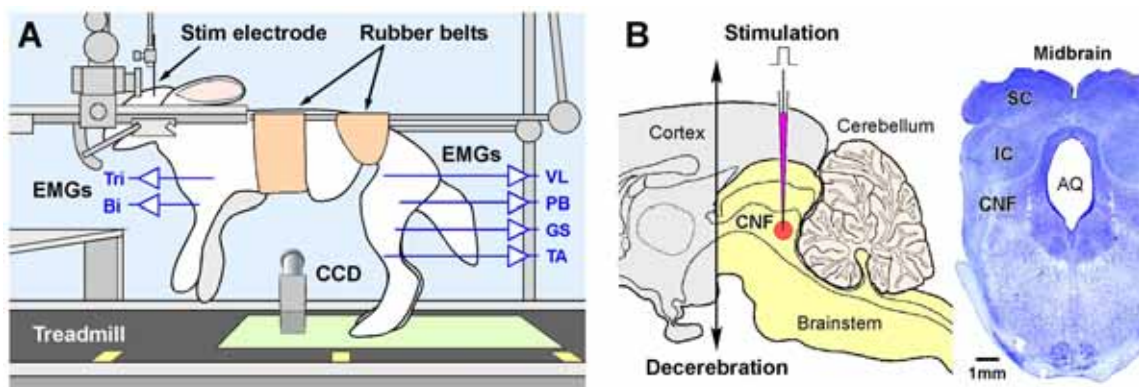


Fig. 1. Decerebrate rabbit locomotor preparation (A) and hopping movement-inducing site in the midbrain (B).

A: Reflex standing posture of the decerebrate rabbit. To record EMGs from extensors and flexors of all limbs, pairs of insulated copper wires were implanted into the biceps brachii (Bi) and triceps brachii (Tri) muscles in the forelimbs, and the vastus lateralis (VL), posterior biceps (PB), gastrocnemius-soleus (GS) and tibialis anterior (TA) muscles in the hindlimbs.

B: Location of the cuneiform nucleus (CNF) in the midbrain.

gas anesthesia with oxygen, the animal was surgically decerebrated at the precollicular-postmammillary level. After decerebration, gaseous anesthesia was discontinued. The head was then fixed in a stereotaxic apparatus, and the chest and abdominal parts were supported by rubber belts to set the body axis in a horizontal position (Fig. 1A). The feet were placed on a treadmill belt or a smooth flooring sheet put on the belt. To maintain the reflex standing posture by the hindlimbs, the forelimbs were floated in the air because their lengths are short.

b. Experimental procedure

A Wood's metal-filled glass microelectrode with a tip replaced with a carbon fiber was inserted stereotaxically into the cuneiform nucleus (CNF) in the midbrain, which corresponds to the mesencephalic locomotor region (MLR) identified in cats [2], and electrical stimuli (50 Hz, 10-110 μ A, 0.2 ms duration) were delivered for 5-15 sec to evoke locomotion (Fig. 1B). The EMGs were recorded by implanting pairs of insulated copper wires (diameter 75 μ m) into selected extensors and flexors of the four limbs (see Fig. 1A). Using a CCD camera and a videotape recorder, movements evoked by CNF stimulation were recorded at 60 frames/sec.

In some cases, after observation of the evoked locomotion, the animals were anesthetized again, and then a complete transection or hemisection of the lower thoracic cord was made at T12. After recovery from anesthesia, we stimulated the CNF, and observed the evoked movements.

3. Results

a. Characteristics of locomotor movements evoked by stimulation to the CNF in decerebrate rabbits

In decerebrate rabbits, when the CNF was stimulated, bilateral hindlimbs consistently exhibited rhythmic, left-right nonalternating (in-phase) gaits, viz. hopping. Such hindlimb hopping movements were evoked not only on a moving belt of the treadmill but also on a still

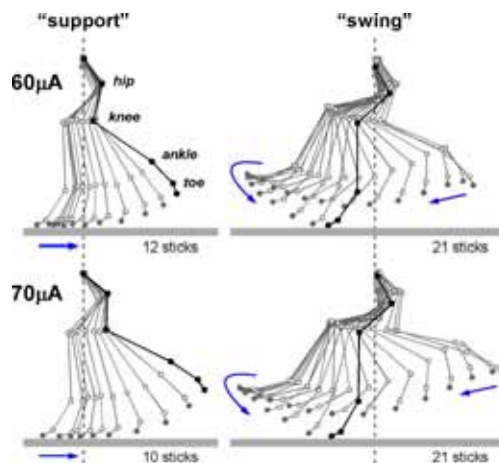


Fig. 2. Gaits of the left hindlimb during hopping movements evoked by 60 and 70 μ A CNF stimulation on a still surface of a smooth flooring sheet. A hopping cycle is divided into support and swing phases, and trajectories of hindlimb movements in each phase are illustrated by stick figures made from video images recorded at 60 frames/sec. The support phase was defined as a period from the beginning of ground contact of the toe to the end of the hindlimb extension (i.e., maximal hindlimb extension). Note that the number of stick figures in the support phase at 70 μ A (n=10) is smaller than that at 60 μ A (n=12).

surface of a smooth flooring sheet (Fig. 2). Left-right alternating gaits as usually seen in decerebrate cats were not evoked at any stimulus intensity. At stronger CNF stimulation, cycle periods of the hindlimb hopping became shorter because of a shortening of support phase in a hopping cycle (Fig. 2).

In addition to the hindlimbs, as shown in Fig. 3A, during CNF stimulation, rhythmic movements of the forelimbs were also evoked. But unlike the hindlimbs, they basically exhibited left-right alternating movements. Despite such differences, rhythm cycles of the forelimbs were consistent with those of the hindlimbs.

Fig. 3B shows patterns of activities of the fore- and

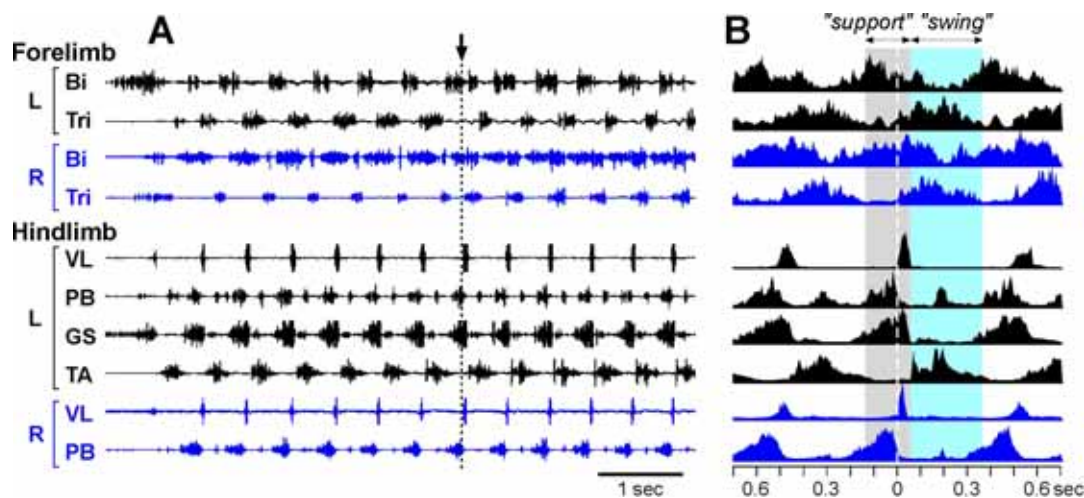


Fig. 3. EMG recordings from fore- and hind-limb muscles during hopping movements evoked by CNF stimulation.

A: Untreated traces of fore- and hind-limb extensor and flexor EMGs during hopping movements evoked by 70 μ A stimulation on a still smooth surface. EMGs of left and right limb muscles are shown by black and blue, respectively. A dotted line with a downward arrow indicates a timing after which coordination patterns between left and right forelimbs changed (see below). **B:** Integrated and averaged EMGs representing patterns of EMG activities in a single hopping cycle. These are aligned with the onset of burst of the left VL EMG (indicated by a white broken line). Support and swing phases in a single step cycle are highlighted by gray and blue, respectively. The timing of transition from the support phase to the swing phase corresponds to the timing of the end of VL-EMG burst.

hindlimb muscles in a single step cycle. In the hindlimbs, the posterior biceps (PB) and gastrocnemius-soleus (GS) muscles gradually increased their activities in the stance phase. Their activities reached peak levels in the late stance phase. The vastus lateralis (VL) muscles showed strong transient bursts just before the end of the stance phase. Such strong GS, PB and VL bursts in the late stance phase characterize powerful backward extensions of the hindlimbs, necessary for producing strong propulsive forces during hopping.

Extensor (Triceps brachii) and flexor (Biceps brachii) in an individual forelimb were active in opposite phase (Fig. 3A,B), and homonymous muscles on both sides were active in opposite phase (Fig. 3A). These represent left-right alternating and simple extension-flexion movements of the forelimbs during locomotion.

b. Interlimb coordination during locomotion

In decerebrate rabbits, the hindlimbs always exhibited left-right in-phase gaits during CNF stimulation at any stimulus intensity. However, their coordination patterns between the left and right forelimbs and between the fore- and hind-limbs were altered by strong CNF stimulation.

As shown in a plot in Fig. 4A, reflecting the left-right alternation of the forelimbs during locomotion, phase differences of activities of left and right Tri muscles at 60 μ A CNF stimulation were distributed around 180 degree.

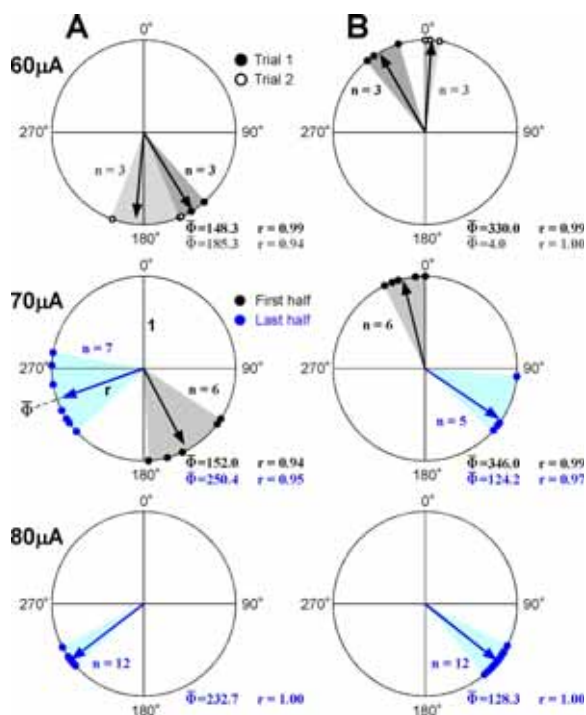


Fig. 4. Circular plot representations of the phase relationships between the onsets of extensor EMG bursts of two different limbs during hopping evoked by 60, 70 and 80 μ A CNF stimulation. **A:** Relationships between the left and right forelimb extensors (R-Tri - L-Tri). **B:** Relationships between the left forelimb and left hindlimb extensors (L-Tri - L-VL). In the circular plots of 70 and 80 μ A, the relationships in single trials are shown, but in the plots of 60 μ A, those in 2 trials are superimposed. The phase relationships in the first and last halves of 70 μ A stimulation are represented by black and blue, respectively. In each circular plot, the mean phase ($\bar{\phi}$) is indicated by a directional vector (arrow) with the origin from the center of the circle and ranges from 0 to 1.

Table 1. Stimulus intensity vs. mean hopping cycle periods

| Stimulus intensity | Mean hopping cycle period (sec) |
|-------------------------|---------------------------------|
| 60 μ A | 0.52 ± 0.03 (n = 3 + 4) |
| 70 μ A (First half) | 0.51 ± 0.01 (n = 6) |
| 70 μ A (Last half) | 0.49 ± 0.01 (n = 6) |
| 80 μ A | 0.46 ± 0.01 (n = 14) |

The mean value at 60 μ A stimulation was obtained from 2 trials. The mean cycle period at 70 μ A stimulation was shorter in the last half of the trial than the first half.

Similar distributions were found in the first half of 70 μ A stimulation. In the last half of this stimulation, however, the phase differences suddenly shifted to around 250 degree. These phase changes were sustained at 80 μ A stimulation. As shown in Fig. 4B, the phase relationships between the fore- and hindlimbs also changed in the last half of 70 μ A stimulation. These changes were also sustained at 80 μ A stimulation.

Since hopping cycle periods were shortened at higher stimulus intensity (Table 1), rabbits also might change interlimb coordination patterns when they move at high speed.

c. Neural mechanisms for interlimb coordination

In quadrupeds, propriospinal (PS) systems projecting over several segments in the spinal cord are essential neural substrates for coordinating activities of locomotor pattern generators (CPGs) for fore- and hind-limb locomotion, which are located in the cervical and lumbar spinal cord, respectively [3,4]. To know functional roles of PS systems in the generation of coordinated locomotion in rabbits, we transected PS pathways partially or totally at the lower thoracic cord in decerebrate rabbits, and investigated characteristics of fore- and hind-limb movements evoked by CNF stimulation

In a decerebrate rabbit with a complete transection at T12, CNF stimulation evoked rhythmic, left-right alternating movements in the forelimbs (Fig. 5). Phase differences of activities of the left and right Tri muscles

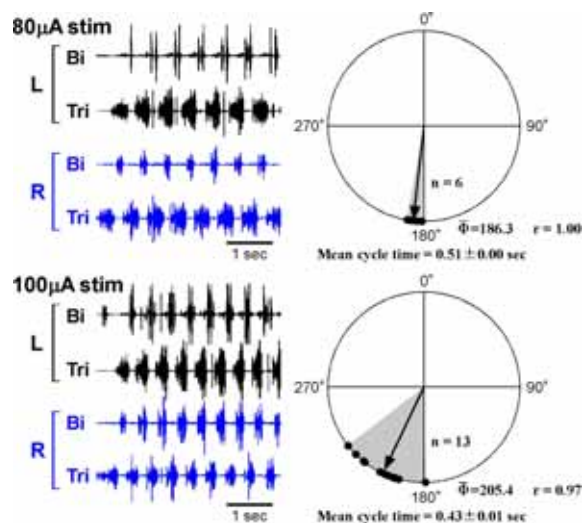


Fig. 5. **Right:** EMGs of extensors and flexors of the forelimbs during 80 and 100 μ A CNF stimulation in a decerebrate rabbit with a complete transection at T12. **Left:** Phase relationships between the onsets of bursts of the left and right Tri EMGs (R-Tri - L-Tri) during 80 and 100 μ A stimulation.

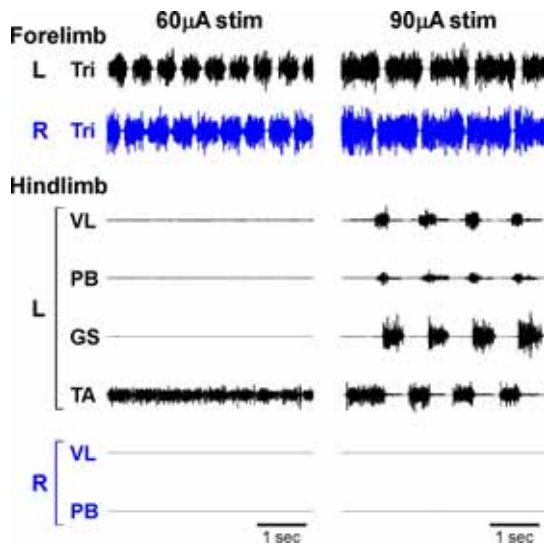


Fig. 6. EMGs of fore- and hind-limb muscles during 60 and 90 μA stimulation to the left CNF in a decerebrate rabbit with a right hemisection at T12.

evoked at 80 μA stimulation were distributed around 180 degree (right panel in Fig. 5). At 100 μA stimulation, although cycle periods were shortened, distributions of the phase differences were similar to those at 80 μA (left in Fig. 5). The phase shifts, as seen in the spinal cord intact animals at strong stimulation (Fig. 4A), were not observed. This suggests that left and right forelimb CPGs act essentially in opposite phase each other.

In a decerebrate rabbit with a right hemisection at T12, the left CNF stimulation at 60 μA evoked rhythmic, left-right alternating movements in the forelimbs but not in the hindlimbs (left in Fig. 6). At 90 μA stimulation, all limbs except the right hindlimb exhibited rhythmic movements at the same cycle (right in Fig. 6). Despite such strong intensity, cycle periods of the forelimb movements were prolonged to circa twice of those at 60 μA stimulation. Rather, rhythms of the forelimb movements appeared to be entrained to slow rhythms of the left hindlimb movements. This indicates that neural signals ascending from the lumbar spinal cord on one side modify activities of forelimb CPGs on both sides.

4. Discussion

It is known that a basic neural circuitry involved in the generation of coordinated quadrupedal locomotion is comprised from neural subsystems located in the brainstem and spinal cord [2]. That is, as shown in Fig. 7, reticulospinal (RS) pathways convey locomotor driving signals, e.g. those arising from the CNF in decerebrate animals, to fore- and hind-limb CPGs that are located in the bilateral cervical and lumbar spinal cord, respectively. Commissural neurons (CNs) project across the midline and densely innervate the contralateral spinal cord at the same segmental level, thus suggesting that left and right CPGs are mutually connected via CNs on both sides [5]. Although each CPG can generate locomotor rhythm, such mutual connections would be necessitated to synchronize rhythmic activities of left and right CPGs [6]. Since many CNs receive RS inputs and exhibit locomotor-related rhythmic activities, a part of them are assumed to act as a primary component of CPGs [7].

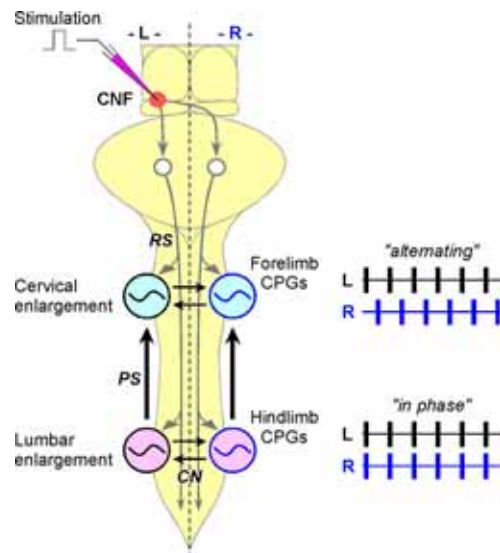


Fig. 7. Scheme of a putative basic neural circuitry involved in the generation of coordinated hopping movements in rabbits. CN, commissural neurons; PS, propriospinal pathways; RS, reticulospinal pathways.

During hopping evoked in decerebrate rabbits in this study, the fore- and hind-limbs showed different left-right coordination patterns, i.e., left-right alternation in the forelimbs and left-right in-phase in the hindlimbs (see Figs. 3 and 7). This may be due to functional differences of cervical and lumbar CN circuits connecting the left and right spinal cord.

Further, the hindlimb movements are characterized by strong backward extension in the late stance phase, while the forelimb movements by simple flexion-extension movements, indicating that fore- and hind-limb CPGs are constituted functionally in a different manner. Despite such differences, locomotor cycles of the forelimbs were synchronized with those of the hindlimbs when the hindlimb hopping was evoked. This suggests that fore- and hind-limb CPGs are tightly coupled possibly via ascending propriospinal (PS) systems (see Fig. 7). Such divergent coordination of fore- and hind-limb CPGs imposed by ascending PS systems would be suitable for elaborating wider motor synergies of all limbs during locomotion in rabbits.

References

1. Cao Y, Matsuyama K, Fujito Y, Aoki M (2006) Involvement of medullary GABAergic and serotonergic raphe neurons in respiratory control: electrophysiological and immunohistochemical studies in rats. *Neurosci Res* 56:322-331.
2. Grillner S (1981) Control of locomotion in bipeds, tetrapods, and fish. In: *Handbook of Physiology, Section 1, The Nervous system, Vol.2 Motor Control*, pp.1179-1236.
3. Jankowska E (1992) Interneuronal relay in spinal pathways from proprioceptors. *Prog Neurobiol* 38:335-378.
4. Juvin L, Simmers J, Morin D (2005) Propriospinal circuitry underlying interlimb coordination in mammalian quadrupedal locomotion. *J Neurosci* 25:6025-6035.
5. Matsuyama K, Kobayashi S, Aoki M (2006) Projection patterns of lamina VIII commissural neurons in the lumbar spinal cord of the adult cat: an anterograde neural tracing study. *Neuroscience* 140:203-218.
6. Cowley KC, Schmidt BJ (1997) Regional distribution of the locomotor pattern-generating network in the neonatal rat spinal cord. *J Neurophysiol* 77:247-259.
7. Matsuyama K, Nakajima K, Mori F, Aoki M, Mori S (2004) Lumbar commissural interneurons with reticulospinal inputs in the cat: morphology and discharge patterns during fictive locomotion. *J Comp Neurol* 474:546-561.

A Locomotor CPG Model based on Phase Dynamics

Ikuko Nishikawa, Ritsumeikan University

Abstract—A network of limit cycle oscillators is used as a model of a central pattern generator (CPG) for a multiped locomotion. Each oscillator controls an oscillatory movement of one limb, and receives a motor control input from higher motor centers. A complex-valued artificial neuron is used to describe each oscillator, and a spinal CPG is modeled by a mutually connected network, which is a mathematical extension of a conventional real-valued Hopfield network. The network dynamics of the phase is known to be reduced to a coupled system of phase oscillators. First, for a bipedal gait, a pair of identical oscillators are used as a CPG model, to analyze the dependency of a gait dynamics on a constant input from higher motor centers. Numerical calculations show the system successfully expresses some characteristic behaviors, which were obtained by more complicated Fitzhugh-Nagumo oscillator model, and which were found in clinical data of disordered interlimb coordination caused by Parkinson's disease. The observed results of symmetric anti-phase synchronization, asymmetric synchronization, and breakdown of the synchronization can be explained by the existence condition of the network energy function, and by the synchronization condition of a coupled system of phase oscillators. Second, for a quadrupedal gait, four identical oscillators connected with a simple symmetry are used as a CPG model. A condition on the coupling parameters for the existence of attractors, which correspond to walk, bound, pronk, trot and pace, is clarified both through a simple analysis and numerical calculations.

I. INTRODUCTION

A network of limit cycle oscillators is used to model a spinal CPG for a bipedal or quadrupedal gait. Each oscillator controls an oscillatory movement of one limb. In this report, a complex-valued artificial neuron is used to model each oscillator. And a mutually connected network of the oscillators, which can be described as a mathematical extension of a conventional real-valued Hopfield network, is used to model a CPG.

II. COMPLEX-VALUED HOPFIELD NEURAL NETWORK

A. Fundamental Equation and Equilibrium of the Dynamics

i -th oscillator of CPG is described by a complex-valued artificial neuron $z_i(t)$, whose autonomous dynamics contains a rotational motion in a complex plane. The dynamics of a mutually connected network is given by[3], [4],

$$\begin{cases} \frac{dz_i(t)}{dt} &= \left(-\frac{1}{\tau_i} + i\omega_i \right) z_i(t) + \sum_{j=1}^N w_{ij} u_j(t) + \theta_i(t) , \\ u_i(t) &= f(z_i(t)), \quad i = 1, \dots, N , \end{cases} \quad (1)$$

where N is the number of neurons in a network, $u_i(t)$, $z_i(t)$ and $\theta_i(t) \in \mathbf{C}$ are the output, the internal state and the external input of the i -th neuron, respectively. The coefficient of the linear term of z_i is a complex value $-1/\tau_i + i\omega_i$,

where i is an imaginary unit. When $\tau_i > 0$, the neuron has a stable fixed point $z_i = 0$ and $\tau_i \in \mathbf{R}$ is a time constant. The imaginary part $\omega_i \in \mathbf{R}$ gives an angular frequency of the rotation in a complex plane. $w_{ij} \in \mathbf{C}$ is the connection weight from the j -th neuron to the i -th neuron.

Activation function $f : \mathbf{C} \rightarrow \mathbf{C}$ is common to all neurons. We restrict the functional form of f to assure the existence of the network energy function. To give the explicit form of f , let us rewrite the complex variable $z_i(t)$ by the amplitude $r_i(t) \geq 0$ and the phase $\phi_i(t)$; $z_i(t) = r_i(t) \exp(i\phi_i(t))$. Then, we restrict the form of f as

$$f(z_i(t)) = f_R(r_i(t)) \cdot \exp(i\phi_i(t)) , \quad (2)$$

where $f_R(\cdot)$ is a nonlinear real function, and here we assume $f_R : R_+ \rightarrow R_+$, where $R_+ = \{r \geq 0, r \in \mathbf{R}\}$. For this type of f , the following sufficient conditions are derived[3] for the existence of the energy function under the restriction of $\forall i, \omega_i = 0$. First, the condition on the connection weight w_{ij} is expressed as the Hermitian condition on the connection weight matrix $W = (w_{ij})$. Then, sufficient conditions on the activation function f are given as follows. When $f_R(r)$ is bounded and continuously differentiable with respect to $r \in R_+$, then the network possesses an energy function if, $\forall r \in R_+$, $\frac{df_R(r)}{dr} > 0$, and $\lim_{r \rightarrow 0} \frac{f_R(r)}{r} > 0$.

If a network (1) is homogeneous with $\forall i, \omega_i = \omega$ and the activation function f takes the form of Eq.(2), then a network of rotating neurons $\omega \neq 0$ can be transformed to the equation with $\omega = 0$ through a rotational transformation by ω for $\forall \omega$. Therefore, the above sufficient conditions are applicable for $\forall \omega$ in this type of the network.

B. Dynamics of Phase and Amplitude

Let us rewrite the complex-valued connection weight w_{ij} which satisfies the Hermitian condition by an amplitude $K_{ij} \geq 0$ and a phase δ_{ij} in the following form;

$$\begin{aligned} w_{ij} &= \frac{1}{2} \{ K_{ij} \exp(-i\delta_{ij}) + K_{ji} \exp(i\delta_{ji}) \} \\ &= w_{ij}^* . \end{aligned}$$

The complex-valued input $\theta_i(t)$ is also rewritten as $\theta_i(t) = \Theta_i(t) \exp(i\gamma_i(t))$.

Then, Eq.(1) is decomposed into the dynamics of the amplitude and the phase of each neuron as follows, by taking the real and imaginary parts of Eq.(1), respectively.

Real part for the amplitude dynamics:

$$\begin{aligned} \frac{dr_i}{dt} &= -\frac{1}{\tau_i} \cdot r_i + \sum_j \frac{1}{2} f(r_j) \{ K_{ij} \cos(\phi_j - \phi_i - \delta_{ij}) \\ &\quad + K_{ji} \cos(\phi_j - \phi_i + \delta_{ji}) \} + \Theta_i \cos(\gamma_i - \phi_i) . \end{aligned} \quad (3)$$

Imaginary part for the phase dynamics:

$$\frac{d\phi_i}{dt} = \omega_i + \sum_j \frac{1}{2} \frac{1}{r_i} f(r_j) \{K_{ij} \sin(\phi_j - \phi_i - \delta_{ij}) + K_{ji} \sin(\phi_j - \phi_i + \delta_{ji})\} + \frac{1}{r_i} \Theta_i \sin(\gamma_i - \phi_i). \quad (4)$$

Eq.(4) for the phase can be seen as a coupled system of N phase oscillators[1] with a modification of the coupling strength by the amplitude r_j . Therefore, a phase synchronization emerges in such a network, just as is well known in a phase oscillator system. And the authors have successfully applied this phase synchronization mechanism for an area-wide urban traffic flow control[2], [4], [5].

III. CPG MODEL FOR BIPEDAL LOCOMOTION

In this section, a pair of oscillators under a control input are used to model a CPG for a bipedal locomotion. A motor control input from higher motor centers works as a bifurcation parameter for the Hopf Bifurcation. The framework follows the CPG model proposed by Asai et al. 2003 [7]. First, let us remind Poincaré normal form for the Hopf bifurcation, and then model the dynamics after the Hopf bifurcation by a complex-valued artificial neuron.

A. Poincaré Normal Form for the Hopf Bifurcation

Generic two-dimensional system undergoing a Hopf bifurcation can be transformed into Poincaré normal form[6], as is briefly reviewed in the followings.

Consider a two-dimensional system of $\mathbf{x} = (x, y)^T \in \mathbf{R}^2$, $\frac{d\mathbf{x}}{dt} = \mathbf{f}(\mathbf{x}, \alpha)$, $\alpha \in \mathbf{R}$, with a smooth function f , which has at $\alpha = 0$ the equilibrium $\mathbf{x}_0 = 0$ with pure imaginary eigenvalues $\lambda_{1,2} = \pm i\omega_0$, $\omega_0 > 0$. There is an α -dependent invertible transformation for sufficiently small $|\alpha|$, which transforms the above equation into the following Poincaré normal form for a complex variable z with only the resonant cubic term;

$$\frac{dz}{dt} = \lambda(\alpha)z + c_1(\alpha)z^2\bar{z} + O(\|z\|^4), \quad (5)$$

where $\lambda_{1,2}(\alpha) = \mu(\alpha) \pm i\omega(\alpha)$, $c_1(\alpha) \in \mathbf{C}$ can be explicitly calculated from $\mathbf{f}(\mathbf{x}, \alpha)$.

If we rewrite the complex variable z in a polar coordinate by the amplitude $r \geq 0$ and the phase ϕ ; $z = r \exp(i\phi)$, the lowest order in α and r of the normal form (5) in a polar coordinate is given as,

$$\frac{dr}{dt} = \tilde{d} \cdot \alpha r + \tilde{a} r^3 + \text{higher order}, \quad (6)$$

$$\frac{d\phi}{dt} = \omega_0 + \tilde{c} \cdot \alpha + \tilde{b} \cdot r^2 + \text{higher order}. \quad (7)$$

by using new constants $\tilde{a} = \Re c_1(0)$, $\tilde{b} = \Im c_1(0)$, $\tilde{c} = \omega'(0)$ and $\tilde{d} = \mu'(0)$.

B. Model by a Complex-valued Neuron

For the supercritical Hopf bifurcation $\tilde{d} > 0$ and $\tilde{a} < 0$, the equilibrium r_0 of Eq.(6) is

$$r_0(\alpha) = \begin{cases} 0 & \text{for } \alpha \leq 0, \\ \sqrt{\tilde{d}\alpha/|\tilde{a}|} & \text{for } \alpha > 0. \end{cases} \quad (8)$$

On the other hand, if we consider an external input with $\gamma_i(t) = \phi_i(t)$ and $\Theta_i(t) = \Theta$ (const.) for a non-interacting complex-valued artificial neuron (3),(4), the dynamics becomes,

$$\begin{aligned} \frac{dr}{dt} &= -r + \Theta, \\ \frac{d\phi}{dt} &= \omega, \end{aligned}$$

which exponentially converges to the equilibrium $r_0 = \Theta$ (let set $\tau = 1$ for a simplicity). Therefore, by the comparison with Eq.(8), we use the following external input to express the dynamics of $r(t, \alpha)$ near the Hopf bifurcation;

$$\Theta(\alpha) = \begin{cases} 0 & \text{for } \alpha \leq 0, \\ \sqrt{\tilde{d}\alpha/|\tilde{a}|} & \text{for } \alpha > 0. \end{cases}$$

The dynamics of the phase is expressed by the α , r -dependent frequency ω , which is given by Eq.(7), namely, $\omega(r, \alpha) = \omega_0 + \tilde{c} \cdot \alpha + \tilde{b} \cdot r^2$ for $\alpha > 0$.

C. CPG Model by a pair of Complex-valued Neurons

Asai et al.[7] considered a simple CPG model consisting of two identical oscillators with a mutual inhibitory coupling. Each oscillator controls an oscillatory movement of one limb, and receives a motor control input from higher motor centers. They used a model to describe a coordination between two limbs during cyclic movements, and compared with several types of clinical data of disordered interlimb coordination which were observed in patients with Parkinson's disease. The interlimb coordination is characterized by the amplitudes and the phase difference of two oscillators. Fitzhugh-Nagumo equation was used to describe each oscillator, and two oscillators were coupled in a following way;

$$\begin{cases} \frac{dx_i}{dt} = c(x_i - \frac{1}{3}x_i^3 - y_i + \alpha_i) + \delta(x_j - x_i), \\ \frac{dy_i}{dt} = \frac{1}{c}(x_i - by_i + a) + \varepsilon x_j, \quad i, j = 1, 2, \quad i \neq j. \end{cases} \quad (9)$$

α_i models a constant input to i -th oscillator, and works as a bifurcation parameter, which moves the nullcline $\dot{x}_i = 0$ in a vertical direction. The term with ε is a main inhibitory anti-phase coupling, and we assume $0 < b < 1$ and $c > 1$. Then, the system undergoes a supercritical Hopf bifurcation at $\alpha = \alpha_*$ to possess a stable limit cycle. The Poincaré normal form (6),(7) is given explicitly as

$$\begin{aligned} \alpha_* &= \frac{1}{b} \left\{ a - \left(1 - \frac{2}{3}b - \frac{b^2}{3c^2} \sqrt{1 - \frac{b}{c^2}} \right) \right\}, \\ \omega_0 &= \sqrt{1 - \frac{b^2}{c^2}} > 0, \\ \tilde{d} &= \frac{bc\sqrt{1 - \frac{b}{c^2}}}{1 - \frac{b^2}{c^2}}, \quad \tilde{c} = \frac{b^2\sqrt{1 - \frac{b}{c^2}}}{(1 - \frac{b^2}{c^2})^{\frac{3}{2}}} > 0, \end{aligned}$$

and so on.

Therefore, a system of Eqs.(3),(4) with $N = 2$ is used to model the above CPG. We assume the symmetry of the coupling and identical natural frequencies ω_0 for $i = 1, 2$.

Here we consider inhibitory anti-phase type coupling, which corresponds to the negative sign of $w = K \cos \delta$, which is redefined as $w = -K$ by $K > 0$, to result in the following set of equations. α_i is a bifurcation parameter for i -th oscillator ($i = 1, 2$), and α_1 and α_2 can be set different.

$$\begin{cases} \frac{dr_i}{dt} = -r_i - Kf(r_j) \cos(\phi_j - \phi_i) + \Theta_i(\alpha_i), \\ \frac{d\phi_i}{dt} = \omega_i(r_i, \alpha_i) - K \frac{1}{r_i} f(r_j) \sin(\phi_j - \phi_i), \end{cases}$$

where $\Theta_i(\alpha) = A \cdot \alpha^{1/2}$, (10)

$\omega_i(r, \alpha) = \omega_0 + C \cdot \alpha + B \cdot r^2$, $i, j = 1, 2$, $i \neq j$.

D. Numerical Calculations

$f_R(r) = \tanh(r)$ is used to meet the existence condition of the network energy function. However, the sufficient condition for the existence is not satisfied if the angular frequencies ω_1 and ω_2 become different, when different values of α_i are given for $i = 1$ and 2 . Parameter values are $A = 1.0$, $B = 0$, $C = 0.51$, $\omega_0 = 0.73$ and $K = 0.1$ in the following. Let $\alpha_1 = \alpha$, and $\alpha_2 = \alpha + \Delta\alpha$. Then $\Delta\alpha$ is set to 0.0 or -0.2 , while changing α from 0 to 10.0.

The results are shown in Figs.1(a) for $\Delta\alpha = 0$, and 1(b) for $\Delta\alpha = -0.2$. For $\Delta\alpha = 0$, the system converges to the state with constant values of r_1, r_2 and $\Delta\phi = \phi_2 - \phi_1 = \pi$, namely, two oscillators are anti-phase. However for $\Delta\alpha = -0.2$, Fig.1(b) shows the constant value $\Delta\phi$ is not equal to π , and decreases according to the increase of α . If α increases

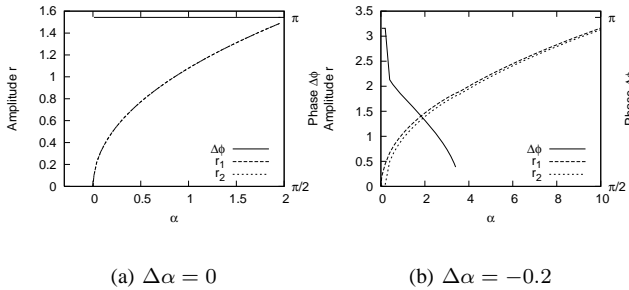


Fig. 1. r_1, r_2 and $\Delta\phi$ for $\alpha = 0 - 2.0$ or 10.0 with $C = 0.51$ up to 10.0, constant r_1, r_2 and $\Delta\phi$ end at $\alpha = \alpha^* \simeq 3.6$, and two oscillators begin to rotate with different frequencies. That is, the frequency synchronization breaks for $\alpha > \alpha^*$. Fig.2 shows that $\Delta\phi(t)$ decreases monotonically, and $r_i(t)$ slightly oscillates with a long period ($\simeq 2\pi / |\frac{d\Delta\phi}{dt}|$), as the effect of the coupling term for r_i in Eq.(10). r_i value in Fig.1(b) for $\alpha > \alpha^*$ is the average of oscillating $r_i(t)$.

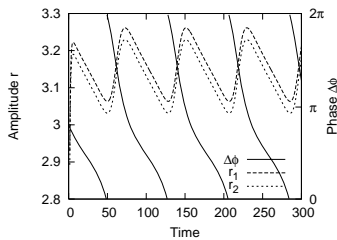


Fig. 2. $r_1(t), r_2(t)$ and $\Delta\phi(t)$ for $t = 0 - 300$ with $C = 0.51$, $\Delta\alpha = -0.2$ and $\alpha = 10.0$

The obtained results are summarized in Table.I. Moreover, three types of behavior (i) $\Delta\phi = \pi$, (ii) $\Delta\phi = \text{const.} \neq \pi$

and (iii) monotonically changing $\Delta\phi(t)$ are summarized in Table.II. These correspond to the types 1, 2 and 3 in the figure 1 in [7], each data of which is shown for both CPG model (9) and clinical data of Parkinson's disease patients. Therefore, for the disordered types of 2 and 3, frequency difference $\omega_1 \neq \omega_2$ is essential, as the result of input difference $\Delta\alpha \neq 0$ to the system with $C \neq 0$.

TABLE I
SATISFACTION OF THE SUFFICIENT CONDITIONS FOR THE EXISTENCE OF THE NETWORK ENERGY OF EQ.(10)

| System Parameter | External Input | $\omega_i(r_i, \alpha_i)$ | Sufficient Conditions | r_i and ϕ_i | |
|------------------|--------------------|----------------------------------|-----------------------|--------------------|--------------|
| | | | | r_i | $\Delta\phi$ |
| $C = 0$ | $\Delta\alpha = 0$ | $\omega_1 = \omega_2 = \omega_0$ | ○ | $r_1 = r_2$ | π |
| | $\Delta\alpha < 0$ | $\omega_1 = \omega_2 = \omega_0$ | ○ | $r_1 > r_2$ | π |
| $C > 0$ | $\Delta\alpha = 0$ | $\omega_1 = \omega_2 > \omega_0$ | ○ | $r_1 = r_2$ | π |
| | $\Delta\alpha < 0$ | $\omega_1 > \omega_2$ | × | $r_1 > r_2$ | |

TABLE II
THREE TYPES OF BEHAVIORS CLASSIFIED BY THE PHASE DIFFERENCE

| $C, \Delta\alpha$ | α | $\Delta\phi$ | Type in [7] |
|--------------------------------|------------------------|------------------------------|-------------|
| $C = 0$ or $\Delta\alpha = 0$ | $\forall \alpha$ | $\Delta\phi = \pi$ | 1 |
| $C > 0$ and $\Delta\alpha < 0$ | $\alpha \leq \alpha^*$ | $\Delta\phi \neq \pi$ | 2 |
| | $\alpha > \alpha^*$ | $\frac{d\Delta\phi}{dt} < 0$ | 3 |

More complicated chaotic dynamics shown as types 4 and 5 in the figure 1 in [7] can not be expressed by Eq.(10), which only describes the dynamics near Hopf bifurcation without higher order terms.

IV. CPG MODEL FOR QUADRUPEDAL LOCOMOTION

A system of Eqs.(3),(4) with $N = 4$ is used to model a CPG for a quadrupedal locomotion. We assume a symmetry of the connection and identical natural frequencies ω for $i = 1, \dots, 4$. In subsection IV-A, a network with C_2 symmetry connection is used, and the existence of the attractors corresponding to various gait patterns are investigated in a parameter space. The consideration on the possible symmetry of the connection is given in subsection IV-B.

A. Ring Network with C_2 Symmetry

Collins et al.[8] modeled a quadrupedal locomotor CPG as a network of four coupled nonlinear oscillators by a ring connection with C_4 symmetry (Cyclic group C_4 of Order 4) as is shown in Fig.3(a), where $i = 1, 2, 3$ and 4 correspond to the left front, left hind, right hind and right front limbs, respectively. Moreover, they considered three different oscillator models, that is, Stein neuronal model, Van der Pol model and Fitzhugh-Nagumo model, and the numerical calculations showed that all models produced three quadrupedal gaits of walk, trot and bound, and the transitions between them depending on the model parameters.

In this subsection, we use a system of Eqs.(3),(4) with identical natural frequency ω , by using a ring connection with C_2 symmetry shown in Fig.3(b). Then, the dynamics is written by the following Eq.(11), where we consider an external input with $\gamma_i(t) = \phi_i(t)$ and $\Theta_i(t) = \Theta$. Contrary to the previous bipedal case with a simple symmetry, the coupling parameters δ, δ' play an essential role, as shown in Fig.4.

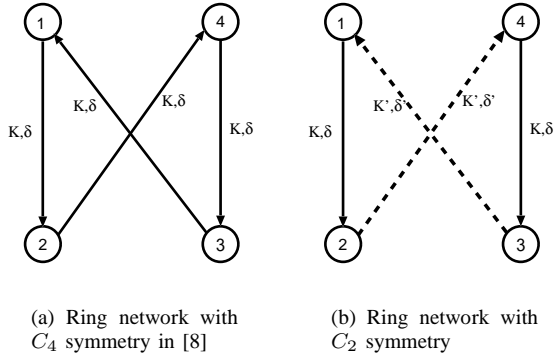


Fig. 3. Connection in a CPG for a quadrupedal locomotion

$$\left\{ \begin{array}{l}
 \dot{r}_1 = -cr_1 + \frac{1}{2} \{ K' f(r_3) \cos(\phi_3 - \phi_1 - \delta') \\
 \quad + K f(r_2) \cos(\phi_2 - \phi_1 + \delta) \} + \Theta \\
 \dot{r}_2 = -cr_2 + \frac{1}{2} \{ K f(r_1) \cos(\phi_1 - \phi_2 - \delta) \\
 \quad + K' f(r_4) \cos(\phi_4 - \phi_2 + \delta') \} + \Theta \\
 \dot{r}_3 = -cr_3 + \frac{1}{2} \{ K f(r_4) \cos(\phi_4 - \phi_3 - \delta) \\
 \quad + K' f(r_1) \cos(\phi_1 - \phi_3 + \delta') \} + \Theta \\
 \dot{r}_4 = -cr_4 + \frac{1}{2} \{ K' f(r_2) \cos(\phi_2 - \phi_4 - \delta') \\
 \quad + K f(r_3) \cos(\phi_3 - \phi_4 + \delta) \} + \Theta \\
 \dot{\phi}_1 = \omega + \frac{1}{2} \frac{1}{r_1} \{ K' f(r_3) \sin(\phi_3 - \phi_1 - \delta') \\
 \quad + K f(r_2) \sin(\phi_2 - \phi_1 + \delta) \} \\
 \dot{\phi}_2 = \omega + \frac{1}{2} \frac{1}{r_2} \{ K f(r_1) \sin(\phi_1 - \phi_2 - \delta) \\
 \quad + K' f(r_4) \sin(\phi_4 - \phi_2 + \delta') \} \\
 \dot{\phi}_3 = \omega + \frac{1}{2} \frac{1}{r_3} \{ K f(r_4) \sin(\phi_4 - \phi_3 - \delta) \\
 \quad + K' f(r_1) \sin(\phi_1 - \phi_3 + \delta') \} \\
 \dot{\phi}_4 = \omega + \frac{1}{2} \frac{1}{r_4} \{ K' f(r_2) \sin(\phi_2 - \phi_4 - \delta') \\
 \quad + K f(r_3) \sin(\phi_3 - \phi_4 + \delta) \}
 \end{array} \right. \quad (11)$$

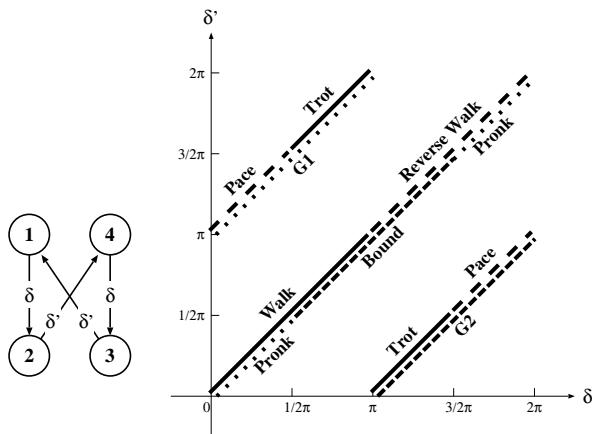


Fig. 4. Attractors for the gaits in a parameter space (δ, δ') with $K = K'$

Fig.4 shows the attractors corresponding to various gaits in a parameter space (δ, δ') when $K = K'$. The amplitude parameter K/K' just modifies the straight lines of the attractors into curves. The gait patterns are given in Table III. Thus, a family of walk, bound and pronk, and a family of trot and pace cannot coexist in the present model under the C_2 symmetry connection.

TABLE III

PHASE DIFFERENCES IN VARIOUS GAITS

| Gait | ϕ_1 | ϕ_2 | ϕ_4 | ϕ_3 |
|--------------|----------|----------|----------|----------|
| Pronk | 0 | 0 | 0 | 0 |
| Walk | 0 | 0.75 | 0.5 | 0.25 |
| Bound | 0 | 0.5 | 0 | 0.5 |
| Reverse Walk | 0 | 0.25 | 0.5 | 0.75 |
| G1 | 0 | 0.75 | 0 | 0.75 |
| Trot | 0 | 0.5 | 0.5 | 0 |
| G2 | 0 | 0.25 | 0 | 0.25 |
| Pace | 0 | 0 | 0.5 | 0.5 |

B. $D_{N/2}$ Symmetry of the Connection

Biological plausibility and the consideration of the symmetry are indispensable to design the connection of an oscillator network. The group theoretic notation is useful to describe the symmetries of the gaits, especially for the periodic oscillations in systems with symmetry, which requires to consider both spatial and temporal symmetries[9]. The spatial symmetry means permutations of N oscillators (i.e. N legs), while the temporal symmetry considers a phase shift on circle group $S^1 = \mathbf{R}/\mathbf{Z}$.

Cyclic group C_N of order N is relevant when we consider a network of N oscillators with a ring or similar types of connection, while dihedral group $D_{N/2}$ of order N is important for the N -legged gait with the left and right symmetry. For the bipedal case of $N = 2$, finite group of order 2 is uniquely given as $C_2 = D_1$. For the quadrupedal case of $N = 4$, there are two finite groups of order 4, C_4 and $D_2 = C_2 \times C_2$, and the latter is important for the gait.

V. FUTURE WORKS

Possible network for a quadrupedal gait will be clarified based on the discussion in IV-B, and the dynamic transition between the gaits will be analyzed as a mechanism of an adaptation. The next extensions of the present model include addition of external inputs, a change of a functional form for the coupling, and a CPG model for $2n$ -legged locomotions.

REFERENCES

- [1] Y. Kuramoto, "Chemical Oscillations, Waves and Turbulence", Springer-Verlag (1984).
- [2] I. Nishikawa, S. Nakazawa and H. Kita, "Area-wide Control of Traffic Signals by a Phase Model," *Transactions of the Society of Instrument and Control Engineers*, **39**, pp.199–208 (2003).
- [3] Y. Kuroe, M. Yoshida and T. Mori, "On activation functions for complex-valued neural networks", ed. Okyay Kaynak et.al., LNCS **2714**, pp.985–992, Springer (2003).
- [4] I. Nishikawa and Y. Kuroe, "Dynamics of Complex-Valued Neural Network and Its Relation to a Phase Oscillator System", ed. Nikhil Pal et.al., LNCS **3316**, pp.122–129, Springer (2004).
- [5] I. Nishikawa, T. Iritani and Y. Kuroe, "Phase Dynamics of Complex-valued Neural Networks and Its Application to Traffic Signal Control", *International Journal of Neural Systems*, **15**, pp.111–120 (2005).
- [6] T. A. Kuznetsov, "Elements of Applied Bifurcation Theory", Applied Mathematical Sciences 112, Third Edition, Springer (2004).
- [7] Y. Asai, T. Nomura, S. Sato, A. Tamaki, Y. Matsuo, I. Mizukawa and M. Abe, "A coupled oscillator model of disordered interlimb coordination in patients with Parkinson's disease", *Biological Cybernetics*, **88**, pp.152–162 (2003).
- [8] J.J. Collins, S.A. Richmond, "Hard-wired central pattern generators for quadrupedal locomotion", *Biological Cybernetics*, **71**, pp.375–385 (1994).
- [9] J.J. Collins and N. Stewart, "Coupled Nonlinear Oscillators and the Symmetries of Animal Gaits", *Nonlinear Science*, **3**, pp.349–392 (1993).

Sensing while moving: exploring a neural correlate of sensorimotor gating during voluntary movement

Kazuhiko SEKI

Background—Animals need to detect the information about the external world surrounding them for survival, and it is known that there are two mode of sensory detection, namely passive and active detection. While it is just needed for animal to pay an attention to their sensory input for the passive detection, animal is also needed to move their body toward the external environment for the active detection. This active sensory detection should be one key concept for “Mobilligence”, but this is computationally challenging since animals brain have to regulate sensory and motor nervous system simultaneously. Exact neural mechanism for this dual regulation is not well understood. Since sensory flow and motor command is known to merge at various structure in our central nervous system (CNS), it has been assumed that sensorimotor integration would be occur in these areas. Theoretically, sensorimotor integration can be occurred by integrating sensory signal into motor command, *vice versa*, or both. Classic physiology has been focused on the integration or transformation of sensory signals into motor command (e.g. spinal- or posture reflexes) and neural mechanism for elucidating these integration has been well documented. On the other hand, several recent report suggest that the neural mechanism for integrating sensory input into motor command . For example, visual receptive field [1] or auditory map [2] is shown to be modulated by the motor system for controlling eye movement. Therefore, against the classical view, sensory processing during movement is not passive, but highly dynamic process since it can be modulated as a function of dynamics of ongoing movement by motor command. In this sense, movement itself may be an element for the initial stage of sensory detection. Our research project focuses on the neural mechanism for modulating sensory input during movement, particularly by motor command signals. In this report, I would like summarize our approach to elucidate this mechanism by focusing on presynaptic inhibition on the primary sensory afferents.

I. INTRODUCTION

Normal motor behavior stimulates peripheral receptors, generating self-induced recurrent activity. For example, moving our limbs produces time-varying afferent input from cutaneous and proprioceptive receptors that is transmitted to the central nervous system (CNS), where it potentially interacts with motor commands and cognitive processes. The extent to which this re-afferent input is incorporated into ongoing motor and sensory processing remains a key issue in understanding mechanisms of voluntary movement and perception.

Movement-induced feedback arrives via afferent fibers that make synaptic contact with so-called first-order “relay”

neurons in spinal cord that transmit activity to local neural circuits [3] and to higher centers via ascending pathways [4]. These relay neurons represent one of the first stages at which peripheral input could be modulated, so any task-dependent changes in their responsiveness during normal behavior would have significant consequences. Responses of the relay neurons may be modulated by either presynaptic or postsynaptic mechanisms. Postsynaptic modulation via synaptic inputs would affect the neurons’ responses to many inputs, peripheral and descending, while presynaptic inhibition could reduce sensory inputs more selectively, since it can modify the efficacy of transmitter release from specific afferents [5]. Presynaptic inhibition operates in various relays of the visual, olfactory and somatosensory system and it is mainly mediated by axo-axonic GABAergic synapses which produce “primary afferent depolarization” (PAD) of the afferent fibers [5]. PAD reduces the amount of transmitter released by action potentials invading the presynaptic terminals, thus reducing the size of responses evoked in first-order and subsequent relay neurons. In spinal cord, PAD in peripheral afferent fibers are typically evoked experimentally by a synchronous volley in other afferents or in descending pathways. To date, the degree to which PAD occurs during normal behavior could only be inferred from indirect

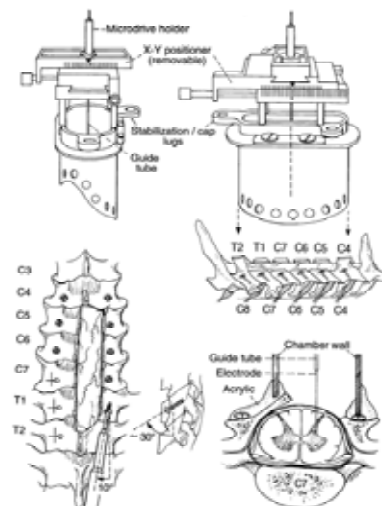


Fig. 1. Schematic diagrams of the surgical procedure for implanting a stainless steel chamber over a unilateral laminectomy of the C₅-T₁ vertebrae and of the system for advancing metal recording electrodes through the chamber into the spinal cord

This work was supported in part by the Ministry of Education, Culture, Sports, Science, and Technology, Grant-in-Aid for Scientific Research on Priority Areas (No.454).

K. SEKI is with Department of developmental physiology, the National Institute for physiological sciences, Okazaki, Aichi 444-8585 JAPAN (phone: 0564-55-7757; fax: 0564-55-7766; e-mail: kazuseki@nips.ac.jp).

evidence. Consequently, the occurrence and role of presynaptic inhibition in normal voluntary behavior remains to be tested directly in intact, behaving animals.

Using new techniques to record the activity of spinal interneurons in awake behaving (Fig.1, [6]), we found the most direct evidence to date that presynaptic inhibition operates in a behaviorally relevant manner during voluntary movement. Presynaptic inhibition reduces afferent input to the primate spinal cord during active voluntary movement, with potential effects on movement control and sensory perception. Data also suggests that this mechanism is evoked either by asynchronous volley from peripheral afferent (Experiment II) and descending motor commands (Experiment I and III).

II. METHODS AND RESULTS

A. Experiment I

Modulation of monosynaptic afferent input during voluntary movement

Voluntary limb movements are controlled by many descending and sensory signals; descending systems send commands to spinal cord for the execution of specific movement, and afferent systems feed back the results of its execution to spinal cord and to higher centers. Interaction of these two systems is essential for proper execution of intended movements, and it is now widely accepted that most sensory and descending pathways share common spinal interneurons, many of which project to motoneurons.

The evidence that sensory and descending pathways share common spinal interneurons came from studies conducted exclusively in anaesthetised or decerebrated cats; and the activity of the "shared" interneurons is known to be modulated corresponding to the functional demand in each phase of movement. From this evidence, one can assume that several pathways controlling voluntary limb movement also share some spinal interneuron, and that the activity of the interneuron is modulated during voluntary movement in the primate, including human. However, activity of spinal interneurons under normal conditions of active behavior have rarely been examined. We, therefore, studied the activity of neurons in the spinal cord of awake behaving monkey to investigate the interaction between descending and sensory signals at spinal interneurons during voluntary movement.

We documented afferent input to C6-T1 spinal interneurons (n=284) and their rate modulation in a monkey performing wrist flexion/extension movements in an instructed delay task. Cutaneous inputs (n=221) were evoked by electrical stimulation of the superficial radial nerve through a cuff electrode (2.6 ± 1.5 x threshold for an afferent volley recorded in another proximal cuff). Muscle inputs (n=87) were evoked by bipolar stimulation of forearm muscle afferents through wire electrode implanted in forearm muscles. The amplitude of the responses of interneurons and their mean firing rate was calculated separately for from peristimulus time histograms (PSTH) for twenty-four epochs of task. EMGs were recorded from 12-forearm muscles with pairs of indwelling electrodes. Cord dorsum potentials were recorded near the cord surface in each recording track (n=104) from the IN recording electrode.

We found that the firing rate of interneuron which receive the cutaneous input (n=118) was higher ($p < 0.01$) during movement than during hold or rest phases of

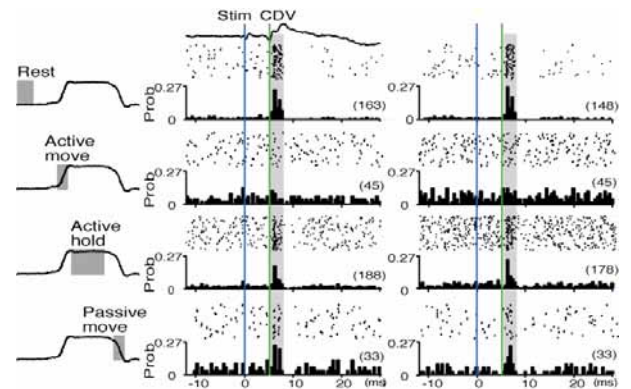


Fig. 2. Peristimulus time histograms (PSTH; bin width, 0.5 ms) below raster plots of the action potentials. Each plot was aligned with the SR stimuli (blue line). Trace above shows the CDP with afferent volley (CDV) marked by vertical green line. Height of each PSTH bin represents the normalized probability of spike occurrence per stimulus. From top to bottom, responses compiled during different task epochs (indicated on torque traces to left): rest, active movement, active hold, and passive movement. Number of stimuli delivered in each epoch shown above each PSTH.

flexion/extension movements. We also found that the responsiveness of interneurons from the stimulation on cutaneous afferent modulated as a function of task, and surprisingly the amplitude of responses were drastically decreased ($p < 0.01$) during active movement (Fig.2). Since the first-order interneuron (n=38), which receive monosynaptic input from cutaneous afferents also exhibit the same characteristics ($p < 0.01$), the depression of responsiveness during active movement was most likely to be induced by the presynaptic inhibition of afferent terminal onto the first-order interneurons. Furthermore, this suppression started 300- 400ms before the onset of muscle activity, suggesting that a part of suppression is induced by motor command, not only reafference.

These results suggested that the peripheral information from cutaneous receptors are strongly gated during active movement by presynaptic inhibition. These mechanisms could be useful for brain to eliminate interference of peripheral sensory input with descending motor commands at spinal level.

B. Experiment II

Modulation of PAD by natural stimulation

Electrical stimuli are known to activate multiple sensory afferent simultaneously, and natural stimuli induced during normal behavior of animals always activate their sensory receptors asynchronously. For example, electrical stimulation of muscle afferents activates all sub-threshold afferent simultaneously and they strongly activate postsynaptic neuron in spinal cord in a synchronous timing. In contrast, stretching skeletal muscle (natural stimulus) stimulates a number of intrafusal fibers in an asynchronous timing and which results in an asynchronous activation of multiple Ia afferents. Function of presynaptic inhibition in spinal cord has been studied in a number of early studies and electrical stimulation to the primary afferent has been used almost exclusively for inducing presynaptic inhibition. However, it is not known whether the natural stimulation to peripheral receptors could modulate the PAD and presynaptic inhibition in the monkey spinal cord. To investigate this issue, we delivered repetitive stimuli (5-20 μ A; 10Hz) to the cervical spinal

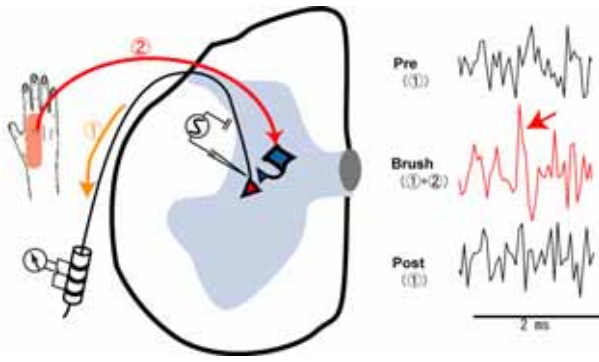


Fig. 3. Primary afferent depolarization evoked by natural stimulation (brushing stimuli). While stimulating afferent terminal (1), dorsal surface of hand were lightly brushed by an experimenter (2). Note that the larger antidromic volley was evoked during brushing.

cord [C6-T1] through an oval chamber implanted over vertebrae and recorded antidromic volleys (AVs) in the superficial radial (SR) and median (M) nerves through tripolar cuff electrodes implanted at the level of forearm. In each electrode track, we monitored orthodromic responses evoked by the electrical stimulation to M and/or SR, and the microstimuli were delivered to the site where the maximal size of orthodromic responses were recorded. By increasing stimulus current (5 to $20\mu\text{A}$), the size of AVs increased progressively and multiple AVs (2-3) were frequently recruited at stronger currents. The stimulus current just above the threshold for each AV tested ($11.4\pm 1.7\mu\text{A}$) was selected for the following test. Then, while delivering microstimuli (10Hz) to the spinal cord, we applied sustained mechanical stimuli (10s) to the receptive field of M (glabrous skin) or SR (hairy skin) alternatively by lightly brushing the radial aspect of the ipsilateral hand, and their effects on the AVs evoked in M and SR were examined (excitability testing). Result indicated that the size of AVs was altered by the mechanical stimulation in 59% ($n=13$) of AVs tested ($n=22$). The effect was either facilitation (50%; $n=11$; Fig. 2) or suppression (9%; $n=2$), and, in average, the size of AVs was increased to 164% of the control ($p < 0.05$). No obvious differences observed between the effect of brushing to the inside and outside of AV's receptive field. We conclude that the asynchronous volley induced by the mechanical stimulation to the cutaneous afferent is strong enough to induce and modulate the PAD in the cervical spinal cord of monkey. The modulation of PAD may suggest that the PI induced by the natural stimulation could modify the sensory input from homonymous/heteronymous afferents.

C. Experiment III

Modulation of PAD during voluntary movement

Result from Experiment I and II indicates that presynaptic inhibition decreases the ability of afferent impulses to activate first-order spinal interneuron (IN) by descending motor command and natural stimulation to peripheral receptor. To further investigate this phenomenon, we examined the modulation of primary afferent depolarization (PAD) in monkeys performing a wrist flexion-extension task. We stimulated the superficial radial (SR) nerve (containing purely cutaneous afferents) and recorded evoked responses of single INs and local field potentials (LFP) in spinal cord [C6-T1]. When a monosynaptic response was observed (73 intraspinal sites; 55 sites near INs, 18 with LFPs), we delivered microstimuli

($1-20\mu\text{A}$; 3-10Hz) continuously through the recording microelectrode and recorded antidromic volleys (AVs) in the SR through a tripolar cuff electrode. Single stimuli sometimes evoked multiple (2-8) AVs, possibly by activating afferent terminals with different conduction velocity. We calculated the size (area) of individual volleys ($n=270$) and averaged in each behavioral epoch [rest, cue, delay, movement, hold, etc]. In specific phases of the behavioral task the size of most volleys (58%) increased or decreased significantly relative to control period, indicating that PAD was modulated in a task-dependent manner. AVs showing modulation had faster conduction velocities than those without modulation (57.04 ± 13.04 vs. 53.20 ± 13.65 , $p < 0.01$), suggesting the primary target of PAD modulation could be faster conducting fibers (i.e. A-beta). The size of many volleys increased during active wrist movement against an elastic load, when monosynaptic unit responses and LFPs decreased. These data suggest that low-threshold cutaneous input can be modulated presynaptically by changing the amount of PAD in a behaviorally relevant way (Fig.3).

III. DISCUSSION

To detect informations about an external world, animal first make an active movement toward the environmental object of interest, and as a result, their peripheral receptor could capture the profile of object which is moved inside to their receptive field by movement. In this sequence of event, two kind of sensory information would be detected by brain; 1) information regarding to the target in their external world (object) and 2) sensory feedback generated by their own movement (reafference). Beside the former is essential for the feature detection of target, the later is essential for guiding their movement toward the target since they provides brain a real-time information about

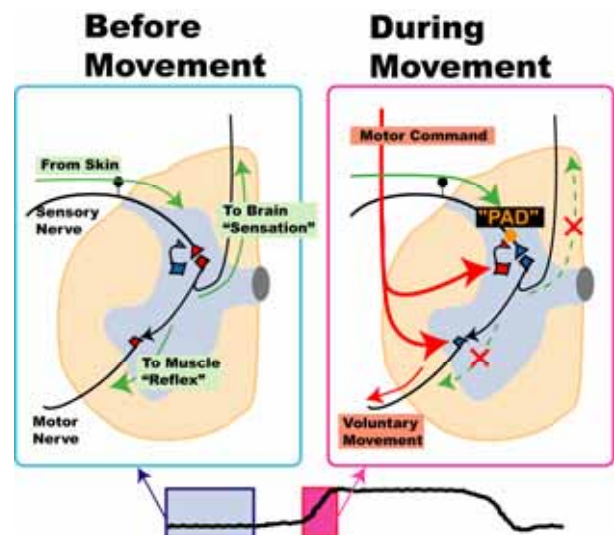


Fig. 4. Summary of Experiment I and III

During active movement, sensory input from cutaneous afferent are suppressed by motor command.

body position and current condition of movement. However, it is big challenge for brain to deal with reafference since they supply abundant information into central nervous system. For example, firing rate of single muscle afferent during locomotion achieves to 200Hz, and

sum of input supplying from muscle afferents to CNS is estimated to be more than 800kHz [7].

In our series of study, we found that the presynaptic inhibition on peripheral cutaneous afferent was maximal during active movement period in a voluntary motor task. From an anatomical and physiological perspective, spinal cord is one of the first relay of peripheral input, and the sensory information transmitted to the first order spinal interneuron affects the computation process in post synaptic systems for guiding their movement and detecting feature of object significantly. Therefore, attenuating sensory input at very early stage of sensory processing may have an advantage for reducing computational load for CNS. Our hypothesis is that abundant informations conveyed by peripheral afferent activated active voluntary movement is needed to be attenuated for reducing computational load of postsynaptic systems, and presynaptic inhibition may effectively suppress the sensory

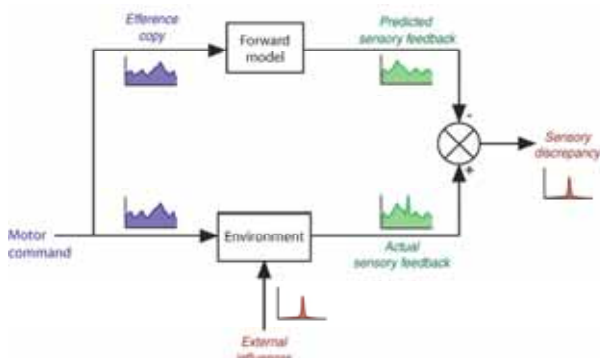


Fig. 5. Cancellation of actual reafference by "predicted" reafference

feedback before they arrived at the very early stage of sensory processing.

Next important question to be asked is the context of sensory information which is suppressed or *not* suppressed by presynaptic inhibition. Besides attenuating sensory input is advantageous for reducing computational load, losing sensory feedback is obvious drawback for the future detection and movement guidance, two critical components of "Mobilligence". It may be important for brain to reduced computational load without losing valuable sensory information. It is possible that presynaptic inhibition may act as a filter for selecting valuable information among abundant sensory input, rather than attenuating them in nonselective manner. One idea which may support this hypothesis is shown in Fig. 5 [8]. According to this model, self-induced "reafference" could be predicted by "efference copy" within the "internal model" of ongoing movement, and brain uses this "predicted" sensory feedback for guiding ongoing movement. Importantly, "predicted" and "actual" sensory feedback is matched at a comparator, where the "external influence" to sensory system is supposed to be extracted and a fragment of actual sensory feedback which has been matched with the predicted feedback are cancelled out. In this case, the comparator acts as a dynamic filter for canceling expected sensory input (reafference) and extracting an external event which are added during active movement (profile of object). In past, several experimental data has been suggested that the internal model for generating "predicted" sensory feedback may be localized in Cerebellum [9]. However, neural

correlate of the comparator is not identified. We speculate that the comparator may exist in the early stage of sensory processing (eg. Spinal cord and brainstem) and presynaptic may work for filtering sensory input within these comparator. We are now planning a new experiment to confirm this hypothesis.

REFERENCES

- [1] Armstrong, KM, Fitzgerald, JK, Moore, T, Changes in visual receptive fields with microstimulation of frontal cortex., *Neuron*, **50**, 791-8, (2006).
- [2] Winkowski, DE, Knudsen, EI, Top-down gain control of the auditory space map by gaze control circuitry in the barn owl., *Nature*, **439**, 336-9, (2006).
- [3] Baldissera, F., Hultborn, H. & Illert, M. in *Handbook of Physiology* (ed. Brooks, V. B.) 509-595 (American Physiological Society, Bethesda, Maryland, 1981).
- [4] Willis, W.D. & Coggeshall, R.E. *Sensory Mechanisms of the Spinal Cord* (Plenum Press, New York, 1991)
- [5] Rudomin, P. & Schmidt, R.F. Presynaptic inhibition in the vertebrate spinal cord revisited. *Exp. Brain Res.* **129**, 1-37 (1999).
- [6] Perlmutter, S.I., Maier, M.A. & Fetz, E.E. Activity of spinal interneurons and their effects on forearm muscles during voluntary wrist movements in the monkey. *J. Neurophysiol.* **80**, 2475-2494 (1998).
- [7] Prochazka, A, Gorassini, M, Ensemble firing of muscle afferents recorded during normal locomotion in cats., *J Physiol.* **507**,293-304 (1998) .
- [8] Bays, PM, Wolpert, DM, Computational principles of sensorimotor control that minimize uncertainty and variability, *J Physiol.* **578**, 378-396 (2007).
- [9] Imamizu H, Miyachi S, Tamada T, Sasaki Y., Takino R., Prutz B., Yoshioka T., Kawato M. Human cerebellar activity reflecting an acquired internal model of a new tool, *Nature*, 403, 192-195 (2000).

Group C: Social Adaptation

Hitoshi Aonuma, Research Institute for Electronic Science, Hokkaido University

I. INTRODUCTION

THE aim of the research project of group C is to elucidate mechanisms underlying social adaptation in animals. In this year, subscribed research groups joined in this project in addition to the planned research groups.

There are various organisms living on the earth, and they have succeeded to survive in the ever-changing environment. As the result of long history of evolution, the organisms have diverged into such a huge number of species. In their process of evolution, animals have acquired a nervous system to exhibit an adaptive behavior as the environment changes. It is important to understand the mechanism underlying the adaptive behavior to get an insight how the organisms have evolved. In addition, it is also important to elucidate the information processing system as a result of long evolutionary history, and to apply them to engineering and our lives. We consider a society, which is a population of individuals, as one of the important environmental factors and try to elucidate the mechanism underlying social adaptation.

II. CONTENTS OF THE PROJECT

Participation of the subscribed research groups in addition to the planned research groups accelerate to promote our research project systematically using both invertebrates and vertebrates including humans. We are to reveal social adaptation mechanisms of animals by the following two approaches; 1) detailed biological studies at entire level of biological hierarchy, from genes and cells to behavior of individuals and/or populations, and 2) system engineering approaches using dynamical models and simulations of the biological phenomena found by biological researches.

The research project is divided into the following four categories; 1) studies of the mechanism underlying socially adaptive behavior using insects as model animals, 2) studies of birds' communication to elucidate the acquisition process of socially adaptive behavior, 3) studies of socially adaptive behavior in primates, such as monkeys and humans, especially focusing on social hierarchy and others understanding, 4) studies of interfaces between humans and machines (artificial substances) to understand the mechanism underlying social adaptation. Each research group consists of both biologists and engineers and they always interact each other. In the following paragraphs, research contents of each group are briefly introduced.

A. Studies of the mechanism underlying socially adaptive behavior using insects as model animals.

In the research groups using insects as model animals, both solitary insects, such as crickets or silkworm moths, and social insects, such as honeybees, ants or termites, are employed in our project. An insect brain consists of only 10^5 neurons, which is less than 10^6 compared with those of mammals. That is why an insect brain is also called a "microbrain". In spite of such a small number of neurons, insects have very sophisticated adaptive capability, e.g. higher brain function including learning and sociality. On the other hand, any present artificial systems and also present robots still do not have such a capability. We believe that the elucidation of the brain mechanism underlying insect adaptive behavior is quite useful for construction of adaptive system such as a distributed autonomous system.

Aonuma and Kanzaki *et al.* have investigated how pheromone-induced behaviors in insects are modulated by the various environmental factors, including social communications. In the crickets, it is known that a male cricket show aggressive behavior to other males, and they start to fight each other. Once it loses, it shows avoidance behavior to others instead of aggression. They are to reveal the neural mechanism of this behavioral selection and elucidate the basic neural mechanism underlying social adaptation. In the silkworm moths, they are to understand the mechanism of adaptive behavior by testing animals' behavioral responses to an artificially changed environment.

Nagao *et al.* have studied the contribution of social experience to the development of instinctive behavior. In the cricket, the behavioral pattern to other crickets, especially aggression, is strongly affected by the socially environmental factor during their developmental processes.

These biological research findings described above are shared with the groups of engineers, Ota, Kawabata, Asama *et al.* and Kurabayashi *et al.*, and study of the social adaptation mechanism in insects is systematically promoted.

Ota, Kawabata, Asama *et al.* simulate a dynamical behavioral model of the population of the male crickets and investigate the behavioral modulation of individuals in the population. In addition, a neural network model of the brain, in which the functions of nitric oxide system and biogenic amine system are involved, is also under construction.

Kurabayashi *et al.* estimate the role of oscillators in the neuronal network. They consider that the function-structure relationship of the oscillator network plays a crucial role in the quick behavioral changing process.

Social insects, including ants, honeybees and termites, organize a colony based on division of labor, trophallaxis and formation of caste. A colony is often referred as a “superorganism” because the colony itself behaves as like an organism. They try to elucidate the mechanism of colony formation from the aspects of recognition of nest mates, maintenance of the caste and learning of the social environment.

Miura *et al.* have studied morphological and brain-functional differentiation during the developmental process in social insects. Using molecular biological approach, they try to reveal how these differentiations take place, and the effect of them to the performance of the colony.

Ito *et al.* have investigated how honey bees transfer their information, which one learned during her foraging, to her nest mates after returning to the hive from flowers. They are also attempting to construct a model from behavioral observation. They are trying to reveal the socially adaptive mechanism by understanding of colony maintenance and information propagation in the insect colony.

Tsuji *et al.* have studied what kind of interactions among individual ants regulates their colony. They focus on the regulation of population density in the nest and the recognition of the size of the colony. Sugawara *et al.* together with Tsuji *et al.*, perform simulation of a dynamical model of the ants’ behavior in the nest.

B. Studies of birds’ communication to elucidate the acquisition process of socially adaptive behavior.

Communication, emotion and others understanding are important issues for the social adaptive mechanism. We try to tackle these issues using vertebrates including humans. Birds (zebra finch) are used for studying the acquisition process of the social adaptation mechanism. Japanese macaques are used for studying the process of social hierarchy formation. And for studying others understanding, humans and machines are used as the research objects.

Oka *et al.* are constructing a neural network model for a song discrimination mechanism in zebra finches. In birds, the hippocampal complex of the brain plays a crucial role for special memory, imprinting and song discrimination. The hippocampal complex is located on the surface of the brain, and because of this morphological feature birds have an advantage for the experiments such as molecular genetics, optical imaging and electrophysiology. They are trying to reveal the process of social learning in birds focusing on the hippocampal complex.

C. Studies of socially adaptive behavior in primates, focusing on social hierarchy and others understanding.

To reveal the neural mechanism underlying others understanding is important for elucidation of the mechanism of socially adaptive behavior in humans. The schizophrenic disorder, which is one of the social problems presently, is considered as a functional deficit of the brain mechanism for others understanding.

Kato *et al.* have focused on the social neuroscientific study of others understanding and adaptive motion in humans. In

the behavioral study using an agency task, it is found that the patients with schizophrenic disorder have a problem with the sense of agency. They are now investigating the neural basis of visual line recognition and transductive effect of attention based on it using fMRI recordings and neuropsychological tests. They also try to develop a robot that recognizes visual line and behaves based on it.

Fujii *et al.* have studied social adaptive behaviors based on the social hierarchy among individuals of Japanese macaques. They are aiming to elucidate the brain mechanism underlying the selection of socially adaptive behavior. In addition, they try to find a new algorithm to detect an intention of the monkey from its behavior. Using this algorithm, they also try to develop a new brain machine interface (BMI) by understanding nonverbal information expressed by humans.

D. Studies of interfaces between humans and machines to discuss the mechanism underlying social adaptation.

Interfaces between humans and machines are useful tools to understand the mechanism of socially adaptive behavior. In particular, it is important to understand how we learn to use a machine as a tool, or in other words how we understand others, for establishing coordination between humans and automated machines.

Sawaragi and Horiguchi *et al.* have studied the design theory of mobile interfaces based on the social communication model. They try to investigate the process in which a human (an operator) get used to handle an automatic machine. The result of this study will lead to the elucidation of the common mechanism of others understanding in organisms and machines.

That is the brief description of the contents of the project. Detailed results of each research group are summarized by each group leader in the following chapter, respectively.

Systematic understanding of neuronal mechanisms for adaptive behavior in changing environment

Hitoshi AONUMA, Hokkaido University, Ryohei KANZAKI, The University of Tokyo

Abstract: Design principle of formation of sociality and that of adaptation in a society have been investigated. This project is to understand neuronal mechanisms of socially adaptive behaviors in animals. Insect communication behaviors such as pheromone behaviors provide great model system to investigate this issue. We have focused on cricket fighting behavior and silkworm moth orientation behavior that are both released by pheromones. Our biologist group mainly concentrated on revealing behavioral and physiological aspects of insect socially adaptive behaviors. Based on the results of our experiments, we collaborate with engineering groups to establish dynamic models to reveal mechanisms of social adaptation.

I. Introduction

Animals have evolved nervous systems as an adaptive function through long evolutionary history of the organisms. Animals perceive many kinds of signals in changing environments and they quickly select and adjust their behaviors to the environments by choosing and switching neuronal program in the central nervous system. Animals do not always respond the same way to the same stimuli, which indicates that the state of central nervous system must be modified depending on their experiences as well as internal and/or external conditions. Environment is composed by lots of factors and we think society is also one of the important factors of animals' adaptive functions.

Insects have rather simple and identical nervous systems. Mammalians have about 10^{12} neurons in a brain. On the other hand, an insect brain has about 10^6 neurons and so it is called a "micro-brain". Such insect brains allow us to access each neuron easily, which accelerate us to investigate how animals show socially adaptive behavior from cellular level to behavioral level analysis. We have here investigated mechanisms for formation of social status and socially adaptive behaviors, which are emerged from individual interactions among animals.

One of the common goals of biologists and engineering researchers is to understand how nervous systems adjust animal behaviors to changing external environments including society. We will combine neuroethological approaches and system engineering approaches to understand how animals form social communities, how they learn and retain previous experiences and how they alter their behavior depending on dynamically changing environments, which will help us to unravel the universal design of central nervous systems.

II. Aims

The aim of our project is to unravel the neuronal mechanism of socially adaptive behavior to understand

mobility of social adaptation. To understand how animals establish social organization and adapt the society, we have investigated 1) how animals show socially adaptive behavior in the changing environment, 2) how they recognize and distinguish each other, 3) how they divide labor and share knowledge. As a first step, we have focused on mechanisms that animals alter their behaviors in order to respond to the demands of changing circumstances.

Insects have identical nervous systems and provide us a good model system to resolve our questions. Communication behavior using pheromones in insects must be one of the greatest model systems to investigate neuronal mechanisms of animal adaptive behavior. Most of pheromone induced behaviors in insects have been thought to be hard-wired: a behavior that could be turn on and off but with no plasticity. For example, male moths respond with a highly stereotyped response when they detect a pheromone plume released by females. However, some of pheromone behaviors are revealed to be modified by their previous experiences. Cricket aggressive behavior is an example of such pheromone induced behaviors. The response of males to the pheromone can be modified by the previous fighting experiences ⁽¹⁾. Insects perceive information from changing environment and the signals perceived are processed in the microbrain to show adaptive behavior. The behavior of insects has been understood that internal factor such as internal timer, experiences and external environments drastically mediate threshold of releasing a behavior or behavioral pattern. In particular, previous social behavior such as mating behavior and agonistic behavior modulate following behaviors. In this study, we have focused on insect communication behavior using silkworm moths and crickets. We systematically construct dynamic models with collaborators belonging to C02 and C03 groups where we use results from cellular level experiments, neuronal network level experiments and behavioral level experiments to reveal neuronal mechanisms of socially adaptive behaviors.

III. Achievements

We have investigated neuronal mechanisms of pheromone induced behavior in silkworm moth (*Bombyx mori*) and cricket (*Gryllus bimaculatus*). Insects' behaviors seem to stereo-typed behavior; however most of behaviors can be modified by their social experiences, internal factor of individuals and different modality of stimuli etc. We focus on how animals alter their behaviors in order to respond to the demands of changing environments.

III-1. Pheromone experience and behavior threshold in silkworm moth

Habituation was observed when male moths continuously perceive sex pheromone from female moth. We have focused on the effect of serotonin (5HT) on neuronal mechanisms of habituation and dishabituation during pheromone induced behavior of male moths.

Puff stimulation using bombykol (1000ng at 500ms) for 30min significantly decreased responded behavior of male moth. This habituation to the sex pheromone continued for more than 30 min and recovered after 1.5 hr rest. Dishabituation was observed when odor stimuli using linalool (860µg, 500ms ×3) were given 5min after the bombykol stimulus. However inter stimulus interval was 28 min, dishabituation did not occur (Fig. 1). To investigate the role of biogenic amines in the brain, we measured changes of biogenic amine levels in the brain of moths that showed habituation, and found that 5-HT level significantly decreased in the brain.

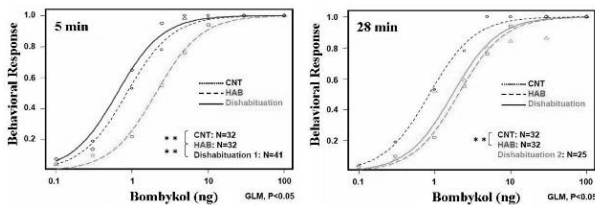


Fig. 1. Dishabituation caused by linalool stimulation

These results showed that pheromone stimuli evoked habituation in insects and that ordinary odor could evoke dishabituation in animals. Furthermore, the timing of stimuli was important factor to evoke dishabituation.

III-2. Convergence of visual information to pheromone processing circuit

The effects of visual information on pheromone induced behavior in male silkworm moth were investigated. The neuronal activities of neck motor neurons were recorded during orientation behavior that was released by sex pheromones from female. As a visual stimulus, optic flow was performed using a stripe pattern. When the stripe pattern was moved without any other stimulus, neuronal activity of neck motor neurons changed depending on the movement direction of the pattern (Fig. 2A). This indicates that the moth shows visual-motor reflection to correct differences of motor output using visual feedback.

Optical flow from a particular direction strongly inhibited motor response to pheromone stimuli (Fig. 2B). This suggested that visual information converge onto the neuronal circuit of pheromone processing in the moth brain. Furthermore, this indicates that stereo-typed behavior that released by pheromone can be modified by environmental conditions including internal factors and external factors.

In the central nervous system in insects, threshold releasing a behavior or behavioral pattern itself can be modified to adapt changing environment. Neuronal modulation must be an important factor in this mechanism. Pheromone is one of the important factors to evoke a particular behavior; however,

previous experiences of perceiving pheromone or ordinary odor dynamically modify the priority of releasing behavior program. This suggests that different stimulus modality can be a trigger of switching behavior program in the brain.

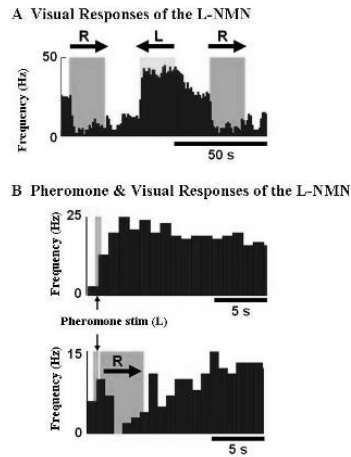


Fig. 2. Effects of visual stimulus on neck motor neurons. A: Response of left-side neck motor neurons (L-NMNs) to the optic flow stimulus from left to right. B: Inhibitory effect of visual stimulus on the activity of neck motor neurons.

III-3. Construction of robot driven by insect

We are proposing a novel approach to reveal adaptation mechanism of animals using a robot system that is controlled by insects. It is important to evaluate interactions between adaptive behavior and environment. Using this robot system, we can manipulate motor output of insect behavior, which make us easy to evaluate the effects of different modality information on programmed behavior.

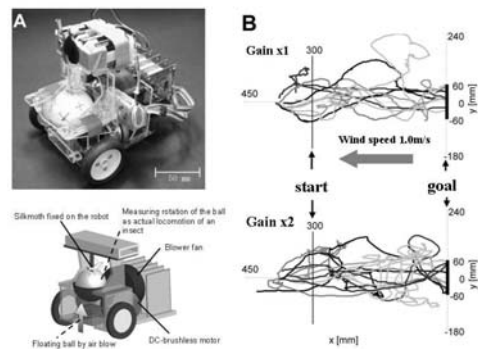


Fig. 3. Wheel robot manipulated by silkworm moth. A: Overview of the robot. B: Orientation to the sex pheromones. The speed of wheel can be changed.

The robot has wheels to move any direction. The speed and direction of robot is controlled by a silkworm moth that is put on a treadmill ball (Fig. 3A). The movement of the treadmill ball was used as input of both side motor control of the robot. The movement of the robot represented moth behavior and the accuracy was 93%. Using this robot, we tested pheromone orientation behavior of the moth. The robot that was controlled by the moth orientated the source of the pheromone like male moths did. When motor output was manipulated to change speed twice faster than the movement by the moth control, the moth changed its movement to adjust

the speed of the robot and correctly orientated to the source of the pheromone (Fig 3B).

This study demonstrated that using this kind of robot system we can manipulate motor function of insects and this allows us to reveal adaptive mechanisms of the nervous system in insects.

III-4. Social experience induced behavior in crickets

Cricket fighting behavior is focused to investigate how animals alter and adjust their behavior in order to respond to the demands of social environments. Male crickets suddenly start fighting against conspecific males as soon as they come across each other (Fig. 4A). This behavior is released when animals detect cuticular substances on the surface of male body. Once male cricket lose fighting, it is likely to avoid fighting again for 30-40 min (Fig. 4B).

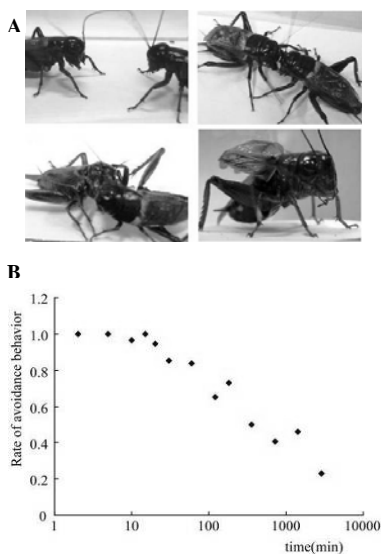


Fig. 4. Cricket fighting behavior. A: When male crickets meet each other, they suddenly start threatening, antennal fencing, and biting each other. B: Obligation of lost memory. Two round fighting was perform after different period of interval.

The cuticular substance is thought to be a complex of hydrocarbons on the surface of cricket body⁽²⁾. At moment the component of hydrocarbons that release aggressive behavior in male crickets has not been clear. To reveal the nature of the cuticular substance that release aggressive behavior, we isolated forewing of male cricket to show other males. The forewing removed and kept for 3hr did not evoke aggressive behavior in males. Furthermore, if isolated forewing was treated heat with hot air condition for 20-30min, the effect of the cuticular substance on evoking aggressive behavior was vanished (Fig. 5). This demonstrated that the component of hydrocarbons in the cuticular substances that evoked aggressive behavior in males could be volatile or quickly degraded substances. It is importance to isolate a component of the cuticular substance that evokes aggression in males to study further neuronal mechanisms of fighting behavior of cricket. Then we have continued to analyze the nature of cuticular pheromone using biochemical methods with Yamaoka.

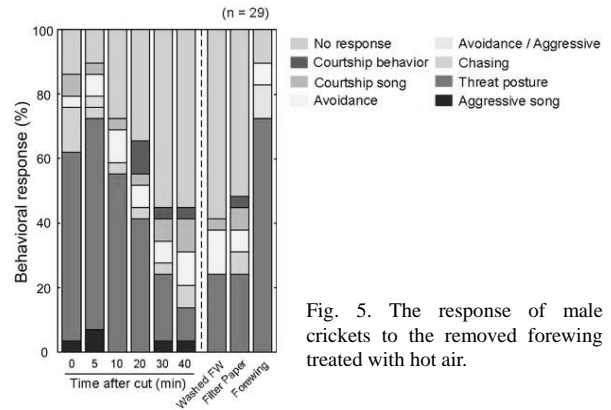


Fig. 5. The response of male crickets to the removed forewing treated with hot air.

Social experiences such as fighting and mating alter following behaviors of animals. To investigate the neuronal mechanism of social adaptation in insect, the response of the male cricket to the cuticular substance that evokes aggression was examined after fight experiences as a first step. The male cuticular substances were extracted by chloroform. This extract evoked aggression in naïve males. However, males that lost fighting previously showed avoidance behavior to the extract (Fig 6). This demonstrated that the social experience drastically changes following behaviors in crickets. As a next step, we are planning to investigate neuronal mechanisms of socially adaptive behavior using cricket fighting behavior. The threshold of behavioral program or behavior selection mechanisms in the brain must be modified after social experience.

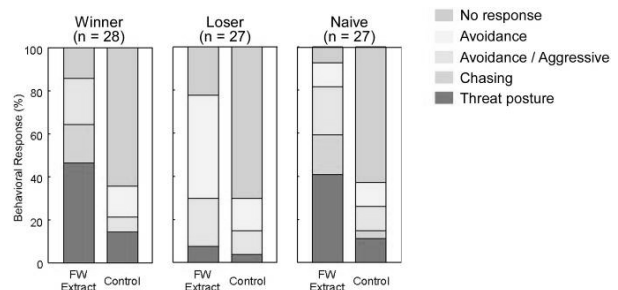


Fig. 6. Response of male cricket that previously experienced fighting to the extract of cuticular substances.

III-5. Memory of fight experience in male crickets

Social experience influences following behavior⁽³⁾. In Male crickets, previous lost experience of fighting changed response behavior against male cuticular substances from aggression to avoidance⁽¹⁾. Pheromone information is processed in the antennal lobe in the brain and then the encoded signals transferred to higher region of the brain such as the mushroom body and the lateral lobe to select behavior program. The detail of the neuronal network that controls aggressive behavior has not been cleared. At moment we are to identify the neuronal circuit controlling aggressive and avoidance behaviors that are evoked by cuticular substances from male crickets.

Pharmacological and behavioral experiments demonstrated that nitric oxide (NO) signaling system mediates aggression

level of male crickets and formation of social hierarchy. It is also demonstrated that the biogenic amine level in hemolymph mediates cricket aggression⁽⁴⁾. Our previous work demonstrated that the stimulation to antenna using male forewing increased NO release around the antennal lobe in the cricket brain. Histochemical analysis showed that the distribution of putative NO releasing neurons and octopaminergic neurons overlapped in similar region of the brain (Fig. 7). We here hypothesize that NO/cGMP system mediate biogenic amine system in the cricket brain. NO and biogenic amines could work as neuromodulators in the nervous systems, which would mediate behavioral selection in the brain.

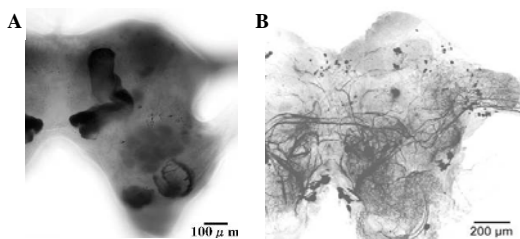


Fig. 7. A: NADPH-diaaphorase histochemistry on cricket brain. B: Octopamine like immunohistochemistry on cricket brain.

In order to examine this hypothesis, we performed pharmacological and biochemical experiments with Murakami and Nagao. Biogenic amine levels of the brain changed after fighting behavior. Octopamine, serotonin, and dopamine levels seemed to slightly decrease in both winner and loser crickets. In the loser cricket octopamine levels significantly decrease in the brain if it was beaten 3 times within short period (Fig. 8A). This suggests that the octopamine level could decrease just after they start fighting. Male crickets release fighting behavior, if they detect cuticular pheromones, which increase releasing of NO in the brain. Thus NO could decrease octopamine level in the brain. As a next step, in order to examine NO can mediate biogenic system in the cricket brain; we measured biogenic amine levels using high-performance liquid chromatography (HPLC) after cricket brains were treated with NO-donor or NO synthase inhibitor. Head injection of NO-donor NOR3 increases NO level in the brain, which activates soluble guanylyl cyclase to increase second messenger cGMP in the target cells of NO⁽⁵⁾. After NOR3 treatment, the level of octopamine in the brain significantly decreased (Fig. 8B). On the other hand, NO synthase inhibitor L-NAME and soluble guanylyl cyclase inhibitor ODQ significantly increase octopamine level in the brain. This strongly suggests that NO decreases octopamine level in the cricket brain.

Our previous experiment showed that head injection of L-NAME partly inhibits retaining of the beaten experience. The cricket treated with L-NAME challenged to attack the winner cricket in the previous fight. Together with the results we got, we suggest that NO system induced biogenic amine system in the brain and that it could play important role to maintain socially adaptive behavior in insect. Now we need

further experiments to understand neuronal mechanisms of fighting behavior of the cricket. By sharing these biological achievements with members of group C02 and C03, we are building a behavioral model and internal models.

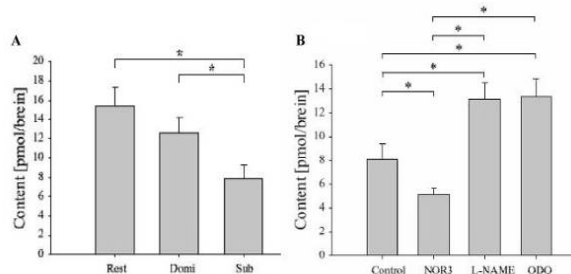


Fig. 8. Octopamine levels in the cricket brain. A: Octopamine level decreased significantly after losing fight 3 times. B: Effect of NO-donor NOR3, NOS inhibitor L-NAME and soluble guanylyl cyclase inhibitor ODQ on the level of octopamine in the cricket brain.

IV. Conclusion and future plan

Neuronal mechanisms of communication behavior in insects have been investigated to reveal socially adaptive function in animals. The study of pheromone induced behavior of the silkworm moth indicated that both internal and external factors of environment modulate pheromone behaviors that have been believed hard-wired. These results propose it is important to consider effects of the interaction between environment and socially adaptive behaviors. The study of cricket fighting demonstrated neuronal mechanisms of formation of social hierarchy. NO/cGMP system deeply link with biogenic amine system in the brain. These results indicate that NO induced biogenic amine system would play important roles to maintain socially adaptive behaviors.

As for the next plan, we will continue to study adaptive behaviors, in particular, neuronal mechanisms that produce socially adaptive behaviors. We will also evaluate established dynamic models by C02 and C03 groups to perform further biological experiments and will feed back the biological achievement to improve each model.

V. References

- (1) Aonuma H., Iwasaki M. and Niwa K. (2004) Role of NO signaling in switching mechanisms in the nervous system of insect. *Proc. SICE Ann. Conf.*, 2477-2482, CD-ROM. ISBN 4-907764-22-7.
- (2) Nagamoto J, Aonuma H., Hisada M. 2005. Discrimination of conspecific individuals via cuticular pheromones by males of the cricket *Gryllus bimaculatus*. *Zool Sci*, 22: 1079-1088.
- (3) Delago A. and Aonuma H. (2006). Experience based agonistic behavior in female crickets, *Gryllus bimaculatus*. *Zool. Sci.* 23: 775-783.
- (4) Adamo SA, Linn CE, Hoy RR. 1995. The role of neurohormonal octopamine during 'fight or flight' behaviour in the field cricket *Gryllus bimaculatus*. *J Exp Biol* 198:1691-1700.
- (5) Aonuma H, Niwa K. 2004. Nitric oxide regulates the levels of cGMP accumulation in the cricket brain, *Act Biol Hung*, 55(1-4): 65-70

Modeling of Neuronal Mechanism of Fighting Behavior in Crickets

Jun OTA, Hajime ASAMA, The Univ. of Tokyo, Kuniaki KAWABATA, RIKEN

Abstract: We have investigated how animals behave in a social population. Insects provide good model systems to investigate neuronal mechanism underlying adaptive social behaviors of crickets. Cricket agonistic behavior must be a good model system to understand the mechanism how circumstances change animal behavior depending on previous experiences. Here we perform mathematical modeling of male-male interaction among cricket population. We propose a behavioral model of crickets and a neuronal mechanism model of them. As application of the proposed models, we propose a foraging algorithm of multiple mobile robots as one application of the proposed models. We show the effectiveness of the proposed models through simulations.

Keywords: crickets, adaptive behavior, multi-agent robot systems

1. Introduction

Many living things in the natural world consists a kind of societies through the interaction with each other. They are surviving themselves with cooperation and competition. This fact shows that each individual has the ability of generating adaptive social behavior in complicated and diversified environments. We believe that it is very important to clarify the underlying mechanism of the adaptation.

Insects provide good model systems to investigate neuronal mechanism underlying adaptive behaviors. We focus on crickets, which generates characteristic social behaviors such as pheromone behaviors, avoiding behaviors, and fighting behaviors. We focus on fighting behaviors of male crickets as a first step of the study. We set the purpose of our study as modeling neuronal mechanism of the fighting behavior in crickets through the system engineering approach.

2. The effect of social population

Aggressive behavior of male crickets is released by cuticular substances on the body surface of male cricket and the aggressive levels escalate until one of male crickets evacuate from the fighting. This agonistic behavior establishes social status between two male crickets.

Subordinate males retained previous losses as short- or mid-term memory. We observed the behavior of loser male cricket that lost in the first fighting. The subordinate crickets avoid fighting against dominant males if inter-engagement interval is short. This avoidance behavior changed to aggressive behavior if the interval is getting longer.

When the crickets interact with each other, we can find very interesting group structure. That is: (a) when the density of crickets was low, fighting behavior showed rather random pattern. (b) When the density was middle, only one cricket beat other crickets to keep dominant status. (c) When the density was high, almost all crickets always moved to avoid interaction among other crickets. We call such a dynamic group structure as “the effect of social population.”

3. Neuronal mechanism of crickets having social adaptive behavior

We seek for modeling social adaptive behavior of crickets. We are going to model with the following two steps.

1. Behavioral modeling of crickets that verifies how the group structure can be self-organized from individual behavior of crickets
2. Neuronal modeling of the individual cricket that connects the sensor signal input and primitive behavior output.

Each modeling is discussed in the next two sections.

3 . 1 Behavior Modeling of artificial crickets

First of all, observation ability and motion ability are assumed as shown in Fig. 1. This is determined based on real characters of crickets. We defined a personal field of crickets. We focused on male-male interactions and established a modeling of cricket agonistic behavior. The cricket behaviors were simplified to three major primitive patterns that were wandering, avoiding and fighting as shown in Fig. 2. We simulate our model by changing the density of the artificial cricket population.

The rules of artificial cricket behaviors are as follows:

- a) Wandering: The cricket walks around randomly with

going straight, turning left or right, and stopping and staying at the same position.

b) Avoiding obstacle: Artificial crickets sense objects using their antennae. When one of antennae touches a wall of obstacle, they will turn opposite side. In case, the antennae touch an obstacle at the same time, they will turn left or right randomly. When they arrive at a corner, both of their antennae will touch the obstacle and then they will again to turn left or right side.

c) Fighting: If another cricket comes into its personal field, one will turn to the alien to start fighting. The fighting will not finish until one of them gives up continuing fighting. Subordinate turns and escapes from dominant opponent. The subordinate will avoid opponent for a while. On the other hand, dominant recognize its win if opponent cricket goes apart from his personal field.

Crickets change their behavior based on their experiences. Hence, we need at least one internal state variables for the cricket model. The probability (P) of losing at cricket fighting depends on a parameter α that runs from 0 through 1. The parameter α describes an internal state of the cricket. We determined this parameter from the behavior experiments of crickets. The value of α decreases gradually depending on time. Losing at fight increases the value of fight but decreases while winning at the fight.

$$P = \alpha(0 \leq \alpha \leq 1) \quad (1)$$

The value of α is revised with the following equation.

$$\alpha_{n+1} = (1 - \omega)\alpha_n + \varepsilon_{lose}\eta_{lose} - \varepsilon_{win}\eta_{win} \quad (2)$$

Here,

$$\eta_{lose} = \begin{cases} 1 & \text{if lose} \\ 0 & \text{else} \end{cases}, \eta_{win} = \begin{cases} 1 & \text{if win} \\ 0 & \text{else} \end{cases}$$

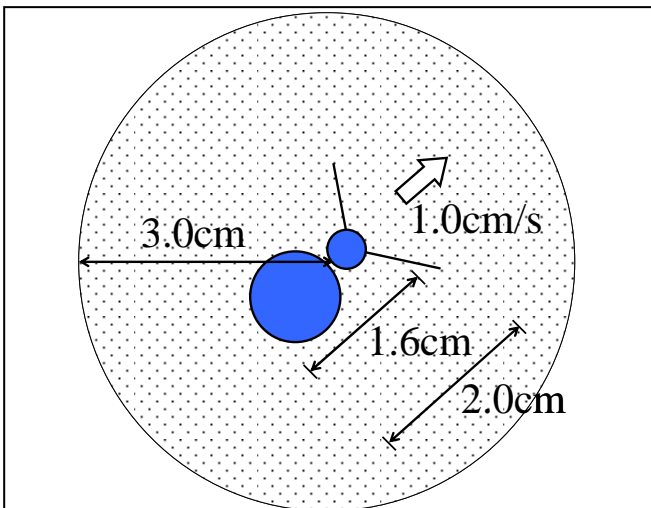


Fig.1 Shape of the artificial cricket and its personal field

$\omega, \varepsilon_{win}, \varepsilon_{lose}$: design parameters

We simulate how crickets change their behavior depending on the density of animal population. Three kinds of fields (128×128(pix) , 256×256(pix) and 512×512(pix)) are utilized for simulations. The number of crickets is fixed to four. Fig. 3 (a) shows the results of the simulation with higher density. The value of α converged to rather high values and most of animals avoided each other. Fig. 3 (b) shows the simulation results of middle density. Only one cricket usually increased its α value, which means that the cricket becomes dominant. Fig.3 (c) shows the situation of the low density. In that condition, α did not converge. The rate of taking aggressive behavior of each cricket becomes almost the same and those values are not so low.

The simulation results indicate that the proposed simulation model can demonstrate that cricket behavior can be modified by the previous experiences. The behavior of the artificial crickets was described by using a probability that is defined by the parameter α . Optimization of the simulation model suggests that the cricket behaviors among males were mainly influenced by the previous fighting experience in the particular previous losses. The simulation results are similar to that of behavior observation results of crickets, suggesting that the parameter α must contain internal model that must be neuronal modulation system in animals.

3.2 Neuronal circuit modeling of the cricket's brain - from sensory input to behavior selection -

There are many scientific research related to neuronal cells of the cricket's brain and it is well-known thing that Nitric Oxide/cyclic Guanosine MonoPhosphate (NO / cGMP) cascade and amine system like Octopamine(OA), Dopamine(DA) and Tyramine(TA) affect to the aggressiveness of the cricket. Actually, in cricket fighting behavior, the amount of OA significantly differs among

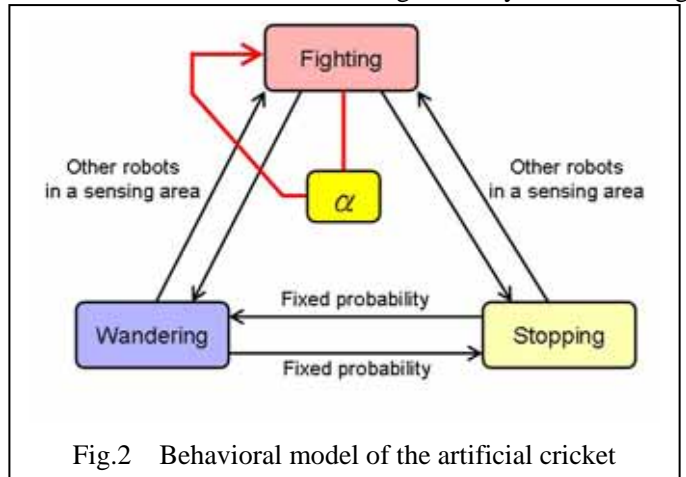


Fig.2 Behavioral model of the artificial cricket

no-fighting one, before and after fighting (Aonuma's data, not published). It is important to construct a neuronal circuit model based on biological knowledge and data with no contradiction for understanding dynamic activities in the cricket's brain. In reference [3], an adaptive behavior selection method is proposed (Fig. 4) and it adopts the function of neuromodulator in the brain of the cricket as a model. The model consists of a diffusion equation for NO concentration, differential equations for cGMP and OA concentrations and a threshold model for behavior selection utilizing OA concentration. The se components are connected in series. Since the hypothesis which OA concentration will affect behavior, we assume that fighting behavior is selected when OA is over the threshold (0.5) and avoidance behavior is selected when OA is under that. By the computer simulations, we observe that a rising trend in cGMP concentration by the upturn in NO concentration and a consumption in OA concentration by a rising trend in cGMP concentration. As memory mechanism of defeat experience in fighting behavior, it assumes that OA concentration of the winner increases by a certain value and the one of the loser reduces by another certain value in proportion to fighting period. Figure 5 shows the response of internal state of the winner and the loser in a time series. The winner continually takes the aggressive state because OA concentration is over the threshold. The loser takes the negative state (under the threshold) for a

short time. These results indicate that proposed model is not to contradict to biological data and is an explicable one for an internal structure of the cricket's brain. As future work, we consider applying the effect of other factors in the brain to proposed neuronal circuit model and also examine to construct an explicable model both of internal physiological state and swarm behavior based on the interaction among individuals.

4. Foraging task realization by multiple mobile robots

We have proposed the model for neural mechanism of cricket fighting behavior. The problem statement in this section consists of the following two motivations:

- We would like to discuss the reason and the rationality of the adaptive behaviors of crickets depending on the density of the crickets.
- We would like to apply the adaptive behavior of crickets to behavior generation problems of multiple mobile robots.

There have been many studies regarding modeling behaviors of biotic communities (for example, ref.[4]). The characteristic of the proposed model in the former section is that animal behaviors become varied based on the density of the animals, and that the dynamical change of the animal behaviors can also be modeled. We have

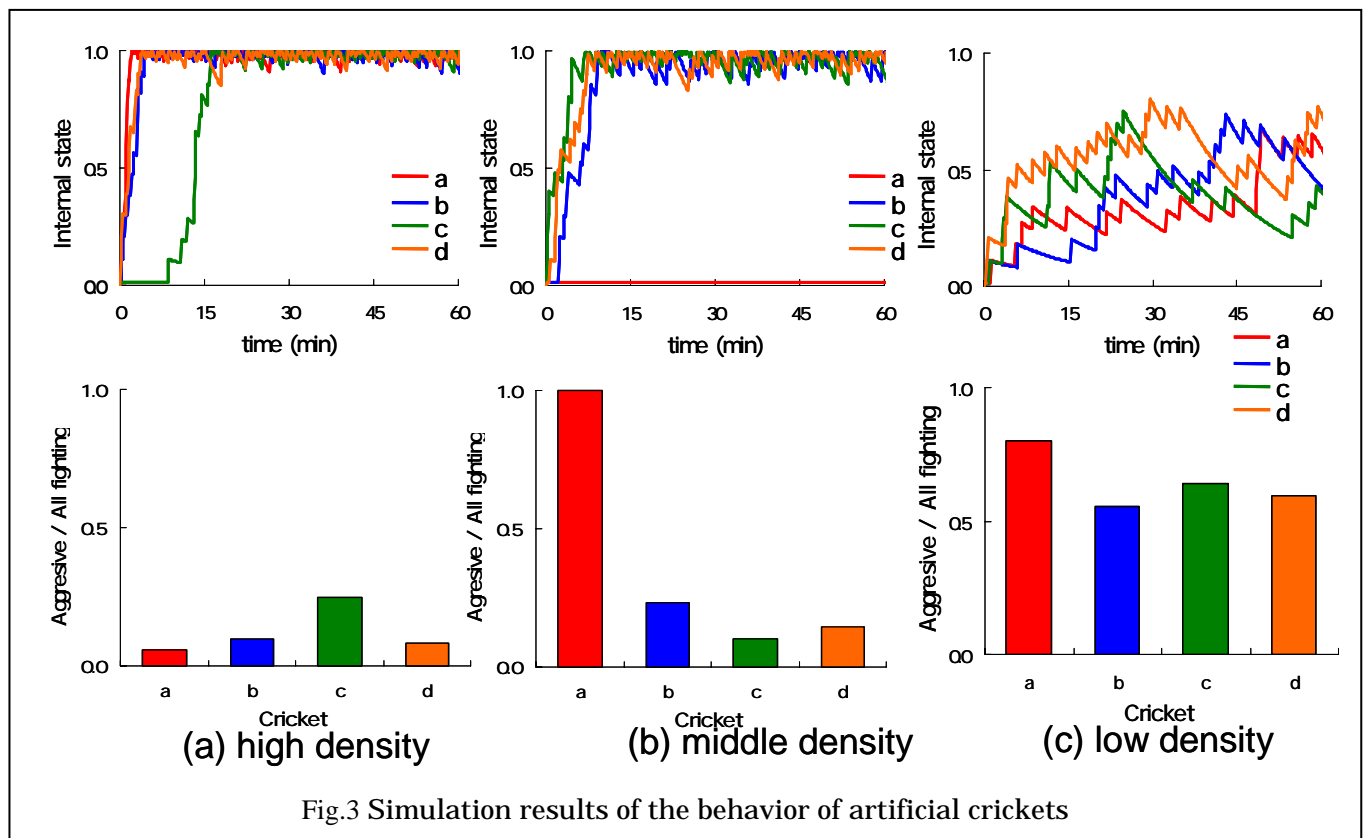


Fig.3 Simulation results of the behavior of artificial crickets

proposed foraging behavior of multiple robots in consideration of the working efficiency in [5]. The model is proposed for a foraging task of multiple mobile robots based on their activities, The performance index is defined to examine the working efficiency per movement distance of all the robots. We show the effectiveness of the model with the comparison model through computer simulations. In the comparison model called fixed number model, only the fixed number of robots can move actively. The simulation results show that the proposed model produces better working efficiency than the comparison model in average. The average of the performance index PI is 22% higher than the maximum in the comparison model. The robots in the proposed model can change their activities adequately based on mutual interaction and interaction with foods. This result

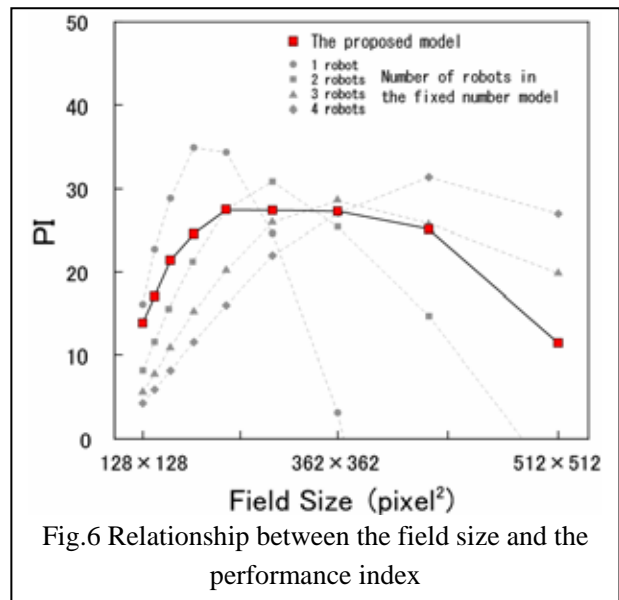


Fig.6 Relationship between the field size and the performance index

shows the effectiveness of the proposed behavior model of multiple mobile robots.

5. Conclusion

We have investigated how crickets behave in a social population. We have proposed the behavioral model and the neuronal model of crickets, and have shown the effectiveness of the models through simulations. We have also extent the model to the foraging task realization of multiple mobile robots.

References

- (1) Aonuma, H and Niwa, K., Nitric Oxide Regulates the Levels of cGMP Accumulation in the Cricket Brain, *Acta Biologica Hungrica*, 55, 65/70 (2004).
- (2) M. Ashikaga, T. Hiraguchi, M. Sakura, H. Aonuma, and J. Ota: Modeling of Adaptive Behaviors in Crickets, 18th SICE Symposium on Decentralized Autonomous Systems, 189-194 (2006). (in Japanese)
- (3) T. Fujiki, K. Kawabata, Y. Ikemoto, H. Aonuma, and H. Asama: A Study on Neural Circuit Model for Adaptive Behavior Selection of Insects – A Model of Adaptive Action Selection from NO/cGMP Cascade -, Prepr. 16th Intelligent System Symposium, 23-26 (2006). (in Japanese).
- (4) Hemelrijk, C. K., Self-organising properties of primate social behaviour. A hypothesis on intersexual rank-overlap in chimpanzees and bonobo's. In: *Primateology and Anthropology: Into the Third Millennium*. Evolutionary Anthropology, volume 11, Supplement 1 (Ed. by Soligo, C., Anzenberger, G., Martin R.D.), Wiley, 91/94 (2002).
- (5) M. Ashikaga, M. Kikuchi, T. Hiraguchi, M. Sakura, H. Aonuma, and J. Ota: Foraging task of multiple mobile robots in a dynamic environment using fighting behavior in crickets, Prepr. 16th Intelligent System Symposium, 17-22 (2006). (in Japanese).

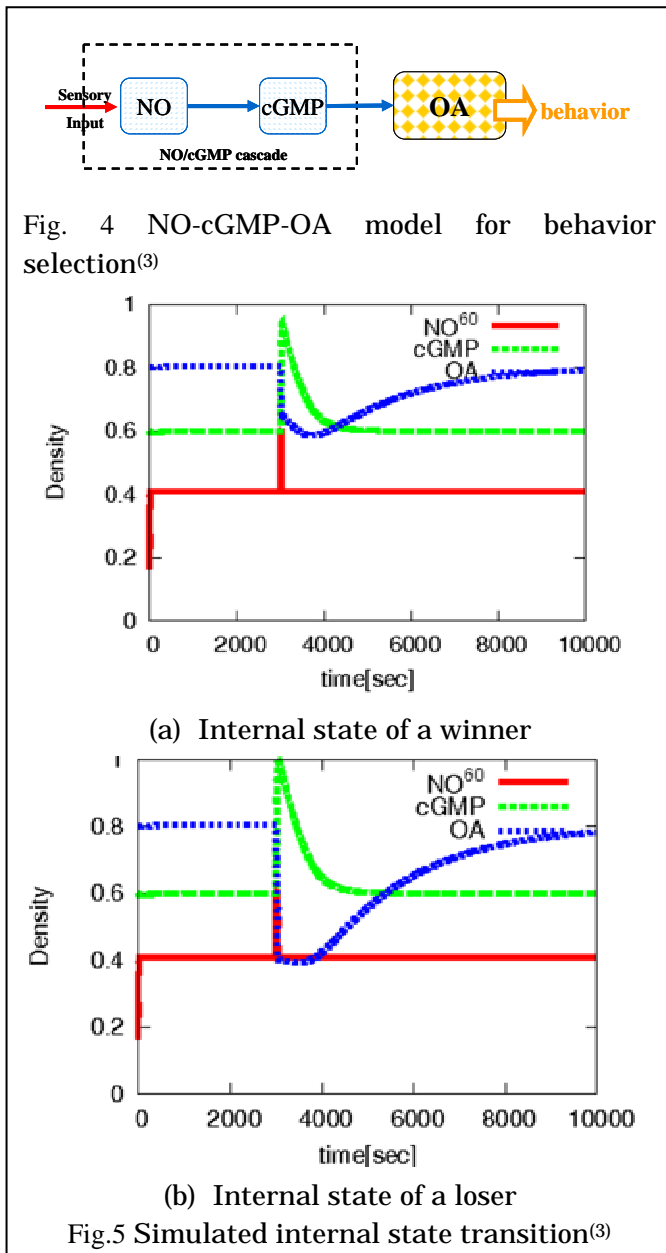


Fig.5 Simulated internal state transition⁽³⁾

Analysis of adaptive behaviors emerged by functional structures in interaction networks

Daisuke Kurabayashi, Tetsuro Funato

Abstract– Insects have only a little brain but the behavior is highly adaptive. We consider that physical structure of the interaction network works on the creation of the brain function and model the behavioral processor that controlled by its structural disposition. In this research, we investigate mechanisms for intelligent behaviors from the viewpoint of network property. We focus on (i) modeling of behavior-switching by nonlinear oscillator network, (ii) direct feedback system employing actual brain of silkworm, (iii) extended pheromone model for emergence of transportation network.

Key Words: Network, oscillator, virtual body

1 Introduction

In this study, we investigate adaptive behavior switching mechanism. A moving individual obtains many types of information through interactions with other individuals and environments. Creatures can adaptively feed back conditions around it to adaptive behaviors.

Robots, artificial products can work perfectly only in limited environment. Insects have high adaptability with limited resources. So, we have focused on the aspect of network property in some levels observed in creatures.

Nowadays, the graph theory indicates functionality of network structure[1]-[4]. Some researchers have insisted some structural functionality in creatures[1][5]. In this research, we investigate mechanisms for intelligent behaviors from the viewpoint of network property. We focus on (i) modeling of behavior-switching by nonlinear oscillator network, (ii) direct feedback system employing actual brain of silkworm, (iii) extended pheromone model for emergence of transportation network.

2 Oscillator network model for behavioral processing

2.1 Input from antenna robe

We have construct a behavior switching mechanism employing nonlinear oscillator network[6]. We have considered correspondence among artificial mobile robot and natural behavioral processing by realizing analog processing system.

Odor information obtained by antenna is categorized by glomeruli in antennal lobe. Then, the signal is transferred to mushroom body and pre-motor neurons by projection neurons (PN)[7]. PN are connected with local inter neurons (LIN). We simplify the signal flow as Fig. 1.

Some researches say that the odor information is coded by oscillate signals around 15-30[Hz][8], and it causes synchronization effects[9]. Therefore, we employ nonlinear oscillator network to model the effect. Figure 2 shows the model, where a small circle indicates an oscillator.

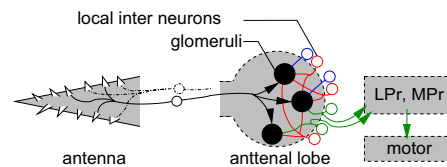


Fig. 1: Information flow through antennal lobe

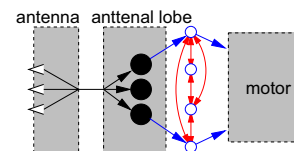


Fig. 2: Connection of oscillators

2.2 Behavior changing model with oscillator

We regard that network structure is connection between oscillators, a behavior corresponds a set of synchronized oscillators, respectively. When oscillators have different eigen frequencies, as Fig. 3(a), they do not synchronize without external input. When we feed cyclic signal into the black circle, oscillators may synchronize.

Synchronization depends on both difference between eigen frequencies and weight of connection[10]. So, we can design a network as Fig. 3 where 6 oscillators have 0.5-1.0 eigen frequency and they can synchronize input signal within ± 0.05 difference of frequency.

Network structure effects the synchronization condition[11]. When we change the network as Fig. 3(b), supposing the effect of neuromodulators, the sets of synchronized oscillators are changed as Table 1.

2.3 Output of network

The formulated network does not depend on any specific oscillator. Here we employ van der Pol (VDP) oscillator (1) that is the most well-known one.

$$\ddot{x}_1 - \varepsilon_1(1 - x_1^2)\dot{x}_1 + \omega_1^2 x_1 = 0 \quad (1)$$

The synchronization effect is represented as (2).

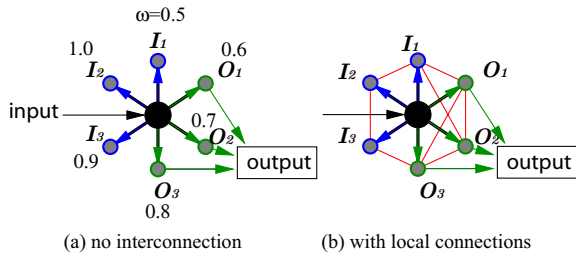


Fig. 3: Network with and without local connections

Table 1: Synchronization among oscillators

| Input w | Sync. Osci. | |
|-----------|-------------|---------------|
| | (a) | (b) |
| 0.55 | None | None |
| 0.65 | O_1+O_2 | $O_1+O_2+O_3$ |
| 0.75 | O_2+O_3 | None |

$$x_i(t+1) = \tilde{x}_i(t) + \varepsilon \left\{ \frac{1}{N_i(t)} \sum_{j=1}^{N_i(t)} x_j(t) - x_i(t) \right\} \quad (2)$$

,where $\tilde{x}_i(t)$ shows the state variable after calculation by (1).

We can implement VDP oscillator by analog circuit with tunnel diode (Fig. 4) Structure manipulation corresponds to addition of R1 and R2. Terminal out 1, out 2, out 3 correspond to O_1, O_2, O_3 in Fig. 3. Figure 5 shows the implemented system realizes behavior switching as Table 1. When we make out 1+out 2 (or out 2+out 3) and then avoid under certain threshold level, we can make output signal high duty ratio when oscillators are synchronized, low when they do not, respectively.

We can realize behavior switching between aggressive and avoidance state by applying the circuit to a simple mobile robot like Braitenberg vehicle[12](Fig. 6).

3 Behavior feedback system with insect brain

3.1 Feedback behaviors to neural system

We are investigating the mechanism and the performance of insect brain. We build direct control system of robotic/simulated body by neural system of silkworm in order to emulate feedback of behavioral outputs.

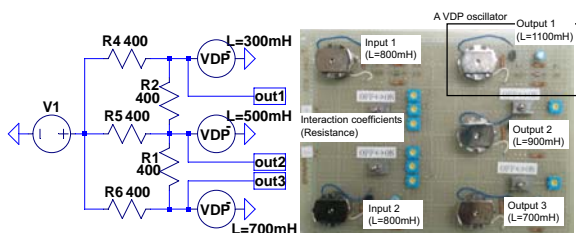


Fig. 4: Implementation of oscillators

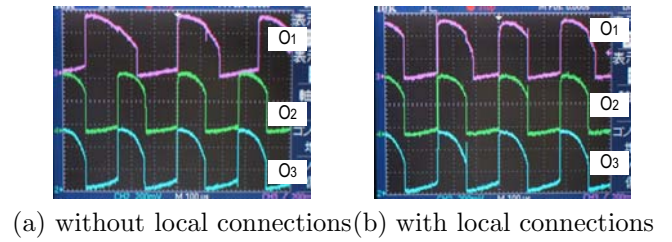


Fig. 5: Outputs depend on the local connections

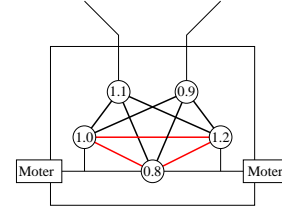


Fig. 6: Model for simple mobile robot

A male silkworm searches a female as odor-source. Because odor information is not smooth in the air, the searching procedure is not trivial problem. We can regard that the brain of silkworm is adaptive controller against complex airflow.

Kanzaki et al. (group C01-01) inspect biological properties of the silkworm's brain, and they have investigated emergence of adaptive motion by a mobile robot[13]. However, we still can find difference among the model and a living silkworm.

Here, we directly connect silkworm's brain to robotic body, and then investigate its adaptability by manipulating properties of body and environment.

3.2 Combining virtual body

Steering of a silkworm is controlled by its brain. Motion commands are translated into the movement of six legs, then silkworm body moves. According to the motion, antenna may encounter new odor information, then it generate next motion command. We observe neck motor neuron (NMN) that has high correspondence with motion commands to legs.

We have implemented preliminary experimental system indicated in Fig. 7, 8. In this system, we incorporate signal of NMN into PC. It decodes the command signal into two motions; left or right turn. According to the motion commands, robotic

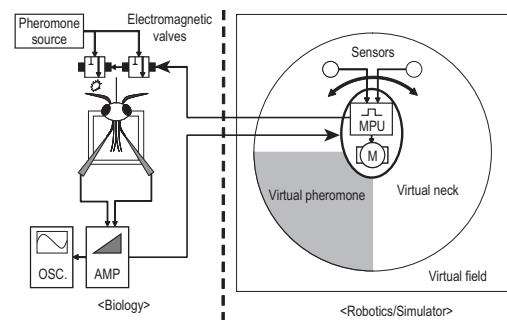


Fig. 7: Schematic view of the experimental system

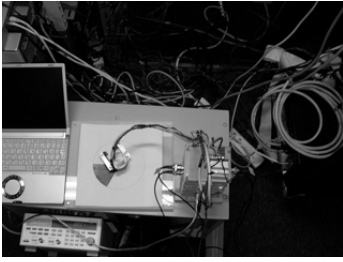


Fig. 8: Virtual neck system

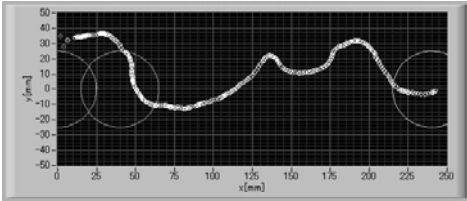


Fig. 9: Odor-searching of virtual body driven by brain (white dots indicate the trajectory)

head with sensor moves on an simple field on which pheromone plume. When the sensor finds the plume, electronic valve provide chemical pheromone to actual silkworm’s head. According to this feedback system, we confirm that we can realize odor-searching behavior with robotic body and actual brain.

We also build virtual field and virtual body instead of the mechanical head as a simulator on PC. In the simulation, we set virtual odor-source and provide pheromone plume to virtual body. When an antenna touches the plume in the simulator, we put chemical pheromone to actual silkworm’s antenna. We monitor the output of NMN, then we move the virtual body according to the decoded signal.

By considering airflow by wings of a silkworm, the virtual silkworm achieves the odor-source with around 20% ratio. We can also observe characteristic movement of searching behavior of actual silkworm in the simulator(Fig. 9).

We are now working to put the brain on actual mobile robot in order to investigate adaptive behavior switching during odor-source searching.

4 Network emerged by negotiation with environment

4.1 Emerging network by small agents

Many different networks are found in our environment. In the field of the emergent systems, some former studies have proposed certain models that represent the foraging networks of ants. However most of these studies have only considered movements between the nest and few feeding places. Here, we formulate and examine an autonomous organization system for a transportation network system. We focus on the emergence of network topology through interactions among agents and their environment considering properties of pheromone[14].

We assume a task in which many robots trans-

port objects. The environment is a 2D plane where N_v nodes (cities) are located. We denote a set of nodes as $\mathbf{V} = \{v_1, v_2, \dots, v_{N_v}\}$. We denote a set of possible connections between the nodes as $\mathbf{E} = \{e_1, e_2, \dots, e_{N_e}\}$, where $N_e = N_v C_2$. There are N_a agents. Suppose $N_a > N_e$. A transportation task occurs at random. The probability of generating an order from the i th node to the j th is equal to $\frac{1}{N_e}$.

We assume that an agent decides its route for ordered transportation and uses the Dijkstra algorithm for minimizing the total cost for traversing the network. We denote the route of an agent i as $\mathbf{r}_i = (e_{i1}, e_{i2}, \dots, e_{im})$, where m indicates the number of edges contained in the route. Then, union of routes $\mathbf{W} = \cup_i \mathbf{r}_i$ produces a graph $G(\mathbf{V}, \mathbf{W})$.

4.2 Property of emerging network

By considering density of pheromone, we state that a transportation line (an edge on a graph) that is used by many agents has a low traversing cost, while the one that is used by few agents has a high cost and its use may be discontinued. We formulate the density through a route i of an agent, η_i by (3).

$$\eta_i = \frac{N_a}{N_e} \frac{1}{|\mathbf{r}_i|} \quad (3)$$

where $|\mathbf{r}_i| = \sum_{\{j|e_j \in \mathbf{r}_i\}} |e_j|$.

If an edge is included in many routes, its density increases. The density ρ_j of an edge j is obtained by using (4).

$$\rho_j = \sum_{\{i|e_j \in \mathbf{r}_i\}} \eta_i \quad (4)$$

We can consider that dense pheromone helps an agent navigate efficiently. In (5), we formulate the cost function f_i according to the expected steps need to traverse an edge e_i . This cost function depends on the length of the edge and its connectivity $p_i(\rho_i)$ to the goal.

$$f_i(|e_i|, \rho_i) = \frac{|e_i|}{p_i(\rho_i)} \quad (5)$$

We have carried out some simulations in order to verify the autonomous adaptability of the transportation network by using the proposed model. We have considered the total number of agents as 1000, 3000, 5000, 10000. Figure 10 shows the converged states under these conditions. The number of nodes is 60.

When the number of agents is extremely small (1000), every agent proceeds to its destination directly similar to walkers. In the case of 3000 agents, the transportation network forms a tree graph similar to the flight network of airlines. These results show that agents try to concentrate on edges that require to be maintained. Figures 10(c)-10(d) show that 5000-10000 agents form loops that connect the leaves shown in Fig. 10(b).

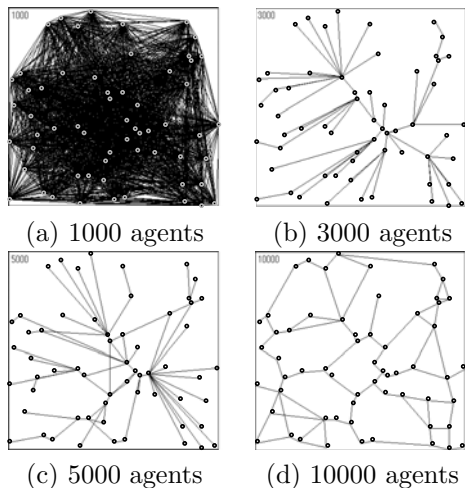


Fig. 10: Emerged Networks

We have found that the emerged networks have small world like property, which provides highly connectivity with low number of edge. We can say that pheromone-like network system is still effective in multi-node environment.

5 Conclusion

In this research, we investigate mechanisms for intelligent behaviors from the viewpoint of network property. Insects have only a little brain but the behavior is highly adaptive. We consider that physical structure of the interaction network works on the creation of the brain function and model the behavioral processor that controlled by its structural disposition. We formulate behavior-switching by nonlinear oscillator network, build direct feedback system employing actual brain of silkworm, and investigate extended pheromone model for emergence of transportation network.

Acknowledgement

The authors thank researchers in group C01-01, C01-02, and C01-12 very much for their kindly providing biological data, experimental system, and comments to the authors.

References

- [1] D.J.Watts: Small Worlds. Princeton Studies in Complexity, 1999.
- [2] S.H.Strogatz: Exploring complex networks. Nature, Vol. 410, 268/276, 2001.
- [3] C.Y.Huang, C.T.Sun, J.L.Hsieh, H.Lin: Simulating sars: Small-world epidemiological modeling and public health policy assessments. Journal of Artificial Societies and Social Simulation, Vol. 7, No. 4, 2004.
- [4] M.Small, P.Shi, C.K.Tse: Plausible models for propagation of the sars virus. IEICE Trans. on Fundamentals of Electronics, Communications

and Computer Sciences, Vol. E87-A, No. 9, 2379/2386, 2004.

- [5] L.F.Lago-Fernandez, R.Huerta, F.Corbacho, J.A.Siguenza: Fast response and temporal coherent oscillations in small-world networks. Physical Review Letters, Vol. 84, No. 12, 2758/2761, 2000.
- [6] T.Funato, H.Aonuma, D.Kurabayashi, M.Nara: Development of oscillator network model for behavioral processing, 2nd International Workshop by Research Group of Invertebrate Nervous System of Japan, 8, Kagawa, Aug. 29-31, 2006.
- [7] R.Okada, M.Sakura, and M.Mizunami: Distribution of dendrites of descending neurons and its implications for the basic organization of the cockroach brain. Ther Journal of Comparative Neurology, Vol. 458, 158/174, 2003.
- [8] M.Stopfer, M.Wehr, K.Macleod, G.Laurent: Neural dynamics, oscillatory synchronisation, and odour codes. In B.S.Hansson, editor, Insect Olfaction, chapter 6, Springer, 1999.
- [9] G.Laurent, M.Wehr, H.Davidowitz: Temporal representations of odors in an olfactory network. The Journal of Neuroscience, Vol. 16, No. 12, 3837/3847, 1996.
- [10] A.Jadbabaie, N.Motee, M.Barahona: On the stability of the Kuramoto model of coupled nonlinear oscillators, in the American Control Conference, 2004.
- [11] T.Funato, D.Kurabayashi, M.Nara: Synchronization Control by Structural Modification of Nonlinear Oscillator Network, 8th International Symposium on Distributed Autonomous Robotic Systems, 41/50, 2006.
- [12] V.Braitenberg: Vehicles :Experiments in synthetic psychology. MIT press, 1984.
- [13] R.Kanzaki, S.Nagasawa, I.Shimoyama: Neural basis of odor-source searching behavior in insect microbrain system evaluated with a mobile robot, Bio-mechanisms of Animals in Swimming and Flying (N. Kato ed.), Springer-Verlag Tokyo, 155/170, 2004.
- [14] D.Kurabayashi, K.Urano, T.Funato: Emergent Transportation Networks by Considering Interactions between Agents and their Environment, Advanced Robotics (in print), 2007.

Analysis on the brain differentiation that regulates the cooperative behaviors in social insects

Toru Miura¹, Hideaki Takeuchi², Mamiko Ozaki³

¹Graduate School of Environmental Science, Hokkaido University, ²Graduate School of Science, University of Tokyo, ³Graduate School of Science, Kobe University

Abstract—In colonies of social insects, there are various castes, among which tasks are allocated. As the results, we can see the elaborate social behavior in those insects. Furthermore, the complicated communication system is also required for the integration of such behavior. Through various approaches, we are investigating the molecular and neurophysiological basis of organized behavior in social insects, to understand the mechanism and evolution of insect society, and to find out new concepts in relation to the autonomous decentralized systems.

I. INTRODUCTION

Termites (Order Isoptera), ants, wasps and bees (Order Hymenoptera) organize colonies, live together with their related individuals, and perform elaborate social behavior [1]. In the colonies, there are reproductive and sterile individuals, and those sterile ones are helpers that are engaged in altruistic tasks such as foraging, nursing, defense, etc. Those types of individuals that specialize in certain tasks are called 'castes'. Although a number of mysteries are found in societies of those insects, one of the fundamental questions is that what mechanisms underlie the caste differentiation. Probably the regulations of this mechanism contribute to the system of social behavior in these insects. In this article, we introduce our studies on the mechanisms regulating social behavior in termites, honeybee, and ants. We are mainly applying molecular and neurophysiological techniques to analyze the social systems such as caste differentiation and nestmate recognition.

II. DIVISION OF LABOR IN TERMITE SOCIETY

We previously investigated on the social behavior of the black marching termite *Hospitalitermes medioflavus*. This termite species make processional columns along tree trunks etc. at forest floors to forage lichens. The workers graze good materials and make foodballs which are carried back to their nests. In this species, the reproductive and sterile castes differentiate at the relatively early stages of postembryonic development. Furthermore, among sterile individuals, castes are differentiated according to their sexes. Because of this special system of caste development, they successfully produce various types of castes based on the sexes and larval stages [2]. As the result of the detailed observation, we found that there are three types of workers, minor (male), medium

(female) and major (female) workers. In addition, tasks of workers are subdivided mainly into two, i.e. gnawers and carriers. Major workers are exclusively engaged in the carrying task, while minor workers are engaged in the gnawing. Medium workers are involved in both tasks (Fig. 1) [2]. This task allocation system is possible in termites, because termites are hemimetabolous so that immature juveniles possess similar body plan to imagos, and because there are both sexes among sterile individuals in termites.

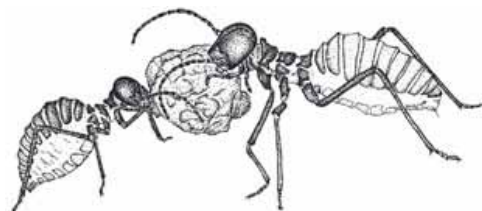


Fig. 1. Division of labor among workers in the black-marching termite.

As seen in the division of labor in the black marching termites, caste differentiation, i.e. morphological and behavioral specialization, is important for the sophisticated social behavior. Therefore, we investigated the detailed mechanisms of caste differentiation in more manageable species under the experimental systems.

III. CASTE DIFFERENTIATION AND ASSOCIATED GENE EXPRESSIONS IN TERMITES

As mentioned above, the termite social behavior is organized elaborately by task allocation and cooperation. In order to accomplish the social behavior, there must be at least two intrinsic mechanisms in termites. The first mechanism is that all individuals possess a set of genes (a genome) that enable them to differentiate into any castes. Similar mechanism is seen in the cell differentiation of multicellular organisms, in which all of the cells include the genomic information that is required for any cells constituting the organismal body. The second mechanism is to regulate the caste ratio in a colony. If all of the individuals differentiate into soldiers, the colony should be destroyed because they lack reproductive options. For this reason, they have flexible options that can change the caste fate during their developmental processes. Namely, each individual can change the physiological status in response to the environmental factors, followed by the change of developmental pathways. Thus, by means of mechanism of "polyphenism" and "feedback", termites can realize the

appropriate caste ratio under a certain environment [4]. In order to uncover the developmental mechanisms of caste differentiation, we investigated the differential gene expressions among different castes in termites.

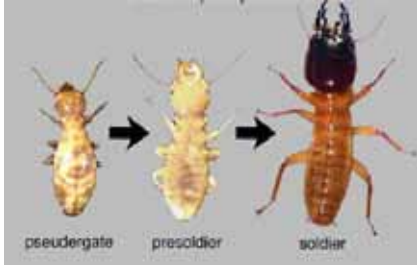


Fig. 2. Soldier differentiation in the damp-wood termite.

As the study material to investigate caste-specific gene expressions, we chose the Japanese damp-wood termite *Hodotermopsis sjostedti*. In this species, soldiers are differentiated from pseudergates, which function as workers, via presoldiers (Fig. 2). In the process of soldier differentiation, the anterior part of the body is exaggerated being suitable for defense and attacking. Especially, the elongation of mandibles is conspicuous. In this process, juvenile hormone (JH) plays important roles as an endocrine factor to regulate the physiological changes, which eventually induce the proliferation of epithelial tissues of mandibles (Fig. 3).

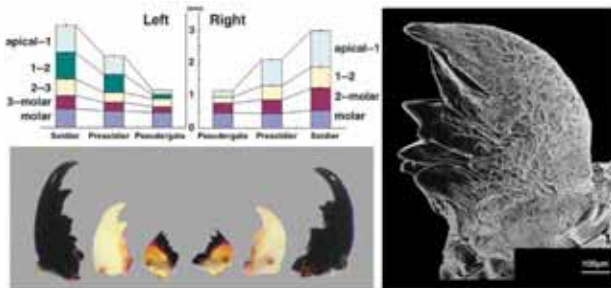


Fig. 3. Elongation of mandibles in the course of soldier differentiation in the damp-wood termite *Hodotermopsis sjostedti*.

So far, we have identified several genes which specifically express during the course of soldier differentiation, and genes specifically express in mature soldiers. The former ones should be required for the building soldier forms, and the latter should be required for the maintenance and/or function of soldiers. For examples, Cytochrome P450 and Ciboulot genes were identified from the individuals that entered the soldier differentiation by the application of juvenile hormone analogue (JHA) [5, 6]. Those genes probably respond to the JH action and induce the special morphogenesis forming the defense morphology. We are now trying to establish the experimental methods using RNAi (RNA interference) that examine the function of these genes. In addition, we are analyzing the expression dynamics of transcription factors and signal transduction factors, which seem to regulate the soldier morphogenesis.

Furthermore, the gene termed 'SOL1' that were identified in mature soldiers, was shown to express extensively in the

mandibular gland which is known as an exocrine gland (Fig. 4) [7]. Recent experimental analyses showed that the product of this gene was a secretory protein, which is secreted externally in a large amount from the mandibular glands (Miura, unpublished data). In addition, based on the prediction of tertiary protein structure, it has been revealed that the SOL1 protein belongs to the lipocalin family, suggesting that this protein is transferred between colony members. From these results, we predict that the SOL1 protein may be involved in the communication among individuals and/or the regulation of caste ratio in termite colonies.

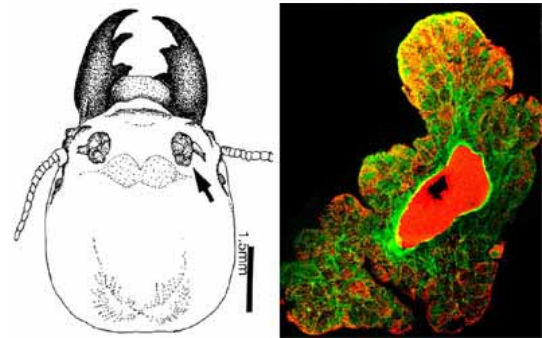


Fig.4. Soldier-specific gene SOL1 is expressed in the mandibular glands.

IV. NEURAL MODIFICATION IN THE SOLDIER DIFFERENTIATION IN TERMITES

Not only morphology but also behavior is changed accompanying the caste differentiation. For example, soldiers aggressively attack against enemies like predators or competitors, while pseudergates rush deep inside nests. To understand the physiological basis underlying the behavioral differences, we compared the central nervous systems, i.e. brains and suboesophageal ganglia (SOG), between pseudergate and soldier in the damp-wood termite *H. sjostedti*. As the result, it was revealed that the size of SOG was significantly larger in soldiers than in pseudergates, whereas no difference was detected in the brains. Histological examinations revealed that there were extremely giant neural somata around the base of mandibular nerves in the soldiers' SOG (Ishikawa and Miura, unpublished data). The retrograde staining using fluoro-dextran showed that those giant neurons were motor neurons for mandibular closer muscles, and approximately 1.5 times larger than those in pseudergate (Fig. 5). It is suggested that the enlargement of mandibular motor neurons enables soldier termites to defense effectively through fast and strong mandibular movements. In addition to the motor neurons, some sensilla are elongated in soldiers, suggesting that the nervous systems, including sensation, integration and motion, are specialized in soldiers at various levels. Based on this hypothesis, we are now identifying genes specifically expressed in relation to the soldier differentiation, using differential display method. So far we obtained several candidate genes that would be responsible for the aggressiveness in soldiers and for the soldier-specific neural modifications.

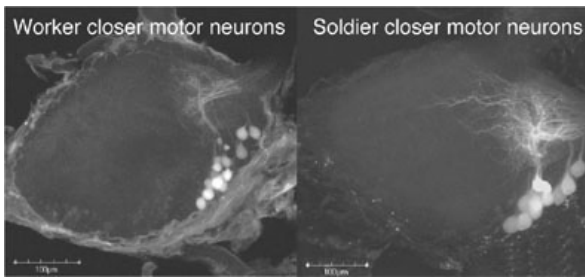


Fig. 5. Soldiers possess larger mandibular motor neurons in the subesophageal ganglion.

V. MOLECULAR BASIS UNDERLYING HONEYBEE SOCIAL BEHAVIORS

The honeybee *Apis mellifera* L. is a eusocial insect, and colony members perform various complex communications and divisions of labor to maintain colony activities. Young workers (nurse bees) labor at in-nest jobs such as cleaning the comb and nursing the brood, while older workers (forager bees) forage for nectar and pollen (age-polyethism). A returning forager bee communicates by dance to inform other workers in the hive of the direction and distance of food. The molecular basis of honeybee social behavior, however, is largely unknown.

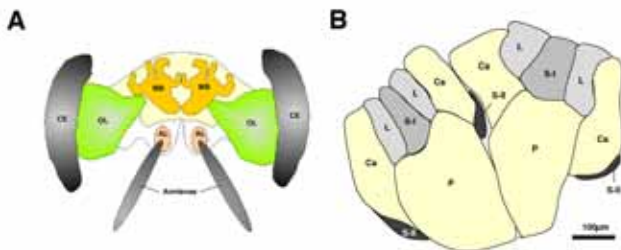


Fig.6 (A). Schematic illustration of the front view of the honeybee brain. (B) Organization in the MB. Dendrites of Kenyon cells compose the calyces (Ca), Kenyon cell axons compose the peduncles (P), which provide both the MB efferents and afferent. Kenyon cells can be subdivided into two types; large and small Kenyon cells. The small-type Kenyon cells are subdivided into two classes: class I and class II. In this figure, clusters of large type, an class I and class II small type Kenyon cell bodies are indicated by L, S-I, and S-II, respectively. OL: Optic lobe, CE: Compound eye, AL: Antennal lobe.

Mushroom bodies (MBs) are insect brain structures that are important for higher-order sensory processing of different sensory modalities (Fig.6). Honeybee MB function is thought to be closely associated with honeybee social behaviors [8]. We have searched genes expressed preferentially in the MBs of the honeybee brain using molecular biologic techniques and showed that genes for ecdysteroid receptor (EcR, HR38, and USP) and ecdysteroid-regulated transcription factors (*Mblk-1/E93*, *E74*, *E75*, *BR-C*) were preferentially expressed in the MBs in the honeybee brain (Fig.7). [8, 9, 10, 11]. During metamorphosis in fruit fly, the EcR/Usp heterodimer binds to ecdysteroids to activate transcription of downstream genes (*Mblk-1/E93*, *E74*, *E75*, *BR-C*). HR38 interacts strongly with EcR directly and consequently disrupts EcR-Usp transactivation. Interestingly the expression of

AmHR38 was selectively expressed in the small-type Kenyon cells and enhanced in the forager brain, which might contribute to switch the mode of ecdysteroid-signaling in the MBs in association with age-polyethism of the workers (Fig.6) [9].

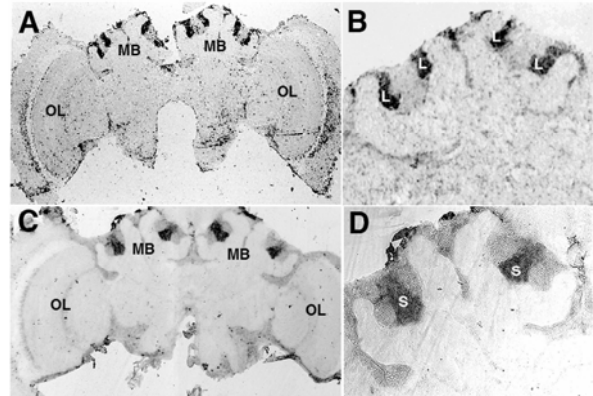


Fig.7 Kenyon cell subtype-selective expression of ecdysteroid-regulated genes (*Mblk-1/E93* and *E74*) in the honeybee MBs. *Mblk-1/E93* expression is shown in (A) and (B). *E74* expression is shown in (C) and (D).

Furthermore the expression of *Mblk-1* was also observed preferentially the cell bodies of differentiating large-type Kenyon cells in pupal worker bee heads, suggesting the expression of genes for ecdysteroid-regulated transcription factors is induced response to ecdysteroid during pupal stage and maintains at the adult stage. During larval and pupal development, the MBs consist of neuroblasts (immature neurons) devoted to the production of Kenyon cells. The MBs of the adult bee have three types of Kenyon cells (Fig.6b: S-I, S-II, and L). During the MB development, S-II Kenyon cells born first and, then L-Kenyon cells born. Last S-I Kenyon cells born and remain nearer the center of neuroblasts. Thus the stage-specific enhancement of gene expression for ecdysteroid-regulated transcription factors might be related to generation of Kenyon cell subtypes, which is characteristic of Hymenoptera (social insects, bees ant ants). Next it will be necessary to show the relation between ecdysteroids signaling and honeybee social behavior.

VI. MECHANISM OF NESTMATE RECOGNITION IN THE ANT *CAMPONOTUS JAPONICUS*

To maintain order in societies, animals including human beings evolved and developed diverse means of communication through various sensory modalities. Social insects rely on chemical communications to recognize sex, species, social status and their colony membership. In the case of ants, they cover their body surface with cuticular hydrocarbons (CHCs) whose combinations were different among species and whose ratios are different among colonies. By sensing such species- and colony-specific CHC profiles of encountered individuals, the ants can exhibit overt aggression toward the non-nestmates but not towards the nestmates.

Although the neural mechanism for this well-defined behavior has been elusive for long time, recently, we found that a CHC-sensitive organ housing about 130 multiple

receptor neurons on the antennae in *Camponotus japonicus* (Fig. 8) [12]. Surprisingly this type of sensilla responded to the non-nestmate CHCs but not to the nestmate CHCs. Thus, the chemical signs of the non-nestmate CHC patterns, which can discriminatively claim the colony identification, would be translated into neuronal signs of the multiple receptor neurons and sent to the antennal lobe, the primary olfactory center in the brain.

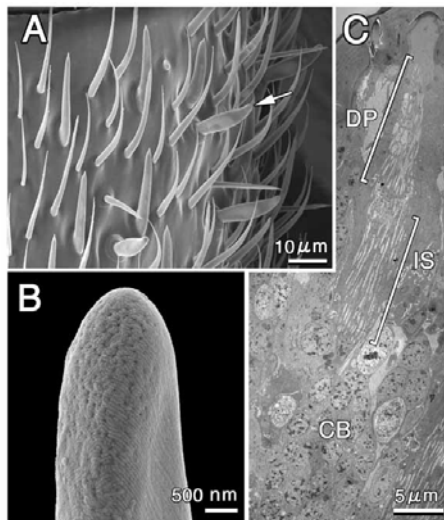


Fig. 8. CHC-sensitive sensillum in the ant *Camponotus japonicus*.

Introducing fluorescent dye through these particular CHC-sensitive sensilla, we identified the innervating region of the CHC-receptor neurons in the antennal lobe. It consisted of 136 glomeruli and located on the Vento-medial part of the antennal lobe (light blue cluster in Fig. 9), which totally consists of 433 glomeruli (Fig. 9). If the neural signs for encounters of non-nestmates came up to the brain, however, aggressive behavior would not automatically be induced. There should be some neural mechanism to determine behavioral threshold for aggressiveness. We suggested such mechanism was regulated by octopamine.

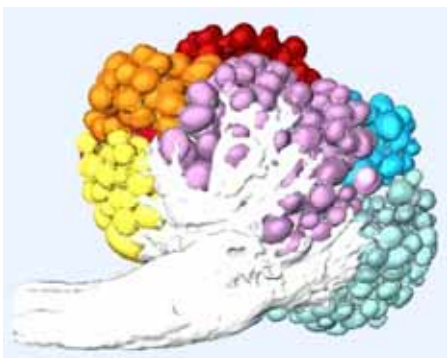


Fig. 9. Seven glomerular clusters of in the antennal lobe of the ant *Camponotus japonicus*.

Furthermore, we made PC analysis of ant locomotion recorded either on nestmate and non-nestmate footprints. From change of the fractal dimension of the walking trail of the ants, which were transferred onto the nestmate or the

non-nestmate footprints, it was suggested that the ants acquire some chemical information either of the nestmates or non-nestmates via their footprints.

VII. PERSPECTIVES

In this article, we introduced our studies on the mechanical basis underlying elaborate social life in termites, honeybee, and ants. Recently, the whole genome of honeybee has been completely sequenced in 2006, and similar genome projects are also launched in other social insects like ants and termites. Molecular techniques are now applicable to non-model organisms like social insects, so that a number of various molecular experiments can be applied to reveal the mechanism of social behavior in various insects. In the near future, it will probably possible to compare genomes between social and non-social insects, providing lots of information on the mechanism of social regulations and the social evolution. Based on the studies on social regulation in these insects, we will probably obtain some clues to find out new concepts of autonomous decentralized systems that can be applied to the area of robotics.

REFERENCES

- [1] Wilson EO (1971) *The Insect Societies*. Belknap Press. Cambridge, Massachusetts.
- [2] Miura T, Roisin Y, Matsumoto T (1998) Developmental pathways and polyethism of neuter castes in the processional nasute termite *Hospitalitermes medioflavus* (Isoptera: Termitidae). *Zoological Science* 15: 843-848.
- [4] Miura T (2005) Developmental regulation of caste-specific characters in social-insect polyphenism. *Evolution & Development* 7: 122-129.
- [5] Cornette R, Koshikawa S, Hojo M, Matsumoto T, Miura T (2006) Caste-specific cytochrome P450 in the damp-wood termite *Hodotermopsis sjostedti* (Isoptera, Termopsidae). *Insect Molecular Biology* 15: 235-244.
- [6] Koshikawa S, Cornette R, Hojo M, Maekawa K, Matsumoto T, Miura T (2005) Screening genes expressed in developing mandibles during soldier differentiation in the termite *Hodotermopsis sjostedti*. *FEBS Letters* 579: 1365-1370.
- [7] Miura T, Kamikouchi A, Sawata M, Takeuchi H, Natori S, Kubo T, Matsumoto T (1999) Soldier caste-specific gene expression in the mandibular glands of *Hodotermopsis japonica* (Isoptera: Termopsidae). *Proceedings of the National Academy of Sciences USA* 96: 13874-13879.
- [8] Takeuchi H (2006) Gene expression in the Honeybee Brain Mushroom Body and its Gene Orthologues. In "Evolution of Nervous Systems. Vol1" Ed by Jpn H Kaas, Elsevier, pp 457-469.
- [9] Yamazaki Y et al. (2006) Differential expression of HR38 in the mushroom bodies of the honeybee brain depends on the caste and division of labor. *FEBS Lett.* 580, 2667-2670.
- [10] Paul RK, Takeuchi H, Kubo T (2006) Expression of two ecdysteroid-regulated genes, Broad-Complex and E75, in the brain and ovary of the honeybee (*Apis mellifera* L.). *Zool. Sci.* 23, 1085-1092.
- [11] Takeuchi, H, Paul, R. K. et al., (2007) EcR-A expression in the brain and ovary of the honeybee (*Apis mellifera* L.). *Zool. Sci.* in press.
- [12] Ozaki M, Wada-Katsumata A, Fujiwara K, Iwasaki M, Yokohari F, Satoji Y, Nisimura T, Yamaoka R (2005) Ant nestmate and non-nestmate discrimination by a chemosensory sensillum. *Science* 309: 311-314.

Brain mechanisms in insects for social adaptation

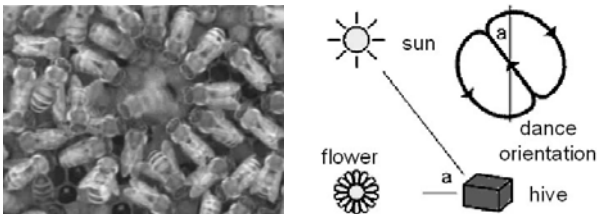
Etsuro Ito¹, Hidetoshi Ikeno² and Ryuichi Okada¹

¹Tokushima Bunri University and ²University of Hyogo

Abstract—A honeybee informs her nestmates of the location of a flower she has visited by a unique behavior called a “waggle dance.” We regard the waggle dance as a good model of the “propagation and sharing of knowledge” that maintains a society, and thus we are attempting to reveal the effects of the waggle dance in terms of the colony’s benefit using mathematical models and computer simulation based on parameters from observations of the bee behavior. This year, we constructed a mathematical model and obtained biological data for the model, e.g., the activity and condition of the hive and the behavior of individual bees. Video analysis showed that the bee does not dance in a single, random place in the hive but waggled several times in one place and several times in another. It also showed that the information of the waggle dance is not so precise. We then succeeded in recording the dance sound, which is considered to be the main signal for information transfer. We made a program to measure the total activity of bees in the hive. Finally, we revealed the distributions of mRNA of nitric oxide synthase and its activity in the brain. In the coming year, we will continue to obtain biological data and try to understand the effects of the waggle dance on the colony through the construction of an improved model incorporating new biological parameters.

I. INTRODUCTION

HIGHLY developed societies such as those of human beings require communication between individuals. The honeybee (*Apis mellifera*), one of the social insect species, is well known to have the ability to communicate with its nestmates, using the so-called “waggle dance” to inform them of the location of a food source (Fig. 1, [1]-[4]). In the waggle dance, the dancer moves in a straight line with her wings beating (waggle run), then circles back to the starting point without wing-beating (the return run). On a vertical comb, the direction of the waggle run (during which the dancer wags her body from side to side and emits sounds) relative to gravity indicates the direction to the food source relative to the sun’s azimuth in the field. The duration of



the waggle run depends on the distance to the food source. A

Fig. 1 Waggle dance (left panel) and the relationship between the dance orientation and food source (right panel).

few follower bees keep close contact with the dancer, and these bees may be recruited to visit the flower the dancer is locating for her nestmates. In the hive, however, it is too dark for followers to “watch” the dance. Hence, they “listen” to and decode the dance, as the sound that is generated by wing vibrations during a waggle run has a carrier frequency of about 260 Hz. The sound amplitude the dancer emits is quickly attenuated with distance, suggesting that information can be transferred within only a very limited area in the hive. This means that only a few bees, compared to the total number of the bees in the hive, will receive the information.

In spite of this fact, bees dance and maintain their colony. How much benefit do honeybees obtain from doing the waggle dance? What strategies for propagation of information are hidden, and how many bees have to share “the information” to maintain their colony? We regard the waggle dance as a good model of the “propagation and sharing of knowledge” that maintains a society, and are attempting to reveal the effect of the waggle dance in terms of its benefits to the colony using mathematical models and computer simulation based on parameters from observations of the bee behavior. This past year, we (1) constructed a mathematical model and simulated foraging behavior, and (2) observed honeybee foraging and dance behavior in the field. Here, we discuss the further parameters necessary for our model, and (3) devise a program for obtaining these parameters from behavioral experiments in the coming year.

II. RESULTS

2-1 Simulation of honeybee foraging

To evaluate the effect of the waggle dance, we first constructed a foraging model. We assumed that honeybee foraging behavior is the result of decision-making after a transition through 3 states: 1) resting, 2) wandering in the hive, and 3) foraging. The transition probabilities among these states were determined based on previous studies. We simulated the efficiency of 3 putative bee colonies with our foraging model. Bees in the first colony neither memorize the location of the food source nor dance. In the second colony, bees memorize but do not inform others of the food source. Bees belonging to the third putative colony memorize and tell

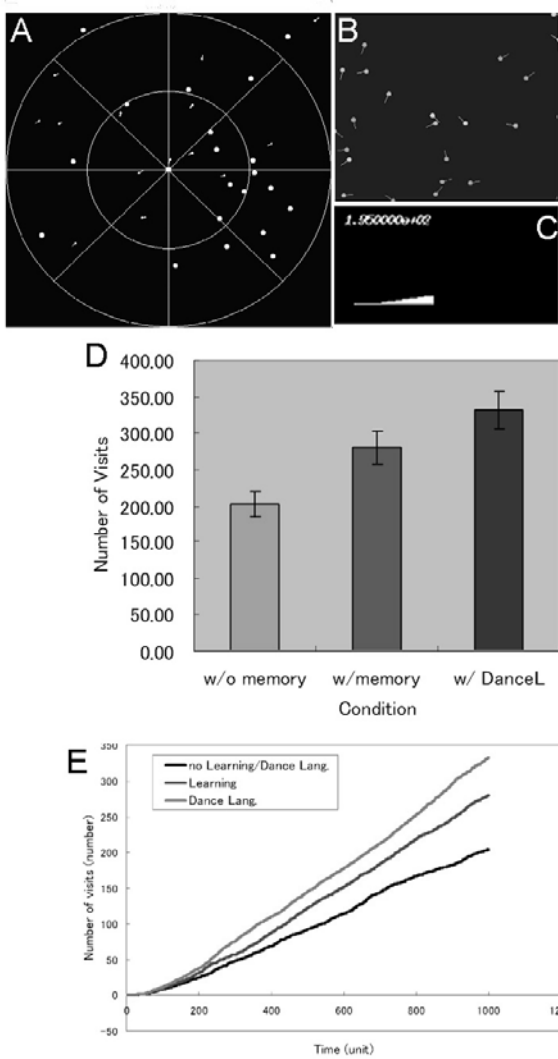


Fig. 2 Simulation of honeybee foraging behavior. A and B: Honeybees fly to feeders from the hive (center). The internal states of individuals differ, as indicated by the different colors. C: The number of visits is counted as a time function. D and E: The numbers of visits in 3 different colonies and its time function.

others of the location of the food source. Our simulation showed little difference among colonies when the total experimental time was short (Fig. 2). After a longer period of the time (corresponding to many foraging expeditions to food sources), the third colony bees made the most visits to the food source, as expected.

We realized that this model is too simple and requires more biological parameters. Hence, we decided to incorporate all of the following parameters into our simulation to improve the model: (A) behavioral patterns of the dancing bees, (B) characteristics of the waggle dance in orientation and duration, (C) behavioral patterns of the dance followers, (D) total activity of the whole hive. Then we observed the waggle dance in the field to obtain these parameters.

2-2 Results of observation of dance behavior

Behavioral studies were performed in Sapporo from 8:30 am to 4 pm on several days in August and September, 2006 (temperature: 25-36 °C in most experiments). One comb was picked up from the hive and monitored by a video camera (JVC, GR-HD1) stored in a digital video tape (30 frames/sec). The location and duration of the dance (waggle run) were analyzed off-line.

2-2-1 Behavioral patterns of dancing bees (A in section 2-1)

A waggle dance consists of more than one waggle run. Observations of 202 waggle runs in 11 bees (an average of 18.4 runs per bee) revealed that a bee performs the waggle run several times at one place on the comb and then moves to another place before resuming the waggle runs. The locations where waggle runs were observed appears to be “clusters” (Fig. 3). All 20 waggle runs of Bee 10 were observed in

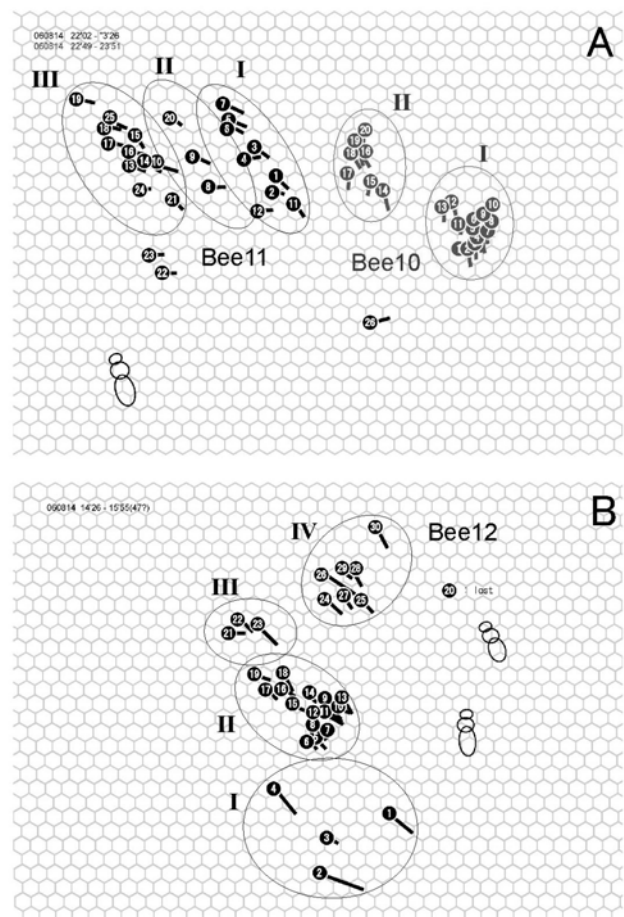


Fig. 3 Locations and orientations of waggle runs. Starting points are indicated by circles. The numbers in the circles indicate the order of the waggle runs. The direction of the line shows the waggle run direction, and its length shows the distance of the run. Scales are different from panel to panel. For reference, honeycombs and honeybees are illustrated in each panel. In A, two bees (Bee 11, black; Bee 10, red) were dancing at the same time. We observed 26 runs in Bee 11 (A), 20 in Bee 10 (A), and 30 in Bee 12 (B).

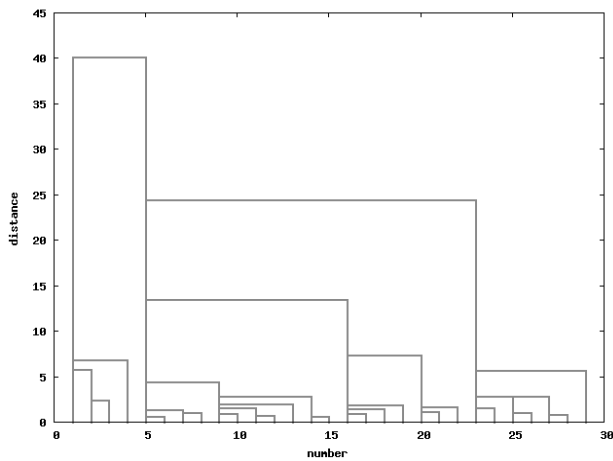


Fig. 4 Dendrogram after cluster analysis in Bee 12.

two clearly distinguishable areas (Fig. 3A, red). Until the 13th run she performed in cluster I; then she moved to cluster II and wagged until she stopped. A similar tendency to "dance and move" was observed in other bees (Fig. 3, Bee 11, and Bee 12). However, some bees did not show this tendency. At present, we are attempting to evaluate the place of dancing quantitatively by using cluster analysis against all bees observed (Fig. 4).

2-2-2 Characteristics of waggle dance in orientation and duration (B in section 2-1)

The durations of 140 waggle runs of the 9 bees that performed more than 10 runs (max, 26 runs; min, 14 runs) were measured, and we found that waggle run duration varied largely from run to run, even in a series of waggle runs by the same individual (Fig. 5). This became clearer from the increments in the durations of the run. In Bee 12, the difference in the duration was at most 0.87 sec (1.47 sec in the 4th run and 0.6 sec in the 3rd run) although the mean duration was 1.08 sec. Bee 3 and Bee 6 exhibited long runs (averaging 8.37 sec in Bee 3 and 11.81 sec in Bee 6). In 16 out of 21 runs for Bee 3 and 9 out of 14 runs for Bee 6, the difference of each run from the mean duration was larger than 1 sec; when

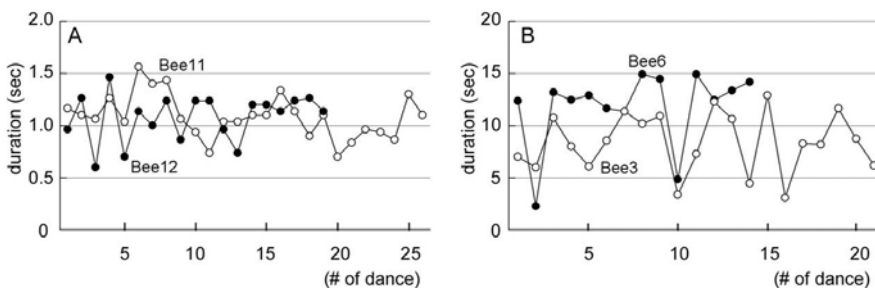


Fig. 5 Duration of each individual waggle run is shown. A: Short run (about 1 sec). B: long run. The mean duration was 8.37 sec in Bee 3, 11.81 sec in Bee 6, 1.08 sec in Bee 11, and 1.08 sec in Bee 12, respectively.

translated into the distance the bee was representing, the difference was more than 200m.

On the other hand, it was found that the orientation of the run also varied from dance to dance even in a series of waggle runs performed by same the individual (Fig. 3). Since followers do not listen to all of the waggle runs performed by a dancer (see "Behavioral patterns of the dance follower"), followers may receive "ambiguous" information about the orientation of the food source, which entails a non-negligible error for foraging.

In all cases, followers have to forage with imprecise information of both orientation and distance.

Automatic measurement of dance information

Various kinds of data are required to improve the reliability of our model, and automation of measurement and analysis is necessary for quick sampling a robust data set. We noticed the dance sound emitted by a dancing bee, and plan to construct an automatic system to get information from the dancer (location, duration, etc of dance) by detecting the sound source with multiple microphones. As an initial trial, we made a small microphone and manually recorded the sound, to evaluate whether the dance sound could indeed be recorded as high-quality sound data that is suitably analyzable.

Figure 6 shows the recorded sound. The temporal structure of the dance sound consists of a sequence of many pulse-like sounds with short intervals (Fig.6A). The time-expanded waveform shows that the dance sound is not a simple "pure tone" but a complex form, suggesting that it contains many frequency components. In fact, FFT analysis revealed a small broad peak at about 260 Hz with a very low SNR, implying that the dance sound appears to be white noise (Fig. 6C). This was consistent with previous works.

We concluded that our microphone can record the dance sound, but that the result is not sufficiently detailed. We need to produce a better microphone. Secondly, because low-frequency components are important, we need to filter the recorded sound. Third, we need to use wavelet transfer, not FFT, because the dance produces a sequence of pulse-like sounds. At present, we are preparing to devise a new microphone, filters and programs for analysis.

2-2-3 Behavioral patterns of dance followers (C in section 2-1)

Followers go out to forage after listening to several waggle runs. Some followers left the dancer after listening to only one waggle run while others followed the dancing bee more than 10 times. Even in

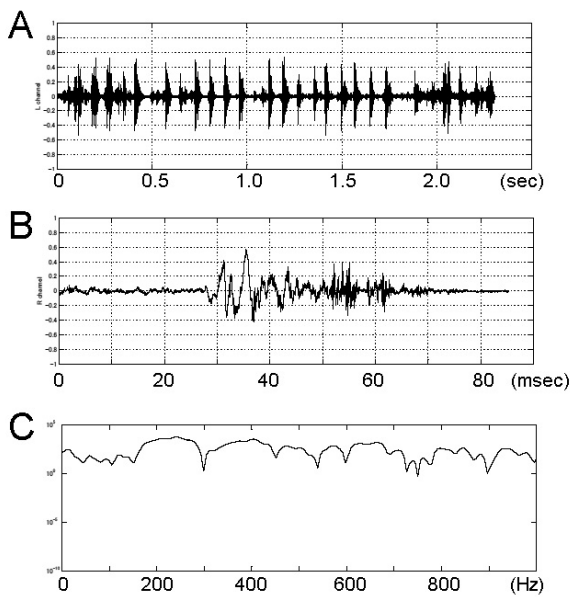


Fig. 6 Dance sound and frequency spectra. A: Recorded dance sound. B: Time-expanded waveform. C: Power spectrum.

a series of waggle runs by the same individual, some waggle runs attracted no followers while others attracted more than 8 bees. We will continue further analysis to incorporate characters of followers into our model.

2-2-4 Total activity of the whole hive (D in section 2-1)

In order to construct a mathematical model and simulation that evaluates the effect of information sharing on foraging behavior, we need to know the total activity of the whole hive, i.e., the total activities of dancers, followers, and other bees, because foraging and maintenance of the colony should depend strongly on the colony conditions, e.g. the number of potential foragers and followers. The activity of dancing bees could be detected with our microphone system because they emit sound. Our system, however, cannot detect both followers and potential followers because they are silent. Hence, we made a program as a first step of extracting the best parameter to express the total activity of the hive. Our program detected places where bees moved with high activity (Fig. 7). The degree of activities is indicated with grey-scale (white is the highest activity and black is lowest). Dancing bees are indicated by intense white in this figure.

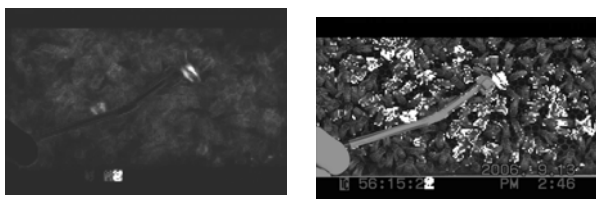


Fig. 7 Distributions of activity in the hive. High activity points are indicated by white dots. Dancing bees are detected here (left panel). Activity patterns were superimposed on the original picture (right panel).

Superimposing the activity distribution on the original picture showed that honeybees near the dancing bees, possibly followers, were also active (Fig. 7) though less active than the dancers. In the near future, we will extract the best parameter(s) to reflect the total activity of the whole hive, and feed it back to the mathematical model.

2-3 Brain regions for dance behavior

Dance behavior is apparently controlled by the nervous system. We examined the distributions of gene expression of gaseous neuromodulators believed to be important for behavior, such as nitric oxide [6]. *In situ* hybridization of the honeybee nitric oxide synthase (NOS) gene showed that Kenyon cells and optic lobe cells were positively labeled. NOS activity was found in the mushroom body, the central complex, the antennal lobe, the optic lobe, and the lateral protocerebral lobe. We are continuing this anatomical work to reveal the neural networks related to dance behavior.

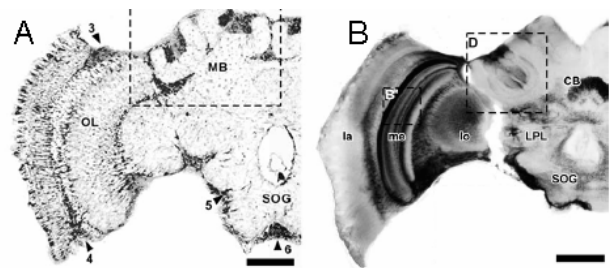


Fig. 8 Distributions of mRNA of NOS gene and NOS activity.

III. FUTURE PLAN

We will improve our mathematical model to reflect natural phenomena more precisely after further detailed biological observation. Then we will examine how well the new mathematical model predicts biological phenomena in nature by behavioral experiments. Finally, we hope to understand the effect of the dance on maintenance of the colony.

We believe that our research is not merely a topic for biology, and that the mechanisms for maintaining a society by the sharing of information will have useful applications to system engineering such as the control of robots under a multi-agent environment.

IV. REFERENCES

- [1] K. von Frisch, *The dance language and orientation of bee*. Harvard University Press, Cambridge, Massachusetts, London, 1993
- [2] J. M. Gould and C. G. Gould, *The honey bee*. Scientific American Library, New York, 1988
- [3] A. Michelsen, "The transfer of information in the dance language of honeybees: progress and problems", *J Comp Physiol* vol. 173, pp. 135-141, 1993
- [4] A. Michelsen, "Signals and flexibility in the dance communication of honeybees", *J Comp Physiol* vol. 189, pp. 165-174, 2003
- [5] A. Michelsen, W. F. Towne, W. H. Kirchner, and P. Kryger "The acoustic near field of a dancing honeybee", *J Comp Physiol* vol. 161, pp. 633-643, 1987
- [6] T. Watanabe, M. Kikuchi, D. Hatakeyama, T. Shiga, T. Yamamoto, H. Aonuma, M. Takahata, N. Suzuki, and E. Ito, "Gaseous neuromodulator-related genes expressed in the brain of honeybee *Apis mellifera*", *Dev. Neurobiol.*, in press, 2007

Constructive Approach to Interface Design by Modeling Human-Automation Interactions Based on Social Communication Model

Tetsuo Sawaragi, Yukio Horiguchi, Tadahiro Taniguchi and Hiroaki Nakanishi

Graduate School of Engineering, Kyoto University.

Abstract— For the purpose of designing a human-automation collaborative system, it is of great importance to clarify how a human gets to grasp the behaviors of the automation when he/she uses that. Many of the current advanced automation are apt to have multiple modes, whose complex transitions are not always transparent to a human user. We regard this mode-recognition problem as analogous to a problem on how a human can recognize the others, one of the key issues for clarifying a human ability of sociality. By introducing a technique of module learning, we implement a computational model of a human mode-recognition process, and the simulation results are discussed.

I. INTRODUCTION

Human and computer subsystems should be structured and designed to work in mutually cooperating ways guaranteeing a user's usability. For this purpose, progressive system redesigns are needed with respect to human computer interactions to increase system reliability and transparency by increasing human-system interactions and especially a human user's proactive participation. Such a *socially-centered view* on the human-machine system design regards a human and an automated agent as equivalent partners, and through their mixed-initiative interactions some novel relations of mutual dependency and reciprocity would emerge. Sharing the recognition on their common task between those partners is an essentially important issue, but the complexity of automation's behaviors embedded by the designer is preventing a human user from correctly grasping the working status and predicting the future behaviors of the automation. This is because the automation is apt to have multiple modes and their output behaviors shown to a human user are quite different according to its active mode. A human user has to learn what transitions among modes are embedded within the automation in order to grasp how the automation behaves and to adapt to that through experiencing the interactions with that. This is actually a process of acquiring an ability of *sociality*.

To many of the biological beings, complexities of the environments they encounter are quite varied depending upon what embodied interactions are allowed and upon the quality of coordination they need for their survival. For instance, the significance environment to insects are quite simple as compared to human, since it is genetically determined what external stimuli to perceive and how to react to that. On the other hand, more social primate beings have to recognize the other's intentions reflected within the

environment in order to make efficient cooperation with their partners; they learn a variety of powerful social rules which minimize interference and maximize their benefit.

In this report, we focus on how a biological being acquires such sociality through the interactions with the others as well as with the surrounding environment. A computational model of a process of recognizing others is build up based upon the findings obtained in the fields of social insects and of social neurology. The final goal of our work is to find out the fundamental design principles of artifacts that can socially behave and collaborate with a human.

In the followings, as collaborating task testbeds we introduce two tasks. One is a simple multi-agent task where two agents have to attain a common goals with their collaboration without any explicit communication but only through their enclosed proactive interpretive efforts on the change of the observed environment. The other is a more practical testbed of human-automation collaboration, where a human driver has to correctly recognize a working status of modes that are embedded within an automated vehicle.

II. SOCIALITY OF HUMAN-IN-THE-LOOP SYSTEMS

What distinguishes a human ability from other lower biological beings is that a human can build up structures by interacting with the unstructured. Through interactions with the surrounding environment he/she can selectively find some cues that are meaningful to their survivals and structurize them into some ordered internal constructs. Humans' social adaptability is to be able to process the others' behaviors acted upon them and to react to them appropriately. This is realized by adaptively rebuilding their internal constructs (i.e., representations) on their social environment as they accumulate the experiences. Wherein, a social environment is more complex and dynamical, thus less predictive as compared with a static physical environment due to a fact that some other living entities may commit into the change of their perceivable environment.

In a general multi-agent environment, an agent should adapt to the diversities of dynamics that are perceived as changes in physical properties of the task environment, from which an agent should be able to recognize a partner's status and shifts of intentions. Not only to recognize the shifts of the partner's intentions, a social agent should be able to explore how to collaborate with the partner's shifts of intentions adaptively. Herein, we do not assume any explicit communication such as verbal commands can be exchanged; they have to interpret the perceived physical cues and have

to infer and identify the invisible intentions of the other. None of such a common code table is shared among them as Shannon-Weaver’s classical communication model.

III. SITUATION-SENSITIVE REINFORCEMENT LEARNING FOR COLLABORATIVE TASK

To implement the above we developed a machine learning architecture called Situation-Sensitive Reinforcement Learning (SSRL) architecture that can flexibly switch among multiple Q-tables of reinforcement learning according to the identified dynamics of the task environment [3] (Fig.1). In addition, an internal goal exploring function is newly added to this SSRL that attempts to attributes an identified situation to one of its own internal goals that is inferred to be consistent with what the partner intends to behave. The details of the model are presented in the followings.

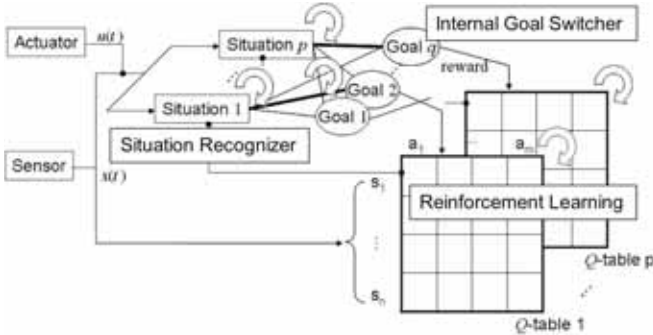


Fig.1 SSRL: Situation Sensitive Reinforcement Learning

Let us assume a couple of collaborative agents, Agent 1 and Agent 2, and their inputs, u_1 and u_2 , respectively, are to be acted upon their common task object, and its effect is observed as output y by Agent 1.

$$y = f(x, u_1, u_2^m) = f(x, u_1, u_2^m(x)) \quad (1)$$

$$= F^m(x, u_1) \quad (2)$$

Here a superscript m represents Agent 2’s input acted with a distinguishable intention m . Here we assume that Agent 1 cannot directly observe Agent 2’s input. In that case, the environment dynamics perceived by Agent 1 is shown as equation (2) showing that Agent 1 perceives a state x as Agent 2’s intention m is reflected upon the task object taking account of his own input u_1 . If we assume that the dynamics of the task object f is time-invariant, Agent 1 can indirectly recognize the shifts of Agent 2’s intention by perceiving the changes of the dynamics F . Thus, by recognizing this, Agent 1 can infer the shifts of Agent 2’s intentions.

Our model internally constructs a multiple functions as prediction models that prescribe how the different intentions are reflected on the change of Agent 1’s perceiving task object. When an agent encounters a situation, those multiple prediction models output their predictions based upon their functions, and from the estimates of the prediction errors, it can identify what is the most plausible situation it is encountering. In case all the prediction errors are not

negligible, the model recognize that it encounters a novel situation, and add a new prediction model to a repertoire of pre-existing models incrementally. This judgment is made based upon the statistical hypothesis testing [4].

With the above mechanism, an agent can get to notice the shifts of the partner’s intentions, but still have no means of behaving adaptively to that inferred intentions. For this purpose, an internal goal exploring function is newly added to SSRL that attempts to attributes an identified situation to one of its own internal goals that is inferred to be consistent with what the partner intends to behave. Here we notice that the intentions inferred by Agent 1 needs not identical to the ones Agent 2 actually intends. Agent 1 is not forming any symbolical representations on the partner’s intentions, but is only recognized as a situation “something different”. Then, Agent 1 attempts to signify this vague situation with its own symbols, which we call *internal goals*. An agent attempts to make up appropriate correspondences between the inferred situations and its internal goals by reinforcement learning. For each of the internal goals, an agent has learned appropriate behaving rules within the respective Q-tables. With this learning architecture, an agent can get to recognize the shifts of the partner’s intentions and to output the appropriate behaviors that are fitted to the partner’s intention.

As a testbed example, a simple truck-pushing task by a pair of agents is considered. They are agents called Leader and Follower, taking different roles to attain the common task goal of pushing a truck to a destination in collaborating with each other without any explicit communications. Leader in the front pulls a truck along its intending direction, while Follower in the rear supports Leader by pushing a truck. The direction of Follower’s pushing should be consistent with the one of Leader’s pulling. Wherein, each agent’s control rules were designed independently, so their collaboration fails initially, which is to be improved through their learning for collaboration.

At first, Leader itself has learned how to reach its intended destination. Being guided by that Leader, Follower has to learn how to collaborate with that, when Follower has to infer the intentions of Leader and behave appropriately without interfering Leader’s destination-reaching actions. Our proposing model is embedded in Follower, which learns how to collaborate with Leader recognizing its intentions from changes of dynamics that appear on a truck. After Follower learned the collaborative behavioral rules, another new task environment is provided to that pair of agents, where they have to attain their common goal in collaboration. At this time, the embodiment of Leader is changed from the one at the initial learning time, and it cannot control a truck as it intends because of the other agent’s (i.e., Follower’s) commitments. In spite of that, a pair of agents gets to improve their performance due to Follower’s collaborative learning ability.

The above organization of the two agents can be mapped onto a relation between a human and an automated assisting

tool such as a wearable power assist device. A human has to attain some task with an assist by the tool. However, commitment by an automated device may sometimes prevent a human from performing his/her task as he/she intends. In that case, an automated device has to be able to adapt its assisting strategies being sensitive to the inferred intentions of a human. Such adaptive device would be a good tool for a human in a sense that he could control a collaborative task performance without being aware of the tool's unexpected interferences (i.e., naturalistic enlargement of his bodily boundary) [5].

IV. CONSTRUCTIVE MODEL OF USER'S DEVELOPING MULTIPLE INTERNAL MODELS OF AUTOMATED SYSTEM

As mentioned in the above, introduction of some automated device does not always improve a human user's task performance, but it may sometimes interfere that. Especially, it is likely that so many functions are installed within a single advanced automated system, thus the design strategy for this requirement is to adopt different control *modes*. The complexity of control logics embedded within those multiple modes would make a human user bothered from a risk of mode-recognition errors; misunderstanding the status of the current active mode, a human user would make a wrong prediction on how the automated system behaves reacting to his/her operation and/or to the environmental changes. Modes are regarded as internal states of the automation system, among which an automation system dynamically transits, but are usually hidden to a user. In this sense, this mode-recognition process is containing a general aspect of *social intelligence* (i.e., how to recognize the others). In the followings of this section, we present a constructive approach to this by developing a computational model of human's mode recognition [6].

During a human uses an automated tool having multiple modes, he/she interacts with that, accumulates the experiences of bodily interactions, and then gets to acquire an internal model on how the tool behaves in each of the modes. Having acquired that, in facing with a behavior of the system, he/she attempts to match that with the model and recognize what mode is currently active. In a field of computational neuroscience and/or machine learning, an idea of module learning, and we attempt to model a human mode recognition process by extending that computational model [2]. Our model is built to represent two concurrent processes of the users. One is a process through which they develop multiple internal models corresponding to system's multiple control modes through interactions with their facing systems and with the external environments. The other is a process that the users recognize current mode by using prediction errors calculated by their developing internal models. First, experiments of observing human user's mode awareness using a driving simulator with ACC (adaptive cruise control) system embedded. Then, the simulation results using our proposing model are presented. Comparative analysis between those will suggest us what and how the model should be improved, thus we can investigate our understanding on how the human recognize

the others having multiple modes and switching them in a constructive fashion.

An automated system with multiple control modes embedded can be modeled as shown in the right of Fig.2. Individual mode is defined as a discrete subsystem that does transit from and to different modes, while each mode has different continuous input-output dynamics. Transitions are made either by a user's intentional operation or in automatically depending upon the status of the environment. A user of the above system may grasp its behaviors as shown in the left of Fig.2, where the dynamics and transition rules among the modes are not always identical with the right one. These two models are referred to as a *user model* and *machine model*, respectively. As mentioned in the above, users grasp the current active mode either by referring to his pre-existing knowledge on mode-transitions or to a display presented to them in the interface, but most of time they do that by referring to the *input-output relations*, i.e., the relationships between input operations by a user and observed responses in the environment where an operation by an automated system is reflected. Each mode is characterized as this input-output relation uniquely.

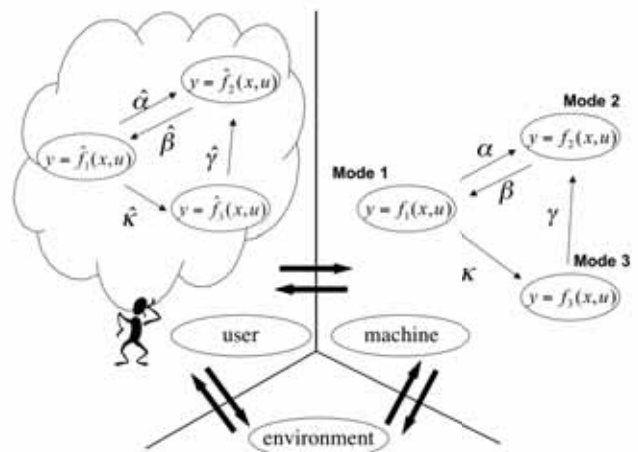


Fig.2 User model grasping actual machine states

We denote the dynamics embedded in each control mode as $y = f_m(x, u)$, where u , x and y represent a user's inputs, states of the environment, and responses observed in the next time step, respectively. For simplicity, all f 's are assumed linear, and superscripts m denote the m -th mode of the multiple modes. Dynamics in the user model are distinguished with $\hat{\cdot}$ attached.

We assume that a user acquires a user model by accumulating interactions with the target system whose dynamic responses are changed depending upon the hidden states (i.e., the active modes) of the automated system. To implement this process, we introduce an idea of *module learning*, and the mode acquisition process and the mode recognition process are done through the estimation of predicted errors as mentioned in the previous section.

At first, a series of experiments using a driving simulator are done and drivers' recognitions of the operating mode of ACC (Adaptive Cruise Control) while driving with it are examined. Within the ACC, dynamics of the machine model

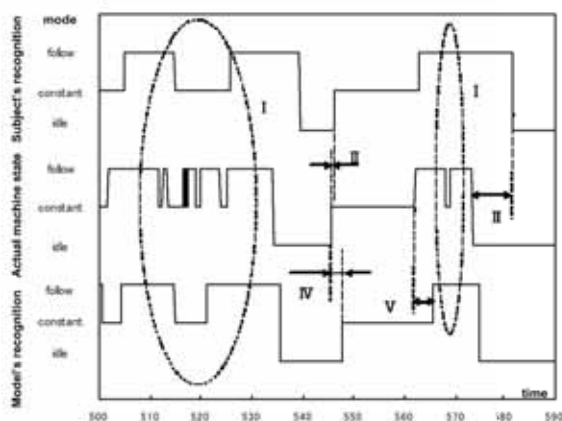


Fig.3 Recognized modes by a subject (top) and a proposed model (bottom) (actual modes are shown in the middle).

are installed. In these experiments, a number of mode-recognition errors are observed actually, so they are *error-prone* behaviors. Then, the same data of the driving situation with the above are input to our implemented user model and it is analyzed what mode the model recognizes and when the recognition is switched. One of the results is shown in Fig.3, and this shows that most of user's error-prone behaviors (encircled in the figure) is replayed by our model although they were not identical. The detailed analysis on how each mode of a user's model is acquired by the model is shown in Fig.4. This is an example of a mode of "idle" and shows the coefficients defining the recognized dynamics particular to this mode. Although the model initially has a rough definition of the mode, the model is improved further by accumulating the experiences of interactions (i.e., outputs approach to the true parameters of A). The spike-type errors show the timings when the mode transits to the other modes. Since our model attempts to interpret the new situation as a behaviors generated under this idle mode, the prediction errors are detected when a mode shifts. Being aware of these misrecognitions, learning continues excluding a latest part of the memory and its quality is recovered to the state before such transitions.

Our model mentioned in the above can predict the current mode state based upon the input-output relations, but does not learn any regularity on mode transitions, i.e., individual modes are learned independently. On the other hand, human mode recognition is partially attributed to such regularity; recognition of the current mode is mostly helped by observed transition events that bridges between the previous mode and the current mode. That is, a user has acquired knowledge on transitions among the multiple nodes. In order to implement this, the above model is extended to another compound computational model that consists of two layers. A role of the bottom layer is the same with the one of the previous model (i.e., to recognize the current mode), and the other upper layer deals with learning the transition events among modes as well as with predicting the following mode when the observations of the transition events are input. Those two layers are connected with each other via sharing the recognized status of current mode. We verified that this

extended model more correctly replays what a human user actually grasps as his/her internal model on the complex mode transitions embedded within the automated system. In this sense, our model can be regarded as a model of recognizing the others' hidden internal states.

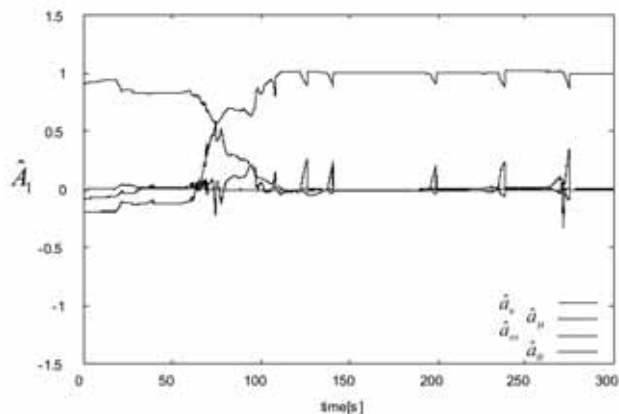


Fig.4 Learning of dynamics embedded in a mode "idle".

V. CONCLUSIONS

Major difference in sociality between insects and humans is an ability to recognize the others and to adapt to them by constructing their representations within them. It is not a simple pattern recognition problem, but is more close to an activity of *interpretation*; what is signified on the provided object is not solely determined by the properties of the objects but also depends upon the internal states of the *interpretant*. In this meaning this is a *semiotic* process. Our research subjects are now extended towards a constructive approach to recognizing biological motions from a viewpoint of *semiosis*.

REFERENCES

- [1] M. Ashikaga, T. Hiraguchi, M. Sakura, H. Aonuma and J. Ota: Modeling of adaptive behaviors in crockets, in Reprints of SICE 18th Symposium on Autonomous Distributed Systems, Fukui, pp.189–194, 2006. (in Japanese).
- [2] K. Doya, et al. Multiple model-based reinforcement learning. *Neural Computation*, Vol. 14, pp. 1347–1369, 2000.
- [3] T. Taniguchi, T. Sawaragi and K. Ogawa: Self-enclosed Estimation of Other' s Intention based on the Situation-Sensitive Reinforcement Learning, 49th Jido Seigyo Rengo Koenaki, Kobe, in CD-ROM, 2006. (in Japanese).
- [4] T. Taniguchi and T. Sawaragi: Incremental Acquisition of Nonlinear Predictors based on Differentiation of Schemata, in Preprints of 15th JNNS, Kagoshima, pp.194–195, 2005 (in Japanese)
- [5] J. Hakamagi, Y. Horiguchi and T. Sawaragi: Introducing Perception-Action Coordination Structure in Human Locomotion to Design of Mobile Robot Teleoperation System, in Reprints of SICE 19th Symposium on Autonomous Distributed Systems, Tokyo, pp. 245-250, 2007. (in Japanese)
- [6] Y. Tanaka, T. Taniguchi, Y. Horiguchi, H. Nakanishi and T. Sawaragi: Constructive Approach to User' s Developing Multiple Internal Models of an Automated System, in Reprints of SICE 19th Symposium on Autonomous Distributed Systems, Tokyo, pp. pp.97–102, 2007. (in Japanese)
- [7] Y. Horiguchi, R. Fukuju, T. Sawaragi: Effects of Similarity in Response Behaviors of Automated Mechanical System on User's Awareness of Operation Modes, in Reprints of HIS2006, pp.109-114, 2006. (in Japanese).

Regulatory dynamics of colony-level adaptive behavior in social insects and its underlying individual-level interaction

Kazuki TSUJI (University of the Ryukyus) , Ryohei YAMAOKA (Kyoto Institute of Technology) ,
Ken SUGAWARA (Tohoku Gakuin University)

Summary: We investigated self-regulatory dynamics of adaptive behavior in social insect colonies. We focused on intra-nest density regulation and colony size recognition. We experimentally showed that both regulations are mediated by physical contacts and movements of individual ants. We also screened chemical substances that bear the key information in the hypothetical regulatory dynamics. We are going to construct mathematical models that can simulate the regulatory dynamics. As the first step we constructed a model for a single worker isolated from social interaction.

Colonies of social insects can behave adaptively. A central idea of social physiology is decentralized control, that is colony-level adaptive functions emerge, even though individual colony members respond to local information that they encounter, according to simple rules. Many studies of social physiology so far have extensively studied division of labor and foraging. Instead, in this study we focus on intra-nest density regulation and colony size recognition. Ants seem to control individual density or the average inter-individual distance within the nest, because when they are kept in a large artificial nest they aggregate, whereas when kept in a small nest they enlarge the nest chamber. An ant colony changes its behavior depending on the number of workers. For example, in small colonies workers are usually timid, whereas in large colonies workers behave more aggressively. For another example an ant colony switches the production of castes related to colony size; sexual castes (queens and males) are usually produced when the colony size exceeds a given threshold. However, regulatory mechanisms of these two phenomena, though

they seem to be general in social insects, are largely unknown. Living in the dark, it is unlikely for individual earth-bound ants directly to obtain global information on colony size and intranest individual density. We assumed that there could be a self-organized and decentralized feedback mechanism mediated by physical contacts between individual colony members. This study consists of three parts. First, we will experimentally show the presence of such regulatory mechanisms. Second, we will identify chemical substances that bear the key information in the hypothetical regulatory dynamics. Last, we will construct mathematical models that can simulate the regulatory dynamics. These models will be also tested by real data. The goal of this study is in the biological sense to understand a general mechanism that regulates animal societies, and in technological sense to accumulate basic information that will be used to develop a control program for decentralized controlled robots.

Density control

We used *Diacamma* sp. from Japan for most experiments. This is the only *Diacamma* species found in Japan. Recently, as a new model organism, its biology has been extensively studied. We observed behavior of individual workers that were placed under different densities: being the size of container (the nest size) constant we varied the number of workers confined in the nest. Almost all workers walk around for a while after placed in an artificial nest, as time passes workers gradually began to stop moving and finally reach a stationary phase where constant but relatively low proportions of workers are moving. In the stationary phase the inter-individual spacing has already been completed. When the density was close to the natural one, workers most quickly became the stationary phase after installed in the nest. When density was higher or lower than this “natural” density, the proportion of workers that were moving fell more slowly. This suggests that ants can sense inter-nest individual density, and when it is inadequate they are more likely to move. When ants are placed under extremely high density, the proportion of workers that were moving after reaching the stationary phase was unusually low. This might be an artifact due to a habituation to unusually high density.

Recognition of the number of workers

The gamergate (functional queen) of *Diacamma* sp. transfers information of her presence to nestmate workers through direct physical contacts (Tsuji et al. 1999). The gamergate regularly walk around in the nest touching workers with her antennae. We defined this active information transmission behavior as patrol. It is predicted that in a large colony the gamergate has to invest more efforts in patrol. In fact, our detailed

observation revealed that as colony grows the gamergate increased the number of patrol bouts per unit time, the proportion of time spent on patrol and the mean duration of patrol. This suggests that gamergates can adaptively change her behavior, as if they can recognize the colony size. But how they can do so? The frequency of the gamergate’s contact per worker per time was almost constant regardless of the colony size, whereas there were more workers that had by chance no contact for a long time in larger colonies. Simultaneously, the frequency of aggressive dominance interaction and that of immobilization (a worker policing behavior directed to ovary-developed workers) has increased as the colony size increased. These behaviors are characteristics of orphaned workers. From these results we set out a hypothetical self-organized feedback system that can control the adaptive shift of patrolling behavior. The hypothesis assumes that the gamergate invests more efforts in patrolling, when she encounters physiologically “orphaned” workers during patrolling. We conducted an experiment that varied the proportion of physiologically orphaned workers under a constant colony size. The gamergates actually respond to the presence of orphaned workers and prolonged the average patrol duration, suggesting that the hypothesis is quantitatively correct. As the next step we are currently developing mathematical model that can simulate the putative feedback mechanism.

Information of gamergate presence

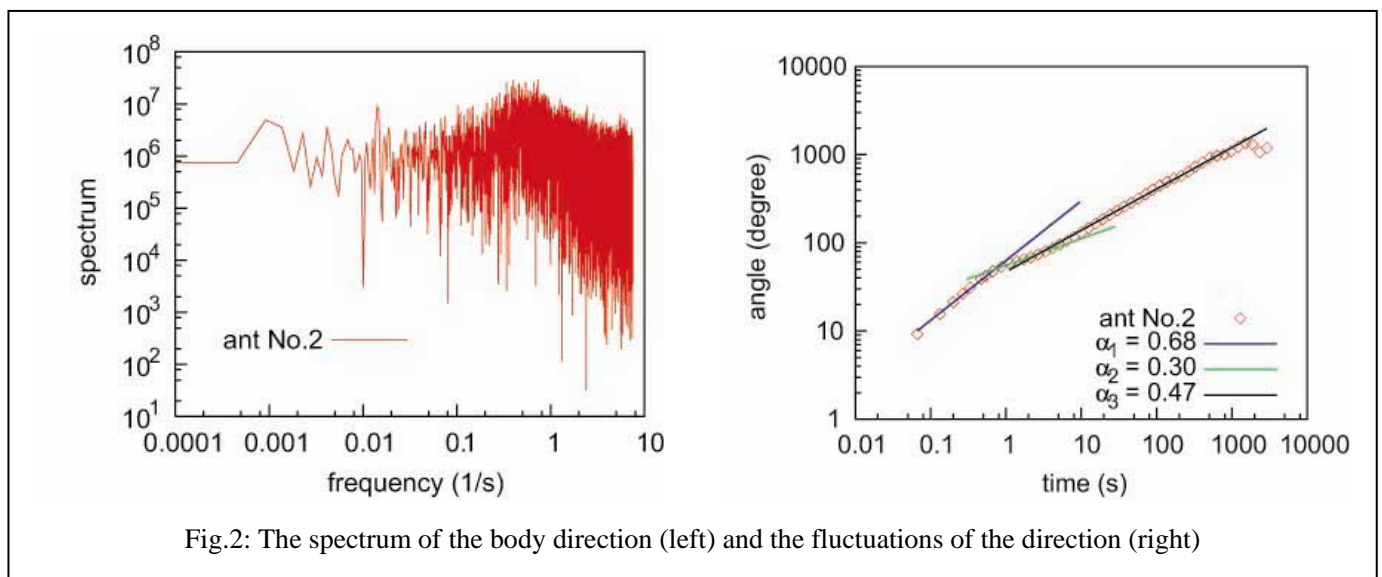
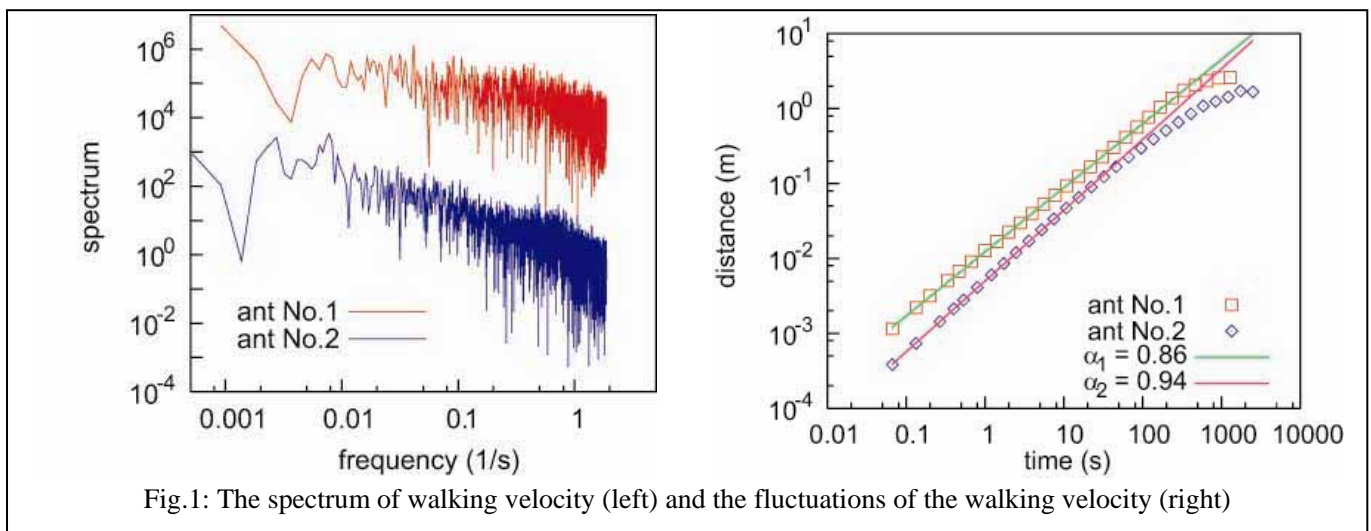
Queens of social insects are considered to produce a queen substance that inhibits self-reproduction of workers. However, in ants such a queen substance has been unidentified yet. Recently, cuticular hydrocarbons (CHCs) are suspected to be the queen substance. In *Diacamma* sp.

from Japan queen information is transferred to workers only through direct contact, suggesting that hardly volatile chemical can bear the information. Furthermore, we found CHC components specific to reproductively active females like gamergates and dominant orphan workers in *Diacamma* sp. Our careful bioassay indicates that among gamergate extracts only CHCs inhibit dominance behavior of orphan workers. This is the first empirical demonstration for the CHCs-queen substance hypothesis. Currently, we are undertaking more sophisticated bioassay separating gamergate's CHCs into long-chained gamergate specific components and short-chained non-specific components.

Movement of individual worker and its fluctuation

Underlying feedback mechanisms mediated by individual movement were suggested both for density regulation and colony size recognition. Before modeling we addressed the question that what characterizes individual ant's movements. As the first step we analyze a single ant's movement without social interaction. Particularly, we focused on fluctuation in movement of individual ant.

It is well known that various fluctuations can be observed in nature from micro scale to macro scales. The fluctuations can be also observed in biological system. An important point is that such fluctuations are not



characterized as white noise, but has a time correlation. In this research, we focused on walk of a single ant and measured the fluctuation of this walk. We found the fluctuations of travel distance and the variance of ant-body direction obey power laws on the time interval. In particular, there was a long-term correlation in the velocity dispersion. On the other hand, there was no long-term correlation longer than 1 sec in the variance of body direction. Based on these results, we also proposed a stochastic model that simulates the walking behavior of an ant, and discussed the foraging behavior of ants.

Descriptions of our experiment for the analysis of ant walk are as follows. We recorded the behavior of a single ant under the environment without a nest and food, and measured the time-series of increments of velocity and body direction by image processing.

(1) Time correlation of walking velocity

From the spectrum of walking velocity, we can see a long-term correlation in the velocity dispersion as shown in Fig.1(left). We also found the fluctuation is in proportion to the time scale ($\propto t^{-\alpha}$), where $\alpha > 0.5$ (Fig.1(right)).

(2) Time correlation of body direction

We also measured the spectrum of body direction. From this result, we found there is a short-term correlation (less than 1 sec), but no long-term correlation here.

Now we are planning/executing the following topics.

- (a) Analysis of the boundary effect.
- (b) Behavioral analysis of the gait of *Diacamma*, especially focusing on the patrol behavior in the nest.
- (c) Analysis of multi-body dynamics of ants behaviors.

Reference

Tsuji, K., Egashira, K., Hölldober, B. (1999) Regulation of worker reproduction by direct physical contact in the ant *Diacamma* sp. from Japan. *Animal Behaviour* 58 (2): 337-343.

Construction of Quantitative Neural Model for Discrimination of Bird Songs in Zebra Finch

Kotaro Oka, Akira Fujimura and Masafumi Hagiwara

Abstract— Neural mechanisms for discrimination and evaluation of conspecific bird songs are important for selecting the future mate for female birds. Neural networks for generation of bird song has been investigated and the computational models are constructed. However, no computational model is presented in female brains. In this study, we focus on the song discrimination mechanisms in female *Zebra finches*. To present the quantitative model, catFISH technique is used for visualizing the functional neural population responding to male songs. These neurons are located in caudal medial mesopallium (CMM) and also hippocampal formation (HF) regions. This finding is useful for understanding the neural coding in female brains.

I. INTRODUCTION

Zebra finches communicate with their songs. Male finches have several kinds of their own songs and female finches choose the male for mating by his song. For understanding the song communication, information processing in the female brains are crucial. However, the neural network for the information processing in female brains has been poorly understood.

On the contrary, how male finches acquire and vocalize their own songs has been investigated by the combination of anatomical, electrophysiological, and molecular biological methods. These investigations reveal the refined neural networks in the male brains (Fig.1) [1].

Recently, neural network mechanism for learning of the song is presented (Fig.2) [2,3]. In this model, the song is divided into notes, and each note is coded as the synchronized firing of a population of neurons. These neurons are assumed to be localized at hyperstriatum ventrale pars caudal (HVC) and robust nucleus of the acropallium (RA). Populations of neurons are tuned by vocalization of their own song via auditory pathways. One of the important presumptions in this learning model is the presence of neural population in the male brain. Unfortunately, no such model and also experimental findings have been reported in the female brains. We, therefore, need to know not only neural architectures but

also the information coding for the discrimination of male songs in female brains. What kinds of approaches are effective for demonstrating the neural mechanism in female brains?

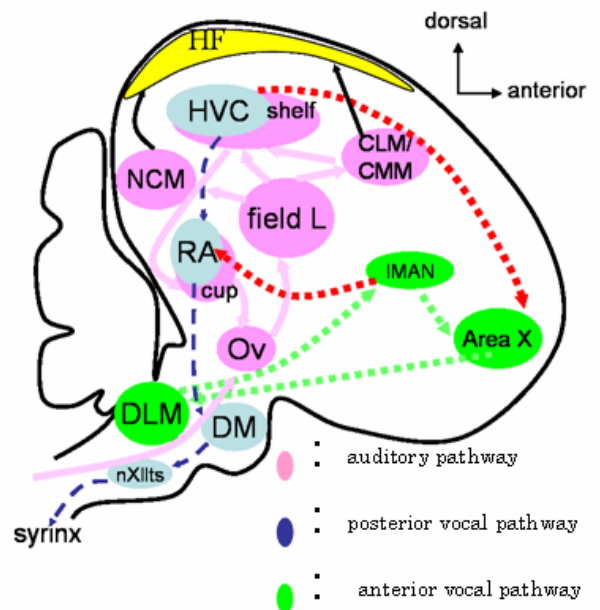


Fig. 1 Brain architecture of male zebra finch

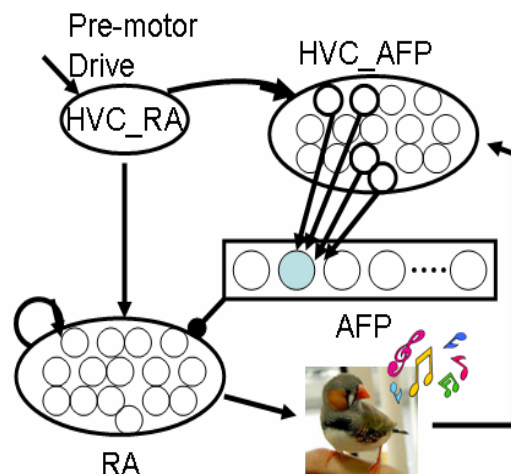


Fig. 2 Neural network model for song learning in male zebra finch.

HVC: Hyperstriatum ventrale pars cauda; RA: Robust nucleus of the acropallium; AFP: Anterior forebrain pathway

Kotaro Oka is with Department of Biosciences and Informatics, Keio University, 3-14-1 Hiyoshi, Kohoku-ku, Yokohama, Kanagawa 223-8522, Japan (phone: 045-566-1728; fax: 045-564-5095; e-mail: oka@bio.keio.ac.jp).

Akira Fujimura is with Department of Biosciences and Informatics, Keio University, 3-14-1 Hiyoshi, Kohoku-ku, Yokohama, Kanagawa 223-8522, Japan.

Masafumi Hagiwara is with Department of Information Engineering, Keio University, 3-14-1 Hiyoshi, Kohoku-ku, Yokohama, Kanagawa 223-8522, Japan

For the first approaches of model construction in female brains, we attempt to find responding regions for song discrimination. Neural activity in the whole brain is studied with several techniques from the classical electrophysiology with multiple electrodes and sophisticated imaging methods including membrane potential imaging, Ca imaging and also functional MRI. These methods have merits and demerits for applying to bird brains. Several imaging techniques are not appropriate because the functional regions are located under in-depth nuclei, and it is very difficult to visualize for conventional optical imaging technique. Another method, including functional MRI, has insufficient spatial resolutions for visualizing single neurons. We, therefore, lay aside the real time imaging, and used a recent molecular biological approach, catFISH (cellular compartment analysis of temporal activity by fluorescent *in situ* hybridization).

II. CATFISH

We used *Arc* (activity-regulated cytoskeletal-associated protein, one of immediate early genes or IEGs) catFISH (cellular compartment analysis of temporal activity by fluorescence *in situ* hybridization). This technique can visualize neural ensembles responded to two stimulations. Worley's group developed this technique for the study of rat hippocampus [4]. Olfactory system of mouse was also studied by this technique [5]. The key point of this technique is time-dependent subcellular localization of *Arc* mRNA. On induction, *Arc* mRNA can be detected first only in the nucleus and later only in the cytoplasm. This property is characteristic for *Arc* mRNA, not like other IEGs used for neural activity marker such as *c-fos* and *zenk* mRNA. Using this property, catFISH is performed by providing two stimulations. Second stimulation provided after appropriate time interval from first stimulation, neurons which respond the first stimulation have *Arc* mRNA in the cytoplasm, which respond the second stimulation have *Arc* mRNA in the nucleus. Thus we can discriminate which neurons respond the first or/and second stimulation. In this study, we used two songs (song A and B) as auditory stimulations (Fig.3).

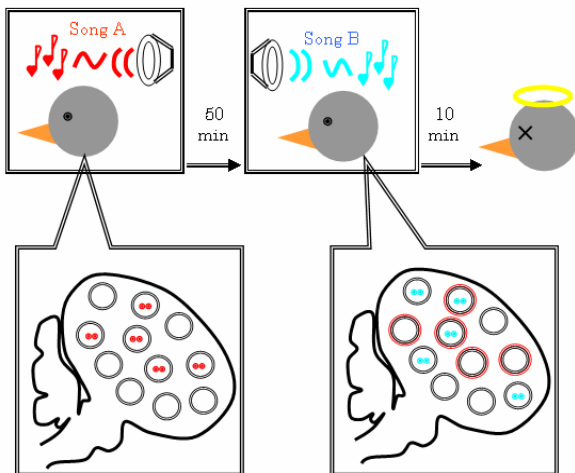


Fig. 3 Neural activity detection by catFISH
After Song A presentation, *Arc* mRNA signals are

localized at the transcription initiation sites in nuclei of responded neurons. During 50 min, the signals are translocated from nucleus to cytoplasm. After the translocation, Song B stimulus induces *Arc* mRNA in nuclei in responded cells again. After the application of 2nd song (in this time, Song B), four types of neurons will be observed; no response neurons, neurons with signals in nuclei (Song B responding neurons), neurons with signals in cytoplasm (Song A responding neurons), and neurons with signals in both nuclei and cytoplasm (Song A & B responding neurons). We, therefore, detect the populations of neurons for responding to two songs.

III. EXPERIMENTAL METHOD

A. Preparation of *Arc* mRNA probe

We synthesized cDNAs from a female zebra finch brain and isolated a partial cds of *Arc* protein mRNA from the cDNAs. For the isolation, we performed nested PCR. Two pairs of PCR primers (first pair, forward: GAGTCCATGGGAGGCAAATA; reverse: TCCACCCACCTGCTTTAAGT, second pair, forward: GGAATTCCTGCCCTGGGGAGCAGGGCA; reverse: CCGCTCGAGATTCCTCCAAGTGGCTCAAG) were designed based on a partial *Arc* sequence (GenBank accession no. AY792623) by using the NCBI ORF finder program (<http://www.ncbi.nlm.nih.gov/gorf/gorf.html>) and Primer 3 (<http://frodo.wi.mit.edu/>). The second pair was added restriction enzyme sites (forward: EcoR I, reverse: Xho I) for inserting into plasmids. PCR reactions were performed with an annealing temperature of 55 C. The amplified product was extracted from the agarose gel using the NucleoSpin[®] Extract II (Macherey Nagel Co.), inserted into pBluescript II SK+ (Toyobo Co.) and used to transform competent cell (Toyobo Co.). Plasmid DNA was extracted using QuickGENE Plasmid kit S (Fuji Film Co.) and linearized with the appropriate restriction enzymes. Sense and antisense digoxigenin-labeled RNA probes were synthesized using T3/T7 primers with DIG labeling mix, linear plasmid DNA, DTT, RNase inhibitor and RNA polymerase.

B. Brain preparation

A female zebra finch is isolated in a soundproof booth for 12 h before the experiment. After present the sound stimulation, the bird was decapitated immediately, and the whole brain was isolated. The isolated brain was embedded in Tissue-tek under -80 C and preserved. Then, the brain was sectioned with 10~12 μ m in thickness, and used for catFISH.

IV. RESULTS

A. Mobilization of *Arc* mRNA in brain

After 10, 30 and 60 min after on set of song stimulation, the localization of *Arc* mRNA was investigated in female brains of zebra finches. The strong signals were observed in the

region of caudal medial mesopallium (CMM). CMM has been known as the region for sound discrimination between bird songs and others, and some neurons in CMM respond to the conspecific bird songs. The *Arc* mRNA signals are located at the specific region of the nuclei after 10 min of the song stimulation (Fig. 4). The specific region is the transcription initiation sites. Then the signal was observed at the cytoplasm around nuclei, and after 60 min, the signal was observed out of the cell bodies as fluorescent spots. This spot may be transported mRNA to the peripheral regions of neurons. These observations confirm us that the *Arc* mRNA is specifically transcribed in specific neurons and transported peripherals as a function of time. This finding also indicates the possibility of catFISH experiments with female brains for visualizing the different populations of neurons with responding to the different song stimulation. And also 60 min is optimal for the interval for song presentation.

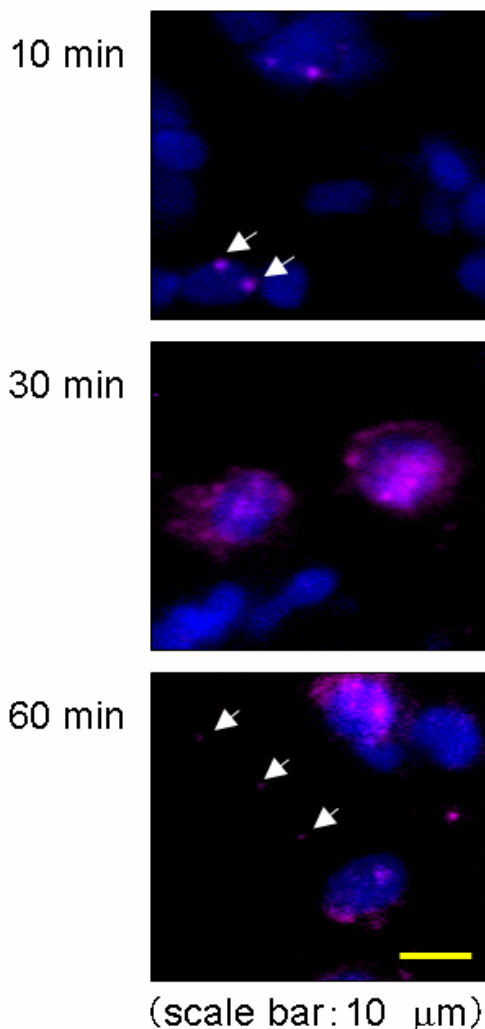


Fig. 4 Translocation of *Arc* mRNA in neurons in CMM region.

After application of song, *Arc* mRNA is transcribed at the transcription sites in nuclei (arrows), and translocated from

the nuclei to the cytoplasm (arrow heads) in 60 min.

B. Responding regions in the brain

We investigated the expression pattern of *Arc* mRNA in female brains, especially hyperpallium, brain stem, cerebellum, hippocampal formation (HF) and caudal medial nidopallium (NCM). The signals from these regions are quite different (Figs. 5 and 6). In brain stem and cerebellum, no signals were observed. The brain stem and cerebellum contribute to the generation of motor patterns of songs, but no relation has been reported for hearing and recognition of bird songs. No responses in these regions are, therefore, reasonable. One of the interesting findings is the responses observed in HF. Although no relationship to the auditory systems and HF has been reported in bird brains, hippocampus can be used for the spatial recognition and memory in several bird species, especially that hide the food during winter season.

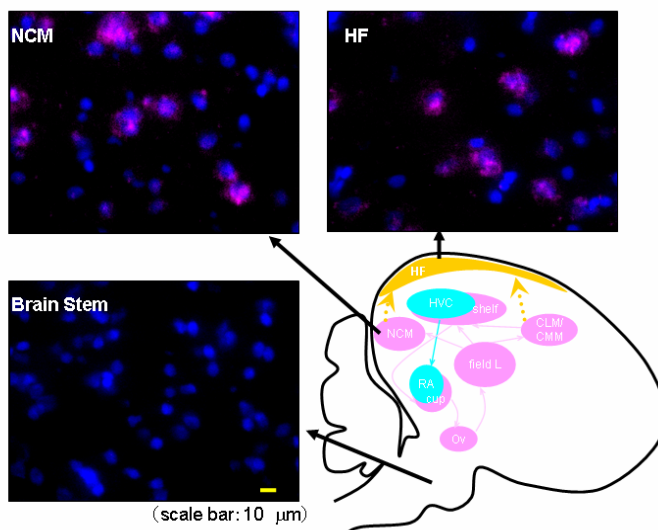


Fig. 5 Regions of *Arc* mRNA expression by song.

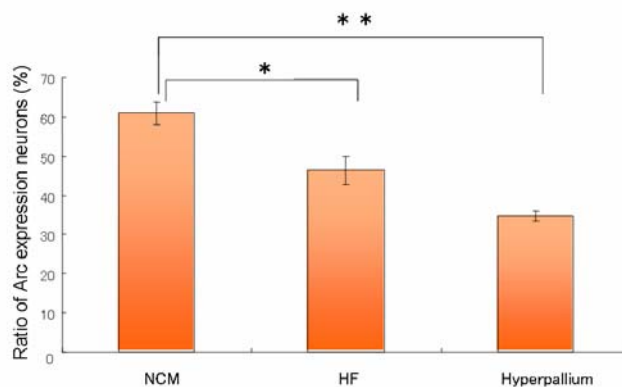


Fig. 6 Different expression levels of *Arc* mRNA

C. Responses to two different songs

Two kinds of male song are presented to the female finches with 50 min interval. After the song presentation, the numbers of cell with *Arc* mRNA signals were counted in CMM and HF (Table 1). Sequential presentation of Song A and Song B induces different populations of neurons in CMM and HF. In signal-detected neurons, about 60% of cells responded to Song A and also Song B. Only 20% of neurons responded to either song. This ratio is almost same in HF. The birds with the same song presented twice showed relative high ratio (73%) of cells with nuclei and cytoplasmic signals. We have to investigate further the meaning of the information coding in CMM and also HF.

Table 1 *Arc* mRNA signals in female zebra finches from different or same song presentation

| Combination of Songs | Brain Region | No. of <i>Arc</i> expression Cells (): % | | | |
|----------------------|--------------|---|--------------|---------|-------|
| | | cyto | nucle & cyto | nucleus | Total |
| (A→B) | CMM | 27 (26) | 59 (56) | 19 (18) | 105 |
| (A→B) | | 22 (24) | 54 (58) | 17 (18) | 93 |
| (A→A) | | 18 (16) | 83 (73) | 12 (11) | 113 |
| (A→B) | HF | 17 (18) | 56 (60) | 20 (22) | 93 |
| (A→B) | | 16 (19) | 51 (60) | 18 (21) | 85 |
| (A→A) | | 10 (16) | 45 (73) | 7 (11) | 62 |

V. DISCUSSION

We found that catFISH with *Arc* mRNA is a feasible technique for detecting the activity of neurons in the brain of female zebra finch. The signal of *Arc* mRNA is observed in the several regions of the brain, especially CMM and HF. This finding indicates a possibility that these regions are used for the information processing of the discrimination of songs.

One of the unlooked-for results is the response in HF because no relation has been reported in auditory systems and HF. We need to show the real neural connections between auditory systems and HF using, for example, retrograde tracing of neurons with dyes. Our finding will become the first step to reveal a new function of HF.

In previous study, CMM is reported to discriminate the conspecific bird songs from the other sounds in male brains [6]. This finding is suitable for our result, and we can suggest that CMM is a first information processing region for discrimination of conspecific bird songs in also female auditory system. Because the population of neurons is responded to the specific bird song, we need a strategy for analyzing the response on CMM. As a future work, the metrics for evaluating the distance or similarity/dissimilarity between two bird songs will be required. Then, we can compare the informational distance and biological coding

distance in information processing of the female finch brains. Carefully prepared experiments will contribute to construct the quantitative model of song discrimination in zebra finches.

VI. CONCLUSION

In this report, we illustrate that catFISH methods with *Arc* mRNA is effective for visualizing the populations of neurons which respond to the specific bird songs. Using this method, we succeed to find the candidates of female brain regions, CMM and HF, in charge of discrimination bird songs. This finding promotes the investigation of neural network analysis and also contributes to construction of quantitative neural models for discrimination of bird songs.

ACKNOWLEDGMENT

We thank Dr. Kazuhiro Wada in Duke University Medical Center, Department of Neurobiology for giving us his FISH protocol. We also thank Dr. Koji Hotta for his helpful suggestion and discussion of molecular biological experiments.

REFERENCES

- [1] Behavioral Neurobiology of birdsong. Annals of The New York Academy of Sciences, vol. 1016, 2004.
- [2] TD. Troyer and A. Doupe, An associational model of birdsong sensorimotor learning I. Efference copy and the learning of song syllables, *J Neurophysiol* 84: 1204–1223, 2000.
- [3] TD. Troyer and A. Doupe, An associational model of birdsong sensorimotor learning II. Temporal Hierarchies and the Learning of Song Sequence, *J Neurophysiol* 84: 1224–1239, 2000.
- [4] JF. Guzowski, BL. McNaughton, CA. Barnes and PF. Worley, Environmental-specific expression of the immediate-early gene *Arc* in hippocampal neuronal ensembles, *Nature Neurosci.* 2, 1120-1124, 1999.
- [5] Z. Zou and LB. Buck, Combinatorial Effects of Odorant Mixes in Olfactory Cortex, *Science*, 311, 1477-1481, 2006.
- [6] TQ. Genter and D. Margoliash, Neuronal populations and single cells representing learned auditory objects, *Nature*, 424, 669-674, 2003.

**Social and cognitive investigation on the neural mechanism of
mind understanding and adaptive behavior
– How do people understand other’s gaze?**

Motoichiro Kato*1, Takaki Maeda*1, Mika Hayashi*1, Mihoko Otake*2

*1 Department of Neuropsychiatry Keio University School of Medicine

*2 The University of Tokyo

Introduction

Gaze understanding and interaction are essential in making humans the uniquely social beings that we are. Its cognition is one of the most primitive of a variety of biological motions, since the motor intention of others can be inferred from their gaze. There are even suggestions for the innateness of gaze cognition, in that newborns show a preference for faces with eyes open versus eyes closed, and that infants as early as 10 weeks of age follow the gaze of others. The behavior of humans toward gaze has recently been enthusiastically studied by applying a spatial cueing paradigm first introduced by Posner (1980)¹⁾, and renewed by Kingstone and colleagues²⁾. In their elegant experiments, central schematic gaze is used as a cue to orient attention in that direction. Normally, subjects shift attention in the direction indicated by the cue gaze, which is reflected as faster reaction times (RTs) in detecting targets presented congruently to the gaze direction, opposed to incongruently presented targets (‘gaze effect’). The tremendousness of the impact that gaze displays on attention is easily imagined when subjects are explicitly instructed to attend opposite to gaze direction in counter-predictive conditions, but simply just cannot, at shorter (300 ms) cue-target intervals. It takes much longer intervals, in this case 700 ms, to strategically inhibit this automatic orientation triggered by gaze direction. An interesting non-biological counterpart to gaze is an arrow sign, which has a directional property just like gaze, but no biological significance. When arrows are used as cues in the same experimental paradigm, normal subjects behave more or less in the same manner as to gaze: faster reaction when targets appear congruent to arrows, slower when incongruent (‘arrow effect’). In this paper, we describe the results of three neuropsychological experiments in which the Kingstone’s paradigm was given to STS patient, amygdala damaged patients and schizophrenics.

Superior temporal sulcus (STS) and Gaze

1 STS

The brain region that is implicated in gaze processing, the

superior temporal sulcus (STS), has repeatedly been activated when viewing gaze in the normal brain. This same region has recently been reported to be smaller in two patient groups that are well-documented for the loss of, or for the lack in acquirement of social abilities, namely schizophrenia and autism, who are without exception impaired in gaze interaction. We have also presented a case, M.J., in a recent report, with a circumscribed lesion in the right superior temporal gyrus (STG) due to a cerebrovascular accident, who manifested a puzzling difficulty in obtaining eye-contact³⁾. As the STG comprises a part of the STS, we investigated her ability in processing gaze in this previous report. Indeed, M.J. demonstrated a unique impairment in discriminating gaze direction, which is the first neuropsychological evidence that establishes the right STS as a gaze processor, so often implicated in animals and human neuroimaging studies⁴⁾.

2 Subjects

The case subject, M.J., is a 60-year-old dextral female with a circumscribed lesion in the right STG due to a cerebral hemorrhage 5 years ago (Fig. 1).



Fig.1. MRI scan of M.J.’s lesion. A rare lesion almost completely circumscribed to the entire right STG, which is indicated by the arrow, is shown in a sagittal slice.

3 Method

The experiment was controlled by Superlab software, and the stimuli were presented on a 14 in. computer monitor. There were two blocks to the experiment: the first block used arrow direction as the cue, and the second block used schematic faces with gaze direction as the cue. The cues were black line drawings as illustrated in Fig. 2. The cue was

presented for either 100, 300 or 700 ms randomly (stimulus onset asynchrony; SOA), after which a target, X, subtending 0.6°, appeared either to the right or left of the cue, 7.1° from the central circle. There were two cue types (arrows and gaze), each in a separate block. The order of the blocks remained fixed among subjects. Within each block, cue-target SOAs (100, 300, 700 ms), cue-target relations (congruent, incongruent, neutral), and target locations (right, left) were randomly selected with equal probability to make up a non-predictive, spatially-cued, target detection test. Subjects were instructed to maintain fixation throughout each trial, and upon target detection, to press the space bar on the keyboard with their dominant index finger.

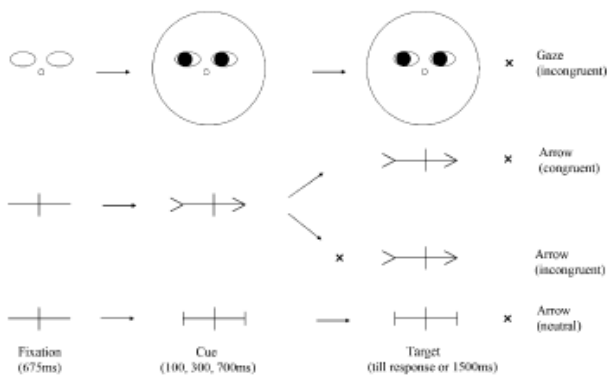


Fig.2. Illustration of the trial sequence in the experiment. A fixation display was presented for 675 ms, followed by a cue display which was either gaze or arrow direction. The cue was displayed for either 100, 300, or 700 ms, then a target was presented, either to the right or left of the cue, and irrespective of cue direction.

4 Results

Mean RTs as a function of congruency and SOA are shown for each cue type in Fig. 3.

ANOVAs were then conducted for M.J. and the control group separately, with cue type (arrows, gaze), cue-target congruency (congruent, incongruent, neutral) and SOA (100, 300 and 700 ms) as the within-subject variables. For the control group, the main effect of cue type, congruency and SOA were all highly significant, but none of the interactions were significant. On the other hand, M.J. demonstrated significant main effect of SOA, but the main effects of cue type nor congruency reached significance. Importantly, there was a significant interaction of congruency \times cue type. Such interaction did not exist for the control group, indicating that M.J. differs from the control group in that cue type modifies congruency effect.

5 Discussion

In this experiment, we have first confirmed that normal

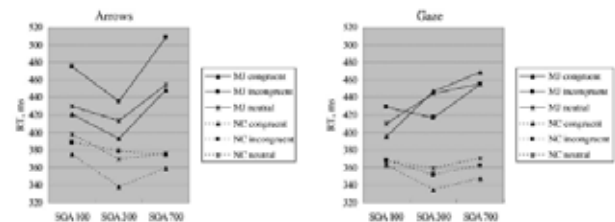


Fig.3. Results of the experiment. The mean RTs of M.J. (line) and normal controls (NC; dotted lines) for each cue type, as a function of cue-target congruency and SOA length. (Note that the results for M.J. include right target trials only.)

subjects demonstrate faster detection of targets when cued by central gaze or arrows that are directionally congruent with target location, opposed to incongruent or neutral cues, as have been previously reported in a number of studies. This facilitation of RTs in congruent conditions might be termed as 'gaze (or arrow) effect', and reflects the significance of such signals in orienting the viewer's attention. In striking contrast, M.J., whose right STG is nearly completely damaged (and thus, right half of whose STS is damaged), has been shown to demonstrate no such gaze effect whatsoever, in the face of a quite normal arrow effect. Her error rates show that she understood the instructions thoroughly, and was attentive throughout the entire experiment. M.J.'s results can be summarized as a dissociative ability in utilizing directional information from biological (gaze) versus non-biological (arrows) signals to orient her attention: impaired for gaze but intact for arrows.

Amygdala and Gaze

1 amygdala function

The amygdala has captured much interest for its intriguing function in processing the emotional valence of a stimulus, and modulating perception, behavior, and memory based on such valence. In the growing field of social cognition, a rather specific role of the amygdala in recognizing fearful faces has been repeatedly demonstrated in both neuropsychological⁵⁾ and neurofunctional⁶⁾ studies. More specifically, the importance of the eye region in fearful faces has been emphasized through functional neuroimaging studies where fearful eyes and even fearful eye-whites have been shown to be sufficient in activating the amygdala. Recently, a further role of the amygdala has been identified in a bilateral amygdala-damaged case, SM, who failed to make gaze fixations on the critical feature of faces, that is, the eyes, thereby hampering her ability to decipher emotion expressed through faces⁷⁾. The finding from this case thus indicates that the amygdala does not merely process incoming emotional stimulus but actually participates in seeking for relevant

stimulus from the environment, and allocating attention toward it. Indeed, a number of functional neuroimaging studies have demonstrated that aversive faces that escape conscious awareness, as when unattended to due to competing stimuli, when subliminally presented, or even when unperceived due to blindsight, are nonetheless captured by the amygdala as seen in its activation. However, to date, few neuropsychological investigations have addressed the impact of amygdala lesion on attention. The outstanding question that we have set out to address in this report is whether amygdala lesion affects attentional orienting triggered by relevant cues, and if so, whether there is any distinction between social and nonsocial cues. Here, we have tested 5 subjects with unilateral amygdala lesions in spatial cueing tasks employing gaze and arrow cues⁸.

2 Subjects and Method

Five subjects with unilateral amygdala lesion (right, 2; left, 3) participated in the study. Magnetic resonance imaging (MRI) slices depicting the amygdala lesion are presented for each subject in Figure 1. We used the same Kingstone's paradigm as in case of STS patient.

3 Results

The mean RTs as a function of congruency and SOA are shown for each cue-type, for each group in Figure 3. Raw RTs were then submitted to ANOVA with a between subject variable of group (amygdala, normal), and within-subject variables of cue-type (Arrows, Eyes, Faces), cue-target congruency (congruent, incongruent, neutral), and SOA (100, 300 and 700 ms). In sum, unilateral amygdala-damaged subjects demonstrated a distinctive difference from the normal subjects in that their response is differentially facilitated by congruent arrow cues but not by congruent gaze cues.

4 Discussions

In this study, we have demonstrated in a group of unilateral amygdala-damaged subjects, a robust deficit in attentional orienting triggered by gaze direction, in the face of a relatively normal orienting to arrow direction. This is evidence for the selective role that the amygdala plays in detecting and analyzing significant social stimuli, and orienting attention accordingly. Such function, when damaged, might underpin many of the intriguing impairments identified in a number of amygdala damaged subjects. Namely, the aforementioned impairment in recognizing fearful faces, the difficulty in discriminating gaze direction, the misjudgment of

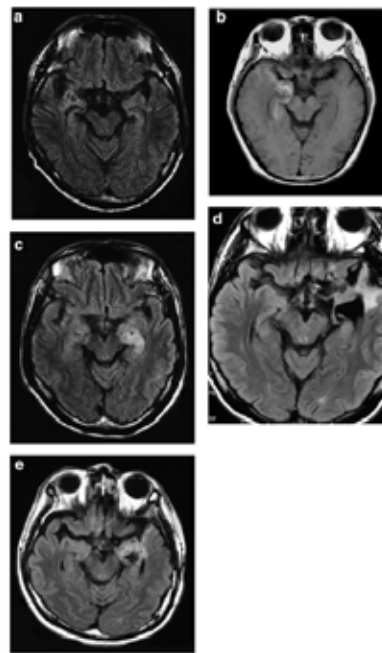


Fig.4. MRI of 1-5 (a-e, respectively), each depicting a lesion in the unilateral (case 1 and 2, right; case 3-5, left) amygdale.

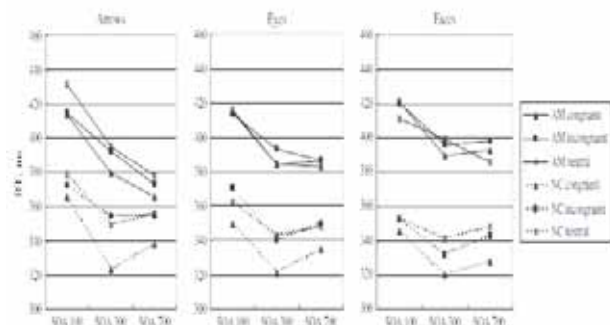


Fig.5. Results of the experiment. The mean RTs of the amygdale group (AM, lines) and normal controls (NC, dotted lines) for each cue type, as a function of cue target congruency and SOA length.

trustworthiness and approachability from unfavorable faces, and the impairment of making fixations on eyes might all be attributed, at least in part, to a common fundamental deficit in exploring for a relevant social signal, allocating attention to it, extracting the critical feature, and guiding behavior accordingly.

The current study answers in the affirmative to the outstanding question of whether the social (or biological) valence of a stimulus (e.g., eyes opposed to arrow signs) is critical for amygdala involvement. In close resemblance is the finding from a case with a lesion to the right superior temporal sulcus (STS) area, where biological motion processing is often implicated. This patient also demonstrated a deficit in gaze-triggered orienting in the face of an intact arrow-triggered orienting. The similar findings from the 2 studies implicate that the amygdala and the STS might work

in concert to selectively process significant social stimuli such as eyes. The amygdala, where very rapid, but coarse information enters, might be in the position to detect potential social stimulus, and crudely evaluate its significance. Through its reciprocal connections with the STS, the amygdala might then relay potentially significant biological stimuli to the STS for finer analysis.

Chronic Schizophrenia and Gaze

Schizophrenia is a neuropsychiatric disorder which can be disabling due to a variety of socio-cognitive impairments. One of its most intriguing symptoms is the abnormal sensitivity to gaze. In a typical course of schizophrenia, the acutely-ill patient often expresses complaints of 'always being watched', reflecting heightened sensitivity to gaze. Through its course into chronicity, however, the patient becomes more and more withdrawn, and hyposensitivity to gaze takes place. This is often observed through the patient's gaze behavior; he/she becomes very reluctant in engaging in mutual eye contact. Some previous studies have highlighted this hyper/hyposensitivity to gaze.

2 Subjects and Method

Twenty-two clinical participants were recruited from a psychiatric hospital in the suburb of Tokyo. We used the same Kingstone's paradigm as in case of STS patient.

3 Results and Discussion

In a spatial cueing experiment using central gaze/arrow direction as cues, we have demonstrated that a relatively uniform population of chronic, medicated schizophrenia differs from normal controls in terms of reduced benefit from congruently directed cues in detecting peripheral targets. Moreover, this benefit reduction in schizophrenia appears to be evident for gaze cues, but not for arrow cues. In the present experiments, we have demonstrated that congruency benefit is reduced in long-term schizophrenia in a spatial cueing paradigm using central directional cues⁹). This finding is indicative of a gaze-specific hyposensitivity in chronic schizophrenia.

Future Direction

In future, we should make a cognitive model of gaze understanding according to the results of above mentioned three experiments, and conduct a computational simulation of recognition of gaze and intention through data obtained. On the other hand, we now examine the mechanism of sense of agency in normal individuals and schizophrenics.

Our experiment was designed to study the abnormal experience of the temporal causal relation or binding between action and sensory consequence in the external world, and aimed to evaluate how patterns of mis-attributions of self-agency differ among normal subjects and schizophrenics. Moreover, we now conduct a computational simulation study through the multiple forward models which explain the results of the agency experiments¹⁰. In cognitive science and robotics, these studies should shed light on the studies for designing and developing user-friendly interaction between human and machines.

References

- 1) Posner, M. I. (1980). Orienting of attention. *Quarterly Journal of Experimental Psychology*, 32(1), 3-25.
- 2) Friesen, C. K., & Kingstone, A. (1998). The eyes have it! Reflexive orienting is triggered by non-predictive gaze. *Psychonomic Bulletin Review*, 5(3), 490-495.
- 3) Tomoko Akiyama, Motoichiro Kato, Taro Muramatsu, Fumie Saito, Ryoko Nakachi, Haruo Kashima: A deficit in discriminating gaze direction in a case with right superior temporal gyrus lesion. *Neuropsychologia* 44:161-170, 2006
- 4) Tomoko Akiyama, Motoichiro Kato, Taro Muramatsu, Fumie Saito, Satoshi Umeda, Haruo Kashima: Gaze but not arrows - a dissociative impairment after right superior temporal gyrus damage.. *Neuropsychologia* 44(10):1804-1810, 2006
- 5) Adolphs R, Tranel D, Damasio AR: The human amygdala in social judgment. *Nature*. 393:470-474, 1998
- 6) Whalen PJ, Rauch SL, Etcoff NL, McInerney SC, Lee MB, Jenike MA. 1998. Masked presentations of emotional facial expressions modulate amygdala activity without explicit knowledge. *J Neurosci*. 18:411-418, 1998
- 7) Adolphs R, Gosselin F, Buchanan TW, Tranel D, Schyns P, Damasio AR: A mechanism for impaired fear recognition after amygdala damage. *Nature*. 433:68-72, 2005
- 8) Tomoko Akiyama, Motoichiro Kato, Taro Muramatsu, Satoshi Umeda, Fumie Saito, Haruo Kashima: Unilateral amygdala lesions hamper attentional orienting triggered by gaze direction. *Cerebral Cortex*, 2007 (in press)
- 9) Tomoko Akiyama, Motoichiro Kato, Taro Muramatsu, Takaki Maeda, Tsunekatsu Hara, Haruo Kashima: Gaze-triggered orienting is reduced in chronic schizophrenia. *Psychiatry Research*, 2007 (in press)
- 10) 新井航平、大武美保子、川端邦明、池本有明、前田貴記、加藤元一郎、浅間一：行為の自他帰属性の解明へのフォワードモデルからのアプローチ、計測自動制御学会 第19回自律分散システムシンポジウム資料、2007年1月29,30日、東京工業大学大岡山キャンパス

Reorganization of the central nervous system responding to changes in social environment in insects

T. Nagao and K. Sasaki

Abstract—Phenotypic plasticity can enhance the survival probability or the reproductive success on an identical genetic background in the species. We investigate the neuro-endocrine systems for the transition of behavioral phenotype in response to changes in social environment in insects. We found the physiological dimorphisms in the brain between different phenotypes: the different levels of brain biogenic amines between the castes in honeybees. Workers can change their reproductive states in the absence of a queen. During the transition, the levels of tyramine and dopamine in the brains increased in reproductive workers. These biogenic amines in the brain can modulate the caste-specific behaviors and these have an important role of the behavioral transition. The process may lead to the formation of morphological caste-specific brain.

I. INTRODUCTION

Phenotypic plasticity can enhance the survival probability or the reproductive success on an identical genetic background in the species. This involves a complex suite of characters, including behavior, color, morphology, endocrine physiology, reproductive development and fecundity. Phenotypic plasticity is known in broad taxa of animals [1], [2], [3], [4]. In social insects, the caste is a phenotypic plasticity with diverse morphological changes. The division of reproduction (reproductive caste) is a behavioral specialization to enhance the efficiency of individual behaviors, and the growth and reproductive success of the colony. Queens engage directly in reproduction, whereas workers perform other tasks, including care of the queen and brood, guarding the nest and foraging. Such a behavioral dimorphism may result from the physiological and morphological differences of the central nervous systems (CNSs) that formed through the developmental program during larval and pupal stages [2], [5]. There have been reported the morphological dimorphism of the CNSs between castes in social insects (Fig. 1) [5], [6], [7], [8]. Adult individuals can not change their morphology of exoskeleton, but they can change the morphology and physiology of the CNSs. Workers can develop the reproductive organs with its motor systems in the absence of a queen and appear the queen-like behaviors. The behavioral transition of reproductive individuals can be a good model for studying the

remodeling of CNSs in response to social environment.

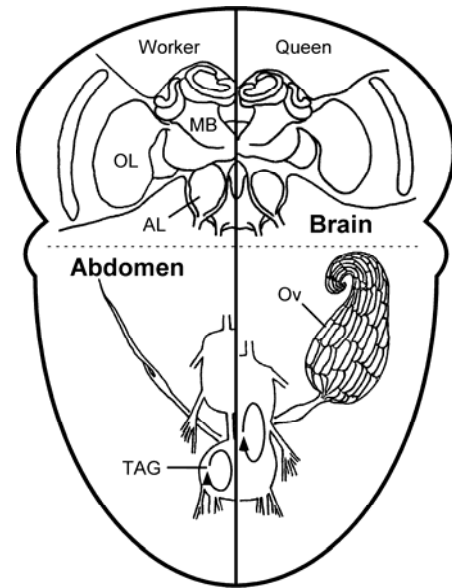


Fig. 1 Morphological dimorphism between castes in honeybees
AL: Antennal lobe, MB: Mushroom body, OL: Optic lobe,
Ov: Ovary, TAG: Terminal abdominal ganglion

II. MODEL

Brain transition from normal workers to reproductive workers seems to be composed of the steps at physiological, behavioral and morphological levels. First step of the caste transition in the brain may be the detection of changes of social environments by sensory systems (Fig. 2). The process follows the changes of endocrine balances within a brain (physiological transition), the appearance of queen-specific behaviors and disappearance of worker-specific behaviors (behavioral transition) and the feedback into the brain morphology by the repetitive queen-specific behaviors (morphological transition). We have the working hypothesis as a model of the remodeling of brains for caste transitions (Fig. 2). This model is partly supported by previous reports [9], [10], [11], [12], [13], [14], [15], but is not fully demonstrated and still controversial.

To test our working hypothesis and to explore the neural mechanisms underlying the caste transition, we would tackle the following topics:

- (1) Physiological and morphological differences of the brain

Both authors are with Kanazawa Institute of Technology, 3-1 Yakkaho, Hakusan, Ishikawa 924-0838, Japan (corresponding author to provide phone: 076-274-8260; fax: 076-274-8251; e-mail: nagao@his.kanazawa-it.ac.jp).

between castes

- (2) Physiological changes of brain during the caste transition
- (3) Effects of biogenic amines on caste-specific behaviors
- (4) Morphological changes of brain during the caste transition

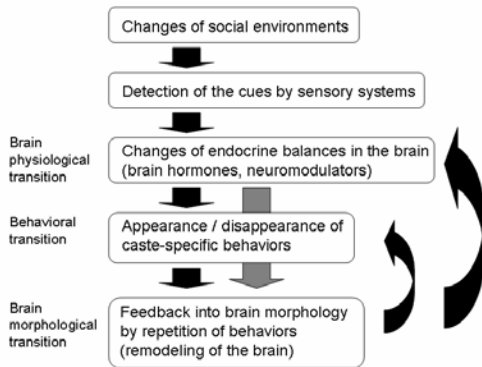


Fig. 2 Transition process of reproductive workers

III. EXPERIMENTS

A. Physiological differences of the brain between castes

To determine whether the brain endocrine condition differs between the caste in honeybees or not, we quantified the brain biogenic amines by HPLC-ECD system and compared the levels between queen and workers. Brain dopamine levels in newly emerged queens were remarkably higher than those in same aged workers (Fig. 3). The dopamine levels in queens were more than 5 times as large as those in workers. These higher dopamine levels were also detected in the haemolymph, suggesting that the higher dopamine levels in queens may affect not only the brain but also the other tissues. Although the behavioral roles of dopamine in the queens remain unknown, dopamine may be involved in the reproductive states or queen-specific behaviors [16]. The distribution dopamine secretory cells in the brain of honeybees have been reported [17][18]. Since morphological differences of the cells between the castes were not found [19], the differences of dopamine levels may result from differences of activities for dopamine synthesis. Pupae of the queens had also the higher levels of brain dopamine. Therefore, the differences of brain dopamine levels between the castes were formed through the developmental program during larval or pupal stages. Dopamine may be a key substance to investigate the physiological dimorphism in the brain between the castes.

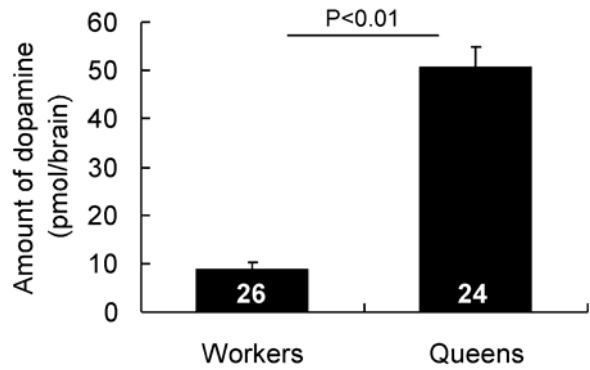


Fig. 3 Brain dopamine levels in workers and queens in honeybees. Values in the bar indicate the sample size that we examined. Differences were examined by Mann-Whitney U-test.

B. Physiological changes of brain during the caste transition

To induce the transition of reproductive states from normal workers to reproductive workers, two cohorts of newly emerged workers were kept under queenless condition. The other two cohorts of the same aged workers were kept under queenright condition as a control. Queenless workers could develop the ovaries with mature eggs and initiate to lay eggs until 15day-old (Fig. 4), whereas queenright workers did not develop the ovaries.

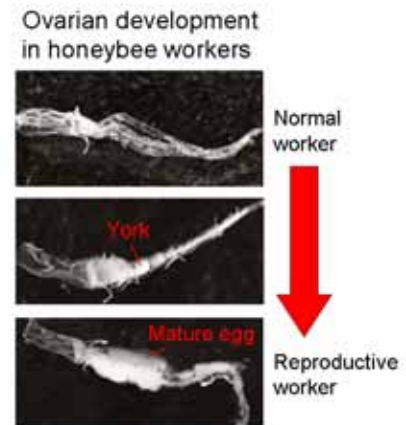


Fig. 4 Ovarian development in honeybee workers

Both 17day-old normal and queenless workers were sampled and quantified the brain dopamine levels. Brain levels of dopamine in queenless workers were significantly higher than those in normal workers (Fig. 5).

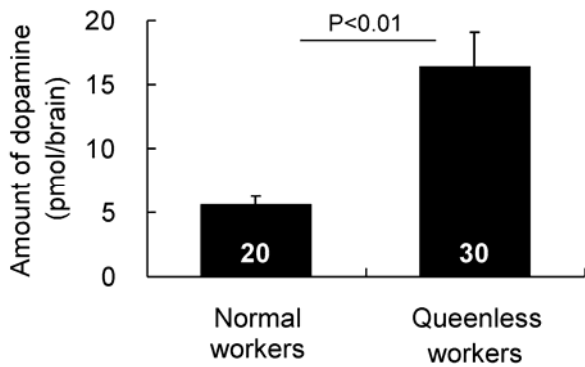


Fig. 5 Brain dopamine levels in both normal workers (17days old) and queenless workers (17days old) in honeybees.

Tyramine is also a candidate of substance for the transition from normal workers to egg-laying workers. Brain tyramine levels in queenless workers were significantly higher than those in normal workers at both 10days and 17days (Fig. 6). This results show the earlier increase of brain levels of tyramine than dopamine. To test whether tyramine levels can respond to the changes in social environment, we transferred the 10day-old queenless workers into the queenright cohort. These transferred individuals (17day-old) showed an intermediate ovarian development in comparison to reproductive workers. The intermediate reproductive workers had intermediate levels of tyramine in the brain (Fig. 6). Thus, brain levels of tyramine seem to be sensitive to changes in social environment, which suggest that tyramine may be involved in a switching of the transition in reproductive workers.

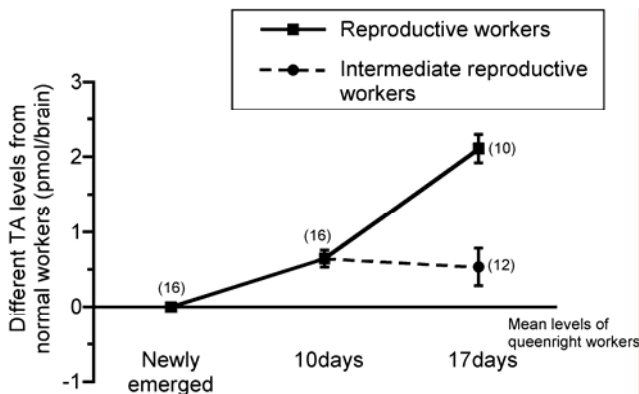


Fig. 6 Relative differences in brain levels of tyramine in reproductive and intermediate reproductive workers.

C. Effects of dopamine or tyramine on the reproductive states

To explore the functional roles of dopamine and tyramine in the transition in reproductive workers, we tried an oral application of dopamine or tyramine to the queenless

workers. Oral treatment with biogenic amines serves as a non-invasive method of reliably elevating the levels of biogenic amines in the brain [20], [21]. For these treatments, newly emerged workers were transferred into plastic cups and given freely a dopamine or tyramine solution for 2 h. As a control, bees were given only 50% sucrose solution for 2 h in another cup. The set of feeding treatments was repeated on the same individuals 4 days old (3 days after the first introduction), 9 days old and 16 days old. Then 17-day-old bees were collected and killed with liquid nitrogen, and used for HPLC analysis. The queenless workers fed dopamine solution had significantly larger levels of brain dopamine and its metabolites (NADA) than control queenless workers (Fig. 7a). This suggests that dopamine can be absorbed from the gut and transferred into the brain. This treatment can accelerate the ovarian development (Fig. 7b). Ovarian diameters in the workers given dopamine were significantly larger than those in control workers. The results of tyramine application were similar to the results of dopamine application. Oral application of tyramine in queenless workers could cause the elevation of brain dopamine levels and accelerate the ovarian development.

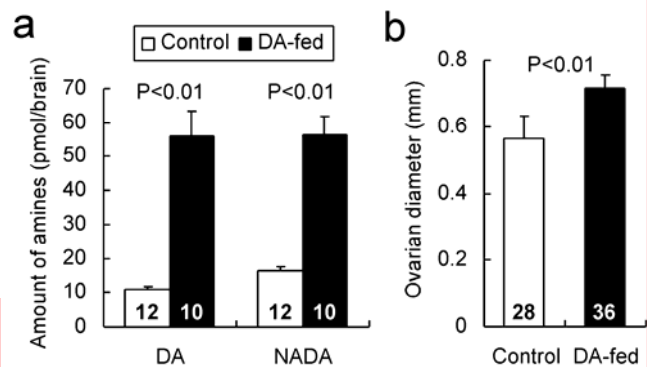


Fig. 7 Effects of dopamine application on the brain amine levels (a) and the ovarian development (b). Values in the bar indicate the sample size that we examined. Differences between groups were examined by Mann-Whitney U-test

D. Behavioral effects of dopamine or tyramine on worker's behaviors

There are several reports on behavioral effects of dopamine or tyramine on worker's behaviors. Dopamine reduces the percentage of bees responding to conditioned stimuli and inhibits information retrieval, but does not affect the storage processes [22], [23], [24]. Tyramine can inhibit the initiation of foraging behavior [21]. These effects seem to be consistent with behaviors of the queenless workers.

We tried to determine the other behavioral effects of tyramine by its oral application. Since honeybee workers respond sucrose solution by the taste sensilla on both the antennae and the tarsi, we examined the behavioral response

to sucrose in queenless workers fed tyramine. The behavioral responses to sucrose by the tarsi were higher in workers fed tyramine than control workers (Fig. 8). The enhanced sucrose response may make the queenless workers intake more food for yolk formation in the ovaries.

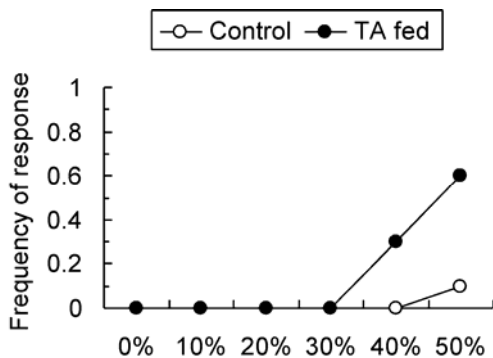


Fig. 8 Behavioral response to sucrose by the tarsi in both tyramine fed (n = 20) and control workers (n = 20).

IV. CONCLUSION AND FUTURE PLAN

A series of our experimental works reveals the neuro-endocrine process of the brain transition to reproductive workers. Biogenic amines, especially tyramine and dopamine may have important roles in the physiological and behavioral transition. Tyramine may be associated with a switching on the initial process of the physiological transition and with an increase the brain dopamine levels. Brain dopamine may be related with ovarian development. These biogenic amines may also affect the caste-specific behaviors. Behavioral effects of these amines still remain unknown. Further investigations of behavioral modulations by the biogenic amines at neural levels are needed. We also plan to determine the brain morphological changes by a repetition of the caste-specific behaviors. Since there have been reported the brain morphological dimorphism between queens and workers [5], [6], [7], [8], we would focus on the dimorphic brain region.

ACKNOWLEDGMENT

We thank Mrs E. Nishida at the Kanazawa Institute of Technology for helping with the maintenance of the HPLC.

REFERENCES

- [1] Shapiro, A.M. 1976. Seasonal Polyphenism. In: Hecht, M.K., Steere, W.C. (eds) *Evolutionary Biology*, vol 9, Plenum, New York, pp259-333.
- [2] Hölldobler, B., Wilson, E.O. 1990. *The ants*. The Belknap Press of Harvard University Press, Cambridge, Mass. 732 pp.
- [3] Simpson, S.J., McCaffery, A.R., Hägele, B.F. 1999. A behavioural analysis of phase change in the desert locust. *Biol. Rev.* 74, 461-480
- [4] Rogers, S.M., Matheson, T., Sasaki, K., Kendrick, K., Simpson, S.J., Burrows, M. 2004. Substantial changes in central nervous system neurotransmitters and neuromodulators accompany phase change in locust. *J. Exp. Biol.*, 207, 3603-3617.
- [5] Winston, M.L. 1987. *The biology of the honeybee*. Harvard University Press, Cambridge, Mass. 281 pp.
- [6] Snodgrass, R.E. 1956. *Anatomy of the Honey Bee*. Cornell Univ. Press, Ithaca, N.Y..
- [7] Wilde, J.de., Beetsma, J. 1982. The physiology of caste development in social insects. *Adv. Insect Physiol.*, 16, 167-246.
- [8] Arnold, G.C., Budharugsa, S., Masson, C. 1988. Organization of the antennal lobe in the queen honey bee, *Apis Mellifera* L. *Int. J. Insect Morphol. Embryol.*, 17, 185-195.
- [9] Withers, G.S., Fahrbach, S.E., Robinson, G.E. 1993. Selective neuroanatomical plasticity and division of labour in the honeybee. *Nature*, 364, 238-240.
- [10] Fahrbach, S.E., Robinson, G.E. 1996. Juvenile hormone, behavioral maturation, and brain structure in the honey bee. *Dev. Neurosci.* 18, 102-114.
- [11] Sigg, D., Thompson, C.M. and Mercer, A.R. 1997. Activity-dependent changes to the brain and behavior of the honey bee, *Apis mellifera* (L.). *J. Neurosci.* 17, 7148-7156.
- [12] Morgan, S.M., Hury, V.M.B., Downes, S.R., Mercer, A.R. 1998. The effects of queenlessness on the maturation of the honey bee olfactory system. *Behav. Brain Res.*, 91, 115-126.
- [13] Gronenberg, W., Liebig, J. 1999. Smaller brains and optic lobes in reproductive workers of the ant *Harpegnathos*. *Naturewissenschaften*, 89, 343-345.
- [14] Sasaki, K., Nagao, T. 2001. Distribution and levels of dopamine and its metabolites in brains of reproductive workers in honeybees. *J. Insect Physiol.*, 47, 1205-1216.
- [15] Sasaki, K., Nagao, T. 2002. Brain tyramine and reproductive states of workers in honeybees. *J. Insect Physiol.*, 48, 1075-1085.
- [16] Harano, K., Sasaki, K., Nagao, T. 2004. Depression of brain dopamine and its metabolite after mating in European honeybee (*Apis mellifera*) queens. *Naturwissenschaften*, 92, 310-313.
- [17] Schäfer, S., Rehder, V. 1989. Dopamine-like immunoreactivity in the brain and suboesophageal ganglion of the honeybee. *J. Comp. Neurol.*, 280, 43-58.
- [18] Schürmann, F. W., Elekes, K., Geffard, M. 1989. Dopamine-like immunoreactivity in the bee brain. *Cell Tissue Res.*, 256, 399-410.
- [19] Blenau, W., Schmidt, M., Faensen, D., Schürmann, F. 1999. Neurons with dopamine-like immunoreactivity target mushroom body Kenyon cell somata in the brain of some hymenopteran insects. *Int. J. Insect Morphol. Embryol.*, 28, 203-210.
- [20] Harris, J.W., Woodring, J. 1999. Effects of dietary precursors to biogenic amines on the behavioural response from groups of caged worker honey bees (*Apis mellifera*) to the alarm pheromone component isopentyl acetate. *Physiological Entomology*, 24, 285-291.
- [21] Schulz, D.J., Robinson, G. 2001. Octopamine influences division of labor in honey bee colonies. *Journal of Comparative Physiology A*, 187, 53-61
- [22] Mercer, A.R., Menzel, R. 1982. The effects of biogenic amines on conditioned and unconditioned responses to olfactory stimuli in the honeybee *Apis mellifera*. *J. Comp. Physiol.*, 145, 363-368.
- [23] Michelsen, D.B. 1988. Catecholamines affect storage and retrieval of conditioned odour stimuli in honey bees. *Comp. Biochem. Physiol.*, 91C, 479-482.
- [24] Menzel, R., Hammer, M., Braun, G., Mauelshagen, J., Sugawa, M. 1991. Neurobiology of learning and memory in honeybees. In: Goodman, L. J., Fisher, R. C. (Eds.), *The behaviour and physiology of bees*, C. A. B. International, Wallingford, pp. 323-353

Revealing Social Brain Functions in Primates

Naotaka Fujii
RIKEN

Abstract

Purpose of this project is aiming to reveal social brain functions in primates at single neuronal level while they are showing social adaptive behaviors. There were two major achievements this year for pursuing the function. One was success in developing new technology, multi-dimensional recording (MDR), which allowed us to record neuronal activity from multiple brain areas and multiple monkeys when they were performing social tasks. The other was starting preliminary studies using the technique. The preliminary results showed dynamic neural adaptation to social environment in parietal cortex and the results led us to employ engineering approach of revealing mechanism of social communication.

● INTRODUCTION

We, human beings, have higher cognitive functions, such as inference and language and are using the functions unconsciously in daily life. Dividing cognitive functions in terms of unconscious and conscious processes, most of the functions might be categorized into unconscious processes. Among our cognitive functions, we could develop complex linguistic communication methods through evolution which other species could not develop. Language has multi-layered structure which can carry complicated information than non-verbal communication. Thus, it is thought to be a one of the major reasons why we could gain outstanding intelligence. On the other hand, social pressure due to our complex social structure that requires heavy cognitive load to adapt our behavior to social demands is another reason why we could gain our intelligence. The function is called social brain function.

There were many challenges that tried to reveal mechanism of the function but still fundamental mechanism of the function is totally unknown. The largest reason why the neuroscientific challenges were

not succeeding was because it was not easy to control social parameters scientifically and quantitatively, which was not the same as studying visual and auditory functions. At the same time, cognitive ethological studies reported that primates showed social adaptive behaviors that suggested the existence of the social brain functions in primates. However, it is not clear if their social brain function is comparable to ours.

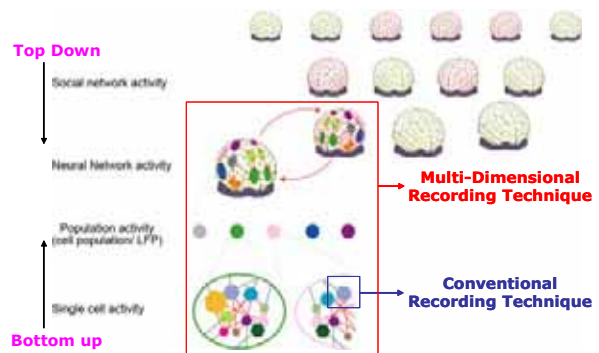


Figure 1 Society consists of multi-tiered networks from neural network to social network.

Figure 1 indicates schematic view of structure of multi-tiered social networks. Society consists of many brains. There is a hierarchical structure between brains that significantly influences on our behavioral choices. The social structure is continuously modulated by action of self and others. In each brain, neural functions are achieved by network function of multiple brain regions. In this network layer, there is anatomical hierarchical structure that regulates the function. The structure could be modulated but less dynamic than social structure. In each brain region, the function is implemented by local neural network. The complex nested neural and social networks are dynamically modulating and thus generating the society.

If we aim to reveal social brain functions at neural level that are implemented by multi-layered networks, conventional approach is not sufficient due to several

reasons. The largest reason is that conventional approach requires strict control of behavioral parameters, but it is not possible to control social parameters in studying social brain. The other major reason is that conventional methods can handle only single-dimensional parameters, while social brain function is dealing multi-dimensional parameters. This is critical problem in studying social brain function but there was no way of solving the problem.

Thus, we developed a new technique, called multi-dimensional recording technique (MDR) and introduced the technique to reveal the mechanism of the social brain function at single cell level which is the aim of our project. There are two different aspects in tackling the issue. One is developing MDR technique and the other is application of the technique in neural recording and analysis to find neural correlates of social brain functions. I will explain current status of the project in terms of these two aspects below.

● MULTI-DIMENSIONAL RECORDING

Current status: I have originally started developing MDR few years before. This is quite a novel approach and essential for revealing social brain mechanism. As I have described above, it is not possible to learn social brain functions in conventional technique. It is because social brain functions can not be described by behavior of single agent or single neurons which conventional methods were dealing. Moreover, social structure is not steady and unpredictable so that controlling the environmental parameters is impossible. Taking these fundamental problems, I concluded that conventional methods were not adequate and thus started development of MDR technique.

For recording neural activity from many neurons in multiple brain regions, I decided to employ chronic multi-electrodes recording system.

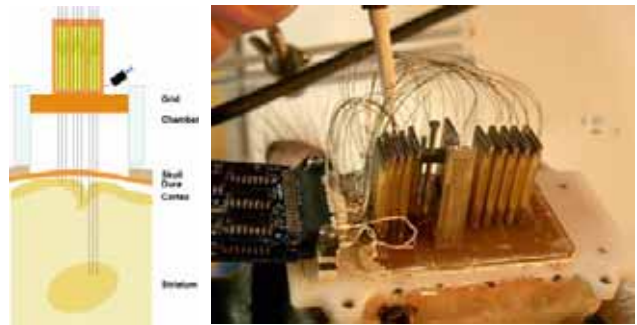


Figure 2. Left) schematic view of chronic implantation of multiple-electrodes. Right) Actual implantation of 72 electrodes in monkey's brain.

Figure 2 indicates chronic implantation of 72 tungsten electrodes (0.12mm diameter, 800K-1.2M Ω) in prefrontal cortex, premotor cortex, primary motor cortex, parietal cortex and caudate nucleus. Each electrode was attached to a micro-manipulator and was independently depth adjustable. Using the method, we could record neuronal activity for 2-3 months. Stability of neural recording was gradually increased during 1-2 weeks after implantation and yield of electrodes collecting neural activity was reached to more than 80% at the best. The best performance lasted for a month and gradually yield decayed over time. After recording was completed, electrodes were pulled out and new set of electrodes will be implanted for next recording session.

The most excellent point of our recording methods is stability of acquiring neural signals. The level of the stability is far beyond conventional technique. In conventional recording technique, head motion always caused loss of neural signal so that head free recording has not been never thought. In conventional methods, head of monkey has to be tightly fixed and number of electrodes used simultaneously was very limited. The electrodes were acutely implanted and not often left chronically.

However, in our recording methods, we succeeded to remove these technical restraints so that we could allow monkeys free head motion. Neuronal activity recorded while monkeys were moving their heads freely was stable and level of the stability was better than conventional technique. We thought that the stability was gained due to chronic implantation in which mechanical stress between tip of electrode and surrounding brain tissue was minimized.

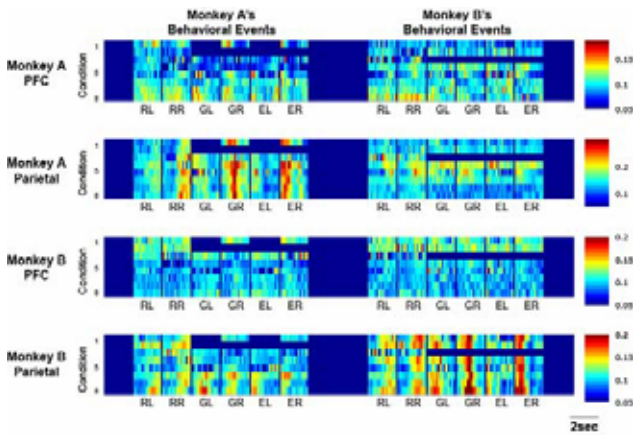


Figure 3 Population histograms of Parietal and prefrontal neurons of two monkeys

Using the method, we succeeded recording neuronal activity from two monkeys simultaneously. Figure 3 shows population histograms of parietal and prefrontal neurons recorded from two monkeys simultaneously. During the recording, there was no behavioral constraint. Monkeys could move head, torso and arms freely. There was no report that record neuronal activity from multiple monkeys while they were showing natural social behaviors.

Allowing natural behavior caused new problem that there was no controlled motion so that association between behavior and neural activity was difficult. Therefore, we decided to introduce motion capture system to monitor and record any behavioral episodes during the task instead of controlling and monitoring specific task parameters. Motion capture system is a non-invasive technique that records three-dimensional location of reflective markers attached on subject's body. We designed custom made motion capture suit for each monkey and succeeded reconstructing monkeys' behaviors on computer.

Combining these two methods, chronic multi-electrodes recording and motion capture systems, provided huge advantages in revealing social brain functions in primates.

Potential problems : A current quality of MDR technique has been reached to certain level that convinced us to start actual experiment. However, there are many issued which have to be solved. As for chronic recording, there is limitation in days of recording and depth of the electrodes has to be adjusted at daily basis. It suggests that there is a problem in biocompatibility between electrode and brain tissue. To solve the problem, we have to find better materials of

electrode and insulation. And also changing diameter and stiffness of the electrode may be other issues to gain biocompatibility. Moreover, immune suppressive substances administrated by coating the tip of the electrode may reduce immune reaction.

Another issue is physical wiring problem in our recording system in which monkeys have to be wired to record neuronal activity. The cable restrains monkeys' behaviors slightly and sometimes monkeys pull out the cables and break expensive cables. To avoid the risks due to the cable issue, we have to consider introducing telemetry system.

● REVEALING NEURAL MECHANISM OF SOCIAL BRAIN

Current status: In parallel with development of MDR system, we recorded neuronal activity from two monkeys simultaneously this year while they were performing social tasks as a preliminary study. The task they performed was simple food grab task. In each trial, a piece of food was place on a table where monkeys were sitting around, in three different relative positions. If monkeys could reach to the food, they could take the food. There was no cue provided that told who should take the food. Figure 4 indicates how monkeys behaved in the task.

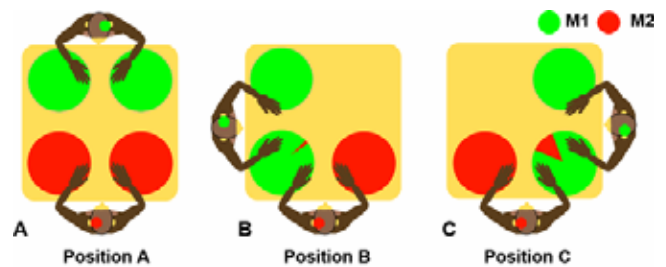


Figure 4 Two monkeys (M1 and M2) were located around the table in three relative positions. M1 took all of available food without hesitation but M2 suppressed responding to the food where M1 could reach.

In position A, where two monkeys were facing each other and no conflict occurred, they reached to all of reachable food without hesitation and ignored each other. However, in position B and C, where conflicting space emerged at the corner between them, M2 changed his behavior. He stopped reaching to the food if M1 could reach the food. In contrast, M1 still took all of available food without hesitation. In these positions, M1 was still ignoring M2 but M2 surreptitiously

watched M1. Based on these findings in their behaviors, we concluded that there was significant hierarchy between them and M2's behavioral selection was narrowed by social suppression due to monkey's hierarchical status.

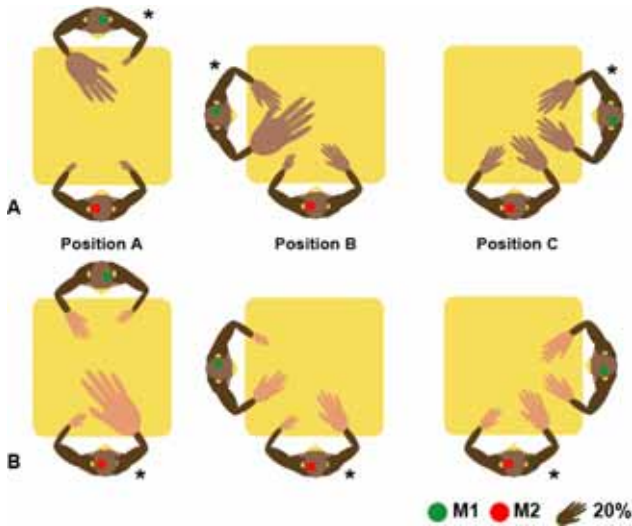


Figure 5 Proportion of motion related parietal neurons of two monkeys at three relative positions.

Figure 5 indicates proportion of motion related parietal neurons while monkeys were performing food grab task at three relative positions. The figure shows that in both monkeys, parietal neurons tended to respond to motion of self and right hand but smaller response to other motions. However, the laterality that was shown in position A was decayed in position B and C. Neurons that were mainly responded to self right hand motion started to respond to motion of others. The findings suggested that neural modulation occurred in response to modulation of social context which was subjectively defined depending on monkey's internal social hierarchical status.

The result of preliminary study showed that monkey switched behavioral strategy if they started sharing a social space and, at the same time, neuronal response properties were also modulated in response to social contextual modulation.

Potential problems: In the preliminary study, we found that neurons were responding to many parameters that were not expected to analyze. For instance, motion of experimenter was not thought to be important when we started the study, but it turned out that experimenter's action showed large impact on monkeys' behavioral choices. It suggested in study of social brain function that we should monitor and record

any available parameters in the social environment as much as possible.

Monitoring eye movement is other important issue which we have to deal, because eye position is an important behavioral parameter that reflects attention. However, there is no available recording system in the market for monitoring accurate eye position in primates if monkeys are moving freely.

● PLANS FOR NEXT YEAR

We have completed basic preparation for pursuing social brain functions in primates and applied the technique for preliminary study. Through the preliminary study, it turned out that MDR technique we invented this year would provide sufficient information for revealing social brain functions at single cell level. We will improve the MDR technique in stability and accuracy of signals. We will continue the study and add more features in the task such like motivation, emotion, sympathy and empathy. We will also widen recorded areas from association cortices to sub-cortical areas, including basal ganglia and limbic system. These expansions may help understanding a realistic network mechanism of social brain functions.

One more important expansion of our project is integration of physiological approach and engineering approach. We started collaboration project with Kuniyoshi Lab at Tokyo Univ. in finding a way of retrieving intention of subjects by estimating from subject's behaviors. The project was started last summer and it is providing very interesting findings. We are expecting the integration study will open totally novel filed and may help understanding social brain functions from different view.

Group D: On Common Principle of Mobiligence

Koichi OSUKA Kobe Univ. , Akio ISHIGURO Tohoku Univ. and Zheng, Xin-Zhi ASTEM

Abstract— In this note, we consider a basic structure of adaptive mechanism of Mobiligence. Concretely, considering the results of passive dynamic walk, we propose a primitive-template-structure of the adaptive structure. The simplest structure consists of a passive part and a active part. More complicated structure is built by these structures and constructs a multi-layered structure.

1. INTRODUCTION

In this note, we discuss a common principle of Mobiligence. To do so, we have to consider both (a) Structure of adaptive mechanism and (b) Algorithm of adaptive function. Here, we discuss the structure of the adaptive mechanism as the first step.

Concretely, as an example, we research an embedded adaptive function in phenomenon of passive dynamic walking. Then, expanding the considered results, we propose a kind of primitive template structure of an adaptive mechanism of Mobiligence. The template consists of “Passive Adaptive Function” and “Active Adaptive Function”. Furthermore, we insist that a general adaptive function may be constructed by multi structured templates.

According to the consideration, it is conjectured that the adaptive function at various levels in various seeds can be expressed by the difference of the contents of the template or the number of the nest of template structure.

The contents of the note are as the following. In Chapter 2, we consider the passive adaptive mechanism (passive adjustment function and passive canalization) that the passive movement walking has. In Chapter 3, focusing on the concept proposed in Chapter 2, we propose the basic structure of the adaptive mechanism of Mobiligence. We summarize the consideration in Chapter 4.

2. ADAPTIVE FUNCTION IN PASSIVE DYNAMIC WALKING

From our previous researches, the following results concerned with passive dynamic walking are known. See Fig. 1.

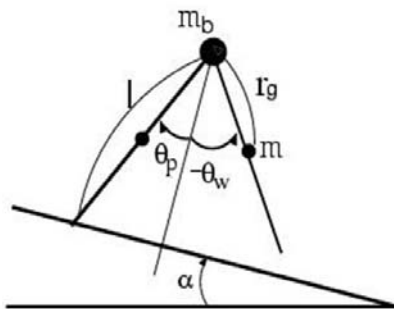


Fig.1 Passive dynamic walker

Here, the parameters are set as the following. M : mass of the hip = 10.0[kg], m : mass of the leg = 1.0[kg], l : length of the leg = 0.3 [m], r : distance between the hip and the center of gravity of the leg = 0.15 [m], g : acceleration of gravity = 9.8[m/s²], α : slope angle of the slope [rad], θ_p : angle of the support leg measured from perpendicular from the waist to the slope [rad], θ_w : angle of the swing leg measured from perpendicular from the waist to the slope [rad] .

1) Implicit Feedback Structure: Phenomenon of passive dynamic walking is stable in the sense of walking. The reason of the stability is the existence of the implicit feedback structure in the Poincare map.

2) Adaptive function: Passive dynamic walker can robustly walk under small variation in the angle of the slope or the parameters of the body. These variations can be regarded as a kind of variation of environment. If the variations become larger, then the passive dynamic walker changes the walking pattern autonomously so as to continue the walking (selection of feedback structure : see Fig.2). We regard the function as a kind of passive adaptive function embedded in the passive dynamic walking system.

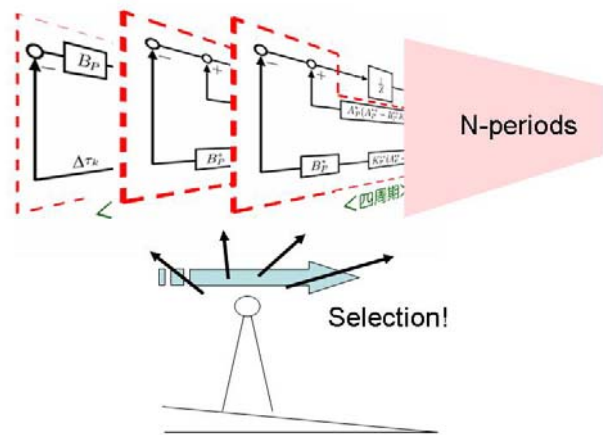


Fig.2 Implicit Feedback Structure in PDW

When we see the passive adaptive function to continuous environmental change from another viewpoint, the following can be seen. That is, once achieve a one-period walking which can be easily gotten, gradually change a parameter. Then we can easily have multi-period walking pattern which is usually difficult to achieve. This implies "Canalization" well known in the embryology.

Summarize from the above, we can have the following finding.

FINDING: The passive adjustment function (Passive Canalization is naturally included) exists inside the passive movement walking. In addition, to deal with a big environmental change, it only has to

construct an active adaptive function on the high layer of this function. □

3. A CONJECTURE ON STRUCTURE OF MOBILIGENCE

In this chapter, expanding the considerations of the previous results, we try to construct a primitive template structure of the adaptive structure. To do so, at first, in 3.1, we list up some characteristic features which can be seen in many species. Then, in 3.2, we show a candidate of structure of Mobiligence.

3.1 Understanding of situations

Observing many living things, we can see the following basic restrictions in the constructing of the structure of Mobiligence.

Embodiment: Living things have its own body. The body is always dynamical.

Brain structure: The structure of brain is multi-layered. The lowest layer brain has very strong connection with the body movement. The upper layer brain exists with the suitable matching on a lower brain.

Transference: The upper layer brain tends to transfer the processing which can be treated by a lower layer brain to the lower layer brain as much as possible.

Complexity: : A complex adaptive function exists in the action of one individual.

Sociality: A hierarchical adaptive function exists in the action of the individual and the action of the society.

Optimality: In the appearance of Mobiligence, optimization to various levels (scale of the time or a complexity) works.

Canalization: The evolution of the living thing has the tendency to persist in the route. The concept of canalization

3.2 Conjectures on Structure of Mobiligence

First of all, "Hierarchy" is recollected from the consideration of the paragraph in the above. At that time, from the consideration that the nature likes simple, we think that a kind of Hierarchy by the same structure is reasonable.

And if we go down the lowest level of the structure, the function has a strong relationship with the dynamics of the body. One example of the lowest passive adaptive function can be seen in the passive dynamic walking. That is, we can consider the adaptive function in walking as the following. Based on the passive adaptive function and passive canalization, active adaptive function and active canalization are constructed. See Fig.3.

Based of the considerations, we can propose a candidate of primitive template of Mobiligence as the following.

Primitive Template of Mobiligence: The template has 2-layered structure. The lower layer can be considered as a passive element and the upper layer can be considered as an active element. See Fig.4.

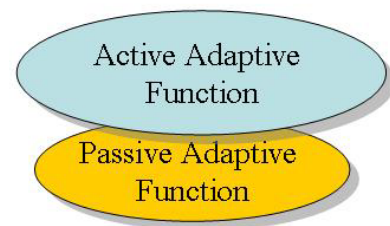


Fig.4 Primitive Template of Mobiligence

Start with this template, then we can construct more complicated Mobiligence by multi-layered as shown in Fig.5.

Multi-layered Dynamical Structure of Mobiligence: Our proposed model of Mobiligence can be shown in Fig.5.

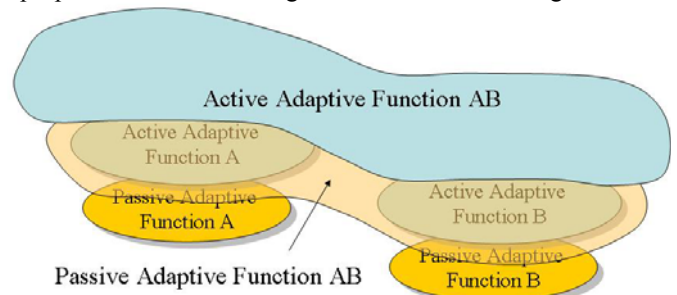


Fig.5 Multi-layered Dynamical Structure of Mobiligence

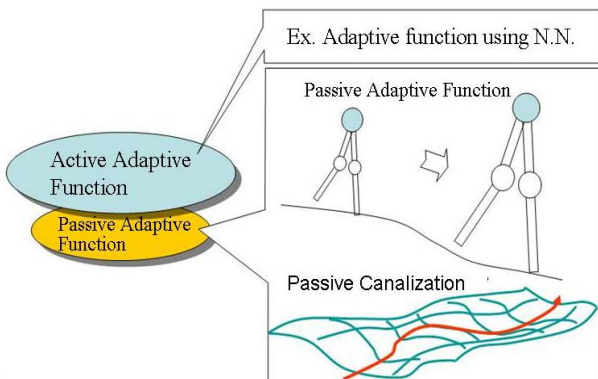


Fig.3 Example: Passive Adaptive Function in PDW

4. CONCLUSION

In this note, we discussed a candidate of structure of adaptive structure in Mobiligence. The point of this discussion is the following. (a) We started the discussion from the lower dynamics instead of the high intelligence. (b) We assumed that the adaptive function consists of Passive part and Active part.

Problem in the future is to justify the conjecture. To do so, we aggressively discuss with Group A, B and C.

Discovery and Progressing of Dynamical Common Principle of Mobiligence

— Common Understanding of Artificial Thing and Living Thing —

Koichi Osuka(Kobe Univ.), Akio Ishiguro(Tohoku Univ.) and Xin-Zhi Zheng(ASTEM)

Abstract: In this note, the activity report of the Group D01 in 2006 is shown. The group has been organized for searching the common principle of Mobiligence. Concretely speaking, we show the considerations from the following three points. A. Walking principle in passive dynamic walking. B. Realtime shape control of the modular robot whose degree of freedom is big. And finally, we discuss the structure of Mobiligence.

1. Introduction

In Group D, we mainly consider the concept of Balance as a common principle in Mobiligence. That is to say, we think that there exists some kind of feedback structure in Mobiligence of many situations (for example, GroupA, GroupB and GroupC). The result is expected to be reduced to the design principle of movement wisdom in the robot including the living thing.

2. Tow approach to Mobiligence

Searching for basic logic from a minimum setting is important to understand the appearance principle and the construction principle of Mobiligence in the composition theory. It is called, so-called "Minimal design" or "KISS (Keep- It- Stupidly- Simple) principle".

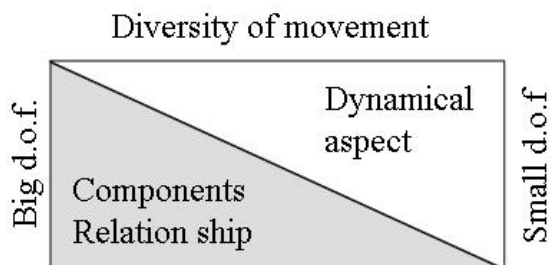


Fig.1 Approach to Mobiligence

In our group, we start from the following two meanings of minimal design. See Fig.1.

A) Diversity of movement which can be seen in

passive dynamic walking that reduces degree of freedom ultimately

B) The component is simplified ultimately, and the diversity of the movement that appears by enlarging the number of the components ultimately.

3. Adaptive Function in PDW

In this chapter, we review some interesting phenomenon in PDW. At first, it is well known that the PDW is stable. And furthermore, we can observe the bifurcation phenomenon in the PDW. In the simulation would, these facts have been known since 1986. We show the bifurcation phenomenon occurs in the real world in 2000. See Fig.2..

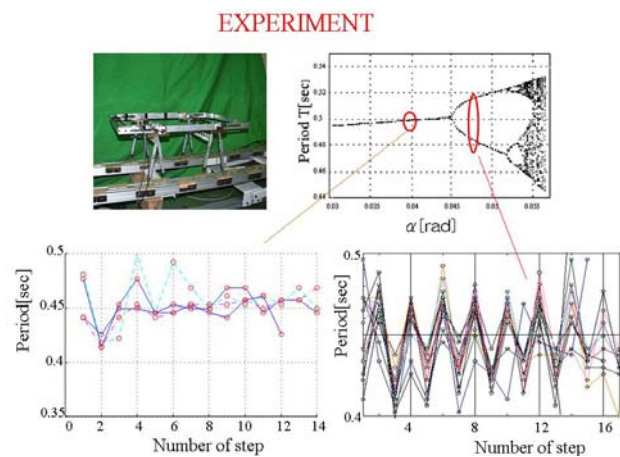


Fig.2 Stability and bifurcation in PDW

To know the reason of the stability, we have to study the Poincare Map P_k which expresses the model of walking of PDW analytically. As the results, we found that the Implicit Feedback Structure is embedded in the Poincare Map. See Fig.3.

Furthermore, we also found that the similar feedback structure can be seen in the Poincare Map in the multi-periodic walking. See Fig.4.

Recently, we carried out some interesting simulations. In the next, we introduce the simulation results. In this chapter, we introduce the simulated results and propose a concept of Passive Adaptive Function.

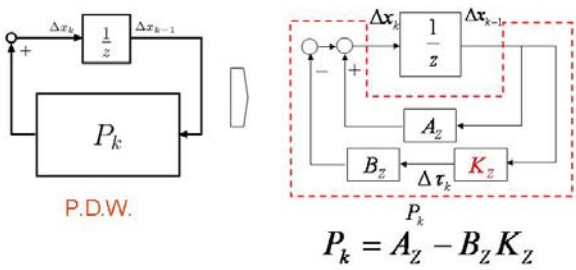


Fig.3 Implicit Feedback Structure

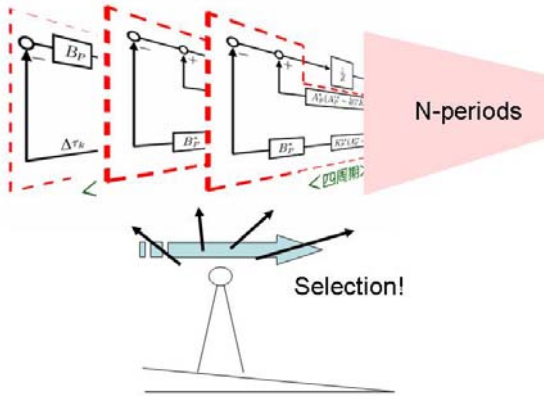


Fig.4 Multi Structured I.F.S.

3.1 Simulated Results

C1) Environment : Slowly varying slope angle

It is easy to find the stable initial condition for 1-period walking. And, it is difficult to find the initial condition for 2-4..period walking. But, if the slope angle $\alpha(t)$ varies slowly, we can easily have the multi-periodic walking very easily. See Fig.5.

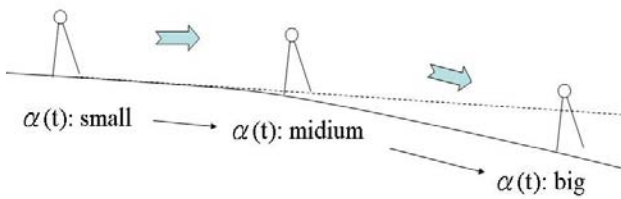


Fig.5 Slowly varying slope angle

C2) Embodiment: Slowly varying body parameter

It is easy to find the stable initial condition for small robot. And, it is difficult to find the stable initial condition for big robot. Here, the difference between the small robot and the big robot is the mass ratio μ . The mass ratio is $\mu=m/M$. Here M is the mass of the body and m is the mass of the leg. The mass ratio μ of the small robot is smaller than that of the big robot. See Fig.6.

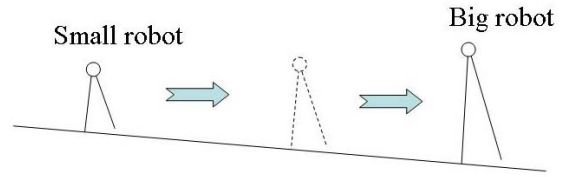


Fig.6 slowly growing up robot

Fig.7 shows the simulated results indicated in Fig.5 and Fig.6. From the results, we can see the searching of the initial condition is carried out.

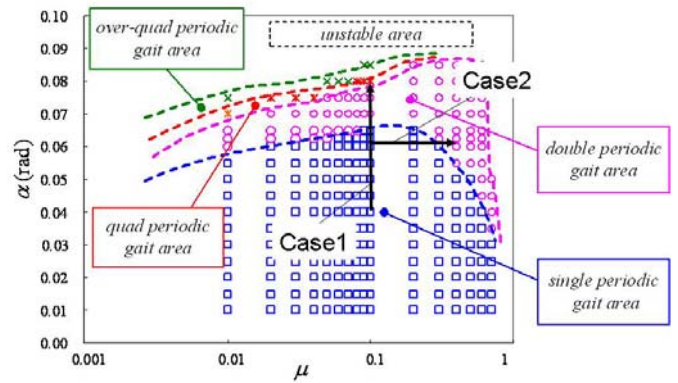


Fig.7 Simulated results

3.2 Passive Adaptive Function

From the above considerations, we propose a kind of structure of intelligence in the living things.

At first, we think that the simulated results shown in 3.1 imply the validity of a concept of canalization well known in the field of Embryology. And these simulated results show that the passive dynamic walker walks down on the slope changing the walking pattern automatically. This implies the existence of a kind of adaptive functions in the dynamics of the passive dynamic walker itself. We call this function as Passive Adaptive Function. Of course, the ability of the passive adaptive function is insufficient for the living things to live in the environment which is variously changed. Therefore, we propose the adaptive function of the living thing as the following. That is, the adaptive function consists of the two adaptive functions. One is the passive adaptive function mentioned in the above. And the other is the Active Adaptive Function. This is constructed from neural networks, for example. See Fig.8.

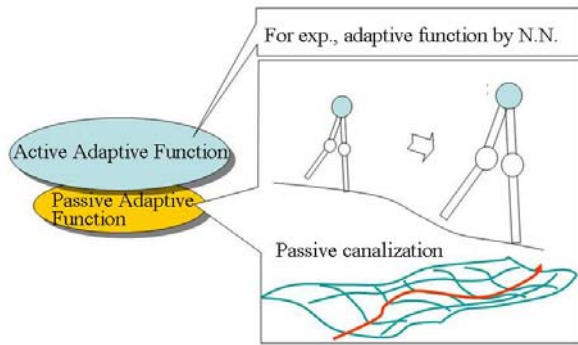


Fig.8 Passive and Active Adaptive Function

4. Adaptive Function in Slimebot

Here we are try to construct a module robots. Nonlinear oscillator is used for the control scheme.

4.1 The way of thinking

Based on the concept “Minimal Design”, the following restrictions have been intentionally imposed.

- The unit robot is very simple. This robot can not move by itself. Only very simple movement and nonlinear oscillator are embedded in the robot.
- The communication between elements is local and divergence.
- The entire module has the same body.

Using this Slime, we research the balance between body and control. That is, under the hypothesis that the adaptive function of living thing stand up in the mid of the figure.

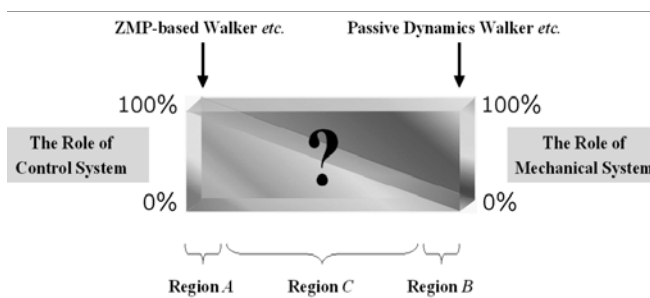


Fig.9 Balance between body and control

4.2 Slimebot

This note discusses a fully decentralized algorithm able to control the morphology of a two-dimensional modular robot called “Slimebot”, consisting of many identical modules, according to the environment encountered. The Slimebot consists of many unified module robot. See Fig.10.

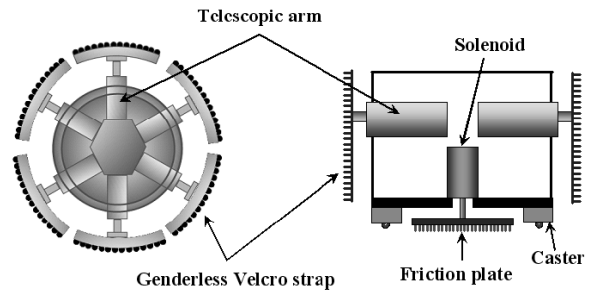


Fig.10 Slimebot

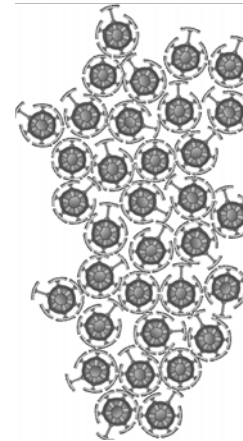


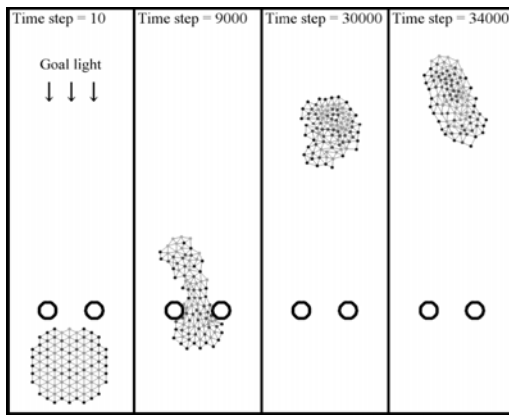
Fig.11 Concept of modular robot

In order to generate appropriate locomotion that effectively drives all the modules toward the goal light while maintaining the coherence of the entire system, the following two things have to be carefully considered in developing a control algorithm:

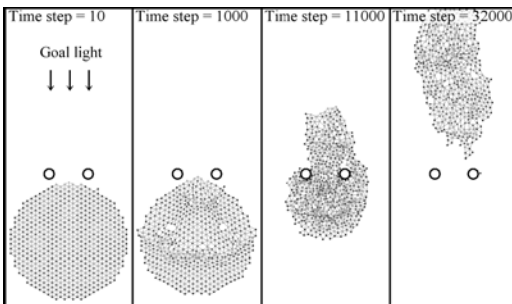
- The mode alternation in each module.
- The extension/contraction of each telescopic arm in a module.

To this end, we have focused on nonlinear oscillators, since they exhibit an interesting phenomenon called the mutual entrainment when they interact each other. In other word, they can create global information through local interaction. Another important aspect to be noted is that they can be used as rhythm generators. In this study, we have implemented a nonlinear oscillator onto each module of the modular robot. We then create phase gradient inside the modular robot through the mutual entrainment among the locally interacting nonlinear oscillators. This is done by a local communication among the physically-connected modules, the detail of which will be explained below.

Fig.12 shows the simulated results. These figure indicate the effectiveness of our control method. Fig.13 shows our developing Slimebot.



(a) Number of module: 100



(b) Number of module: 500

Fig. 12 Simulation

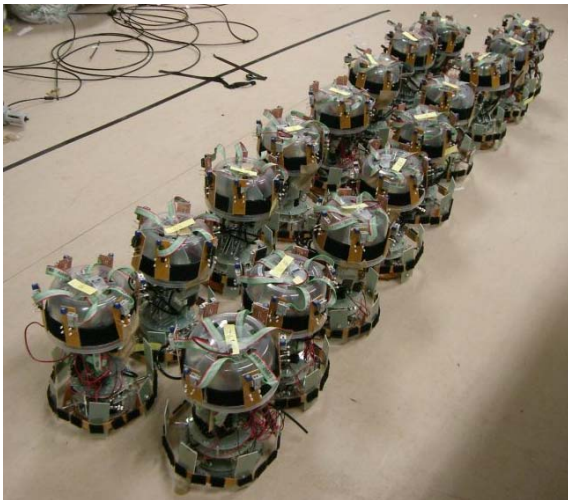


Fig. 13 Slimebot

5. Conclusion

As viewed in the previous sections, an understanding to the intrinsic behavioral emergence ability or adaptability mechanisms in Mobiligence can be based on the idea of the multi-layered active/passive adaptive template structure. The "Intelligence" (defined here as the behavioral emergence ability and the emergent behaviors in some specific environments) acquired through "Moving" (defined as any behavior to achieve dynamic and informatic interaction with the environments) in all living and human beings, may appears in an inherent

or an acquired nature through short-term, middle-term, and/or long-term adaptations.

The inherent intelligence also shows mutational nature in gene information or mature growth nature as in muscle-skeletons, both of which may be regarded invariant or with very large time-constant during single generation, which therefore may be addressed as passive adaptation in our multi-layered adaptive structure. Meanwhile locomotion on irregular ground, skill mastery/ acquisition in sports/ skillful tasks, and antibody development against new disease germs are all adaptive abilities to the newly emerging environments, which may be addressed as active adaptation in our multi-layered adaptive structure. The latter three are obviously under quite different scales, and are categorized here as short-term, middle-term, and long-term adaptations following the periods of their adaptations.

Especially in the mastery/acquisition of skillful sports, the iteration of motion in drills/practices induces the emergence of adapted behaviors that meets the dynamic properties of the "environments", the specific sports, and of the human body. Here some criterion (adaptive principle) are obeyed and refinement of the feed forward motion instruction are achieved through the iteration, which is addressed here as a type of function of the passive adaptation. Playing tennis or baseball will be good examples. In these sports, however, more underlying and distinguished characteristics are observed; it is known that the adaptations in so-called discrete motions, such as the individual practices for forehand and backhand swings in tennis or for left-field and right-field batting in baseball, are much different with those in so-called compound motions where the practices are performed under the random mixtures of the above individual tennis swings or baseball batting. Moreover, the adaptive or behavioral emerging abilities in these situations are having to be discussed within some new theoretic frameworks different with the conventional ones in existing control theories such as learning control for single/discrete trajectory tracking or repetitive control for periodical trajectory following. These characteristics suggest active adaptation ability in Mobiligence.

The engineering understanding and designing of structure and relationship for the above adaptive mechanisms are on-going, and the mutual verification of the results with the finding and knowledge obtained in exercise physiology may useful and inevitable in future researching.

Fractals in Dynamical Systems excited by External Inputs

Kazutoshi Gohara

Graduate School of Engineering, Department of Applied Physics,
Hokkaido University, Sapporo 060-8628, Japan

Abstract—In this paper the dynamical system is defined by a continuous dynamical system discretely switched by external temporal inputs. A theory developed by the author suggests that the dynamics of ordinary differential equations, which is stochastically excited by external temporal inputs, is characterized by a set of continuous trajectories with a fractal structure in hyper-cylindrical phase space. After the theory is reviewed, a simple example and a preliminary multi-fractal formalism are given.

1. Introduction

A *Hybrid Dynamical System* (HDS) [1] is a dynamical system that involves an interaction of discrete and continuous dynamics. Control strategies introduced for HDS have been applied to various design problems for realizing desired behavior in power plants [2], chemical plants [3], etc.

The dynamical evolution of HDS can be described by a differential equation involving a number of vector fields that are switched one after another [4]. It has been shown that HDS displays very complex behaviors such as chaotic behavior [5]. Branicky [6] and the author [7] have independently demonstrated numerical experiments of HDS described by simple linear equations and shown that the state of the system moves around on the Sierpinski gasket, a very well-known fractal set. These results suggest that the fractals may universally appear in some classes of HDS. In this paper a theory for continuous dynamical systems with temporal inputs are presented from hybrid dynamical systems point of view.

We focus on dissipative, continuous, and non-autonomous dynamical systems defined by the following ordinary differential equations:

$$\begin{aligned}\dot{x} &= f(x, t), \\ x &\in R^N,\end{aligned}\tag{1}$$

where x , t and f are state, time, and vector field, respectively. Equation (1) implies that the vector field depends on time. In general, this suggests that a system is influenced by other systems. To emphasize that the vector fields depend on time throughout the input $I(t)$, we rewrite Eq. (1) as follows:

$$\begin{aligned}\dot{x} &= f(x, I(t)), \\ x, I &\in R^N.\end{aligned}\tag{2}$$

2. Dynamics with Periodic Inputs

We will begin by considering a dynamics with a periodic input:

$$I(t) = I(t + T),$$

where T is the period of the input. The vector field f is also periodic with the same period T :

$$f(t) = f(t + T).$$

Introducing the angular variable $\theta = \frac{2\pi}{T}t \bmod 2\pi$ and new state variable $y = (x, \theta)$, we can transform the non-autonomous system expressed by Eq. (2) into the following autonomous system:

$$\begin{aligned}\dot{y} &= f_I(y), \\ y &\in R^N \times S^1.\end{aligned}\tag{3}$$

The vector field f_I is defined on a manifold $\mathcal{M} : R^N \times S^1$ that is a hyper-cylindrical space. In other words, Eq. (3) expresses a continuous dynamical system D_c defined by the manifold \mathcal{M} and the vector field f_I :

$$D_c = (\mathcal{M}, f_I).\tag{4}$$

In the hyper-cylindrical space \mathcal{M} , we can define the Poincaré section:

$$\Sigma = \{(x, \theta) \in R^N \times S^1 | \theta = 2\pi\},$$

where a trajectory starting from an initial state at $\theta = 0$ returns at $\theta = 2\pi$. On the section Σ , a mapping can be defined which transforms a state x_τ to another state $x_{\tau+1}$ after interval T :

$$\begin{aligned}x_{\tau+1} &= g_I(x_\tau), \\ x_\tau &\in R^N,\end{aligned}\tag{5}$$

where g_I is an iterated function. In other words, Eq. (5) expresses a discrete dynamical system D_d defined by the manifold Σ and the iterated function g_I :

$$D_d = (\Sigma, g_I).\tag{6}$$

We can summarize the dynamics with a periodic input as follows. The periodic input I defines two dynamical systems, a continuous one D_c and a discrete one D_d defined by Eqs. (4) and (6), respectively. In order to emphasize the relation among I , D_c and D_d , we use the following schematic expression:

$$I \rightarrow D_c \rightarrow D_d.\tag{7}$$

3. Dynamics with Switching Inputs

3.1. A Set of Inputs

In this section, we consider a dynamics in which plural input patterns are stochastically fed into the system one after the other. Let us suppose that *each input is one period of a periodic function*. For example, we can define the periodic function by the following Fourier series:

$$I(t) = \frac{a_0}{2} + \sum_{m=1}^M \left(a_m \cos \frac{2\pi m}{T} t + b_m \sin \frac{2\pi m}{T} t \right), \quad (8)$$

where $a_0, a_m, b_m \in \mathbb{R}^N$ are vectors for Fourier coefficients, and T is the period. The set of these parameters defines the *input space*:

$$\mathcal{I} = \left\{ a_0, \{a_m, b_m\}_{m=1}^M, T \right\},$$

$$\mathcal{I} : \mathbb{R}^{N+2 \times N \times M+1}.$$

Within this space, an arbitrary point represents an external temporal input. We consider the input as a set $\{I_l\}_{l=1}^L$ of time functions I_l sampled on the parameterized space \mathcal{I} . In the following sections, we abbreviate subscripts and express individual sets as $\{\cdot\}$ for simplicity.

3.2. Two Sets of Dynamical Systems

Much as in the case of periodic input, we can define two sets of dynamical systems corresponding to the set $\{I_l\}$. One is the set of continuous dynamical systems:

$$\{D_{cl}\} = (\mathcal{M}, \{f_l\}), \quad (9)$$

where $\{f_l\}$ is the set of vector fields on the hyper-cylindrical space \mathcal{M} . The other is the set of discrete ones:

$$\{D_{dl}\} = (\Sigma, \{g_l\}), \quad (10)$$

where $\{g_l\}$ is the set of iterated functions on the global Poincaré section Σ . We also use the following schematic expression, which is similar to expression (7):

$$\{I_l\} \rightarrow \{D_{cl}\} \rightarrow \{D_{dl}\}. \quad (11)$$

3.3. Excited Attractor

In this paper, we are considering a continuous dynamical system that is dissipative and has an attractor for a periodic input. When an input pattern is fed into the system repeatedly, i.e., in the case of periodic input, a trajectory converges to an attractor. But how do we describe the dynamics when the inputs are switched stochastically? Even for an input with finite interval, we can assume an attractor corresponding to a periodic input with infinite interval. We call this an *excited attractor* in order to emphasize that the attractor is excited by the external input. Although a trajectory tends to converge to a corresponding excited attractor, the trajectory cannot reach the excited attractor due

to the finite time interval. If the next input is the same as the previous one, the trajectory again goes toward the same excited attractor. If the next input is different from the previous one, the trajectory changes its direction and goes toward an excited attractor distinct from the previous one. Continuing this process, the trajectory takes a transient path to the excited attractors. Intuitively, the trajectory will be spread out around excited attractors in the hyper-cylindrical phase space \mathcal{M} . How, then, do we characterize the properties of the transient trajectory?

4. Fractal Transition

4.1. Iterated Function System

In the following two sections, we focus on the set $\{g_l\}$ of iterated functions on the global Poincaré section Σ .

4.1.1. Hutchinson's Theory

Hutchinson [8] has proved that a set $\{h_l\}$ of iterated functions, which are not limited on the Poincaré section, defines a unique and invariant set C that satisfies the following equation:

$$C = \bigcup_{l=1}^L h_l(C), \quad (12)$$

where

$$\bigcup_{l=1}^L h_l(C) = h_1(C) \cup h_2(C) \cup \dots \cup h_L(C),$$

and

$$h_l(C) = \bigcup_{x \in C} h_l(x).$$

Such an invariant set C is often a fractal or sometimes used as a mathematical definition of various fractals.

A sufficient condition for satisfying Eq. (12) is the *contraction* property of h_l for all $l = 1, 2, \dots, L$. The contraction for h_l is definitely defined by the Lipschitz constant $Lip(h_l)$:

$$Lip(h_l) = \sup_{x_i \neq x_j} \frac{d(h_l(x_i), h_l(x_j))}{d(x_i, x_j)}, \quad (13)$$

where d is a distance on a metric space. When

$$Lip(h_l) < 1,$$

the map $h_l : x \rightarrow x$ is called the *contraction* or the *contraction map*.

4.1.2. Iterated Function System with Probabilities

Barnsley has named a set $\{h_l\}$ as the IFS (*Iterated Function System*) [9]. He introduced the *IFS with probabilities* as follows:

$$(\{h_l\}, \{p_l\}), \quad (14)$$

where $\{p_l\}$ is a set of probabilities corresponding to $\{h_l\}$.

Based on the IFS with probabilities, he proposed an alternative method for constructing the invariant set C that satisfies Eq. (12). The iterated functions h_l are switched with probabilities p_l for $l = 1, 2, \dots, L$ as follows. Choose an initial point and then choose recursively and independently $x_{\tau+1} \in \{h_1(x_\tau), h_2(x_\tau), \dots, h_L(x_\tau)\}$ for $\tau = 0, 1, 2, \dots, \infty$, where the probability of the event $x_{\tau+1} = h_l(x_\tau)$ is p_l . Thus a sequence constructs a set $\{x_n\}_{n=0}^\infty$. Using Hutchinson's theory, Barnsley has shown that the set $\{x_n\}_{n=0}^\infty$ constructed by random sequence, and here assumed to have equal probability, "converges to" the set C defined by Eq. (12) when all iterated functions are the contractions. The set $\{x_n\}_{n=0}^\infty$ is thus an approximation of C .

4.2. Vector Field System

We are now ready to consider the trajectory of continuous dissipative dynamical systems excited by the temporal inputs. When the inputs I_l are stochastically fed into the system one after another, the vector fields f_l and the iterated functions g_l are also stochastically switched as explained in Sec. 3. To emphasize the relation among the set $\{I_l\}$, $\{f_l\}$ and $\{g_l\}$, we use the following schematic expression instead of expression (11):

$$\{I_l\} \rightarrow \{f_l\} \rightarrow \{g_l\}. \quad (15)$$

We call the set $\{f_l\}$ the *Vector Field System (VFS)*, which is similar to the *Iterated Function System (IFS)* for the set $\{g_l\}$. The discrete dynamics on the Poincaré section Σ correspond to the random iteration algorithm using the IFS with probabilities. That is, when all iterated functions g_l are the contractions, the state x_τ on the Poincaré section approximately changes on the invariant set C defined by Eq. (12) after sufficient random iterations. The property of the set C having the fractal structure affects the trajectory in the hyper-cylindrical phase space \mathcal{M} .

The trajectory set $\Gamma(C)$ corresponding to the input set $\{I_l\}$ is obtained by the union of the trajectory set $\gamma_l(C)$ for each input I_l :

$$\begin{aligned} \Gamma(C) &= \bigcup_{l=1}^L \gamma_l(C), \\ &= \gamma_1(C) \cup \gamma_2(C) \cup \dots \cup \gamma_L(C). \end{aligned} \quad (16)$$

We can conclude that the dissipative dynamical systems excited by plural temporal inputs are characterized by the trajectory set $\Gamma(C)$ starting from the initial set C defined by Eq. (12). All of the trajectories are considered to represent the transition between the excited attractors. We call this the *fractal transition between the excited attractors*. At this point, we should emphasize that the contraction property of iterated functions defined on the Poincaré section is a *sufficient*, but not *necessary*, condition for the fractal transition.

5. Simple Example

In this section a simple example is shown using the solvable class of the following two dimensional linear ODE with additive input [7].

$$\dot{x} = Ax + I_l(t), \quad (17)$$

where

$$A = \begin{pmatrix} \lambda & 0 \\ 0 & \lambda \end{pmatrix}, \quad I_l(t) = \sin \frac{2\pi}{T_l} t \begin{pmatrix} b_{1,l} \\ b_{2,l} \end{pmatrix},$$

$$\lambda < 0.$$

The corresponding mapping at period T_l can be easily obtained:

$$x_{\tau+1} = A_l x_\tau + B_l, \quad (18)$$

where

$$A_l = \begin{pmatrix} e^{\lambda T_l} & 0 \\ 0 & e^{\lambda T_l} \end{pmatrix}, \quad B_l = \frac{2\pi T_l}{\lambda^2 T_l^2 + 4\pi^2} (e^{\lambda T_l} - 1) \begin{pmatrix} b_{1,l} \\ b_{2,l} \end{pmatrix}.$$

The Lipschitz constant is obtained as follows:

$$\text{Lip}(g_l) = e^{\lambda T_l} < 1. \quad (19)$$

This shows that the map is a contraction. Therefore a fractal is constructed on the Poincaré section. The similarity dimension, one of fractal dimension, is obtained as follows:

$$d = \frac{-\ln 3}{\lambda T}. \quad (20)$$

This shows that the dimension is proportional to $1/\lambda T$ while it is independent of input amplitude b . Figure 1 is the λ -dependence of the dimension d . The solid curve is the dimension calculated by Eq. (20), which shows good agreement with the correlation dimension obtained numerically using log-log plot in the totally disconnected region.

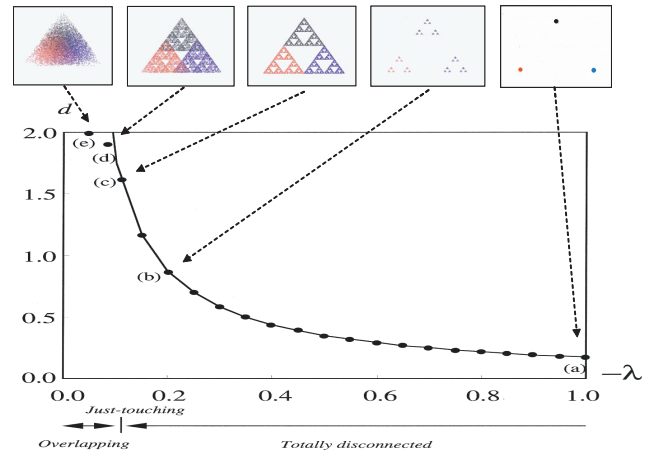


Figure 1: λ -dependence of the dimension d .

In the overlapping region, however, the solid curve gradually deviated from the correlation dimension. This is because the dimension of the Poincaré section is the ceiling of 2. The above figures denoted (a), (b), (c), (d), and (e) are examples obtained at the Poincaré section. (a) and (b) are totally disconnected, i.e., clusters of the same color are completely separated from each other. (d) and (e) are overlapping, i.e., the clusters partially overlap each other. (c) is just-touching, i.e., the clusters touch each other at a single point. Although this is a simple example using a linear equation, a nonlinear equation also shows similar characteristics of fractals [10]. Recently we derived multi-fractal formalism under some condition. The result is as follows:

$$D_q = \frac{n}{q-1} \frac{\ln \sum_{i=1}^N p_i^q}{\lambda T}, \quad (21)$$

where D_q , n , N , λ , T , and p_i are general dimension of q , number of states, number of inputs, statistical contraction, time length of inputs, and probability of i -th input, respectively.

6. Discussion

In this paper a theoretical framework is reviewed for the continuous dynamical systems stochastically excited by external temporal inputs. In this section we discuss some related works. More general theory has been presented in order to model complex systems that interact strongly with other systems. It has been revealed that these dynamics are generally characterized by fractals when the iterated functions are not the contractions [10]. The hierarchical structure of fractals and the noise effect of inputs have been investigated [7]. The fractals generated by switching vector fields have been observed in different domains such as a forced damped oscillator [11], an electronic circuit [12], artificial neural networks [13], and human behavior [14]. Closure of the fractals in both linear [15] and non-linear systems [16] has been also presented. A set of attractors obtained by periodic inputs can approximate trajectories of fractals [17]. These works show that fractals are indispensable for understanding of dynamics observed in the Hybrid Dynamical Systems as a complex system.

References

- [1] A. S. Matvee and A. V. Savkin, *Qualitative theory of hybrid dynamical systems*, Birkhauser, Boston, 2000.
- [2] H. E. Garcia, A. Ray, and R. M. Edwards, "A reconfigurable hybrid systems and its application to power plant control," *IEEE Trans. Control Systems Technology*, Vol.3, pp.157-170, 1982.
- [3] B. Lennartson, B. Egardt, and M. Tittus, "Hybrid systems in process control", *Proc. 33rd CDC*, pp.3587-3592, 1994.
- [4] J. Guckenheimer and S. D. Johnson, "Planar hybrid systems", in *Hybrid Systems II: Lecture Notes in Computer Science*, vol.999, pp.202-225, Springer-Verlag, 1995.
- [5] S. D. Johnson, "Simple hybrid systems", *Int. J. Bifurcation and Chaos*, vol.4, pp.1655-1665, 1994.
- [6] M. S. Branicky, "Multiple Lyapunov functions and other analysis tools for switched and hybrid systems", *IEEE Trans. Automatic Control*, vol.43, pp.475-482, 1998.
- [7] K. Gohara and A. Okuyama, "Fractal Transition - Hierarchical Structure and Noise Effect", *Fractals*, vol.7(3), pp.313-326, 1999.
- [8] J. Hutchinson, "Fractals and self-similarity", *Indiana Journal of Mathematics*, vol.30, pp.713-747, 1981.
- [9] M. F. Barnsley, *Fractals Everywhere*, Academic Press, Boston, 1988.
- [10] K. Gohara and A. Okuyama, "Dynamical Systems Excited by Temporal Inputs: Fractal Transition between Excited Attractors", *Fractals*, vol.7(2), pp.205-220, 1999.
- [11] K. Gohara, H. Sakurai, and S. Sato, "Experimental Verification for Fractal Transition Using a Forced Damped Oscillator", *Fractals*, vol.8(1), pp.67-72, 2000.
- [12] J. Nishikawa and K. Gohara, "Fractals in an Electronic Circuit Driven by Switching Inputs", *Int. J. Bifurcation and Chaos*, vol.12(4), pp.827-834, 2002.
- [13] S. Sato and K. Gohara, "Fractal Transition in Continuous Recurrent Neural Networks", *Int. J. Bifurcation and Chaos*, vol.11(2), pp.421-434, 2001.
- [14] Y. Yamamoto and K. Gohara, "Continuous Hitting Movements Modeled from the Perspective of Dynamical Systems with Temporal Input", *Human Movement Science*, vol.19(3), pp.341-371, 2000.
- [15] R. Wada and K. Gohara, "Fractals and Closures of Linear Dynamical Systems Stochastically Excited by Temporal Inputs", *Int. J. Bifurcation and Chaos*, vol.11(3), pp.755-779, 2001.
- [16] R. Wada and K. Gohara, "Closures of Fractal Sets in Non-linear Dynamical Systems with Switched Inputs", *Int. J. Bifurcation and Chaos*, vol.11(8), pp.2205-2215, 2001.
- [17] H. Oka and K. Gohara, "Approximation of the Fractal Transition Using Attractors Excited by Periodic Inputs", *Int. J. Bifurcation and Chaos*, vol.13(4), pp.943-950, 2003.

The Role of Limbic System for Mobiligence

Ichiro Tsuda* and Yutaka Yamaguti**

**Research Institute for Electronic Science, Hokkaido University, Sapporo, 060-0812, Japan

***Department of Mathematics, School of Science, Hokkaido University, Sapporo, 060-0810, Japan

Abstract—Motivated by Freeman’s theory on the creation of intentional intelligence which is represented by five specific loops of information flow, we develop the theory on the mechanism of creation and annihilation of mobiligence in terms of the modified loops of information called “mobiligence loop”. In order to establish the embodiment, which is assumed to appear in the process of formation of the sense of “now” in the body, we introduced a new concept, refference copy, and describe its relation with efference copy of von Holst. Based on this theory, we developed a mathematical model for the hippocampus since the hippocampus plays a decisive role of the formation of episodic memory that is viewed as a remembering process of past experience and imagining process of future as well. This suggests that the hippocampus may create a sense of “now”. We found a Cantor set in a model CA1 neural nets, where the Cantor set represents the time series of events hierarchically, according to the history of time series. We further observed affine transformations which are emerged in the network so as to produce a Cantor set.

I. INFORMATION LOOP IN MOBILIGENCE

The aim of this study is to obtain a new insight for the mechanism of creation and annihilation of intelligence by movements, that is, “mobiligence”, taking into account the role of limbic system in that mechanism. As is shown in Fig. 1, Walter J. Freeman considered five specific loops of information flow by which the acquisition of intelligence becomes possible. Animals and men search the environment actively by using motor cortex, cerebellum cortex, or basal ganglia, and sense its response from environment via receptors. This information is sent to the entorhinal cortex as sensory information and back to the motor system. This is called a motor loop. Since the body is used for movement, a control loop must act to control the body via the motor system. Furthermore, a refferent loop to the sensory systems from the body works as a proprioceptive loop. A spatio-temporal loop as an interaction system between the entorhinal cortex and the hippocampus participates in these processes.

Based on this Freeman’s idea, we tried to construct

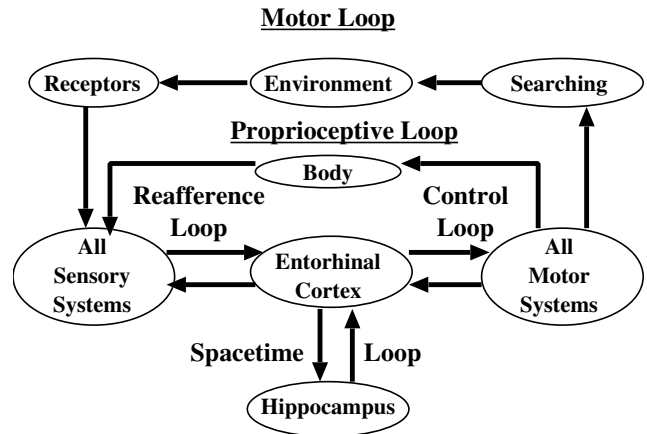


Fig. 1. The multiple feedback loops of the limbic system. (Modified from Freeman[1].)

a “mobiligence loop”, as shown in Fig. 2. For the first time, we introduced efference copy as an internal image as for the response of the receptors to the body movement in the environment. This definition seems to be slightly different from the original definition of von Holst that the sensory systems utilize exactly negative image of the response in order to match the response with the anticipated one[2], but essentially the same in the following sense. An efference copy can be used not only for the judgment of the correctness of the present motor pattern, but also for extracting the difference of the effect to the body between in active and voluntary movements and in passive movements, by which the embodiment as harnessing of sensory-motor systems can be established.

There seems to be at least two roles of efference copy. One is to copy the response stemming from the existence of body in order to distinguish it from the response stemming purely from the environment. Other one is to find the difference between subjective embodiment and objective response of the body to stimulus. However, the latter seems to be difficult to be established only by efference copy in the above sense. Then, we need another concept, say called “refference

copy " as information for the control of body by interpreting efference copy. For the establishment of these loops, not only proprioceptive loop but interoceptive loop is necessary.

Based on this theory, we developed a mathematical model for the hippocampus since the hippocampus plays a decisive role of the formation of episodic memory that is viewed as a remembering process of past experience and imagining process of future as well. This suggests that the hippocampus may create a sense of "now". We constructed, in particular, a neural network model for CA1, thereby we studied a mechanism of coding of time series of temporal patterns.

II. MATHEMATICAL MODEL FOR THE HIPPOCAMPAL CA1

A. Network

Fig. 3(a) shows the CA1 network which receives the CA3 output. We assume that the input temporal series of firing patterns to CA1 is a temporal series of evoked attractors embedded in CA3, which may represent a series of events, that is, an episode. In the present model of CA3 which consists of N_{ca3} pyramidal cells, it is assumed that M firing patterns denoted by $X(0), \dots, X(M-1)$ is stored in the networks via Hebbian learning algorithm as event memories. Each stored pattern can be represented by an attractor in the state space of neural activity.

The pyramidal cells of CA1 receive such activity via both AMPA- and NMDA- receptors. We also assume that the synaptic strengths from CA3 to CA1 is accomplished by Hebbian learning. More specifically, the synaptic strength, w_{ij} of j -th neuron of CA1 from the i -th neuron of CA3 is given by the following expression:

$$w_{ij} = S_{\max} \sum_{k=0}^{M-1} X_i(k)Y_j(k), \quad (1)$$

where $X_i(k)$ denotes the activity of i -th neuron in CA3, and $Y_j(k)$ the activity of j -th neuron in CA1 for both input pattern k , and S_{\max} is an adjustable parameter for controlling the input strength. Here, we treat only the case that the network consists of only pyramidal cells and no explicit connections between CA1 neurons.

B. Neuron model

We used two-compartment model proposed by Pinsky and Rinzel[6]. This model can represent the electric properties of dendrite and cell body, each of which is

assumed to be electrically uniform. The equations of model neuron are given as follows:

$$C_m V_s' = -I_{Leak}(V_s) - I_{Na}(V_s, h) - I_{K-DR}(V_s, n) + (g_c/p)(V_d - V_s) + I_s/p \quad (2a)$$

$$C_m V_d' = -I_{Leak}(V_d) - I_{Ca}(V_d, s) - I_{K-AHP}(V_d, q) - I_{K-C}(V_d, Ca, c) - I_{Syn}/(1-p) + (g_c/(1-p))(V_s - V_d) + I_d/(1-p), \quad (2b)$$

where V_s and V_d are the membrane potential of cell body and dendrite, respectively. C_m is conductance of membrane, each I_z is an ionic current associated with each kind of ionic channels, I_{Syn} is a synaptic current, g_c is a conductance, and p is a ratio of the surface area of cell body with the whole cell area.

C. Encoding of sequences

We investigated how the temporal sequences can be encoded in the membrane potential and/or spike events of CA1 neurons. It turns out that this system can be described by Iterated Function System (IFS)[7], because this CA1 neural network receives the input pattern series whose elementary pattern is selected with a certain probability.

III. RESULTS

A. Cantor coding

We obtained Cantor sets in membrane potential of CA1 neurons, each element of which actually represented a temporal series of input patterns. A Cantor set, generally, consists of self-similar clusters of the subsets. In this case, this hierarchical clustering of the subsets represent a depth of the temporal series, that is, history of event-series. This is typically shown in Fig. 4. Here, one question arises: how could the Cantor coding be generated? We investigated the return maps of the 1st and the 2nd principal components of membrane potentials. We obtained linear transformations, according to the input patterns, in both principal components. These are actually affine transformations, so that IFS (Iterated Function Systems)-like mechanism, which are generated in the network dynamics as one of the emergent properties of the system, yields the Cantor sets of membrane potential.

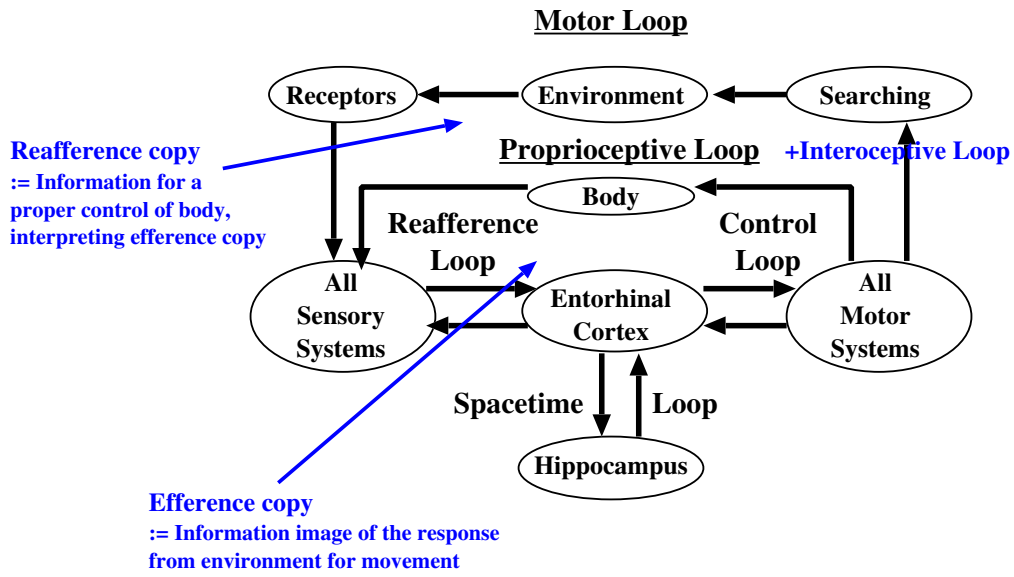


Fig. 2. The mobiligence loop.

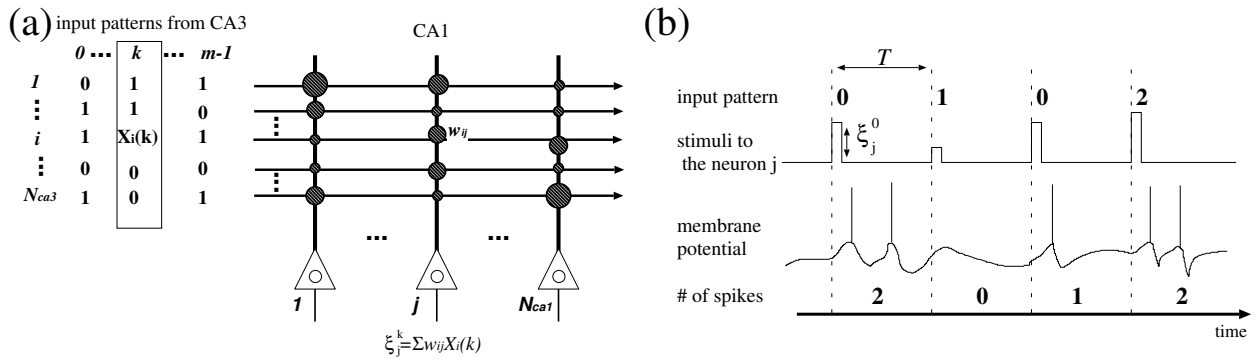


Fig. 3. The schematic representation of the CA1 model. (a) Network connections. (b) Inputs and responses of a CA1 neuron.

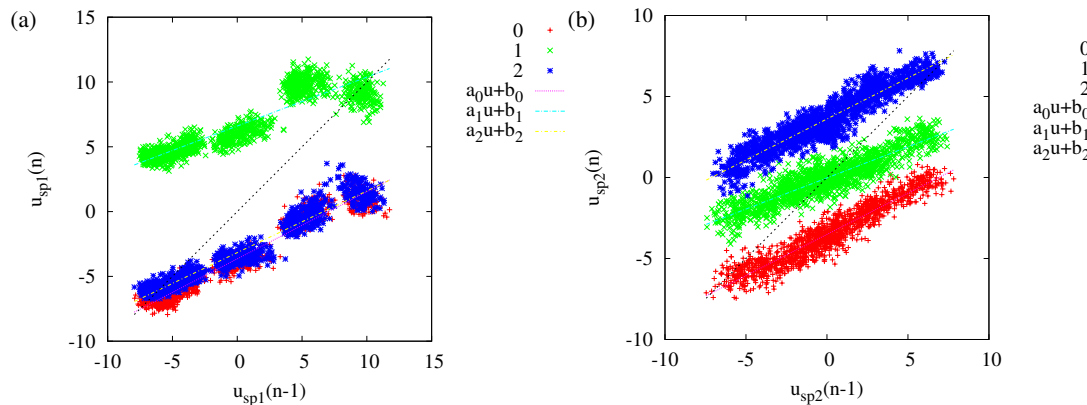


Fig. 5. Return maps of the principal components. First(a) and second(b) components. $m = 3, T = 80$, and $S_{max} = 1.2$.

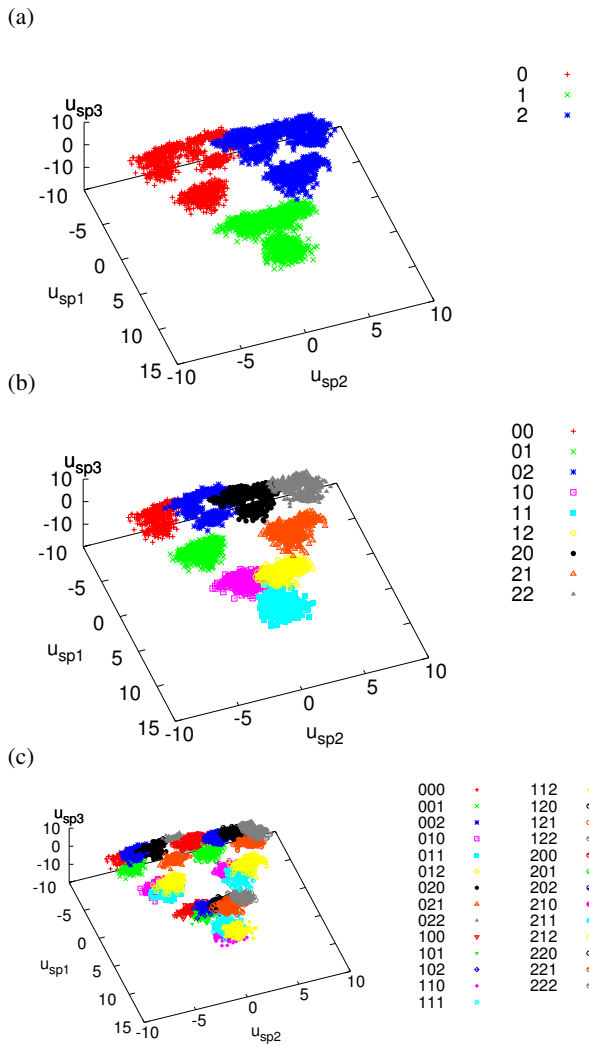


Fig. 4. An example of Cantor coding in CA1 model. Self-similar structures are shown in the phase space. $m = 3, T = 80$, and $S_{max} = 1.2$.

B. Performance

Fig. 6 shows the performance of the coding scheme obtained here. It turned out that the Cantor coding sensitively depends on the input strength and the interval of input sequence. This suggests that the strength of episode and the timing of input events in the hippocampus will be decisive for the learning of episode.

REFERENCES

[1] W. J. Freeman, *How Brains Make up Their Minds*, London, Weidenfeld & Nicolson, 1999.
 [2] E. von Holst and H. Mittelstaedt, "Das Reafferenzprinzip", *Naturwissenschaften*, 37, 1950, pp 464-476.
 [3] I. Tsuda and S. Kuroda, "Cantor coding in the hippocampus", *Japan J. of Industrial and Applied Mathematics*, 18, 2001, pp 249-258.

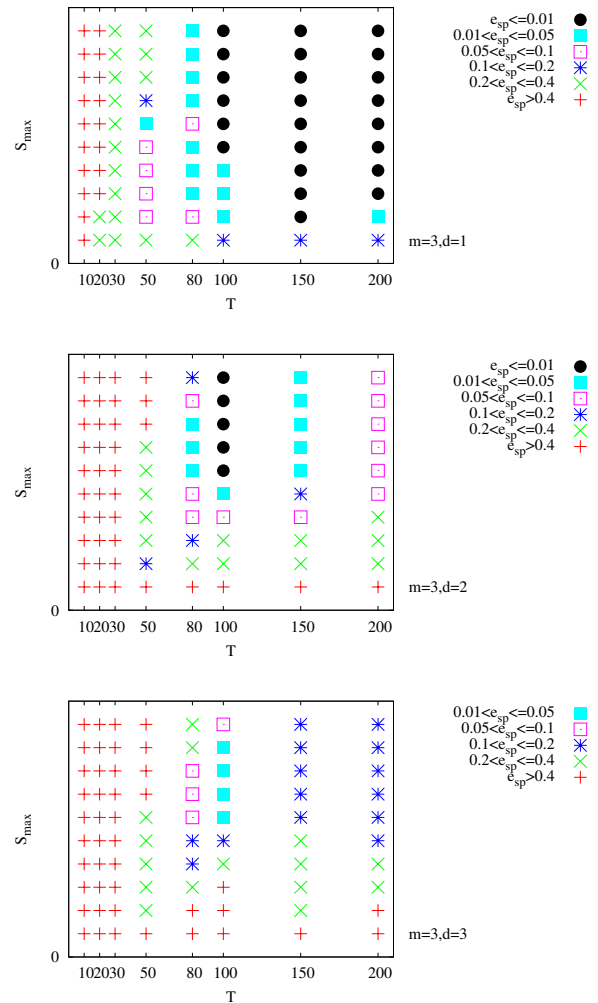


Fig. 6. Performance of the Cantor coding in the model as a function of interval of input sequences and input strength. A smaller value of e means better performance.

[4] I. Tsuda, "Toward an interpretation of dynamic neural activity in terms of chaotic dynamical systems", *Behavioral and Brain Sciences* 24, 2001, pp 793-847.
 [5] J. K. Ryeu, K. Aihara and I. Tsuda, "Fractal encoding in a chaotic neural network", *Phys. Rev. E*, 64, 2001, 046202:1-6.
 [6] P. F. Pinsky and J. Rinzel, Intrinsic and Network Rhythmogenesis in a Reduced Traub Model for CA3 Neurons, *J. Comp. Neurosci.*, 1, 1994, pp39-60.
 [7] M. F. Barnsley, *Fractals Everywhere*, Academic Press, 1988.

Computational model of neural systems for learning causality of external events and performing actions

Toshio Aoyagi

Department of Applied Analysis and Complex Dynamical Systems, Graduate School of Informatics,
Kyoto University, Kyoto, Japan

Abstract

Many theoretical and experimental studies of the brain address understanding of how the brain works. For this purpose, one of the most important challenges in neuroscience is to discover a way to decode the neuronal activity, for example, to translate the signals into action. Among various neuronal activity patterns, synchronous activity associated with behaviour and cognition has been observed in many neuronal systems. In this study, we first demonstrate that a network organized under spike-timing dependent plasticity (STDP), not only is capable of memorizing the activity patterns of the external stimulus, but also exhibits a systematic transition behavior among the memorized patterns in response to uniform external synchronized spikes. Next, we attempt to decode multi-neuronal spike activities which were recorded from the hippocampus CA1 region of rats, in which the rats were trained to perform a conditional discrimination task. In this analysis, we use two statistical methods: a kernel k-means clustering and a kernel PCA. As a result, we found that the behaviors of rats can be predicted by suitable finite sequences of the multi-neuronal spiking patterns.

I. INTRODUCTION

One of the most important challenges in neuroscience is to discover a way to decode the neuronal activity, for example, to predict the decisions, choices, behaviors. In particular, synchronous activity associated with behavior and cognition has been observed in many neuronal systems [1], [2], [3]. However, its functional role remains unclear [4], [5]. It is reasonable to assume that such generated synchronous spikes drive certain cortical networks as input signals and thereby affect their functions. Another related phenomenon is spike-timing dependent plasticity (STDP) [6], [7], [8], which allows cortical networks to learn the causality of experienced events through the coding of the temporal structures of neuronal activity. Considering that both phenomena affect the functioning of cortical neurons, it is natural to ask what effect synchronous inputs have on a neural network organized under STDP learning. For this purpose, let us consider the specific situation in which a model network of spiking neurons, whose synaptic connections are modified through STDP, receives an activity pattern as an external stimulus as a result of the experiencing of some external events.

II. EXPLORING ROLE OF SYNCHRONY IN BRAIN SYSTEMS

A. A network of spiking neurons with STDP

Figure 1a presents a schematic illustration of the model network we consider, in which leaky integrate-and-fire neurons are recurrently connected by excitatory synapses whose coupling strengths are modified according to the STDP rule. Thus, if a presynaptic spike and a postsynaptic spike occur at times t_{pre} and t_{post} , the peak synaptic conductance g is modified by the addition of the value of the STDP window function $F(t_{\text{pre}} - t_{\text{post}})$ as shown in Figure 1b. The synaptic conductance g is restricted to lie within the range 0 to g_{max}^E . To enforce this restriction, if the STDP rule would cause g to take a value outside this range, it is reset to the appropriate limiting value. In addition, a globally uniform inhibition without modification of learning is included in an all-to-all manner.

We employ two types of controllable external inputs. One is a stimulus input, in which an initial stimulus-pattern and a training stimulus-pattern are presented during a trial and a learning session, respectively. For learning, we use a simple training stimulus-pattern, as depicted in Figure 1c. This pattern is divided into three

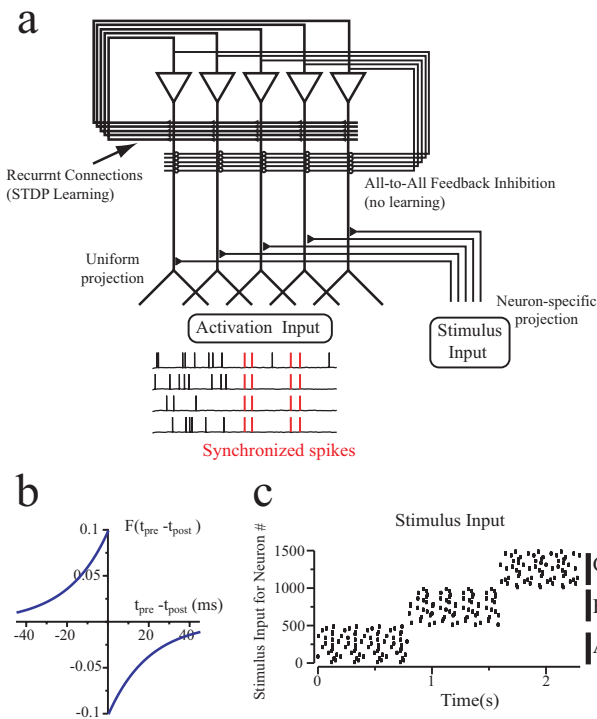


Fig. 1. (A) Structure of the network model with spike-timing dependent plasticity (STDP). (B) The STDP window function. (C) The activity pattern presented by the stimulus input during learning. Each dot represents a spike presented in the corresponding stimulus input. This whole pattern consists of three basic firing patterns in the fixed order A,B,C,A,B,C...

parts consisting of firing patterns referred to as A, B and C, in which each composed of a particular set of active neurons. These neurons that are active for a given pattern fire periodically, and in each pattern, there are certain fixed phase relationships among the active neurons. During learning, these three patterns are presented as the stimulus input (Figure 1a) in the fixed order (A,B,C,A,B,C...). This can be regarded as representing a certain external sequence of events that the network is to learn, in other words, the causality of certain external events.

The other type of controllable input is an activation input, which projects to all neurons uniformly. This input is introduced to examine the effect of synchrony on the neuronal dynamics. This uniform background input serves to activate the entire network and to allow each neuron to be in a firing state under suitable conditions. There are two modes of neuronal activity for the activation input: asynchronous and synchronous modes. In the asynchronous mode, spike trains are randomly generated by a Poisson process. During learning, the activation input is always in the asynchronous mode.

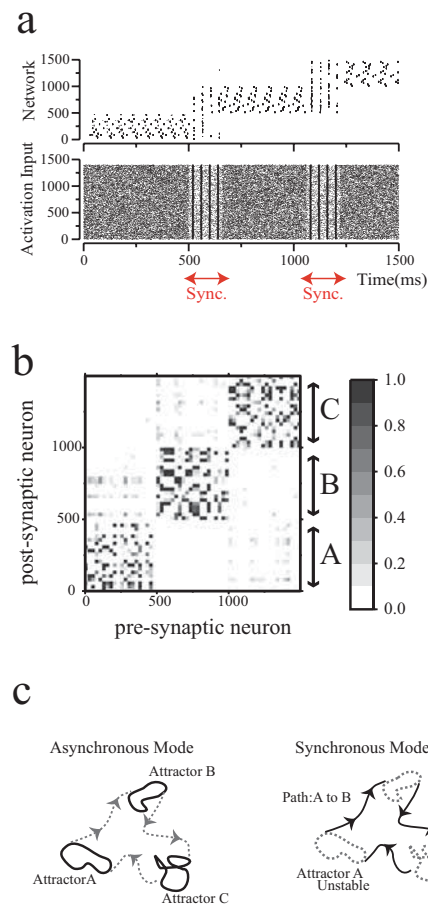


Fig. 2. Typical effect of a uniformly synchronized spike input on the network of spiking neurons organized under the STDP learning rule. a. Synchrony-induced switching behavior of the network realized through the STDP learning rule. b. Grayscale plot of the normalized strengths of excitatory synapses between neurons after the STDP learning. c. Interpretation of the synchrony-induced switching behavior from the point of view of dynamical systems.

In the synchronous mode, some of the neurons fire synchronously, while the other neurons remain in the asynchronous firing state. The fraction of neurons firing synchronously represents the degree of synchrony. To remove the influence of firing rate modulation, in both modes, the average firing rate is set to the same constant value, 25Hz.

B. A role of uniformly synchronous inputs

The main question of interest in this study is the following: after the STDP learning process described above has been completed, what activity pattern does the resultant network exhibit? To answer this question, we first examine the case in which the activation input is initially set in the asynchronous mode, with the level of the total current such that the neurons are in

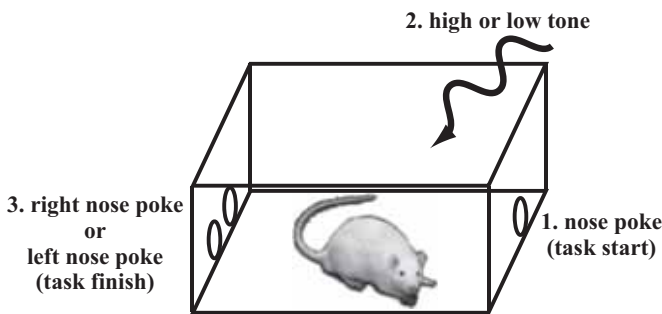


Fig. 3. Schematic illustration of the conditional discrimination task

an active state in response to an appropriate stimulus input and maintain an active state through recurrent excitatory synapses organized under the STDP. Figure 2a illustrates some typical activity patterns displayed by the network (top) and the activation input (bottom) as rasterplots. First, the network exhibits the pattern A, which is stable when the activation input is in the asynchronous mode. Thus, in this case, the network exhibits ordinary associative memory. In Figure 2b, we can see clearly that three diagonal blocks of major synaptic connections, which are formed by the three basic stimulus patterns (A,B,C), enable the network to retrieve each pattern in an associative manner. In addition, there are three off-diagonal blocks of weak synaptic connections arising from the less frequent transitions among the stimulus patterns as shown in Figure 1c. Because the synaptic connections for transitions are relatively weak, under ordinary conditions, each individual pattern is sufficiently stable that no transition among patterns occurs.

Interestingly, Figure 2a demonstrates that a brief period of synchrony in the uniform activation input can enhance this weak effect embedded in the synaptic matrix and can thereby cause a transition from the one pattern to another. Therefore, when the activation input is switched for a brief time to the synchronous mode, a transition from the pattern A to the pattern B occurs. Hence, the retrieval of a learned sequence in the presented order can be triggered by globally uniform synchronous inputs. From the perspective of dynamical systems, when the network is activated by a uniformly asynchronous spike input, the system possesses some attractors formed by the STDP learning rule (Figure 2c left). However, a brief uniformly synchronous input activates the paths between attractors, leading to a transition to the next pattern in the learned order (Figure 2c right).

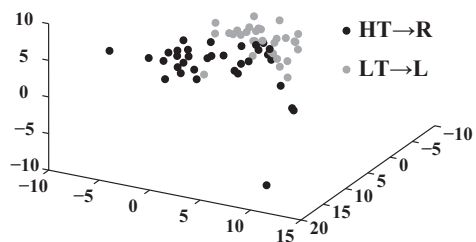


Fig. 4. Results obtained by applying the kernel PCA

III. DECODING REAL NEURONAL SIGNALS IN BRAIN

Multiple electrodes are currently standard tools in neuroscience, which enable us to study the simultaneous activity of multiple neurons in a given brain regions. The information coding in the brain is still a controversial issue, particularly, how does multiple neurons work in concert to realize specific brain functions? In this context, we need to design statistical methods that allow us to perform multivariate analysis of multiple spike train data. Multi-neuronal spike trains of behavioral animals can be obtained on-line [9]. Furthermore, the brain machine interfaces, the technologies for directly controlling robots by decoding the brain activities, have been developed intensively, although coding scheme in higher brain functions is left unknown [10]. This experimental new paradigm is very important not only from the medical point of view, but also for providing us a clue to reveal the coding mechanism in the brain.

A. Experimental Data

The data used in this study were recorded from a tetrode introduced in the hippocampus CA1 region of rats. In the learning periods, the rats were conditioned to poke the right (left) hole when they heard a high (low) tone, as illustrated in Figure 3. During the recording periods, rats performed the conditional discrimination task after the learning was completed. The sampling rate of the recording was 20kHz. The multi-neuronal spike activities were obtained by applying the spike sorting technique to the raw data [9].

B. Statistical Analysis

The kernel method, one of the powerful methods for discovering a common feature among data sets, has been studied and applied widely to various real problems, for example, bio-informatics, character recognition, pattern recognition and so on [11][12]. In this study, we apply the kernel method to multi-neuronal spike data recorded from rats, in which the rats are

trained to perform a conditional discrimination task. We here use the kernel developed by Shpigelman et al. [13]. This kernel (Spikernel) is designed to measure a similarity between two of multi-neuronal spike sequences in a natural sense (See [13] in detail).

C. Result

First, the matrix of the kernel functions calculated from a multi-neuronal spike count data set. we pre-processed a raw multi-neuronal spike data into multi-neuronal spike count data with bin of 100ms. We apply the kernel k-means clustering method by using this kernel matrices. Examining some available sample data sets, at the best performance, we found that two discrimination behaviors (high-tone to right-poke and low-tone to left-poke) can be separated with 76% accuracy.

In this best case, the kernel-PCA is applied so as to visualize how the two behaviors are expressed in the kernel feature space. In Fig. 4, we plot two behaviors in three dimensional feature space spanned by the eigenvectors corresponding to the three largest eigenvalues obtained from the kernel PCA. We can see that, even if we do not know a behavior of rats, the behavior of the rat could be predicted from seeing which cluster the data point belongs to in the feature space.

IV. CONCLUSIONS AND FUTURE WORKS

The first results suggest that synchronous spikes may act as a signal in biological systems, serving to link learned sequences of actions in response to some external stimuli [2], [14]. Our results suggest that one possible functional role of neuronal synchrony is to control the flow of information by changing the nature of the dynamical system constituted by a set of neuronal circuits. We believe that some experimental results can be more clearly reinterpreted using our results.

Second, we demonstrated the kernel based analysis with two data sets recorded from the hippocampus CA1 region of rats performing the conditional discrimination task. As a result, we found that the behavior of the rats can be predicted on the kernel feature space mapped from multi-neuronal spike trains, However, we have to admit that the more data is needed for the reliable conclusion and the kernel parameters should be searched for the best performance. We will study these issues in the near future.

V. ACKNOWLEDGMENTS

I thank M. Nomura and T. Aoki who participated in this study. I am also grateful to Y. Sakurai for conducting the preliminary BMI experiments..

REFERENCES

- [1] C. M. Gray, P. Konig, A. K. Engel, and W. Singer, "Oscillatory responses in cat visual cortex exhibit inter-columnar synchronization which reflects global stimulus properties." *Nature*, vol. 338, pp. 334–337, 1989.
- [2] A. Riehle, S. Grun, M. Diesmann, and A. Aertsen, "Spike synchronization and rate modulation differentially involved in motor cortical function." *Science*, vol. 278, pp. 1950–1953, 1997.
- [3] P. Fries, J. H. Reynolds, A. E. Rorie, and R. Desimone, "Modulation of oscillatory neuronal synchronization by selective visual attention." *Science*, vol. 291, pp. 1560–1563, 2001.
- [4] A. K. Engel, P. Fries, and W. Singer, "Dynamic predictions: oscillations and synchrony in top-down processing." *Nat. Rev. Neurosci.*, vol. 2, pp. 704–716, 2001.
- [5] E. Salinas and T. J. Sejnowski, "Correlated neuronal activity and the flow of neural information." *Nat. Rev. Neurosci.*, vol. 2, pp. 539–550, 2001.
- [6] G. Q. Bi and M. M. Poo, "Synaptic modifications in cultured hippocampal neurons: dependence on spike timing, synaptic strength, and postsynaptic cell type." *J. Neurosci.*, vol. 18, pp. 10464–10472, 1998.
- [7] L. I. Zhang, H. W. Tao, C. E. Holt, W. A. Harris, and M. Poo, "A critical window for cooperation and competition among developing retinotectal synapses." *Nature*, vol. 395, pp. 37–44, 1998.
- [8] H. Markram, J. Lubke, M. Frotscher, and B. Sakmann, "Regulation of synaptic efficacy by coincidence of postsynaptic apss and epsps." *Science*, vol. 275, pp. 213–215, 1997.
- [9] S. Takahashi and Y. Sakurai, "Real-time and automatic sorting of multi-neuronal activity for sub-millisecond interactions in vivo." *Neurosci.*, vol. 134, pp. 301–315, 2005.
- [10] M. A. L. Nicolelis, "Actions from thoughts," *Nature*, vol. 409, pp. 403–407, 2001.
- [11] B. Scholkopf and A. J. Smola, *Learning With Kernels: Support Vector Machines, Regularization, Optimization and Beyond*, ser. Adaptive Computation and Machine Learning. MIT Press, 2001.
- [12] J. Shawe-Taylor and N. Cristianini, *Kernel Methods for Pattern Analysis*. Cambridge University Press, 2004.
- [13] L. Shpigelman, Y. Singer, R. Paz, and E. Vaadia, "Spikernels: Predicting arm movements by embedding population spike rate patterns in inner-product spaces," *Neural Comput.*, vol. 17, pp. 671–690, 2005.
- [14] D. Lee, "Coherent oscillations in neuronal activity of the supplementary motor area during a visuomotor task." *J. Neurosci.*, vol. 23, pp. 6798–6809, 2003.

Basic strategy for trajectory planning in human movements

Jun NISHII
Yamaguchi University

I. INTRODUCTION

Living bodies show various kinds of movements in order to acquire energy, and the return which is determined by the balance of the energy cost of movements and obtained energy determines the probability of survival. The intelligence in movements and behaviors would be something which living bodies acquired through natural selection or learning in order to raise the return. In order to investigate the “something” in movements and behavior authors have investigated the problems: (1) how cooperative and altruistic behaviors can be explained from a view point of natural selection, and (2) what is an intelligence in movements of living bodies. In this paper I’ll introduce our recent results about the second topic.

In order to investigate the intelligence in movements of living bodies, it would be necessary to understand the movement itself, in other words, we should understand the basic strategy of living bodies to determine a movement by solving the problem of redundancy. The understanding of the basic strategy would be also necessary to investigate the adaptive or learning mechanisms which realize optimal movements under various environments.

If living bodies have accomplished many optimization through natural selection, the minimization of energy cost would be a candidate of basic strategy for the selection of a movement trajectory. The following sections introduce three studies of which purpose are to investigate the optimality of movements and to understand learning mechanism. (1) Does the swing trajectory during walking can be explained by the criteria of the minimization of the energy cost. (2) Does the reaching trajectory can be explained by the criteria of the minimization of the energy cost. (3) How do higher centers and the central pattern generator (CPG) cooperate and realize desired locomotor patterns.

II. OPTIMALITY OF LEG SWING TRAJECTORY DURING WALKING

How is the swing trajectory during human walking is planned? According to Becket and Chang (1967) [1], a study for this problem was found in 1830s and a hypothesis that is called as a pendulum hypothesis or a ballistic model was proposed. The hypothesis assumes that no joint torque is produced during swing and the leg swing motion is a kind of pendulum motion. This idea has attracted many researchers not only in biomechanics but also in robotics, which brought

Yamaguchi University, Faculty of Science, Yamaguchi University 1677-1 Yoshida, 753-8512 Yamaguchi, JAPAN, nishii@sci.yamaguchi-u.ac.jp

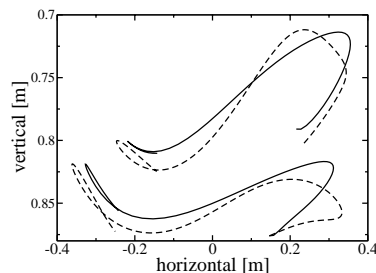


Fig. 1. Horizontal view of the trajectories of ankle joint (upper lines) and toe (lower lines) during 3 km/h walking. Walking direction is the left side of the figure. Solid lines show the measured trajectories and dashed lines shows the optimal ones which minimize the energy cost.

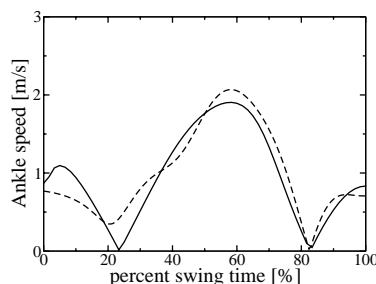


Fig. 2. Ankle speed during 3 km/h walking. Solid line shows the measured trajectory and dashed line shows the optimal one which minimizes the energy cost.

the idea of the passive walker by McGeer (1990) [2]. On the other hand, especially in recent years many experimental and computational analysis for the swing phase show the counterarguments for the ballistic model, e.g., the large joint torque at the end of swing causes the retraction of the foot [3], [4], which has been suggested as an important feature to obtain the stability of locomotion [5].

Authors have computed the optimal leg trajectory that minimizes the energy cost during the swing phase under the boundary condition that enables the smooth taking off and the grounding. The computed optimal trajectory is well coincident with measured trajectory in many aspects [6], [7]. However, the energy cost was estimated by assuming that the metabolic cost of a muscle activity shows the same property as a DC-motor, because the relation between the cost and a muscle activity during locomotion has not been known in physiological studies. Such estimation seems to show essential features of energy cost which consists of mechanical energy and heat energy loss, however, the computation of the optimal trajectory with other estimation

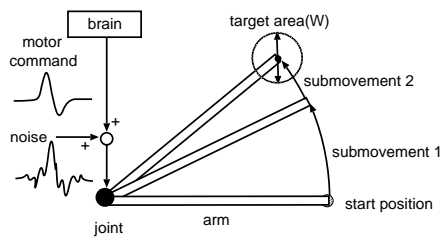


Fig. 3. Schematic view of an arm reaching movement.

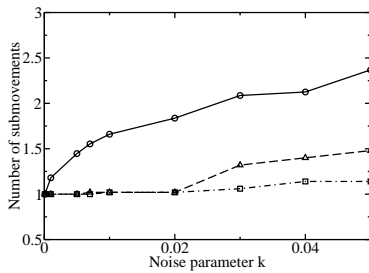


Fig. 4. Average numbers of corrective sub-movements required to reach the target area by criteria of minimization of the energy cost (○), the endpoint variance (△) and the torque change (□). The movement duration was determined by Fitts' law. The error bar shows the standard deviation.

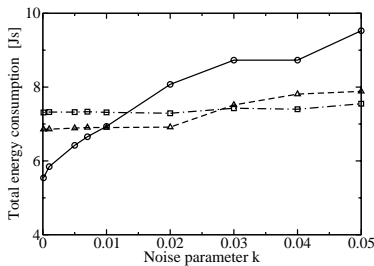


Fig. 5. Energy consumptions required to reach the target area by criteria of minimization of the energy cost (○), the endpoint variance (△) and the torque change (□). The movement duration was determined by Fitts' law. The error bar shows the standard deviation.

method of energy cost would be necessary in order to understand the essential feature of the optimal trajectory and to discuss the optimality of human leg swing trajectory. From such reason, we recomputed the optimal one by using the muscle model proposed by Alexander [8]. The results are well coincident with actual trajectories (Fig. 1 and 2), which suggest that the leg swing trajectory is well optimized on the energy cost. However, slight difference between optimal trajectory and actual one was observed at the leg trajectory during kick-off phase, which might reflect the spring factor of tendon. Therefore, the computation of optimal trajectory for total walking cycle including stance phase by considering the effect of tendon is an important future task.

III. OPTIMALITY OF ARM REACHING TRAJECTORY

It has been reported that arm trajectories during reaching movements are slightly curved and their speed profiles take bell shapes [9]. As criteria which determines such trajectory, minimum jerk model [10], minimum torque change model

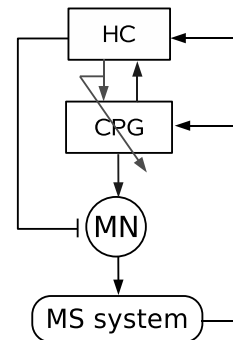


Fig. 6. A hierarchical control learning model by a higher center and the CPG. The higher center evaluates the result of movements and learns the control signal to the CPG. The CPG tunes its parameters so as to decrease the control signal from the higher center.

[11], and minimum end-point variance model [12] has been proposed. Especially the last criterion is interesting at the point that the noise could have a great influence on the planning of the trajectory.

On the other hand, minimum energy cost model was also investigated as a criterion which determines the reaching trajectory [8], [13], however, it has been reported that the trajectory which minimizes the energy cost differ from actual one in some aspects, e.g., the speed profile does not take a bell shape [13]. Does this result mean that reaching trajectories are determined by the factor of the smoothness or the noise, and independent of the energy cost?

In actual reaching movements, corrective sub-movements so as to compensate for the positional error are often observed. In this study, we paid attention to the existence of the sub-movements, and investigated which criterion, minimization of end-point variance or that of energy cost or that of torque change, have an advantage in the total energy cost when we consider signal-dependent noise and corrective sub-movements (Fig. 3) [14].

The results show that the trajectory which minimizes energy cost without considering noise effect is very sensitive to the noise (Fig. 4). Therefore, when noise is large the trajectories which minimize the end-point variance and the torque change require smaller cost than that by minimum energy cost model (Fig. 5). This result indicates that the planning of the reaching trajectory is not independent of the minimization of the energy cost and the optimization is done so as to suppress the expected value of the energy cost.

For further analysis of the optimality of the reaching movement we are computing the optimal trajectory which minimizes energy cost under noise effect [15].

IV. A HIERARCHICAL LEARNING MODEL OF LOCOMOTOR PATTERNS

Most animal locomotor patterns present cyclic movement, e.g., walking and swimming. Such locomotor patterns are controlled by the cooperation of the Central Pattern Generator (CPG) which shows autonomous periodic activity and higher control centers which trigger the activity of the

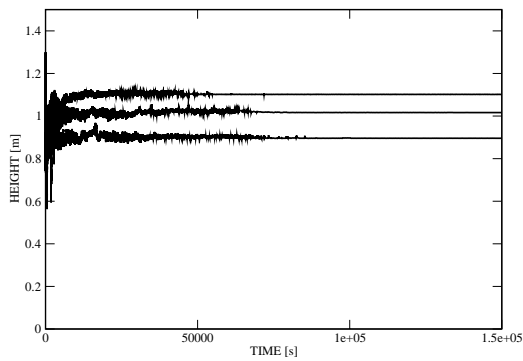


Fig. 7. Height of hopping robot during learning. By learning the height approaches to each target height 0.9, 1.0, 1.1 m.

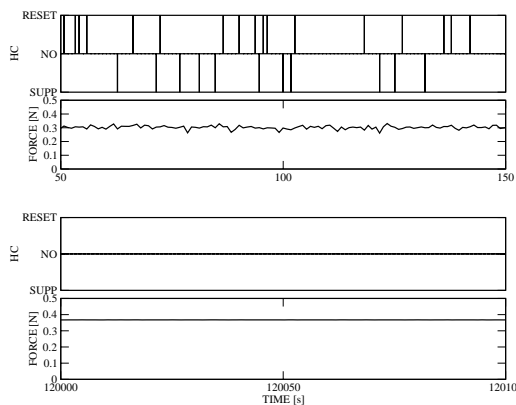


Fig. 8. Activity of the higher center during learning of the target height 1.0 m. Upper figure and lower one show the activity in the beginning of the learning and after a sufficient learning time, respectively. In each subfigure, upper graph shows the control signal, i.e., excitatory signal and the inhibitory signal, from the higher center to the CPG and lower shows the amplitude of the motor command which is determined by the higher center. In the beginning of the learning ($t = 50 - 150$ s in Fig. 7), higher center searches an appropriate signal set. After a sufficient learning time ($t = 120000 - 120100$ s in Fig. 7), desired hopping is realized without control signal to the CPG and without fluctuation of the amplitude of the motor command.

CPG and respond to a perturbation for the locomotion. Authors have studied about three problems concerning the control system by the CPG and higher centers based on previous studies [16]. (1) How do motor commands from the CPG and a higher centers realize an organized locomotor pattern without conflict? (2) In order that the CPG generates motor commands to realize a desired motor-pattern, three parameters, the period, the phase and the amplitude of motor command must be well adjusted. How are these parameters adjusted independently? (3) How do control systems, the CPG and higher centers, acquire adequate motor commands to realize target motions. Although the firing pattern of the CPG is genetically determined at some level, learning of a desired firing pattern would be necessary to respond the change of body parameters due to growth and injury. How is the CPG in the spinal cord able to evaluate the performance of the locomotion and learn adequate motor command. Considering these problems, we proposed a hierarchical learning

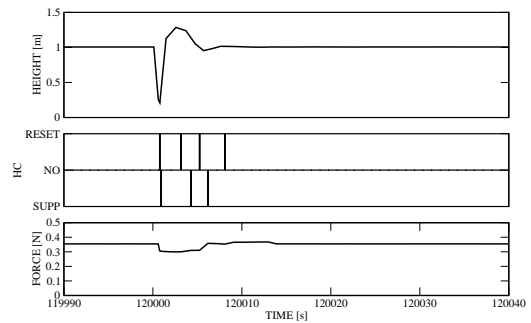


Fig. 9. Response to perturbation. Upper graph shows the height of robot, middle one shows the control signal to the CPG and bottom one shows the amplitude of motor command.

model.

Many projections from brainstem and cortex to spinal cord are reported and are suggested to contribute to send motor commands to respond with sensory signals from such as optic and equilibrium organs. However, if higher centers send control signals to motor neurons independent with the activity of the CPG, the control signals from higher center and the CPG would conflict each other. Therefore, we hypothesize that higher centers control the CPG by sending signals which cause immediate firings or a delay of the firing of the CPG in response to the states of the musculo-skeletal system and the CPG so as to enable the control of the musculo-skeletal system with adjusting the state of the CPG. In fact it is reported that many neural projections into spinal cord from higher centers do not directly project to motor neurons but to interneurons which consist of the CPG [17]. It is also reported that brainstem and cerebellum monitor the activity of the CPG [17]. These facts seem to support the idea that higher centers send control signals to the activity of the CPG according to the states of the CPG.

In order to generate a desired locomotor pattern, the period, timing and amplitude of a motor signal should be tuned. Authors have reported that locomotor parameters, such as stance length and duty ratio, are well selected so as to minimize energy cost [7], [18], [19]. This result suggests that control parameters for locomotion are independently tuned, however, it would be difficult to tune the timing and amplitude of motor commands by the CPG itself. Neurophysiological experiments have reported that inhibition of the primary motor cortex (M1) during bipedal locomotion of Japanese monkey results in the decrease of a joint torque, such as an ankle [20], and inhibition of the supplementary motor area (SMA) results in the decrease of muscle tone of whole body [21]. It is also reported that there exists spinal projection from pedunculo-pontine tegmental nucleus (PPN) and mesencephalic locomotor region (MLR) which do not affect the activity of the CPG but the muscle tone [22]. Therefore, it would not be unnatural assumption that the CPG determines the timing of motor signal and the amplitude of motor command is regulated by higher centers.

Concerning to the learning mechanism, the control signals

from higher center can work as a teacher signal for the CPG, and if the parameters of the CPG are tuned so as to decrease the control signal, the CPG would acquire the ability to generate an adequate firing pattern to realize a target action.

Figure 6 shows the schematic view of a hierarchical learning control model which summarizes above considerations. We applied this model to the control of a one-dimensional hopping robot [23]. Reinforcement learning is used for the learning of the higher center and a learning model for coupled oscillators by Nishii [24] was used for the learning of the CPG. As learning proceeds, the hopping height approaches the target height (Fig. 7). In the beginning of the learning, higher center explores adequate control signal to the CPG. However, after a sufficient learning time the control signal from the higher center to the CPG becomes silent because the CPG learned the timing of the motor command, and the amplitude of motor command becomes constant (Fig. 8). When a disturbance is added to the robot, the higher center send control signals to the CPG in order to respond to the disturbance and the robot can recover the original height (Fig. 9). It was also confirmed that the cooperative control by the CPG and the higher center enables more stable control than that by the CPG without the higher center.

V. LEARNING AND TIME SCALE

In the learning of locomotion, the adequate time scale for the learning depends on locomotor parameters. For instance, the intrinsic frequency of the CPG should be tuned in short duration in order to synchronize with the physical system, and the phase relation between the CPG and the physical system should be tuned by slower time scale. Although the choice of such adequate time scale might be a problem, if it can be chosen, many locomotor parameters can be separately learned by different time scales.

Individuals show behaviors which consist of a series of movements. Adequate selection of a behavior cannot be possible if the component movement is not optimized. Therefore, adequate time scale for the optimization of a behavior is also different from that of a movement, and the criteria of the optimization is given from selection pressure of the environment. The optimization mechanism in and between each layer of such time scales would be a kind of intelligence which living bodies have acquired through natural selection, and studies about the mechanism would be an important problem in order not only to understand the intelligence in movements and behaviors but also to understand the essential definition of living bodies from a view point of informatics.

VI. CONCLUSION

In this paper we have reported our current studies about the problems; (1) what is the basic strategy for living bodies to plan a locomotion, (2) how do living bodies control and learn a locomotion. These studies suggest that locomotor patterns and movement trajectories be well optimized on the energetic cost and nervous system precisely control our bodies by hierarchical control systems. As future problems, we are planning to investigate the trick which living bodies use

to optimize movements and behaviors, and to consider the learning control mechanism to obtain the optimal movements with considering the time-scale problem.

REFERENCES

- [1] R. Becket and K. Chang, "An evaluation of the kinematics of gait by minimum energy," *J Biomech*, vol. 1, pp. 147–159, 1967.
- [2] R. B. McGeer, "Passive dynamic walking," *Int J Robotics Res*, vol. 9, no. 2, pp. 62–82, 1990.
- [3] S. N. Whittlesey, R. E. A. van Emmerik, and J. Hamill, "The swing phase of human walking is not a passive movement," *Motor control*, vol. 4, pp. 273–292, 2000.
- [4] R. W. Selles, J. B. J. Bussmann, R. C. Wagenaar, and H. J. Stam, "Comparing predictive validity of four ballistic swing phase models of human walking," *J Biomech*, vol. 34, pp. 1171–1177, 2001.
- [5] A. Seyfarth, H. Geyer, and H. Herr, "Swing-leg retraction: a simple control model for stable running," *J Exp Biol*, vol. 206, pp. 2547–2555, 2003.
- [6] M. Nakamura, M. Mori, and J. Nishii, "Trajectory planning for a leg swing during human walking," *Proc of IEEE SMC 2004*, pp. 784–790, 2004.
- [7] J. Nishii and M. Nakamura, "A determinant of the leg swing trajectory during walking," *Proc of 3rd international symposium on adaptive motion in animals and machines*, pp. CD-ROM, 2005.
- [8] R. McN. Alexander, "A minimum energy cost hypothesis for human arm trajectories," *Biol Cybern*, vol. 76, pp. 97–105, 1997.
- [9] C. G. Atkeson and J. M. Hollerbach, "Kinematic feature of unrestrained vertical arm movements," *The Journal of Neuroscience*, vol. 5, pp. 2318–2330, Sep 1985.
- [10] T. Flash and N. Hogan, "The coordination of arm movements: An experimentally confirmed mathematical model," *J. Neurosci.*, vol. 5, pp. 1688–1703, 1985.
- [11] Y. Uno, M. Kawato, and R. Suzuki, "Formation and control of optimal trajectory in human multijoint arm movement: minimum torque-change model," *Biol Cybern*, vol. 61, pp. 89–101, 1989.
- [12] C. M. Harris and D. M. Wolpert, "Signal-dependent noise determines motor planning," *nature*, vol. 394, pp. 780–784, 1998.
- [13] J. Nishii and T. Murakami, "Energetic optimality of arm trajectory," *Proc Int Conf on Biomech of Man 2002*, pp. 30–33, 2002.
- [14] Y. Tani ai and J. Nishii, "Optimality of the minimum endpoint variance model based on energy consumption," in *Brain-inspired IT II: Decision and Behavioral Choice Organized by Natural And Artificial Brains, 1291*, K. Ishii, K. Natsume, and A. Hanazawa, Eds., pp. 101–104. Elsevier, 2006.
- [15] Y. Tani ai and J. Nishii, "Optimality of reaching movements based on energetic cost under the influence of signal-dependent noise," *Tech. Rep. of IEICE*, in press.
- [16] T. Hioki, T. Yamasaki, and J. Nishii, "A hierarchical learning model for the cpg and a higher center to obtain a basic locomotor pattern," *Proc of 3rd international symposium on adaptive motion in animals and machines*, pp. CD-ROM, 2005.
- [17] S. Grillner, P. Wallen, and L. Brodin, "Neuronal network generating locomotor behavior in lamprey: circuitry, transmitters, membrane properties and simulation," *Ann Rev of Neurosci*, vol. 14, pp. 169–199, 1991.
- [18] J. Nishii, "Legged insects select the optimal locomotor pattern based on energetic cost," *Biol Cybern*, vol. 83, no. 5, pp. 435–442, 2000.
- [19] J. Nishii, "An analytical estimation of the energy cost for legged locomotion," *J Theor Biol*, vol. 238, pp. 636–645, 2006.
- [20] K. Nakajima, F. Mori, A. Tachibana, A. Nambu, and S. Mori, "Cortical mechanisms for the control of bipedal locomotion in Japanese monkeys: I. local inactivation of the primary motor cortex (M1)," *Neurosci Res*, vol. 46 (suppl. 1), pp. S156, 2003.
- [21] K. Nakajima, F. Mori, A. Tachibana, A. Nambu, and S. Mori, "Cortical mechanisms for the control of bipedal locomotion in Japanese monkeys: II. local inactivation of the supplementary motor area (SMA)," *Neurosci Res*, vol. 46 (suppl. 1), pp. S157, 2003.
- [22] K. Takakusaki, K. Saitoh, H. Harada, and M. Kashiwayanagi, "Role of basal ganglia-brainstem pathways in the control of motor behaviors," *Neurosci Res*, vol. 50, pp. 137–151, 2004.
- [23] Y. Miyazaki, To. Hioki, and J. Nishii, "A hierarchical learning model to obtain a periodic movement," *Tech. Rep. of IEICE*, in press.
- [24] J. Nishii, "A learning model for oscillatory networks," *Neural Networks*, vol. 11, pp. 249–257, 1998.

Network Geometry of Plasmodial Slime Mold and Emergence of Biological Function

Atsuko Takamatsu*, Masateru Ito, and Yuki Kagawa
Department of Electrical Engineering and Bioscience, Waseda University,
3-4-1, Okubo, Shinjuku-ku, Tokyo, 168-8555, Japan

Abstract—Morphology and mobility of plasmodium of true slime mold, *Physarum polycephalum*, dramatically depends on environmental conditions, which can be considered as one of adaptations by "mobiligence". In this study, we analyzed the dynamical behavior of the plasmodium by focusing on the morphology of the tubular network, in order to investigate the relation of the network geometry and the biological function. We assumed the plasmodial network consists of vertices and edges, namely, we consider only network topology. The network topology were analyzed from viewpoint of complex networks in various environmental conditions. We found that the topology does not have scall-free like structure. From our preliminary experimental results, it is suggested that this kind of characteristics might be embedded in the connectivities among the elements. For further analysis, we tried to reconstruct the plasmodial network system using a cellular automaton model with a simple rule for edge generation to simulate the growing process of the plasmodia. The systematic and synthetic approach would provide one of useful algorithm that describe adaptation by morphology where the system consists of distributed simple elements.

I. INTRODUCTION

Plasmodium of true slime mold, *Physarum polycephalum*, is an oscillatory amoeba-like unicellular organism. The cell crawls on various environment oscillating the cell thickness, while the cell transforms its morphology to adapt to the environment. The organism is primitive and peculiar, however, it is one of the ideal biological model systems to investigate "mobiligence" with synthetic and systematic approach. In this study, we analyze the dynamical behavior of the plasmodium by focusing on the morphology of the tubular network, and investigate the relation of the network geometry and the biological function.

A. A collective of oscillatory units -distributed sensors, actuators and processor-

The single cell size of the plasmodium is relatively large and ranges $10\mu\text{m} - 1\text{m}$. To keep such a large body, the plasmodium developed multinucleated system, where a single cell contains numerous nuclei. Therefore, the cell can be cut and divided into multiple parts without losing the original biological functions of the organism. On the other hand, multiple cells can fuse into a single cell. So to speak, each divided unit is individually equipped with sensors, actuators and processor and the unit can also independently function. The plasmodium itself is merely a collective of those partial bodies. These points are quite different from

those of higher organisms or animals that are highly differentiated and can never cut into partial bodies keeping with normal function. Differently from the higher animals that have brains, namely, center-dependent-processing systems, the plasmodium process the environment information using the whole body consisting of distributed units. In this way, the plasmodium shows sophisticated biological functions such as gathering and escaping behaviors in response to attractants and repellents [1].

These biological functions might be understood through intrinsic oscillation phenomena observed in plasmodia, e.g., oscillations in concentrations of intracellular chemicals such as ATP and Ca^{2+} , and contraction and relaxation rhythms that drive thickness oscillation in plasmodia [2]. A minimum unit generating such oscillating phenomena is definable as an oscillator. Therefore, plasmodia can be treated as a collective of oscillators [3], [4].

Partial bodies of a plasmodium as oscillators are interconnected by tubular structures, through which protoplasm streams periodically as a result of the pressure difference generated by the contraction/relaxation rhythm [5]. The plasmodium oscillators, therefore, are considered to interact through protoplasmic streaming.

B. Adaptation by morphological transformation

Plasmodia dramatically change their morphology depending on environmental condition as shown in Fig. 1 [6]. The plasmodium spreads into dendritic formation where clear tubular structures are observed, when the environment is unpleasant for the plasmodium, e.g., the condition with harmful chemicals such as KCl. On the other hand it spreads into disc formation with thin sheets where microscopic tubular structures are highly interconnected, when the environment is pleasant, e.g., the condition with nutrients such as oat flakes. It takes several hours for the morphological transformation.

In short time range (a few times of oscillation period; one period is 1-2 min.), the period of the oscillation changes longer/shorter in unpleasant/pleasant environment [7]–[9], which could correspond coding of input from environmental condition. The local change of period in the plasmodium by local input propagates through the tubular structure among partial bodies of the cell then propagate through the whole body. Then frequency gradient of phase gradient of oscillation generates, which is considered to determine the behavior of the cell whether escape or approach in short time range. This can be said as an short-time-scale adaptation.

*Corresponding author, atsuko.ta@waseda.jp

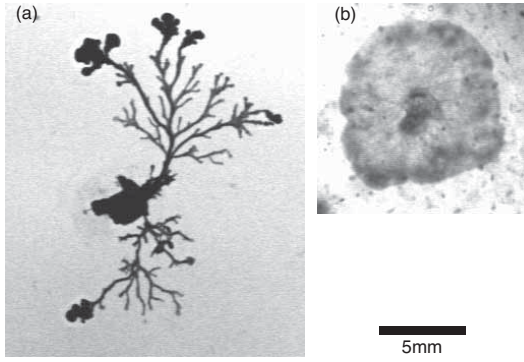


Fig. 1. Morphology of plasmodial slime mold depending on environment. (a) Dendritic formation on unpleasant environment, 0.3% agar medium with 10 mM KCl. (b) Disk formation on pleasant environment, 1.5% agar medium with 0.1 g/ml oat flakes ground into powder.

On the contrary, morphological transformation, which also results from the local input from the environment, could be considered as long-time-scale adaptation to the environment.

It would be important to know characteristics of network geometry or topology of tubular structure in the plasmodium for investigation of the adaptation by the morphology. Our goal is to bring out the relation between network geometry and biological function from the viewpoint of complex network dynamics. As the first step, here we report quantitative characteristics of plasmodial network and propose a simple cellular automaton model to describe environment dependent morphology of the plasmodium.

II. ANALYSIS OF NETWORK STRUCTURE

Recent development of study on complex networks, e.g., World Wide Web, gene regulation networks in cells, network of epidemic routes, and etc., provides us with useful tools to analyze dynamical complex systems where a huge number of dynamical elements are interconnected [10]–[12]. We analyzed the plasmodial networks by using this tool in two typical environmental conditions, cultured on 1.5% and 0.3% agar media that correspond pleasant and unpleasant conditions, respectively¹ [6].

A. A network composed of vertices and edges

First, we assume that the plasmodial network consists of vertices and edges without information on length and interaction strength for simplicity as shown in Fig.2. The vertices were defined at junctions of tubes where more than two protoplasmic streams confluent. The edges were defined for tubes interconnecting the junctions, namely, the vertices. Quantities to characterize networks are, e.g., total number of vertices n , total number of edges m , mean degree² $\langle k \rangle$, degree distribution $p(k)$, mean vertex-vertex distance³ l ,

¹Morphology of plasmodia depend not only on chemicals but also on surface condition of culture media, i.e., soft or hard. The plasmodia prefer 1.5% agar media (hard) to 0.3% agar media (soft).

²Degree k is number of edges connecting to a vertex

³Minimum number of edges to connect any two vertices

clustering coefficient⁴ C , and etc [10]–[12]. These quantities were estimated.

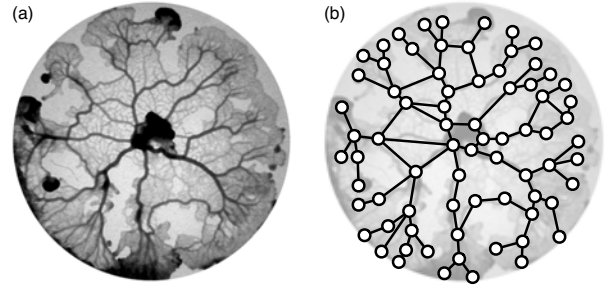


Fig. 2. Analysis of network structure. (a) Disk formation on 1.5% agar medium without chemicals. (b) Schematic diagram for extraction of network structure; circles denote vertices and lines denote edges. Original binary images were skeletonized with an image processing method using an image processing software, Image J [13] and searched coordinates of junctions and end points, and relation of links. Then characteristics of the network were analyzed by a software Pajek [14]

About 10 samples for each condition of 0.3% (unpleasant) or 1.5% (pleasant) agar media after 7 hours cultivation were analyzed as shown in Fig.3. Figure 3(a) shows that m is proportional to n irrespective of the conditions. The numbers of vertices were larger in pleasant medium than in unpleasant medium.

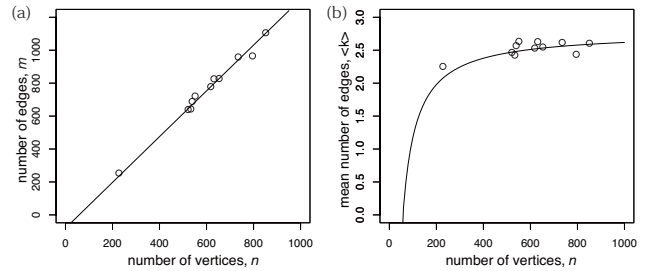


Fig. 3. Relations between numbers of vertices and edges. Open circles denote data for networks on 1.5% agar medium (11 samples), closed circles denote data for networks on 0.3% agar medium (10 samples). Data were taken from the sample images after 7 hours cultivation. (a) Relation between total number of vertices n and total number of edges m in each network. The line was fitted one with the relation $m = (-1.39 \pm 0.04)n + (-80.0 \pm 19.7)$ calculated by linear regression analysis. (b) Relation between total number of vertices n and mean degree $\langle k \rangle$. The line was calculated with the relation $\langle k \rangle = 2m/n$ using the relation described in (a).

B. Edges in network

The mean degree $\langle k \rangle$ can be defined with the relations $\langle k \rangle = 2m/n$. A calculated line with coefficients estimated from the data of Fig.3(a) by linear regression analysis and the data analyzed directory from the original image data were compared in Fig.3(b). $\langle k \rangle$ is almost 2.5 and slightly increases depending on n . The number 2.5 of $\langle k \rangle$ is agree with an intuition where streams almost always split into two branches to make three edges per a vertex and the plasmodial networks include end vertices at terminals.

⁴Rate of closed local network

Then we analyzed degree distributions, $p(k)$, that showed binomial distribution apparently different from scale-free distribution. It is natural as long as we consider only connections between vertices without information on strength and length of connectivities because these systems spread on 2-dimension along with networks of roads, railways, and power lines. To get additional information on the edges, we roughly estimated distribution of tube diameter in each network, which seems to follow exponential or power distribution. This means that the tube diameter is hierarchical in wide range, which might function as scale-free like network.

C. Other network properties

We also analyzed vertex-vertex distance l and clustering coefficient C . Dependence of mean distance $\langle l \rangle$ on n indicates how compact the network is and observation of $\langle l \rangle$ in network growing process provides us with information on what kind of graph topology the network has. Our preliminary analysis suggested that plasmodial networks in pleasant condition is lattice-like and one in unpleasant condition is tree-like. These results also agree with the direct observation of the original images.

Clustering coefficient C indicates connectivities of local network and is estimated by using triangle relations among vertices as simple standard geometry that corresponds local connection. They were estimated to be very low value for the plasmodial networks irrespective of environmental conditions. C ranged 0.01–0.03, which is smaller than those of standard social networks (0.1–0.6, small world type network) and almost same level as technological networks such as Internet [10]. This suggests the plasmodial network is not a small-world type. However, it can be expected that higher C in the pleasant condition than in the unpleasant condition because the vertices are highly connected. Method for analysis should be improved by changing standard geometry for estimation of relation, e.g. square, pentagon, and etc.

D. Vertices as oscillators

At this stage, we have not considered characteristics of vertices as oscillators. The period of oscillation affected by environment as already mentioned. Therefore it is important to know how oscillation phenomena for the each vertices and synchronization of whole network perform biological functions. This would be one of important future works.

III. CELLAR AUTOMATON MODEL FOR PATTERN FORMATION

To proceed synthetic and systematic approach, we tried to reconstruct of the plasmodial system with a cellar automaton model. As mentioned above, the network structure depends on environmental condition and two extreme examples are dendrite and disc formations. To understand what is essential parameters to control the dramatical difference of the geometrical patterns, we tried to put an simple assumption: When once a tube formed in the growing process of dendrite formations, the growing direction is kept. On the contrary,

there is no direction preference in the growing process of disc formation.

A. Rules

For simplicity, we prepare hexagonal lattice. At first step, a single vertex is set on the center and new edges to connect to new vertices are put with probability p_o for each direction (6 directions on hexagonal lattice). For the next step, the probability P_j to connect to a new vertex j from each existing vertex, which has not been not occupied by six edges yet, are calculated according to the following equation:

$$P_j = \prod_{h=1}^6 p_j^{(h)}, \quad (1)$$

where h is edge number and $\mathbf{p}^{(h)} = (p_j^{(h)}) = (p_1^{(h)}, p_2^{(h)}, \dots, p_6^{(h)})$ is a probability vector taking into account the directivity that depends on occupied edges h . $\mathbf{p}^{(h)}$ is defined as follows. For example, when a edge $h = 3$ exists, $\mathbf{p}^{(3)} = (q(1), q(2), 0, q(-2), q(-1), q(0))$, where $q(i)$ is defined by the following equation:

$$q(i) = p_o \exp(-a|i|). \quad (2)$$

Here, $i = 0, \pm 1, \pm 2$ is the relative direction number of the possible edge. Note that $p_{j=h}^{(h)} = 0$ because the edge h has already existed. The example is shown in Fig.4(a) when edge numbered as $h = 3$ has already existed. The edge at the opposite direction of the existing edge is numbered as $i = 0$, the neighboring edges are defined as $i = \pm 1$, and the second neighbors are as $i = \pm 2$. In Eq. (2), a is a parameter of directivity, e.g. as show in Fig.4(b). When a is large, the edges grows anisotropically, and when a is small the edges grows isotropically. p_o is maximum probability among all directions when there has been existed an only one edge. When a edge does not exist at edge number h , $\mathbf{p}^{(h)} = (1, 1, 1, 1, 1, 1)$. Finally, the probability P_j , is defined by Eq.(1) considered directivity resulting from all the existing edges. Figure 4(c), (d) shows an example when edges $h = 1, 3$ have already existed. This method is repeated to grow the network.

B. Results

Figure 5 shows results of computer simulation with the cellular automata. These show good agreement with experimental results: Dendritic formation with small number of vertices and edges is shown in Fig. 5(a) as simulated one for unpleasant condition, and disc formation with large number of vertices and highly connected edges is shown in in Fig. 5(b) as simulated one for pleasant condition. We have not analyzed characteristic quantities of the simulated networks such as degree, vertex-vertex distance, and clustering coefficient yet. In addition, the growing speeds of the network do not show good agreement with those of the experimental system. While it is faster in unpleasant condition than in pleasant condition in plasmodia. Further analysis, e.g., consideration of dependence of oscillation period on environmental condition will be needed.

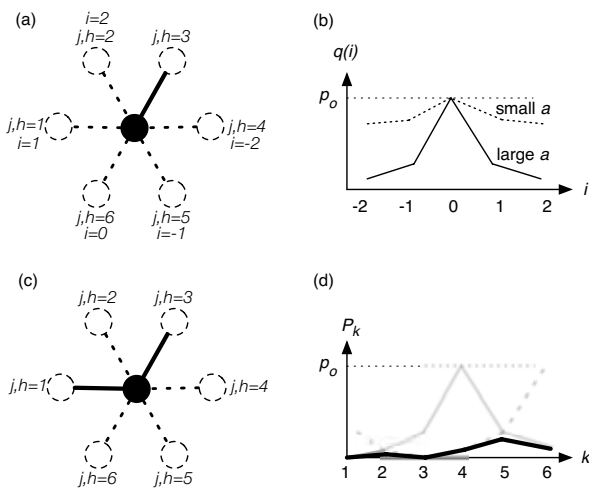


Fig. 4. Schematic diagrams of the rules for the cellular automaton model considering directivity. (a) Numbering of edges when the edge number $h = 3$ exists. (b) Probability considering directivity for the case of Fig. (a). (c),(d) Probability considering directivity when plural edges $h = 1, 3$ exist.

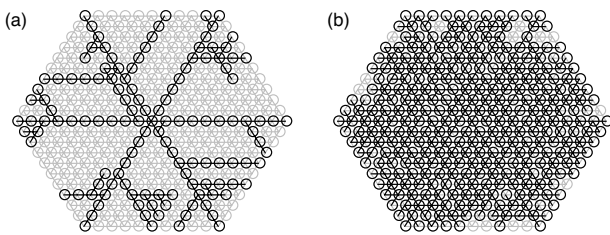


Fig. 5. Simulation results with the cellular automaton model. Open circles denote vertices and lines denote edges. (a) Dendritic formation when $a = 2$ and $p_o = 1$, (b) Disk formation when $a = 0.5$ and $p_o = 1$.

IV. CONCLUSIONS AND FUTURE WORKS

A. Conclusions

We analyzed network topology of plasmodium of true slime mold in various environment using the method recently developed for analysis of complex networks. We found there are some tendencies in topology of the network depending on environment. Those appear in relation among number of the vertices, the degrees, vertex-vertex distance, and etc. However, only the topological information of the plasmodial network without considering connectivities among vertices such as tube diameter and length can not capture fundamental characteristics of the biological networks.

Second, we tried to reconstruct the plasmodial network system using a cellular automaton model with a simple assumption, directivity of edge generation probability. The geometrical patterns obtained with this model showed good agreement with those of experimental results. However, the dynamics include "time" will be needed to capture the system as dynamical biological systems that adapt environment.

B. Future Works

To proceed toward our research goal, the following subjects are left:

For experiment, following quantities should be measured:

- characteristics of edges, i.e., tubes in the plasmodium, such as tube diameter, length, flux of protoplasmic streaming,
- characteristics of vertices such as oscillation period, amplitude for each tube or junction,
- additional characteristics of networks in each environmental condition such as fractal dimensions,
- biological activities such as metabolic rate, growing speed, and etc.

For cellular automaton model, following assumption should be considered:

- oscillating vertices,
- edges considering interaction strength, time delay⁵
- growing networks taking into account feedback by information of oscillation.

From viewpoint of engineering, information obtained from this research would provide one of useful algorithm that describe adaptation by morphology where the system consists of distributed simple elements.

REFERENCES

- [1] D. J. C. Knowles and M. J. Carlike, The chemotactic response of plasmodia of the myxomycete *Physarum polycephalum* to sugars and related compounds, *J. Gen. Microbiol.* 108 (1978) 17-25.
- [2] Y. Yoshimoto and N. Kamiya, ATP- and calcium-controlled contraction in a saponin model of *Physarum polycephalum*, *Cell Struct. Funct.* 9 (1984) 135-41.
- [3] A. Takamatsu and T. Fujii, Construction of a living coupled oscillator system of plasmodial slime mold by a microfabricated structure, in *Sensors Update*, Wiley-VCH, Weinheim (2002), Vol. 10, pp. 33.
- [4] A. Takamatsu, T. Fujii, and I. Endo, Time delay effect in a living coupled oscillator system with the plasmodium of *Physarum polycephalum*, *Phys. Rev. Lett.* 85 (2000) 2026.
- [5] N. Kamiya, The rate of protoplasmic flow in the myxomycete plasmodium. *Cytologia* 15 (1950)183-193.
- [6] A. Takamatsu, A cell behavior depends on morphology ?Pattern formation in plasmodium of true slime mold, *Physarum polycephalum*-, *Katachi no Kagaku*, 20(1) (2005) 47-48. (in Japanese)
- [7] A.C. Durham and E.B. Ridgway, Control of chemotaxis in *Physarum polycephalum*. *J. Cell, Biol.* 69 (1979)218-223.
- [8] Y. Miyake, H. Tada, M. Yano, and H. Shimizu, Relationship between intracellular period modulation and external environment change in *Physarum polycephalum*. *Cell Struct. Funct.* 19 (1994)363-370.
- [9] K. Takahashi, G. Uchida, Z.-S. Hu, and Y. Tsuchiya, Entrainment of the self-sustained oscillation in a *Physarum polycephalum* strand as a one-dimensionally coupled oscillator system, *J. theor. Biol.*, 184,(1997) 105-110.
- [10] M. E. J. Newman, The structure and function of complex networks., *SIAM review* 45 (2003) 167-256.
- [11] S. Boccaletti, V. Latora, Y. Moreno, M. Chavez, D.-U. Hwang, Complex networks: Structure and dynamics., *Physics Reports* 424 (2006) 175-308.
- [12] R. Albert and A.-L. Barabasi, Statistical mechanics of complex networks., *Rev. Mod. Phys.* 74 (2003) 47-97.
- [13] W.S. Rasband, ImageJ, U. S. National Institutes of Health, Bethesda, Maryland, USA, <http://rsb.info.nih.gov/ij/>, 1997-2006.
- [14] V. Batagelj, A. Mrvar: Pajek - Analysis and Visualization of Large Networks. in Jünger, M., Mutzel, P., (Eds.) *Graph Drawing Software*. Springer, Berlin (2003) pp. 77-103

⁵It has been reported time delay effect among oscillators can not be neglected in the plasmodium of true slime mold [4].

Members

■=Director ■=Planned Research Groups ■=Subscribed Research Groups

| | Name | Organization | |
|------------|---------------------|---|---|
| Director | Hajime Asama | The University of Tokyo | ■ |
| A01 | Masafumi Yano | Tohoku University | ■ |
| A01 | Kazuhiro Sakamoto | Tohoku University | ■ |
| A01 | Yoshinari Makino | Tohoku University | ■ |
| A02 | Koji Ito | Tokyo Institute of Technology | ■ |
| A02 | Toshiyuki Kondo | Tokyo Institute of Technology | ■ |
| B01 | Kaoru Takakusaki | Asahikawa Medical College | ■ |
| B01 | Masahiko Inase | Kinki University | ■ |
| B01 | Shigeru Kitazawa | Juntendo University | ■ |
| B01 | Kazuya Saito | Asahikawa Medical College | ■ |
| B01 | Taizo Nakazato | Juntendo University | ■ |
| B01 | Katsumi Nakajima | Kinki University | ■ |
| B01 | Futoshi Mori | Yamaguchi University | ■ |
| B01 | Dai Yanagihara | The University of Tokyo | ■ |
| B02 | Naomichi Ogihara | Kyoto University | ■ |
| B02 | Kazuo Tsuchiya | Kyoto University | ■ |
| B02 | Yasuhiro Sugimoto | Kyoto University | ■ |
| B02 | Shinya Aoi | Kyoto University | ■ |
| B03 | Koh Hosoda | Osaka University | ■ |
| B03 | Kousuke Inoue | Ibaraki University | ■ |
| B03 | Hiroshi Kimura | The University of Electro-Communications | ■ |
| B03 | Katsuyoshi Tsujita | Osaka Institute of Technology | ■ |
| C01 | Hitoshi Aonuma | Hokkaido University | ■ |
| C01 | Ryohei Kanzaki | The University of Tokyo | ■ |
| C02 | Jun Ota | The University of Tokyo | ■ |
| C02 | Hajime Asama | The University of Tokyo | ■ |
| C02 | Kuniaki Kawabata | RIKEN | ■ |
| C03 | Daisuke Kurabayashi | Tokyo Institute of Technology | ■ |
| D01 | Koichi Osuka | Kobe University | ■ |
| D01 | Akio Ishiguro | Tohoku University | ■ |
| D01 | Xin-Zhi Zheng | ASTEM | ■ |
| D01 | Masahiro Shimizu | Tohoku University | ■ |
| Evaluation | Shinzo Kitamura | Kobe University | ■ |
| Evaluation | Ryoji Suzuki | Kanazawa Institute of Technology | ■ |
| Evaluation | Shigemi Mori | National Institute for Physiological Sciences | ■ |
| Evaluation | Rolf Pfeifer | University of Zurich | ■ |
| Evaluation | Sten Grillner | Karolinska Institutet | ■ |
| Evaluation | Avis H. Cohen | University of Maryland | ■ |
| A01-11 | Satoshi Shioiri | Tohoku University | ■ |
| A01-12 | Tetsuya Inamura | National Institute of Informatics | ■ |
| A01-13 | Yasuharu Koike | Tokyo Institute of Technology | ■ |
| A01-14 | Yusuke Maeda | Yokohama National University | ■ |
| A01-15 | Toshiya Matsushima | Hokkaido University | ■ |
| A01-16 | Yasuji Sawada | Tohoku Institute of Technology | ■ |

| | | | |
|--------|------------------|---|---|
| A01-17 | Sumiaki Ishikawa | Tokyo University of Science, Suwa | ■ |
| A01-18 | Akira Murata | Kinki University | ■ |
| A01-19 | Jun Tani | RIKEN | ■ |
| B01-11 | Yoshimasa Koyama | Fukushima University | ■ |
| B01-12 | Takafumi Suzuki | The University of Tokyo | ■ |
| B01-13 | Yoshio Sakurai | Kyoto University | ■ |
| B01-14 | Takashi Hanakawa | National Center of Neurology and Psychiatry | ■ |
| B01-15 | Kiyoji Matsuyama | Sapporo Medical University | ■ |
| B01-16 | Ikuko Nishikawa | Ritsumeikan University | ■ |
| B01-17 | Kazuhiko Seki | National Institute for Psychological Problems | ■ |
| C01-11 | Toru Miura | Hokkaido University | ■ |
| C01-12 | Etsuro Ito | Tokushima Bunri University | ■ |
| C01-13 | Tetsuo Sawaragi | Kyoto University | ■ |
| C01-14 | Nuzuki Tsuji | University of Ryukyus | ■ |
| C01-15 | Kotaro Oka | Keio University | ■ |
| C01-16 | Motojiro Kato | Keio University | ■ |
| C01-17 | Takashi Nagao | Kanazawa Institute of Technology | ■ |
| C01-18 | Naotaka Fujii | RIKEN | ■ |
| D01-11 | Kazutoshi Gohara | Hokkaido University | ■ |
| D01-12 | Ichiro Tsuda | Hokkaido University | ■ |
| D01-13 | Toshio Aoyagi | Kyoto University | ■ |
| D01-14 | Jun Nishii | Yamaguchi University | ■ |
| D01-15 | Atsuko Takamatsu | Waseda University | ■ |

Publications, Awards

Publications

1. Yoshinari Makino, Masafumi Yano, Pictorial Cues Constrain Depth in the Vinci Stereopsis, *Vision Research*, 46, 1-2, 91-105, 2006
2. Naohiro Saito, Hajime Mushiake, Kazuhiro Sakamoto, Yasuto Itoyama, Jun Tanji, Representation of Immediate and Final Behavioral Goals in the Monkey Prefrontal Cortex during an Instructed Delay Period, *Cerebral Cortex*, 15, 10, 1535 - 1546, 2005
3. Kazuhiro SAKAMOTO, Takayuki SUGIURA, Toshihiko KAKU, Toru ONIZAWA and Masafumi YANO, Spatiotemporal balance in competing apparent motion is not predicted from the strength of the single-motion percept, *Perception*, 35, 947-957, 2006
4. Hajime Mushiake, Naohiro Saito, Kazuhiro Sakamoto, Yasuto Itoyama, and Jun Tanji, Activity in the Lateral Prefrontal Cortex Reflects Multiple Steps of Future Events in Action Plans, *Neuron*, 50, 631-641, 2006
5. Yoshinari Makino, Hisanori Makinae, Tsukasa Obara, Haruki Miura and Masafumi Yano, Observations of Olfactory Information Flows within Brain of the Terrestrial Slug, *Inciralia fruhstorferi*, *Proceeding of 2006 International Joint Conference on Neural Networks*, 7605-7612, 2006
6. Masashi Ito, Masafumi Yano, High-quality voice modification based on Local Vector Coding, *Proceeding of AES Japan Conference*, P-17,
7. Taiichiro Watanabe, Keita Motonami, Kazuhiro Sakamoto, Jun Deguchi, Risato Kobayashi, Ken Komiya, Keiji Okumura, Takafumi Fukushima, Hiroyuki Kurino, Hajime Mushiake, and Mitsumasa Koyanagi, Intelligent Neural Implant Microsystem Fabricated Using Multi-Chip Bonding Technique, *2005 International Conference on Solid State Device and Materials*, 462-463, 2005
8. Masashi Ito, Masafumi Yano, Pitch determination and sinusoidal modeling for time-varying voiced speech, *The Journal of the Acoustical Society of America* (4th joint meeting of ASA/ASJ), 120, 5, 3376, 2006
9. YOSHIHARA Yuki, TOMITA Nozomi, ASANO Tomotaka, MAKINO Yoshinari, YANO Masafumi, Control of Reaching Movement in Unpredictably Changing Environment by Constraints Emergence and Satisfaction, *Proc. of SICE-ICASE International Joint Conference 2006*, SP02-2, 2006
10. TOMITA Nozomi, YANO Masafumi, Real-time Control of Bipedal Movement based on Basal ganglia and Brainstem Systems, *Proc. of SICE-ICASE International Joint Conference 2006*, 4499-4502, 2006
11. Masashi Ito, Masafumi Yano, A Local Vector Coding for High Quality Voice Analysis/Synthesis, *The Journal of the Acoustical Society of America* (150th Meeting of the Acoustical Society of America), 118, 3, 2024, 2005
12. Kazuhiro Sakamoto, Toru Onizawa, Masafumi Yano, Competition Between Spatial and Temporal Factors in Simple Apparent Motion is Modulated by Laterality, *Proceedings of the 4th IEEE International Conference on Development and Learning (ICDL-05)*, 175-179, 2005
13. Yoshinari Makino, Hisanori Makinae, Tsukasa Obara, Masafumi Yano, Brain Regions Related to Odor Learning and Memory in Terrestrial Slug, *Inciralia fruhstorferi*: Two Lobes of the Cerebral Ganglion Show Different Spatiotemporal Activities, *Proceedings of the 11th International Symposium on Artificial Life and Robotics*, OS7-1, 2006
14. Kazuhiro Sakamoto, Hajime Mushiake, Naohiro Saito, Jun Tanji, Transient Synchrony and Dynamical Representation of Behavioral Goals of the Prefrontal Cortex, *Proceedings of the 4th IEEE International Conference on Development and Learning (ICDL-05)*, 207-211, 2005
15. Ikuo Matsuo, and Masafumi Yano, A Computational Model of Echolocation: Restoration of an Acoustic Image from a Single-Emission Echo, *The Journal of the Acoustical Society of America* (149th Meeting of the Acoustical Society of America), 117, 4, 2553, 2005
16. Koji Ito, Takahiro Shioyama and Toshiyuki Kondo, Lower-limb Joint Torque and Position Controls by Functional Electrical Stimulation (FES), in J. L. Wu et al (eds.): *Complex Medical Engineering*, Springer, 240-249, 2006
17. Shunsuke Iida, Toshiyuki Kondo, Koji Ito, An Environmental Adaptation Mechanism for a Biped Walking Robot Control Based on Elicitation of Sensorimotor Constraints, *From Animals to Animats 9*, Lecture Notes in Computer Science, *Proceedings of 9th International Conference on Simulation of Adaptive*

- Behavior (SAB'06),4095, 174-184,2006
18. Toshiyuki Kondo, Evolutionary design and behavior analysis of neuromodulatory neural networks for mobile robots control, *Applied Soft Computing*, 7, 189-202, 2007
 19. J.L.Wu, K.Ito, S. Tobimatsu, T. Nishida, F. Fukuyama, *Complex Medical Engineering*, Springer, 2007
 20. Toshiyuki Kondo, Koji Ito, A Proposal of Continuous Time Recurrent Neural Networks with Neuromodulatory Bias for Adaptation to Un-experienced Environments, *SICE-ICASE Joint Conference 2006 (SICE-ICCAS'06)*, 5067-5070, 2006
 21. Koji Ito, Tsutomu Imai, Naoki Tomi and Toshiyuki Kondo, Decomposition of Internal Models in Motor Learning Under Mixed Dynamic Environments, *SICE-ICASE Joint Conference 2006 (SICE-ICCAS'06)*, 5061-5066, 2006
 22. Tomoaki Nagano, Toshiyuki Kondo and Koji Ito, A Distributed Motor Control System based on Spinal Cord and Musculoskeletal Mechanisms, *Proceedings of IEEE/RSJ International Conference on Intelligent Robots and Systems*, 192-197, 2006
 23. Koji Ito, Tsutomu Imai and Toshiyuki Kondo, Motor Adaptation to Dynamic Environments in Arm Reaching Motions, *Proceedings of XVIII IMEKO WORLD CONGRESS*, 2006
 24. Toshiyuki Kondo, Koji Ito, A design principle of adaptive neural controllers for realizing anticipatory behavior in reaching movement under un-experienced environments, *Proceedings of The Third Workshop on Anticipatory Behavior in Adaptive Learning Systems (ABiALS'06)*, 2006
 25. Toshiyuki Kondo, Koji Ito, A Neuromodulatory Neural Networks Model for Environmental Cognition and Motor Adaptation, *Proceedings of IEEE World Congress on Computational Intelligence (WCCI2006)*, 9865-9870, 2006
 26. Jun Izawa, Takahito Shimizu, Toshiyuki Aodai, Toshiyuki Kondo, Hiroaki Gomi, Shigeki Toyama, Koji Ito, MR Compatible Manipulandum with Ultrasonic Motor for fMRI Studies, *Proceedings of IEEE International Conference on Robotics and Automation (ICRA2006)*, 3850-3854, 2006
 27. Tetsunari Inamura, Naoki Kojo, Masayuki Inaba, Situation Recognition and Behavior Induction based on Geometric Symbol Representation of Multimodal Sensorimotor Patterns, *IEEE/RSJ International Conference on Intelligent Robots and Systems*, 5147--5152, 2006
 28. Tetsunari Inamura, Naoki Kojo, Kazuyuki Sakamoto, Masayuki Inaba, Interactive intent imitation for humanoid robots based on dynamic attention prediction and control, *50th Anniversary Summit of Artificial Intelligence*, 2006
 29. Ei-Ichi Izawa, Naoya Aoki, Toshiya Matsushima, Neural correlates of the proximity and quantity of anticipated food rewards in the ventral striatum of domestic chicks, *European Journal of Neuroscience*, 22, 1502-1512, 2005
 30. Naoya Aoki, Ryuhei Suzuki, Ei-Ichi Izawa, Andras Csillag, Toshiya Matsushima, Localized lesions of ventral striatum, but not arcopallium, enhanced impulsiveness in choices based on anticipated spatial proximity of food rewards in domestic chicks, *Behavioural Brain Research*, 168, 1-12, 2006
 31. Naoya Aoki, Andras Csillag, Toshiya Matsushima, Localized lesions of arcopallium intermedium of the lateral forebrain caused a handling-cost aversion in the domestic chick performing a binary choice task, *European Journal of Neuroscience*, 24, 2314-2326, 2006
 32. Toshiya Matsushima, Neural control of foraging decision making in the domestic chicks, *International IBRO workshop (International Brain Research Organization, Budapest, 26 January, 2006)*, 2006
 33. Fumihiko Ishida, Yasuji E Sawada, Semianalytical transient solution of a delayed differential equation and its application to the tracking motion in the sensory-motor system, *Physical Review E*, 75, 12901, 2007
 34. Kenshi Watanabe, Kenichi Ohkubo, Sumiaki Ichikawa, and Fumio Hara, Classification of Object Shapes Utilizing Tactile Spatiotemporal Differential Information Obtained from Grasping by Single-Finger Robot Hand with Soft Tactile Sensor Array, *Journal of Robotics and Mechatronic*, 19, 1, 2007
 35. Akira Murata, Hiroaki Ishida, Representation of bodily self in the multimodal parieto-premotor network, In: *Representation and Brain*, edited by Shintaro Funahashi, Springer Verlag, (in press)
 36. Raos, V., Umiltà, M-A., Murata, A., Fogassi, L. & Gallese V, Functional properties of grasping-related neurons in ventral premotor area F5 of the Macaque monkey., *J Neurophysiol.* 95, 2, 709-729, 2006
 37. M. Ito, K. Noda, Y. Hoshino, J. Tani, Dynamic and interactive generation of object handling behaviors by a small humanoid robot using a dynamic neural network model, *Neural Networks*, 19, 323-337, 2006
 38. K. Noda, M. Ito, Y. Hoshino, J. Tani, Dynamic generation and switching of object handling behaviors by a humanoid robot using a recurrent neural network model, *Lecture Notes in Artificial*

- Intelligence(SAB2006),4095, 185-196,2006
39. H. Arie, J. Namikawa, T. Ogata, J. Tani, S. Sugano, Reinforcement learning algorithm with CTRNN in continuous action space, *Lecture Notes in Computer Science(ICONIP2006)*,4232, 387-396,2006
 40. Oshio Kenichi, Atsushi Chiba, Masahiko Inase, Delay Period Activity of Monkey Prefrontal Neurons during Duration-Discrimination Task, *European Journal of Neuroscience*,23,10,2779-2790,2006
 41. Atsushi Chiba, Kenichi Oshio, Masahiko Inase, Cue and Delay Responses of Monkey Striatal Neurons during a Duration Discrimination Task, *Proceedings of Neuroscience 2006, 36th Annual Meeting of Society for Neuroscience*, 572.2,2006
 42. Takakusaki K, Saitoh K and Kashiwayanagi M . ,The pedunculopontine nucleus and the basal ganglia in locomotion., In: *Recent Breakthroughs in Basal Ganglia Research*, (ed by E. Bezdard), 133-149,2006
 43. Takakusaki K, Saitoh K, Nonaka S, Okumura T, Miyokawa N, Koyama Y. ,Neurobiological basis of state-dependent control of motor behavior. ,*Sleep and Biological Rhythms*,4, 87-104,2006
 44. Yamada H, Tanno S, Takakusaki K, Okumura T., Intracisternal injection of orexin-A prevents ethanol-induced gastric mucosal damage in rats, *Journal of Gastroenterology* (in press),
 45. Takakusaki K, ,Forebrain control of locomotor behaviors, *Brain Research Review*, (in press),
 46. Adachi M, Nonaka S, Katada A, Arakawa T, Ota R, Harada H, Takakusaki K, Harabuchi Y., Carbachol injection into the pontine reticular formation depresses laryngeal muscle activity and airway reflexes in decerebrate cats, *Neuroscience Research* (in press),
 47. Takakusaki K, ,What are the Neurophysiologic Substrates of Normal and Abnormal Gait? ,*Journal of Neurology* (in press),
 48. Takakusaki K, Forebrain control of locomotor behaviors, *Wenner-Gren Foundations International Symposium: "Networks in Motion"*, 2006
 49. F. Mori, K. Nakajima, A. Tachibana, and S. Mori., Obstacle clearance and prevention from falling in the bipedally walking Japanese monkey, *Macaca fuscata*. ,*Age and Aging*,35,S2,19-23,2006
 50. F. Mori, K. Nakajima, and S. Mori., Control of bipedal walking in the Japanese monkey, *M. fuscata*, Reactive and anticipatory control mechanisms, In: Kimura, H., Tsuchiya, Ishiguro, A., and Witte, H. (Eds.), *Adaptive Motion of Animals and Machines*, Springer, p.249-p.250 (2006), 249-250,2006
 51. F. Mori, K. Nakajima, Tachibana, A., Tsukada, H., and S. Mori., Primary, supplementary and premotor cortices are involved in the execution and control of operant-trained bipedal treadmill walking in Japanese monkey (*M. fuscata*). ,*The 1st International Congress on Gait and Mental Function*,
 52. Satoshi Shibuya, Toshimitsu Takahashi, Shigeru Kitazawa, Effects of visual stimuli on temporal order judgments of unimanual finger stimuli, *Experimental Brain Research*, DOI 10.1007/s00221-006-0829-4.,2007
 53. Kenji Yamamoto, Mitsuo Kawato, Shinya Kotosaka, Shigeru Kitazawa, Encoding of movement dynamics by Purkinje cell simple spike activity during fast arm movements under resistive and assistive force fields., *Journal of Neurophysiology*,97,2,1588-1599,2007
 54. Makoto Miyazaki, Shinya Yamamoto, Sunao Uchida, Shigeru Kitazawa , Bayesian calibration of simultaneity in tactile temporal order judgment., *Nature Neuroscience* ,9,7,875-877,2006
 55. Makoto Wada, Kenji Yoshimi, Noriyuki Higo, Yong-Ri Ren, Hideki Mochizuki, Yoshikuni Mizuno, Shigeru Kitazawa, Statistical parametric mapping of immunopositive cell density. , *Neuroscience Research*,28,11,96-102,2006
 56. Nakazato T, Kagohashi M, Yoshimi M. ,Influence of pH on voltammetric measurement of dopamine. , *Biogenic Amines*, 20, (in press),2006
 57. Shigeru Kitazawa, Reversal of subjective temporal order due to sensory and motor integrations, *Attention and Performance XXII Sensorimotor foundations of higher cognition*. , 2006
 58. Shigeru Kitazawa, Where tactile signals are ordered in time, *Cognition and Action*, The 29th Annual Meeting of the Japan Neuroscience Society, 2006
 59. Shigeru Kitazawa, Discussion from a neurophysiological viewpoint, *Developing cross-modal representation of objects and space International Conference on Infant Studies 2006*, 2006
 60. Kagohashi M., Moizumi S Yoshimi K. Nakazato T, Kitazawa S., Wireless voltammetry: dopamine measurement in the freely moving rat., *Soc. Neurosci.*, (Suppl) 592.1., 2006
 61. Yoshimi K., Kagohashi M., Moizumi S, Hattori N, Nakazato T, Kitazawa, Week-long voltammetric recording in the rat striatum: circadian rhythm of dopamine level., *Soc. Neurosci.*, (Suppl) 469.1., 2006
 62. Futoshi Mori, Katsumi Nakajima, Atsumichi Tachibana, Shigemi Mori , Obstacle Clearance and

- Prevention from Falling in the Bipedally Walking Japanese Monkey, *Macaca fuscata*, Age and Aging, 35, S2, 19-23, 2006
63. Dai Yanagihara, Role of the cerebellum in adaptive control of locomotion., Proceedings of SICE-ICASE International Joint Conference, 4493-4494, 2006
 64. Nakatsukasa, M., Hirasaki, E., Ogihara, N., Energy expenditure of bipedal walking is higher than that of quadrupedal walking in Japanese macaques, *American Journal of Physical Anthropology*, 131, 33-37, 2006
 65. S. Aoi, K. Tsuchiya, Bifurcation and Chaos of a Simple Walking Model Driven by a Rhythmic Signal, *International Journal of Non-Linear Mechanics*, 41, 3, 438-446, 2006
 66. S. Aoi, K. Tsuchiya, Stability Analysis of a Simple Walking Model Driven by an Oscillator With a Phase Reset Using Sensory Feedback, *IEEE Transactions on Robotics*, 22, 2, 391-397, 2006
 67. S. Aoi, K. Tsuchiya, Self-stability of a Simple Walking Model Driven by a Rhythmic Signal, *Nonlinear Dynamics*, 48, 1-2, 1-16, 2007
 68. S. Aoi, K. Tsuchiya, Gait Transition from Quadrupedal to Bipedal Locomotion of an Oscillator-driven Biped Robot, *International Journal of Advanced Robotic Systems*, (in press),
 69. S. Aoi, H. Sasaki, K. Tsuchiya, A Multi-legged Modular Robot That Meanders: Investigation of Turning Maneuvers Using its Inherent Dynamic Characteristics, *SIAM Journal on Applied Dynamical Systems*, (in press),
 70. Nakatsukasa, M., Hirasaki, E., Ogihara, N., Energy expenditure of bipedal walking is higher than that of quadrupedal walking in Japanese macaques, *American Journal of Physical Anthropology*, 131, 33-37, 2006
 71. S. Aoi, K. Tsuchiya, Bipedal Locomotion Control Using Nonlinear Oscillators, *Dynamic Walking 2006*, 2006
 72. S. Aoi, K. Tsuchiya, Feedback Control of a Simple Walking Model Driven by an Oscillator, *IEEE International Conference on Robotics and Automation*, 1990-1996, 2006
 73. S. Aoi, K. Tsuchiya, Turning Maneuvers of a Multi-legged Modular Robot Using Its Inherent Dynamic Characteristics, *IEEE/RSJ International Conference on Intelligent Robots and Systems*, 180-185, 2006
 74. Y. Sugimoto, K. Osuka, Implicit Feedback Structure in Passive Dynamic Walking, *Dynamic Walking 2006*, 2006
 75. Ogihara, N., Nakatsukasa, M., Sugimoto, Y., Aoi, S., Tsuchiya, K., Adaptive locomotion mechanisms inherent in the musculoskeletal structure, *SICE-ICASE International Joint Conference 2006*, 2006
 76. Hase, K., Obinata, G., Nakayama, A., Ogihara, N., Usui, T., Tasaki, Y., Large-scale forward dynamics simulation with a whole-body musculoskeletal model, *5th World Congress of Biomechanics*, 2006
 77. Zu Guang Zhang, Hiroshi Kimura and Yasuhiro Fukukoka, Autonomously generating efficient running of a quadruped robot using delayed feedback control, *Advanced Robotics*, 20, 6, 607-629, 2006
 78. Zu Guang Zhang, Hiroshi Kimura and Kunikatsu Takase, delayed feedback control, *Journal of Vibration and Control*, 12, 12, 1361-1383, 2006
 79. Takashi Takuma, Koh Hosoda, Controlling the Walking Period of a Pneumatic Muscle Walker, *International Journal of Robotics Research*, 25, 9, 861-866, 2006
 80. Hiroshi Kimura, Yasuhiro Fukuoka and Avis H. Cohen, Biologically Inspired Adaptive Walking of a Quadruped Robot, *Philosophical Transactions of the Royal Society A*, 365, 1850, 153-170, 2007
 81. Zu Guang Zhang, Hiroshi Kimura, and Yasuhiro Fukuoka, Self-Stabilizing Dynamics for a Quadruped Robot and Extension Towards Running on Rough Terrain, *Journal of Robotics and Mechatronics*, 19, 1, 2007
 82. K. Tsujita and T. Masuda, Simulation Study on Acquisition Process of Locomotion by using an Infant Robot, *International Journal of Advanced Robotic Systems*, (in press), 2006
 83. K. Tsujita, A. Morioka, K. Nakatani, K. Suzuki and T. Masuda, Oscillator-controlled Bipedal Walk with Pneumatic Actuators, *KSME International Journal*, (in press), 2006
 84. Takashi Takuma, Koh Hosoda, Controlling Walking Velocity of a Pneumatic Actuated Biped by Changing Hip Passivity, *Dynamic Walking 2006*, Poster-22, 2006
 85. Koh Hosoda, Takashi Takuma, and Athushi Nakamoto, Design and Control of a Running Biped with Pneumatic Artificial Muscles, *Dynamic Walking 2006*, 2006
 86. Tsuyoshi UENO, Yutaka NAKAMURA, Takashi TAKUMA, Tomohiro SHIBATA, Koh HOSODA, Shin ISHII, Fast and Stable Learning of Quasi-Passive Dynamic Walking by an Unstable Biped Robot based on Off-Policy Natural Actor-Critic, *International Conference on Intelligent Robots and Systems*, 5226-5231, 2006

87. Koh Hosoda, Takashi Takuma, and Atsushi Nakamoto, Design and Control of 2D Biped that can Walk and Run with Pneumatic Artificial Muscles, IEEE-RAS/RSJ International Conference on Humanoid Robots (Humanoids 2006), CD-ROM, 2006
88. K. Tsujita, A. Morioka, K. Nakatani, K. Suzuki and T. Masuda, Oscillator-controlled Bipedal Walk with Pneumatic Actuators, Proc. of Int. Conf. of Motion and Vibration Control, 670-675, 2006
89. K. Tsujita and T. Masuda, Simulation of Acquisition of Locomotion of an Infant Robot, Proc. of IEEE/RSJ IROS 2006, 4929-4934, 2006
90. Takaaki SUMI, Kousuke INOUE, Norikazu SATO, Shugen MA, Development of an Environmentally Adaptable Snake-Like Robot --Construction of a Neural Oscillator Network Capable of Changing Ground Friction--, Proceedings of 3rd International Conference on Brain-inspired Information Technology, 82, 2006
91. Y. Ninomiya, Y. Kayama, Y. Koyama, Postnatal development of cholinergic neurons in the mesopontine tegmentum revealed by histochemistry, Internatl J Develop Neurosci, 23, 711-721, 2005
92. K. Takahashi, Q.-P. Wang, J.-L. Guan, Y. Kayama, S. Shioda and Y. Koyama, State-dependent effects of orexin on the serotonergic dorsal raphe neurons in the rat, Reg. Peptide, 126, 43-47, 2005
93. Q.-P. Wang, Y. Koyama, J.-L. Guan, Y. Kayama, K. Takahashi, and S. Shioda, The orexinergic synaptic innervation of serotonin- and orexin 1 receptor-containing neurons in the dorsal raphe nucleus, Reg. Peptide, 126, 35-42, 2005
94. Y. Yasoshima, N. Kai, S. Yoshida, S. Shiosaka, Y. Koyama, Y. Kayama Y., K. Kobayashi, Subthalamic neurons coordinate basal ganglia function through differential neural pathways, J. Neurosci., 25, 7743-7753, 2005
95. K. Takakusaki, K. Takahashi, K. Saitoh, H. Harada, T. Okumura, Y. Kayama, Y. Koyama, Orexinergic projections to the midbrain mediate alternation of emotional behavioral states from locomotion to cataplexy, J. Physiol., 568, 1003-1020, 2005
96. T. Sakurai, R. Nagata, A. Yamanaka, H. Kawamura, N. Tsujino, Y. Muraki, H. Kageyama, S. Kunita, S. Takahashi, K. Goto, Y. Koyama, S. Shioda, M. Yanagisawa, Input of orexin/hypocretin neurons revealed by genetically encoded tracer in mice, Neuron, 46, 297-308, 2005
97. T. Kodama, S. Usui, Y. Honda, M. Kimura, High Fos expression during the active phase in orexin neurons of a diurnal rodent, *Tamias sibiricus barberi*, Peptides, 26, 4, 631-638, 2005
98. T. Kodama, and Y. Koyama, Nitric oxide from the laterodorsal tegmental neurons: Its possible retrograde modulation on norepinephrine release from the axon terminal of the locus coeruleus neurons, Neuroscience, 138, 245-256, 2006
99. K. Takakusaki, K. Saito, T. Nonaka, T. Okumura, N. Miyokawa, Y. Koyama, Neurobiological basis of state-dependent control of motor behaviors, Sleep and Biological Rhythms, 4, 87-104, 2006
100. Y. Tamakawa, A. Karashima, Y. Koyama, N. Katayama and M. Nakao, A Quartet Neural System Model Orchestrating Sleep and Wakefulness Mechanisms, J Neurophysiol, 95, 2055-2069, 2006
101. K. Takahashi, J.S. Lin, K. Sakai, Neuronal activity of histaminergic tuberomammillary neurons during wake-sleep states in the mouse, J. Neuroscience, 26, 40, 10292-10298, 2006
102. K. Nakamura, Y. Koyama, K. Takahashi, et al., Requirement of tryptophan hydroxylase during development for maturation of sensorimotor gating, J Mol Biol, 363, 345-354, 2006
103. Osamu Fukayama, Noriyuki Taniguchi, Takafumi Suzuki, Kunihiro Mabuchi, Estimation of Locomotion Speed and Directions Changes to Control a Vehicle Using Neural Signals from the Motor Cortex of Rat, Proceedings of the 28th IEEE EMBS Annual International Conference, 1138-1141, 2006
104. Yasuhiro Kato, Itsuro Saito, Takayuki Hoshino, Takafumi Suzuki, Kunihiro Mabuchi, Preliminary Study of Multichannel Flexible Neural Probes Coated with Hybrid Biodegradable Polymer, Proceedings of the 28th IEEE EMBS Annual International Conference, 660-663, 2006
105. Takashi Sato, Takafumi Suzuki, Kunihiro Mabuchi, A new multi-electrode array design for chronic neural recording, with independent and automatic hydraulic positioning, Journal of Neuroscience Methods, 160, 45-51, 2007
106. Sakurai, Y., How can we detect ensemble coding by cell assembly, Representation and Brain, 2007 (in press)
107. Sakurai, Y., Takahashi, S., Dynamic synchrony of firing in the monkey prefrontal cortex during working memory tasks, Journal of Neuroscience, 26, 10141-10153, 2006
108. Koike, Y., Hirose, H., Sakurai, Y., Iijima, T., Prediction of arm trajectory from a small number of neuron

- activities in the primary motor cortex.,*Neuroscience Research*,56, 146-153,2006
109. Takahashi, S., Sakurai, Y. ,Sub-millisecond synchronization among pyramidal neurons in hippocampal CA1 of rats during delayed non-matching to sample task.,36th Society for Neuroscience Annual Meeting., 2006
 110. Hirokawa, J., M. Bosch, Sakata, S., Sakurai, Y., Yamatori, T.,A distinct area of rat visual cortex mediates behavioral enhancement by audiovisual integration.,36th Society for Neuroscience Annual Meeting., 2006
 111. Sakurai, Y.,Brain plasticity revealed with brain-machine interfaces,1st International Conference on Advanced Medical Engineering and Informatics. , 2006
 112. Nomura, M., Sakurai, Y., Kitano, K. & Aoyagi, T.,Applying the kernel method to multi-neuronal spike trains.,1st Symposium on Complex Medical Engineering. ,2006
 113. Aso T, Hanakawa T, Matsuo K, Toma K, Shibasaki H, Fukuyama H, Nakai T.,Subregions of human parietal cortex selectively encoding object orientation.,*Neuroscience Letters*, (in press),
 114. Sawamoto N, Honda M, Hanakawa T, Aso T, Inoue M, Toyoda H, Ishizu K, Fukuyama H, Shibasaki H. ,Role of the striatum in cognitive slowing in Parkinson's disease. ,*Neurology*, (in press),
 115. Yamada M, Namiki C, Hirao K, Hanakawa T, Fukuyama H, Hayashi T, Murai T,Social cognition and frontal lobe pathology in schizophrenia: A voxel-based morphometric study. ,*Neuroimage*, (in press),
 116. Mikuni N, Okada T, Nishida N, Taki J, Enatsu R, Ikeda A, Miki Y, Hanakawa T, Fukuyama H, Hashimoto N ,Comparison between motor evoked potential recording and fiber tracking for estimating pyramidal tracts near brain tumors. ,*Journal of Neurosurgery*,106,1,128-133,2007
 117. Yamamoto A, Miki Y, Urayama S, Fushimi Y, Okada T, Hanakawa T, Fukuyama H, Togashi K.,Diffusion tensor fiber tractography of the optic radiation: analysis with 6-, 12-, 40- and 81-directional motion probing gradients; a preliminary study. ,*American Journal of Neuroradiology* ,28,1,92-96,2007
 118. Mikuni N, Okada T, Taki J, Matsumoto R, Nishida N, Enatsu R, Hanakawa T, Ikeda A, Miki Y, Urayama SI, Fukuyama H, Hashimoto N.,Fibers from the dorsal premotor cortex elicit motor-evoked potential in a cortical dysplasia. ,*Neuroimage*,34,1,12-18,2007
 119. Takaya S, Hanakawa T, Hashikawa K, Ikeda A, Sawamoto N, Nagamine T, Ishizu K, Fukuyama H. ,Prefrontal hypofunction in patients with intractable mesial temporal lobe epilepsy. ,*Neurology* ,67,9,1674-1676,2006
 120. Kikuta K, Takagi Y, Fushimi Y, Ishizu K, Okada T, Hanakawa T, Miki Y, Fukuyama H, Nozaki K, Hashimoto N,“Target bypass”: a method for preoperative targeting of a recipient artery in superficial temporal artery-to-middle cerebral artery anastomoses.,*Neurosurgery*,59,4,ONS-320-327,2006
 121. Okada T, Miki Y, Mikuni N, Kikuta K, Urayama S, Hanakawa T, Fukuyama H, Hashimoto N, Togashi K,Diffusion tensor tractography of corticospinal tract using 3-T combined with white matter stimulation mapping: an integrated approach to validate the corticospinal tract localization.,*Radiology*,240,3,849-857,2006
 122. Fukui H, Murai T, Shinozaki J, Aso T, Fukuyama H, Hayashi T, Hanakawa T.,The neural basis of social tactics: An fMRI study.,*Neuroimage*,32, 913-920,2006
 123. Bohlhalter S, Goldfine A, Matteson A, Garraux G, Hanakawa T, Kansaku K, Wurzman R, Hallett M.,Neural correlates of tic generation in Tourette syndrome: an event-related functional MRI study.,*Brain*,129,8, 2029-37,2006
 124. Callan D, Tsytsarev V, Hanakawa T, Callan A, Katsuhara M, Fukuyama H, Turner R.,Perception and covert generation of song and speech.,*Neuroimage*,31,3,1327-1342,2006
 125. Crinion J, Turner R, Grogan A, Hanakawa T, Noppeney U, Devlin JT, Aso T, Urayama S, Fukuyama H, Stockton K, Usui K, Green D, Price CJ.,Language control in the bilingual brain.,*Science*,312,5779,1537-1540,2006
 126. Hanakawa T, Honda M, Zito G, Dimyan MA, Hallett M. ,Brain activity during motor behavior triggered by arbitrary cues and spatially-constrained cues: An fMRI study in humans. ,*Experimental Brain Research*,172,2,275-282,2006
 127. Le Bihan D, Urayama S, Aso T, Hanakawa T, Fukuyama H,Direct and fast detection of neuronal activation in the human brain with diffusion MRI.,*Proceedings of National Academy of Science USA*,103,21,8263-8268,2006
 128. Fushimi Y, Miki Y, Kikuta K, Okada T, Kanagaki M, Yamamoto A, Nozaki K, Hashimoto N, Hanakawa T, Fukuyama H, Togashi K,Comparison of 3.0- and 1.5-T three-dimensional time-of-flight MR angiography in moyamoya disease: a preliminary experience.,*Radiology*,239,1,232-237,2006

129. Kikuta K, Takagi Y, Nozaki K, Hanakawa T, Okada T, Fushimi Y, Miki Y, Fukuyama H, Hashimoto N, Early experience with 3-tesla magnetic resonance tractography in the surgery of cerebral AVMs in and around the visual pathway. *Neurosurgery*, 58,2,331-337,2006
130. Garraux G, Goldfine A, Bohlhalter S, Lerner A, Hanakawa T, Hallett M. The midbrain hypothesis in Tourette's syndrome: a reappraisal using voxel-based morphometry. *Annals of Neurology* ,59,2,381-385,2006
131. Okada T, Miki Y, Fushimi Y, Hanakawa T, Kanagaki M, Yamamoto A, Urayama S, Fukuyama H, Hiraoka M, Togashi K, Diffusion tensor fiber tractography: Intra-individual comparison using 3 T and 1.5 T MRI. *Radiology*, 238,2,668-678,2006
132. Fridman E, Immisch I, Hanakawa T, Bohlhalter S, Waldvogel D, Kansaku K, Wheaton L, Wu T, Hallett M, The role of the dorsal stream for gesture production. *Neuroimage*, 29,2,417-428,2006
133. Hanakawa T, Neuroimaging of standing and walking: Special emphasis on Parkinsonian gait. *Parkinsonism and Related Disorders* , 12, Suppl 2, S70-75, 2006
134. Ihara M, Tomimoto H, Ishizu K, Yoshida H, Sawamoto N, Hashikawa K, Fukuyama H, Association of vascular parkinsonism with impaired neuronal integrity in the striatum. *Journal of Neural Transmission*, (in press),
135. Miyamoto JJ, Honda M, Saito DN, Okada T, Ono T, Ohyama K, Sadato N., The representation of the human oral area in the somatosensory cortex: a functional MRI study. *Cerebral Cortex*, 16,5,669-675,2006
136. Qiu Y, Noguchi Y, Honda M, Nakata H, Tamura Y, Tanaka S, Sadato N, Wang X, Inui K, Kakigi R, Brain processing of the signals ascending through unmyelinated C fibers in humans: an event-related functional magnetic resonance imaging study. *Cereb Cortex*, 16,9,1289-1295,2006
137. Aramaki Y, Honda M, Okada T, Sadato N., Neural correlates of the spontaneous phase transition during bimanual coordination. *Cereb Cortex*, 16,9,1338-1348,2006
138. Aramaki Y, Honda M, Sadato N., Suppression of the non-dominant motor cortex during bimanual symmetric finger movement: a functional magnetic resonance imaging study. *Neuroscience*, 141,4,2147-2153,2006
139. Saito DN, Okada T, Honda M, Yonekura Y, Sadato N., Practice makes perfect: the neural substrates of tactile discrimination by Mah-Jong experts include the primary visual cortex. *BMC Neurosci*, 5,7,79,2006
140. Kiyoji Matsuyama K, Suguru Kobayashi, Mamoru Aoki, Projection patterns of lamina VIII commissural neurons in the lumbar spinal cord of the adult cat: an anterograde neural tracing study. *Neuroscience*, 140,1,203-218,2006
141. Ying Cao, Yutaka Fujito, Kiyoji Matsuyama, Mamoru Aoki. Effects of electrical stimulation of the medullary raphe nuclei on respiratory movements in rats. *Journal of Comparative Physiology A: Sensory, Neural, and Behavioral Physiology*, 192,5,497-505,2006
142. Ying Cao, Kiyoji Matsuyama, Yutaka Fujito, Mamoru Aoki. Involvement of medullary GABAergic and serotonergic raphe neurons in respiratory control: electrophysiological and immunohistochemical studies in rats. *Neuroscience Research*, 56,3,322-331,2006
143. Kiyoji Matsuyama, Masanori Ishiguro, Suguru Kobayashi, Mamoru Aoki, Characteristics of the interlimb coordination between fore- and hindlimbs during hopping movements in decerebrate rabbits. *Neuroscience Meeting Planner of Neuroscience 2006 (36th Annual Meeting of the Society for Neuroscience)*, 648.14,2006
144. M. Nakanishi, T. Nomura, S. Sato, Stumbling with optimal phase reset during gait can prevent a humanoid from falling. *Biological Cybernetics*, 95,5,503-515,2006
145. Y. Yasutake, S. Taniguchi, T. Nomura, Non-Asymptotical Postural Stabilization Strategy during Human Quiet Stance. *Proceedings of the 28th IEEE EMBS Annual International Conference, New York City, USA, Aug 30-Sept 3, 1189-1192,2006*
146. T. Ishikawa, Y. Kaji, T. Nomura, Sensory perception of unexpected sudden changes in floor level during human gait. *Proceedings of the 28th IEEE EMBS Annual International Conference, New York City, USA, Aug 30-Sept 3, 4474-4477,2006*
147. Kazuhiko SEKI, Tomohiko Takei, Primary afferent depolarization evoked by natural stimulation of cutaneous afferent in monkey. *006 Neuroscience Meeting Planner. Atlanta, GA: Society for Neuroscience, 2006. Online., 627-54.8/P13628,2006*
148. Tomohiko Takei, Kazuhiko SEKI, Involvement of the primate spinal neurons in the control of precision grip. *006 Neuroscience Meeting Planner. Atlanta, GA: Society for Neuroscience, 2006. Online.,*

- 54.9/P14,2006
149. Tomohiko Takei, Kazuhiko SEKI, Spinomuscular coherence in monkey performing a precision grip task, Society for neural control of movement annual meeting abstract booklet, (in press), 2007
 150. Ott S. R., Aonuma H., Newland P.L. and Elphick M.R. Nitric oxide synthase in crayfish walking leg ganglia: segmental differences in chemo-tactile centers argue against a generic role in sensory integration, *J. Comp. Neurol.*, 501, 381-399, 2007
 151. Watanabe T., Kikuchi M., Hatakeyama D., Shiga T., Yamamoto T., Aonuma H., Takahata M., Suzuki N. and Ito E., Gaseous neuromodulator-related genes expressed in the brain of honeybee *Apis mellifera*, *Develop. Neurobiol.*, (in press), 2007
 152. Ikeno H., Nishioka T., Hachida T., Kanzaki R., Seki Y., Ohzawa I., Usui S., Development and application of CMS based database modules for neuroinformatics. *Neurocomputing*, (in press), 2007
 153. Wagatsuma A., Azami S., Sakura M., Hatakeyama D., Aonuma H. and Ito E., De novo synthesis of CREB in a presynaptic neuron is required for synaptic enhancement involved in memory consolidation, *J. Neurosci. Res.*, 84, 954-960, 2006
 154. Matsumoto Y., Unoki S., Aonuma H. and Mizunami M., Nitric oxide-cGMP signaling is critical for cAMP-dependent long-term memory formation, *Learn. Mem.*, 13, 1, 35-44, 2006
 155. Delago A. and Aonuma H. Experience based agonistic behavior in female crickets, *Gryllus bimaculatus*, *Zool. Sci.*, 23, 775-783, 2006
 156. Iwasaki M., Delago A., Nishino H. and Aonuma H., Effects of previous experiences on the agonistic behaviour of male crickets *Gryllus bimaculatus*, *Zool. Sci.*, 23, 863-872, 2006
 157. Niwa K., Sakai J., Karino T., Aonuma H., Watanabe T., Ohyama T., Inanami O. and Kuwabara M., Reactive oxygen species mediate shear stress-induced fluid-phase endocytosis in vascular endothelial cells, *Free Radical Res.*, 40, 2, 167-174, 2006
 158. Yamasaki T., Isokawa T., Matsui M., Ikeno H. and Kanzaki R., Reconstruction and simulation for three-dimensional morphological structure of insect neurons. *Neurocomputing*, 69, 1043-1047, 2006
 159. Kitamura Y., Aonuma H., Oka K. and Ogawa H., Acetylcholine enhances nitric oxide production in the terminal abdominal ganglion of the cricket, *Gryllus bimaculatus*, Society for Neuroscience, 351, 2006
 160. Suzuki M., Kimura T., Ogawa H., Aonuma H., Kitamura Y., Hotta K. and Oka K., Peripheral nervous plexuses control squid chromatophore organs, Society for Neuroscience, 353, 2006
 161. Tomohisa Fujiki, Kuniaki Kawabata, Hajime Asama, Adaptive Action Selection of Body Expansion Behavior in Multi-Robot System using Communication, *Journal of Advanced Computational Intelligence and Intelligent Informatics*, 11, 2, 2007
 162. Yusuke Fukazawa, Chomchana Trevai, Jun Ota and Tamio Arai, Acquisition of Intermediate Goals for an Agent Executing Multiple Tasks, *IEEE Transactions on Robotics*, 22, 5, 1034/1040, 2006
 163. T. Fujiki, K. Kawabata, H. Aonuma, H. Asama, A Computational Model of the Adaptive Action Selection in Cricket Fighting Behavior by NO/cGMP Cascade, The 2nd International Workshop by Research Group of Invertebrate Nervous System of Japan, 8, 2006
 164. Ashikaga, M., Hiraguchi, T., Sakura, M., Aonuma, H. and Ota, J., Modeling of Adaptive Behaviors of Crickets, 5th Forum of European Neuroscience Abstract Book (FENS Forum Abstracts), 3, A129.1, 2006
 165. M. Ashikaga, M. Kikuchi, T. Hiraguchi, M. Sakura, H. Aonuma and J. Ota, Modeling of fighting behaviors in crickets, The 2nd International Workshop by Research Group of Invertebrate Nervous System of Japan, 7, 2006
 166. Yusuke Tamura, Masao Sugi, Jun Ota and Tamio Arai, Prediction of Target Object Based on Human Hand Movement for Handing-Over between Human and Self-Moving Trays, *Proc. 15th IEEE Int. Symp. Robot and Human Interactive Communication (RO-MAN06)*, 189/194, 2006
 167. Yusuke Tamura, Masao Sugi, Jun Ota and Tamio Arai, Handling-over between Human and Self-Moving Tray, *Proc. XVIII IMEKO World Congress Metrology for a Sustainable Development*, 2006
 168. Daisuke Kurabayashi, Katsunori Urano, Tetsuro Funato, Tetsuro Funato: Emergent Transportation Networks by Considering Interactions between Agents and their Environment, *Advanced Robotics*, (in press), 2007
 169. Daisuke Kurabayashi, Kunio Okita, Tetsuro Funato, Obstacle avoidance of a mobile robot group using a nonlinear oscillator network, *IEEE/RSJ International Conference on Intelligent Robots and Systems*, 186-191, 2006
 170. Tetsuro Funato, Hitoshi Aonuma, Daisuke Kurabayashi, Masahito Nara, Development of oscillator

- network model for behavioral processing,nd International Workshop by Research Group of Invertebrate Nervous System of Japan, 29-31,2006
171. Tetsuro Funato, Daisuke Kurabayashi, Masahito Nara, Synchronization Control by Structural Modification of Nonlinear Oscillator Network, 8th International Symposium on Distributed Autonomous Robotic Systems, 41-50, 2006
 172. Daisuke Kurabayashi, Tomohiro Inoue, Akira Yajima, Tetsuro Funato, Emergence of small-world in Ad-hoc communication network among individual agents, Intelligent Autonomous Systems 9, 605-612, 2006
 173. Cornette R, Koshikawa, S, Hojo M, Matsumoto T, Miura T, A caste-specific cytochrome P450 in the damp-wood termite *Hodotermopsis sjostedti* (Isoptera, Termopsidae), Insect Molecular Biology, 15, 235-244, 2006
 174. Garcia J, Maekawa K, Constantino R, Matsumoto T, Miura T, Analysis of the genetic diversity of *Nasutitermes coxipoensis* (Isoptera: Termitidae) in natural fragments of Brazilian cerrado savanna using AFLP markers. , Sociobiology, 48, 267-279, 2006
 175. Miura T, Caste development and division of labor in the processional nasute termite *Hospitalitermes medioflavus* in Borneo. , TROPICS, 15, 275-278, 2006
 176. Okada Y, Tsuji K, Miura T, Morphological differences between sexes in the ponerine ant *Diacamma* sp. (*Diacamma*: Ponerinae), Sociobiology, 48, 527-541, 2006
 177. Hojo M, Matsumoto T, Miura T, Cloning and expression of a geranylgeranyl diphosphate synthase gene - Insights into the synthesis of termite defense secretion. , Insect Molecular Biology, 16, 121-131, 2007
 178. Katoh H, Matsumoto T, Miura T, Alate differentiation and compound-eye development in the dry-wood termite *Neotermes koshunensis* (Isoptera, Kalotermitidae). , Insectes Sociaux, 54, (in press), 2007
 179. T. Miura, Heterochrony and modularity of the caste polyphenism in termites, XV Congress IUSI Proceedings, 103, 2006
 180. R. Cornette, S. Koshikawa, T. Matsumoto, T. Miura, Juvenile hormone and caste differentiation in the damp-wood termite *Hodotermopsis sjostedti*: histological and molecular approaches focused on the soldier differentiation, XV Congress IUSI Proceedings, 36-37, 2006
 181. S. Koshikawa, T. Miura, Gene expression analysis during caste differentiation in the damp-wood termite - perspective for genome-wide analysis, XV Congress IUSI Proceedings, 104, 2006
 182. S. Miyazaki, T. Murakami, N. Azuma, S. Higashi, T. Miura, Soldier-specific modification of the mandibular motor neurons in termites, XV Congress IUSI Proceedings, 255, 2006
 183. Y. Ishikawa, T. Miura, Soldier-specific modification of the mandibular motor neurons in termites, XV Congress IUSI Proceedings, 872-873, 2006
 184. A. Ishikawa, T. Miura, Developmental regulation of the wing polyphenism in aphids, XV Congress IUSI Proceedings, 229, 2006
 185. M. Hojo, T. Matsumoto, T. Miura, Geranylgeranyl diphosphate synthesis is related to the biosynthesis of defence secretion in *Nasutitermes takasagoensis* (Isoptera: Termitidae), XV Congress IUSI Proceedings, 222, 2006
 186. K. Maekawa, S. Mizuno, S. Koshikawa, T. Miura, Compound eye development during caste differentiation in the termite *Reticulitermes speratus* (Isoptera: Rhinotermitidae), XV Congress IUSI Proceedings, 225, 2006
 187. T. Matsumoto, T. Miura, S. Koshikawa, R. Cornette, K. Maekawa, O. Kitade, T. G. Myles, Phylogeny, evolution and colony composition of the primitive damp-wood termites (Termopsinae, Termopsidae, Isoptera) in Asia and North America, XV Congress IUSI Proceedings, 178-179, 2006
 188. Takeuchi, H., Paul, R. K., Matsuzaka, E., and Kubo, T. , EcR-A expression in the brain and ovary of the honeybee, Zool. Sci., (in press), 2007
 189. Uno, Y., Fujiyuki, T., Takeuchi, H., Morioka, M. and Kubo, T., Identification of proteins whose expression is up- or down-regulated in the mushroom bodies in the honeybee brain using proteomics, FEBS Lett., 581, 1, 97-101, 2007
 190. Hideaki Takeuchi, Gene expression in the Honeybee Brain Mushroom Body and its Gene Orthologues. , Evolution of Nervous Systems (Elsevier), 1, 457-469, 2006
 191. Fujiyuki, T., Ohka, S., Takeuchi, H., Ono, M., Nomoto, A., and Kubo, T. , Prevalence and phylogeny of Kakugo virus, a novel insect picorna-like virus that infects the honeybee (*Apis mellifera* L.), under various colony conditions. , J. Virol. , 80, 23, 11528-11538, 2006

192. Paul, R. K., Takeuchi, H. and Kubo, T. ,Expression of two ecdysteroid-regulated genes, Broad-Complex and E75, in the brain and ovary of the honeybee (*Apis mellifera* L.),*Zool. Sci.*,23,12,1085-1092,2006
193. Kunieda, T. Fujiyuki, T. Kucharski, R. Foret, S., Ament, S. A., Toth, A.L., Ohashi, K, Takeuchi, H, Kamikouchi, A., Kage, E., Morioka, M., Beye, M., Kubo, T., Robinson, G.E., Maleszka, R.,Carbohydrate metabolism genes and pathways in insects: insights from the honey bee genome. *Insect Mol. Biol.*,15,5,563-576,2006
194. Yamazaki, Y., Shirai, K., Paul, R. K., Fujiyuki, T., Wakamoto, A., Takeuchi, H., and Kubo, T.,Differential expression of HR38 in the mushroom bodies of the honeybee brain depends on the caste and division of labor. *FEBS Lett.*,580,11,2667-2770,2006
195. Hori, S.,Takeuchi, H., Arikawa, K., Kinoshita, M., Ichikawa, N., Sasaki, M., and Kubo, T.,Associative visual learning, color discrimination, and chromatic adaptation in the harnessed honeybee *Apis mellifera* L. *J. Comp.Physiol. A*,192,7,691-700,2006
196. Lehman, H. K., Schulz, D. J., Barron, A. B., S. A., Wraight, L., Hardison, C., Whitney, S., Takeuchi, H., Paul, R. K., and Robinson, G. E.,Division of labor in the honey bee (*Apis mellifera*): The role of tyramine beta-hydroxylase, *J. Exp.Biol.*,209,14,2774-2784,2006
197. The Honeybee Genome Sequencing Consortiu,Insights into social insects from the genome of the honey bee *Apis mellifera*. *Nature*,443,7114,931-949,2006
198. Mamiko Ozaki,Ant nestmate and non-nestmate discrimination by a sensillum,15th Internatoinal Union for the Study of Social Insects , 130,2006
199. Wakako Omura, Mamiko Ozaki, Ryohei Yamaoka,Behabioral and electrophysiopogical investigation on taste response of the termite *Zootermopsis nevadensis* to wood extractives,*J. Wood Sci.*,52, 261-264,2006
200. Kazumitsu Hanai, Mamiko Ozaki, Daigo Yamauchi, Yasuhiro Nakatomi, Chihiro Yokoyama and Keniji Fukui,Scale free dynamics involved in the locomotion activity of ant and mouse,WSEAS Transactions on Biology and Biomedicine,3, 511-515,2006
201. Takayuki Watanabe, Mika Kikuchchi, Dai Hatakeyama, Takumi Shiga, Takehiro Yamamoto, Hitoshi Aonuma, Masakazu Takahata, Norio Suzuki, and Etsuro Ito,Gaseous neuromodulator-related genes expressed in the brain of honeybee *Apis mellifera*,*Developmental Neurobiology*, (in press),
202. Takayuki Yamasaki, Teijiro Isokawa, Nobuyuki Matsui, Hidetoshi Ikeno, Ryohei Kanzaki,Reconstruction and simulation for three-dimensional morphological structure of insect neurons,*Neurocomputing*,69, 1043-1047,2006
203. Hidetoshi Ikeno, Takuto Nishioka, Takuya Hachida, Ryohei Kanzaki, Yoichi Seki, Izumi Ohzawa, Shiro Usui,Development and application of CMS based database modules for neuroinformatics,Annual Computational Neuroscience Meeting 2006, 60,2006
204. Tadahiro Taniguchi, Tetsuo Sawaragi,Incremental Acquisition of Behaviors and Signs based on Reinforcement Learning Schema Model and STDP, *Advanced Robotics*, (in press),2007
205. Tetsuo Sawaragi, Yukio Horiguchi and Yuji Kuroda,Editing and Distributing Human Skills within community via Fragmentary Annotations on Image Data,Preprints of the 8th IFAC Symposium on Automated Systems Based on Human Skill and Knowledge, CD-ROM,2006
206. Tetsuo Sawaragi and Yukio Horiguchi,Human-Robot Collaboration: Technical Issues from a Viewpoint of Human-Centered Automation,Proc. of International Symposium on Automation and Robotics in Construction 2006, CD-ROM,2006
207. Tetsuo Sawaragi, Yukio Horiguchi and Akihiro Hina,Safety Analysis of Systemic Accidents Triggered by Performance Deviation,Proceedings of SICE-ICASE International Joint Conference 2006, 1778-1781 ,2006
208. Yukio Horiguchi, Ryuichi Fukuju and Tetsuo Sawaragi,An Estimation Method of Possible Mode Confusion in Human Work with Automated Control Systems,Proceedings of SICE-ICASE International Joint Conference 2006, 943-948,2006
209. T. Taniguchi, T. Sawaragi,Symbol emergence by combining a reinforcement learning schema model with asymmetric synaptic plasticity,Proceedings in 5th International Conference on Development and Learning, CD-ROM,2006
210. T. Taniguchi, T. Sawaragi,Incremental Acquisition of Compositional Schemata based on Behavioral Learning,Proceedings of 6th International Workshop on Epigenetic Robotics, 187,2006
211. Kazuki Tsuji , Tomonori Sasaki , Hideaki Mori,Shigeto Dobata, Eisuke Hasegawa —,Evolutionary Dynamics of altruists vs. social parasites in the ant *Pristomyrmex punctatus*,XV IUSSI (the International

- Union for the study of social insects) Congress Proceedings, 122,2006
212. Kazuki Tsuji, Hisashi Ohtsuki, Reproductive allocation conflict causes worker policing in hymenopteran societies, XV IUSSI Congress Proceedings, 131,2006
 213. Yasukazu Okada, Kazuki Tsuji, Toru Miura, Behavioral ontogeny followed by reproductive division of labor in the Japanese ponerine ant *Diacamma* sp., XV IUSSI Congress Proceedings, 246,2006
 214. Shigeto Dobata, Tomonori Sasaki, Masakazu Shimada, Kazuki Tsuji, Spatially explicit model for altruist-cheater population dynamics in the ant *Pristomyrmex punctatus*, XV IUSSI Congress Proceedings, 256,2006
 215. Mayuko Suwabe, Hitoshi Ohnishi, Tomonori Kikuchi, Kazuki Tsuji, Distributional and seasonal activity patterns of exotic and native ants in Okinawa island, XV IUSSI Congress Proceedings, 263,2006
 216. J. Le Breton, G. Takaku, K. Tsuji, Brood parasitism in an invasive population of the pest ant *Pheidole megacephala*, *Insectes Sociaux*, 53,2, 168-171,2006
 217. Kikuchi, T., Tsuji, K., Ohnishi, H., Le Breton, J., Caste-biased acceptance of non-nestmates in a polygynous ponerine ant, *Animal Behaviour*, (in press),2007
 218. Kazuki Tsuji, Life history strategy and evolution of insect societies: age structure, spatial distribution and density dependence. V. E. Kipyatkov (ed.): *Life Cycles in Social Insects: Behaviour, Ecology and Evolution*. St. Petersburg University Press, St. Petersburg, 156 p., 21-36,2006
 219. K. Oka, A. Fujimura, K. Hotta, H. Ogawa, Analysis of vocal communication between male and female zebra finches, Fifth East Asian Biophysics Symposium & Forty-Fourth Annual Meeting of the Biophysical Society of Japan, 2P370,2006
 220. Tomoko Akiyama, Motoichiro Kato, Taro Muramatsu, Satoshi Umeda, Fumie Saito, Haruo Kashima, Unilateral amygdala lesions hamper attentional orienting triggered by gaze direction, *Cerebral Cortex*, (in press),2007
 221. Tomoko Akiyama, Motoichiro Kato, Taro Muramatsu, Takaki Maeda, Tsunekatsu Hara, Haruo Kashima, Gaze-triggered orienting is reduced in chronic schizophrenia. *Psychiatry Research*, (in press),2007
 222. K. Sasaki and K. Asaoka, Swallowing motor pattern triggered and modified by taste information in larvae of the silkworm, *Bombyx mori*, *Journal of Insect Physiology*, 52, 528-537,2006
 223. H. Shiga, J. Murakami, T. Nagao, M. Tanaka, K. Kawahara, I. Matsuoka and E. Ito, Glutamate release from astrocytes is stimulated via the appearance of exocytosis during cyclic AMP-induced morphologic changes, *Journal of Neuroscience Research*, 84, 338-347,2006
 224. K. Sasaki and K. Harano, Potential effects of tyramine on the transition of reproductive workers in honeybees (*Apis mellifera* L.), *Physiological Entomology*, 32, (in press),2007
 225. K. Harano, M. Sasaki and K. Sasaki, Effects of reproductive state on rhythmicity, locomotor activity and body weight in European honeybee, *Apis mellifera* (Apidae: Hymenoptera) queens, *Sociobiology*, 49, (in press),2007
 226. J. Murakami, H. Aonuma and T. Nagao, Nitric oxide mediated biogenic amine system in the agonistic behavior of cricket, KIT International Symposium on Brain and Language 2005, 23,2006
 227. K. Harano, K. Sasaki and T. Nagao, Dopamine levels associated with physiological and behavioral changes after mating in European honeybee queens, 8th Asian Australian Apicultural Conference Proceedings, 32,2006
 228. K. Harano, K. Sasaki, T. Nagao and M. Sasaki, Decline of dopamine levels after mating and its association with behavioral changes in European honeybee queens, 11th Biological Sciences Graduate Congress Proceedings, 18,2006
 229. K. Sasaki, K. Yamasaki and T. Nagao, Physiological correlates of brain biogenic amines with dominance and reproductive behaviors in primitive paper wasps *Polistes chinensis*, KIT International Symposium on Brain and Language Proceedings, 28-29,2006
 230. K. Harano, K. Sasaki and T. Nagao, Dopamine levels associated with physiological and behavioral changes after mating in European honeybee queens, KIT International Symposium on Brain and Language Proceedings, 24-25,2006
 231. T. Narita, K. Harano and K. Sasaki, Involvement of dopamine and its receptor with transition of reproductive states in honeybee workers, KIT International Symposium on Brain and Language Proceedings, 21-22,2006
 232. M. Sugiyama, K. Sasaki, T. Nagao and K. Iwabuchi, Involvement of biogenic amines with escape

- behaviors of host *Acanthoplistia* agnate parasitized by endoparasitic wasp *Glyptapanteles pallipes*,KIT International Symposium on Brain and Language Proceedings, 26-27,2006
233. Y Tamori and N Tomita,Orbital representation of auditory perception,The 10th meeting of Association for the Scientific Study of Consciousness, 2006
 234. K Mogi and Y Tamori,Making good hidden figures,The 29th European Conference on Visual Perception, 2006
 235. K. Sasaki,Reorganization of the central nervous system responding to changes in social environment in insects,ESB Special Seminar, 2007
 236. Hihara S, Notoya T, Tanaka M, Ichinose S, Ojima H, Obayashi s, Fujii N, Iriki A,Extension of corticocortical afferents into the anterior bank of the intraparietal sulcus by tool-use training in adult monkeys.,*Neuropsychologia*,44,13,2636-46,2006
 237. N. FUJII, S. HIHARA, A. IRIKI,Conflicting social environment represented in primate parietal cortex,Atlanta, GA: Society for Neuroscience, 2006., 63.6,2006
 238. N. FUJII, D. ABLA, N. KUDO, S. HIHARA, K. OKANOYA, A. IRIKI, Prefrontal cortex manipulates abstract odour knowledge,Atlanta, GA: Society for Neuroscience, 2006., 263.17,2006
 239. M. Iribe, K. Osuka,Analogy between Passive walking robot and Phase Locked Loop circuit,Proceedings of the SICE-ICASE International Joint Conference 2006 (SICE-ICCAS 2006), C D,2006
 240. M. Iribe, K. Osuka,Analysis and stabilization of the passive walking robot via analogy with the Phase Locked Loop circuits,Proceedings of the IEEE-RAS/RSJ International Conference on Humanoid Robots (Humanoids 2006), C D,2006
 241. M. Iribe, K. Osuka,A designing method of the passive dynamic walking robot via analogy with the Phase Locked Loop circuits,Proceedings of the 2006 IEEE International Conference on Robotics and Biomimetics (ROBIO2006), C D,2006
 242. Akio Ishiguro,Hiroaki Matsuba,Tomoki Megawa,Masahiro Shimizu,A Modular Robot That Self-Assembles,*Intelligent Autonomous Systems*,9, 585-594,2006
 243. Akio Ishiguro,Masahiro Shimizu,Toshihiro Kawakatsu,A Modular Robot That Exhibits Amoebic Locomotion,*Robotics and Autonomous Systems*,54, 641-650,2006
 244. Akio Ishiguro,Mobiligence: The Emergence of Adaptive Motor Function through Interaction Among the Body, Brain, and Environment,50th Anniversary Summit of Artificial Intelligence, 2006
 245. Masahiro Shimizu, Takafumi Mori, Akio Ishiguro,A Development of a Modular Robot That Enables Adaptive Reconfiguration ,2006 IEEE/RSJ International Conference on Intelligent Robots and Systems, 174-179,2006
 246. Akio Ishiguro, Tomoki Maegawa,Self-Assembly Through the Interplay between Control and Mechanical Systems ,2006 IEEE/RSJ International Conference on Intelligent Robots and Systems, 631-638,2006
 247. Takuya Umedachi, Akio Ishiguro,A Development of a Fully Self-contained Real-time Tunable Spring ,2006 IEEE/RSJ International Conference on Intelligent Robots and Systems, 1662-1667,2006
 248. Dai Owaki, Akio Ishiguro,Enhancing Stability of a Passive Dynamic Running Biped by Exploiting a Nonlinear Spring ,2006 IEEE/RSJ International Conference on Intelligent Robots and Systems, 4923-4928,2006
 249. Tomoki Maegawa, Akio Ishiguro,Self-reconfiguration by a Modular Robot That Has a Cell-differentiation Ability,SICE-ICASE International Joint Conference 2006, 2073-2077,2006
 250. Masahiro Shimizu, Takafumi Mori, Toshihiro Kawakatsu, Akio Ishiguro,An Adaptive Morphology Control of a Modular Robot,SICE-ICASE International Joint Conference 2006, 4509-4514,2006
 251. Dai Owaki, Akio Ishiguro,Enhancing Self-stability of a Passive Dynamic Runner by Exploiting Nonlinearity in the Leg Elasticity ,SICE-ICASE International Joint Conference 2006, 4532-4537,2006
 252. H. Shioya, K. Gohara,Generalized phase retrieval algorithm based on information measures ,*Optics Communications*,266,1,88-93,2006
 253. M. Nagayama, T. Uchida, K. Gohara,Temporal and Spatial variations of Lipid Droplets during Adipocyte Division and Differentiation,*J. Lipid Res.*,48,1,9-18,2007
 254. K. Gohara,Fractals in Hybrid Systems,Proceedings of Nonlinear Theory and Application, 171-174,2006
 255. M. Uchida, Y. Maehara, H. Shioya and W.T. Huang,Unsupervised Weight Parameter Estimation Method for Ensemble Learning,Proceedings of Joint 3rd International conference on Soft computing and Intelligent systems and 7th International Symposium on advanced Intelligent Systems (SCIS & ISIS 2006), 416-421,2006

256. D. Kitakoshi, H. Shioya and R. Nakano, Stochastic Information Expressed in an Mixture Model of Bayesian Networks - Applying to Adaptive Learning for Mobile Robots in Actual Environments, Proceedings of Joint 3rd International conference on Soft computing and Intelligent systems and 7th International Symposium on advanced Intelligent Systems (SCIS & ISIS 2006), 636-643, 2006
257. H. Diebner and I. Tsuda, Fundamental Interfaciology: Indistinguishability and Time's arrow, Proceedings of the Foundation of Information Science 2005, 1-16, 2005
258. H. Fujii and I. Tsuda, Interneurons: their cognitive roles - A perspective from dynamical systems view, The Fourth IEEE International Conference in Development and Learning - from Interaction to Cognition., 1-6, 2005
259. Y. Yamaguti, S. Kuroda and I. Tsuda, A mathematical model for the hippocampus: Toward the understanding of episodic memory, Abstracts: The 8th RIES-Hokudai International Symposium on [bi], 108-109, 2006
260. K. Matsumoto and I. Tsuda, Controlling engine data: Nonperiodic fluctuations in a spark ignition engine of motorcycle and its stabilization, Abstracts: The 8th RIES-Hokudai International Symposium on [bi], 110-111, 2006
261. S. Tadokoro, Y. Yamaguti, I. Tsuda and H. Fujii, Chaotic itinerancy in gap junction-coupled class I* neurons, Abstracts: The 8th RIES-Hokudai International Symposium on [bi], 112-113, 2006
262. Masaki Nomura, Toshio Aoyagi, Stability of Synchronous Solutions in Weakly Coupled Neuron Networks, Progress of Theoretical Physics, 113, 911-925, 2005
263. Takashi Takekawa, Toshio Aoyagi, Tomoki Fukai, Synchronization properties on slow oscillatory activity in a cortex network model, Progress of Theoretical Physics Supplement, S161, 356-359, 2006
264. Masaki Nomura, Takuma Tanaka, Takeshi Kaneko Toshio Aoyagi, Phase analysis of inhibitory neurons involved in the thalamocortical loop, Progress of Theoretical Physics Supplement, S161, 310-313, 2006
265. Takaaki Aoki, Toshio aoyagi, A Possible Role of Incoming Spike Synchrony in Associative Memory Model with STDP Learning rule, International Symposium on Oscillation, Progress of Theoretical Physics Supplement, S161, 152-155, 2006
266. Takaaki Aoki, Toshio aoyagi, Synchrony-induced switching behavior of spike-pattern attractors created by spike-timing dependent plasticity, Neural Computation, (in press),
267. Takaaki Aoki, Toshio aoyagi, Self-Organizing maps with Asymmetric Neighborhood function, Neural Computation, (in press),
268. Masaki Nomura, Toshio Aoyagi, Stability Analysis of Synchronous and Asynchronous Behavior in Periodically Spiking Neurons, The First International Conference on Complex Medical Engineering-CME2005, OS06.4, CD-ROM, 2005
269. Y. Tani, J. Nishii, Optimality of the minimum endpoint variance model based on energy consumption, Brain-inspired IT II: Decision and Behavioral Choice Organized by Natural And Artificial Brains, 1291, 101-104, 2006
270. Takeuchi, H., Paul, R. K., Matsuzaka, E., and Kubo, T. , EcR-A expression in the brain and ovary of the honeybee, Zool. Sci., in press, , 2007
271. Uno, Y., Fujiyuki, T., Takeuchi, H., Morioka, M. and Kubo, T., Identification of proteins whose expression is up- or down-regulated in the mushroom bodies in the honeybee brain using proteomics., FEBS Lett., 581, 1, 97-101, 2007
272. Hideaki Takeuchi, Gene expression in the Honeybee Brain Mushroom Body and its Gene Orthologues. , Evolution of Nervous Systems (Elsevier), 1, 457-469, 2006
273. Fujiyuki, T., Ohka, S., Takeuchi, H., Ono, M., Nomoto, A., and Kubo, T. , Prevalence and phylogeny of Kakugo virus, a novel insect picorna-like virus that infects the honeybee (*Apis mellifera* L.), under various colony conditions. , J. Virol. , 80, 23, 11528-11538, 2006
274. Paul, R. K., Takeuchi, H. and Kubo, T. , Expression of two ecdysteroid-regulated genes, Broad-Complex and E75, in the brain and ovary of the honeybee (*Apis mellifera* L.), Zool. Sci., 23, 12, 1085-1092, 2006
275. Kunieda, T. Fujiyuki, T. Kucharski, R. Foret, S., Ament, S. A., Toth, A.L., Ohashi, K., Takeuchi, H., Kamikouchi, A., Kage, E., Morioka, M., Beye, M., Kubo, T., Robinson, G.E., Maleszka, R., Carbohydrate metabolism genes and pathways in insects: insights from the honey bee genome. , Insect Mol. Biol., 15, 5, 563-576, 2006
276. Yamazaki, Y., Shirai, K., Paul, R. K., Fujiyuki, T., Wakamoto, A., Takeuchi, H., and Kubo, T., Differential

- expression of HR38 in the mushroom bodies of the honeybee brain depends on the caste and division of labor. *FEBS Lett.*,580,11,2667-2770,2006
277. Hori, S., Takeuchi, H., Arikawa, K., Kinoshita, M., Ichikawa, N., Sasaki, M., and Kubo, T., Associative visual learning, color discrimination, and chromatic adaptation in the harnessed honeybee *Apis mellifera* L. *J. Comp. Physiol. A*, 192, 7, 691-700, 2006
 278. Lehman, H. K., Schulz, D. J., Barron, A. B., S. A., Wraight, L., Hardison, C., Whitney, S., Takeuchi, H., Paul, R. K., and Robinson, G. E., Division of labor in the honey bee (*Apis mellifera*): The role of tyramine beta-hydroxylase. *J. Exp. Biol.*, 209, 14, 2774-2784, 2006
 279. Yasuaki Kuroe and Kei Miura, Generation of Oscillatory Trajectories with Specified Stability Degree Using Recurrent Neural Networks, Proc. of International Joint Conference on Neural Networks, 6510-6517, 2006
 280. Yasuaki Kuroe and Yuriko Taniguchi, Models of Self-Correlation Type Complex-Valued Associative Memories and Their Performance Comparison, Proc. of International Joint Conference on Neural Networks, 605-609, 2006
 281. Yasuaki Kuroe and Hitoshi Iima, A Learning Method for Synthesizing Spiking Neural Oscillators, Proc. of International Joint Conference on Neural Networks, 7613-7617, 2006
 282. Yoshihiro Mori, Yasuaki Kuroe and Takehiro Mori, A Synthesis Method of Gene Networks Based on Gene Expression by Network Learning, Proc. of SICE-ICASE International Joint Conference, 4545-4550, 2006
 283. Nishikawa I., Iritani T., Sakakibara K., and Kuroe Y., "Phase Synchronization in Phase Oscillators and Complex-Valued Neural Networks and its Application to Traffic Flow Control", *Progress of Theoretical Physics Supplement*, 161, "302-305", 2006
 284. "Nishikawa I., Iritani T., and Sakakibara K.", "Improvements of the Traffic Signal Control by Complex-valued Neural Networks", *Proceedings of IEEE World Congress on Computational Intelligence 2006*, "1186-1191", 2006
 285. Nishikawa I., Sakamoto H., Nouno I., Iritani T., Sakakibara K. and Ito M., "Prediction of the O-glycosylation sites in Protein by Layered Neural Networks and Support Vector Machines", *Lecture Notes in Artificial Intelligence 4252*, Part II, "953-960", 2006
 286. Nouno, I., Sakamoto, H., Iritani, T., Sakakibara, K., Nishikawa, I. and Ito, M., "Prediction of Mucin-type O-glycosylation by Layered Neural Networks and Support Vector Machines", *Proceedings of the 17th International Conference on Genome Informatics 2006*, P111_1-2, 2006
 287. Sakakibara K., Noishiki M., Watanabe S., Tamaki H. and Nishikawa I., "Hierarchical Approach with Informational Feedback for Pickup and Delivery Problems", *Proceedings of the International Symposium on Scheduling 2006*, 48-53, 2006
 288. Khoa N.L.D., Noishiki M., Sakakibara K., and Nishikawa I., "Stock Price Forecasting using Neural Networks with Inputs selected by Genetic Algorithm", *Proceedings of the 5th International Conference on Research, Innovation and Vision for the Future*, 2007
 289. Khoa, N. L. D., Sakakibara, K., Nishikawa, I., "Stock price forecasting using back propagation neural networks with time and profit based adjusted weight factors", *Proceedings of SICE-ICASE 2006*, 5484-5488, 2006
 290. "Noishiki M., Sakakibara K., Nishikawa I., Tamaki H. and Nakayama K.", "Autonomous Distributed Genetic Approach for Route Planning Problems", *Proceedings of SICE-ICASE 2006*, 6075-6079, 2006
 291. Sakakibara K., Noishiki M., Tamaki H. and Nishikawa I., "A Study on Distributed Meta-Heuristic Approach for Route Planning", *Proceedings of SICE-ICASE 2006*, 4977-4980, 2006

Awards

1. Masashi Ito and Masafumi Yano 4th joint meeting of ASA/ASJ, 28 November--2 December 2006, Honolulu, Hawaii, The second place winner of the Best Student Paper in Speech Communication, "Pitch determination and sinusoidal modeling for time-varying voiced speech," *J. Acoust. Soc. Am.* 120(5), pp.

3376.

2. Yasuaki Kuroe and Hitoshi Iima: World Congress of Computational Intelligence, Best Session Paper Award, A Learning Method for Synthesizing Spiking Neural Oscillators, July 20, 2006, Proc. of International Joint Conference on Neural Networks, pp.7613-7617, 2006
3. Takuya Umedachi, Akio Ishiguro: 2006 IEEE Robotics and Automation Society Japan Chapter Young Award (IROS) 「Development of a Fully Self-contained Real-time Tunable Spring」, 2006年10月11日 Proc. of 2006 IEEE/RSJ International Conference on Intelligent Robots and Systems, WP2-6(3), 2006

Activity Record

| | |
|-------|---|
| Date | April 10th, 2006 |
| Place | Room 316, Bld. P, University of Electro-Communications |
| Name | Explanation about walking control using CPGs and mobiligence activity for media |

| | |
|-------|--|
| Date | April 24th, 2006 |
| Place | Room 321, Bld.14, Faculty of Engineering, The Univ. of Tokyo |
| Name | A group general meeting |

| | |
|-------|---|
| Date | April 27-28th, 2006 |
| Place | Nagoya University |
| Name | D group meeting (planned research groups) |

| | |
|-------|---|
| Date | May 18th, 2006 |
| Place | Dept. of Mechanical Engineering , Kobe University |
| Name | D group meeting (planned research groups) |

| | |
|-------|---|
| Date | May 21st, 2006 |
| Place | Research Institute for Electronic Science , Hokkaido University |
| Name | 1 st C group general meeting |

| | |
|-------|---|
| Date | May 27th, 2006 |
| Place | Okubo Campus, Waseda University |
| Name | Organized session "Mobiligence" in The Japan Society of Mechanical Engineers Conference on Robotics and Mechatronics (ROBOMECH2006) (in Japanese) |

| | |
|-------|---|
| Date | June 9th, 2006 |
| Place | Asahikawa Medical College |
| Name | Study session on Biology-Engineering integrating research |

| | |
|-------|---|
| Date | June 10th, 2006 |
| Place | Campus Plaza Kyoto |
| Name | 1 st D group general meeting |

| | |
|----------|--|
| Date | June 23rd-25th, 2006 |
| Place | Toya SunPalace, Hokkaido |
| Name | Mobiligence Symposium |
| Schedule | <p>June 23rd 13:30-17:30 A, B, C, D Group general meeting (individually)</p> <p>June 24th 09:00-09:30 Director of the Project: Hajime Asama (Univ. Tokyo) 09:30-10:30 A group leader: Koji Ito (Tokyo Institute of Technology) 11:00-12:00 B group leader: Kazuo Tsuchiya (Kyoto University) 13:00-14:00 C group leader: Hitoshi Aonuma (Hokkaido University) 14:00-15:00 D group leader: Koichi Osuka (Kobe University) 15:30-16:30 Invited speaker: Prof. Tateo Shimozawa (Hokkaido University) 16:30-17:30 Invited speaker: Prof. Hiroaki Gomi (NTT Communication Science Labs.)</p> <p>June 25th 09:00-11:00 Subscribed researchers: Toshiya Matsushima (Hokkaido University) Yasuharu Koike (Tokyo Institute of Technology) Takashi Hanakawa (National Center of Neurology and Psychiatry) Naotaka Fujii (RIKEN) Ken Sugawara (Tohoku Gakuin University) Kazutoshi Gohara (Hokkaido University) 11:00-11:30 General Meeting 12:00-14:00 Steering Committee</p> |

| | |
|-------|--|
| Date | July 21st, 2006 |
| Place | Research Institute for Electronic Science, Hokkaido University |
| Name | C group study session |

| | |
|-------|-----------------------------|
| Date | July 22nd, 2006 |
| Place | Kyoto University |
| Name | 3rd B group general meeting |

| | |
|-------|---|
| Date | September 4th, 2006 |
| Place | Tokyo Institute of Technology |
| Name | 1st Mobiligence Engineering Seminar "Measurement and Signal Processing Seminar" |

| | |
|-------|--|
| Date | September 14th, 2006 |
| Place | Tsuyama Campus, Okayama University |
| Name | Organized Session “Mobiligence” in The 24 th Annual Conference of the Robotics Society of Japan (in Japanese) |

| | |
|-------|--|
| Date | September 18th, 2006 |
| Place | Shikotsuko lake |
| Name | C group study session on social behaviors in insects |

| | |
|-------|---|
| Date | September 26th, 2006 |
| Place | RACE (Research into Artifacts, Center for Engineering), The University of Tokyo |
| Name | Organized session “Mobiligence” in the 16 th Intelligent Systems Symposium (FAN Symposium) (in Japanese) |

| | |
|-------|---|
| Date | September 28th, 2006 |
| Place | Okubo Campus, Waseda University |
| Name | 3 rd D group general meeting |

| | |
|----------|---|
| Date | October 11th, 2006 |
| Place | Beijing, China |
| Name | Organized session “Mobiligence” in IEEE/RSJ International Conference on Intelligent Robots and Systems 2006 |
| Schedule | <p>Time: 9:30-10:45 Chairs: Akio Ishiguro, Hajime Asama #1 (9:30~9:48) Title: A Development of a Modular Robot That Enables Adaptive Reconfiguration, Authors: Masahiro Shimizu, Takafumi Mori, Akio Ishiguro #2 (9:48~10:06) Title: Turning Maneuvers of a Multi-legged Modular Robot Using Its Inherent Dynamic Characteristics, Authors: Shinya Aoi, Hitoshi Sasaki, Kazuo Tsuchiya #3 (10:06~10:24) Title: Obstacle Avoidance of a Mobile Robot Group Using a Nonlinear Oscillator Network, Authors: Daisuke Kurabayashi, Kunio Okita, Tetsuro Funato #4 (10:24~10:42) Title: A Distributed Motor Control System based on Spinal Cord and Musculoskeletal Mechanisms, Authors: Tomoaki Nagano, Toshiyuki Kondo, Koji Ito</p> |

| | |
|-------|------------------------------------|
| Date | October 31st, 2006 |
| Place | DIST - University of Genova, Italy |
| Name | Seminar |

| | |
|-------|---|
| Date | November 20th, 2006 |
| Place | Research Institute of Electrical Communication, Tohoku University |
| Name | A & B group joint meeting |

| | |
|-------|--|
| Date | November 21st, 2006 |
| Place | BEXCO, Busan, Korea |
| Name | Organized Session "Mobiligence" in SICE-ICASE International Joint Conference 2006 (SICE-ICCAS2006) |

| | |
|----------|--|
| Schedule | <p>October 21 , 2006(Sat) 09:00 -- 11:00 SA02 Mobiligence (1) , Adaptive Locomotion SA02-1 "Role of the Cerebellum in Adaptive Control of Locomotion" , Prof. Dai Yanagihara SA02-2 "Adaptive Locomotion Mechanisms Inherent in the Musculoskeletal Structure" , Dr. Naomichi Ogihara SA02-3 "Real-time Control of Bipedal Movement based on Basal ganglia and Brainstem" , Dr. Tomita Nozomi SA02-4 "Enhancing Self-stability of a Passive Dynamic Runner by Exploiting Nonlinearity in the Leg Elasticity" , Mr. Dai Owaki SA02-5 "An Adaptive Morphology Control of a Modular Robot" , Mr. Masahiro Shimizu</p> |
| | <p>October 21 , 2006(Sat) 13:30 -- 15:30 SP02 Mobiligence (2) , Adaptive Movements SP02-1 "Computational Models to Understand Sensorimotor Control and Adaptation Performance" , Prof. Vittorio Sanguineti SP02-2 "Control of Reaching Movement in Unpredictably Changing Environment by Constraints Emergence and Satisfaction" , Mr. Yuki Yoshihara SP02-3 "Speed Characteristic of A New Type Ultrasonic-motor and Impedance Matching System by Novel Method" Dr. Dong-Ok Kim SP02-4 "Decomposition of Internal Models in Motor Learning Under Mixed Dynamic Environments" , Prof. Koji Ito SP02-5 "A Proposal of Continuous Time Recurrent Neural Networks with Neuromodulatory Bias for Adaptation to Un-experienced Environments , Dr. Toshiyuki Kondo</p> |

| | |
|-------|---|
| Date | November 28th, 2006 |
| Place | Otsuka Campus, Tsukuba University |
| Name | Organized session “Thinking of Mobiligence with walking dynamics as a breakthrough” (in Japanese) |

| | |
|-------|---|
| Date | December 6th, 2006 |
| Place | Human Information System Laboratory, Kanazawa Institute of Technology |
| Name | C group study session on cricket modeling |

| | |
|-------|---|
| Date | December 25th, 2006 |
| Place | Sapporo Convention Center (SORA) |
| Name | Organized session “Mobiligence (1) – (3)” in SICE SI2006 Conference (in Japanese) |

| | |
|-------|---|
| Date | January 9th, 2007 |
| Place | KKR Yamaguchi Asakura |
| Name | 4 th D group general meeting |

| | |
|-------|---|
| Date | January 29th, 2007 |
| Place | Tokyo Institute of Technology |
| Name | Organized session “Mobiligence” in SICE 19 th SICE Symposium on Decentralized Autonomous Systems (in Japanese) |

| | |
|-------|---|
| Date | February 10th, 2007 |
| Place | 50th Anniversary Memorial Hall, Ryukyu University |
| Name | C group general meeting |